Dynamics of Nondegenerate Vector Bright Solitons in Certain Nonlinear Media

A thesis submitted to Bharathidasan University
for the award of the degree of

DOCTOR OF PHILOSOPHY

in

PHYSICS

by

Mr. R. RAMAKRISHNAN, M. Sc.

CSIR - Direct Senior Research Fellow (Theoretical Physics)

[Reg. No.:40000/Ph.D.K2/Physics/Full-Time/January-2017/Date:06.03.2017]

Under the supervision of

Prof. M. LAKSHMANAN

Professor of Eminence & DST-SERB National Science Chair

Department of Nonlinear Dynamics

School of Physics

Bharathidasan University

Tiruchirappalli - 620 024

Tamilnadu, India

FEBRUARY 2022

DEPARTMENT OF NONLINEAR DYNAMICS
SCHOOL OF PHYSICS
BHARATHIDASAN UNIVERSITY
TIRUCHIRAPPALLI - 620 024
TAMILNADU, INDIA

Prof. M. LAKSHMANAN
Professor of Eminence & DST-SERB National Science Chair

CERTIFICATE

Certified that the work reported in this thesis entitled "**Dynamics of Nondegenerate Vector Bright Solitons in Certain Nonlinear Media**" is based on the bonafide work done by **Mr. R. Ramakrishnan** under my guidance in the Department of Nonlinear Dynamics, School of Physics, Bharathidasan University, Tiruchirappalli - 620 024, during the period 2017-2021 and has not been included in any other thesis submitted previously for the award of any degree.

TIRUCHIRAPPALLI - 620 024
15 FEBRUARY 2022

[M. LAKSHMANAN]
RESEARCH SUPERVISOR

SCHOOL OF PHYSICS
BHARATHIDASAN UNIVERSITY
TIRUCHIRAPPALLI - 620 024
TAMILNADU, INDIA

Prof. S. RAJASEKAR
Professor of Physics & Dean of Sciences (Former)

CERTIFICATE

Certified that the work reported in this thesis entitled "**Dynamics of Nondegenerate Vector Bright Solitons in Certain Nonlinear Media**" is based on the bonafide work done by **Mr. R. Ramakrishnan** under my Co-guidance in the Department of Nonlinear Dynamics, School of Physics, Bharathidasan University, Tiruchirappalli - 620 024, during the period 2017-2021 and has not been included in any other thesis submitted previously for the award of any degree.

TIRUCHIRAPPALLI - 620 024
15 FEBRUARY 2022

[S. RAJASEKAR]
RESEARCH CO-SUPERVISOR

DEPARTMENT OF NONLINEAR DYNAMICS
SCHOOL OF PHYSICS
BHARATHIDASAN UNIVERSITY
TIRUCHIRAPPALLI - 620 024
TAMILNADU, INDIA

DECLARATION

Declared that the work presented in this thesis is based on the original work done by me under the guidance of **Prof. M. LAKSHMANAN**, Professor of Eminence & DST-SERB National Science Chair, Department of Nonlinear Dynamics, School of Physics, Bharathidasan University, Tiruchirappalli - 620 024, during the period 2017-2021 and has not been included in any other thesis submitted previously for the award of any degree.

TIRUCHIRAPPALLI - 620 024
15 FEBRUARY 2022

[R. RAMAKRISHNAN]
RESEARCH SCHOLAR

Dedicated to my Research Supervisor
Prof. M. LAKSHMANAN
and
MY PARENTS

PREFACE

The field of soliton research has been started in recent times from the work of E. Fermi, J. Pasta and S. Ulam through their investigation of the famous anharmonic lattice problem in early 1950s. The energy of the fundamental mode returns after every recurrence time. This result has stimulated various research problems in different areas, ranging from statistical mechanics of nonlinear oscillators, nonlinear normal modes and integrable systems, and so on. The continuum limit of the above anharmonic lattice problem leads to the very celebrated Korteweg de-Vries equation and it admits solitary wave solutions. The beauty of this solitary wave solution is that the amplitude of the wave is directly proportional to the velocity. This means that the higher amplitude waves move faster than the lower amplitude counterparts. This special kind of waves undergo elastic collision and so M. Kruskal and N. Zabusky termed these waves as solitons. Later such solitons were observed in different fields, including plasma physics, Bose–Einstein condensation and nonlinear optics, etc.

Optical solitons have been initially identified in nonlinear optical fibers by Hasegawa and Tappert in both the anomalous and normal dispersion regimes. Wave propagation in nonlinear optical fibers is governed by the standard nonlinear Schroedinger equation and its generalizations. Until the paper by R. Radhakrishnan, M. Lakshmanan, J. Hietarinta (Phys. Rev. E **56**, 2213 (1997)) appeared, people thought that solitons can admit only shape preserving collisions. The shape changing collision property of vector solitons associated with integrable coupled nonlinear Schrödinger equations lead to the construction of optical logic gates (optical computing applications) and soliton switches. This is all possible through the linear fractional transformations associated with the vector soliton collisions. Very surprisingly, we noticed that the vector solitons studied so

far in the literature have identical wave numbers in their individual components (degenerate solitons). Then the obvious questions we got in our mind was what happens if nonidentical wave numbers are characterizing the nature of vector solitons? What kind of collision behaviour do they exhibit? We have initially identified the existence of such vector solitons in two coupled nonlinear Schrödinger equations and their collision properties and then extended the studies to other related systems. Through our series of works, we have studied the properties of this new class of solitons, namely nondegenerate solitons. This thesis is a summary of the results of our studies on nondegenerate solitons on various coupled nonlinear Schrödinger equations.

In Chapter I, we have given a general introduction to solitons and, in particular, solitons in nonlinear optical systems. Chapter II deals with the existence and collision behaviour of nondegenerate solitons in two coupled nonlinear Schroedinger system/Manakov system. In Chapter III, the role of four wave mixing effect on nondegenerate vector solitons has been studied using generalized coupled nonlinear Schroedinger system. Chapter IV elaborates the nature of nondegenerate solitons and their collision dynamics in two component long wave – short wave resonance interaction (LSRI) system familiarly named as Yajima - Oikawa system. In Chapter V, we have studied the existence of nondegenerate solitons in mixed two coupled nonlinear Schroedinger system, coherently coupled nonlinear Schroedinger system and N-coupled nonlinear Schroedinger system. Finally we summarize the results and mention some of the future directions in Chapter VI.

TIRUCHIRAPPALLI **R. RAMAKRISHNAN**
15 FEBRUARY 2022

Acknowledgements

First and foremost, I wish to express my profound gratefulness to my Research Supervisor, **Prof. M. Lakshmanan**, Professor of Eminence & DST-SERB National Science Chair, for introducing me to this wonderful field of integrable nonlinear dynamical systems and optical solitons, his scientific guidance, his moral and human support and for stimulating and enthusiastic discussions during the entire course of research.

I express my sincere thanks to my Research Co-supervisor **Prof. S. Rajasekar**, Dean of Sciences (Former) & Professor of Physics, Bharathidasan University for his moral support and advice during the entire period of research.

It is my great pleasure to thank my doctoral committee members **Dr. T. Kanna**, Associate Professor, Bishop Heber College, Tiruchirappalli and **Dr. A. Venkatesan**, Associate Professor, Nehru Memorial College, Puthanampatti for periodically appraising the progress of my research works and giving various suggestions to improve them.

I express my special and heartiest thanks to my Research Collaborator **Dr. S. Stalin**, Post Doctoral Fellow, Department of Mathematics, Khalifa University, Abu Dhabi, United Arab Emirates for his continuous, tireless help and care during my entire course of research.

It is my great pleasure to thank **Prof. P. Muruganandam**, Head of the Department of Physics, for his help in verifying the stability of nondegenerate solitons numerically.

It is my pleasure to thank **Prof. M. Senthilvelan**, Head of the Department of Nonlinear Dynamics, for his support and encouragement.

My sincere thanks to **Prof. M. Daniel**, CEO, SNS group of institutions, Coimbatore, **Prof. K. Porsezian** (Deceased), Department of Physics, Pondicherry University, **Prof. K. Murali**, Department of Physics, Anna University, Chennai, and **Prof. R. Sahadevan**, Former Director of Ramanujan Institute for Advanced Study in Mathematics, University of Madras, Chennai for their enthusiastic words and motivation during the various workshops, conferences and meetings.

It is a great pleasure to thank my PG teachers **Prof. S. Dhanuskodi** (Retired), **Prof. K. Tamilmaran** (Retired), **Prof. S. Arumugam** (Director,

CHPR), **Prof. K. Jeganathan**, (Director, CNST), **Dr. R. Ramesh Babu**, **Dr. T. C. Sabari Girisun** and **Dr. L. C. Nehru** for their support and encouragement.

It is a great pleasure to thank my Higher Secondary School Physics Teachers, **Mr. S. Soundara Rajan**, National Best Teacher Awardee (1986) & Director, Sri Maha Bharathi Higher Secondary School, Namakkal and **Mr. R. Palani**, Sri Maha Bharathi Higher Secondary School, Namakkal for motivating me to take physics as my career. I extend my sincere thanks to my Higher Secondary School Teachers, **Dr. S. Thangaraja, Mrs. R. Pushpa, Mrs. R. R. Papathi, Mrs. M. Ananthi** and **Mrs. R. Vasanthi**, for their encouragement.

It is my pleasure to thank my Undergraduate mentor, **Dr. P. Christuraj**, Assistant Professor, Department of Physics, St. Joseph College, Tiruchirappalli for his constant support and encouragement.

I thank my lab seniors and colleagues, **Dr. A. Ishaq Ahamed, Dr. B. Subash, Dr. R. Gopal, Dr. A. Durga Devi, Dr. R. Arun, Dr. V. Chithiika Ruby, Dr. K. Sakkaravarthi, Dr. A. Govindarajan, Dr. A. K. Shafeeque Ali, Dr. K. Sathiyadevi** and **Dr. M. Sathish Aravindh** for their support and encouragement.

I wish to express my thanks to **Dr. Shamik Gupta** (Associate Professor, Department of Physics, Ramakrishna Mission Vivekananda University, Belur and now at Tata Institute for Fundamental Research, Mumbai), **Dr. Abhik Mukherjee** (Indian Statistical Institute, Kolkata) and **Dr. Theophile Fonzin Fozin** (Lecturer, Department of EEE, University of Buea, Cameroon) for motivating me during their visits to Bharathidasan University.

I wish to thank my lovable friends, **Mr. M. Isacfranklin, Mrs. S. Preethi, Mrs. R. Kanmani, Mr. M. Durairaj, Mr. S. Harikrishnan, Mr. S. Sudharsan, Mr. J. Praveen Kumar, Dr. S. Christopher Jeyaseelan, Mrs. R. Sowmiya, Mrs. G. Sindhu, Mr. S. Thamizharasan, Dr. T. Anandh, Mr. S. Muthukumar, Mr. M. Sathishkumar, Mr. K. Thirunaukkarasu, Mr. K. Vignesh Balaji, Mr. S. Dinesh Vijay, Mr. T. Ajaykamal, Mr. S. Vignesh, Dr. Patil Nikil Nishikant, Dr. G. Karthi, Mr. A. P. Hari Arvinth, Mr. S. Hariharan, Mr. R. Gokul, Miss. S. Sugapriya, Miss. S. Megavathi, Mr. P. Raju, Mr. V. Gowthambabu, Mr. M. Thiagarajan, Mr. M. Syed Marjuk**

and **Mr. K. Thulasidharan**, for their help and making my period of Ph. D. an enjoyable one.

I wish to thank **Mrs. S. Sumathi**, Section Officer, and the non-teaching staff of School of Physics for their timely help and support.

I sincerely acknowledge the **Department of Science and Technology, Department of Atomic Energy** and **Council of Scientific and Industrial Research, India** for providing me financial support in the form of Project Assistant, Junior Research Fellowship and CSIR-Direct Senior Research Fellowship.

My special and heartiest thanks to my parents, **Mr. K. Ratchagan, Mrs. K. Kantha** and family members, **Mr. M. Subramaniyan, Mrs. R. Devi, Mr. S. Rishanth** and **Mr. S. Kavin**, for their unconditional love, care and support.

TIRUCHIRAPPALLI **R. RAMAKRISHNAN**
15 FEBRUARY 2022

List of Publications

1. *Nondegenerate solitons in Manakov system*, S Stalin, **R Ramakrishnan**, M Senthilvelan, M Lakshmanan, Physical Review Letters 122 (4), 043901 (2019).

2. *Nondegenerate soliton solutions in certain coupled nonlinear Schrödinger systems*, S Stalin, **R Ramakrishnan**, M Lakshmanan, Physics Letters A 384 (9), 126201 (2020).

3. *Nondegenerate solitons and their collisions in Manakov systems*, **R Ramakrishnan**, S Stalin, M Lakshmanan, Physical Review E 102 (4), 042212 (2020).

4. *Multihumped nondegenerate fundamental bright solitons in N-coupled nonlinear Schrödinger system*, **R Ramakrishnan**, S Stalin, M Lakshmanan, Journal of Physics A: Mathematical and Theoretical 54 (14), 14LT01 (2021).

5. *Nondegenerate Bright Solitons in Coupled Nonlinear Schrödinger Systems: Recent Developments on Optical Vector Solitons*, S Stalin, **R Ramakrishnan**, M Lakshmanan, Photonics 8 (7), 258 (2021).

6. *Dynamics of nondegenerate solitons in long-wave short-wave resonance interaction system*, S Stalin, **R Ramakrishnan**, M Lakshmanan, Accepted for Publication in Physical Review E, arXiv:2108.13736 (2022).

7. *General coupled nonlinear Schrödinger system: Role of four-wave mixing effect on nondegenerate vector solitons*, **R Ramakrishnan**, S Stalin, M Lakshmanan, Submitted for publication (2021).

8. *Collision properties of nondegenerate vector solitons in Manakov system*, S. Stalin, **R. Ramakrishnan**, M. Lakshmanan, Submitted for publication (2021).

Contents

Chapter 1

Introduction

1.1 Nonlinear dynamical systems and solitons

The behaviour of physical systems in nature can be well understood by studying their underlying dynamics. Dynamics is the study of change of the state of a physical system as time evolves. According to Newton's laws of motion, any future state of the dynamical system can be predicted with enough accuracy when the force acting on the system is exactly identified and initial conditions are appropriately specified. Based on the types of forces acting on the system, one can classify the dynamics as linear or nonlinear. Linear dynamics is a branch of science of systems which deal with linear forces whereas nonlinear dynamics encompasses systems that are acted upon by nonlinear forces [1]. Nonlinear systems are realized in all branches of sciences including physical, chemical and biological sciences, and they are especially important in the understanding of the interesting problem of wave phenomena. A wave is a disturbance which carries energy from one place to another. Examples include water waves, sound waves, electromagnetic waves and so on which we experience in our daily life. Any wave phenomena can be mathematically modelled using linear or nonlinear partial differential equations. Linear differential equations obey linear superposition principle but the nonlinear differential equations do not obey it.

In the study of nonlinear wave propagation, the observation of the great wave of translation in the Union Canal connecting the cities of Edinburgh

and Glasgow in Scottland by a Victorian Naval Architect John Scott Russel (1834) has played a crucial role. While stopping of a boat (when riding on a horse-back), he observed the water lump which originated in that canal travels a large distance without changing its shape and velocity. Based on further experiments, he proposed that the velocity of the lump of water is directly proportional to its amplitude. The higher amplitude water lumps move faster than the lower amplitude lumps. Later in 1895, two Dutch physicists Korteweg and de Vries have deduced the dynamical equation for the above water wave of translation which is now famously known as the Korteweg-de Vries equation (KdV equation)[2].

In 1965, Norman Zabuski and Martin Kruskal [3] obtained the same KdV equation in the continuum limit of nonlinear lattice of anharmonic oscillators to explain the famous Fermi-Pasta-Ulam (FPU) phenomenon [4]. This KdV equation is a nonlinear dispersive type partial differential equation in (1+1) dimensions. The dispersion property makes the wave to spread out because each Fourier component in the wave travels with different velocities, whereas the nonlinearity steepens the wave. In the case of KdV equation, there is an exact balance between the nonlinearity and dispersion which makes this equation to admit localized wave solutions, namely solitary waves. These solitary waves are often called solitons when they retain their identity even under collision with similar kind of waves. Mathematically, solitons are the solutions of integrable nonlinear partial differential equations and also certain coupled nonlinear ordinary differential equations. This integrability nature of the differential equations can be examined through two methods (among several others), namely Painlevé singularity structure analysis and Lax formalism. Painlevé analysis ensures the existence of solutions of nonlinear differential equations without movable critical point singularities whereas the Lax method provides the possibility of writing the nonlinear equation into a linear eigen value problem and a corresponding linear time evolution equation through a Lax pair. Existence of such stable nonlinear waves are also identified in several branches of physics like shallow/deep water waves in hydrodynamics, light pulse propagation in nonlinear optics, matter waves in condensed matter physics in the form of Bose-Einstein Condensation, nonlinear waves in plasma physics and even in biophysics. It is very important

to understand the underlying structures of nonlinear waves and their dynamics within the framework of integrable/non-integrable nonlinear wave models.

1.2 Solitons in nonlinear optical systems

1.2.1 Linear Effects

In optics, in general, an optical pulse or a beam has a natural tendency to spread while it propagates in a linear medium because the Fourier components of the pulse or the beam start to travel with distinct velocities. The spreading occurs in the temporal domain because of the material dispersion while in the spatial domain it is due to diffraction. In some cases, the spreading takes place due to the combined effects of dispersion and diffraction. The spreading of velocities is called group velocity dispersion (GVD). This dispersion occurs due to material dispersion or waveguide dispersion. In multimode fibers, along with the intramodal dispersion which we mentioned above, intermodal dispersions also occurs. This dispersion may cause attenuation of information or loss in the energy of pulses.

1.2.2 Nonlinear Effects

The invention of LASER is one of the most important milestones in the history of scientific devolepment, because it has very interesting properties like coherence, high intensity, high directionality and strict monochromaticity. This high intense electromagnetic field of the LASER can be able to induce some peculiar and useful properties in the medium in which it propagates. One such important phenomenon is the one which can be induced due to change of polarization of the medium. Nonlinearity in optical systems may be easily understood by learning the change of polarization of the medium due to the strength of applied electromagnetic field. In the linear limit or with low intensity light, the polarization of the medium only depends on the first order suceptibility, $\vec{P_L} = \epsilon_0 \chi \vec{E}$. In the case of high intensity light like LASER's, the total polarization is no longer dependent

only on the first order suceptibility but it also depends on its higher orders, $\vec{P_T} = \vec{P_L} + \vec{P_{NL}}$. In optical fibers the second order suceptibility is zero due to the centre of symmetry exhibited by silica (SiO_2), so the lowest higher order nonlinearity is third order suceptibility and the main role of $\chi^{(3)}$ is to change the refractive index of the medium as proportional to the intensity of light. This intensity dependant refractive index is responsible for the optical Kerr effect. The underlying nonlinear effect eventually induces a self phase shift during the propagation of optical pulse and the phenomenon is known as self phase modulation (SPM). In multimode fibers or even in single mode fibers, due to birefringence property the given light pulse splits into two parts as ordinary and extraordinary rays. Thus there is a possibility of interaction between the two copropagating fields. As a result, nonlinear phase shift is induced by the copropagating fields. This phenomenon is called cross phase modulation (XPM). Very interstingly one more additional nonlinearity occurs due to the optical Kerr effect and it is called four wave mixing (FWM) in which two different frequency components (say ν_1 and ν_2) generate two additional frequency components (ν_3=2ν_1-ν_2 and ν_4=2ν_2-ν_1) by refractive index modulation. These additional frequency components can amplify the already existing frequency components. Practically this parametric amplification process yeilds low power signals due to the lack of phase matching conditions.

However, a stable localized wave packet forms when this linear effect is balanced by the nonlinear response of the medium. Such a stable light wave envelope is known as the optical soliton. Optical soliton can be further classified as (i) spatial soliton, (ii) temporal soliton and (iii) spatio-temporal soliton depending on the nature of formation mechanism [5]. The evolution of optical soliton, whether it is a spatial or temporal one, in $(1+1)$-dimensional setting is described by the ubiquitous nonlinear Schrödinger (NLS) equation. For instance, the dimensionless NLS equation, derived from the Maxwell's equations under slowly varying envelope approximation, for the optical field propagation in a single mode optical fiber turns out to be [6]

$$iq_z - \mathrm{sgn(K'')}q_{tt} + 2|q|^2 q = 0,\ K'' = \left(\frac{\partial^2 K}{\partial \omega^2}\right)_{\omega=\omega_0} = \frac{1}{v_g^2}. \tag{1.1}$$

In the temporal soliton case, where the soliton evolution is confined along the optical fiber, $q(z,t)$ is the complex wave amplitude and the independent variables z and t denote normalized distance along the fiber and retarded time, respectively. Also $q_z = \frac{\partial q}{\partial z}$ and $q_{tt} = \frac{\partial^2 q}{\partial t^2}$. Here, the sign of the group velocity dispersion (GVD) or simply the coefficient of the second derivative in time, in Eq. (1.1), characterizes the nature of the fiber dispersion. If $K'' < 0$, then the dispersion is anomalous whereas the dispersion is normal for $K'' > 0$. The nonlinearity in Eq. (1.1) arises due to the self phase modulation (SPM), where the intensity of light induces a change in the refractive index of the medium $\Delta n(I) = n_0(\omega) + n_2|E|^2 = n_0 + n_2 I$, where n_0 refers to the linear refractive index and n_2 is the nonlinear refractive index of the medium due to Kerr effect, which gives rise to an intensity-dependent phase modulation. On the other hand, the spatial soliton is a self-trapped optical beam that guides itself by inducing a waveguide during the stable propagation in a photorefractive medium without diffraction. Here, the diffraction is exactly balanced by the nonlinearly induced self-focusing effect. In this context, the independent variables, z and t in Eq. (1.1), correspond to transverse spatial coordinates. Since this thesis will focus on the theoretical aspects of vector bright solitons of certain coupled integrable field models that emerge in optical fiber systems, one can find a detailed discussion on the development and advancement of both spatial and spatio-temporal solitons in the interesting review articles by Chen et al [7] and by Malomed et al [8], respectively.

In 1973, Hasegawa and Tappert theoretically demonstrated that the lossless fibers can admit bright soliton structure, which exhibits an intensity maximum in the time domain when the GVD regime is anomalous [9]. They have also shown that the dark soliton, with the intensity minimum or dip on a constant wave background field, arises in the normal GVD regime [10]. After this theoretical work, in 1980, Mollenauer and his coworkers succeeded experimentally in observing the optical soliton in a fiber [11]. These discoveries clearly demonstrated how an abstract mathematical concept can turn into a practical use. Both these theoretical and experimental works have opened up a new possibility of using the ultrashort optical pulses in long distance communication applications [12]. On

the other hand, the mathematical interest in understanding the analytical structure of the underlying integrable models intensified after the NLS equation was solved by Zakharov and Shabat through a more sophisticated inverse scattering transform (IST) method [13], developed earlier by Gardner et al. for the celebrated Korteweg-de Vries equation [14]. Now, it is well known that the NLS equation (1.1) is a completely integrable infinite dimensional Hamiltonian system having special mathematical properties like an infinite number of conserved quantities and Lax pair [15]. We note that in [13] the authors had derived a double-pole solution, which has recently received attention in the theory of rogue-waves for describing the Peregrine breather on the zero background field of the NLS equation [16], by considering the merging of two simple poles in the complex plane. The interesting fact of the temporal bright solitons of the scalar NLS equation is that they exhibit particle-like elastic collision.

Apart from the above fundamental aspects, in 1983, Gordon had predicted that when two or more light pulses propagate in a nonlinear optical fiber, they exert forces, either attractive or repulsive, on their neighbors [17]. This has been experimentally verified by Mitschke and Mollenauer in [18]. Such a study brought out a special kind of soliton state, namely bound soliton state or soliton molecule [19]. A soliton molecule is a bound soliton state that can be formed when two solitons persist at a stable equilibrium separation distance, where the interaction force is zero among the individuals. Such a stable equilibrium manifests as this bound state structure, reminiscent of a diatomic molecule in chemical physics. The binding force arises between the constituents of the soliton composite due to the Kerr nonlinearity [17, 18] and the detailed mechanism can be found in Ref. [20]. This special kind of soliton state has been extensively studied in non-dispersion managed fibers [21–27]. Recently, the existence of soliton molecules in dispersion-managed fiber [19] and their usefulness in optical telecommunications with enhanced data carrying capacity have been pointed out [28, 29]. However, in order to elevate the transmission capacity of the optical telecommunication systems, it is necessary to consider multichannel bit-parallel wavelength fiber networks and wavelength division multiplexing schemes, where the light pulses propagate in multi channels simultaneously. In fact, practically even in a single mode fiber

the bending and strains or birefringence induce two orthogonal polarization modes. To pursue this kind of practical applications, one has to essentially understand the problem of intermodal interaction of solitons. Therefore the contribution of the interaction of copropagating modes must be taken into account. In fact, there is no surprise other than the standard elastic collision of the bright solitons in single mode optical fibers. In contrast to this, the bright soliton structure in two mode fibers or in a single mode fiber with birefringence property or even in multimode fibers display rich propagation and collisional properties. Due to these fascinating features and intriguing collision dynamics, vector solitons (which are solutions of coupled NLS type equations) are receiving intense attention among researchers. Apart from the several interesting properties, vector solitons have also been found in a variety of applications, including soliton based optical computing [30, 31], multi-level optical communication with enhanced bit-rate transmission [32], soliton based signal processing systems [33] and so on.

Vector solitons are fascinating nonlinear objects in which a given soliton is split among two or more components. In other words, a vector soliton with two or more polarization components coupled together maintains its shape during propagation. Such vector solitons are also named as multicolour solitons. The dynamics of vector solitons is usually understandable within the framework of coupled nonlinear Schrödinger (CNLS) equations. In general, the CNLS equations are non-integrable and they become integrable for specific choices of parameters [34]. Therefore, mathematically vector solitons arise as solutions of the CNLS equations. Like in the scalar NLS equation, the optical vector solitons are formed due to an exact balance between the dispersion/diffraction and the self-phase modulation and cross-phase modulation. This interesting class of optical solitons has been first predicted by Manakov in 1974, where he has derived the one-soliton solution and made an asymptotic analysis for the two-soliton solution through the IST method, by introducing a set of two CNLS equations for the nonlinear interaction of the two orthogonally polarized optical waves in birefringent fibers [35]. The Manakov system is essentially an integrable system, where the strength of the nonlinear interactions within

and between the components are equal. Vector optical solitary wave propagation in birefringent fiber has been first theoretically studied by Menyuk by considering a pair of non-integrable CNLS equations [36]. Very interestingly Lakshmanan along with Radhakrishnan and Hietarinta theoretically predicted that the bright solitons of the Manakov model exhibit novel energy sharing collision through intensity redistribution [37]. They have explicitly demonstrated this fascinating collision scenario by analysing the two bright soliton solution derived through the Hirota bilinear method. Then this study has been extended to N-CNLS equations by Kanna and Lakshmanan in [38], where there is a lot of exciting possibilities for the occurrence of energy redistribution among the N-modes that have been reported. This theoretical development was experimentally verified in [39–41] and subsequently, it gave rise to the possibility of constructing all optical logic gates [30, 31, 42–44]. The discovery of photorefractive solitons [45–48] and the subsequent experimental developments [49–52] have substantially enriched our knowledge on vector solitons. It is known that a set of N-CNLS equations describes the beam propagation in a Kerr-like photorefractive medium [53–56]. Further, the experimental studies on vector solitons in photorefractive media as well as in dispersive media during the past three decades demand investigation of physical and mathematical aspects of CNLS equations even more rigorously.

It is very important to point out there exist many types of vector solitons that have been reported so far for both integrable and non-integrable CNLS type equations. For instance, in the non-integrable cases, a temporal light pulse composed of orthogonally polarized components propagate with common group velocity and it is called group velocity-locked soliton [57]. On the other hand, if the two polarization components of the soliton are locked in phase, then such a vector soliton has been called a phase-locked soliton [58], whereas for the polarization-locked vector soliton [59], the relative phase between the components is locked at $\pm\frac{\pi}{2}$ but across the pulse, and the polarization state profile is not uniform. However, the corresponding profile is invariant with propagation. Apart from the above, other types of vector solitary waves have been reported in birefringent fibers [60–63] and in saturable nonlinear medium [64, 65], where the stability of multi-hump solitons has been reported. In the integrable cases,

bright-bright solitons [35, 37, 38, 66], bright-dark or dark-bright solitons [67–71] and dark-dark solitons [72, 73] were documented in the context of nonlinear optics and their novel properties in multicomponent BECs have also been investigated considerably [74]. In a photorefractive medium, partially coherent solitons or soliton complexes were identified in the N-CNLS system, and their special properties were revealed by Akhmediev and his collaborators in [32, 53–56]. Apart from the above, during the last decade, a large volume of work has been dedicated to the temporal optical solitons (both theoretically and experimentally) by considering the fiber lasers, which has been reported as a very useful nonlinear system to study the dynamics and formation of temporal optical solitons [75]. There exist different types of optical solitons in dissipative systems too and their various properties have been explored in [76].

From the above studies on vector solitons, especially in integrable coupled nonlinear Schrödinger models, we have identified that there exists a degeneracy in the structure of the bright solitons as we have explained below in Section 1.4. That is, the solitons in two-mode fibers or in multimode fibers propagate with identical wave numbers. In order to avoid this degeneracy, we introduce two non-identical propagation constants appropriately in the structure of the fundamental bright solitons of the 2-CNLS equation to start with. Consequently, the degeneracy is removed and it leads to a new class of fundamental bright solitons, namely nondegenerate fundamental vector bright solitons [77]. For the first time, we have shown that such an inclusion of additional distinct propagation constants brings out a general form of vector bright soliton solution to the several integrable CNLS systems [78, 79], namely Manakov system or 2-CNLS system, mixed 2-CNLS system (with one mode in the anomalous dispersion regime and the other mode in the normal dispersion regime), 2-component coherently coupled NLS system, generalized CNLS system, and 2-component long-wave short-wave resonance interaction system [79]. We note that very recently the nondegenerate solitons have also been studied in other contexts as well. For instance, in multi-component BECs [80] using the Darboux transformation method, in coupled Fokas-Lenells system [81] and in AB-system [82] such nondegenerate solitons have been identified. We also note that multi-valley dark nondegenerate soliton has been studied in the

context of multicomponent repulsive BECs [83]. In this thesis, we critically study, the existence and their salient novel features of the general form of nondegenerate vector bright solitons in the above class of 2-component nonlinear Schrödinger systems. Then we also critically analyse their novel collision properties with the Manakov system as an example. Further, we also discuss in detail the corresponding already known degenerate vector bright solitons and their intriguing collisional properties. Additionally, we also illustrate the multi-hump nature of the nondegenerate fundamental bright solitons in N-CNLS system [84].

1.3 Derivation of CNLS equations and other integrable CNLS type models

In general, the interaction between two or more co-propagating optical modes is governed by the coupled nonlinear Schrödinger family of equations. The derivation of one such CNLS equations starts from the Maxwell's equations for electromagnetic wave propagation in a dielectric medium,

$$\nabla^2\vec{E} - \frac{1}{c^2}\frac{\partial^2\vec{E}}{\partial t^2} = -\mu_0\frac{\partial^2\vec{P}}{\partial t^2}, \tag{1.2}$$

where $\vec{E}(\vec{r},t)$ is the electric field, $\vec{P}(\vec{r},t)$ is the induced polarization, μ_0 is the permeability of free space and c is the velocity of light. The induced polarization $\vec{P}(\vec{r},t)$ contains both a linear part and a nonlinear part. That is $\vec{P}(\vec{r},t) = \vec{P}_L(\vec{r},t) + \vec{P}_{NL}(\vec{r},t)$. The linear and nonlinear induced polarizations can be further written as

$$\vec{P}_L(\vec{r},t) = \epsilon_0\int_{-\infty}^{+\infty}\chi^{(1)}(t-t')\vec{E}(\vec{r},t')dt', \tag{1.3a}$$

$$\vec{P}_{NL}(\vec{r},t) = \epsilon_0\int_{-\infty}^{+\infty}\int_{-\infty}^{+\infty}\int_{-\infty}^{+\infty}\chi^{(3)}(t-t_1,t-t_2,t-t_3)\vec{E}(\vec{r},t_1)\vec{E}(\vec{r},t_2)\vec{E}(\vec{r},t_3)dt_1dt_2dt_3. \tag{1.3b}$$

Here, ϵ_0 is the permitivity of the free space and $\chi^{(j)}$ is the jth order susceptibility tensor of rank $(j+1)$ [6, 85]. For elliptically birefringent fibers, the electric field $\vec{E}(\vec{r},t)$ can be written as

$$\vec{E}(\vec{r},t) = \frac{1}{2}\Big(\hat{e}_1 E_1(z,t) + \hat{e}_2 E_2(z,t)\Big)e^{-i\omega_0 t} + c.c. \tag{1.4}$$

In the above, the variables z and t denote the direction of propagation and retarded time, respectively and $c.c$ stands for complex conjugation. The orthonormal vectors $\hat{e}_1$ and $\hat{e}_2$ are expressed as, $\hat{e}_1 = \frac{\hat{x}+ir\hat{y}}{\sqrt{1+r^2}}$ and $\hat{e}_2 = \frac{r\hat{x}-i\hat{y}}{\sqrt{1+r^2}}$, where r is a measure of the extent of ellipticity and $\hat{x}$ and $\hat{y}$ are unit polarization vectors along x and y directions, respectively. In Eq. (1.4), E_1 and E_2 are complex amplitudes of the polarization components at frequency ω_0. The nonlinear polarization can be obtained by substituting the expression of the electric field $\vec{E}(\vec{r},t)$ from Eq. (1.4) in Eqs. (1.3a) and (1.3b). The electric-field components are written under slowly varying approximation as

$$E_j(z,t) = F_j(x,y)Q_j(z,t)e^{iK_{0j}z},\ j = 1,2, \tag{1.5}$$

where $F_j(x,y)$ are the fiber distribution function in the transverse directions x and y and K_{0j}, $j = 1,2$, are the propagation constants for the two modes. By doing so, the following coupled equations are obtained for $Q_j(z,t)$:

$$iQ_{1,z} + \frac{i}{v_{g1}}Q_{1,t} - \frac{k''}{2}Q_{1,tt} + \mu(|Q_1|^2 + B|Q_2|^2)Q_1 = 0, \tag{1.6}$$

$$iQ_{2,z} + \frac{i}{v_{g2}}Q_{2,t} - \frac{k''}{2}Q_{2,tt} + \mu(|Q_1|^2 + B|Q_2|^2)Q_2 = 0. \tag{1.7}$$

Here, $k'' = \left(\frac{\partial^2 k}{\partial\omega^2}\right)_{\omega=\omega_0}$ accounts for the group velocity dispersion, μ is the nonlinearity coefficient and v_{g1} and v_{g2} are the group velocities of the two co-propagating modes, respectively. The constant $B = \frac{2+2\sin^2\theta}{2+\cos^2\theta}$ is the cross-phase modulation coupling parameter, where θ is the angle of ellipticity which varies between 0 and $\frac{\pi}{2}$. Here, we have assumed that the fiber is having a strong birefringent nature. Under three sets of consecutive transformations (detailed derivation can be found in [85]), we obtain the following dimensionless 2-CNLS equation with the integrability restriction

$B = 1$ [34], which is obtained from the Painlevé analysis,

$$iq_{1,z} + q_{1,tt} + 2\mu(|q_1|^2 + |q_2|^2)q_1 = 0, \tag{1.8}$$
$$iq_{2,z} + q_{2,tt} + 2\mu(|q_1|^2 + |q_2|^2)q_2 = 0. \tag{1.9}$$

The above set of CNLS equations constitute the completely integrable system introduced by Manakov to describe the propagation of an intense electromagnetic pulse in a birefringent fiber [35]. The system (1.8)-(1.9) is well discussed in nonlinear optics and in other areas of physics. In this thesis, we also wish to consider another 2-CNLS equation which is a variant of the Manakov system, namely the mixed coupled nonlinear Schrödinger system or Zakharov and Schulman system [66, 86]. One can write both the mixed CNLS equation and Manakov equation in a unified form as given below:

$$iq_{j,z} + q_{j,tt} + 2\left(\sigma_1|q_1|^2 + \sigma_2|q_2|^2\right)q_j = 0, \qquad j = 1, 2. \tag{1.10}$$

In Eq. (1.10), σ_1 and σ_2 are the strength of the SPM and cross-phase modulation (XPM) nonlinearities. If $\sigma_1 = \sigma_2 = +1$, the above equation becomes the Manakov equation (focusing type 2-CNLS equations), where the two optical fields q_1 and q_2 propagate in the anomalous dispersion regimes [35], whereas for $\sigma_1 = \sigma_2 = -1$, they propagate in the normal dispersion regimes or in other words, the resultant model (1.10) turns out to be the defocusing Manakov system [72]. For the other choice, $\sigma_1 = +1$ and $\sigma_2 = -1$, the system (1.10) becomes the mixed-CNLS system [66], in which the SPM is positive and the XPM is negative in both the modes, where the first mode q_1 is propagating in the anomalous dispersion regime while the second mode q_2 is propagating in the normal dispersion regime. Both the focusing and defocusing Manakov models also find applications in attractive and repulsive multicomponent BECs [74]. We note that the soliton trapping and daughter wave (shadow) formation have been reported [87] using the bright soliton solutions of the Manakov system. Radhakrishnan and Lakshmanan have derived the dark-dark soliton solution [72] and Sheppard and Kivshar have obtained bright-dark soliton solution [68] to

the above system. In the latter case, the authors have pointed out the existence of breathing bound states. Further, it has been shown that the mixed CNLS system models the electromagnetic pulse propagation in isotropic and homogeneous nonlinear left handed materials [88]. By taking into account the electron-phonon interaction and in the long-wavelength approximation, the mixed-CNLS system can also be obtained as the modified Hubbard model (Lindner-Fedyanin system) [89–91]. The mixed CNLS system is also realized in two species BECs for a suitable choice of interspecies and intraspecies interactions [92]. We point out that the IST method and Darboux transformation method have been rigorously developed to obtain the bright-bright, dark-dark and bright-dark soliton solutions of the multicomponent focusing, defocusing and mixed CNLS systems [93–105].

Next, we consider the two-component coherently coupled nonlinear Schrödinger equation, which arises due to the coherent effects of the coupling among the copropagating optical fields. In general, an ultrashort pulse propagation in non-ideal weakly birefringent multimode fibers and optical beam propagation in low anisotropic Kerr type nonlinear media are described by the following two-component non-integrable CCNLS system, [5, 106, 107];

$$iq_{1,z} + \delta q_{1,tt} - \mu q_1 + (|q_1|^2 + \sigma|q_2|^2)q_1 + \lambda q_2^2 q_1^* = 0, \tag{1.11}$$

$$iq_{2,z} + \delta q_{2,tt} + \mu q_2 + (\sigma|q_1|^2 + |q_2|^2)q_2 + \lambda q_1^2 q_2^* = 0. \tag{1.12}$$

The above equation also appears in isotropic Kerr-type nonlinear gyrotropic medium [108]. In the above q_1 and q_2 are two coherently coupled orthogonally polarized modes, z and t are the propagation direction and transverse direction, respectively, μ is the degree of birefringence, σ and λ are the incoherent and coherent coupling parameters, respectively, and δ is the group velocity dispersion. The nonlinearities arise in Eq. (1.11) and Eq. (1.12) due to SPM ($|q_j|^2 q_j$, $j = 1, 2$), XPM ($\sigma|q_k|^2 q_j$, $j, k = 1, 2$, $j \neq k$) and four-wave mixing effect ($\lambda q_k^2 q_j^*$, $j, k = 1, 2$, $j \neq k$). Equations (1.11) and (1.12) are shown to be integrable for a specific choice of system parameters (δ, μ, σ and λ) [107] and soliton solutions were derived by linearly superposing the soliton solutions of the two nonlinear Schrödinger equations

through a transformation. The corresponding integrable two-component CCNLS system (2-CCNLS system) is

$$iq_{1,z} + q_{1,tt} + \gamma(|q_1|^2 + 2|q_2|^2)q_1 - \gamma q_2^2 q_1^* = 0, \tag{1.13}$$
$$iq_{2,z} + q_{2,tt} + \gamma(2|q_1|^2 + |q_2|^2)q_2 - \gamma q_1^2 q_2^* = 0. \tag{1.14}$$

Interestingly, Kanna et al [109] have derived the fundamental and two bright soliton solutions of (1.13), (1.14) and its multicomponent version [110] by developing a non-standard Hirota bilinearization procedure. They have classified the fundamental bright soliton as incoherently coupled soliton (ICS) and coherently coupled soliton (CCS) based on a condition on the parameters in the auxiliary function. A novel double-hump soliton profile arises in these CCNLS systems due to the coherent coupling among the two copropagating optical fields. Further, they have also demonstrated a fascinating energy switching collision during the interaction of ICS and CCS [109, 110]. We remark that the CCNLS type equations are useful in studying the dynamics of solitons in spinor BECs and coherently coupled BECs [111–113]also. A similar type of CCNLS equation has been identified in the context of spinor BEC and is shown to be integrable [114–116].

Next, we wish to examine the bright soliton solutions of the general coupled nonlinear Schrödinger (GCNLS) system [117], namely

$$iq_{1,z} + q_{1,tt} + 2(a|q_1|^2 + c|q_2|^2 + bq_1q_2^* + b^*q_1^*q_2)q_1 = 0, \tag{1.15}$$
$$iq_{2,z} + q_{2,tt} + 2(a|q_1|^2 + c|q_2|^2 + bq_1q_2^* + b^*q_1^*q_2)q_2 = 0. \tag{1.16}$$

In the above GCNLS equations, a and c account for the strength of the SPM and XPM nonlinearities whereas the complex parameter b in the phase dependent terms, $bq_1q_2^* + b^*q_1^*q_2$, describes the four-wave mixing effect that arises in multichannel communication systems [6]. When $a = c$ and $b = 0$ the system (1.15)-(1.16) reduces to the Manakov system (or Eq. (1.10) with $\sigma_1 = \sigma_2 = +1$). Then, if $a = -c$ and $b = 0$ the GCNLS system becomes the mixed-CNLS model.

This GCNLS system has received considerable attention recently in

both mathematical and physical aspects [117–120]. The integrability properties of the system (1.15) and (1.16) have been studied in [117] in which the N-soliton solution was obtained through the Riemann-Hilbert method. The GCNLS system is shown to be integrable through Weiss-Tabor-Carnevale (WTC) Painlevé test [118]. In [119], bright and dark-soliton solutions were obtained through the Hirota bilinear method. By relating the GCNLS system with the Manakov and Makhankov vector models using a transformation ($q_1 = \psi_1 - b^*\psi_2$ and $q_2 = a\psi_2$), the authors in [120] have constructed bright-bright, dark-dark and a quasibreather-dark soliton solutions.

Finally, for our investigation, we also wish to take into account the following coupled nonlinear Schrödinger type equations, namely the two-component long-wave short-wave resonance interaction system,

$$iS_t^{(1)} + S_{xx}^{(1)} + LS^{(1)} = 0,\ iS_t^{(2)} + S_{xx}^{(2)} + LS^{(2)} = 0,\ L_t = \sum_{l=1}^{2}(|S^{(l)}|^2)_x. \quad (1.17)$$

In the above, $S^{(l)}$'s, $l = 1, 2$, are short-wave (SW) components, L is the long-wave (LW) component and suffixes x and t denote partial derivatives with respect to spatial and temporal coordinates, respectively. The above LSRI system arises whenever the phase velocity of the low-frequency long-wave matches with the group velocity of the high-frequency short-waves [121, 122]. In Eq. (1.17), the formation of soliton in the SW components is due to the exact balance between its dispersion by the nonlinear interaction of the LW with the SW. At the same time, the formation and evolution of the soliton in the LW components is determined by the self-interaction of the SWs. The above LSRI system (1.17) has considerable physical relevance in nonlinear optics [123–126], plasma physics [127, 128], hydrodynamics [122, 129–133] and BECs [134–136]. The LSRI system originally arose from the pioneering study of nonlinear resonant interaction of the plasma waves by Zakharov [121], where generalized Zakharov equations were deduced to describe Langmuir waves. Such generalized Zakharov equations were reduced to $(1+1)$-dimensional Yajima-Oikawa equation for describing the one-dimensional two-layer fluid flow [128] for which soliton solutions were obtained through the IST method. Benney has also derived a single-component LSRI system for modelling the dynamics of

short capillary gravity waves and gravity waves in deep water [122]. After these works, there have been a large amount of work in the direction of LSRI involving $(1+1)$ and $(2+1)$-dimensional single component and multi-component cases [137–154]. In nonlinear optics, the single component LSRI system was deduced from the coupled nonlinear Schrödinger equations describing the interaction of two optical modes under small amplitude asymptotic expansion [123]. In the negative refractive index media, the LSRI process has been investigated [124]. We wish to point out that the bright soliton solutions for the general multi-component LSRI system have been derived through the Hirota bilinear method [138]. In this thesis, we have demonstrated two types of energy sharing collisions for two different choices of nonlinearity coefficients. Considering the collisions of solitons in these cases one finds that the solitons appearing in the LW component always exhibit elastic collision whereas the solitons in the SW components always undergo energy sharing collisions.

1.4 Motivation of the present thesis

As we have pointed out in Section 1.2, the fundamental (even higher order) bright soliton solutions which have been already reported for the integrable coupled nonlinear Schrödinger family of equations are degenerate. Here, by degenerate, we mean that the fundamental bright soliton nature is characterized by a single wave number in all the modes or components. The presence of identical wave number in all the modes restricts the motion as well as the structure of the fundamental bright soliton in most of the CNLS type equations. Thus, the bright solitons propagate in all the modes with identical velocity apart from the distinct polarization vector constants. Such a constrained motion always persists in most of the fundamental bright soliton solutions of various CNLS systems. As a consequence of this degeneracy, a single-hump structure only emerges in the fundamental bright soliton profile. In order to demonstrate this clearly, in the following, we consider the fundamental bright soliton solution of the Manakov system:

$$q_j = \frac{\alpha_1^{(j)} e^{\eta_1}}{1 + e^{\eta_1 + \eta_1^* + R}} \equiv A_j k_{1R} e^{i\eta_{1I}} \mathrm{sech}(\eta_{1R} + \frac{R}{2}),\ j = 1, 2. \tag{1.18}$$

Here A_j's are the unit polarization vectors, $A_j = \frac{\alpha_1^{(j)}}{(|\alpha_1|^2 + |\beta_1|^2)^{1/2}}$, $j = 1, 2$, the wave variable η_1 $(= \eta_{1R} + i\eta_{1I})$, $\eta_{1R} = k_{1R}(t - 2k_{1I}z)$, $\eta_{1I} = k_{1I}t + (k_{1R}^2 - k_{1I}^2)z$ and $e^R = \frac{(|\alpha_1|^2 + |\beta_1|^2)}{(k_1 + k_1^*)^2}$. From the above expression for the one-soliton solution, it is evident that the fundamental soliton is described by only one complex wave number k_1. Consequently, the single-hump soliton propagates in the two modes, q_1 and q_2, with identical velocity $v = 2k_{1I}$. A similar situation always persists in the other coupled field models mentioned above and their generalizations. For instance, the N-component Manakov type system [38], the mixed N-CNLS system [66], the GCNLS system [117, 119], and the multi-component LSRI system [128, 138] are such cases. However, in contrast to such cases, the coherent coupling among the copropagating optical fields induces a special type of double-hump vector bright soliton in the CCNLS system [109, 110]. In this four wave mixing physical situation also the coherently coupled soliton is governed by an identical propagation constant in all the modes. Therefore it is clear that the above mentioned degeneracy in propagation constants always persist in all the previously reported vector bright solitons.

In order to differentiate the above class of vector bright solitons from more general fundamental solitons, we classify them as degenerate and nondegenerate solitons based on the absence or presence of more than one wave numbers in the multi-component soliton solution. We call the solitons which propagate in all the modes with identical wave number as degenerate vector solitons whereas the solitons with nonidentical wave numbers as nondegenerate vector solitons. From the above literature, it is clear that the vector bright solitons with identical wave numbers have been well understood. However, the studies on solitons with non-identical propagation constants in all the modes have not been considered until recently. Therefore one would like to investigate the role of additional wave number(s) on the vector bright soliton structures and collision scenario

as well. With this motivation, we plan to look for a class of fundamental soliton solutions, in a more general form, which possesses more than one distinct propagation constants. Recently, we have successfully identified such a general class of fundamental vector bright soliton solutions for a wide class of physically important CNLS type equations using the Hirota bilinear method. In this thesis, we elaborately describe the novel properties, including the various collision properties, associated with the nondegenerate vector bright solitons of the Manakov system by deriving their analytical forms through the bilinearization method. Then we point out the existence of such nondegenerate solitons in other coupled systems, namely N-CNLS system, mixed 2-CNLS system, 2-CCNLS system, GCNLS system and two-component LSRI system. In these systems, we also specify how the degenerate bright soliton solution arises as a special case of the nondegenerate soliton solution and point out their fascinating energy sharing collisions.

1.5 Methodology

The present work is mainly concerned with theoretical calculations and we have carried out the above mentioned objectives by using the following analytical techniques.

(i) Hirota bilinearization method:

The standard Hirota bilinear method is adopted to bring out the exact analytical form of the nondegenerate fundamental vector solitons in all the CNLS family of systems mentioned above except for the CCNLS system and to derive the higher-order nondegenerate soliton solutions in the Manakov system, the GCNLS system and the 2-LSRI system. The standard Hirota bilinear procedure has the following steps.

- First one has to bilinearize the given coupled nonlinear partial differential equations using the dependant variable transformations which comes as a result of Painleve' singularity structure analysis.

- Then for the unkown functions present in the bilinear forms of the associated coupled nonlinear partial differential equations, one needs to substitue suitable power series expansion with a small expansion parameter.
- Collecting the various powers of the small expansion parameter leads to a set of linear coupled partial differential equations, where the lowest order partial differential equations are of homogenous type while the higher orders are of inhomogenous types.
- Now one can consider the admissible seed solutions, for the lowest-order linear partial differential equations, as the starting solution.Then proceeding in a standard way, solving the successive inhomogeneous linear partial differential equations, we deduce the full series solution.
- Explicit forms of the complex or real functions which appeared in the bilinear transformations constitue the soliton solution of the given coupled nonlinear partial differential equation.

(ii) Nonstandard bilinearization procedure:

It is known that to derive the soliton solutions for the CCNLS system one has to adopt the non-standard Hirota bilinearization procedure rather than considering the standard bilinearization procedure. Since to get the nontrivial solutions as well as to make the number of bilinear equations to be equal to the number of unknown functions it is very much essential to introduce an appropriate number of auxiliary variables to get the correct bilinear forms of the CCNLS system. Once the bilinearization is achieved we assume the more general form of admissible seed solutions for the lowest-order linear PDEs and then perform the calculations in the standard way.

(iii) Asymptotic analysis:

Asymptotic analysis is used to investigate the collision dynamics of nondegenerate solitons. By using this analysis, we deduce the explicit forms of individual nondegenerate solitons at the asymptotic limits z (or t) $\rightarrow \pm\infty$. To do so, we have incorporated the asymptotic

behaviour of the wave variables in the obtained two-soliton solution and from which we have deduced the asymptotic forms of individual solitons. Then based on the obtained asymptotic forms we have analyzed the collision among the two nondegenerate solitons and the collision scenario between degenerate and nondegenerate solitons.

1.6 Plan of the present thesis

Our original findings are presented in the next four chapters (chapter 2 to chapter 5). In the final Chapter 6, a summary of results obtained in the present thesis along with the possible future directions are given.

Chapter 2: Nondegenerate solitons in Manakov system

In this chapter, we show that the Manakov equation can admit a more general class of nondegenerate vector solitons, associated with distinct wave numbers, besides the already known energy exchanging solitons corresponding to identical wave numbers. To bring out these details, we derive the exact forms of such vector one-, two- and three-soliton solutions through Hirota bilinear method and they are rewritten in more compact forms using Gram determinants. The presence of distinct wave numbers allows the nondegenerate fundamental soliton to admit various profiles such as double-hump, flat-top and single-hump structures. We explain the formation of double-hump structure in the fundamental soliton when the relative velocity of the two modes tends to zero. More critical analysis shows that the nondegenerate fundamental solitons can undergo three-types of collision scenarios: (i) shape preserving collision, (ii) shape altering collision and (iii) shape changing collision, for appropriate parametric choices. However, they belong to elastic collision only. Then we observe the coexistence of degenerate and nondegenerate solitons in the Manakov system when the wave numbers are restricted appropriately in the obtained two-soliton solution. In such a situation we find the degenerate soliton induces shape changing behavior of nondegenerate soliton during the collision process. By performing suitable asymptotic analysis we analyze the consequences that occur in each of the collision scenario. Finally

we point out that the previously known class of energy exchanging vector bright solitons, with identical wave numbers, turns out to be a special case of the newly derived nondegenerate solitons.

Chapter 3: Nondegenerate solitons in GCNLS system

We investigate the role of the four-wave mixing effect on the structure of nondegenerate vector solitons and their collision dynamics. For this purpose, we consider the generalized coupled nonlinear Schrödinger (GCNLS) system, which describes the evolution and nonlinear interaction of the two optical modes. The fundamental, as well as higher-order nondegenerate vector soliton solutions, are derived through the Hirota bilinear method and their forms are rewritten in a compact way using Gram determinants. Very interestingly, we find that the presence of four-wave mixing effect provokes the breathing vector soliton state in both the optical modes. Such breather formation is not possible in the fundamental vector solitons of the Manakov system. Then, we observe that the nondegenerate solitons in the GCNLS system undergo, in general, novel shape changing collision when the four-wave mixing effect strength is strong enough. On the other hand, for the weak four-wave mixing effect they undergo mere shape preserving (or shape altering) collision. Further, we analyze the degenerate soliton collision induced novel shape shaping property of nondegenerate vector soliton by deriving the partially nondegenerate two-soliton solution. We believe that the results reported in this chapter will be useful in nonlinear optics for manipulating light by light through collision.

Chapter 4: Nondegenerate solitons in two-component LSRI system

In this chapter, we study the dynamics of an interesting class of nondegenerate vector solitons in the long wave-short wave resonance interaction (LSRI) system. The model that we consider here describes the nonlinear interaction of the long-wave and two-short waves and it generically appears in several physical settings. To derive this class of nondegenerate vector soliton solutions we adopt the Hirota bilinear method with the more general form of admissible seed solutions with nonidentical distinct

propagation constants. We express the resultant fundamental as well as multi-soliton solutions in a compact way using Gram-determinants. The general fundamental vector soliton solution possesses several interesting properties. For instance, the double-hump or a single-hump profile structure including a special flattop profile form results in when the soliton propagates in all the components with identical velocities. Interestingly, in the case of nonidentical velocities, the soliton number is increased to two in the long-wave (LW) component, while a single-humped soliton propagates in the two short-wave (SW) components. We establish through a detailed analysis that the nondegenerate multi-solitons in contrast to the already known vector solitons (with identical wave numbers) can undergo three types of elastic collision scenarios: (i) shape preserving, (ii) shape altering, and (iii) a novel shape changing collision, depending on the choice of the soliton parameters. Very importantly, the later shape changing behaviour of the nondegenerate vector solitons is observed in the long-wave mode also, along with corresponding changes in the short-wave modes, and this nonlinear phenomenon has not been observed in the already known vector solitons. In addition, we point out the coexistence of nondegenerate and degenerate solitons simultaneously along with the associated physical consequences. We also indicate the physical realizations of these general vector solitons in nonlinear optics, hydrodynamics, and Bose-Einstein condensates.

Chapter 5: Existence of nondegenerate solitons in other coupled nonlinear Schrödinger family of systems

We investigate the existence of nondegenerate vector solitons in certain class of physically important CNLS systems. In particular N-CNLS system, mixed 2-CNLS system and two-component CCNLS system are considered. Very interestingly, the obtained nondegenerate fundamental vector soliton solutions admits novel geometrical structurs. For example, in N-CNLS system, it admits multi-humped intensity profiles. This specific property is illustrated by considering the nondegenerate soliton solutions for 3 and 4-CNLS systems. In addition, we also point out the existence of a special class of partially nondegenerate soliton solutions by imposing

appropriate restrictions on the wavenumbers in the already obtained completely nondegenerate soliton solution. Such class of soliton solutions can also exhibit multi-hump profile structures. The stability analysis associated with the nondegenerate fundamental soliton of the 3-CNLS system is examined. The numerical results confirm the stability of triple-humped profile nature against perturbations of 5% and 10% white noise. The multi-hump nature of nondegenerate fundamental soliton solution will be useful in multi-level optical communication applications with enhanced flow of data in multi-mode fibers. In the mixed 2-CNLS system, the nondegenerate fundamental soliton always admits a singularity due to the presence of defocusing nonlinearity of the system. Finally, we briefly discuss the properties of nondegenerate vector solitons in the 2-CCNLS system.

Chapter 6: Summary and Future works

In this chapter, a summary of the important results of our investigations is given. Also possible future works along the direction of the above study are also suggested.

Chapter 2

Nondegenerate solitons in Manakov system

2.1 Introduction

Coupled nonlinear Schrödinger (CNLS) equations are the fundamental dynamical models for representing the propagation of optical field in multimode optical fibers. As discussed earlier, CNLS equations consist of self phase and cross phase modulation effects unlike the scalar NLS equation which has only the self phase modulation nonlinearity. Among the various CNLS equations, the simplest one is the two coupled nonlinear Schrödinger system which describes the optical pulse propagation in two mode optical fibers or birefringence fibers. This system of two coupled nonlinear Schrödinger equations is not integrable in general except for very special choices of parameters. One such integrable case is the Manakov system. This celebrated Manakov system is of the form,

$$\begin{aligned} iq_{1,z} + q_{1,tt} + 2\left(|q_1|^2 + |q_2|^2\right) q_1 = 0, \\ iq_{2,z} + q_{2,tt} + 2\left(|q_1|^2 + |q_2|^2\right) q_2 = 0. \end{aligned} \tag{2.1}$$

Here q_j, $j = 1, 2$, are the complex wave envelops which propagate in the two mode optical fiber, z and t denote the normalized distance and

retarded time, respectively. It is very important to understand the properties of nondegenerate solitons in such simplest coupled field model like the Manakov system. We present the results of our investigations on the system (2.1) in this chapter.

This chapter is structured as follows: In Sec. 2.2, we discuss the Hirota bilinearization procedure in order to derive nondegenerate soliton solutions of Eq. (2.1). Using this procedure we obtain nondegenerate one- and two-soliton solutions and also identify the coexistence of nondegenerate and degenerate solitons in Sec. 2.3.1 and Sec. 2.3.2, respectively. In Sec. 2.3.3, we discuss various collision properties of nondegenerate solitons. Sec. 2.3.4 and Sec. 2.3.5 deal with the collision between nondegenerate solitons and degenerate solitons. We recover the degenerate one- and two-soliton solutions from the nondegenerate one- and two-soliton solutions by suitably restricting the wave numbers and then study the underlying collision dynamics in Sec. 2.3.6. We point out the possible experimental realization of nondegenerate solitons in Sec. 2.3.7. In Sec. 2.4 we provide the stability analysis for nondegenerate double hump solitons under perturbation. Gram determinant form of nondegenerate three-soliton solution is given in Sec. 2.5.

2.2 Hirota Bilinearization of Manakov system

To derive the nondegenerate soliton solutions for the Manakov system we adopt the same Hirota bilinear procedure that has been already used to get degenerate vector bright soliton solutions but with appropriate form of initial seed solutions. We point out later how such a simple form of new seed solutions will produce remarkably new physically important class of soliton solutions. In general, the exact soliton solutions of Eq. (2.1) can be obtained by introducing the bilinearizing transformation, which can be identified from the singularity structure analysis of Eq. (2.1) [34] as

$$q_j(z,t) = \frac{g^{(j)}(z,t)}{f(z,t)}, \quad j = 1,2, \tag{2.2}$$

to Eq. (2.1). This results in the following set of bilinear forms of Eq. (2.1),

$$(iD_z + D_t^2)g^{(j)} \cdot f = 0, j = 1, 2, \tag{2.3a}$$

$$D_t^2 f \cdot f = 2\sum_{n=1}^{2} g^{(n)} g^{(n)*}. \tag{2.3b}$$

Here $g^{(j)}$'s are complex functions whereas f is a real function and $*$ denotes complex conjugation. The Hirota's bilinear operators D_z and D_t are defined [155] by the expressions,

$$D_z^m D_t^n (a \cdot b) = \left(\frac{\partial}{\partial z} - \frac{\partial}{\partial z'}\right)^m \left(\frac{\partial}{\partial t} - \frac{\partial}{\partial t'}\right)^n a(z,t) b(z',t')\big|_{z=z',\ t=t'}.$$

Substituting the standard expansions for the unknown functions $g^{(j)}$ and f,

$$\begin{aligned} g^{(j)} &= \epsilon g_1^{(j)} + \epsilon^3 g_3^{(j)} + ..., \ j = 1, 2, \\ f &= 1 + \epsilon^2 f_2 + \epsilon^4 f_4 + ..., \end{aligned} \tag{2.4}$$

in the bilinear Eqs. (2.3a)-(2.3b) one can get a system of linear partial differential equations (PDEs). Here ϵ is a formal series expansion parameter. The set of linear PDEs arises after collecting the coefficients of same powers of ϵ. By solving these linear PDEs recursively (at an appropriate order of ϵ), the resultant associated explicit forms of $g^{(j)}$'s and f constitute the soliton solutions to the underlying system (2.1). We note that the truncation of series expansions (2.4) for the nondegenerate soliton solutions is different from degenerate soliton solutions. This is essentially due to the general form of seed solutions assigned to the lowest order linear PDEs.

2.3 A new class of nondegenerate soliton solutions

To study the role of additional wave numbers on the structural, propagational and collisional properties of nondegenerate soliton, it is very much important to find the exact analytical form of it systematically. In this section by exploiting the procedure described above we intend to construct nondegenerate one- and two-soliton solutions which can be generalized to arbitrary N-soliton case. In principle this is possible because of the existence of nondegenerate N-soliton solution ensured by the complete integrability property of Manakov Eq. (2.1). Then we point out the possibility of coexistence of degenerate and nondegenerate solitons by imposing certain restriction on the wave numbers in the obtained nondegenerate two-soliton solution. Further we also point out the possibility of deriving this partially nondegenerate two-soliton solution through Hirota bilinear method. We note that to avoid too many mathematical details we provide the final form of solutions only since the NDS solution construction process is a lengthy one.

2.3.1 Nondegenerate fundamental soliton solution

In order to deduce the exact form of nondegenerate one-soliton solution we consider two different seed solutions for the two modes as

$$g_1^{(1)} = \alpha_1^{(1)} e^{\eta_1}, \;\; g_1^{(2)} = \alpha_1^{(2)} e^{\xi_1}, \tag{2.5}$$

where $\eta_1 = k_1 t + i k_1^2 z$ and $\xi_1 = l_1 t + i l_1^2 z$, to the following linear PDEs

$$i g_{1z}^{(j)} + g_{1tt}^{(j)} = 0, \; j = 1, 2. \tag{2.6}$$

In (2.5) the complex parameters $\alpha_1^{(j)}$, $j = 1, 2$, are arbitrary. The above equations arise in the lowest order of ϵ. The presence of two distinct complex wave numbers k_1 and l_1 ($k_1 \neq l_1$, in general) in the seed solutions (2.5) makes the final solution as nondegenerate one. This construction procedure is different from the standard one that has been followed in earlier

works on degenerate vector bright soliton solutions [37, 38] where identical seed solutions of Eq. (2.1) (solutions (2.5) with $k_1 = l_1$ and distinct $\alpha_1^{(j)}$'s, $j = 1, 2$) have been used as starting seed solutions for Eq. (2.6). We note that such degenerate seed solutions only yield degenerate class of vector bright soliton solutions [37, 38, 77].

With the starting solutions (2.5) we allow the series expansions (2.4) to terminate by themselves while solving the system of linear PDEs. From this recursive process, we find that the expansions (2.4) get terminated for the nondegenerate fundamental sliton solution as, $g^{(j)} = \epsilon g_1^{(j)} + \epsilon^3 g_3^{(j)}$ and $f = 1 + \epsilon^2 f_2 + \epsilon^4 f_4$. The explicit expressions of $g_1^{(j)}$, $g_3^{(j)}$, f_2 and f_4 constitute a general form of new fundamental one-soliton solution to Eq. (2.1) as

$$
\begin{aligned}
q_1 &= \frac{g_1^{(1)} + g_3^{(1)}}{1 + f_2 + f_4} = (\alpha_1^{(1)} e^{\eta_1} + e^{\eta_1 + \xi_1 + \xi_1^* + \Delta_1^{(1)}})/D_1 \\
q_2 &= \frac{g_1^{(2)} + g_3^{(2)}}{1 + f_2 + f_4} = (\alpha_1^{(2)} e^{\xi_1} + e^{\eta_1 + \eta_1^* + \xi_1 + \Delta_1^{(2)}})/D_1.
\end{aligned} \tag{2.7}
$$

Here $D_1 = 1 + e^{\eta_1 + \eta_1^* + \delta_1} + e^{\xi_1 + \xi_1^* + \delta_2} + e^{\eta_1 + \eta_1^* + \xi_1 + \xi_1^* + \delta_{11}}$,
$e^{\Delta_1^{(1)}} = \frac{(k_1 - l_1)\alpha_1^{(1)} |\alpha_1^{(2)}|^2}{(k_1 + l_1^*)(l_1 + l_1^*)^2}$, $e^{\Delta_1^{(2)}} = -\frac{(k_1 - l_1)|\alpha_1^{(1)}|^2 \alpha_1^{(2)}}{(k_1 + k_1^*)^2 (k_1^* + l_1)}$,
$e^{\delta_1} = \frac{|\alpha_1^{(1)}|^2}{(k_1 + k_1^*)^2}$, $e^{\delta_2} = \frac{|\alpha_1^{(2)}|^2}{(l_1 + l_1^*)^2}$ and $e^{\delta_{11}} = \frac{|k_1 - l_1|^2 |\alpha_1^{(1)}|^2 |\alpha_1^{(2)}|^2}{(k_1 + k_1^*)^2 (k_1^* + l_1)(k_1 + l_1^*)(l_1 + l_1^*)^2}$.

In the above one-soliton solution two distinct complex wave numbers, k_1 and l_1, occur in both the expressions of q_1 and q_2 simultaneously. This confirms that the obtained solution is nondegenerate. We also note that the solution (2.7) can be rewritten in a more compact form using Gram determinants as

$$g^{(1)}=\begin{vmatrix} \frac{e^{\eta_1+\eta_1^*}}{(k_1+k_1^*)} & \frac{e^{\eta_1+\xi_1^*}}{(k_1+l_1^*)} & 1 & 0 & e^{\eta_1} \\ \frac{e^{\xi_1+\eta_1^*}}{(l_1+k_1^*)} & \frac{e^{\xi_1+\xi_1^*}}{(l_1+l_1^*)} & 0 & 1 & e^{\xi_1} \\ -1 & 0 & \frac{|\alpha_1^{(1)}|^2}{(k_1+k_1^*)} & 0 & 0 \\ 0 & -1 & 0 & \frac{|\alpha_1^{(2)}|^2}{(l_1+l_1^*)} & 0 \\ 0 & 0 & -\alpha_1^{(1)} & 0 & 0 \end{vmatrix}, \tag{2.8a}$$

$$g^{(2)}=\begin{vmatrix} \frac{e^{\eta_1+\eta_1^*}}{(k_1+k_1^*)} & \frac{e^{\eta_1+\xi_1^*}}{(k_1+l_1^*)} & 1 & 0 & e^{\eta_1} \\ \frac{e^{\xi_1+\eta_1^*}}{(l_1+k_1^*)} & \frac{e^{\xi_1+\xi_1^*}}{(l_1+l_1^*)} & 0 & 1 & e^{\xi_1} \\ -1 & 0 & \frac{|\alpha_1^{(1)}|^2}{(k_1+k_1^*)} & 0 & 0 \\ 0 & -1 & 0 & \frac{|\alpha_1^{(2)}|^2}{(l_1+l_1^*)} & 0 \\ 0 & 0 & 0 & -\alpha_1^{(2)} & 0 \end{vmatrix}, \tag{2.8b}$$

$$f=\begin{vmatrix} \frac{e^{\eta_1+\eta_1^*}}{(k_1+k_1^*)} & \frac{e^{\eta_1+\xi_1^*}}{(k_1+l_1^*)} & 1 & 0 \\ \frac{e^{\xi_1+\eta_1^*}}{(l_1+k_1^*)} & \frac{e^{\xi_1+\xi_1^*}}{(l_1+l_1^*)} & 0 & 1 \\ -1 & 0 & \frac{|\alpha_1^{(1)}|^2}{(k_1+k_1^*)} & 0 \\ 0 & -1 & 0 & \frac{|\alpha_1^{(2)}|^2}{(l_1+l_1^*)} \end{vmatrix}. \tag{2.8c}$$

The above Gram determinant forms satisfy the bilinear Eqs. (2.3a) and (2.3b) as well as Manakov Eq. (2.1).

To investigate the various properties associated with the above fundamental soliton solution, we rewrite Eq. (2.7) as

$$q_1=e^{i\eta_{1I}}e^{\frac{\Delta_1^{(1)}+\rho_1}{2}}\{\cosh(\xi_{1R}+\frac{\phi_{1R}}{2})\cos(\frac{\phi_{1I}}{2})+i\sinh(\xi_{1R}+\frac{\phi_{1R}}{2})\sin(\frac{\phi_{1I}}{2})\}/D_2, \tag{2.9a}$$

$$q_2=e^{i\xi_{1I}}e^{\frac{\Delta_1^{(2)}+\rho_2}{2}}\{\cosh(\eta_{1R}+\frac{\phi_{2R}}{2})\cos(\frac{\phi_{2I}}{2})+i\sinh(\eta_{1R}+\frac{\phi_{2R}}{2})\sin(\frac{\phi_{2I}}{2})\}/D_2, \tag{2.9b}$$

where $D_2=e^{\frac{\delta_{11}}{2}}\cosh(\eta_{1R}+\xi_{1R}+\frac{\delta_{11}}{2})+e^{\frac{\delta_1+\delta_2}{2}}\cosh(\eta_{1R}-\xi_{1R}+\frac{\delta_1-\delta_2}{2})$,

$\eta_{1R} = k_{1R}(t - 2k_{1I}z)$, $\eta_{1I} = k_{1I}t + (k_{1R}^2 - k_{1I}^2)z$, $\xi_{1R} = l_{1R}(t - 2l_{1I}z)$, $\xi_{1I} = l_{1I}t + (l_{1R}^2 - l_{1I}^2)z$, $\rho_j = \log \alpha_1^{(j)}$, $j = 1, 2$. Here, ϕ_{1R}, ϕ_{1I}, ϕ_{2R} and ϕ_{2I} are real and imaginary parts of $\phi_1 = \Delta_1^{(1)} - \rho_1$ and $\phi_2 = \Delta_1^{(2)} - \rho_2$, respectively, and also k_{1R}, l_{1R}, k_{1I} and l_{1I} are the real and imaginary parts of k_1 and l_1, respectively. From the above, we can write $\phi_{1R} = \frac{1}{2}\log\frac{|k_1-l_1|^2|\alpha_1^{(2)}|^4}{|k_1+l_1^*|^2(l_1+l_1^*)^4}$, $\phi_{1I} = \frac{1}{2}\log\frac{(k_1-l_1)(k_1^*+l_1)}{(k_1^*-l_1^*)(k_1+l_1^*)}$, $\phi_{2R} = \frac{1}{2}\log\frac{|l_1-k_1|^2|\alpha_1^{(1)}|^4}{|k_1+l_1^*|^2(k_1+k_1^*)^4}$ and $\phi_{2I} = \frac{1}{2}\log\frac{(l_1-k_1)(k_1+l_1^*)}{(l_1^*-k_1^*)(k_1^*+l_1)}$. The profile structures of solution (2.9a)-(2.9b) are described by the four complex parameters k_1 , l_1 and $\alpha_1^{(j)}$, $j = 1, 2$.

For the nondegenerate fundamental soliton in the first mode, the amplitude, velocity and central position are found from Eq. (2.9a) as $2k_{1R}$, $2l_{1I}$ and $\frac{\phi_{1R}}{2l_{1R}}$, respectively. Similarly for the soliton in the second mode they are found from Eq. (2.9b) as $2l_{1R}$, $2k_{1I}$ and $\frac{\phi_{2R}}{2k_{1R}}$, respectively. Note that $\alpha_1^{(j)}$, $j = 1, 2$, are related to the unit polarization vectors of the nondegenerate fundamental solitons in the two modes. They constitute different phases for the nondegenerate soliton in the two modes as $A_1 = (\alpha_1^{(1)}/\alpha_1^{(1)*})^{1/2}$ and $A_2 = (\alpha_1^{(2)}/\alpha_1^{(2)*})^{1/2}$.

To explain the various properties associated with solution (2.9a)-(2.9b) further we consider two physically important special cases where the imaginary parts of the wave numbers k_1 and l_1 are either identical with each other ($k_{1I} = l_{1I}$) or nonidentical with each other ($k_{1I} \neq l_{1I}$). Physically this implies that the former case corresponds to solitons in the two modes travelling with identical velocities $v_1 = v_2 = 2k_{1I}$ but with $k_1 \neq l_1$ whereas the latter case corresponds to solitons which propagate in the two modes with non-identical velocities $v_1 \neq v_2$. In the identical velocity case, the quantity ϕ_{jI}, $j = 1, 2$ becomes zero in (2.9a)-(2.9b) when $k_{1I} = l_{1I}$. This results in the following expression for the fundamental soliton propagating with single velocity, $v_{1,2} = 2k_{1I}$, in the two modes,

$$
\begin{aligned}
q_1 &= e^{i\eta_{1I}} e^{\frac{\Delta_1^{(1)}+\rho_1}{2}} \cosh(\xi_{1R} + \frac{\phi_{1R}}{2})/D_2, \\
q_2 &= e^{i\xi_{1I}} e^{\frac{\Delta_1^{(2)}+\rho_2}{2}} \cosh(\eta_{1R} + \frac{\phi_{2R}}{2})/D_2,
\end{aligned} \tag{2.10}
$$

where $D_2 = e^{\frac{\delta_{11}}{2}} \cosh(\eta_{1R} + \xi_{1R} + \frac{\delta_{11}}{2}) + e^{\frac{\delta_1+\delta_2}{2}} \cosh(\eta_{1R} - \xi_{1R} + \frac{\delta_1-\delta_2}{2})$

with $\eta_{1R} = k_{1R}(t - 2k_{1I}z)$, $\eta_{1I} = k_{1I}t + (k_{1R}^2 - k_{1I}^2)z$, $\xi_{1R} = l_{1R}(t - 2k_{1I}z)$, $\xi_{1I} = k_{1I}t + (l_{1R}^2 - k_{1I}^2)z$. Note that the constants that appear in the above solution becomes equivalent to the one that appear in the solution (2.9a)-(2.9b) after imposing the condition $k_{1I} = l_{1I}$ in it. The solution (2.10) admits four types of symmetric profiles (satisfying appropriate conditions on parameters, see below) and also their corresponding asymmetric profiles. The symmetric profiles are: (i) double-humps in both the modes (or a double-hump in q_1 mode and a M-type double-hump in q_2 mode), (ii) a flat-top in one mode and a double-hump in the other mode, (iii) a single-hump in the first mode and a double-hump in the second mode (or vice versa), (iv) single-humps in both the modes. The corresponding four types of asymmetric wave profiles can be obtained by tuning the real parts of wave numbers k_1 and l_1 and the arbitrary complex parameters $\alpha_1^{(j)}$'s, $j = 1, 2$.

To illustrate the symmetric and asymmetric nature of the nondegenerate soliton in the identical velocity case we fix $k_{1I} = l_{1I} = 0.5$ in Figs. 2.1 and 2.2. The symmetric profiles are displayed in Fig. 2.1. The asymmetric profiles are depicted in Fig. 2.2 for the values of parameters indicated in Fig. 2.2. From Figs. 2.1 and 2.2 we observe that the transition which occurs from double-hump to single-hump is through a special flat-top profile. The flat-top profile has been considered as an intermediate soliton state. It is noted that flattop soliton is also observed in a complex Ginzburg-Landau equation [156]. In Ref. [77] we have discussed symmetric and asymmetric nature of solution (2.10) by incorporating the condition $k_{1R} < l_{1R}$ supplementary material of [77]. However to exhibit the generality of these structures, in the present thesis, we discuss these properties for $k_{1R} > l_{1R}$. It should be pointed out here that in Ref. [80] the authors have derived this solution in the context of multi-component BEC using Darboux transformation and they have classified density profiles as we have reported in Ref. [77] for $k_{1R} < l_{1R}$ in the context of nonlinear optics. They have also studied the stability of double-hump soliton using Bogoliubov-de Gennes excitation spectrum.

The symmetric nature of all the four cases can be confirmed by finding the extremum points of the nondegenerate one-soliton solution (2.10). For instance, to show that the double-hump soliton profile displayed in

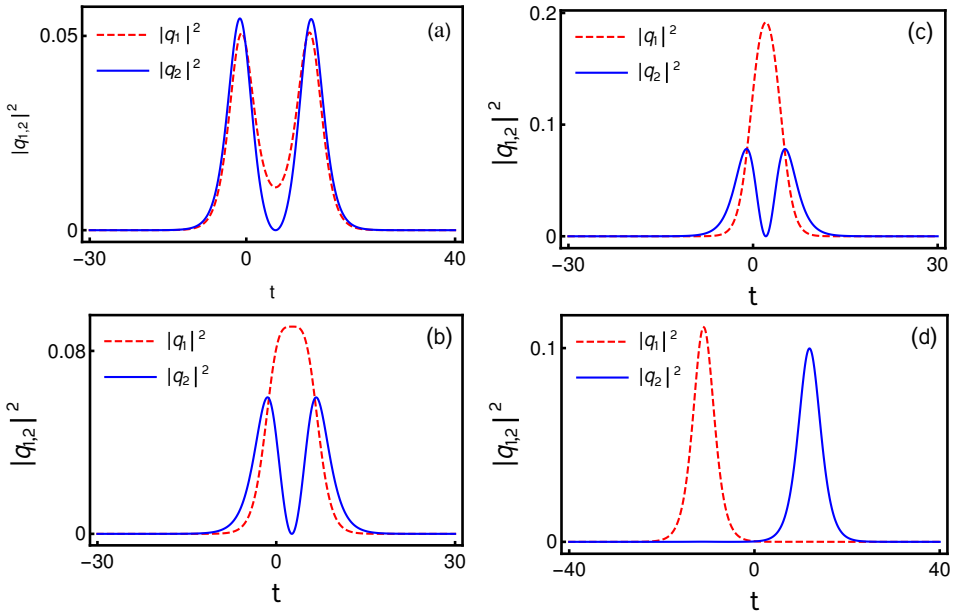

FIGURE 2.1: Various symmetric intensity profiles of nondegenerate fundamental soliton: While (a) denotes double-hump solitons in both the modes (b) and (c) represent flat-top-double-hump solitons and single-hump-double-hump solitons, respectively. Single-hump solitons in both the modes are illustrated in (d). The parameter values of each figures are: (a): $k_1 = 0.333 + 0.5i$, $l_1 = 0.315 + 0.5i$, $\alpha_1^{(1)} = 0.45 + 0.45i$, $\alpha_1^{(2)} = 0.49 + 0.45i$. (b): $k_1 = 0.425 + 0.5i$, $l_1 = 0.3 + 0.5i$, $\alpha_1^{(1)} = 0.44 + 0.51i$, $\alpha_1^{(2)} = 0.43 + 0.5i$. (c): $k_1 = 0.55 + 0.5i$, $l_1 = 0.333 + 0.5i$, $\alpha_1^{(1)} = 0.5 + 0.5i$, $\alpha_1^{(2)} = 0.5 + 0.45i$. (d): $k_1 = 0.333 + 0.5i$, $l_1 = -0.316 + 0.5i$, $\alpha_1^{(1)} = 0.45 + 0.5i$, $\alpha_1^{(2)} = 0.5 + 0.5i$.

Fig. 2.1(a) is symmetric, we find the corresponding local maximum and minium points by applying the first derivative test ($\{|q_j|^2\}_t = 0$) and the second derivative test ($\{|q_j|^2\}_{tt} < 0$ or > 0) to the expression of $|q_j|^2$, $j = 1, 2$, at $z = 0$. For the first mode, the three extremal points are identified, namely $t_1 = -0.9$, $t_2 = 5.5$ and $t_3 = 11.9$. We find another set of three extremal points for the second mode, namely $t_4 = -1.2$, $t_5 = 5.5$ and $t_6 = 12.2$ by setting $\{|q_2|^2\}_t = 0$. The points t_1 and t_3 correspond to the maxima (at which $\{|q_1|^2\}_{tt} < 0$) of the double hump soliton whereas t_2 corresponds to the minimum of the double hump soliton. Similarly the extremal points t_4 and t_6 represent the maxima and t_5 corresponds to the minimum of the double hump soliton in the q_2 mode. In the first component the two maxima t_1 and t_3 are symmetrically located about the

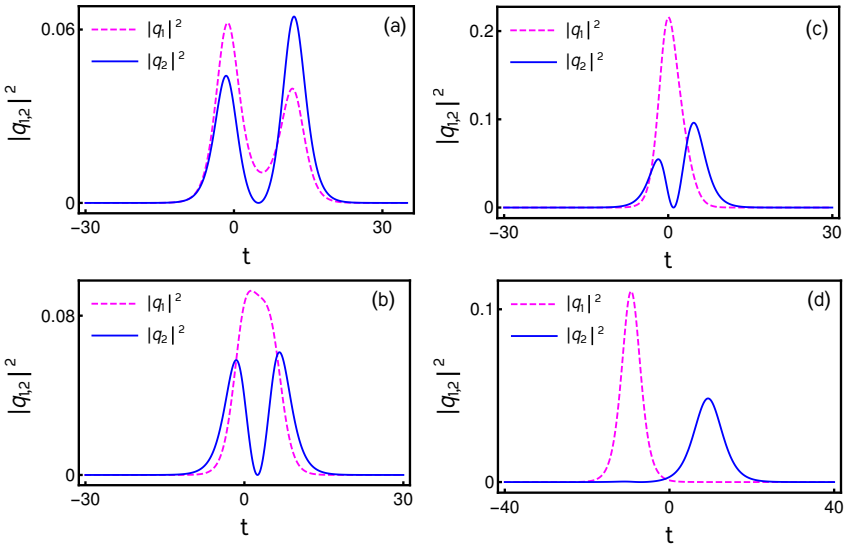

FIGURE 2.2: Various asymmetric intensity profiles of nondegenerate fundamental soliton: Figures (a), (b), (c) and (d) represent each of figures asymmetric intensity profiles as against the symmetric profiles of Figs.2.1(a)-(d). The corresponding parameter values of each figures are: (a): $k_1 = 0.333 + 0.5i, l_1 = 0.315 + 0.5i$, $\alpha_1^{(1)} = 0.65 + 0.45i$, $\alpha_1^{(2)} = 0.49 + 0.45i$. (b): $k_1 = 0.425 + 0.5i, l_1 = 0.3 + 0.5i$, $\alpha_1^{(1)} = 0.5 + 0.51i$, $\alpha_1^{(2)} = 0.43 + 0.5i$. (c): $k_1 = 0.55 + 0.5i, l_1 = 0.333 + 0.5i$, $\alpha_1^{(1)} = 1.2 + 0.5i$, $\alpha_1^{(2)} = 0.5 + 0.45i$. (d): $k_1 = 0.333 + 0.5i, l_1 = -0.22 + 0.5i$, $\alpha_1^{(1)} = 0.45 + 3i$, $\alpha_1^{(2)} = 0.5 + 0.5i$.

minimum point t_2. This can be easily confirmed by finding the difference between t_2 and t_1 and t_3 and t_2, that is $t_2 - t_1 = 6.4 = t_3 - t_2$. This is true for the second component also, that is $t_5 - t_4 = 6.7 = t_6 - t_5$. This implies that the two maxima t_4 and t_6 are located symmetrically from the minimum point t_5. Then the magnitude ($|q_1|^2$) of each hump (of the double hump soliton) corresponding to the maxima t_1 is equal to 0.051 and t_3 is equal to 0.051. In the second mode, the magnitude ($|q_2|^2$) corresponding to t_4 is equal to 0.054 and t_6 is equal to 0.054. This confirms that the magnitude of each hump of double hump soliton in both the modes are equal. Therefore it is evident that the double hump soliton drawn in Fig. 2.1(a) is symmetric. One can easily verify from the Figs. 2.1(c) and 2.1(d) that the single-hump soliton is symmetric about the local maximum point (and checking the half widths as well). As far as the flat-top soliton case is concerned, we have confirmed that the first derivative $\{|q_j|^2\}_t$ very slowly

tends to zero near the corresponding maximum for certain number of t values. This also confirms that the presence of almost flatness and symmetric nature of the one-soliton.

We also derive the conditions analytically to corroborate the symmetric and asymmetric nature of soliton solution (2.10) in another way. For this purpose, we intend to calculate the relative separation distance Δt_{12} between the minima of the two components (modes)

$$\begin{aligned} \Delta t_{12} &= \bar{t}_1 - \bar{t}_2 = (t - t_1) - (t - t_2), \\ &= \frac{\phi_{1R}}{2l_{1R}} - \frac{\phi_{2R}}{2k_{1R}}. \end{aligned} \tag{2.11}$$

If the above quantity $\Delta t_{12} = 0$ then the solution (2.10) exhibits symmetric profiles otherwise it admits asymmetric profiles. The explicit form of relative separation distance turns out to be

$$\Delta t_{12} = \frac{1}{2l_{1R}} \log \frac{(k_{1R} - l_{1R})|\alpha_1^{(2)}|^2}{4l_{1R}^2(k_{1R} + l_{1R})} - \frac{1}{2k_{1R}} \log \frac{(l_{1R} - k_{1R})|\alpha_1^{(1)}|^2}{4k_{1R}^2(k_{1R} + l_{1R})}. \tag{2.12}$$

We have explicitly calculated the relative separation distance values and confirmed the displayed profiles in Fig. 2.1 and 2.2 are symmetric and asymmetric, respectively. For instance, the Δt_{12} value corresponding to the symmetric double-hump soliton in both the modes (Fig. 2.1(a)) is 0.002 (to get the perfect zero value one has to fine tune the parameters suitably) and for asymmetric double-hump solitons the value is equal to 0.6493. The above calculated values reaffirm that the obtained figures are symmetric in Fig. 2.1(a) and asymmetric in Fig. 2.2(a). Similarly one can easily confirm the symmetric and asymmetric nature of other profiles in Figs. 2.1 and 2.2 also.

In addition to the above, for the general nonidentical velocity case ($k_{1I} \neq l_{1I}$), $v_1 \neq v_2$, the distinct wave numbers k_1 and l_1 influence drastically the propagation of nondegenerate solitons in the two modes. If the relative velocity ($\Delta v_{12} = v_1 - v_2$) of the solitons between the two modes is large, then there is a node created in the structure of the fundamental

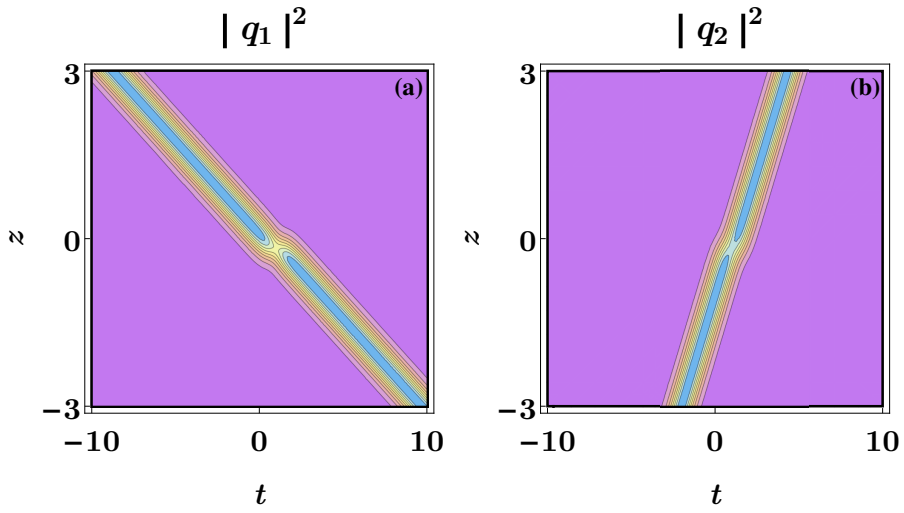

FIGURE 2.3: Node formation in the nonidentical velocity case. The parameter values are $k_1 = 1 + 1.5i, l_1 = 1.5 + 0.5i$, $\alpha_1^{(1)} = 1.5 + 0.5i$, $\alpha_1^{(2)} = 0.45 + 0.5i$.

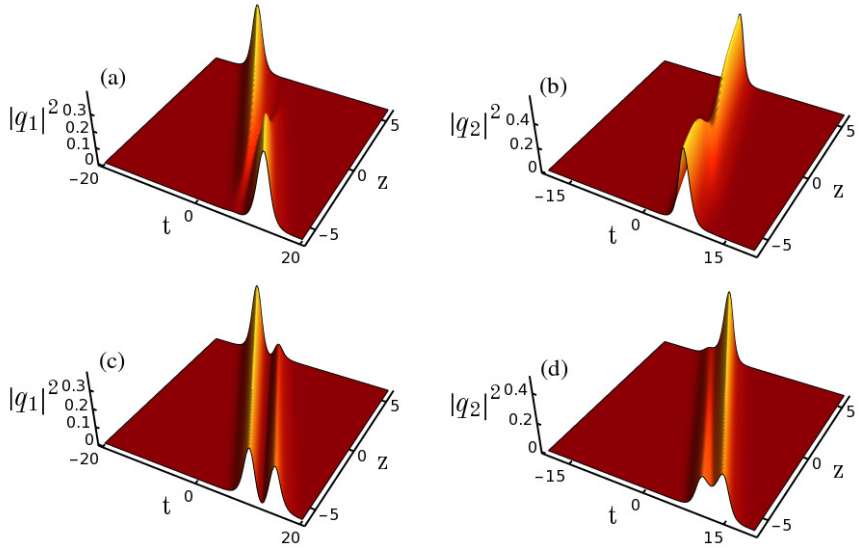

FIGURE 2.4: Double-hump formation in the profile structure of nondegenerate fundamental soliton: (a) and (b) represent the node formation in soliton profiles. (c) and (d) denote the emergence of double-hump in both the modes. The corresponding parameter values for (a) and (b) are: $k_1 = 0.65 - 0.85i$, $l_1 = 0.78 - 0.5i$, $\alpha_1^{(1)} = 1$ and $\alpha_1^{(2)} = 0.5$; For figures (c) and (d) the values are chosen as $k_1 = 0.65 - 0.8i$, $l_1 = 0.78 - 0.8i$, $\alpha_1^{(1)} = 1$ and $\alpha_1^{(2)} = 0.5$.

solitons of both the modes [80]. This is due to the cross phase modulation between the modes. In this situation the intensity of the fast moving

soliton ($v_1 = 2l_{1I} > 0$) in the first mode starts to decrease and it gets completely suppressed after $z = 0$. At the same value of z the fast moving soliton reappears in the second mode after a finite time. Similarly this fact is true in the case of slow moving soliton ($v_2 = 2k_{1I} < 0$) as well. Consequently the intensity of solitons is unequally distributed among the two modes. This is clearly demonstrated in Fig. 2.3 and Figs. 2.4(a)-2.4(b). On the otherhand, if the relative velocity tends to zero ($\Delta v_{12} \to 0$), then the total intensity, $I_{\text{total}} = |q_1|^2 + |q_2|^2$, of nondegenerate solitons starts to get distributed equally among the two components. As a consequence of this, a double-hump profile starts to emerge in each of the modes as displayed in Fig. 2.4(c)-2.4(d). At perfect zero relative velocity ($\Delta v_{12} = 0$), the double-hump fundamental soliton emerges completely in both the modes. As we have already pointed out in [77] the nondegenerate soliton solution exhibits symmetric and asymmetric profiles in the nonidentical velocity case also but the relative velocity of the solitons should be minimum. We have not displayed their plots here for brevity.

Recently we found that the occurence of multi-humps depends on the number of distinct wave numbers and modes [78] apart from the nonlinearities. In the present two component case, the resultant nondegenerate fundamental soliton solution (2.9a)-(2.9b) yields only a double-hump soliton. However a triple-hump soliton and a quadruple hump soliton are also observed in the cases of 3 and 4 component Manakov system cases, respectively. For the N-component case one may expect a more complicated profile, as mentioned in the case of theory of incoherent solitons [157, 158], involving N-number of humps which are characterized by $2N$-complex parameters. Very recently we have also reported the existence of nondegenerate fundamental solitons and their various novel profile structures in other integrable coupled NLS type systems [79] as well. It should be pointed out that the multi-hump nature of nondegenerate fundamental soliton is somewhat analogous to partially coherent solitons/soliton complexes [53, 55] where such partially coherent solitons can be obtained when the number of modes is equal to the number of degenerate vector soliton solution [37, 43]. We also note here that the 2-partially coherent

soliton can be deduced from the double-humped nondegenerate fundamental soliton (2.9a)-(2.9b) in the Manakov system by imposing the restrictions $\alpha_1^{(1)} = e^{\eta_{10}}$, $\alpha_1^{(2)} = -e^{\eta_{20}}$, $k_1 = k_{1R}$, $l_1 = k_{2R}$, $k_{1I} = l_{1I} = 0$, where η_{10} and η_{20} are real constants, in solution (2.7) [43]. The soliton complex reported in [159] is a special case of nondegenerate fundamental soliton solution (2.7) when the parameters k_1 and l_1 are chosen as real constants and $\alpha_1^{(1)} = \alpha_1^{(2)} = 1$.

2.3.2 Nondegenerate two-soliton solution

To get the nondegenerate two-soliton solution of Manakov Eq. (2.1) we proceed with the procedure given in the previous subsection along with the following seed solutions, $g_1^{(1)} = \alpha_1^{(1)} e^{\eta_1} + \alpha_2^{(1)} e^{\eta_2}$ and $g_1^{(2)} = \alpha_1^{(2)} e^{\xi_1} + \alpha_2^{(2)} e^{\xi_2}$, $\eta_j = k_j t + i k_j^2 z$ and $\xi_j = l_j t + i l_j^2 z$, $j = 1, 2$. We find that the series expansions for $g^{(j)}$, $j = 1, 2$, and f get terminated as $g^{(j)} = \epsilon g_1^{(j)} + \epsilon^3 g_3^{(j)} + \epsilon^5 g_5^{(j)} + \epsilon^7 g_7^{(j)}$ and $f = 1 + \epsilon^2 f_2 + \epsilon^4 f_4 + \epsilon^6 f_6 + \epsilon^8 f_8$. Here we assume that all the k_j's and l_j's, $j = 1, 2$, are distinct. The explicit forms of the obtained unknown functions in the truncated series expansions constitute the following nondegenerate two-soliton solution and it can be expressed using Gram determinants in the following way:

$$g^{(N)} = \begin{vmatrix} A & I & \phi \\ -I & B & \mathbf{0}^T \\ \mathbf{0} & C_N & 0 \end{vmatrix}, \quad f = \begin{vmatrix} A & I \\ -I & B \end{vmatrix}, \quad N = 1, 2. \tag{2.13}$$

Here the matrices A and B are of the order (4×4) defined as

$$A = \begin{pmatrix} A_{mm'} & A_{mn} \\ A_{nm} & A_{nn'} \end{pmatrix}, \; B = \begin{pmatrix} \kappa_{mm'} & \kappa_{mn} \\ \kappa_{nm} & \kappa_{nn'} \end{pmatrix}, \; m, m', n, n' = 1, 2.$$

The various elements of the matrix A can be obtained from the following, $A_{mm'} = \frac{e^{\eta_m + \eta^*_{m'}}}{(k_m + k^*_{m'})}$, $A_{mn} = \frac{e^{\eta_m + \xi^*_n}}{(k_m + l^*_n)}$, $A_{nn'} = \frac{e^{\xi_n + \xi^*_{n'}}}{(l_n + l^*_{n'})}$, $A_{nm} = \frac{e^{\eta^*_n + \xi_m}}{(k^*_n + l_m)}$, $m, m', n, n' = 1, 2$. The elements of the matrix B are $\kappa_{mm'} = \frac{\psi^\dagger_m \sigma \psi_{m'}}{(k^*_m + k_{m'})}$, $\kappa_{mn} = \frac{\psi^\dagger_m \sigma \psi'_n}{(k^*_m + k_n)}$, $\kappa_{nm} = \frac{\psi'^\dagger_n \sigma \psi_m}{(l^*_n + k_m)}$, $\kappa_{nn'} = \frac{\psi'^\dagger_n \sigma \psi'_{n'}}{(l^*_n + l_{n'})}$. In the latter, the column matrices are defined as

$\psi_j = \begin{pmatrix} \alpha_j^{(1)} \\ 0 \end{pmatrix}$, $\psi_j' = \begin{pmatrix} 0 \\ \alpha_j^{(2)} \end{pmatrix}$, $j = m, m', n, n' = 1, 2$, $\eta_j = k_j t + i k_j^2 z$ and $\xi_j = l_j t + i l_j^2 z$, $j = 1, 2$. The other matrices in Eq. (2.13) are defined as $\phi = \begin{pmatrix} e^{\eta_1} & e^{\eta_2} & e^{\xi_1} & e^{\xi_2} \end{pmatrix}^T$, $C_1 = -\begin{pmatrix} \alpha_1^{(1)} & \alpha_2^{(1)} & 0 & 0 \end{pmatrix}$, $C_2 = -\begin{pmatrix} 0 & 0 & \alpha_1^{(2)} & \alpha_2^{(2)} \end{pmatrix}$, $\mathbf{0} = \begin{pmatrix} 0 & 0 & 0 & 0 \end{pmatrix}$ and $\sigma = I$ is a (4×4) identity matrix. The presence of eight arbitrary complex parameters k_j, l_j, $\alpha_1^{(j)}$ and $\alpha_2^{(j)}$, $j = 1, 2$, define the profile shapes of the nondegenerate two solitons and their interesting collision scenarios. In addition to the above, we also find that the Manakov system also admits degenerate and nondegenerate solitons simultaneously under the wave numbers restriction $k_1 = l_1$ (or $k_2 = l_2$) but $k_2 \neq l_2$ (or $k_1 \neq l_1$). Such a special kind of partially nondegenerate two-soliton solution can be deduced by fixing the latter wave number restriction in the completely nondegenerate two-soliton solution (2.13). This partially nondegenerate soliton solution can also be derived through the Hirota bilinear method. To derive this solution one has to assume the following seed solutions, $g_1^{(1)} = \alpha_1^{(1)} e^{\eta_1} + \alpha_2^{(1)} e^{\eta_2}$ and $g_1^{(2)} = \alpha_1^{(2)} e^{\eta_1} + \alpha_2^{(2)} e^{\xi_2}$, $\eta_j = k_j t + i k_j^2 z$ and $\xi_2 = l_2 t + i l_2^2 z$, $j = 1, 2$, in the solution construction process. The resultant coexistence soliton solution and its dynamics are characterized by only seven complex parameters k_j, l_2, $\alpha_1^{(j)}$ and $\alpha_2^{(j)}$, $j = 1, 2$.

2.3.3 Various types of collision dynamics of nondegenerate solitons

In order to understand the interesting collision properties associated with the nondegenerate solitons, one has to analyze the asymptotic forms of the complete nondegenerate two-soliton solution (2.13) of the Manakov equation. By doing so, we observe that the nondegenerate solitons in general exhibit three types of collision scenarios, namely shape preserving, shape altering and shape changing collision behaviours, for either of the two cases (i) Equal velocities: $k_{1I} = l_{1I}$, $k_{2I} = l_{2I}$ and (ii) Unequal velocities: $k_{1I} \neq l_{1I}$, $k_{2I} \neq l_{2I}$. To facilitate the understanding of these collision properties, here we present the asymptotic analysis for the case of equal

velocities only and it can be performed for unequal velocities case also in a similar manner.

2.3.3.1 Asymptotic analysis

We perform a careful asymptotic analysis for the nondegenerate two soliton solution (2.13) in order to understand the interaction dynamics of the nondegenerate solitons completely. We deduce the explicit expressions for the individual solitons at the aymptotic limits $z \to \pm\infty$. To explore this, we consider as a typical example $k_{jR}, l_{jR} > 0$, $j = 1, 2$, $k_{1I} > k_{2I}$, $l_{1I} > l_{2I}$, $k_{1I} = l_{1I}$ and $k_{2I} = l_{2I}$, that corresponds to head-on collision between the two nondegenerate solitons. In this situation the two fundamental solitons S_1 and S_2 are well separated and subsequently the asymptotic forms of the individual nondegenerate solitons can be deduced from the solution (2.13) by incorporating the following asymptotic nature of the wave variables $\xi_{jR} = l_{jR}(t - 2l_{jI}z)$ and $\eta_{jR} = k_{jR}(t - 2k_{jI}z)$, $j = 1, 2$, in it. The wave variables η_{jR} and ξ_{jR} behave asymptotically as (i) Soliton 1 (S_1): η_{1R}, $\xi_{1R} \simeq 0$, η_{2R}, $\xi_{2R} \to \mp\infty$ as $z \mp \infty$ and (ii) Soliton 2 (S_2): η_{2R}, $\xi_{2R} \simeq 0$, η_{1R}, $\xi_{1R} \to \mp\infty$ as $z \pm \infty$. Correspondingly these results lead to the following asymptotic expressions of nondegenerate individual solitons.

(a) Before collision: $z \to -\infty$

Soliton 1: In this limit, the asymptotic forms of q_1 and q_2 are deduced from the two soliton solution (2.13) for soliton 1 as below:

$$q_1 \simeq \frac{2A_1^{1-}k_{1R}e^{i\eta_{1I}}\cosh(\xi_{1R}+\phi_1^-)}{\left[a_{11}\cosh(\eta_{1R}+\xi_{1R}+\phi_1^-+\phi_2^-+c_1)+\frac{1}{a_{11}^*}\cosh(\eta_{1R}-\xi_{1R}+\phi_2^-+\phi_1^-+c_2)\right]}, \tag{2.14a}$$

$$q_2 \simeq \frac{2A_2^{1-}l_{1R}e^{i\xi_{1I}}\cosh(\eta_{1R}+\phi_2^-)}{\left[a_{12}\cosh(\eta_{1R}+\xi_{1R}+\phi_1^-+\phi_2^-+c_1)+\frac{1}{a_{12}^*}\cosh(\eta_{1R}-\xi_{1R}+\phi_2^-+\phi_1^-+c_2)\right]}. \tag{2.14b}$$

Here, $a_{11} = \frac{(k_1^*-l_1^*)^{\frac{1}{2}}}{(k_1^*+l_1)^{\frac{1}{2}}}$, $a_{12} = \frac{(k_1^*-l_1^*)^{\frac{1}{2}}}{(k_1+l_1^*)^{\frac{1}{2}}}$, $\phi_1^- = \frac{1}{2}\log\frac{(k_1-l_1)|\alpha_1^{(2)}|^2}{(k_1+l_1^*)(l_1+l_1^*)^2}$, $\phi_2^- = \frac{1}{2}\log\frac{(l_1-k_1)|\alpha_1^{(1)}|^2}{(k_1^*+l_1)(k_1+k_1^*)^2}$, $A_1^{1-} = [\alpha_1^{(1)}/\alpha_1^{(1)^*}]^{1/2}$ and $A_2^{1-} = i[\alpha_1^{(2)}/\alpha_1^{(2)^*}]^{1/2}$. In the latter, superscript $(1-)$ represents soliton S_1 before collision and subscript $(1,2)$ denotes the two modes q_1 and q_2 respectively.

Soliton 2: The asymptotic expressions for soliton 2 in the two modes before collision turn out to be

$$q_1 \simeq \frac{2k_{2R}A_1^{2-}e^{i(\eta_{2I}+\theta_1^-)}\cosh(\xi_{2R}+\varphi_1^-)}{\left[a_{21}\cosh(\eta_{2R}+\xi_{2R}+\varphi_1^-+\varphi_2^-+c_3)+\frac{1}{a_{21}^*}\cosh(\eta_{2R}-\xi_{2R}+\varphi_2^--\varphi_1^-+c_4)\right]}, \tag{2.15a}$$

$$q_2 \simeq \frac{2l_{2R}A_2^{2-}e^{i(\xi_{2I}+\theta_2^-)}\cosh(\eta_{2R}+\varphi_2^-)}{\left[a_{22}\cosh(\eta_{2R}+\xi_{2R}+\varphi_1^-+\varphi_2^-+c_3)+\frac{1}{a_{22}^*}\cosh(\eta_{2R}-\xi_{2R}+\varphi_2^--\varphi_1^-+c_4)\right]}. \tag{2.15b}$$

In the above, $a_{21} = \frac{(k_2^*-l_2^*)^{\frac{1}{2}}}{(k_2^*+l_2)^{\frac{1}{2}}}$, $a_{22} = \frac{(k_2^*-l_2^*)^{\frac{1}{2}}}{(k_2+l_2^*)^{\frac{1}{2}}}$, $c_3 = \frac{1}{2}\log\frac{(k_2^*-l_2^*)}{(l_2-k_2)}$, $c_4 = \frac{1}{2}\log\frac{(k_2-l_2)(k_2^*+l_2)}{(l_2-k_2)(k_2+l_2^*)}$, $\varphi_1^- = \frac{1}{2}\log\frac{(k_2-l_2)|\alpha_2^{(2)}|^2}{(k_2+l_2^*)(l_2+l_2^*)^2} + \Psi_1$, $\Psi_1 = \frac{1}{2}\log\frac{|k_1-l_2|^2|l_1-l_2|^4}{|k_1+l_2^*|^2|l_1+l_2^*|^4}$, $\varphi_2^- = \frac{1}{2}\log\frac{(l_2-k_2)|\alpha_2^{(1)}|^2}{(k_2^*+l_2)(k_2+k_2^*)^2} + \Psi_2$, $\Psi_2 = \frac{1}{2}\log\frac{|k_2-l_1|^2|k_1-k_2|^4}{|k_2+l_1^*|^2|k_1+k_2^*|^4}$, $e^{i\theta_1^-} = \frac{(k_1-k_2)(l_1-l_2)(l_1^*+l_2)(k_2-l_1)^{\frac{1}{2}}(k_1+k_2^*)(k_2^*+l_1)^{\frac{1}{2}}}{(k_1^*-k_2^*)(l_1+l_2^*)(l_1^*-l_2^*)(k_2^*-l_1^*)^{\frac{1}{2}}(k_1^*+k_2)(k_2+l_1^*)^{\frac{1}{2}}}$, $A_1^{2-} = [\alpha_2^{(1)}/\alpha_2^{(1)^*}]^{1/2}$, $A_2^{2-} = [\alpha_2^{(2)}/\alpha_2^{(2)^*}]^{1/2}$, $e^{i\theta_2^-} = \frac{(l_1-l_2)(k_1-l_2)^{\frac{1}{2}}(k_1+l_2^*)^{\frac{1}{2}}(l_1+l_2^*)}{(k_1^*-l_2^*)^{\frac{1}{2}}(l_1^*-l_2^*)(k_1^*+l_2)^{\frac{1}{2}}(l_1^*+l_2)}$. Here, superscript $(2-)$ refers to soliton S_2 before collision.

(b) After collision: $z \to +\infty$

Soliton 1: The asymptotic form for soliton 1 after collision is deduced as,

$$q_1 \simeq \frac{2k_{1R}A_1^{1+}e^{i(\eta_{1I}+\theta_1^+)}\cosh(\xi_{1R}+\phi_1^+)}{\left[a_{11}\cosh(\eta_{1R}+\xi_{1R}+\phi_1^++\phi_2^++c_1)+\frac{1}{a_{11}^*}\cosh(\eta_{1R}-\xi_{1R}+\phi_2^+-\phi_1^++c_2)\right]}, \tag{2.16a}$$

$$q_2 \simeq \frac{2l_{1R}A_1^{2+}e^{i(\xi_{1I}+\theta_2^+)}\cosh(\eta_{1R}+\phi_2^+)}{\left[a_{12}\cosh(\eta_{1R}+\xi_{1R}+\phi_1^++\phi_2^++c_1)+\frac{1}{a_{12}^*}\cosh(\eta_{1R}-\xi_{1R}+\phi_2^+-\phi_1^++c_2)\right]}. \tag{2.16b}$$

Here, $\phi_1^+ = \phi_1^- + \psi_1$, $\psi_1 = \frac{1}{2}\log\frac{|k_2-l_1|^2|l_1-l_2|^4}{|k_2+l_1^*|^2|l_1+l_2^*|^4}$, $\phi_2^+ = \phi_2^- + \psi_2$, $\psi_2 = \frac{1}{2}\log\frac{|k_1-l_2|^2|k_1-k_2|^4}{|k_1+l_2^*|^2|k_1+k_2^*|^4}$, $e^{i\theta_1^+} = \frac{(k_1-k_2)(k_1-l_2)^{\frac{1}{2}}(k_1^*+k_2)(k_1^*+l_2)^{\frac{1}{2}}}{(k_1^*-k_2^*)(k_1^*-l_2^*)^{\frac{1}{2}}(k_1+k_2^*)(k_1+l_2^*)^{\frac{1}{2}}}$, $e^{i\theta_2^+} = \frac{(l_1-l_2)(k_2-l_1)^{\frac{1}{2}}(k_2+l_1^*)^{\frac{1}{2}}(l_1^*+l_2)}{(k_2^*-l_1^*)^{\frac{1}{2}}(l_1^*-l_2^*)(k_2^*+l_1)^{\frac{1}{2}}(l_1+l_2^*)}$, $A_1^{1+} = [\alpha_1^{(1)}/\alpha_1^{(1)^*}]^{1/2}$ and $A_2^{1+} = [\alpha_1^{(2)}/\alpha_1^{(2)^*}]^{1/2}$, in which superscript (1+) denotes soliton S_1 after collision.

Soliton 2: The expression for soliton 2 after collision deduced from the two soliton solution is

$$q_1 \simeq \frac{2A_2^{1+}k_{2R}e^{i\eta_{2I}}\cosh(\xi_{2R}+\varphi_1^+)}{[a_{21}\cosh(\eta_{2R}+\xi_{2R}+\varphi_1^++\varphi_2^++c_3)+\frac{1}{a_{21}^*}\cosh(\eta_{2R}-\xi_{2R}+\varphi_2^+-\varphi_1^++c_4)]}, \quad (2.17a)$$

$$q_2 \simeq \frac{2A_2^{2+}l_{2R}e^{i\xi_{2I}}\cosh(\eta_{2R}+\varphi_2^+)}{[a_{22}\cosh(\eta_{2R}+\xi_{2R}+\varphi_1^++\varphi_2^++c_3)+\frac{1}{a_{22}^*}\cosh(\eta_{2R}-\xi_{2R}+\varphi_2^+-\varphi_1^++c_4)]}, \quad (2.17b)$$

where $\varphi_1^+ = \frac{1}{2}\log\frac{(k_2-l_2)|\alpha_2^{(2)}|^2}{(k_2+l_2^*)(l_2+l_2^*)^2}$, $\varphi_2^+ = \frac{1}{2}\log\frac{(l_2-k_2)|\alpha_2^{(1)}|^2}{(k_2^*+l_2)(k_2+k_2^*)^2}$, $\varphi_3^+ = \frac{1}{2}\log\frac{|k_2-l_2|^2|\alpha_2^{(1)}|^2|\alpha_2^{(2)}|^2}{|k_2+l_2^*|^2(k_2+k_2^*)^2(l_2+l_2^*)^2}$, $\varphi_4^+ = \frac{1}{2}\log\frac{|\alpha_2^{(1)}|^2(l_2+l_2^*)^2}{|\alpha_2^{(2)}|^2(k_2+k_2^*)^2}$, $A_1^{2+} = [\alpha_2^{(1)}/\alpha_2^{(1)^*}]^{1/2}$ and $A_2^{2+} = i[\alpha_2^{(2)}/\alpha_2^{(2)^*}]^{1/2}$. In the latter, superscript (2+) represents soliton S_2 after collision.

In the above, $\eta_{jI} = k_{jI}t + (k_{jR}^2 - k_{jI}^2)z$, $\xi_{jI} = l_{jI}t + (l_{jR}^2 - l_{jI}^2)z$, $j = 1, 2$, and that the phase terms φ_j^-, $j = 1, 2$, can also be rewritten as $\varphi_1^- = \varphi_1^+ + \Psi_1$, $\varphi_2^- = \varphi_2^+ + \Psi_2$. The above asymptotic analysis clearly shows that there is a definite drastic alteration in the phase terms only. It can be identified from the following relations among the phase terms before and after collisions. That is,

$$\phi_1^+ = \phi_1^- + \psi_1,\ \phi_2^+ = \phi_2^- + \psi_2,\ \varphi_1^+ = \varphi_1^- - \Psi_1,\ \varphi_2^+ = \varphi_2^- - \Psi_2. \quad (2.18)$$

The above relations imply that the initial structures of the nondegenerate two solitons are preserved except for the phase terms. From this, we infer that they undergo either shape preserving collision with zero phase shift or shape changing collision with a finite phase shift. In addition to

this, a special shape altering collision can also occur with a small phase shift. The zero phase shift condition, deduced from Eq. (2.18), turns out to be

$$\phi_j^+ = \phi_j^-, \ \varphi_j^+ = \varphi_j^-, \ j = 1, 2. \tag{2.19}$$

In order to follow the above condition, the additional phase constants $\psi_j's$ and Ψ_j's should be maintained as zero. That is,

$$\psi_1 = \frac{1}{2}\log\frac{|k_2 - l_1|^2|l_1 - l_2|^4}{|k_2 + l_1^*|^2|l_1 + l_2^*|^4} = 0, \ \psi_2 = \frac{1}{2}\log\frac{|k_1 - l_2|^2|k_1 - k_2|^4}{|k_1 + l_2^*|^2|k_1 + k_2^*|^4} = 0. \tag{2.20}$$

$$\Psi_1 = \frac{1}{2}\log\frac{|k_1 - l_2|^2|l_1 - l_2|^4}{|k_1 + l_2^*|^2|l_1 + l_2^*|^4} = 0, \ \Psi_2 = \frac{1}{2}\log\frac{|k_2 - l_1|^2|k_1 - k_2|^4}{|k_2 + l_1^*|^2|k_1 + k_2^*|^4} = 0. \tag{2.21}$$

From the above, we deduce the following criterion, corresponding to the conditions (2.19), for the occurrence of shape preserving collision with zero phase shift,

$$\frac{|k_2 + l_1^*|^2}{|k_2 - l_1|^2}| - \frac{|k_1 + l_2^*|^2}{|k_1 - l_2|^2} = 0. \tag{2.22}$$

As a result, whenever the conditions (2.19) or equivalently the criterion (2.22), are satisfied the nondegenerate bright solitons exhibit shape preserving collision with a zero phase shift. Otherwise, they undergo shape altering and shape changing collisions, as discussed in the following. Further, the shape changing (and altering) collision scenario also belongs to the elastic collision as we describe below.

The above analysis clearly demonstrates that during the collision process the initial phase of each of the soliton gets changed. The total phase shift of soliton S_1 in the two modes after collision becomes

$$\begin{aligned} \Delta\Phi_1 &= (\phi_1^+ + \phi_2^+) - (\phi_1^- + \phi_2^-) = \psi_1 + \psi_2 \\ &= \frac{1}{2}\log\frac{|k_2 - l_1|^2|l_1 - l_2|^4|k_1 - l_2|^2|k_1 - k_2|^4}{|k_2 + l_1^*|^2|l_1 + l_2^*|^4|k_1 + l_2^*|^2|k_1 + k_2^*|^4}. \end{aligned} \tag{2.23}$$

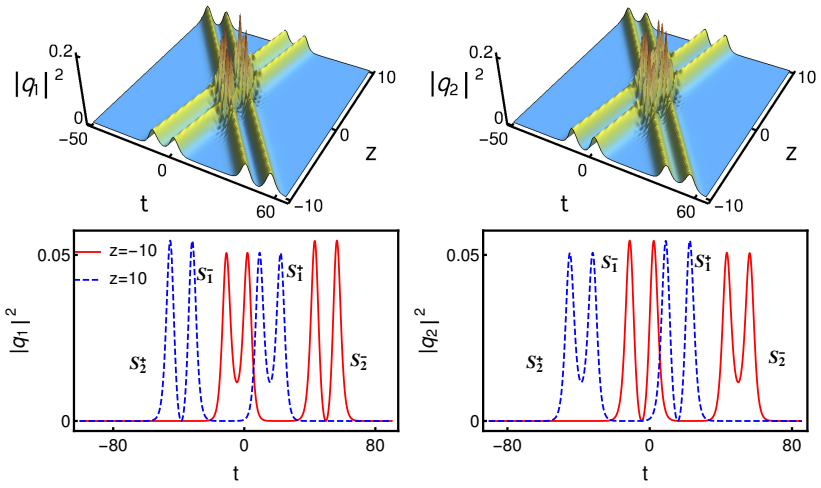

FIGURE 2.5: Shape preserving collision of two symmetric double-hump solitons - The energy does not get exchanged among the nondegenerate solitons during the collision process. The parameter values are $k_1 = 0.333 + 0.5i$, $l_1 = 0.315 + 0.5i$, $k_2 = 0.315 - 2.2i$, $l_2 = 0.333 - 2.2i$, $\alpha_1^{(1)} = 0.45 + 0.45i$, $\alpha_2^{(1)} = 0.49 + 0.45i$, $\alpha_1^{(2)} = 0.49 + 0.45i$ and $\alpha_2^{(2)} = 0.45 + 0.45i$.

Similarly the total phase shift suffered by soliton S_2 in the two modes is

$$\begin{aligned}\Delta\Phi_2 &= (\varphi_1^+ + \varphi_2^+) - (\varphi_1^- + \varphi_2^-) = -(\Psi_1 + \Psi_2) \\ &= -\frac{1}{2}\log\frac{|k_1 - l_2|^2|l_1 - l_2|^4|k_2 - l_1|^2|k_1 - k_2|^4}{|k_1 + l_2^*|^2|l_1 + l_2^*|^4|k_2 + l_1^*|^2|k_1 + k_2^*|^4} = -(\psi_1 + \psi_2) = -\Delta\Phi_1. \quad (2.24)\end{aligned}$$

From the above expressions, we conclude that the phases of all the solitons are mainly influenced by the wave numbers k_j and l_j, $j = 1, 2$, and not by the complex parameters $\alpha_1^{(j)}$'s and $\alpha_2^{(j)}$'s, $j = 1, 2$. This peculiar property of nondegenerate solitons is different in the case of degenerate vector bright solitons [37, 38], see also Section. 2.3.6 below, where the complex parameters $\alpha_1^{(j)}$'s and $\alpha_2^{(j)}$'s, associated with polarization constants, play a crucial role in shifting the position of solitons after the collision.

2.3.3.2 Elastic collision: shape preserving, shape altering and shape changing collisions

From the above asymptotic analysis, we observe that the intensities of nondegenerate solitons S_1 and S_2 in the two modes are the same before and after collision in the equal velocities case, $k_{1I} = l_{1I}$ and $k_{2I} = l_{2I}$. To confirm this, we calculate the transition intensities (using the expressions for the transition amplitudes $T_j^i = \frac{A_j^{i+}}{A_j^{i-}}$, $i,j = 1,2$), $|T_1^1|^2 = \frac{|A_1^{1+}|^2}{|A_1^{1-}|^2}$, $|T_2^1|^2 = \frac{|A_2^{1+}|^2}{|A_2^{1-}|^2}$, $|T_1^2|^2 = \frac{|A_1^{2+}|^2}{|A_1^{2-}|^2}$ and $|T_2^2|^2 = \frac{2|A_2^{2+}|^2}{2|A_2^{2-}|^2}$. The various expressions deduced for the different A_j^i's previously confirm that the transition intensities are unimodular. That is, $|T_j^l|^2 = 1$, $j,l = 1,2$. Thus, the collision scenario that occurs among the nondegenerate solitons, in general, is always elastic. So, the nondegenerate solitons, for $k_{1I} = l_{1I}$, $k_{2I} = l_{2I}$, (but $k_1 \neq l_1$, $k_2 \neq l_2$) corresponding to two distinct wave numbers in general undergo elastic collision without any intensity redistribution between the modes q_1 and q_2. However, it is clear from Eq. (2.18), the changes that occur in the phase terms do alter the structure of the nondegenerate solitons during the collision scenario. Consequently, there is a possibility of shape altering and shape changing collisions occurring, without violating the unimodular conditions of transition intensities, in the equal velocities case, apart from the earlier mentioned shape preserving collision. A typical shape-preserving collision is displayed in Figure 2.5, in which we set two well separated symmetric double-hump soliton profiles as initial profiles in both the modes at $z = -10$. The initial structures of the two double-hump solitons are preserved after the collision. It is evident from the dashed red curves drawn at $z = +10$ in Figure 2.5. In addition to this, we have also verified that the wave parameters k_j and l_j, $j = 1,2$, that are given in the caption of Figure 2.5, satisfy the zero phase shift criterion (2.22). The obtained numerical value from Eq. (2.22) is equal to -0.0064 (nearly equal to) 0. This value physically implies that during the collision the two double-humped nondegenerate bright solitons pass through one another without a phase shift and emerge from the collision unaltered in shape, amplitude and velocity. This remarkable property has not been observed earlier in the cases of scalar NLS bright solitons as well as in the degenerate vector

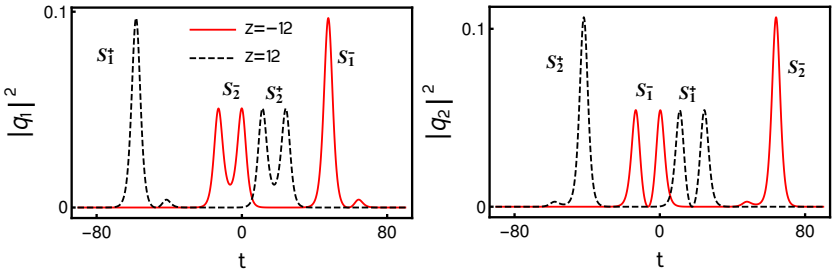

FIGURE 2.6: Shape preserving collision between a symmetric double-hump soliton and an asymmetric double-hump soliton: The parameter values are $k_1 = 0.333 + 0.5i$, $l_1 = 0.315 + 0.5i$, $k_2 = 0.315 - 2.2i$, $l_2 = 0.333 - 2.2i$, $\alpha_1^{(1)} = 0.45 + 0.45i$, $\alpha_2^{(1)} = 2.49 + 2.45i$, $\alpha_1^{(2)} = 0.49 + 0.45i$ and $\alpha_2^{(2)} = 0.45 + 0.45i$.

bright solitons [37, 38]. Very interestingly, a similar zero phase shift shape preserving collision also occurs even when the symmetric double-hump soliton interacts with an asymmetric double-hump soliton. Such collision is illustrated in Figure 2.6.

In this case, the total intensity of each soliton is conserved which can be verfied from the relations $|A_j^{l-}|^2 = |A_j^{l+}|^2$, $j, l = 1, 2$. In addition to this, the total intensity in each of the modes is also conserved, that is $|A_j^{1-}|^2 + |A_j^{2-}|^2 = |A_j^{1+}|^2 + |A_j^{2+}|^2 =$ constant.

Then, we also come across another type of elastic collision, namely shape altering collision for certain sets of parametric choices again with $k_{1I} = l_{1I}$ and $k_{2I} = l_{2I}$. To demonstrate such collision scenario in Figure 2.7, we fix the parameter values as $k_1 = 0.425 + 0.5i$, $l_1 = 0.3 + 0.5i$, $k_2 = 0.3 - 2.2i$, $l_2 = 0.425 - 2.2i$, $\alpha_1^{(1)} = \alpha_2^{(2)} = 0.5 + 0.5i$ and $\alpha_2^{(1)} = \alpha_1^{(2)} = 0.45 + 0.5i$. From this figure, one can observe that a symmetric (or asymmetric) flattop soliton collides with an asymmetric (or symmetric) double-hump soliton in the q_1 (or q_2) component. As a result, the symmetric flattop profile in the q_1 mode gets modified slightly as the asymmetric flattop profile and slightly asymmetric double-hump soliton S_2^- becomes symmetric double-hump soliton. Similarly, while the symmetric double-hump soliton S_1^- in the q_2 mode changes slightly into an asymmetric structure, the asymmetric flattop soliton S_2^- becomes symmetric. As we have pointed out earlier, this kind of shape alteration essentially arises in the structures of nondegenerate bright solitons is due to the phase conditions

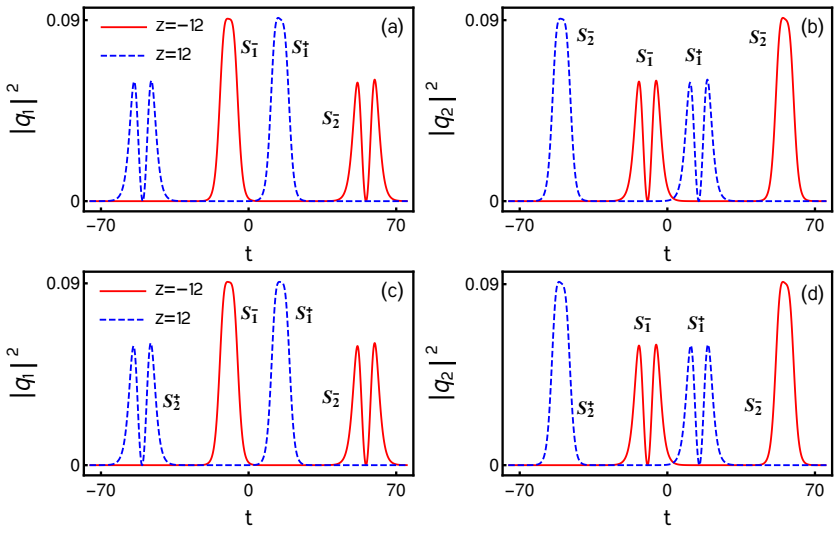

FIGURE 2.7: A typical shape altering collision is displayed in the top panels. Their corresponding shape preserving nature is brought out in the bottom panels after taking a pair of postion shifts, ($z' = z - \frac{\psi_1}{2l_{1R}k_{1I}} = 12.3053$, $z' = z - \frac{\psi_2}{2k_{1R}k_{1I}} = 12.27$) and ($z' = z + \frac{\Psi_1}{2l_{2R}k_{2I}} = 12.0614$, $z' = z + \frac{\Psi_2}{2k_{2R}k_{2I}} = 12.0694$) in the expressions (2.16a)-(2.16b) of soliton 1 and the expressions (2.17a)-(2.17b) of soliton 2, respectively.

(2.18). However, the shape preserving nature of the nondegenerate solitons can be brought out by taking appropriate position shifts based on the expressions (2.16a)-(2.16b) and (2.17a)-(2.17b). For example, the expressions (2.16a) and (2.16b) of soliton 1 after collision exactly coincides with the expressions (2.14a) and (2.14b) after substituting $z' = z - \frac{\psi_1}{2l_{1R}k_{1I}}$ and $z' = z - \frac{\psi_2}{2k_{1R}k_{1I}}$, respectively, in it. Similarly, for the soliton 2, the expressions (2.17a)-(2.17b) exactly matches with the expressions (2.15a) and (2.15b) after taking the position shifts $z' = z + \frac{\Psi_1}{2l_{2R}k_{2I}}$ and $z' = z + \frac{\Psi_2}{2k_{2R}k_{2I}}$, respectively. Correspondingly the shapes of the nondegenerate solitons are preserved. A typical example of this transition is illustrated in Figures 2.7 (c) and (d), where the initial profiles are retained after taking the shifts in the positions of solitons. This is also true in the case of shape changing collision. Here, we have not displayed the shape changing collision and their corresponding position shift plots for brevity.

2.3.4 Collision between nondegenerate and degenerate solitons

In this sub-section, we discuss the collision among the degenerate and nondegenerate solitons admitted by the two-soliton solution (2.13) of the Manakov system (2.1) in the partial nondegenerate limit $k_1 = l_1$ and $k_2 \neq l_2$. The following asymptotic analysis assures that there is a definite energy redistribution occurs among the modes q_1 and q_2.

2.3.4.1 Asymptotic analysis

To elucidate this new kind of collision behaviour, we analyze the partially nondegenerate two-soliton solution (2.13) in the asymptotic limits $z \to \pm\infty$. The resultant action yields the asymptotic forms corresponding to degenerate and nondegenerate solitons. To obtain the asymptotic forms for the present case we incorporate the asymptotic nature of the wave variables $\eta_{jR} = k_{jR}(t - 2k_{Ij}z)$ and $\xi_{2R} = l_{2R}(t - 2l_{2I}z)$, $j = 1, 2$, in the solution (2.13). Here the wave variable η_{1R} corresponds to the degenerate soliton and η_{2R}, ξ_{2R} correspond to the nondegenerate soliton. In order to find the asymptotic behaviour of these wave variables we consider the parametric choice as $k_{1R}, k_{2R}, l_{2R} > 0$, $k_{1I} > 0$, $k_{2I}, l_{2I} < 0$, $k_{1I} > k_{2I}$, $k_{1I} > l_{2I}$. For this choice, the wave variables behave asymptotically as follws: (i) degenerate soliton S_1: $\eta_{1R} \simeq 0$, η_{2R},$\xi_{2R} \to \mp\infty$ as $z \to \mp\infty$ (ii) nondegenerate soliton S_2: $\eta_{2R}, \xi_{2R} \simeq 0$, $\eta_{1R} \to \pm\infty$ as $z \to \pm\infty$. By incorporating these asymptotic behaviours of wave variables in the solution (2.13), we deduce the following asymptotic expressions for degenerate and nondegenerate solitons.

(a) Before collision: $z \to -\infty$

Soliton 1: In this limit, the asymptotic form for the degenerate soliton deduced from the partially nondegenerate two soliton solution (2.13) is

$$q_j \simeq \begin{pmatrix} A_1^{1-} \\ \\ A_2^{1-} \end{pmatrix} k_{1R} e^{i\eta_{1I}} \mathrm{sech}(\eta_{1R} + \frac{R}{2}),\ j = 1, 2, \tag{2.25}$$

where $A_j^{1-} = \alpha_1^{(j)}/(|\alpha_1^{(1)}|^2 + |\alpha_1^{(2)}|^2)^{1/2}$, $j = 1, 2$, $R = \ln \frac{(|\alpha_1^{(1)}|^2 + |\alpha_1^{(2)}|^2)}{(k_1 + k_1^*)^2}$. Here, in A_j^{1-} the superscript $1-$ denotes soliton S_1 before collision and subscript j refers to the mode number.

Soliton 2: The asymptotic expressions for the nondegenerate soliton S_2 which is present in the two modes before collision are obtained as

$$q_1 \simeq \frac{2k_{2R}A_1^{2-}}{D}\left(e^{i\xi_{2I}+\Lambda_1}\cosh(\eta_{2R} + \frac{\Phi_{21} - \Delta_{21}}{2}) + e^{i\eta_{2I}+\Lambda_2}\cosh(\xi_{2R} + \frac{\lambda_2 - \lambda_1}{2})\right), \tag{2.26a}$$

$$q_2 \simeq \frac{2l_{2R}A_2^{2-}}{D}\left(e^{i\eta_{2I}+\Lambda_7}\cosh(\xi_{2R} + \frac{\Gamma_{21} - \gamma_{21}}{2}) + e^{i\xi_{2I}+\Lambda_6}\cosh(\eta_{2R} + \frac{\lambda_7 - \lambda_6}{2})\right), \tag{2.26b}$$

$$D = e^{\Lambda_5}\cosh(\eta_{2R} - \xi_{2R} + \frac{\lambda_3 - \lambda_4}{2}) + e^{\Lambda_3}\cosh(i(\eta_{2I} - \xi_{2I}) + \frac{\vartheta_{12} - \varphi_{21}}{2}) + e^{\Lambda_4}\cosh(\eta_{2R} + \eta_{3R} + \frac{\lambda_5 - R}{2}).$$

Here, $A_1^{2-} = [\alpha_2^{(1)}/\alpha_2^{(1)^*}]^{1/2}$, $A_2^{2-} = [\alpha_2^{(2)}/\alpha_2^{(2)^*}]^{1/2}$. In the latter the superscript $2-$ denote nondegenerate soliton S_2 before collision. The various other constants appearing in Eq. (2.26a-2.26b) are defined below.

(b) After collision: $z \to +\infty$

Soliton 1: The asymptotic forms for degenerate soliton S_1 after collision deduced from the solution (2.13) (with $k_1 = l_1$ and $k_2 \neq l_2$) as,

$$q_j \simeq \begin{pmatrix} A_1^{1+} \\ \\ A_2^{1+} \end{pmatrix} e^{i(\eta_{1I}+\theta_j^+)} k_{1R}\ \mathrm{sech}(\eta_{1R} + \frac{R' - \varsigma_{22}}{2}),\ j = 1, 2, \tag{2.27}$$

where $A_1^{1+} = \alpha_1^{(1)}/(|\alpha_1^{(1)}|^2 + \chi|\alpha_1^{(2)}|^2)^{1/2}$, $A_2^{1+} = \alpha_1^{(2)}/(|\alpha_1^{(1)}|^2\chi^{-1} + |\alpha_1^{(2)}|^2)^{1/2}$,
$\chi = (|k_1 - l_2|^2|k_1 + k_2^*|^2)/(|k_1 - k_2|^2|k_1 + l_2^*|^2)$, $e^{i\theta_1^+} = \frac{(k_1-k_2)(k_1^*+k_2)(k_1-l_2)^{\frac{1}{2}}(k_1^*+l_2)^{\frac{1}{2}}}{(k_1^*-k_2^*)(k_1+k_2^*)(k_1^*-l_2^*)^{\frac{1}{2}}(k_1+l_2^*)^{\frac{1}{2}}}$,
$e^{i\theta_2^+} = \frac{(k_1-k_2)^{\frac{1}{2}}(k_1^*+k_2)^{\frac{1}{2}}(k_1-l_2)(k_1^*+l_2)}{(k_1^*-k_2^*)^{\frac{1}{2}}(k_1+k_2^*)^{\frac{1}{2}}(k_1^*-l_2^*)(k_1+l_2^*)}$. Here $1+$ in A_1^{1+} refers to degenerate soliton S_1 after collision.

Soliton 2: Similarly the expression for the nondegenerate soliton, S_2, after collision deduced from the two soliton solution (2.13) (with $k_1 = l_1$ and $k_2 \neq l_2$) is

$$q_1 \simeq \frac{2k_{2R}A_1^{2+}e^{i\eta_{2I}}\cosh(\xi_{2R} + \frac{\Lambda_{22}-\rho_1}{2})}{\big[\frac{(k_2^*-l_2^*)^{\frac{1}{2}}}{(k_2^*+l_2)^{\frac{1}{2}}}\cosh(\eta_{2R} + \xi_{2R} + \frac{\varsigma_{22}}{2}) + \frac{(k_2+l_2^*)^{\frac{1}{2}}}{(k_2-l_2)^{\frac{1}{2}}}\cosh(\eta_{2R} - \xi_{2R} + \frac{R_3-R_6}{2})\big]}, \quad (2.28a)$$

$$q_2 \simeq \frac{2l_{2R}A_2^{2+}e^{i\xi_{2I}}\cosh(\eta_{2R} + \frac{\mu_{22}-\rho_2}{2})}{\big[\frac{(k_2^*-l_2^*)^{\frac{1}{2}}}{(k_2+l_2^*)^{\frac{1}{2}}}\cosh(\eta_{2R} + \xi_{2R} + \frac{\varsigma_{22}}{2}) + \frac{(k_2^*+l_2)^{\frac{1}{2}}}{(k_2-l_2)^{\frac{1}{2}}}\cosh(\eta_{2R} - \xi_{2R} + \frac{R_3-R_6}{2})\big]}. \quad (2.28b)$$

where $\rho_j = \log\alpha_2^{(j)}$, $j = 1, 2$, $A_1^{2+} = [\alpha_2^{(1)}/\alpha_2^{(1)^*}]^{1/2}$, $A_2^{2+} = i[\alpha_2^{(2)}/\alpha_2^{(2)^*}]^{1/2}$.
The explicit expressions of all the undefined constants are given below.
The various constants which arise in the asymptotic analysis of collision between degenerate and nondegenerate solitons.

$$e^{\Lambda_1}=\frac{i\alpha_1^{(1)}(k_1-k_2)^{\frac{1}{2}}(k_1-l_2)^{\frac{1}{2}}(k_1^*+k_2)^{\frac{1}{2}}(k_1+k_1^*)(k_2+l_2^*)^{\frac{1}{2}}|k_1+l_2^*|^2}{\alpha_2^{(1)}(k_1^*-l_2^*)^{\frac{1}{2}}(k_2^*-l_2^*)^{\frac{1}{2}}}e^{R_5^*+\frac{R_3-R_6}{2}},$$

$$e^{\Lambda_2}=\frac{(k_1-k_2)^{\frac{1}{2}}(k_2^*+l_2)^{\frac{1}{2}}(k_1+k_2^*)\hat{\Lambda}_1\hat{\Lambda}_2}{(k_1^*-k_2^*)^{\frac{1}{2}}(k_2^*-l_2^*)^{\frac{1}{2}}(k_1^*+k_2)},\ e^{\Lambda_3}=\frac{|\alpha_1^{(1)}||\alpha_1^{(2)}|(k_1+k_1^*)(k_2+k_2^*)(l_2+l_2^*)}{|k_2-l_2|},$$

$$e^{\Lambda_4}=(|\alpha_1^{(1)}|^2+|\alpha_1^{(2)}|^2)^{1/2}(|\alpha_1^{(1)}|^2|k_1-k_2|^2|k_1+l_2^*|^2+|\alpha_1^{(2)}|^2|k_1-l_2|^2|k_1+k_2^*|^2)^{1/2},$$

$$e^{\Lambda_5}=\frac{|k_2+l_2^*|}{|k_2-l_2|}(|\alpha_1^{(1)}|^2|k_1+l_2^*|^2+|\alpha_1^{(2)}|^2|k_1-l_2|^2)^{1/2}(|\alpha_1^{(1)}|^2|k_1-k_2|^2+|\alpha_1^{(2)}|^2|k_1+k_2^*|^2)^{1/2},$$

$$e^{\Lambda_6}=\frac{(k_1-l_2)^{\frac{1}{2}}(k_2+l_2^*)^{\frac{1}{2}}(k_1+l_2^*)\hat{\Lambda}_3\hat{\Lambda}_4}{(k_1^*-l_2^*)^{\frac{1}{2}}(k_2^*-l_2^*)^{\frac{1}{2}}(k_1^*+l_2)},\ \hat{\Lambda}_1=(|\alpha_1^{(1)}|^2(k_1-k_2)-|\alpha_1^{(2)}|^2(k_1^*+k_2))^{1/2},$$

$$e^{\Lambda_7}=\frac{\alpha_1^{(2)}(k_1-k_2)^{\frac{1}{2}}(k_1-l_2)^{\frac{1}{2}}(k_1^*+l_2)^{\frac{1}{2}}(k_1+k_1^*)(k_2^*+l_2)^{\frac{1}{2}}|k_1+k_2^*|^2}{\alpha_2^{(2)}(k_1^*-k_2^*)^{\frac{1}{2}}(k_2^*-l_2^*)^{\frac{1}{2}}}e^{R_2^*+\frac{R_6-R_3}{2}},$$

$$\hat{\Lambda}_2=(|\alpha_1^{(1)}|^2(k_1-k_2)|k_1+l_2^*|^2-|\alpha_1^{(2)}|^2|k_1-l_2|^2(k_1^*+k_2))^{1/2},$$

$$\hat{\Lambda}_4=(|\alpha_1^{(1)}|^2|k_1-k_2|^2(k_1^*+l_2)-|\alpha_1^{(2)}|^2(k_1-l_2)|k_1+k_2^*|^2)^{1/2},$$

$$\hat{\Lambda}_3=(|\alpha_1^{(2)}|^2(k_1-l_2)-|\alpha_1^{(1)}|^2(k_1^*+l_2))^{1/2},$$

$$e^{\frac{\Phi_{21}-\Delta_{21}}{2}}=\frac{|\alpha_2^{(1)}|(k_1-k_2)(k_2^*-k_1^*)^{\frac{1}{2}}(k_2-l_2)^{\frac{1}{2}}}{(k_1+k_2^*)(k_2+k_2^*)(k_2+k_1^*)^{\frac{1}{2}}(k_2^*+l_2)^{\frac{1}{2}}},\ e^{\frac{\lambda_2-\lambda_1}{2}}=\frac{|\alpha_2^{(2)}||k_1-l_2|(k_2-l_2)^{\frac{1}{2}}\hat{\Lambda}_2}{(k_2+l_2^*)^{\frac{1}{2}}|k_1+l_2^*|^2(l_2+l_2^*)\hat{\Lambda}_1},$$

$$e^{\frac{\lambda_5-R}{2}}=\frac{|k_1-k_2||k_1-l_2||k_2-l_2|\hat{\Lambda}_5}{|k_1+k_2^*|^2|k_1+l_2^*|^2|k_2+l_2^*|(|\alpha_1^{(1)}|^2+|\alpha_1^{(2)}|^2)^{1/2}}e^{\frac{R_3+R_6}{2}},$$

$$e^{\frac{\vartheta_{12}-\varphi_{21}}{2}}=\frac{(k_2-k_1)^{\frac{1}{2}}(k_1^*-l_2^*)^{\frac{1}{2}}(k_2^*+l_2)^{\frac{1}{2}}}{(k_2+l_2^*)^{\frac{1}{2}}(k_2^*-k_1^*)^{\frac{1}{2}}(k_1-l_2)^{\frac{1}{2}}}e^{\frac{R_2^*+R_5-(R_2+R_5^*)}{2}},\ e^{\frac{\lambda_3-\lambda_4}{2}}=\frac{|k_1-k_2|\hat{\Lambda}_6|k_1+l_2^*|^2e^{\frac{R_3-R_6}{2}}}{|k_1+k_2^*|^2|k_1-l_2|\hat{\Lambda}_7},$$

$$e^{\frac{\Gamma_{21}-\gamma_{21}}{2}}=\frac{(k_2-l_2)^{\frac{1}{2}}(k_1-l_2)(k_1^*-l_2^*)^{\frac{1}{2}}}{(k_2+l_2^*)^{\frac{1}{2}}(k_1+l_2^*)(k_1^*+l_2)^{\frac{1}{2}}}e^{\frac{R_6}{2}},\ e^{\frac{\lambda_7-\lambda_6}{2}}=\frac{(k_1-k_2)(k_2-l_2)^{\frac{1}{2}}\hat{\Lambda}_4}{|k_1+k_2^*|^2(k_2^*+l_2)^{\frac{1}{2}}\hat{\Lambda}_3}e^{\frac{R_3}{2}},$$

$$\hat{\Lambda}_5=(|\alpha_1^{(1)}|^2|k_1-k_2|^2|k_1+l_2^*|^2+|\alpha_1^{(2)}|^2|k_1-l_2|^2|k_1+k_2^*|^2)^{1/2},$$

$$e^{\frac{R'-\varsigma_{22}}{2}}=\frac{|k_1-k_2||k_1-l_2|\hat{\Lambda}_5}{|k_1+k_2^*|^2|k_1+l_2^*|^2(k_1+k_1^*)},\ e^{\frac{\varsigma_{22}}{2}}=\frac{|k_2-l_2|}{|k_2+l_2^*|}e^{\frac{R_3+R_6}{2}},\ e^{\frac{R_3-R_6}{2}}=\frac{|\alpha_2^{(1)}|(l_2+l_2^*)}{|\alpha_2^{(2)}|(k_2+k_2^*)},$$

$$\hat{\Lambda}_6=(|\alpha_1^{(1)}|^2|k_1-k_2|^2+|\alpha_1^{(2)}|^2|k_1+k_2^*|^2)^{1/2},\ \hat{\Lambda}_7=(|\alpha_1^{(1)}|^2|k_1+l_2^*|^2+|\alpha_1^{(2)}|^2|k_1-l_2|^2)^{1/2},$$

$$e^{\frac{\Lambda_{22}-\rho_1}{2}}=\frac{(k_2-l_2)^{\frac{1}{2}}}{(k_2+l_2^*)^{\frac{1}{2}}}e^{\frac{R_6}{2}},\ e^{\frac{\mu_{22}-\rho_2}{2}}=\frac{(l_2-k_2)^{\frac{1}{2}}}{(k_2^*+l_2)^{\frac{1}{2}}}e^{\frac{R_3}{2}},\ e^{R_1}=\frac{|\alpha_1^{(1)}|^2}{(k_1+k_1^*)^2},\ e^{R_2}=\frac{\alpha_1^{(1)}\alpha_2^{(1)*}}{(k_1+k_2^*)^2},$$

$$e^{R_3}=\frac{|\alpha_2^{(1)}|^2}{(k_2+k_2^*)^2},\ e^{R_4}=\frac{|\alpha_1^{(2)}|^2}{(k_1+k_1^*)^2},\ e^{R_5}=\frac{\alpha_1^{(2)}\alpha_2^{(2)*}}{(k_1+l_2^*)^2},\ e^{R_6}=\frac{|\alpha_2^{(2)}|^2}{(l_2+l_2^*)^2}.$$

2.3.5 Degenerate soliton collision induced shape changing scenario of nondegenerate soliton

The coexistence of nondegenerate and degenerate solitons can be realized from the partially nondegenerate limit of the soliton solution (2.13) (with $k_1 = l_1$ and $k_2 \neq l_2$). Such coexisting solitons undergo a novel collision property, that has been illustrated in Figure. 2.8. From this figure, one can observe that the intensity of the degenerate soliton S_1 is enhanced after collision in the q_1 mode and it gets suppressed in the q_2 mode. As we expected, like in the complete degenerate case [37, 43], the degenerate soliton undergoes energy redistribution among both the modes. In this case, the polarization vectors, $A_j^l = \alpha_l^{(j)}/(|\alpha_1^{(1)}|^2 + |\alpha_1^{(2)}|^2)^{1/2}$, $l, j = 1, 2$, play a crucial role in changing the shape of the degenerate solitons under collision, where the intensity redistribution occurs between the modes q_1 and q_2. As we have pointed out below in the next subsection, the shape preserving collision arises in the pure degenerate case when the polarization parameters obey the condition, $\frac{\alpha_1^{(1)}}{\alpha_2^{(1)}} = \frac{\alpha_1^{(2)}}{\alpha_2^{(2)}}$, where $\alpha_i^{(j)}$'s, $i, j = 1, 2$, are complex parameters related to the polarization vectors as given above. However, this collision property is not true in the case of nondegenerate solitons as we have depicted in Figure. 2.8. As a result, the nondegenerate soliton S_2 switches its asymmetric double-hump profile into a single-hump profile along with a phase shift. In addition, we also noticed from the asymptotic expressions (2.26a)-(2.26b) and (2.28a)-(2.28b) the asymmetric double-hump profile of nondegenerate soliton gets transformed into another form of an asymmetric double-hump profile when it interacts with a degenerate soliton for a specific choice of parameter values. In the nondegenerate case, the relative separation distances (or phases) are in general not preserved during the collision. Therefore the mechanism behind the occurrence of shape preserving and shape changing collisions in the nondegenerate solitons is quite new. These novel collision properties can be understood from the corresponding asymptotic analysis given in the previous subsection. The analysis reveals that energy redistribution occurs between the modes q_1 and q_2. In order to confirm the shape changing nature of this interesting collision scenario we obtain the following expression for the transition amplitudes,

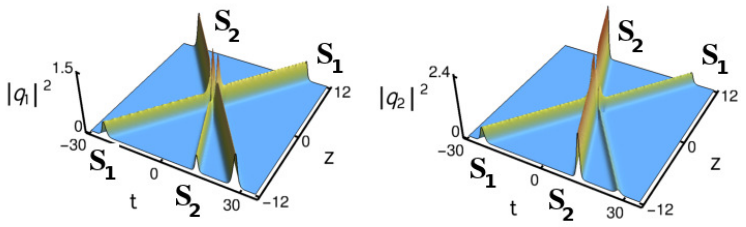

FIGURE 2.8: Shape changing collision between degenerate and nondegenerate soliton: $k_1 = l_1 = 1 + i$, $k_2 = 1 - i$, $l_2 = 1.5 - 0.5i$, $\alpha_1^{(1)} = 0.8 + 0.8i$, $\alpha_2^{(2)} = 0.6 + 0.6i$, $\alpha_2^{(1)} = 0.25 + 0.25i$, $\alpha_1^{(2)} = 1 + i$.

$$T_1^1 = \frac{(|\alpha_1^{(1)}|^2 + |\alpha_1^{(2)}|^2)^{1/2}}{(|\alpha_1^{(1)}|^2 + \chi|\alpha_1^{(2)}|^2)^{1/2}}, \; T_2^1 = \frac{(|\alpha_1^{(1)}|^2 + |\alpha_1^{(2)}|^2)^{1/2}}{(|\alpha_1^{(1)}|^2\chi^{-1} + |\alpha_1^{(2)}|^2)^{1/2}}. \tag{2.29}$$

In general, the transition amplitudes are not equal to unity. If the quantity T_j^l is not unimodular (for this case the constant $\chi \neq 1$) then the degenerate and nondegenerate solitons always exhibit shape changing collision. The standard elastic collision can be recovered when $\chi = 1$. One can calculate the shift in the positions of both degenerate and nondegenerate solitons after collision from the asymptotic analysis. This new kind of collision property has not been observed in the degenerate vector bright solitons of the Manakov system [37, 43].

2.3.6 Degenerate bright solitons and their shape changing/energy redistribution collision in Manakov system

The already reported degenerate vector one-bright soliton solution of the Manakov system (2.1) can be deduced from the one-soliton solution (2.7) by imposing the condition $k_1 = l_1$ in it. The forms of q_j given in Eq. (2.7) degenerate into the standard bright soliton form [37, 43]

$$q_j = \frac{\alpha_1^{(j)} e^{\eta_1}}{1 + e^{\eta_1 + \eta_1^* + R}}, \; j = 1, 2, \tag{2.30}$$

which can be rewritten as

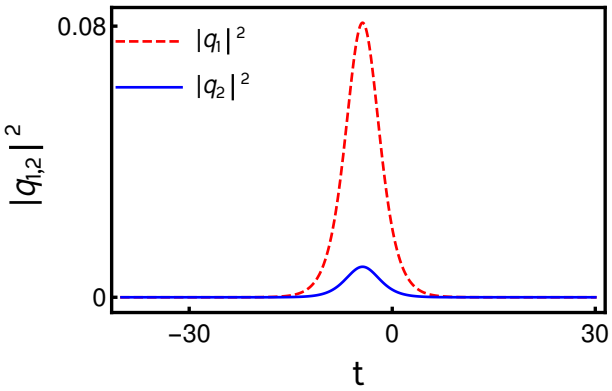

FIGURE 2.9: Degenerate one-soliton of the Manakov equation: The values of the parameters are $k_1 = 0.3 + 0.5i$, $\alpha_1^{(1)} = 1.5 + 1.5i$, $\alpha_1^{(2)} = 0.5 + 0.5i$.

$$q_j = k_{1R}\hat{A}_j e^{i\eta_{1I}}\text{sech}(\eta_{1R} + \frac{R}{2}), \tag{2.31}$$

where $\eta_{1R} = k_{1R}(t - 2k_{1I}z)$, $\eta_{1I} = k_{1I}t + (k_{1R}^2 - k_{1I}^2)z$, $\hat{A}_j = \frac{\alpha_1^{(j)}}{\sqrt{(|\alpha_1^{(1)}|^2 + |\alpha_1^{(2)}|^2)}}$, $e^R = \frac{(|\alpha_1^{(1)}|^2 + |\alpha_1^{(2)}|^2)}{(k_1 + k_1^*)^2}$, $j = 1, 2$.

Note that the above fundamental bright soliton always propagates in both the modes q_1 and q_2 with the same velocity $2k_{1I}$. The polarization vectors $(\hat{A}_1, \hat{A}_2)^\dagger$ have different amplitudes and phases, unlike the case of nondegenerate solitons where they have only different unit phases. The presence of a single wave number k_1 in the solution (2.31) restricts the degenerate soliton to have a single-hump form only. A typical profile of the degenerate soliton is shown in Figure 2.9. As already pointed out in [37, 43] the amplitude and central position of the degenerate vector bright soliton are obtained as $2k_{1R}\hat{A}_j$, $j = 1, 2$ and $\frac{R}{2k_{1R}}$, respectively.

2.3.6.1 Degenerate two-soliton solution and its energy sharing collision

Further, the degenerate two-soliton solution can be deduced from the nondegenerate two-soliton solution (2.13) by applying the degenerate limits

$k_1 = l_1$ and $k_2 = l_2$. Such degenerate two-soliton solution of the Manakov system is obtained in [37]. The two-soliton solution can be compactly written in terms of Gram determinants as

$$q_j = \frac{g^{(j)}}{f}, \quad j = 1, 2, \tag{2.32a}$$

where

$$g^{(j)} = \begin{vmatrix} A_{11} & A_{12} & 1 & 0 & e^{\eta_1} \\ A_{21} & A_{22} & 0 & 1 & e^{\eta_2} \\ -1 & 0 & B_{11} & B_{12} & 0 \\ 0 & -1 & B_{21} & B_{22} & 0 \\ 0 & 0 & -\alpha_1^{(j)} & -\alpha_2^{(j)} & 0 \end{vmatrix}, \quad f = \begin{vmatrix} A_{11} & A_{12} & 1 & 0 \\ A_{21} & A_{22} & 0 & 1 \\ -1 & 0 & B_{11} & B_{12} \\ 0 & -1 & B_{21} & B_{22} \end{vmatrix}, \tag{2.32b}$$

in which $A_{ij} = \dfrac{e^{\eta_i + \eta_j^*}}{k_i + k_j^*}$, and $B_{ij} = \kappa_{ji} = \dfrac{\left(\alpha_j^{(1)} \alpha_i^{(1)*} + \alpha_j^{(2)} \alpha_i^{(2)*}\right)}{(k_j + k_i^*)}$, $i, j = 1, 2$. The above degenerate bright two-soliton solution is characterized by six arbitrary complex parameters k_1, k_2, $\alpha_1^{(j)}$ and $\alpha_2^{(j)}$, $j = 1, 2$.

By fixing the wave numbers as $k_i = l_i, i = 1, 2, ..., N$, the N degenerate vector bright soliton solution can be recovered from the nondegenerate N-soliton solutions. In passing we also note that the nondegenerate one-soliton solution (2.7) can arise when we fix the parameters $\alpha_2^{(1)} = \alpha_1^{(2)} = 0$ in Eqs. (2.32a) and (2.32b) and rename the constants k_2 as l_1 and $\alpha_2^{(2)}$ as $\alpha_1^{(2)}$ in the resultant solution. We also note that the above degenerate two-soliton solution (2.32a)-(2.32b) can also be rewritten from the Gram determinant forms of nondegenerate two-soliton solution (2.13).

As reported in [37, 38, 43], the degenerate fundamental solitons ($k_i = l_i$, $i = 1, 2$) in the Manakov system undergo shape changing collision due to the intensity redistribution among the modes. The energy redistribution occurs in the degenerate case because of the polarization vectors of the two modes combine with each other in a specific way. This shape changing collision illustrated in Figure 2.10 where the intensity redistribution occurs because of the enhancement of soliton S_1 in the first mode and the corresponding suppression of the intensity of the same soliton in the

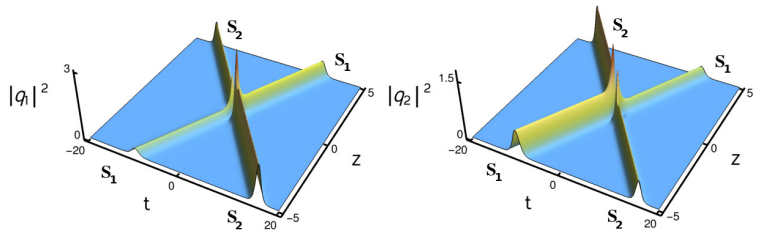

FIGURE 2.10: Shape changing collision of degenerate two-solitons: $k_1 = l_1 = 1 + i$, $k_2 = l_2 = 1.51 - 1.51i$, $\alpha_1^{(1)} = 0.5 + 0.5i$, $\alpha_2^{(1)} = \alpha_1^{(2)} = \alpha_2^{(2)} = 1$.

second mode.

To hold the conservation of energy between the modes, the intensity of the soliton S_2 gets suppressed in the first mode and it is enhanced in the second mode. The standard elastic collision occurs (as already noted) for the very special choice of parameters, namely $\frac{\alpha_1^{(1)}}{\alpha_2^{(1)}} = \frac{\alpha_1^{(2)}}{\alpha_2^{(2)}}$ [37, 38].

2.3.7 Possible experimental realization of nondegenerate solitons

To experimentally observe the nondegenerate vector solitons (single hump/ double hump solitons) in the Manakov system one may adopt the mutual-incoherence method that has been used to observe the multi-hump multi-mode solitons experimentally (Ref. [52]). The Manakov solitons (degenerate solitons) can also be observed by the same experimental procedure with appropriate modifications (Ref. [39]). In the following, we briefly envisage how the procedure is given in Ref. [52] can be redesigned to generate the double-humped nondegenerate soliton as it has been discussed in our work [78].

To observe the nondegenerate vector solitons experimentally it is essential to consider two laser sources with different properties so that the wavelength of the second laser beam is different from the first one. Using polarizing beam splitters, each one of the laser beams can be split into ordinary and extraordinary beams. The extraordinary beam coming out from the first source can be further split into two individual fields F_{11} and F_{12} by allowing it to fall on a beam splitter. These two fields are nothing

but the reflected and transmitted extraordinary beams coming out from the beam splitter. The intensities of these two fields are different. Similarly, the second beam which is coming out from the second source can also be split into two fields F_{21} and F_{22} by passing through another beam splitter. The intensities of these two fields are also different. As a result, one can generate four fields that are incoherent to each other. To set the incoherence in phase among these four fields one should allow them to travel a sufficient distance before the coupling is performed. The fields F_{11} and F_{12} now become nondegenerate two individual solitons in the first mode whereas F_{21} and F_{22} form another set of two nondegenerate solitons in the second mode. The coupling between the fields F_{11} and F_{21} can be performed by combining them using another beam splitter. Similarly, by suitably locating another beam splitter, one can combine the fields F_{12} and F_{22}, respectively. After appropriate coupling is performed the resultant optical field beams can now be focused through two individual cylindrical lenses and the output may be recorded in an imaging system, which consists of a crystal and CCD camera. The collision between the nondegenerate two-solitons in both the modes can now be seen from the recorded images.

To observe the elastic collision between double-humped nondegenerate solitons, one must make arrangements to vanish the mutual coherence property between the solitons F_{11} and F_{12} in the first mode q_1 and F_{21} and F_{22} in the second mode q_2 (Ref. [39]). The four optical beams are now completely independent and incoherent with one another. The collision angle at which the nondegenerate solitons interact should be sufficiently large enough. Under this situation, no energy exchange is expected to occur between the nondegenerate solitons of the two modes. This experimental procedure can also be used to realize multi-humped nondegenerate vector solitons in N-CNLS system but with appropriate modification in the initial conditions.

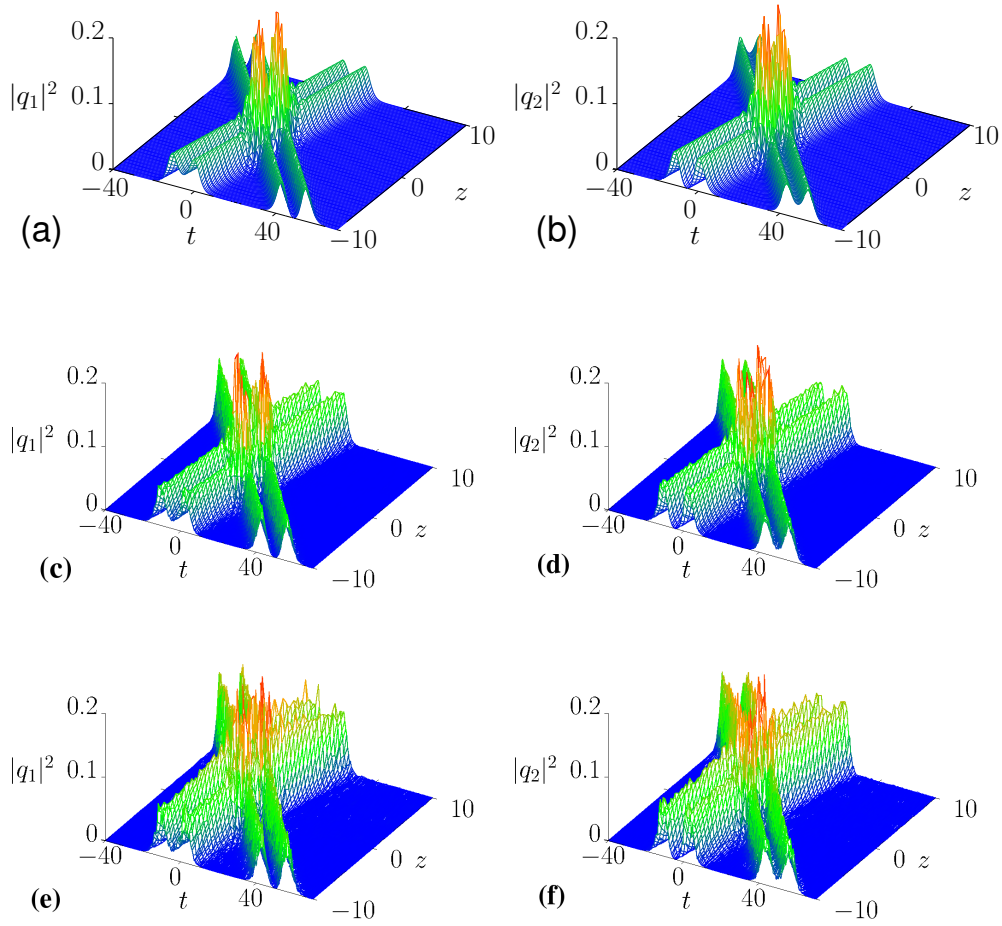

FIGURE 2.11: Numerical plots of shape preserving collision of nondegenerate symmetric double hump solitons with 10% and 20% white noise as perturbations: (a) and (b) denote the elastic collision of two symmetric double hump solitons without perturbation. (c) and (d) denote the collision with 10% white noise. (e) and (f) represent the collision with 20% strong white noise as perturbation.

2.4 Numerical stability analysis corresponding to Figs. 2.5 under perturbation

In this section, we wish to point out the stability nature of the obtained nondegenerate soliton solutions numrerically using Crank-Nicolson procedure even under the addition of suitable white noise or Gaussian noise to the initial conditions. Specifically we consider the shape preserving collision of symmetric double hump solitons discussed in Figs. 2.5. For this purpose, we have considered the Manakov system (2.1) with the initial

conditions,

$$q_j(0,t) = [1 + A\zeta(t)]q_{j,0}(t),\ j = 1,2. \tag{2.33}$$

In the above, $q_{j,0}$'s, $j = 1,2$, are the initial conditions obtained from the nondegenerate two-soliton solution Eqs. (2.13) at $z = -10$. Here A is the amplitude of the white noise and $\zeta(t)$ represents the noise or fluctuation function. The white noise was created by generating random numbers in the interval $[-1,1]$. To fix the initial conditions in the numerical algorithm, we consider the same complex parameter values which are given for the figures 2.5 in Sec. IV. We also consider the space and time step sizes, respectively, as $dz = 0.1$ and $dt = 0.001$ in the numerical algorithm. To study the collision scenario of double-hump solitons (Figs. 2.11(a) and 2.11(b)) under perturbation we fix the domain ranges for t and z as $[-45,45]$ and $[-10,10]$, respectively.

First, we consider 10% ($A = 0.1$) of random perturbation on the intial solution of Manakov system. For this strength of perturbation, we do not observe any significant change in the profile as well as in the dynamics of the nondegenerate solitons apart from a slight change, which is insignificant, in the amplitudes of double-hump solitons after the collision. This is illustrated in Figs. 2.11(c) and 2.11(d). Then we study the stability with 20% white noise ($A = 0.2$), which is a stronger perturbation, for the double-hump solitons. Such a study is demonstrated in Figs. 2.11(e) and 2.11(f). The numerical analysis shows that the double-hump soliton profiles still survive after the collision under as strong as 20% perturbation apart from a slight distortion in the amplitudes. This ensures the stability of nondegenerate solitons against perturbations of the above type of noise.

Similarly we have also verified the stability of nondegenerate solitons with Gaussian noise perturbation as well.

2.5 Nondegenerate three-soliton solution

The explicit form of nondegenerate three-soliton solution of Eq. (2.1) can be deduced by proceeding with the Eqs. (2.4) using the series representation upto orders ϵ^{11} for $g^{(N)}$ and ϵ^{12} for f. Then the solution can be expressed using Gram determinant in the following way:

$$g^{(N)} = \begin{vmatrix} A & I & \phi \\ -I & B & \mathbf{0}^T \\ \mathbf{0} & C_N & 0 \end{vmatrix}, \quad f = \begin{vmatrix} A & I \\ -I & B \end{vmatrix}, \quad N = 1, 2. \tag{2.34a}$$

Here the matrices A and B are of the order (6×6) defined as

$$A = \begin{pmatrix} A_{mm'} & A_{mn} \\ A_{nm} & A_{nn'} \end{pmatrix}, \quad B = \begin{pmatrix} \kappa_{mm'} & \kappa_{mn} \\ \kappa_{nm} & \kappa_{nn'} \end{pmatrix}, m, m', n, n' = 1, 2, 3. \tag{2.34b}$$

The various elements of matrix A are obtained from the following,

$$A_{mm'} = \frac{e^{\eta_m + \eta^*_{m'}}}{(k_m + k^*_{m'})}, \; A_{mn} = \frac{e^{\eta_m + \xi^*_n}}{(k_m + l^*_n)}, \tag{2.34c}$$

$$A_{nn'} = \frac{e^{\xi_n + \xi^*_{n'}}}{(l_n + l^*_{n'})}, \; A_{nm} = \frac{e^{\eta^*_n + \xi_m}}{(k^*_n + l_m)}, \; m, m', n, n' = 1, 2, 3. \tag{2.34d}$$

The elements of matrix B is defined as

$$\kappa_{mm'} = \frac{\psi^\dagger_m \sigma \psi_{m'}}{(k^*_m + k_{m'})}, \; \kappa_{mn} = \frac{\psi^\dagger_m \sigma \psi'_n}{(k^*_m + l_n)}, \; \kappa_{nm} = \frac{\psi'^\dagger_n \sigma \psi_m}{(l^*_n + k_m)}, \; \kappa_{nn'} = \frac{\psi'^\dagger_n \sigma \psi'_{n'}}{(l^*_n + l_{n'})}. \tag{2.34e}$$

In (2.34e) the column matrices are $\psi_j = \begin{pmatrix} \alpha^{(1)}_j \\ 0 \end{pmatrix}$, $\psi'_j = \begin{pmatrix} 0 \\ \alpha^{(2)}_j \end{pmatrix}$, $j = m, m', n, n' = 1, 2, 3$, $\eta_j = k_j t + i k_j^2 z$ and $\xi_j = l_j t + i l_j^2 z$, $j = 1, 2, 3$. The other matrices in Eq. (2.34a) are defined below:

$\phi = \begin{pmatrix} e^{\eta_1} & e^{\eta_2} & e^{\eta_3} & e^{\xi_1} & e^{\xi_2} & e^{\xi_3} \end{pmatrix}^T$, $C_1 = -\begin{pmatrix} \alpha^{(1)}_1 & \alpha^{(1)}_2 & \alpha^{(1)}_3 & 0 & 0 & 0 \end{pmatrix}$, $C_2 =$

$-\begin{pmatrix} 0 & 0 & 0 & \alpha_1^{(2)} & \alpha_2^{(2)} & \alpha_3^{(2)} \end{pmatrix}$, $\mathbf{0} = \begin{pmatrix} 0 & 0 & 0 & 0 & 0 & 0 \end{pmatrix}$ and $\sigma = I$ is a (6×6) identity matrix.

2.6 Conclusion

We have derived the nondegenerate one- and two- soliton solution of Manakov system using the standard Hirota bilinearization method. Such new class of solitons admits novel profile structure namely double hump soliton structure which is not possible in its degenerate soliton version. The double hump formation of nondegenerate solitons is explained using the relative velocities of the modes of the solitons. The coexistence of degenerate and nondegenerate solitons simultaneously in both the modes was identified by imposing wave number restrictions on the nondegenerate two-soliton solution. Then we have elaborated an interesting interaction dynamics of the nondegenerate solitons. Especially they undergo shape preserving, shape altering and shape changing collision behaviours. However all these three types of collisions are classified under elastic collision based on our detailed asymptotic analysis. They also undergo energy sharing interactions for appropriate choice of parameters. We have recaptured the degenerate one- and two-soliton solutions from our more general nondegenerate one- and two-soliton solutions by imposing constraints on their wave numbers. Also we have shown the energy sharing interactions between the degenerate solitons. Further we have pointed out the possibility of realizing nondegenerate Manakov solitons experimentally, and then the numerical stability of the nondegenerate two-solitons was studied under perturbation. At the end, nondegenerate three-soliton solution has been given in the Gram determinant form.

Chapter 3

Nondegenerate solitons in general coupled nonlinear Schrödinger system

3.1 Introduction

In the previous chapter, we have studied the existence and collision properties of the nondegenerate vector bright solitons in the celebrated Manakov system. In the present chapter, we intend to investigate the role of four-wave mixing effect on the structure of the nondegenerate vector solitons and their collision dynamics. For this purpose, we consider the generalized coupled nonlinear Schrödinger (GCNLS) system,

$$\begin{aligned} iq_{1,z} + q_{1,tt} + 2(a|q_1|^2 + c|q_2|^2 + bq_1q_2^* + b^*q_1^*q_2)q_1 = 0, \\ iq_{2,z} + q_{2,tt} + 2(a|q_1|^2 + c|q_2|^2 + bq_1q_2^* + b^*q_1^*q_2)q_2 = 0. \end{aligned} \tag{3.1}$$

which in general describes the evolution and nonlinear interaction of the two optical modes. As we have pointed out in the first chapter, the GCNLS system contains the additional phase dependent terms, $(bq_1^*q_2 + b^*q_1q_2^*)q_j$, $j = 1, 2$, which arise essentially because of the four-wave mixing effect. The complex constant b represents the strength of the four-wave mixing effect. By taking into account this nonlinearity, as well as SPM

and XPM, we aim to derive the fundamental as well as higher-order non-degenerate vector soliton solutions through the Hirota bilinear method. In addition to this, we also obtain a special type of two-soliton solution, which contains both degenerate and nondegenerate solitons simultaneously, namely partially nondegenerate two-soliton solution. It can be deduced by imposing a condition on the wave numbers in the completely nondegenerate two-soliton solution. Then we analyze the effect of FWM parameter b on the structures of nondegenerate vector bright solitons and their dynamics. Very interestingly, we find that the presence of four-wave mixing effect provokes the breathing vector soliton state in both the optical modes. Such breather formation is not possible in the fundamental vector solitons of the Manakov system (2.1). Then, we observe that the nondegenerate solitons in the GCNLS system undergo, in general, novel shape changing collision when the four-wave mixing effect strength is strong enough. On the other hand, for the weak four-wave mixing effect they undergo mere shape preserving or shape altering collision. Further, we also analyze the degenerate soliton collision induced novel shape changing property of nondegenerate vector solitons using the partially nondegenerate two-soliton solution.

The plan of this chapter is given as follows: In Section 3.2, we present the fundamental as well as the higher-order nondegenerate soliton solutions of the system (3.1) in Gram determinant forms in a compact manner apart from pointing out the complete degenerate two-soliton solution. Then in this section we also analyze the properties of nondegenerate fundamental soliton with special attention to FWM parameter b. Section 3.3 deals with the investigation of novel collision scenarios of nondegenerate solitons with appropriate asymptotic analysis. In Section 3.4, we analyze the degenerate soliton collision induced novel shape changing collision property of the nondegenerate soliton. Then, in this section we also indicate the collision properties of the degenerate solitons.

3.2 Nondegenerate vector soliton solutions

To derive the non-degenerate soliton solutions, we adopt again the well known Hirota bilinear method, in which the considered coupled nonlinear

evolution equation (3.1) should be written in the so-called bilinear form. To do so, the bilinear transformation, namely $q_j(z,t) = \frac{g^{(j)}(z,t)}{f(z,t)}$, $j = 1,2$, is introduced in Eqs. (3.1). As a result, the following bilinear forms are obtained. That is,

$$(iD_z + D_t^2)g^{(j)} \cdot f = 0, \ j = 1,2, \tag{3.2a}$$
$$D_t^2 f \cdot f = 2(ag^{(1)}g^{(1)*} + cg^{(2)}g^{(2)*} + bg^{(1)}g^{(2)*} + b^*g^{(1)*}g^{(2)}). \tag{3.2b}$$

In the above, $g^{(j)}(z,t)$'s are complex functions and $f(z,t)$ is a real function. Before proceeding further, one has to substitute the series expansions, $g^{(j)} = \epsilon g_1^{(j)} + \epsilon^3 g_3^{(j)} + ...$, and $f = 1 + \epsilon^2 f_2 + \epsilon^4 f_4 + ...$, of the unknown functions $g^{(j)}$ and f in the appropriate places of the above bilinear forms and deduce a system of linear partial differential equations (PDEs) at various orders of ϵ. Solving the resultant set of linear PDEs sucessively one can arrive at either the degenerate or non-degenerate multi-soliton solutions of Eqs. (3.1) under appropriate choices of initial seed solutions.

3.2.1 Nondegenerate fundamental vector soliton solution

To obtain the nondegenerate fundamental soliton solution of Eq. (3.1), we start with the general form of seed solutions, $g_1^{(1)} = \alpha_1^{(1)} e^{\eta_1}$, $g_1^{(2)} = \alpha_1^{(2)} e^{\xi_1}$, $\eta_1 = k_1 t + ik_1^2 z$ and $\xi_1 = l_1 t + il_1^2 z$, $k_1 \neq l_1$, as the starting solutions to the lowest order linear PDEs, $ig_{1z}^{(j)} + g_{1tt}^{(j)} = 0$, $j = 1,2$. We remark here that the previously known class of fundamental vector soliton solution of the GCNLS system (3.1) can be obtained by considering the restricted form of the seed solutions, $g_1^{(1)} = \alpha_1^{(1)} e^{\eta_1}$, $g_1^{(2)} = \alpha_1^{(2)} e^{\eta_1}$, $\eta_1 = k_1 t + ik_1^2 z$, , which can be easily deduced from the above general choice with $k_1 = l_1$. Then, by following the standard procedure of the Hirota method, we arrive at the nondegenerate fundamental bright soliton solution of the system (3.1) as

$$q_1 = \left(\alpha_1^{(1)} e^{\eta_1} + e^{\eta_1+\eta_1^*+\xi_1+\Delta_1^{(1)}} + e^{\eta_1+\xi_1+\xi_1^*+\Delta_2^{(1)}}\right)/D, \tag{3.3}$$

$$q_2 = \left(\alpha_1^{(2)} e^{\xi_1} + e^{\eta_1+\eta_1^*+\xi_1+\Delta_1^{(2)}} + e^{\eta_1+\xi_1+\xi_1^*+\Delta_2^{(2)}}\right)/D, \tag{3.4}$$

$$D = 1 + e^{\eta_1+\eta_1^*+\delta_1} + e^{\eta_1^*+\xi_1+\delta_2} + e^{\eta_1+\xi_1^*+\delta_2^*} + e^{\xi_1+\xi_1^*+\delta_3} + e^{\eta_1+\eta_1^*+\xi_1+\xi_1^*+\delta_4}.$$

Here, $e^{\Delta_1^{(1)}} = \frac{b^*(k_1-l_1)|\alpha_1^{(1)}|^2\alpha_1^{(2)}}{(k_1+k_1^*)(k_1^*+l_1)^2}$, $e^{\Delta_2^{(1)}} = \frac{c(k_1-l_1)\alpha_1^{(1)}|\alpha_1^{(2)}|^2}{(k_1+l_1^*)(l_1+l_1^*)^2}$, $e^{\Delta_1^{(2)}} = -\frac{a(k_1-l_1)|\alpha_1^{(1)}|^2\alpha_1^{(2)}}{(l_1+k_1^*)(k_1+k_1^*)^2}$, $e^{\Delta_2^{(2)}} = -\frac{b(k_1-l_1)\alpha_1^{(1)}|\alpha_1^{(2)}|^2}{(l_1+l_1^*)(k_1+l_1^*)^2}$, $e^{\delta_1} = \frac{a|\alpha_1^{(1)}|^2}{(k_1+k_1^*)^2}$, $e^{\delta_2} = \frac{b^*\alpha_1^{(1)*}\alpha_1^{(2)}}{(k_1^*+l_1)^2}$, $e^{\delta_3} = \frac{c|\alpha_1^{(2)}|^2}{(l_1+l_1^*)^2}$, $e^{\delta_4} = \frac{|k_1-l_1|^2|\alpha_1^{(1)}|^2|\alpha_1^{(2)}|^2\left[ac|(k_1+l_1^*)|^2-|b|^2(k_1+k_1^*)(l_1+l_1^*)\right]}{(k_1+k_1^*)^2|k_1+l_1^*|^4(l_1+l_1^*)^2}$. The nature of the above solution is described by four arbitrary complex parameters, k_1, l_1, $\alpha_1^{(j)}$, $j = 1,2$, and three system parameters a, c and b. The solution (3.3)-(3.4) is non-singular for $\left(ac|(k_1+l_1^*)|^2 - |b|^2(k_1+k_1^*)(l_1+l_1^*)\right) > 0$, for which the strength of SPM and XPM should be always positive ($a, c > 0$). For $b = 0$, the solution (3.3)-(3.4) exactly coincides with the nondegenerate fundamental bright soliton solution of the Manakov system and mixed 2-CNLS system by further fixing $a = c = 1$ and $a = -c = 1$, respectively, in it. The previously reported three-parameter vector soliton solution of the GCNLS system (3.1) [119] arises as a special case when we impose the restriction $k_1 = l_1$ in the above four-parameter solution (3.3)-(3.4). As a result, the explicit form of the three-parameter bright soliton solution turns out to be

$$q_j = \frac{\alpha_1^{(j)} e^{\eta_1}}{1 + e^{\eta_1+\eta_1^*+R}} \equiv k_{1R}\hat{A}_j e^{i\eta_{1I}}\mathrm{sech}(\eta_{1R} + \frac{R}{2}),\ j = 1,2, \tag{3.5}$$

where $\eta_1 = k_1 t + ik_1^2 z = \eta_{1R} + i\eta_{1I} = [k_{1R}(t - 2k_{1I}z)] + i[k_{1I}t + (k_{1R}^2 - k_{1I}^2)z]$, the unit polarization vectors are $\hat{A}_j = \alpha_1^{(j)}/[a|\alpha_1^{(1)}|^2 + c|\alpha_1^{(2)}|^2 + b\alpha_1^{(1)}\alpha_1^{(2)*} + b^*\alpha_1^{(1)*}\alpha_1^{(2)}]^{\frac{1}{2}}$, $e^R = \frac{(a|\alpha_1^{(1)}|^2+c|\alpha_1^{(2)}|^2+b\alpha_1^{(1)}\alpha_1^{(2)*}+b^*\alpha_1^{(1)*}\alpha_1^{(2)})}{(k_1+k_1^*)^2}$, the amplitude of the two modes are $k_{1R}\hat{A}_j$, the velocity of the degenerate soliton is $2k_{1I}$ and the central position of the soliton is found to be $\frac{R}{2k_{1R}} =$

$\frac{1}{k_{1R}}\log\frac{(a|\alpha_1^{(1)}|^2+c|\alpha_1^{(2)}|^2+b\alpha_1^{(1)}\alpha_1^{(2)*}+b^*\alpha_1^{(1)*}\alpha_1^{(2)})^{\frac{1}{2}}}{(k_1+k_1^*)}$. The above degenerate bright soliton solution always admits single-hump '*sech*' soliton profile.

To bring out the special properties associated with the solution (3.3)-(3.4) further, we rewrite it as follows:

$$q_1 = \frac{2k_{1R}}{D_1}\Big(c_{11}e^{i\eta_{1I}}\cosh(\xi_{1R}+\phi_1)+c_{21}e^{i\xi_{1I}}[\cosh(\eta_{1R}+\phi_2-\phi_1+c_2) + \sinh(\eta_{1R}+\phi_2-\phi_1+c_2)]\Big), \tag{3.6}$$

$$q_2 = \frac{2l_{1R}}{D_1}\Big(c_{12}e^{i\xi_{1I}}\cosh(\eta_{1R}+\phi_2)+c_{22}e^{i\eta_{1I}}[\cosh(\xi_{1R}-(\phi_2-\phi_1)+c_2) + \sinh(\xi_{1R}-(\phi_2-\phi_1)+c_2)]\Big), \tag{3.7}$$

$$D_1 = \Lambda_1\cosh(\eta_{1R}+\xi_{1R}+\phi_2+\phi_1+c_1)+\cosh(\eta_{1R}-\xi_{1R}+\phi_2-\phi_1+c_2) + \Lambda_2[\cosh\phi_3\cos(\eta_{1I}-\xi_{1I})+i\sinh\phi_3\sin(\eta_{1I}-\xi_{1I})].$$

Here, $\eta_{1R} = k_{1R}(t-2k_{1I}z)$, $\xi_{1R} = l_{1R}(t-2l_{1I}z)$, $\eta_{1I} = k_{1I}t+(k_{1R}^2-k_{1I}^2)z$, $\xi_{1I} = l_{1I}t+(l_{1R}^2-l_{1I}^2)z$, $\phi_1 = \frac{1}{2}\log\frac{c(k_1-l_1)|\alpha_1^{(2)}|^2}{(k_1+l_1^*)(l_1+l_1^*)^2}$, $\phi_2 = \frac{1}{2}\log\frac{a(l_1-k_1)|\alpha_1^{(1)}|^2}{(k_1^*+l_1)(k_1+k_1^*)^2}$, $\phi_3 = \frac{1}{2}\log\frac{b\alpha_1^{(1)}\alpha_1^{(2)*}(k_1^*+l_1)^2}{b^*\alpha_1^{(1)*}\alpha_1^{(2)}(k_1+l_1^*)^2}$, $c_{11} = [\frac{\alpha_1^{(1)}(k_1-l_1)}{a\alpha_1^{(1)*}(k_1+l_1^*)}]^{1/2}$, $c_{21} = \frac{1}{2}[\frac{b^*\alpha_1^{(2)}(k_1-l_1)}{a(k_1^*+l_1)^2}]$, $c_{12} = [\frac{\alpha_1^{(2)}(l_1-k_1)}{c\alpha_1^{(2)*}(k_1^*+l_1)}]^{1/2}$, $c_{22} = \frac{1}{2}[\frac{b\alpha_1^{(1)}(l_1-k_1)}{c(k_1+l_1^*)^2}]$, $c_1 = \frac{1}{2}\log\frac{(k_1^*-l_1^*)[ac|k_1+l_1^*|^2-|b|^2(k_1+k_1^*)(l_1+l_1^*)]}{ac(l_1-k_1)|k_1+l_1^*|^2}$, $c_2 = \frac{1}{2}\log\frac{(k_1-l_1)(k_1^*+l_1)}{(l_1-k_1)(k_1+l_1^*)}$, $\Lambda_1 = \frac{|k_1-l_1|[ac|k_1+l_1^*|^2-|b|^2(k_1+k_1^*)(l_1+l_1^*)]^{1/2}}{(ac)^{1/2}|k_1+l_1^*|^2}$, and $\Lambda_2 = \frac{|b|(k_1+k_1^*)(l_1+l_1^*)}{(ac)^{1/2}|k_1+l_1^*|^2}$. The presence of additional wave number k_1 or l_1 provides the additional degree of freedom to the motion as well as the structure of the soliton in the two modes q_1 and q_2. For instance, the following two possibilities are always allowed. The solitons in the two modes can propagate either with equal velocities: $v_1 = v_2$, $v_1 = 2k_{1I}$, $v_2 = 2l_{1I}$ or with unequal velocities: $v_1 \neq v_2$. As we describe below, these two choices reveal the new geometrical structures associated with the solution (3.3)-(3.4) of the GCNLS system (3.1).

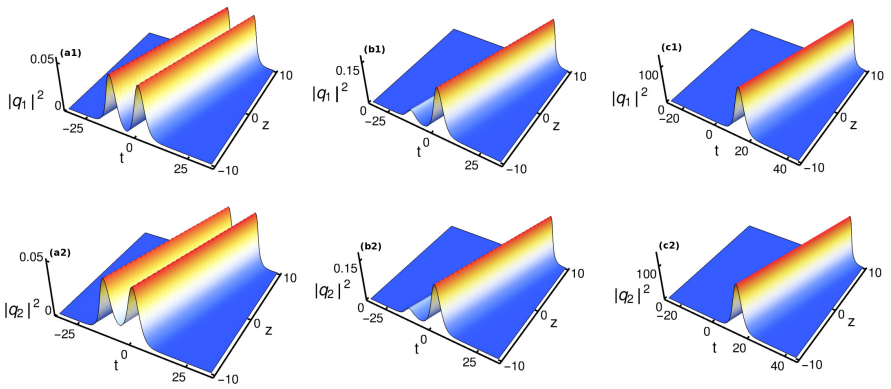

FIGURE 3.1: The role of FWM effect on the double-hump soliton structure of the nondegenerate one-soliton solution is demonstrated by fixing the parameter values as $k_1 = 0.333 - 0.5i$, $l_1 = 0.315 - 0.5i$, $k_2 = 0.315 + 2.2i$, $l_2 = 0.333 + 2.2i$, $\alpha_1^{(1)} = 0.45 + 0.45i$, $\alpha_2^{(1)} = 2.49 + 2.45i$, $\alpha_1^{(2)} = 0.49 + 0.45i$ and $\alpha_2^{(2)} = 0.45 + 0.45i$. The strength of FWM for each of the figures. (a1)-(a2): $b = 0$, (b1)-(b2): $b = 0.5 + 0.5i$ and (c1)-(c2): $b = 1$.

3.2.1.1 Role of FWM effect on one-soliton solution

The nondegenerate fundamental soliton solution (3.3)-(3.4) with $v_1 = v_2$ admits double-hump profile when the FWM effect is zero. Such profiles are displayed in Figs. 3.1(a1) and (a2) for $b = 0$ and $a = c = 1$. However, the symmetric nature of such intensity profiles disappears and the asymmetric double-hump profiles emerge in both the modes q_1 and q_2 when we incorporate the FWM effect ($b \neq 0$) along with the real part of k_1 is slightly greater than the real part of l_1 ($k_{1R} > l_{1R}$). Such a profile transition is displayed in Figs. 3.1(b1) and (b2). Further, increasing the value of b, we find that the first-hump is completely suppressed in both the modes and the second-hump only persists throughout the evolution with an enhancement in the amplitude or intensity, which is illustrated in Figs. 3.1(c1) and (c2).

Interestingly, we also find that the presence of the FWM parameter generates the breathing state in the structure of nondegenerate fundamental soliton of the GCNLS system (3.1). It can be identified from the expressions (3.6)-(3.7) with $v_1 = v_2$, where periodic functions explicitly appear because of FWM parameter b. Such the novel breathing state is depicted in Figs. (3.2) and (3.3), where the oscillations occur along the propagation

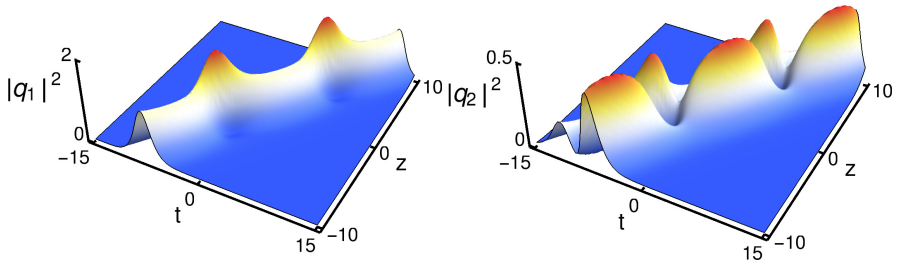

FIGURE 3.2: Breather formation with strong FWM effect is demonstrated by fixing the parameter values as $a = c = 1$, $b = 0.5 + 0.5i$, $k_1 = 1 + 0.5i$, $l_1 = 0.5 + 0.5i$, $\alpha_1^{(1)} = 0.65$, and $\alpha_1^{(2)} = 1 + i$.

direction z only. From these figures, we observe that the strong breathing nature appears when the FWM effect is high enough (see Fig. (3.2)) along with a parameteric condition $k_{1R} >> l_{1R}$, in which case the value of k_{1R} should be considerably larger than l_{1R}. On the other hand, for a weak strength of the FWM effect, the small oscillations appear in the intensity peaks only (see Fig. (3.3)). The period of oscillation is calculated as

$$T = \frac{2\pi}{\omega} = \frac{2\pi}{(k_{1R}^2 - l_{1R}^2)}. \tag{3.8}$$

The above expression shows that the period of oscillation mainly depends on the real parts of the wave numbers k_1 and l_1 apart from the influence of the FWM nonlinearity. This type of special property has not been observed in the degenerate counterparts, where the real part of the single wave number k_1 is responsible for the amplitude of the degenerate vector bright soliton of Eq. (3.1) accompanying the unit polarization vectors. For completeness, in Fig. 3.4, we also demonstrate the breathing soliton state by considering the mixed type nonlinearity $a = 1$, $c = -1$. However, the singularity essentially arises in the breathing state because of the negative sign of the XPM nonlinearity.

Next, we consider the solution (3.3)-(3.4) with unequal velocities: $v_1 \neq v_2$. In this situation, it admits two types of two-soliton like collision patterns as we have illustrated in Figs. (3.5) and (3.6). In these figures, two distinct single-hump profiles at different positions start to interact at $z = 0$.

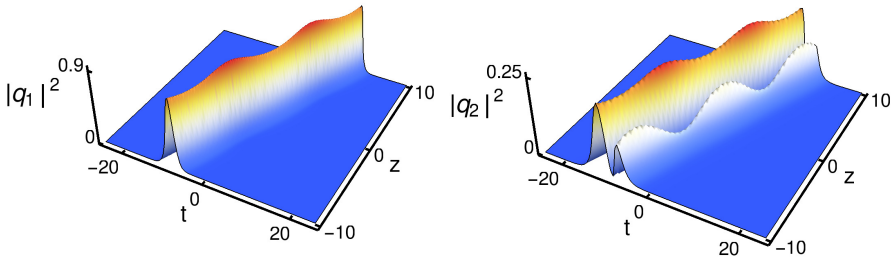

FIGURE 3.3: Breathing state is demonstrated for the low strength of FWM effect. The parameter values are the same as in Fig. 3.2 except now $b = 0.15 + 0.15i$.

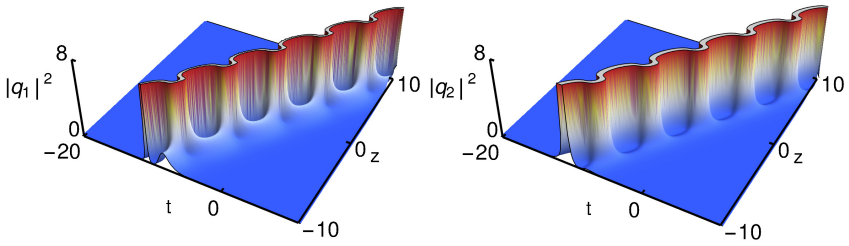

FIGURE 3.4: Singular breathing state is demonstrated for the strong strength of FWM effect. The parameter values are $b = 0.5 + 0.5i$, $k_1 = 1.3 + 0.5i$, $l_1 = -0.5 + 0.5i$, $\alpha_1^{(1)} = 0.65$, and $\alpha_1^{(2)} = i$.

As a result, these interaction patterns appear due to the exchange of intensities among the modes. This kind of switching of intensities among the waveguides could be relevant to optical switching applications.

3.2.2 Completely/partially nondegenerate two-soliton solution

Depending on the choices of seed solutions, consideration along with the following conditions on the wave numbers, namely (i) $k_1 \neq l_1$, $k_2 \neq l_2$, (ii) $k_1 = l_1$ and $k_2 \neq l_2$ (or $k_1 \neq l_1$ and $k_2 = l_2$), and (iii) $k_1 = l_1$ and $k_2 = l_2$, the GCNLS system (3.1) also admits three-types of two-soliton solutions, namely (i) completely nondegenerate two-soliton solution, (ii)

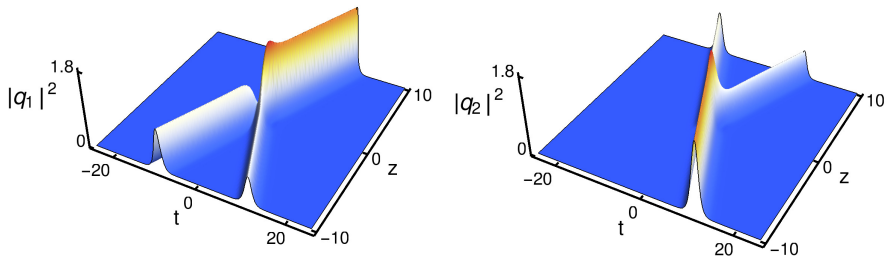

FIGURE 3.5: Nondegenerate fundamental soliton with unequal-velocity by fixing the parameter values as $k_1 = 0.333 - 0.5i$, $l_1 = 0.315 - 0.5i$, $k_2 = 0.315 + 2.2i$, $l_2 = 0.333 + 2.2i$, $\alpha_1^{(1)} = 0.45 + 0.45i$, $\alpha_2^{(1)} = 2.49 + 2.45i$, $\alpha_1^{(2)} = 0.49 + 0.45i$ and $\alpha_2^{(2)} = 0.45 + 0.45i$.

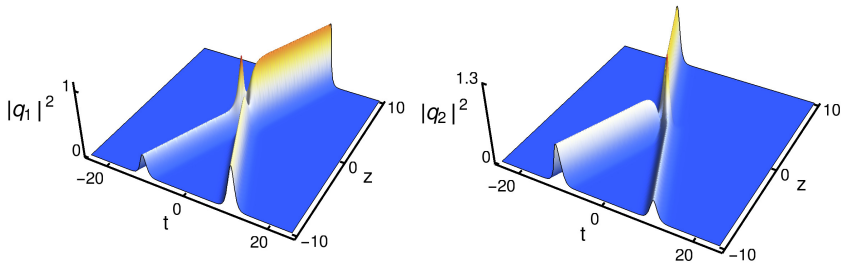

FIGURE 3.6: Nondegenerate fundamental soliton with unequal-velocity by fixing the parameter values as $k_1 = 0.333 - 0.5i$, $l_1 = 0.315 - 0.5i$, $k_2 = 0.315 + 2.2i$, $l_2 = 0.333 + 2.2i$, $\alpha_1^{(1)} = 0.45 + 0.45i$, $\alpha_2^{(1)} = 2.49 + 2.45i$, $\alpha_1^{(2)} = 0.49 + 0.45i$ and $\alpha_2^{(2)} = 0.45 + 0.45i$.

partially nondegenerate two-soliton solution, and (iii) completely degenerate two-soliton solution, respectively. For instance, the two-soliton solution, with the complete nondegeneracy property, is obtained as a result of finding the unknown functions in the truncated series expansions, $g^{(j)} = \epsilon g_1^{(j)} + \epsilon^3 g_3^{(j)} + \epsilon^5 g_5^{(j)} + \epsilon^7 g_7^{(j)}$, $j = 1, 2$, and $f = 1 + \epsilon^2 f_2 + \epsilon^4 f_4 + \epsilon^6 f_6 + \epsilon^8 f_8$. To get the explicit forms of the unknown functions that are present in the latter series expansions, we assume the initial solutions as

$$\begin{aligned} &g_1^{(1)} = \alpha_1^{(1)} e^{\eta_1} + \alpha_2^{(1)} e^{\eta_2} \text{ and } g_1^{(2)} = \alpha_1^{(2)} e^{\xi_1} + \alpha_2^{(2)} e^{\xi_2}, \\ &\eta_j = k_j t + i k_j^2 z,\ \xi_j = l_j t + i l_j^2 z,\ j = 1, 2. \end{aligned} \tag{3.9}$$

Here, the wave numbers k_j and l_j and the constants $\alpha_1^{(j)}$ and $\alpha_2^{(j)}$, $j =$

1,2, are in general complex. We find that the other unknown functions, $g_9^{(j)}$, $g_{11}^{(j)}$, $j = 1,2$, f_{10}, f_{12} and etc., all exactly vanish. The remaining non-vanishing functions constitute the nondegenerate two-soliton solution, which is rewritten using the Gram determinants in the following way:

$$g^{(s)} = \begin{vmatrix} A & I & \phi \\ -I & B & \mathbf{0}^T \\ \mathbf{0} & C_s & 0 \end{vmatrix}, \; f = \begin{vmatrix} A & I \\ -I & B \end{vmatrix}, \; s = 1,2, \tag{3.10a}$$

where the other elements in the above determinants are defined as given below:

$$A = \begin{pmatrix} \frac{e^{\eta_1+\eta_1^*}}{(k_1+k_1^*)} & \frac{e^{\eta_1+\eta_2^*}}{(k_1+k_2^*)} & \frac{e^{\eta_1+\xi_1^*}}{(k_1+l_1^*)} & \frac{e^{\eta_1+\xi_2^*}}{(k_1+l_2^*)} \\ \frac{e^{\eta_2+\eta_1^*}}{(k_2+k_1^*)} & \frac{e^{\eta_2+\eta_2^*}}{(k_2+k_2^*)} & \frac{e^{\eta_2+\xi_1^*}}{(k_2+l_1^*)} & \frac{e^{\eta_2+\xi_2^*}}{(k_2+l_2^*)} \\ \frac{e^{\xi_1+\eta_1^*}}{(l_1+k_1^*)} & \frac{e^{\xi_1+\eta_2^*}}{(l_1+k_2^*)} & \frac{e^{\xi_1+\xi_1^*}}{(l_1+l_1^*)} & \frac{e^{\xi_1+\xi_2^*}}{(l_1+l_2^*)} \\ \frac{e^{\xi_2+\eta_1^*}}{(l_2+k_1^*)} & \frac{e^{\xi_2+\eta_2^*}}{(l_2+k_2^*)} & \frac{e^{\xi_2+\xi_1^*}}{(l_2+l_1^*)} & \frac{e^{\xi_2+\xi_2^*}}{(l_2+l_2^*)} \end{pmatrix}, \tag{3.10b}$$

$$B = \begin{pmatrix} \frac{a\alpha_1^{(1)}\alpha_1^{(1)*}}{(k_1+k_1^*)} & \frac{a\alpha_2^{(1)}\alpha_1^{(1)*}}{(k_2+k_1^*)} & \frac{b^*\alpha_1^{(2)}\alpha_1^{(1)*}}{(l_1+k_1^*)} & \frac{b^*\alpha_2^{(2)}\alpha_1^{(1)*}}{(l_2+k_1^*)} \\ \frac{a\alpha_1^{(1)}\alpha_2^{(1)*}}{(k_1+k_2^*)} & \frac{a\alpha_2^{(1)}\alpha_2^{(1)*}}{(k_2+k_2^*)} & \frac{b^*\alpha_1^{(2)}\alpha_2^{(1)*}}{(l_1+k_2^*)} & \frac{b^*\alpha_2^{(2)}\alpha_2^{(1)*}}{(l_2+k_2^*)} \\ \frac{b\alpha_1^{(1)}\alpha_1^{(2)*}}{(k_1+l_1^*)} & \frac{b\alpha_2^{(1)}\alpha_1^{(2)*}}{(k_2+l_1^*)} & \frac{c\alpha_1^{(2)}\alpha_1^{(2)*}}{(l_1+l_1^*)} & \frac{c\alpha_2^{(2)}\alpha_1^{(2)*}}{(l_2+l_1^*)} \\ \frac{b\alpha_1^{(1)}\alpha_2^{(2)*}}{(k_1+l_2^*)} & \frac{b\alpha_2^{(1)}\alpha_2^{(2)*}}{(k_2+l_2^*)} & \frac{c\alpha_1^{(2)}\alpha_2^{(2)*}}{(l_1+l_2^*)} & \frac{c\alpha_2^{(2)}\alpha_2^{(2)*}}{(l_2+l_2^*)} \end{pmatrix}, \tag{3.10c}$$

$$\phi = \begin{pmatrix} e^{\eta_1} & e^{\eta_2} & e^{\xi_1} & e^{\xi_2} \end{pmatrix}^T, \; C_1 = -\begin{pmatrix} \alpha_1^{(1)} & \alpha_2^{(1)} & 0 & 0 \end{pmatrix},$$
$$C_2 = -\begin{pmatrix} 0 & 0 & \alpha_1^{(2)} & \alpha_2^{(2)} \end{pmatrix}, \; \mathbf{0} = \begin{pmatrix} 0 & 0 & 0 & 0 \end{pmatrix},$$

and I is a (4×4) identity matrix. The above solution consists of eight arbitrary complex parameters k_j, l_j, $\alpha_1^{(j)}$ and $\alpha_2^{(j)}$, $j = 1,2$. The profile shapes of the nondegenerate solitons and their various novel collision scenarios are governed by these eight nontrivial soliton parameters and the three system parameters a, c and b.

Further, we wish to point out that the GCNLS system (3.1) also admits

another class of two-soliton solution containing both degenerate and non-degenerate vector solitons simultaneously. This additional possibility always exists in the newly derived two-soliton solution (3.10a)-(3.10c). Such possibility arises by restricting the sets of wave numbers as $k_1 = l_1$ and $k_2 \neq l_2$ or $k_1 \neq l_1$ and $k_2 = l_2$ in Eq. (3.10a)-(3.10c). Here, we have considered the former choice. By doing so, the seed solutions (3.9) get reduced as

$$\begin{aligned} &g_1^{(1)} = \alpha_1^{(1)} e^{\eta_1} + \alpha_2^{(1)} e^{\eta_2} \text{ and } g_1^{(2)} = \alpha_1^{(2)} e^{\eta_1} + \alpha_2^{(2)} e^{\xi_2}, \\ &\eta_j = k_j t + i k_j^2 z,\ \xi_2 = l_2 t + i l_2^2 z,\ j = 1, 2. \end{aligned} \tag{3.11}$$

With the above choice of initial solutions one can also derive the partial nondegenerate two-soliton solution through the Hirota bilinear method. We obtain the following form of the partial nondegenerate two-soliton solution as a final product. However, the resultant form is the same as the one given in Eq. (3.10a)-(3.10c) except the following changes that occur in the elements of matrices A, B and ϕ:

$$A = \begin{pmatrix} \frac{e^{\eta_1+\eta_1^*}}{(k_1+k_1^*)} & \frac{e^{\eta_1+\eta_2^*}}{(k_1+k_2^*)} & \frac{e^{\eta_1+\eta_1^*}}{(k_1+k_1^*)} & \frac{e^{\eta_1+\xi_2^*}}{(k_1+l_2^*)} \\ \frac{e^{\eta_2+\eta_1^*}}{(k_2+k_1^*)} & \frac{e^{\eta_2+\eta_2^*}}{(k_2+k_2^*)} & \frac{e^{\eta_2+\eta_1^*}}{(k_2+k_1^*)} & \frac{e^{\eta_2+\xi_2^*}}{(k_2+l_2^*)} \\ \frac{e^{\eta_1+\eta_1^*}}{(k_1+k_1^*)} & \frac{e^{\eta_1+\eta_2^*}}{(k_1+k_2^*)} & \frac{e^{\eta_1+\eta_1^*}}{(k_1+k_1^*)} & \frac{e^{\eta_1+\xi_2^*}}{(k_1+l_2^*)} \\ \frac{e^{\xi_2+\eta_1^*}}{(l_2+k_1^*)} & \frac{e^{\xi_2+\eta_2^*}}{(l_2+k_2^*)} & \frac{e^{\xi_2+\eta_1^*}}{(l_2+k_1^*)} & \frac{e^{\xi_2+\xi_2^*}}{(l_2+l_2^*)} \end{pmatrix}, \tag{3.12a}$$

$$\phi = \begin{pmatrix} e^{\eta_1} & e^{\eta_2} & e^{\eta_1} & e^{\xi_2} \end{pmatrix}^T, \tag{3.12b}$$

$$B = \begin{pmatrix} \frac{a\alpha_1^{(1)}\alpha_1^{(1)*}}{(k_1+k_1^*)} & \frac{a\alpha_2^{(1)}\alpha_1^{(1)*}}{(k_2+k_1^*)} & \frac{b^*\alpha_1^{(2)}\alpha_1^{(1)*}}{(k_1+k_1^*)} & \frac{b^*\alpha_2^{(2)}\alpha_1^{(1)*}}{(l_2+k_1^*)} \\ \frac{a\alpha_1^{(1)}\alpha_2^{(1)*}}{(k_1+k_2^*)} & \frac{a\alpha_2^{(1)}\alpha_2^{(1)*}}{(k_2+k_2^*)} & \frac{b^*\alpha_1^{(2)}\alpha_2^{(1)*}}{(k_1+k_2^*)} & \frac{b^*\alpha_2^{(2)}\alpha_2^{(1)*}}{(l_2+k_2^*)} \\ \frac{b\alpha_1^{(1)}\alpha_1^{(2)*}}{(k_1+k_1^*)} & \frac{b\alpha_2^{(1)}\alpha_1^{(2)*}}{(k_2+k_1^*)} & \frac{c\alpha_1^{(2)}\alpha_1^{(2)*}}{(k_1+k_1^*)} & \frac{c\alpha_2^{(2)}\alpha_1^{(2)*}}{(l_2+k_1^*)} \\ \frac{b\alpha_1^{(1)}\alpha_2^{(2)*}}{(k_1+l_2^*)} & \frac{b\alpha_2^{(1)}\alpha_2^{(2)*}}{(k_2+l_2^*)} & \frac{c\alpha_1^{(2)}\alpha_2^{(2)*}}{(k_1+l_2^*)} & \frac{c\alpha_2^{(2)}\alpha_2^{(2)*}}{(l_2+l_2^*)} \end{pmatrix}. \tag{3.12c}$$

The structural and the interaction properties associated with this interesting class of solution are described by seven complex parameters k_j, l_2,

$\alpha_1^{(j)}$, and $\alpha_2^{(j)}$, $j = 1, 2$.

We also wish to point out that one can capture the already known completely degenerate two-soliton solution of the GCNLS system (3.1) from the nondegenerate two-soliton solution (3.10a)-(3.10c) for the wave number choices $k_1 = l_1$ and $k_2 = l_2$. The resultant forms again coincide with the one given in Eq. (3.10a)-(3.10c) except for the following changes that occur in the elements of matrices A, B and ϕ:

$$A = \begin{pmatrix} \frac{e^{\eta_1+\eta_1^*}}{(k_1+k_1^*)} & \frac{e^{\eta_1+\eta_2^*}}{(k_1+k_2^*)} & \frac{e^{\eta_1+\eta_1^*}}{(k_1+k_1^*)} & \frac{e^{\eta_1+\eta_2^*}}{(k_1+k_2^*)} \\ \frac{e^{\eta_2+\eta_1^*}}{(k_2+k_1^*)} & \frac{e^{\eta_2+\eta_2^*}}{(k_2+k_2^*)} & \frac{e^{\eta_2+\eta_1^*}}{(k_2+k_1^*)} & \frac{e^{\eta_2+\eta_2^*}}{(k_2+k_2^*)} \\ \frac{e^{\eta_1+\eta_1^*}}{(k_1+k_1^*)} & \frac{e^{\eta_1+\eta_2^*}}{(k_1+k_2^*)} & \frac{e^{\eta_1+\eta_1^*}}{(k_1+k_1^*)} & \frac{e^{\eta_1+\eta_2^*}}{(k_1+k_2^*)} \\ \frac{e^{\eta_2+\eta_1^*}}{(k_2+k_1^*)} & \frac{e^{\eta_2+\eta_2^*}}{(k_2+k_2^*)} & \frac{e^{\eta_2+\eta_1^*}}{(k_2+k_1^*)} & \frac{e^{\eta_2+\eta_2^*}}{(k_2+k_2^*)} \end{pmatrix}, \tag{3.13a}$$

$$\phi = \begin{pmatrix} e^{\eta_1} & e^{\eta_2} & e^{\eta_1} & e^{\eta_2} \end{pmatrix}^T, \tag{3.13b}$$

$$B = \begin{pmatrix} \frac{a\alpha_1^{(1)}\alpha_1^{(1)*}}{(k_1+k_1^*)} & \frac{a\alpha_2^{(1)}\alpha_1^{(1)*}}{(k_2+k_1^*)} & \frac{b^*\alpha_1^{(2)}\alpha_1^{(1)*}}{(k_1+k_1^*)} & \frac{b^*\alpha_2^{(2)}\alpha_1^{(1)*}}{(k_2+k_1^*)} \\ \frac{a\alpha_1^{(1)}\alpha_2^{(1)*}}{(k_1+k_2^*)} & \frac{a\alpha_2^{(1)}\alpha_2^{(1)*}}{(k_2+k_2^*)} & \frac{b^*\alpha_1^{(2)}\alpha_2^{(1)*}}{(k_1+k_2^*)} & \frac{b^*\alpha_2^{(2)}\alpha_2^{(1)*}}{(k_2+k_2^*)} \\ \frac{b\alpha_1^{(1)}\alpha_1^{(2)*}}{(k_1+k_1^*)} & \frac{b\alpha_2^{(1)}\alpha_1^{(2)*}}{(k_2+k_1^*)} & \frac{c\alpha_1^{(2)}\alpha_1^{(2)*}}{(k_1+k_1^*)} & \frac{c\alpha_2^{(2)}\alpha_1^{(2)*}}{(k_2+k_1^*)} \\ \frac{b\alpha_1^{(1)}\alpha_2^{(2)*}}{(k_1+k_2^*)} & \frac{b\alpha_2^{(1)}\alpha_2^{(2)*}}{(k_2+k_2^*)} & \frac{c\alpha_1^{(2)}\alpha_2^{(2)*}}{(k_1+k_2^*)} & \frac{c\alpha_2^{(2)}\alpha_2^{(2)*}}{(k_2+k_2^*)} \end{pmatrix}. \tag{3.13c}$$

The above solution contains only six complex parameters, k_j, $\alpha_1^{(j)}$, $\alpha_2^{(j)}$, $j = 1, 2$. Obviously, it is less general than the nondegenerate two-soliton solution (3.10a)-(3.10c) given above.

3.2.3 Nondegenerate N-soliton solution

By generalizing the procedure given above along with the more general form of seed solutions,

$$g_1^{(1)} = \sum_{j=1}^{N} \alpha_j^{(1)} e^{\eta_j}, \quad g_1^{(2)} = \sum_{j=1}^{N} \alpha_j^{(2)} e^{\xi_j}, \tag{3.14}$$

where $\eta_j = k_j x + ik_j^2 t$, $\xi_j = l_j x + il_j^2 t$, $j = 1, 2, ..., N$, we arrive the nondegenerate N-soliton solution of the GCNLS system (3.1). The following general forms of matrices A, B, I, ϕ and C_s, $s = 1, 2$, which are defined below, constitute the N-soliton solution. They are defined as follows:

$$A = \begin{pmatrix} A_{mm'} & A_{mn} \\ A_{nm} & A_{nn'} \end{pmatrix}, \; B = \begin{pmatrix} K_{mm'} & K_{mn} \\ K_{nm} & K_{nn'} \end{pmatrix}, \; m, m', n, n' = 1, 2, ..., N, \quad (3.15)$$

$$\phi = \begin{pmatrix} e^{\eta_1} & e^{\eta_2} & . & . & e^{\eta_N} & e^{\xi_1} & e^{\xi_2} & . & . & e^{\xi_N} \end{pmatrix}^T,$$

$$C_1 = -\begin{pmatrix} \alpha_1^{(1)} & \alpha_2^{(1)} & . & . & \alpha_N^{(1)} & 0 & 0 & . & . & 0 \end{pmatrix},$$

$$C_2 = -\begin{pmatrix} 0 & 0 & . & . & 0 & \alpha_1^{(2)} & \alpha_2^{(2)} & . & . & \alpha_N^{(2)} \end{pmatrix}, \; \mathbf{0} = \begin{pmatrix} 0 & 0 & . & . & . & 0 \end{pmatrix},$$

where

$$A_{mm'} = \frac{e^{\eta_m + \eta_{m'}^*}}{(k_m + k_{m'}^*)}, \; A_{mn} = \frac{e^{\eta_m + \xi_n^*}}{(k_m + l_n^*)}, \; A_{nn'} = \frac{e^{\xi_n + \xi_{n'}^*}}{(l_n + l_{n'}^*)}, \; A_{nm} = \frac{e^{\eta_n^* + \xi_m}}{(k_n^* + l_m)},$$

$$K_{mm'} = \frac{a\alpha_m^{(1)*}\alpha_{m'}^{(1)}}{(k_m + k_{m'}^*)}, \; K_{mn} = \frac{b^*\alpha_m^{(1)*}\alpha_n^{(2)}}{(k_m^* + l_n)}, \; K_{nn'} = \frac{c\alpha_n^{(2)*}\alpha_{n'}^{(2)}}{(l_n + l_{n'}^*)}, \; K_{nm} = \frac{b\alpha_n^{(2)*}\alpha_m^{(1)}}{(k_n + l_m^*)},$$

and I is a $(N \times N)$ identity matrix. The resultant N-soliton solution contains $4N$-complex parameters, k_j, l_j, $\alpha_1^{(j)}$, and $\alpha_2^{(j)}$, $j = 1, 2, ..., N$.

3.3 Collision dynamics of nondegenerate solitons

We find that the nondegenerate solitons of the GCNLS system (3.1) display interesting collision properties depending on the strength of the FWM effect along with further choices of the velocity conditions. We observe that they exhibit two types of collision scenarios, namely novel shape changing collision and mere shape preserving or shape altering collision for equal velocities $k_{1I} = l_{1I}$, $k_{2I} = l_{2I}$. The novel shape changing collision essentially occurs among two nondegenerate breathing soliton states when the

FWM effect is strong. However, for low strengths of FWM effect we encounter a mere shape preserving collision. To explain these collision properties we again perform appropriate asymptotic analysis, as we have done earlier for the Manakov case. Such interesting collision properties can be analyzed by obtaining the asymptotic forms from the two-soliton solution (3.10a)-(3.10c).

To do so, we consider the parametric choices $k_{jR}, l_{jR} > 0$, $j = 1, 2$, $k_{1I} > k_{2I}$, $l_{1I} > l_{2I}$, $k_{1I} = l_{1I}$ and $k_{2I} = l_{2I}$, which correspond to the case of a head-on collision between the two breathing nondegenerate solitons. In this situation these two breathing solitons S_1 and S_2 are well separated and subsequently the asymptotic forms of the individual solitons can be deduced from the solution (3.10a)-(3.10c) by incorporating the asymptotic nature of the wave variables $\eta_{jR} = k_{jR}(t - 2k_{jI}z)$ and $\xi_{jR} = l_{jR}(t - 2l_{jI}z)$, $j = 1, 2$, in it. The wave variables η_{jR} and ξ_{jR} behave asymptotically as (i) Soliton 1 (S_1): η_{1R}, $\xi_{1R} \simeq 0$, η_{2R}, $\xi_{2R} \to \mp\infty$ as $z \mp \infty$ and (ii) Soliton 2 (S_2): η_{2R}, $\xi_{2R} \simeq 0$, η_{1R}, $\xi_{1R} \to \mp\infty$ as $z \pm \infty$. Correspondingly these results lead to the asymptotic forms of nondegenerate individual solitons as given below.

(a) Before collision: $z \to -\infty$

Soliton 1: In this limit, the asymptotic forms of breathing nondegenerate soliton states are deduced from the two soliton solution (3.10a)-(3.10c) as below:

$$q_1 = \frac{1}{D_1^-}\left(c_{11}^{1-} e^{i\eta_{1I}} \cosh(\xi_{1R} + \phi_1^{1-}) + c_{21}^{1-} e^{i\xi_{1I}}[\cosh\eta_{1R} + \sinh\eta_{1R}]\right), \quad (3.16)$$

$$q_2 = \frac{1}{D_1^-}\left(c_{12}^{1-} e^{i\xi_{1I}} \cosh(\eta_{1R} + \phi_2^{1-}) + c_{22}^{1-} e^{i\eta_{1I}}[\cosh\xi_{1R} + \sinh\xi_{1R}]\right), \quad (3.17)$$

$$\begin{aligned} D_1^- = {} & \Lambda_1^{1-}\cosh(\eta_{1R} + \xi_{1R} + \phi_3^{1-}) + \Lambda_2^{1-}\cosh(\eta_{1R} - \xi_{1R} + \phi_4^{1-}) \\ & + \Lambda_3^{1-}[\cosh\phi_5^{1-}\cos(\eta_{1I} - \xi_{1I}) + i\sinh\phi_5^{1-}\sin(\eta_{1I} - \xi_{1I})]. \end{aligned}$$

In the above, $\phi_1^{1-} = \frac{1}{2}\log\frac{c(k_1-l_1)|\alpha_1^{(2)}|^2}{(l_1+l_1^*)^2(k_1+l_1^*)}$, $\phi_2^{1-} = \frac{1}{2}\log\frac{a(l_1-k_1)|\alpha_1^{(1)}|^2}{(k_1+k_1^*)^2(k_1^*+l_1)}$, $\phi_3^{1-} =$

$\phi_1^{1-}+\phi_2^{1-}+\frac{1}{2}\log\frac{(k_1^*-l_1^*)\left[ac|k_1+l_1^*|^2-|b|^2(k_1+k_1^*)(l_1+l_1^*)\right]}{ac(l_1-k_1)|k_1+l_1^*|^2}$, $\phi_4^{1-}=\frac{1}{2}\log\frac{a|\alpha_1^{(1)}|^2(l_1+l_1^*)^2}{c|\alpha_1^{(2)}|^2(k_1+k_1^*)^2}$,
$\phi_5^{1-}=\frac{1}{2}\log\frac{b\alpha_1^{(1)}\alpha_1^{(2)*}(k_1^*+l_1)^2}{b^*\alpha_1^{(1)*}\alpha_1^{(2)}(k_1+l_1^*)^2}$, $c_{11}^{1-}=[\frac{c|\alpha_1^{(2)}|^2(k_1-l_1)}{(k_1+l_1^*)(l_1+l_1^*)}]^{1/2}$, $c_{21}^{1-}=\frac{1}{2}[\frac{b^*\alpha_1^{(2)}|\alpha_1^{(1)}|^2(k_1-l_1)}{(k_1+k_1^*)(k_1^*+l_1)^2}]$,
$c_{12}^{1-}=[\frac{a\alpha_1^{(2)}|\alpha_1^{(1)}|^2(l_1-k_1)}{(k_1^*+l_1)(k_1+k_1^*)}]^{1/2}$, $c_{22}^{1-}=\frac{1}{2}[\frac{b\alpha_1^{(1)}|\alpha_1^{(2)}|^2(l_1-k_1)}{(k_1+l_1^*)^2(l_1+l_1^*)}]$, $\Lambda_2^{1-}=\lambda_1=[\frac{ac|\alpha_1^{(1)}|^2|\alpha_1^{(2)}|^2}{(k_1+k_1^*)(l_1+l_1^*)}]$,
$\Lambda_1^{1-}=\frac{\lambda_1|k_1-l_1|[ac|k_1+l_1^*|^2-|b|^2(k_1+k_1^*)(l_1+l_1^*)]^{1/2}}{(ac)^{1/2}|k_1+l_1^*|^2}$, and $\Lambda_3^{1-}=\frac{|b||\alpha_1^{(1)}||\alpha_1^{(2)}|}{|k_1+l_1^*|^2}$.

Soliton 2: In this limit, the asymptotic forms of q_1 and q_2 are deduced from the two soliton solution (3.10a)-(3.10c) for soliton 2 as below:

$$q_1=\frac{1}{D_2^-}\left(c_{11}^{2-}e^{i\eta_{2I}}\cosh(\xi_{2R}+\phi_1^{2-})+c_{21}^{2-}e^{i\xi_{2I}}\cosh(\eta_{2R}+\phi_2^{2-})\right), \quad (3.18)$$

$$q_2=\frac{1}{D_2^-}\left(c_{22}^{2-}e^{i\xi_{2I}}\cosh(\eta_{2R}+\phi_7^{2-})+c_{12}^{2-}e^{i\eta_{2I}}\cosh(\xi_{2R}+\phi_6^{2-})\right), \quad (3.19)$$

$$\begin{aligned}D_2^-=&\Lambda_1^{2-}\cosh(\eta_{2R}+\xi_{2R}+\phi_3^{2-})+\Lambda_2^{2-}\cosh(\eta_{2R}-\xi_{2R}+\phi_4^{2-})\\&+\Lambda_3^{2-}[\cosh\phi_5^{2-}\cos(\eta_{2I}-\xi_{2I})+i\sinh\phi_5^{2-}\sin(\eta_{2I}-\xi_{2I})].\end{aligned}$$

Here,
$\phi_1^{2-}=\frac{1}{2}\log\frac{c|k_1-l_2|^2(k_2-l_2)|l_1-l_2|^4|\alpha_2^{(2)}|^2\left[ac|k_1+l_1^*|^2(k_2+l_1^*)|k_1+l_2^*|^2(k_2+l_2^*)-|b|^2(k_1+k_1^*)(k_1^*+k_2)\right]}{|k_1+l_2^*|^4(l_1^*+l_2)^2(k_2+l_2^*)^2(l_1+l_2^*)^2(l_2+l_2^*)^2\left[ac|k_1+l_1^*|^2(k_2+l_1^*)-|b|^2(k_1+k_1^*)(k_1^*+k_2)(l_1+l_1^*)\right]}$,
$\phi_2^{2-}=\frac{1}{2}\log\frac{|k_1-k_2|^4|k_2-l_1|^2(k_2-l_2)\left[|b|^2(k_1+k_1^*)|k_1+k_2^*|^2(k_2+k_2^*)(l_1+l_1^*)(l_1^*+l_2)-ac(k_1+l_1^*)(k_2+l_1^*)\right]}{ac(l_2-k_2)|k_1+k_2^*|^4(k_2^*+l_2)|k_2+l_1^*|^4}$,
$\phi_3^{2-}=\phi_1^{2-}+\phi_2^{2-}+d_1^-$, $d_1^-=\frac{1}{2}\log\frac{(k_2^*-l_2^*)\lambda_2}{ac(l_2-k_2)\lambda_3}$, $\lambda_3=\left[ac|k_1+l_1^*|^2|k_2+l_1^*|^2(k_1^*+l_2)(k_2^*+l_2)-|b|^2(l_1+l_1^*)(l_1^*+l_2)\right]\left[ac|k_1+l_1^*|^2(k_2+l_1^*)|k_1+l_2^*|^2(k_2+l_2^*)-|b|^2(k_1+k_1^*)(k_1^*+k_2)\right]$, $\lambda_2=\left[ac|k_1+l_1^*|^2(k_2+l_1^*)-|b|^2(k_1+k_1^*)(k_1^*+k_2)(l_1+l_1^*)\right]\left[ac(k_1^*+l_2)|k_1+l_1^*|^2-|b|^2(k_1+k_1^*)(l_1+l_1^*)(l_1^*+l_2)\right]\left[|b|^4(k_1+k_1^*)|k_1+k_2^*|^2(k_2+k_2^*)(l_1+l_1^*)|l_1+l_2^*|^2(l_2+l_2^*)+a^2c^2|k_1+l_1^*|^2|k_2+l_1^*|^2|k_2+l_2^*|^2-ac|b|^2\right]$, $\phi_4^{2-}=\phi_2^{2-}-\phi_1^{2-}+d_2^-$, $d_2^-=\frac{1}{2}\log\frac{(k_2-l_2)\lambda_4(k_2^*+l_2)^2}{(l_2-k_2)\lambda_5}$, $\lambda_4=\left[ac|k_1+l_1^*|^2|k_2+l_1^*|^2-|b|^2(l_1+l_1^*)\right]\left[ac|k_1+l_1^*|^2(k_1^*+l_2)-|b|^2(k_1+k_1^*)(l_1+l_1^*)(l_1^*+l_2)\right]\left[ac|k_1+l_1^*|^2(k_2+l_1^*)|k_1+l_2^*|^2(k_2+l_2^*)-|b|^2(k_1+k_1^*)(k_1^*+k_2)\right]$,
$\lambda_5=\left[ac|k_1+l_1^*|^2|k_1+l_2^*|^2-|b|^2(k_1+k_1^*)\right]\left[ac|k_1+l_1^*|^2(k_2+l_1^*)-|b|^2(k_1+k_1^*)(k_1^*+k_2)(l_1+l_1^*)\right]$, $\phi_5^{2-}=\frac{b(k_1-k_2)^2(k_2-l_1)(k_1^*-l_2^*)(l_1-l_2)^2(k_1+k_2^*)^2(k_2^*+l_1)^2\lambda_6}{b^*(k_1^*-k_2^*)^2(k_2^*-l_1^*)(k_1-l_2)(l_1-l_2)^2\lambda_7}$, $\lambda_6=(k_1^*+l_2)^2(k_2^*+l_2)^2(l_1^*+l_2)^2\left[|b|^2(k_1+k_1^*)(k_1^*+k_2)(l_1+l_1^*)(l_1^*+l_2)-ac(k_1^*+l_1)\right]$, $\lambda_7=\left[|b|^2(k_1+k_1^*)(k_1+k_2^*)(l_1+l_1^*)(l_1^*+l_2)-ac(k_1+l_1^*)\right]$, $\phi_6^{2-}=$

$\frac{1}{2}\log\frac{a(l_2-k_2)|\alpha_2^{(1)}|^2|k_1-k_2|^4|k_2-l_1|^2\lambda_8}{(k_2^*+l_2)(k_2+k_2^*)^2|k_1+k_2^*|^4|k_2+l_1^*|^4(k_2^*+l_2)\lambda_8}$, $\lambda_7=\big[ac|k_1+l_1^*|^2|k_2+l_1^*|^2(k_1^*+l_2)(k_2^*+l_2)-|b|^2(l_1+l_1^*)(l_1^*+l_2)\big]$, $\lambda_8=\big[ac|k_1+l_1^*|^2(k_1^*+l_2)-|b|^2(k_1+k_1^*)(l_1+l_1^*)(l_1^*+l_2)\big]$, $\phi_7^{2-}=\frac{1}{2}\log\frac{c(k_2-l_2)|\alpha_2^{(1)}|^2|(k_1-l_2)|^2|l_1-l_2|^4\lambda_9}{ac(k_2+l_2^*)(k_2+k_2^*)^2(k_1^*+l_1)(l_1+l_1^*)\lambda_{10}}$, $\lambda_9=\big[|b|^2(k_1+k_1^*)(k_1^*+k_2)(l_1+l_1^*)|l_1+l_2^*|^2(l_2+l_2^*)-ac(k_1^*+l_1)(k_1^*+l_2)\big]$, $\lambda_{10}=(k_1^*+l_2)^2)(k_1+l_2^*)^2|l_1+l_2^*|^4(l_2+l_2^*)^2(k_1^*-l_1^*)(k_2+l_2^*)$,

$c_{11}^{2-}=\frac{c(k_1-k_2)^2(k_2-l_1)|k_1-l_2||l_1-l_2|^2(k_2-l_2)^{\frac{1}{2}}|\alpha_1^{(1)}|^2|\alpha_1^{(2)}|^2|\alpha_2^{(2)}|\alpha_2^{(1)}|k_1-l_1|^2\lambda_{11}}{(k_1+k_1^*)^2(k_2+k_1^*)^2|k_1+l_1^*|^4(k_2+l_1^*)^2(l_1+l_1^*)^2|k_1+l_2^*|^2|l_1+l_2^*|^2(k_2+l_2^*)(l_2+l_2^*)}$, $\lambda_{11}=\big[ac|k_1+l_1^*|^2(k_2+l_1^*)-|b|^2(k_1+k_1^*)(k_1^*+k_2)(l_1+l_1^*)\big]^{\frac{1}{2}}\big[ac|k_1+l_1^*|^2(k_2+l_1^*)|k_1+l_2^*|^2(k_2+l_2^*)-|b|^2(k_1+k_1^*)(k_1^*+k_2)\big]$,

$c_{21}^{2-}=\frac{b^*c|k_1-k_2|^2|k_1-l_1|^2|k_2-l_1|(k_1-l_2)(k_2-l_2)(l_1-l_2)^2|\alpha_1^{(1)}|^2|\alpha_1^{(2)}|^2|\alpha_2^{(1)}|\alpha_2^{(2)}\lambda_{12}}{(k_1+k_1^*)|k_1+k_2^*|^2(k_1^*+l_1)^2(k_1+l_1^*)(k_2+k_2^*)|k_2+l_1^*|^2(l_1+l_1^*)^2(k_1^*+l_2)^2(k_2^*+l_2)(l_1^*+l_2)^2}$, $\lambda_{12}=\big[|b|^2(k_1+k_1^*)|k_1^*+k_2|^2(k_2+k_2^*)(l_1+l_1^*)(l_1^*+l_2)-ac(k_1+l_1^*)(k_2+l_1^*)\big]^{\frac{1}{2}}$,

$c_{12}^{2-}=\frac{ab(k_1-k_2)^2|k_1-l_1|^2(k_1^*-l_1^*)(k_2-l_1)|k_1-l_2|(k_2-l_2)|l_1-l_2|^2|\alpha_1^{(1)}|^2|\alpha_1^{(2)}|^2\alpha_2^{(1)}|\alpha_2^{(2)}|\lambda_{13}}{(k_1+k_1^*)^2(k_1^*+k_2)^2(k_1^*+l_1)(k_1+l_1^*)^2(k_2+l_1^*)^2(l_1+l_1^*)|k_1+l_2^*|^2|l_1+l_2^*|^2(k_2+k_2^*)(l_2+l_2^*)}$, $\lambda_{13}=\big[|b|^2(k_1+k_1^*)(k_1^*+k_2)(l_1+l_1^*)|l_1+l_2^*|^2(l_2+l_2^*)-ac(k_1^*+l_1)(k_1^*+l_2)\big]^{\frac{1}{2}}$, $c_{22}^{2-}=\frac{a|k_1-k_2|^2|k_1-l_2|^2|k_2-l_1|(k_1-l_2)(k_2-l_2)(l_1-l_2)^2|\alpha_1^{(1)}|^2|\alpha_1^{(2)}|^2|\alpha_2^{(1)}|\alpha_2^{(2)}\lambda_{14}}{(k_1+k_1^*)^2|k_1+k_2^*|^2|k_1+l_1^*|^4(l_1+l_1^*)^2(k_1^*+l_2)^2(k_2+k_2^*)(l_1^*+l_2)^2|k_2+l_1^*|^2(k_2^*+l_2)}$, $\lambda_{14}=\big[|b|^2(k_1+k_1^*)(l_1+l_1^*)(l_1^*+l_2)-ac|k_1+l_1^*|^2(k_1^*+l_2)\big]\big[ac|k_1+l_1^*|^2|k_2+l_1^*|^2(k_1^*+l_2)(k_2^*+l_2)-|b|^2(l_1+l_1^*)(l_1^*+l_2)\big]$.

(b) After collision: $z\to+\infty$

Soliton 1: In this limit, the asymptotic forms of q_1 and q_2 are deduced from the two soliton solution (3.10a)-(3.10c) for soliton 1 as below:

$$q_1=\frac{1}{D_1^+}\Big(c_{11}^{1+}e^{i\eta_{1I}}\cosh(\xi_{1R}+\phi_1^{1+})+c_{21}^{1+}e^{i\xi_{1I}}\cosh(\eta_{1R}+\phi_2^{1+})\Big),\quad(3.20)$$

$$q_2=\frac{1}{D_1^+}\Big(c_{12}^{1+}e^{i\eta_{1I}}\cosh(\xi_{1R}+\phi_6^{1+})+c_{22}^{1+}e^{i\xi_{1I}}\cosh(\eta_{1R}+\phi_7^{1+})\Big),\quad(3.21)$$

$$D_1^+=\Lambda_1^{1+}\cosh(\eta_{1R}+\xi_{1R}+\phi_3^{1+})+\Lambda_2^{1+}\cosh(\eta_{1R}-\xi_{1R}+\phi_4^{1+})+\Lambda_3^{1+}[\cosh\phi_5^{1+}\cos(\eta_{1I}-\xi_{1I})+i\sinh\phi_5^{1+}\sin(\eta_{1I}-\xi_{1I})].$$

$\phi_1^{1+}=\frac{1}{2}\log\frac{c(k_1-l_1)|k_2-l_1|^2|l_1-l_2|^4|\alpha_1^{(2)}|^2\Delta_1}{(k_1+l_1^*)^2|k_2+l_1^*|^4(l_1+l_1^*)^2|l_1+l_2^*|^4\Delta_2}$, $\Delta_1=\big[ac|k_2+l_1^*|^2(k_1+l_1^*)|k_2+l_2^*|^2(k_1+l_2^*)-|b|^2(k_1+k_2^*)(k_2+k_2^*)\big]$, $\Delta_2=\big[ac|k_2+l_2^*|^2(k_1+l_2^*)-|b|^2(k_1+$

$k_2^*)(k_2+k_2^*)(l_2+l_2^*)\big]$, $\phi_2^{1+}=\frac{1}{2}\log\frac{||^4(k_1-l_1)|k_1-l_2|^2|\alpha_1^{(1)}|^2\Delta_3}{c(k_1+k_1^*)^2|k_1+k_2^*|^4(k_2+k_2^*)(k_1^*+l_1)^2|k_1^*+l_2|^4|(k_2+l_2^*)|^2}$,
$\Delta_3=\big[|b|^2(k_1+k_1^*)|k_1+k_2^*|^2(k_2+k_2^*)(l_1+l_2^*)(l_2+l_2^*)-ac(k_1+l_2^*)(k_2+$
$l_2^*)\big]$, $\phi_3^{1+}=\phi_1^{1+}+\phi_2^{1+}+c_1^+$, $c_1^+=\frac{\Delta_4\left[ac|k_2+l_2^*|^2(k_1+l_2^*)-|b|^2(k_1+k_2^*)(k_2+k_2^*)(l_2+l_2^*)\right]}{ac\Delta_5|k_2+l_1^*|^2(k_1+l_1^*)|k_2+l_2^*|^2(k_1+l_2^*)-|b|^2(k_1+k_2^*)(k_2+k_2^*)}$,
$\Delta_4=\big[ac(k_2^*+l_1)|k_2+l_2^*|^2-|b|^2(k_2+l_2^*)(l_1+l_2^*)(l_2+l_2^*)\big]$, $\Delta_5=\big[ac(k_1^*+$
$l_1)(k_2^*+l_1)|k_1+l_2^*|^2|k_2+l_2^*|^2-|b|^2(l_1+l_2^*)(l_2+l_2^*)\big]$, $\phi_4^{1+}=\phi_2^{1+}-\phi_1^{1+}+c_2^+$,
$c_2^+=\frac{1}{2}\log\frac{\left[ac|k_1+l_2^*|^2|k_2+l_2^*|^2-|b|^2(l_2+l_2^*)\right]\Delta_6}{\Delta_7\left[ac|k_2+l_1^*|^2|k_2+l_2^*|^2-|b|^2\right]}$, $\Delta_6=\big[ac(k_2^*+l_1)(k_2^*+l_2)(k_2+$
$l_2^*)-|b|^2(k_2+k_2^*)(l_1+l_2^*)(l_2+l_2^*)\big]\big[ac|k_2+l_2^*|^2(k_1+l_2^*)-|b|^2(l_2+l_2^*)(k_1+$
$k_2^*)(k_2+k_2^*)\big]$, $\Delta_7=\big[ac(k_1^*+l_1)(k_2^*+l_1)|k_1^*+l_2|^2|k_2^*+l_2|^2-|b|^2(l_1+l_2^*)(l_2+$
$l_2^*)\big]\big[ac|k_2+l_1^*|^2|k_2+l_2^*|^2(k_1+l_1^*)(k_1+l_2^*)-|b|^2(k_1+k_2^*)(k_2+k_2^*)\big]$, $\phi_5^{1+}=$
$\frac{1}{2}\log\frac{b(k_1-k_2)^2(k_2^*-l_1^*)(k_1-l_2)(l_1^*-l_2^*)^2\alpha_1^{(1)}\alpha_1^{(2)*}\Delta_8}{b^*(k_1^*-k_2^*)^2(k_2-l_1)(k_1^*-l_2^*)(l_1-l_2)^2\alpha_1^{(1)*}\alpha_1^{(2)}\Delta_9}$, $\Delta_8=\big[|b|^2(k_1+k_2^*)(k_2+k_2^*)(l_1^*+$
$l_2)(l_2+l_2^*)-ac(k_2^*+l_2)\big](k_1^*+k_2)^2(k_1^*+l_1)^2(k_2^*+l_1)^2$, $\Delta_9=\big[|b|^2(k_1^*+k_2)(k_2^*+$
$k_2)(l_1^*+l_2)(l_2^*+l_2)-ac(k_2+l_2^*)\big](k_1+k_2^*)^2(k_1+l_1^*)^2(k_2+l_1^*)^2$,
$\phi_6^{1+}=\frac{1}{2}\log\frac{a|k_1-k_2|^4(k_1-l_1)|k_1-l_2|^2|\alpha_1^{(1)}|^2\Delta_{11}}{(k_1+k_1^*)^2|k_1+k_2^*|^4(k_1^*+l_1)^2(k_1^*+l_2)^2(k_1+l_2^*)^2\Delta_{12}}$, $\Delta_{11}=\big[ac(k_1^*+l_1)(k_2^*+$
$l_1)|k_1^*+l_2|^2|k_2+l_2^*|^2-|b|^2(l_1+l_2^*)(l_2+l_2^*)\big]$, $\Delta_{12}=\big[ac(k_2^*+l_1)|k_2^*+l_2|^2-$
$|b|^2(k_2+l_2^*)(l_1+l_2^*)(l_2+l_2^*)\big]$, $\phi_7^{1+}=\frac{1}{2}\log\frac{(k_1-l_1)|k_2-l_1|^2|l_1-l_2|^4(k_2^*-l_2^*)|\alpha_1^{(2)}|^2\Delta_{13}}{(k_1+l_1^*)^2|k_2+l_1^*|^4(l_1+l_1^*)^2(k_2^*+l_2)(l_2+l_2^*)\Delta_{14}}$
$\Delta_{14}=a(k_1^*-k_2^*)^2|l_1+l_2^*|^4$,
$c_{11}^{1+}=\frac{c(k_1-k_2)^2(k_1-l_2)(k_1-l_1)|k_2-l_2|^2|k_2-l_1||l_1-l_2|^2\alpha_1^{(1)}|\alpha_1^{(2)}||\alpha_2^{(1)}|^2|\alpha_2^{(2)}|^2\Delta_{15}}{(k_1+k_2^*)^2(k_2+k_2^*)^2(k_2^*+l_2)^2(k_1+l_2^*)^2(l_1+l_2^*)^2(l_2+l_2^*)^2(k_2^*+l_1)(k_1+l_1^*)(k_2+l_1^*)(l_1+l_1^*)|l_1+l_2^*|^2}$,
$\Delta_{15}=\big[ac|k_2+l_2^*|^2(k_1+l_2^*)-|b|^2(k_1+k_2^*)(k_2+k_2^*)(l_2+l_2^*)\big]\big[ac|k_2+l_1^*|^2(k_1+$
$l_1^*)(k_2^*+l_2)(k_1+l_2^*)(k_2+l_2^*)-|b|^2(k_1+k_2^*)(k_2+k_2^*)\big]$,
$c_{21}^{1+}=\frac{b^*c|k_1-k_2|^2(k_1-l_1)(k_2-l_1)(k_2-l_2)(k_1-l_2)(l_1-l_2)^2(k_1^*-l_2^*)(k_2^*-l_2^*)|\alpha_1^{(1)}|\alpha_1^{(2)}|\alpha_2^{(1)}|^2|\alpha_2^{(2)}|^2\Delta_{15}}{(k_1+k_1^*)|k_1+k_2^*|^2(k_2+k_2^*)(k_2^*+l_1)^2(k_1^*+l_1)|k_1+l_2^*|^2(k_2^*+l_2)^2(k_2+l_2^*)(l_1+l_2^*)^2(l_2+l_2^*)^2}$,
$\Delta_{16}=\big[|b|^2(k_1+k_1^*)|k_1+k_2^*|^2(k_2+k_2^*)(l_1+l_2^*)(l_2+l_2^*)-ac(k_1+l_2^*)(k_2+$
$l_2^*)\big]$, $c_{12}^{1+}=\frac{ab(k_1-k_2)^2(k_1-l_1)|k_2-l_1|(k_1-l_2)|k_2-l_2|^2|l_1-l_2|^2(k_2^*-l_2^*)\alpha_1^{(1)}|\alpha_1^{(2)}||\alpha_1^{(1)}|^2|\alpha_2^{(2)}|^2\Delta_{17}}{(k_1+k_2^*)^2(k_2+k_2^*)^2|k_2^*+l_1|^2(k_1+l_1^*)(l_1+l_1^*)(k_2^*+l_2)|l_1+l_2^*|^2(k_2+l_2^*)^2(l_2+l_2^*)^2(k_1+l_2^*)^2}$,
$\Delta_{17}=\big[|b|^2(k_1+k_2^*)(k_2+k_2^*)(l_1+l_1^*)|l_1^*+l_2|^2(l_2+l_2^*)-ac(k_2^*+l_1)(k_2^*+l_2)\big]$,
$c_{22}^{1+}=\frac{a|k_1-k_2|^2(k_1-l_1)(k_2-l_1)|k_1-l_2|(k_2-l_2)(l_1-l_2)^2|\alpha_1^{(1)}||\alpha_1^{(2)}||\alpha_2^{(1)}|^2|\alpha_2^{(2)}|^2\Delta_{18}}{(k_1+k_1^*)|k_1+k_2^*|^2(k_2+k_2^*)^2(k_1^*+l_1)(k_2^*+l_1)^2|k_1+l_2^*|^2|k_2+l_2^*|^4(l_1+l_2^*)^2(l_2+l_2^*)^2}$, $\Delta_{18}=\big[ac(k_2^*+$
$l_1)|k_2+l_2^*|^2-|b|^2(k_2+k_2^*)(l_1+l_2^*)(l_2+l_2^*)\big]\big[ac(k_1^*+l_1)(k_2^*+l_1)(k_1^*+l_2)(k_2^*+$
$l_2)(k_1+l_2^*)(k_2+l_2^*)-|b|^2(l_1+l_2^*)(l_2+l_2^*)\big]$.

Soliton 2: In this limit, the asymptotic forms of q_1 and q_2 are deduced from the two soliton solution (3.10a)-(3.10c) for soliton 2 as below:

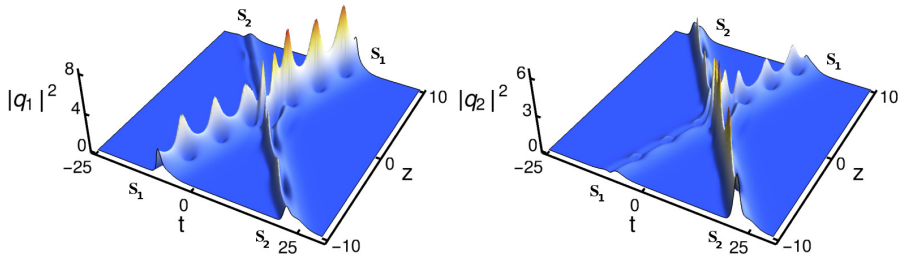

FIGURE 3.7: Interaction between two breathing nondegenerate soliton states is demonstrated by fixing the parameter values as $a = c = 1$, $b = 0.6 + 0.6i$, $k_1 = 1.5 + 0.5i$, $l_1 = 0.45 + 0.5i$, $k_2 = 0.5 - i$, $l_2 = 1.3 - i$, $\alpha_1^{(1)} = 0.55$, $\alpha_2^{(1)} = 0.5 + 0.5i$, $\alpha_1^{(2)} = 0.45 + 0.45i$, and $\alpha_2^{(2)} = 1 + i$.

$$q_1 = \frac{1}{D_2^+}\left(c_{11}^{1+}e^{i\eta_{2I}}\cosh(\xi_{2R}+\phi_1^{2+}) + c_{21}^{2+}e^{i\xi_{2I}}[\cosh\eta_{2R}+\sinh\eta_{2R}]\right), \quad (3.22)$$

$$q_2 = \frac{1}{D_2^+}\left(c_{12}^{2+}e^{i\xi_{2I}}\cosh(\eta_{2R}+\phi_2^{2+}) + c_{22}^{2+}e^{i\eta_{2I}}[\cosh\xi_{2R}+\sinh\xi_{2R}]\right), \quad (3.23)$$

$$D_2^+ = \Lambda_1^{2+}\cosh(\eta_{2R}+\xi_{2R}+\phi_3^{2+}) + \Lambda_2^{2+}\cosh(\eta_{2R}-\xi_{2R}+\phi_4^{2+})$$
$$+\Lambda_3^{2+}[\cosh\phi_5^{2+}\cos(\eta_{2I}-\xi_{2I}) + i\sinh\phi_5^{2+}\sin(\eta_{2I}-\xi_{2I})].$$

In the above, $\phi_1^{2+} = \frac{1}{2}\log\frac{c(k_2-l_2)|\alpha_2^{(2)}|^2}{(l_2+l_2^*)^2(k_2+l_2^*)}$, $\phi_2^{2+} = \frac{1}{2}\log\frac{a(l_2-k_2)|\alpha_2^{(1)}|^2}{(k_2+k_2^*)^2(k_2^*+l_2)}$, $\phi_3^{2+} = \phi_1^{2+}+\phi_2^{2+}+\frac{1}{2}\log\frac{(k_2^*-l_2^*)\left[ac|k_2+l_2^*|^2-|b|^2(k_2+k_2^*)(l_2+l_2^*)\right]}{ac(l_2-k_2)|k_2+l_2^*|^2}$, $\phi_4^{2+} = \frac{1}{2}\log\frac{a|\alpha_2^{(1)}|^2(l_2+l_2^*)^2}{c|\alpha_2^{(2)}|^2(k_2+k_2^*)^2}$, $\phi_5^{2+} = \frac{1}{2}\log\frac{b\alpha_2^{(1)}\alpha_2^{(2)*}(k_2^*+l_2)^2}{b^*\alpha_2^{(1)*}\alpha_2^{(2)}(k_2+l_2^*)^2}$, $c_{11}^{2+} = [\frac{c|\alpha_1^{(2)}|^2(k_2-l_2)}{(k_2+l_2^*)(l_2+l_2^*)}]^{1/2}$, $c_{21}^{2+} = \frac{1}{2}[\frac{b^*\alpha_2^{(2)}|\alpha_2^{(1)}|^2(k_2-l_2)}{(k_2+k_2^*)(k_2^*+l_2)^2}]$, $c_{12}^{2+} = [\frac{a\alpha_2^{(2)}|\alpha_2^{(1)}|^2(l_2-k_2)}{(k_2^*+l_2)(k_2+k_2^*)}]^{1/2}$, $c_{22}^{2+} = \frac{1}{2}[\frac{b\alpha_2^{(1)}|\alpha_2^{(2)}|^2(l_2-k_2)}{(k_2+l_2^*)^2(l_2+l_2^*)}]$, $\Lambda_2^{2+} = \lambda_2 = [\frac{ac|\alpha_2^{(1)}|^2|\alpha_2^{(2)}|^2}{(k_2+k_2^*)(l_2+l_2^*)}]$, $\Lambda_1^{2+} = \frac{\lambda_2|k_2-l_2|[ac|k_2+l_2^*|^2-|b|^2(k_2+k_2^*)(l_2+l_2^*)]^{1/2}}{(ac)^{1/2}|k_2+l_2^*|^2}$, and $\Lambda_3^{2+} = \frac{|b||\alpha_2^{(1)}||\alpha_2^{(2)}|}{|k_2+l_2^*|^2}$.

The above analysis clearly indicates that there are definite changes in the asymptotic forms of the nondegenerate solitons. The profile change of a given soliton S_1 (or S_2) during the collision can be confirmed from the changes that occur in both the constants, $c_{jk}^{1\pm}$, $c_{jk}^{2\pm}$, $j,k = 1,2$, and as well as from the phases, $\phi_j^{1\pm}$, $\phi_j^{2\pm}$, $j = 1,2,3,4,5$. This implies that the structures of the nondegenerate solitons are not preserved during the collision

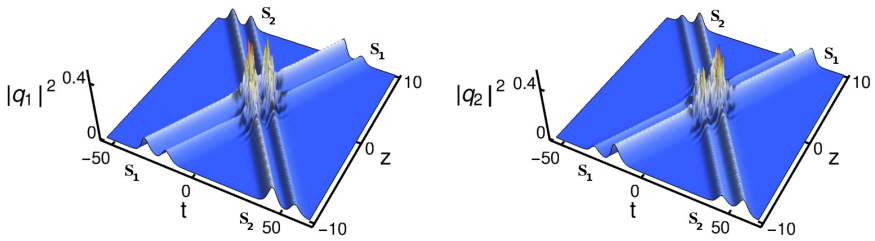

FIGURE 3.8: The collision among the two double-hump solitons is demonstrated for low strength of FWM effect. To draw this figure we fix the parameter values as $a = c = 1$, $b = 0.15 + 0.15i$, $k_1 = 0.333 + 1.5i$, $l_1 = 0.315 + 1.5i$, $k_2 = 0.315 + 2.2i$, $l_2 = 0.333 + 2.2i$, $\alpha_1^{(1)} = 0.6$, $\alpha_2^{(1)} = 0.6$, $\alpha_1^{(2)} = 0.45i$, and $\alpha_2^{(2)} = 0.45i$.

process. However, the period of oscillation, $T_j = \frac{2\pi}{k_{jR}^2 - l_{jR}^2}$, $j = 1, 2$, remains constant during the entire evolution process. A typical shape changing collision is demonstrated in Fig. 3.7. From this figure, we observe that the two breathing nondegenerate solitons are well separated and their structures definitely get drastically varied during the collision. The intensity of breathing nondegenerate soliton, say S_1, is enhanced in both the modes q_1 and q_2 whereas the reverse, that is suppression of intensity, is occurs for soliton S_2. For strong FWM effect, such shape changing collision happens among the two breathing soliton states. It is difficult to calculate transition intensities in order to characterize this shape changing collision. However, a mere shape preserving collision or shape altering collision is observed for low strengths of FWM paramater b. This collision scenario is demonstrated in Fig. 3.8, where the two asymmetric double-hump solitons preserve their structures after collision. In this situation, the phase terms and all the constants do not contribute significantly in the collision dynamics.

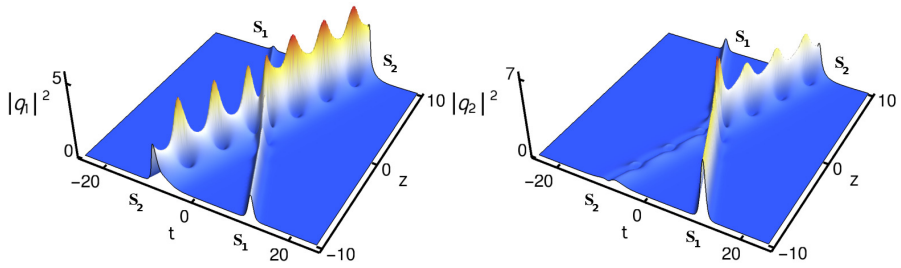

FIGURE 3.9: Degenerate soliton collision induced Type-I shape changing behaviour of the breathing nondegenerate soliton state is illustrated by fixing the parameter values as $a = c = 1$, $b = 0.6 + 0.6i$, $k_1 = 1.5 + 0.5i$, $l_1 = 0.45 + 0.5i$, $k_2 = 1.5 - 0.5i$, $l_2 = 1.5 - 0.5i$, $\alpha_1^{(1)} = 0.55$, $\alpha_2^{(1)} = 0.5 + 0.5i$, $\alpha_1^{(2)} = 0.45 + 0.45i$, and $\alpha_2^{(2)} = 1 + i$.

3.4 Degenerate soliton collision induced shape changing property of nondegenerate soliton

In this section, we discuss the collision between degenerate and nondegenerate solitons admitted by the partially nondegenerate two-soliton solution (3.12a)-(3.12c) of the GCNLS system (3.1) in the partial nondegenerate limit $k_1 = l_1$ and $k_2 \neq l_2$. The following asymptotic analysis ensures that there is a definite energy redistribution occurs among the modes q_1 and q_2. As a consequence, we observe two types of shape changing collisions. We call them as Type-I and Type-II shape changing collisions. In Type-I shape changing collision, the intensity of the nondegenerate soliton S_2 is enhanced in both the modes whereas in Type-II shape changing collision it is reversed. That is the intensity of the nondegenerate soliton S_2 is suppressed in both the components. During these kinds of collisions, the degenerate soliton S_1 loses (or gains) energy to (or from) the nondegenerate soliton. To characterize these collision scenario, we perform suitable asymptotic analysis, as given below, and obtain the asymptotic forms for both the solitons S_1 and S_2. To do so, we incorporate the asymptotic nature of the wave variables $\eta_{jR} = k_{jR}(t - 2k_{Ij}z)$ and $\xi_{2R} = l_{2R}(t - 2l_{2I}z)$, $j = 1, 2$, in the solution (3.12a)-(3.12c). Here also the wave variable η_{1R} corresponds to the degenerate soliton S_1 and η_{2R}, ξ_{2R} correspond to the nondegenerate soliton S_2. In order to find the asymptotic behaviours of

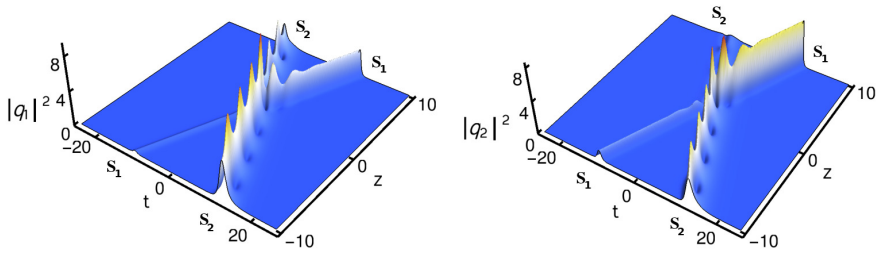

FIGURE 3.10: Degenerate soliton collision induced Type-II shape changing behaviour of the breathing nondegenerate soliton state is illustrated by fixing the parameter values as $a = c = 1$, $b = 0.6 + 0.6i$, $k_1 = 1.5 - 0.5i$, $l_1 = 0.45 - 0.5i$, $k_2 = 1.5 + 0.5i$, $l_2 = 1.5 + 0.5i$, $\alpha_1^{(1)} = 0.55$, $\alpha_2^{(1)} = 0.5 + 0.5i$, $\alpha_1^{(2)} = 0.45 + 0.45i$, and $\alpha_2^{(2)} = 1 + i$.

these wave variables, we consider the parametric choice as $k_{1R}, k_{2R}, l_{2R} > 0$, $k_{1I} > 0$, $k_{2I}, l_{2I} < 0$, $k_{1I} > k_{2I}$, $k_{1I} > l_{2I}$. For this choice, the wave variables behave asymptotically as follws: (i) degenerate soliton S_1: $\eta_{1R} \simeq 0$, $\eta_{2R}, \xi_{2R} \to \mp\infty$ as $z \to \mp\infty$ (ii) nondegenerate soliton S_2: $\eta_{2R}, \xi_{2R} \simeq 0$, $\eta_{1R} \to \pm\infty$ as $z \to \pm\infty$. By incorporating these asymptotic behaviours of wave variables in the solution (3.12a)-(3.12c), we deduce the following asymptotic expressions for both the degenerate and nondegenerate solitons.

(a) Before collision: $z \to -\infty$

Soliton 1: In this limit, the asymptotic form for the degenerate soliton deduced from the partially nondegenerate two soliton solution (3.12a)-(3.12c) is

$$q_j \simeq \begin{pmatrix} A_1^{1-} \\ \\ A_2^{1-} \end{pmatrix} k_{1R} e^{i\eta_{1I}} \mathrm{sech}(\eta_{1R} + \phi^-), \; j = 1, 2, \tag{3.24}$$

where $A_j^{1-} = \alpha_1^{(j)} / (a|\alpha_1^{(1)}|^2 + c|\alpha_1^{(2)}|^2 + b\alpha_1^{(1)}\alpha_1^{(2)*} + b^*\alpha_1^{(1)*}\alpha_1^{(2)})^{1/2}$, $j = 1, 2$, $\phi^- = \frac{1}{2} \ln \frac{(a|\alpha_1^{(1)}|^2 + c|\alpha_1^{(2)}|^2 + b\alpha_1^{(1)}\alpha_1^{(2)*} + b^*\alpha_1^{(1)*}\alpha_1^{(2)})}{(k_1 + k_1^*)^2}$. Here, in A_j^{1-} the superscript $1-$ denotes soliton S_1 before collision and subscript j refers to the

mode number.

Soliton 2: The asymptotic expressions for the nondegenerate soliton S_2 which is present in the two modes before collision are obtained as

$$q_1 = \frac{1}{D}\left(\mu_{11}e^{i\eta_{2I}}\cosh(\xi_{2R}+\varphi_1^{2-}) + \mu_{21}e^{i\xi_{2I}}\cosh(\eta_{2R}+\varphi_2^{2-})\right), \quad (3.25)$$

$$q_2 = \frac{1}{D}\left(\mu_{22}e^{i\xi_{2I}}\cosh(\eta_{2R}+\varphi_7^{2-}) + \mu_{12}e^{i\eta_{2I}}\cosh(\xi_{2R}+\varphi_6^{2-})\right), \quad (3.26)$$

$$D = \lambda_1^{2-}\cosh(\eta_{2R}+\xi_{2R}+\phi_3^{2-}) + \lambda_2^{2-}\cosh(\eta_{2R}-\xi_{2R}+\phi_4^{2-}) + \lambda_3^{2-}[\cosh\phi_5^{2-}\cos(\eta_{2I}-\xi_{2I}) + i\sinh\phi_5^{2-}\sin(\eta_{2I}-\xi_{2I})].$$

In the above, $\varphi_1^{2-} = \frac{1}{2}\log\frac{|k_1-l_2|^2(k_2-l_2)|\alpha_2^{(2)}|^2\chi_1}{(k_1^*+l_2)^2(k_1+l_2^*)^2(k_2+l_2^*)^2(l_2+l_2^*)^2\chi_2}$, $\chi_1 = \big[ac(k_1-k_2)|k_1+l_2^*|^2(k_2+l_2^*)|\alpha_1^{(1)}|^2 - c(k_1^*+k_2)|k_1-l_2|^2(k_2+k_2^*)\alpha_1^{(2)}(b^*\alpha_1^{(1)*}+c\alpha_1^{(2)}) + b(k_2-k_1)\alpha_1^{(1)}\big]$, $\chi_2 = \big[a|\alpha_1^{(1)}|^2(k_1-k_2) - b^*\alpha_1^{(1)*}\alpha_1^{(2)}(k_1^*+k_2) + b\alpha_1^{(1)}(k_1-k_2)\alpha_1^{(2)} - c|\alpha_1^{(2)}|^2(k_1^*+k_2)\big]$, $\varphi_2^{2-} = \frac{1}{2}\log\frac{|k_1-k_2|^2(k_2-l_2)|\alpha_2^{(1)}|^2}{(k_1+k_1^*)|k_1+k_2^*|^4(k_2+k_2^*)^2(k_2^*+l_2)^2\alpha_1^{(2)}(b^*\alpha_1^{(1)*}+c\alpha_1^{(2)*})}$, $\varphi_3^{2-} = \frac{1}{2}\log\frac{|k_1-k_2|^2|k_1-l_2|^2|k_2-l_2|^2|\alpha_2^{(1)}|^2|\alpha_2^{(2)}|^2}{|k_1+k_2^*|^4(k_2+k_2^*)^2(k_1^*+l_2)^2|k_2^*+l_2|^4(k_1+l_2^*)^2(l_2+l_2^*)^2\chi_3}$, $\chi_3 = a|\alpha_1^{(1)}|^2 + c|\alpha_1^{(2)}|^2 + b\alpha_1^{(1)}\alpha_1^{(2)*} + b^*\alpha_1^{(1)*}\alpha_1^{(2)}$, $\varphi_4^{2-} = \frac{1}{2}\log\frac{|\alpha_2^{(1)}|^2|k_1+l_2^*|^4(l_2+l_2^*)^2\chi_4}{|k_1+k_2^*|^4(k_2+k_2^*)^2|k_1-l_2|^2|\alpha_2^{(2)}|^2\chi_5}$, $\chi_4 = \big[ac|k_1+k_2^*|^2 - |b|^2(k_1+k_1^*)(k_2+k_2^*)|\alpha_1^{(2)}|^2\big]$, $\chi_5 = \big[ac|k_1+l_2^*|^2|\alpha_1^{(1)}|^2 + c\alpha_1^{(2)}|k_1-l_2|^2(b^*\alpha_1^{(1)*}+c\alpha_1^{(2)*}) + b\alpha_1^{(1)}(-b^*(k_1+k_1^*)(l_2+l_2^*) + c|k_1-l_2|^2\alpha_1^{(2)*})\big]$, $\varphi_5^{2-} = \frac{1}{2}\log\frac{(k_1-k_2)(k_1^*-l_2^*)\alpha_2^{(1)}\alpha_2^{(2)*}(k_1+k_2^*)^2(k_1^*+l_2)^2(k_2^*+l_2)^2\chi_6}{(k_1^*+k_2)^2(k_1+l_2^*)^2(k_2+l_2^*)^2(k_1^*-k_2^*)(k_1-l_2)\alpha_2^{(1)*}\alpha_2^{(2)}\chi_7}$, $\chi_6 = \big[|b|^2(k_1^*+k_2)(k_1+l_2^*)\alpha_1^{(2)}\alpha_1^{(1)*} + a\alpha_1^{(2)}\alpha_1^{(1)*}(b(k_1-k_2)(k_1^*-l_2^*)\alpha_1^{(1)} - c(k_1+k_1^*)(k_2+l_2^*)\alpha_1^{(2)}) + b(k_1-k_2)(k_1^*-l_2^*)(b\alpha_1^{(1)}+c\alpha_1^{(2)})\alpha_2^{(1)}\alpha_2^{(2)*}\big]$, $\chi_7 = b^*(k_1^*-k_2^*)(k_1-l_2)\alpha_1^{(1)*}(a\alpha_1^{(1)} + b^*\alpha_1^{(2)}) + |b|^2\alpha_1^{(2)}\big[(k_1+k_2^*)(k_1^*+l_2)\alpha_1^{(1)} - ac(k_1+k_1^*)(k_2^*+l_2)\alpha_1^{(1)} + b^*c(k_1^*-k_2^*)(k_1-l_2)\big]$, $\varphi_6^{2-} = \frac{1}{2}\log\frac{|k_1-l_2|^2(k_2-l_2)|\alpha_2^{(2)}|^2}{(k_1+k_1^*)|k_1+l_2^*|^4(k_2+l_2^*)^2(l_2+l_2^*)^2(a\alpha_1^{(1)*}+b\alpha_1^{(2)*})}$, $\varphi_7^{2-} = \frac{1}{2}\log\frac{(k_2-l_2)|\alpha_2^{(1)}|^2\chi_8}{|k_1+k_2^*|^4(k_2+k_2^*)^2(k_2^*+l_2)^2\chi_9}$, $\chi_9 = \big[-a|\alpha_1^{(1)}|^2(k_2^*+l_2) + b^*\alpha_1^{(1)*}\alpha_1^{(2)}(k_1-l_2) - b\alpha_1^{(1)}\alpha_1^{(2)*}(k_1^*+l_2) + c(k_1-l_2)|\alpha_1^{(2)}|^2\big]$, $\chi_8 = \big[a^2|k_1-k_2|^4(k_1^*+l_2)(k_2^*+l_2)|\alpha_1^{(1)}|^2\big]$, $\mu_{11} = \frac{(k_1-k_2)|k_1-l_2|(k_2^*-l_2^*)^{\frac{1}{2}}(\chi_1\chi_2)^{\frac{1}{2}}}{(k_1+k_1^*)(k_1^*+k_2)(k_1^*+l_2)^2(k_1+l_2^*)(k_2+l_2^*)(l_2+l_2^*)}$,

$\mu_{21} = \frac{\chi_3^{\frac{1}{2}}|k_1-l_2|(k_2-l_2)(b^*\alpha_1^{(1)*}+c\alpha_1^{(2)*})}{(k_1+k_1^*)|k_1+k_2^*|^2(k_2+k_2^*)(k_1^*+l_2)^2(k_2^*+l_2)}$, $\mu_{12} = \frac{(k_1-k_2)|k_1-l_2|(k_2-l_2)|\alpha_2^{(2)}|(a\alpha_1^{(1)*}+b\alpha_1^{(2)*})}{(k_1+k_1^*)(k_1^*+k_2)^2(k_1^*+l_2)(k_1+l_2^*)(k_2+l_2^*)(l_2+l_2^*)}$,

$$\mu_{22}=\frac{\sqrt{\chi_8\chi_9}(k_1-l_2)(k_2-l_2)|\alpha_2^{(1)}|\alpha_2^{(2)}}{(k_1+k_1^*)^2(k_1^*+k_2)^2(k_1+k_2^*)(k_2+k_2^*)(k_1^*+l_2)(k_2^*+l_2)},$$
$$\lambda_1^{2-}=\frac{\sqrt{\chi_3}|k_1-k_2||k_1-l_2||k_2-l_2||\alpha_2^{(1)}||\alpha_2^{(2)}|}{(k_1+k_1^*)^2|k_1+k_2^*|^2(k_2+k_2^*)|k_1+l_2^*|^2|k_2+l_2^*|^2(l_2+l_2^*)},$$
$$\lambda_2^{2-}=\frac{\sqrt{\chi_4\chi_5}|\alpha_2^{(1)}||k_1-l_2|}{(k_1+k_1^*)^2|k_1+k_2^*|^2(k_2+k_2^*)(l_2+l_2^*)(k_1^*+l_2)^2},\text{ and }\lambda_3^{2-}=\frac{|k_1-k_2||k_1-l_2||\alpha_2^{(1)}||\alpha_2^{(2)}|}{(k_1+k_1^*)^2|k_1+k_2^*|^2|k_1+l_2^*|^2|k_2+l_2^*|^2}.$$

(b) After collision: $z\to+\infty$

Soliton 1: The asymptotic forms for degenerate soliton S_1 after collision are deduced from the solution (3.12a)-(3.12c) as,

$$q_j\simeq\begin{pmatrix}A_1^{1+}\\ \\ A_2^{1+}\end{pmatrix}e^{i(\eta_{1I}+\theta_j^+)}k_{1R}\operatorname{sech}(\eta_{1R}+\phi^+),\ j=1,2, \tag{3.27}$$

where $A_1^{1+}=\frac{\hat\Lambda_1}{\sqrt{\hat\Lambda_3\hat\Lambda_4}}$, $A_2^{1+}=\frac{\hat\Lambda_2}{\sqrt{\hat\Lambda_3\hat\Lambda_4}}$, $\phi^+=\frac{1}{2}\log\frac{|k_1-k_2|^2|k_1-l_2|^2\hat\Lambda_4}{(k_1+k_1^*)^2|k_1+k_2^*|^4|k_1+l_2^*|^4|\alpha_2^{(1)}|^2\hat\Lambda_3}$, $\hat\Lambda_4=\left[ac|k_2+l_2^*|^2-|b|^2(k_2+k_2^*)(l_2+l_2^*)\right]$, $\hat\Lambda_1=(k_1-k_2)\left[ac(k_1+l_2^*)|k_2+l_2^*|^2-|b|^2(k_1+k_2^*)(k_2+k_2^*)(l_2+l_2^*)\alpha_1^{(1)}-b^*c(k_2+k_2^*)(k_1-l_2)(k_2^*-l_2^*)(k_2+l_2^*\alpha_1^{(2)})\right]$, $\hat\Lambda_3=a|k_1-k_2|^2|\alpha_1^{(1)}|^2\Big[ac|k_1+l_2^*|^2|k_2+l_2^*|^2-|b|^2(l_2+l_2^*)\Big(k_1k_2(k_1^*+k_2^*+l_2-l_2^*)+l_2l_2^*(k_1+k_1^*+k_2+k_2^*)+k_1^*k_2^*(k_1+k_2-l_2+l_2^*)\Big)\Big]+b^*(k_1^*-k_2^*)(k_1-l_2)\alpha_1^{(1)*}\alpha_1^{(2)}\Big[ac(k_2+l_2^*)\Big(k_1l_2(k_1^*+k_2^*+k_2-l_2)+k_2l_2^*(k_1+k_1^*+l_2+k_2^*)+k_1^*k_2^*(k_1-k_2+l_2+l_2^*)\Big)-|b|^2(k_1^*+k_2)(k_2^*+k_2)(k_1+l_2^*)(l_2^*+l_2)\Big]+b(k_1-k_2)(k_1^*-l_2^*)\alpha_1^{(1)}\alpha_1^{(2)*}\Big[ac(k_2^*+l_2)\Big(k_1^*l_2^*(k_1+k_2-l_2+k_2^*)+k_2^*l_2(k_1+k_1^*+k_2+l_2^*)+k_1k_2(k_1^*-k_2^*+l_2+l_2^*)\Big)-|b|^2(k_1+k_2^*)(k_2+k_2^*)(k_1^*+l_2)(l_2+l_2^*)\Big]+c|k_1-l_2|^2|\alpha_1^{(2)}|^2\Big[ac|k_1+k_2^*|^2|k_2+l_2^*|^2-|b|^2(k_2+k_2^*)\Big(k_1^*l_2^*(k_1-k_2+k_2^*+l_2)+k_1l_2(k_1^*+k_2-k_2^*+l_2^*)+k_2k_2^*(k_1+k_1^*+k_2+k_2^*)\Big)\Big]$, $\hat\Lambda_2=\Big[ab(k_1-k_2)(k_2^*+l_2)(k_2^*-l_2^*)(l_2+l_2^*)\alpha_1^{(1)}+(k_1-l_2)\alpha_1^{(2)}\left[ac(k_1+k_2^*)|k_2+l_2^*|^2-|b|^2(k_2+\right.$

$k_2^*)(k_1+l_2^*)(l_2+l_2^*)]\Big]$, $e^{i\theta_1^+} = \frac{(k_1-k_2)^{\frac{1}{2}}(k_1^*+k_2)(k_1-l_2)^{\frac{1}{2}}(k_1^*+l_2)}{(k_1^*-k_2^*)^{\frac{1}{2}}(k_1+k_2^*)(k_1^*-l_2^*)^{\frac{1}{2}}(k_1+l_2^*)}$,
$e^{i\theta_2^+} = \frac{(k_1-k_2)^{\frac{1}{2}}(k_1^*+k_2)(k_1-l_2)^{\frac{1}{2}}(k_1^*+l_2)}{(k_1^*-k_2^*)^{\frac{1}{2}}(k_1+k_2^*)(k_1^*-l_2^*)^{\frac{1}{2}}(k_1+l_2^*)}$. Here $1+$ in A_j^{1+}, $j=1,2$, refers to degenerate soliton S_1 after collision.

Soliton 2: Similarly the expression for the nondegenerate soliton, S_2, after collision deduced from the two soliton solution (3.12a)-(3.12c) is

$$q_1 = \frac{1}{D}\Big(d_{11}e^{i\eta_{2I}}\cosh(\xi_{2R}+\varphi_1) + d_{21}e^{i\xi_{2I}}[\cosh\eta_{2R}+\sinh\eta_{2R}]\Big), \quad (3.28)$$

$$q_2 = \frac{1}{D}\Big(d_{12}e^{i\xi_{2I}}\cosh(\eta_{2R}+\varphi_2) + d_{22}e^{i\eta_{2I}}[\cosh\xi_{2R}+\sinh\xi_{2R}]\Big), \quad (3.29)$$

$$D = \Lambda_1\cosh(\eta_{2R}+\xi_{2R}+\phi_3) + \Lambda_2\cosh(\eta_{2R}-\xi_{2R}+\phi_4)$$
$$+\Lambda_3[\cosh\phi_5\cos(\eta_{2I}-\xi_{2I}) + i\sinh\phi_5\sin(\eta_{2I}-\xi_{2I})].$$

Here, $\varphi_1 = \frac{1}{2}\log\frac{c(k_2-l_2)|\alpha_2^{(2)}|^2}{(l_2+l_2^*)^2(k_2+l_2^*)}$, $\varphi_2 = \frac{1}{2}\log\frac{a(l_2-k_2)|\alpha_2^{(1)}|^2}{(k_2+k_2^*)^2(k_2^*+l_2)}$, $\varphi_3 = \varphi_1+\varphi_2+\frac{1}{2}\log\frac{(k_2^*-l_2^*)\left[ac|k_2+l_2^*|^2-|b|^2(k_2+k_2^*)(l_2+l_2^*)\right]}{ac(l_2-k_2)|k_2+l_2^*|^2}$, $\varphi_4 = \frac{1}{2}\log\frac{a|\alpha_2^{(1)}|^2(l_2+l_2^*)^2}{c|\alpha_2^{(2)}|^2(k_2+k_2^*)^2}$,
$\varphi_5 = \frac{1}{2}\log\frac{b\alpha_2^{(1)}\alpha_2^{(2)*}(k_2^*+l_2)^2}{b^*\alpha_2^{(1)*}\alpha_2^{(2)}(k_2+l_2^*)^2}$, $d_{11} = [\frac{c|\alpha_2^{(2)}|^2(k_2-l_2)}{(k_2+l_2^*)(l_2+l_2^*)}]^{1/2}$, $d_{21} = \frac{1}{2}[\frac{b^*\alpha_2^{(2)}|\alpha_2^{(1)}|^2(k_2-l_2)}{(k_2+k_2^*)(k_2^*+l_2)^2}]$,
$d_{12} = [\frac{a\alpha_2^{(2)}|\alpha_2^{(1)}|^2(l_2-k_2)}{(k_2^*+l_2)(k_2+k_2^*)}]^{1/2}$, $d_{22} = \frac{1}{2}[\frac{b\alpha_2^{(1)}|\alpha_2^{(2)}|^2(l_2-k_2)}{(k_2+l_2^*)^2(l_2+l_2^*)}]$, $\Lambda_2 = [\frac{ac|\alpha_2^{(1)}|^2|\alpha_2^{(2)}|^2}{(k_2+k_2^*)(l_2+l_2^*)}]^{1/2}$,
$\Lambda_1 = \frac{\Lambda_2|k_2-l_2|[ac|k_2+l_2^*|^2-|b|^2(k_2+k_2^*)(l_2+l_2^*)]^{1/2}}{(ac)^{1/2}|k_2+l_2^*|^2}$, and $\Lambda_3 = \frac{|b||\alpha_2^{(1)}||\alpha_2^{(2)}|}{|k_2+l_2^*|^2}$.

The above results confirm the energy redistribution that occurs among the two modes q_1 and q_2. Such a novel collision property is displayed in Figs 3.9 and 3.10. From figure 3.9, that is in Type-I collision, one can observe that the intensity of the degenerate soliton S_1 is suppressed after collision in both the modes. In contrast to this, the intensity of the breathing nondegenerate soliton S_2 gets enhanced in both the modes q_1 and q_2. In addition to the latter case, we also noticed that the nondegenerate soliton loses its energy when it interacts with a degenerate soliton in Type-II collision, which is illustrated in Fig. 3.10. In the nondegenerate case, the phases, φ_j^{2-}, $j=1,2,...,7$ and the constants μ_{jk}, $j,k=1,2$ are in general not

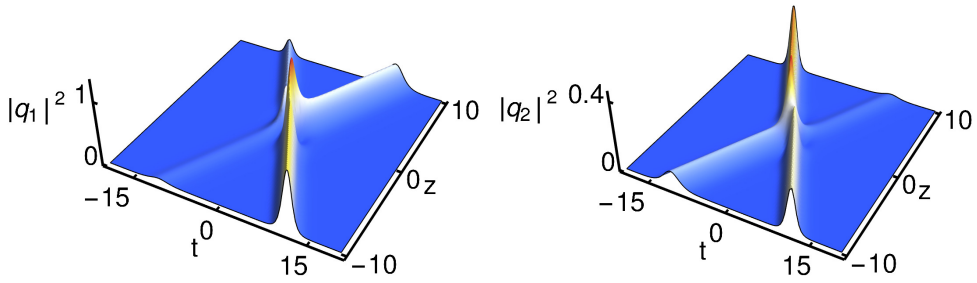

FIGURE 3.11: Manakov type shape changing collision among the two degenerate solitons.

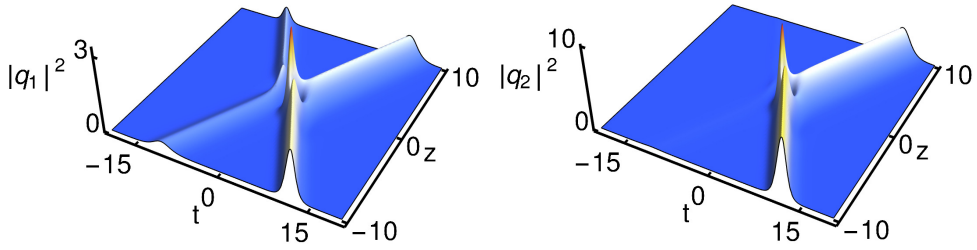

FIGURE 3.12: Mixed type shape changing collision among the two degenerate solitons.

preserved during the collision. Consequently, the shape of the nondegenerate soliton is changed into another form of breather with low oscillations. One can confirm it from Fig. 3.10. To characterize these collision scenarios, we obtain the expression for the transition amplitudes,

$$T_1^1 = \frac{\hat{\Lambda}_1 \chi_3}{\alpha_1^{(1)} \sqrt{\hat{\Lambda}_3 \hat{\Lambda}_4}}, \; T_2^1 = \frac{\hat{\Lambda}_2 \chi_3}{\alpha_1^{(2)} \sqrt{\hat{\Lambda}_3 \hat{\Lambda}_4}}. \tag{3.30}$$

In general, the above expressions are not equal to unity. If the quantity T_j^l is not unimodular then the degenerate and nondegenerate solitons always exhibit shape changing collision. These new kind of collision properties have not been observed in the Manakov case as well as in the degenerate vector bright solitons of the GCNLS system [119].

Next, for completeness, we illustrate the two types of pure degenerate soliton collisions for two different choices of SPM and XPM coefficients, (i)

$a, c > 0$, and (ii) $a > 0$, $c < 0$, for arbitrary values of FWM b values. In Fig. 3.11 we demonstrate the first type of degenerate two-soliton collision for the parametric choices $a = c = b = 1$, $k_1 = 1 - 0.5i$, $k_2 = 0.5 + 0.5i$, $\alpha_1^{(1)} = 0.5 - 0.5i$, $\alpha_1^{(2)} = 0.8 + 0.25i$, $\alpha_2^{(1)} = 0.5 + 0.5i$, $\alpha_1^{(2)} = 0.9$. It is evident from this figure that the degenerate soliton S_1 undergoes an enhancement in its intensity while the soliton S_2 gets suppressed in the q_1 mode and the reverse process takes place in the q_2 mode. This type of shape changing collision behaviour is not possible in the single component NLS system but it is similar to the one observed in the Manakov case. Another type of shape-changing collision among the two degenerate solitons is depicted in Fig. 3.12 for $a = b = 1$ and $c = -1$ with other parameters same as the one fixed in Fig. 3.11, where a given degenerate soliton shows same type of shape change in both the modes.

3.5 Conclusion

In this chapter, we have systematically derived the nondegenerate one- and two-soliton solutions for the general coupled nonlinear Schrödinger system using the standard Hirota bilinearization method. The role of four wave mixing nonlinear effect on vector nondegenerate Manakov type solitons has been understood by analysing the obtained nondegenerate solitons. The nondegenerate one- and two-soliton solutions of GCNLS system have been given in a compact way using the Gram determinant forms. Due to the effect of four wave mixing nonlinearity on vector nondegenerate solitons of Manakov type, they exhibit breathing behaviour in both the modes. We have given the N-soliton solution for the GCNLS system by generalizing the one and two nondegenerate solitons. Also the nondegenerate solitons of the GCNLS system have shown very interesting collision properties. In general they undergoes shape changing collision when the strength of four wave mixing nonlinear parameter is high enough. Further they undergo shape altering or mere shape preserving interaction when the strength of four wave mixing nonlinearity is low. We have deduced the partially nondegenerate two-soliton solution from the pure nondegenerate two-solitons by fixing the wave numbers appropriately. In such a case,

we have analysed the degenerate soliton collision induced shape changing collision of nondegenerate soliton. Then the well studied degenerate solitons have been regained by making the wave numbers identical in the one and two nondegenerate solitons of the GCNLS system and then their interaction properties are identified.

Chapter 4

Nondegenerate solitons in two component long-wave short-wave resonance interaction system

4.1 Introduction

As we have pointed out in the earlier chapters, the study of nonlinear wave interactions is very important and interesting in various field of physics such as plasma physics, hydrodynamics, nonlinear optics and so on. In these areas, nonlinear wave interactions have been observed under various physical situations. One such important wave interaction has been identified in hydrodynamics under the so called resonance conditions. Resonance is a natural phenomenon which occurs in both linear and nonlinear dynamical systems under special conditions on the frequencies [1]. This parametric process has been widely observed ranging from simple harmonic motion in mechanical systems to more complicated ultra-short pulse dynamics in optical systems. In this connection, the interaction among the nonlinear waves induces one such fascinating resonance phenomenon called the long-wave short-wave resonance interaction (LSRI) modelled by a set of coupled nonlinear Schrödinger type equations (4.1). Soliton formation essentially takes place in the evolution equations of SWs, that is the first two of the equations in Eq. (4.1) below, due to the interplay between

the nonlinearities and their corresponding dispersions, namely second order spatial derivative terms. The nonlinearities arise in these equations while the long-wave interacts with the short-waves. At the same time, the self interaction of the SWs defines the soliton formation in the long-wave evolution equation as specified by the last of the equations in Eq. (4.1). Physically the system (4.1) appears whenever the phase velocity of the long-wave ($v_{p,LW}$) almost matches with the group velocity of the short-waves ($v_{g,SW} = \frac{d\omega}{dk}$). This resonance condition is called Zakharov-Benny condition. Later this LSRI process has been reported in the nonlinear optics context also, especially in an optical fibers. In this chapter, we intend to derive a more general form of bright soliton solutions for the following LSRI model, namely two component long-wave short-wave resonance interaction system/two component Yajima-Oikawa system.

The plan of this chapter is as follows: In Section 4.2, we present the nondegenerate one- and two-soliton solutions of the system (4.1) apart from pointing out the existence of partially nondegenerate soliton solution. In this section, we also discuss the various properties associated with the nondegenerate fundamental solitons of Eqn. (4.1). Section 4.3 deals with the investigation of the three types of elastic collision scenarios with appropriate asymptotic analysis and suitable graphical demonstrations. The degenerate soliton collision induced novel shape changing properties of the nondegenerate soliton is analysed in Section 4.4. In Section 4.5, we point out that the degenerate one- and two-soliton solutions can be captured as a limiting case of the nondegenerate one- and two-soliton solutions under appropriate wave number restrictions. Then we bring out the energy sharing collision of degenerate solitons. Finally in section 4.6, we have given the analytical form of nondegenerate three-soliton solution using the Gram determinant form.

4.2 Nondegenerate soliton solutions

We have pointed out in chapter 1, that the two component long-wave short-wave resonance interaction system can be written as,

$$iS_t^{(1)} + S_{xx}^{(1)} + LS^{(1)} = 0,\ iS_t^{(2)} + S_{xx}^{(2)} + LS^{(2)} = 0,\ L_t = \sum_{l=1}^{2}(|S^{(l)}|^2)_x. \quad (4.1)$$

In the above, L is the long-wave and $S^{(l)}$'s, $l = 1, 2$, are the short-waves. The suffixes x and t denote partial derivatives with respect to the spatial and temporal coordinates, respectively.

We construct the nondegenerate multi-soliton solution by bilinearizing Eq. (4.1) through the dependent variable transformations, $S^{(l)}(x,t) = \frac{g^{(l)}(x,t)}{f(x,t)}$, $l = 1, 2$, $L = 2\frac{\partial^2}{\partial x^2}\ln f(x,t)$. This action yields the following bilinear forms of Eq. (4.1),

$$D_1 g^{(l)} \cdot f = 0,\ l = 1, 2,\ D_2 f \cdot f = \sum_{n=1}^{2} |g^{(n)}|^2, \quad (4.2)$$

where $D_1 \equiv iD_t + D_x^2$ and $D_2 \equiv D_x D_t$. Here D_t and D_x are the Hirota bilinear operators defined by [155]

$$D_x^m D_t^n (a \cdot b) = \left(\frac{\partial}{\partial x} - \frac{\partial}{\partial x'}\right)^m \left(\frac{\partial}{\partial t} - \frac{\partial}{\partial t'}\right)^n a(x,t)b(x',t')\Big|_{x=x',\ t=t'}$$

In principle, the soliton solutions (with vanishing boundary condition $S^{(l)} \to 0$, $l = 1, 2$ and $L \to 0$ as $x \to \pm\infty$) of Eq. (4.1) can be derived by solving a system of linear partial differential equations (PDEs), which appear at various orders of ϵ while substituting the series expansions $g^{(l)} = \epsilon g_1^{(l)} + \epsilon^3 g_3^{(l)} + ...$, $l = 1, 2$, $f = 1 + \epsilon^2 f_2 + \epsilon^4 f_4 + ...$ in the bilinear forms (4.2). The explicit forms of the functions $g^{(l)}$'s and f lead to various soliton solutions to the underlying LSRI system (4.1).

4.2.1 Nondegenerate one-soliton solution

To derive the nondegenerate fundamental soliton solution we start with the more general form of seed solutions,

$$g_1^{(1)} = \alpha_1^{(1)} e^{\eta_1},\ g_1^{(2)} = \alpha_1^{(2)} e^{\xi_1},\ \eta_1 = k_1 x + ik_1^2 t,\ \xi_1 = l_1 x + il_1^2 t, \quad (4.3)$$

where $\alpha_1^{(l)}$'s, k_1 and l_1 are arbitrary complex constants, for the lowest order linear PDEs,

$$ig_{1,t}^{(1)} + g_{1,xx}^{(1)} = 0,\ ig_{1,t}^{(2)} + g_{1,xx}^{(2)} = 0. \tag{4.4}$$

From the above, one can notice that the functions $g^{(1)}$ and $g^{(2)}$ considered in Eq. (4.3) are two distinct solutions. This is because of the independent nature of the two linear PDEs specified above in Eq. (4.4) and so their solutions should be expressed in general in terms of two independent functions as given in Eq. (4.3) above with arbitrary wave numbers k_1, l_1, where in general $k_1 \neq l_1$. The general forms of the seed solutions with distinct propagation constants will bring out a physically meaningful class of fundamental soliton solutions as we describe below. Such a possibility has not been considered so far in the literature for the $(1+1)$-dimensional integrable two component LSRI system as far as our knowledge goes except in our earlier papers [77–79, 84, 160]. What has been considered so far is only the restricted class of seed solutions, that is the wave number restricted seed solutions, namely $g_1^{(1)} = \alpha_1^{(1)} e^{\eta_1}$, $g_1^{(2)} = \alpha_1^{(2)} e^{\eta_1}$, $\eta_1 = k_1 x + i k_1^2 t$ (one can get this set of seed solutions straightforwardly by setting the condition $k_1 = l_1$ in (4.3)). Even such restricted seed solutions have been shown to yield interesting energy sharing collision properties of solitons [161]. So what we emphasize here is that the vector bright solitons reported so far in the literature are achieved by considering such a limited class of seed solutions only. With the general forms of seed solutions (4.3), we solve the following system of linear inhomogeneous partial differential equations:

$$O(\epsilon^0) : 0 = 0,\ O(\epsilon^2) : D_2(1 \cdot f_2 + f_2 \cdot 1) = g_1^{(1)} g_1^{(1)*} + g_1^{(2)} g_1^{(2)*}, \tag{4.5}$$

$$O(\epsilon^3) : D_1 g_3^{(l)} \cdot 1 = -D_1 g_1^{(l)} \cdot f_2, \tag{4.6}$$

$$O(\epsilon^4) : D_2(1 \cdot f_4 + f_4 \cdot 1) = -D_2 f_2 \cdot f_2 + g_1^{(1)} g_3^{(1)*} + g_3^{(1)} g_1^{(1)*} + g_1^{(2)} g_3^{(2)*} + g_3^{(2)} g_1^{(2)*}, \tag{4.7}$$

$$O(\epsilon^5) : D_1 g_5^{(l)} \cdot 1 = -D_1(g_1^{(l)} \cdot f_4 + g_3^{(l)} \cdot f_2),\ l = 1, 2, \tag{4.8}$$

$$\begin{aligned} O(\epsilon^6) : D_2(1 \cdot f_6 + f_6 \cdot 1) = {} & -D_2(f_4 \cdot f_2 + f_2 \cdot f_4) + g_1^{(1)} g_5^{(1)*} + g_3^{(1)} g_3^{(1)*} + g_5^{(1)} g_1^{(1)*} \\ & + g_1^{(2)} g_5^{(2)*} + g_3^{(2)} g_3^{(2)*} + g_5^{(2)} g_1^{(2)*}, \end{aligned} \tag{4.9}$$

and etc. By doing so, we find the explicit forms of the unknown functions f_2, $g_3^{(l)}$, $l = 1, 2$, and f_4 as $f_2 = e^{\eta_1 + \eta_1^* + R_1} + e^{\xi_1 + \xi_1^* + R_2}$, $g_3^{(1)} =$

$e^{\eta_1+\xi_1+\xi_1^*+\Delta_1}$, $g_3^{(2)} = e^{\xi_1+\eta_1+\eta_1^*+\Delta_2}$, $f_4 = e^{\eta_1+\eta_1^*+\xi_1+\xi_1^*+R_3}$, where $e^{R_1} = \frac{|\alpha_1^{(1)}|^2}{2i(k_1+k_1^*)^2(k_1-k_1^*)}$, $e^{R_2} = \frac{|\alpha_1^{(2)}|^2}{2i(l_1+l_1^*)^2(l_1-l_1^*)}$,$e^{\Delta_1} = \frac{i\alpha_1^{(1)}|\alpha_1^{(2)}|^2(l_1-k_1)}{2(k_1+l_1^*)(l_1-l_1^*)(l_1+l_1^*)^2}$, $e^{\Delta_2} = \frac{i\alpha_1^{(2)}|\alpha_1^{(1)}|^2(k_1-l_1)}{2(k_1^*+l_1)(k_1-k_1^*)(k_1+k_1^*)^2}$, $e^{R_3} = -\frac{|\alpha_1^{(1)}|^2|\alpha_1^{(2)}|^2|k_1-l_1|^2}{4|k_1+l_1^*|^2(k_1-k_1^*)(l_1-l_1^*)(k_1+k_1^*)^2(l_1+l_1^*)^2}$. We note that the right hand sides of all the remaining linear PDEs identically vanish upon substitution of the obtained functions $g_1^{(l)}$, $g_3^{(l)}$, $l = 1,2$, f_2 and f_4. Consequently, one can take $g_5^{(l)} = g_7^{(l)} = ... = 0$, $l = 1,2$, and $f_6 = f_8 = ... = 0$. Thus in the series all $g_i^{(l)} = 0$ for $i \geq 5$ and all $f_j = 0$, $j \geq 6$. Therefore, ultimately the series converges at the $O(\epsilon^3)$ in the function $g^{(l)}(x,t)$ while the series terminates at the $O(\epsilon^4)$ in $f(x,t)$: $g^{(l)} = \epsilon g_1^{(l)} + \epsilon^3 g_3^{(l)}$, $l = 1,2$, $f = 1 + \epsilon^2 f_2 + \epsilon^4 f_4$. We also note that the small parameter ϵ can be fixed as 1 (as it can be subsumed with the parameters $\alpha_1^{(1)}$ and $\alpha_1^{(2)}$), without loss of generality. Thus the above procedure makes the infinite expansion to terminate with a finite number of terms only and hence the solution can be summed up into an exact one. Finally, the resultant explicit forms of the unknown functions constitute the nondegenerate fundamental soliton solution for the system (4.1), which reads as,

$$S^{(1)}(x,t) = \frac{g_1^{(1)} + g_3^{(1)}}{1 + f_2 + f_4} = \frac{\alpha_1^{(1)} e^{\eta_1} + e^{\eta_1+\xi_1+\xi_1^*+\Delta_1}}{1 + e^{\eta_1+\eta_1^*+R_1} + e^{\xi_1+\xi_1^*+R_2} + e^{\eta_1+\eta_1^*+\xi_1+\xi_1^*+R_3}}, \tag{4.10}$$

$$S^{(2)}(x,t) = \frac{g_1^{(2)} + g_3^{(2)}}{1 + f_2 + f_4} = \frac{\alpha_1^{(2)} e^{\xi_1} + e^{\xi_1+\eta_1+\eta_1^*+\Delta_2}}{1 + e^{\eta_1+\eta_1^*+R_1} + e^{\xi_1+\xi_1^*+R_2} + e^{\eta_1+\eta_1^*+\xi_1+\xi_1^*+R_3}}, \tag{4.11}$$

$$L(x,t) = 2\frac{\partial^2}{\partial x^2} \ln(1 + e^{\eta_1+\eta_1^*+R_1} + e^{\xi_1+\xi_1^*+R_2} + e^{\eta_1+\eta_1^*+\xi_1+\xi_1^*+R_3}). \tag{4.12}$$

Using Gram determinants [162, 163], we can rewrite the above soliton solution in a more compact form as $S^{(1)} = \frac{g^{(1)}}{f}$, $S^{(2)} = \frac{g^{(2)}}{f}$, $L = 2\frac{\partial^2}{\partial x^2} \ln f$, where

$$g^{(1)} = \begin{vmatrix} \frac{e^{\eta_1+\eta_1^*}}{(k_1+k_1^*)} & \frac{e^{\eta_1+\xi_1^*}}{(k_1+l_1^*)} & 1 & 0 & e^{\eta_1} \\ \frac{e^{\xi_1+\eta_1^*}}{(l_1+k_1^*)} & \frac{e^{\xi_1+\xi_1^*}}{(l_1+l_1^*)} & 0 & 1 & e^{\xi_1} \\ -1 & 0 & \frac{|\alpha_1^{(1)}|^2}{2i(k_1^2-k_1^{*2})} & 0 & 0 \\ 0 & -1 & 0 & \frac{|\alpha_1^{(2)}|^2}{2i(l_1^2-l_1^{*2})} & 0 \\ 0 & 0 & -\alpha_1^{(1)} & 0 & 0 \end{vmatrix}, \tag{4.13}$$

$$g^{(2)} = \begin{vmatrix} \frac{e^{\eta_1+\eta_1^*}}{(k_1+k_1^*)} & \frac{e^{\eta_1+\xi_1^*}}{(k_1+l_1^*)} & 1 & 0 & e^{\eta_1} \\ \frac{e^{\xi_1+\eta_1^*}}{(l_1+k_1^*)} & \frac{e^{\xi_1+\xi_1^*}}{(l_1+l_1^*)} & 0 & 1 & e^{\xi_1} \\ -1 & 0 & \frac{|\alpha_1^{(1)}|^2}{2i(k_1^2-k_1^{*2})} & 0 & 0 \\ 0 & -1 & 0 & \frac{|\alpha_1^{(2)}|^2}{2i(l_1^2-l_1^{*2})} & 0 \\ 0 & 0 & 0 & -\alpha_1^{(2)} & 0 \end{vmatrix}, \tag{4.14}$$

$$f = \begin{vmatrix} \frac{e^{\eta_1+\eta_1^*}}{(k_1+k_1^*)} & \frac{e^{\eta_1+\xi_1^*}}{(k_1+l_1^*)} & 1 & 0 \\ \frac{e^{\xi_1+\eta_1^*}}{(l_1+k_1^*)} & \frac{e^{\xi_1+\xi_1^*}}{(l_1+l_1^*)} & 0 & 1 \\ -1 & 0 & \frac{|\alpha_1^{(1)}|^2}{2i(k_1^2-k_1^{*2})} & 0 \\ 0 & -1 & 0 & \frac{|\alpha_1^{(2)}|^2}{2i(l_1^2-l_1^{*2})} \end{vmatrix}. \tag{4.15}$$

We find that the above forms of Gram determinants satisfy the two component LSRI system (4.1) as well as the bilinear equations (4.2). In order to analyse the various special properties of the nondegenerate one-soliton solution of Eq. (4.1), we obtain the following expression for the one-soliton solution by rewriting Eqs. (4.10)-(4.12) in hyperbolic forms,

$$S^{(1)} = \frac{4k_{1R}\sqrt{k_{1I}}A_1 e^{i(\eta_{1I}+\frac{\pi}{2})}[\cosh(\xi_{1R}+\varphi_{1R})\cos\varphi_{1I} + i\sinh(\xi_{1R}+\varphi_{1R})\sin\varphi_{1I}]}{[a_{11}\cosh(\eta_{1R}+\xi_{1R}+\varphi_1+\varphi_2+c_1)+\frac{1}{a_{11}^*}\cosh(\eta_{1R}-\xi_{1R}+\varphi_2-\varphi_1+c_2)]}, \tag{4.16}$$

$$S^{(2)} = \frac{4l_{1R}\sqrt{l_{1I}}A_2 e^{i(\xi_{1I}+\frac{\pi}{2})}[\cosh(\eta_{1R}+\varphi_{2R})\cos\varphi_{2I} + i\sinh(\eta_{1R}+\varphi_{2R})\sin\varphi_{2I}]}{[a_{12}\cosh(\eta_{1R}+\xi_{1R}+\varphi_1+\varphi_2+c_1)+\frac{1}{a_{12}^*}\cosh(\eta_{1R}-\xi_{1R}+\varphi_2-\varphi_1+c_2)]}, \tag{4.17}$$

$$L = \frac{4k_{1R}^2\cosh(2\xi_{1R}+2\varphi_1+c_4)+4l_{1R}^2\cosh(2\eta_{1R}+2\varphi_2+c_3)+\frac{1}{2}e^{R_3'-(\frac{R_1+R_2+R_3}{2})}}{[\Lambda\cosh(\eta_{1R}+\xi_{1R}+\varphi_1+\varphi_2+c_1)+\Lambda^{-1}\cosh(\eta_{1R}-\xi_{1R}+\varphi_2-\varphi_1+c_2)]^2}, \tag{4.18}$$

$$e^{R_3'} = 4(k_{1R}+l_{1R})^2 e^{R_3} + 4(k_{1R}-l_{1R})^2 e^{R_1+R_2},$$

where $a_{11} = \frac{(k_1^*-l_1^*)^{\frac{1}{2}}}{(k_1^*+l_1)^{\frac{1}{2}}}$, $a_{12} = \frac{(k_1^*-l_1^*)^{\frac{1}{2}}}{(k_1+l_1^*)^{\frac{1}{2}}}$, $\Lambda = \frac{1}{2}\log\frac{|k_1-l_1|}{|k_1+l_1^*|}$, $c_1 = \frac{1}{2}\log\frac{(k_1^*-l_1^*)}{(l_1-k_1)}$, $c_2 = \frac{1}{2}\log\frac{(k_1-l_1)(k_1^*+l_1)}{(l_1-k_1)(k_1+l_1^*)}$, $c_3 = \frac{1}{2}\log\frac{(l_1^*-k_1^*)(k_1^*+l_1)}{(k_1+l_1^*)(l_1-k_1)}$, $c_4 = \frac{1}{2}\log\frac{(k_1^*-l_1^*)(k_1+l_1^*)}{(k_1^*+l_1)(k_1-l_1)}$, $\eta_{1R} = k_{1R}(x-2k_{1I}t)$, $\eta_{1I} = k_{1I}x + (k_{1R}^2 - k_{1I}^2)t$, $\xi_{1R} = l_{1R}(x-2l_{1I}t)$, $\xi_{1I} = l_{1I}x + (l_{1R}^2 - l_{1I}^2)t$, $A_1 = [\alpha_1^{(1)}/\alpha_1^{(1)*}]^{1/2}$, $A_2 = i[\alpha_1^{(2)}/\alpha_1^{(2)*}]^{1/2}$, and the other constants can be calculated using the constants that are defined below Eqs. (4.10)-(4.12). Here, φ_{1R}, φ_{2R}, φ_{1I} and φ_{2I} are real and imaginary parts of $\varphi_1 = \frac{\Delta_1-\rho_1}{2}$ and $\varphi_2 = \frac{\Delta_2-\rho_2}{2}$, $e^{\rho_l} = \alpha_1^{(l)}$, $l = 1, 2$, respectively and k_{1R}, l_{1R}, k_{1I} and l_{1I} denote the real and imaginary parts of k_1 and l_1, respectively. The four arbitrary complex parameters, $\alpha_1^{(l)}$'s, $l = 1, 2$, k_1 and l_1, determine the structure of the nondegenerate fundamental soliton solution (4.16)-(4.18) of the two component LSRI system (4.1).

In general, the amplitudes of the soliton in the short-wave components are $4k_{1R}\sqrt{k_{1I}}A_1$ and $4l_{1R}\sqrt{l_{1I}}A_2$, respectively, and their velocities in their respective SW components are $2k_{1I}$ and $2l_{1I}$. On the other hand, the amplitude and the velocity of the soliton in the LW component mainly depend on the real and imaginary parts of both the wave numbers k_1 and l_1, respectively. From the above, one can easily notice that the amplitudes of the SW components explicitly depend on the velocity of the soliton. This interesting amplitude dependent velocity property is analogous to the property of the Korteweg-de Vries (KdV) soliton of the form $u(x,t) = \frac{c}{2}\mathrm{sech}^2\frac{\sqrt{c}}{2}(x-ct)$. Here c is the velocity of the KdV soliton [1, 164]. Consequently, like the degenerate bright solitons, the taller nondegenerate solitons also travel faster than the smaller ones, as pointed out in Section 5 and in Ref. [161]. We note that the nondegenerate fundamental soliton in the Manakov system does not possess this velocity-dependent amplitude property [77, 78]. The solution (4.16)-(4.18) shows both regular and singular behaviour. The singularity property of the solution is determined by the quantities e^{R_1}, e^{R_2} and e^{R_3}. The regular soliton solution arises for the case when both k_{1I} and $l_{1I} < 0$. In this case, the quantities, e^{R_1}, e^{R_2} and $e^{R_3} > 0$ whereas the solution (4.16)-(4.18) displays singularity for k_{1I} and/or $l_{1I} > 0$.

The nondegenerate one-soliton solution (4.16)-(4.18) is classified as follows depending on the choice of the velocity conditions:

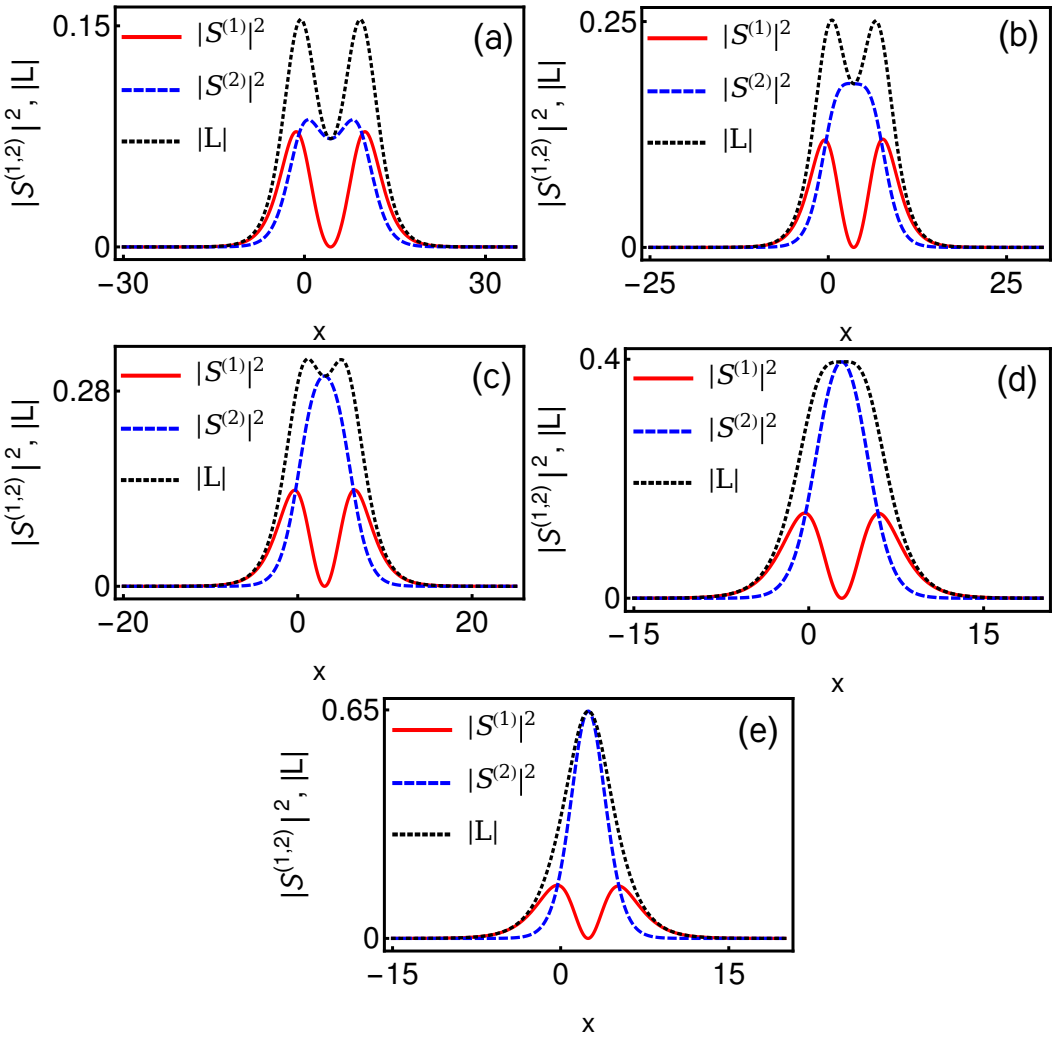

FIGURE 4.1: Five types of symmetric profiles of the nondegenerate fundamental soliton solution (4.16)-(4.18) with $k_{1I} = l_{1I}$ or (4.19)-(4.21): While (a) represents double-hump profiles in all the components, (b) denotes double-hump profiles in $S^{(1)}$ and L components and a flattop profile in $S^{(2)}$ componenet, (c) indicates double-hump profiles in $S^{(1)}$ and L components and a single-hump profile in $S^{(2)}$ componenet, (d) represents double-hump in $S^{(1)}$ component, single-hump in $S^{(2)}$ component and a flattop profile in L componnet and (e) denotes double-hump profile in $S^{(1)}$ and single-hump profiles in both $S^{(2)}$ and L components. The parameter values of each one of the cases are as follows: (a) $k_1 = 0.25 - 0.5i$, $l_1 = 0.315 - 0.5i$, $\alpha_1^{(1)} = 0.5 + 0.5i$ and $\alpha_1^{(2)} = 0.45 + 0.5i$. (b) $k_1 = 0.3 - 0.5i$, $l_1 = 0.425 - 0.5i$, $\alpha_1^{(1)} = 0.43 + 0.55i$ and $\alpha_1^{(2)} = 0.45 + 0.45i$. (c) $k_1 = 0.315 - 0.5i$, $l_1 = 0.5 - 0.5i$, $\alpha_1^{(1)} = 0.5 + 0.5i$ and $\alpha_1^{(2)} = 0.45 + 0.45i$. (d) $k_1 = 0.315 - 0.5i$, $l_1 = 0.545 - 0.5i$, $\alpha_1^{(1)} = 0.5 + 0.5i$ and $\alpha_1^{(2)} = 0.45 + 0.5i$. (e) $k_1 = 0.315 - 0.5i$, $l_1 = 0.65 - 0.5i$, $\alpha_1^{(1)} = 0.5 + 0.5i$ and $\alpha_1^{(2)} = 0.45 + 0.5i$.

(i) For $k_{1I} = l_{1I}$, we designate the one-soliton solution as $(1,1,1)$-soliton solution, where all the components $(S^{(1)}, S^{(2)}, L)$ consist of only one soliton with double-hump or flattop or single-hump structured profile.
(ii) On the other hand, we refer the solution (4.16)-(4.18) with $k_{1I} \neq l_{1I}$ as $(1,1,2)$-soliton solution, where both the short-wave components $S^{(1)}$ and $S^{(2)}$ possess one humped localized structures only while the long-wave component contains two single-hump structured profiles like the 2-soliton solution of the NLS equation. We will discuss each one of these cases separately in the following.

In the equal velocity case, the soliton in the SW components propagates with identical velocities but with different amplitudes. For this case, the imaginary parts of φ_j's are equal to zero. That is, $\varphi_{jI} = 0$, $j = 1,2$. This property reduces the solution (4.16)-(4.18) into the following form of $(1,1,1)$-soliton solution,

$$S^{(1)} = \frac{4k_{1R}\sqrt{k_{1I}}A_1 e^{i(\eta_{1I}+\frac{\pi}{2})}\cosh(\xi_{1R}+\varphi_{1R})}{\left[b_1\cosh(\eta_{1R}+\xi_{1R}+\varphi_1+\varphi_2+c_1)+\frac{1}{b_1}\cosh(\eta_{1R}-\xi_{1R}+\varphi_2-\varphi_1+c_2)\right]}, \tag{4.19}$$

$$S^{(2)} = \frac{4l_{1R}\sqrt{k_{1I}}A_2 e^{i(\xi_{1I}+\frac{\pi}{2})}\cosh(\eta_{1R}+\varphi_{2R})}{\left[b_1\cosh(\eta_{1R}+\xi_{1R}+\varphi_1+\varphi_2+c_1)+\frac{1}{b_1}\cosh(\eta_{1R}-\xi_{1R}+\varphi_2-\varphi_1+c_2)\right]}, \tag{4.20}$$

$$L = \frac{4k_{1R}^2\cosh(2\xi_{1R}+2\varphi_1+c_4)+4l_{1R}^2\cosh(2\eta_{1R}+2\varphi_2+c_3)+4(k_{1R}^2-l_{1R}^2)}{[b_1\cosh(\eta_{1R}+\xi_{1R}+\varphi_1+\varphi_2+c_1)+b_1^{-1}\cosh(\eta_{1R}-\xi_{1R}+\varphi_2-\varphi_1+c_2)]^2}, \tag{4.21}$$

where $b_1 = \frac{(k_{1R}-l_{1R})^{\frac{1}{2}}}{(k_{1R}+l_{1R})^{\frac{1}{2}}}$, $\eta_{1R} = k_{1R}(x-2k_{1I}t)$, $\eta_{1I} = k_{1I}x+(k_{1R}^2-k_{1I}^2)t$, $\xi_{1R} = l_{1R}(x-2k_{1I}t)$, $\xi_{1I} = k_{1I}x+(l_{1R}^2-k_{1I}^2)t$.

From the above solution, we find a relation between the short-wave components and the long-wave component and it turns out to be

$$|S^{(1)}|^2+|S^{(2)}|^2 = -2k_{1I}L. \tag{4.22}$$

The latter relation confirms that the above type of linear superposition of intensities of the two short-wave components accounts for the formation of interesting soliton structure in the long-wave component. The special solutions (4.19)-(4.21) with the condition $k_{1R} < l_{1R}$ admits five types of symmetric profiles which we have displayed in figure 4.1. The symmetric profiles are classified as follows: (i) Double-humps in all the components,

(ii) double-humps in $S^{(1)}$ and long-wave components and a flattop in the $S^{(2)}$ component, (iii) double-humps in $S^{(1)}$ and long-wave components and a single-hump in the $S^{(2)}$ component, (iv) double-hump in $S^{(1)}$ component, single-hump in $S^{(2)}$ component and a flattop profile in the long-wave component and (v) double-hump in $S^{(1)}$ component and single-humps in both the $S^{(2)}$ and long-wave components. In order to demonstrate all the above five cases we fix $k_{1I} = l_{1I} = -0.5 < 0$ in figure 4.1. From figure 4.1, one can observe that the transition which occurs from double-hump to single-hump or from single-hump to double-hump is through a special flattop profile. The corresponding asymmetric profiles are illustrated in figure 4.2 for the parameter values as specified there. This can be achieved by tuning either the real parts of the wave numbers k_1 and l_1 or by tuning the complex parameters $\alpha_1^{(l)}$'s. One can also bring out a double-hump and a flattop profile in the $S^{(1)}$ ($S^{(2)}$ and L as well) component by considering another possibility, namely $k_{1I} = l_{1I} < 0$ and $k_{1R} > l_{1R}$.

Further, one can confirm the symmetric and asymmetric nature of the $(1,1,1)$ solution (4.19)-(4.21), by finding the extremum points as we have analyzed the profile nature of the nondegenerate soliton solution in the Manakov system [78]. In the following, we explain this analysis for the symmetric double-hump soliton profile, displayed in figure 4.1(a), of the LSRI system (4.1): First, we find the local maximum and minimum points by applying the first derivative test ($\{|S^{(j)}|^2\}_x = 0$, $\{|L|\}_x = 0$) and the second derivative test ($\{|S^{(j)}|^2\}_{xx}, \{|L|\}_{xx} < 0$ or > 0) to the expressions of $|S^{(j)}|^2$, $j = 1,2$, and $|L|$, at $t = 0$. As a result, for the first SW component, three extremal points are identified, namely $x_1 = -1.4$, $x_2 = 4.3$ and $x_3 = 9.99$. Then we found another set of three extremal points, $x_4 = 0.6$, $x_5 = 4.3$ and $x_6 = 8.09$, for the second SW component. We also identified another set of three extremal points, $x_7 = -0.6$, $x_8 = 4.29$ and $x_9 = 9.2$, for the LW component by setting $\{|L|\}_x = 0$. While the points x_2, x_5 and x_8 correspond to minima, the points, (x_1, x_3), (x_4, x_6), and (x_7, x_9) correspond to maximum points. In all the components, the minimum points x_2, x_5 and x_8 are located at equal distances from the two maximum points (x_1, x_3), (x_4, x_6) and (x_7, x_9), respectively. This can be easily confirmed by finding their differences. For instance, in the $S^{(1)}$-component, $x_1 - x_2 = -5.7 = x_2 - x_3$. This is true for both the SW component $S^{(2)}$ and the LW component L

also. That is for $S^{(2)}$: $x_4 - x_5 = -3.7 \approx x_5 - x_6 = -3.79$ and for L: $x_7 - x_8 = -4.89 \approx x_8 - x_9 = -4.91$. Then the intensity, $|S^{(1)}|^2$, of each hump, of the double-hump soliton, corresponding to maxima x_1 and x_3 are equal to 0.078. Similarly, in the second SW component, the magnitude of the intensity corresponding to the maximum points x_4 and x_6 are equal to 0.086. We also obtain the magnitudes corresponding to the maxima x_7 and x_8 are equal to 0.154. The above analysis confirms that the double-hump soliton profiles displayed in figure 4.1(a) are symmetric. In addition, one can also verify the symmetric nature of the single-hump soliton about the local maximum point and checking the half widths as well. For the flat-top soliton case, we have confirmed that the first derivative $\{|S^{(l)}|^2\}_x$, $l = 1, 2$, and $\{|L|\}_x$, very slowly tends to zero, for a certain number of x values, near the corresponding maximum. This also confirms that the presence of almost flatness and symmetric nature of the one-soliton. By following the above procedure, one can also verify the asymmetric nature of the solution (4.19)-(4.21).

Next, we consider the $(1, 1, 2)$-soliton solution, that is the solution (4.16)-(4.18) with $k_{1I} \neq l_{1I}$. In this situation, the soliton in the two short-wave components (as well as in the long-wave component) propagate with distinct velocities as we have displayed in figure 4.3. As it is evident from this figure that distinct single-humped one-soliton structures always occur in each of the short-wave components and they propagate from $+x$ to $-x$ direction (but with different localizations). However, surprisingly the two single-hump structured solitons of the SW component emerge in the LW component and they interact like the two soliton solution of the scalar NLS case. Each of the single-humped structures of the soliton in the SW components $S^{(1)}$ and $S^{(2)}$ interact through the LW component as dictated by the nonlinearity of the LW component. This special nonlinear phenomenon occurs because of the nondegeneracy property of the fundamental soliton solution (4.16)-(4.18) of the LSRI system (4.1). To the best of our knowledge, this special kind of phenomenon has not been observed earlier in the present $(1 + 1)$-dimensional two-component LSRI system and its multicomponent version. A similar kind of soliton nature is also observed in the Wronskian solutions, derived by Ohta et al., for the two-component $(2 + 1)$-dimensional LSRI system [142]. Although we have

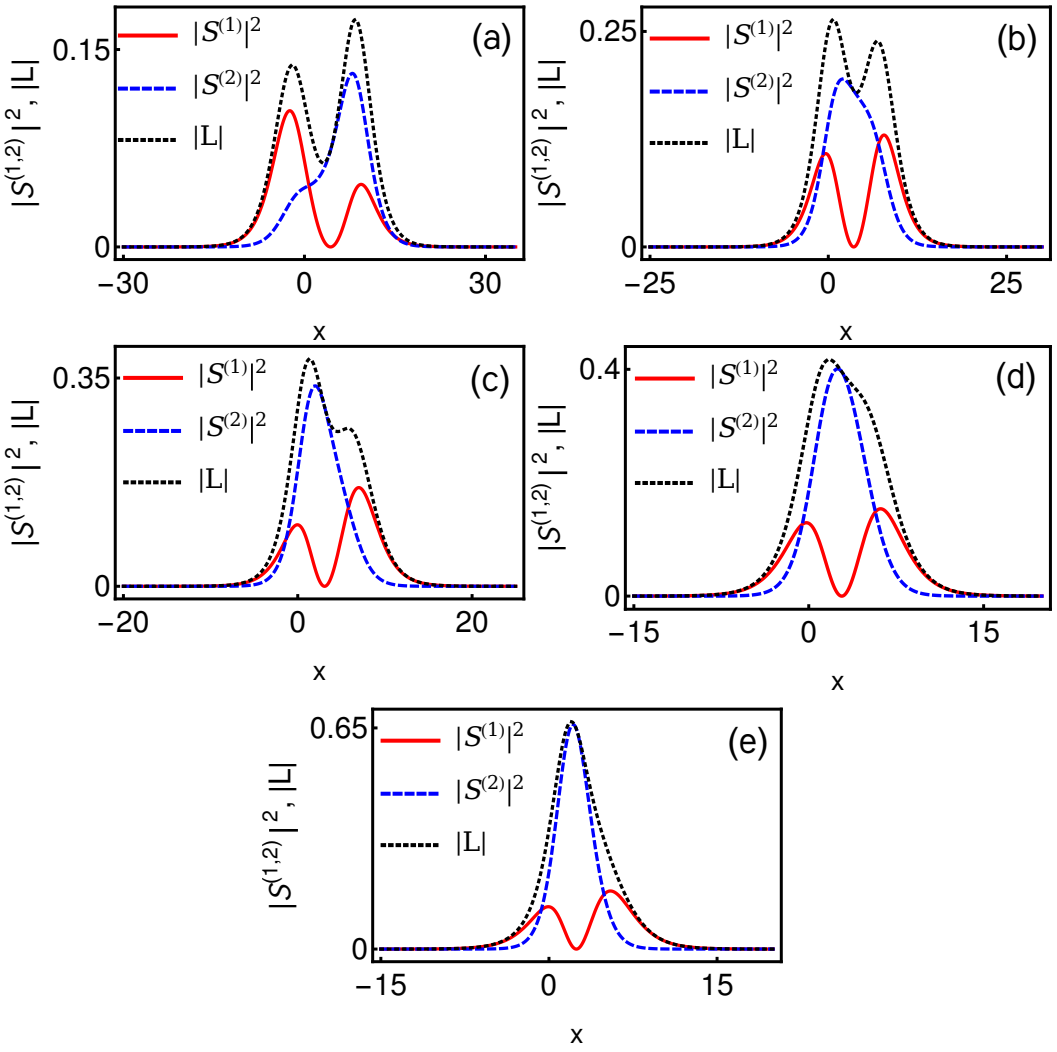

FIGURE 4.2: Panels (a), (b), (c), (d) and (e) denote asymmetric profiles corresponding to the symmetric profiles of Fig. 4.1(a)-4.1(e) with $k_{1I} = l_{1I}$. The parameter values of each of the cases are as follows: (a) $k_1 = 0.25 - 0.5i$, $l_1 = 0.315 - 0.5i$, $\alpha_1^{(1)} = 0.5 + i$ and $\alpha_1^{(2)} = 0.45 + 0.5i$. (b) $k_1 = 0.3 - 0.5i$, $l_1 = 0.425 - 0.5i$, $\alpha_1^{(1)} = 0.3 + 0.55i$ and $\alpha_1^{(2)} = 0.45 + 0.45i$. (c) $k_1 = 0.315 - 0.5i$, $l_1 = 0.5 - 0.5i$, $\alpha_1^{(1)} = 0.15 + 0.5i$ and $\alpha_1^{(2)} = 0.45 + 0.45i$. (d) $k_1 = 0.315 - 0.5i$, $l_1 = 0.545 - 0.5i$, $\alpha_1^{(1)} = 0.38 + 0.5i$ and $\alpha_1^{(2)} = 0.45 + 0.5i$. (e) $k_1 = 0.315 - 0.5i$, $l_1 = 0.65 - 0.5i$, $\alpha_1^{(1)} = 0.25 + 0.5i$ and $\alpha_1^{(2)} = 0.45 + 0.5i$.

graphically demonstrated the $(1, 1, 2)$ and $(2, 2, 4)$ soliton solutions in [142], the complete analysis of such soliton solutions and their associated many novel results are still missing in the literature. We have systematically analyzed the $(1, 1, 2)$ and $(2, 2, 4)$ soliton solutions of the $(2 + 1)$-dimensional

multicomponent LSRI system by expressing their exact analytical forms in terms of Gram determinants and the results will be published elsewhere. Moreover, it is shown in Ref. [144] that the Wronskian solutions $(N, M, N+M)$ reported in [142] have also been deduced from the degenerate soliton solutions (m, m, m). However, the dynamical properties of the Wronskian solutions, as graphically illustrated in [142], are distinct from the degenerate soliton solutions as explained in [144]. We point out that the double-hump soliton profile emerges in all the components when the relative velocity $2(l_{1I} - k_{1I})$ tends to zero. In other words, the double-hump formation will occur if $l_{1I} \approx k_{1I}$.

To experimentally generate the nondegenerate vector solitons one may consider three channels of nonlinear dispersive medium or triple mode nonlinear optical fiber [142], where the two light pulses are in the anomalous dispersion regime and the remaining pulse is in the normal dispersion regime. By introducing the intermodal interactions in such a way one can make the short-wave modes (anamalous dispersion regime) to interact with the long-wave mode (normal dispersion regime). In this situation, it is essential to consider two laser sources of different characters so that the frequency of the first laser beam is different from the second one. By sending the extraordinary mutual incoherent optical beam, coming out from both the sources, to the short-wave channels along with the appropriate coupling on the long-wave channel, it is possible to create the nondegenerate solitons. In this situation, the group velocities $v_g = \frac{d\omega}{dk}$ of the optical beam in the short-wave channels should be equal to the phase velocity v_p of the long-wave channel. Under this resonance condition, the nondegenerate solitons in the short-wave optical modes can be created and made to interact with the soliton in the long-wave mode. In the fluid dynamics context also one can observe the nondegenerate solitons by considering a three-layer system [165] of homogeneous fluids having different densities. In this circumstance, it is possible to achieve the problem of resonance interaction of a long interfacial wave and a short surface waves. By a proper choice of the various densities and layer thicknesses, one may tune the three-layer system to a resonant condition whereby the group velocity of the shorter surface waves and the phase velocity of the longer interfacial

wave are nearly equal. Thus, all of the physics relevant to the nondegenerate solitons can be identified from this simple three-layer fluid system. On the other hand, it is also possible to create the nondegenerate solitons in spinor BECs by tuning the hyperfine states of the ^{87}Rb atoms [166] whenever the group velocities of the short-waves are equal to the phase velocity of the long-wave.

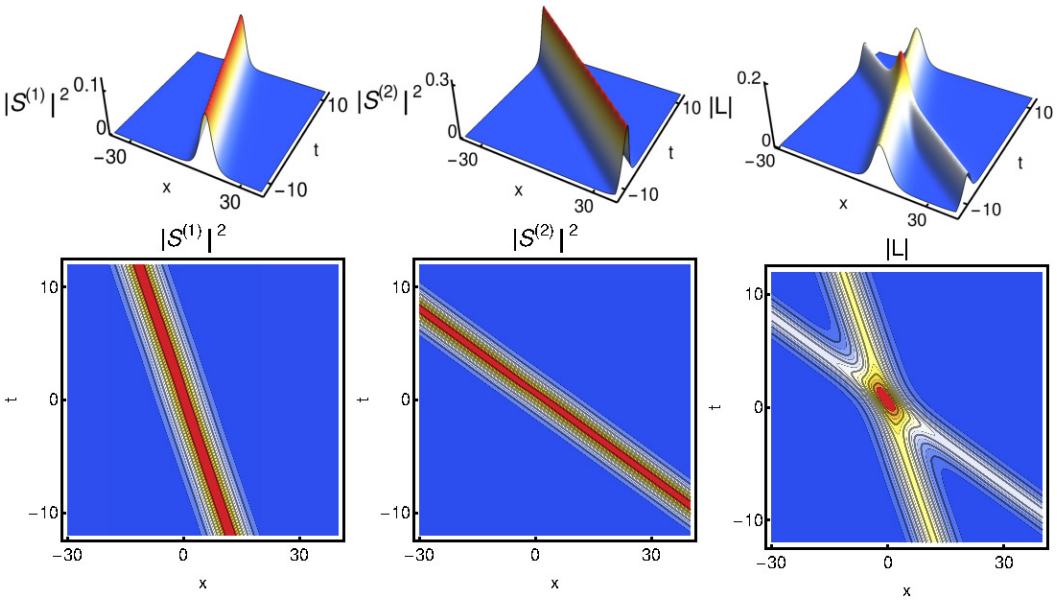

FIGURE 4.3: Nondegenerate one-soliton $(1,1,2)$ with unequal velocities. The parameter values are $k_1 = 0.25 - 0.5i$, $l_1 = 0.2 - 2i$, $\alpha_1^{(1)} = 0.45 + 0.5i$ and $\alpha_1^{(2)} = 0.5 + 0.5i$.

4.2.2 Completely nondegenerate two-soliton solution

To construct the completely nondegenerate two-soliton solution, we consider the seed solutions of the following forms,

$$\begin{aligned} g_1^{(1)} &= \alpha_1^{(1)} e^{\eta_1} + \alpha_2^{(1)} e^{\eta_2},\ \eta_1 = k_1 x + i k_1^2 t,\ \eta_2 = k_2 x + i k_2^2 t, \\ g_1^{(2)} &= \alpha_1^{(2)} e^{\xi_1} + \alpha_2^{(2)} e^{\xi_2},\ \xi_1 = l_1 x + i l_1^2 t,\ \xi_2 = l_2 x + i l_2^2 t, \end{aligned} \tag{4.23}$$

for Eqs. (4.4). Here we treat the four arbitrary constants k_1, k_2, l_1 and l_2 as distinct from one another, in general, apart from the other four distinct

complex constants $\alpha_1^{(l)}$ and $\alpha_2^{(l)}$, $l = 1, 2$. For the two-soliton solution, we find that the above seed solutions terminate the series expansions as $g^{(l)} = \epsilon g_1^{(l)} + \epsilon^3 g_3^{(l)} + \epsilon^5 g_5^{(l)} + \epsilon^7 g_7^{(l)}$, $l = 1, 2$, $f = 1 + \epsilon^2 f_2 + \epsilon^4 f_4 + \epsilon^6 f_6 + \epsilon^8 f_8$, while solving the resulting inhomogeneous linear partial differential equations recursively. The explicit Gram determinat forms of $g^{(l)}$'s and f can be written as

$$g^{(1)} = \begin{vmatrix} A_{mm'} & A_{mn} & I & \mathbf{0} & \phi_1 \\ A_{nm} & A_{nn'} & \mathbf{0} & I & \phi_2 \\ -I & \mathbf{0} & \kappa_{mm'} & \kappa_{mn} & \mathbf{0'}^T \\ \mathbf{0} & -I & \kappa_{nm} & \kappa_{nn'} & \mathbf{0'}^T \\ \mathbf{0'} & \mathbf{0'} & C_1 & \mathbf{0'} & 0 \end{vmatrix}, \; f = \begin{vmatrix} A_{mm'} & A_{mn} & I & \mathbf{0} \\ A_{nm} & A_{nn'} & \mathbf{0} & I \\ -I & \mathbf{0} & \kappa_{mm'} & \kappa_{mn} \\ \mathbf{0} & -I & \kappa_{nm} & \kappa_{nn'} \end{vmatrix} \tag{4.24}$$

$$g^{(2)} = \begin{vmatrix} A_{mm'} & A_{mn} & I & \mathbf{0} & \phi_1 \\ A_{nm} & A_{nn'} & \mathbf{0} & I & \phi_2 \\ -I & \mathbf{0} & \kappa_{mm'} & \kappa_{mn} & \mathbf{0'}^T \\ \mathbf{0} & -I & \kappa_{nm} & \kappa_{nn'} & \mathbf{0'}^T \\ \mathbf{0'} & \mathbf{0'} & \mathbf{0'} & C_2 & 0 \end{vmatrix}. \tag{4.25}$$

The various elements are defined as

$$\begin{aligned} A_{mm'} &= \frac{e^{\eta_m + \eta^*_{m'}}}{(k_m + k^*_{m'})}, \; A_{mn} = \frac{e^{\eta_m + \xi^*_n}}{(k_m + l^*_n)}, A_{nn'} = \frac{e^{\xi_n + \xi^*_{n'}}}{(l_n + l^*_{n'})}, \; A_{nm} = \frac{e^{\eta^*_n + \xi_m}}{(k^*_n + l_m)}, \\ \kappa_{mm'} &= \frac{\psi^\dagger_m \sigma \psi_{m'}}{2i(k^2_m - k^{*2}_{m'})}, \; \kappa_{mn} = \frac{\psi^\dagger_m \sigma \psi'_n}{2i(l^2_m - k^{*2}_n)}, \kappa_{nm} = \frac{\psi'^\dagger_n \sigma \psi_m}{2i(k^2_n - l^{*2}_m)}, \; \kappa_{nn'} = \frac{\psi'^\dagger_n \sigma \psi'_{n'}}{2i(l^2_n - l^{*2}_{n'})}, \\ & \qquad\qquad\qquad\qquad\qquad\qquad\qquad\qquad\qquad\qquad m, m', n, n' = 1, 2. \end{aligned}$$

The other elements are defined below:

$$\phi_1 = \begin{pmatrix} e^{\eta_1} & e^{\eta_2} \end{pmatrix}^T, \phi_2 = \begin{pmatrix} e^{\xi_1} & e^{\xi_2} \end{pmatrix}^T, \psi_j = \begin{pmatrix} \alpha_j^{(1)} & 0 \end{pmatrix}^T, \psi'_j = \begin{pmatrix} 0 & \alpha_j^{(2)} \end{pmatrix}^T,$$

$\mathbf{0}' = \begin{pmatrix} 0 & 0 \end{pmatrix}, I = \sigma = \begin{pmatrix} 1 & 0 \\ 0 & 1 \end{pmatrix}, \mathbf{0} = \begin{pmatrix} 0 & 0 \\ 0 & 0 \end{pmatrix}$ and $C_N = -\begin{pmatrix} \alpha_1^{(N)} & \alpha_2^{(N)} \end{pmatrix}$,

$j, N = 1, 2$. Note that in the above the $g^{(j)}$'s are (9×9) determinants and f is a (8×8) determinant. The collision dynamics and the structure of the nondegenerate two-solitons are characterized by eight arbitrary complex constants, $\alpha_1^{(j)}$, $\alpha_2^{(j)}$, k_j and l_j, $j = 1, 2$. The singularity of the two-soliton solution mainly depends on the function f. To get the non-singluar solution, the function f should be positive definite ($f > 0$). This restricts the imaginary parts of the wave numbers, k_{jI} and l_{jI}, $j = 1, 2$ as negative. That is $k_{jI}, l_{jI} < 0$. Further, the complete nondegenerate two-soliton solution (4.24) and (4.25) is classified as $(2, 2, 2)$-soliton solution ($k_{jI} = l_{jI}$, $j = 1, 2$) and $(2, 2, 4)$-soliton solution ($k_{jI} \neq l_{jI}$, $j = 1, 2$). We have also given the completely nondegenerate three-soliton solution in section 2.6 for the system (4.1) using the Gram-determinants.

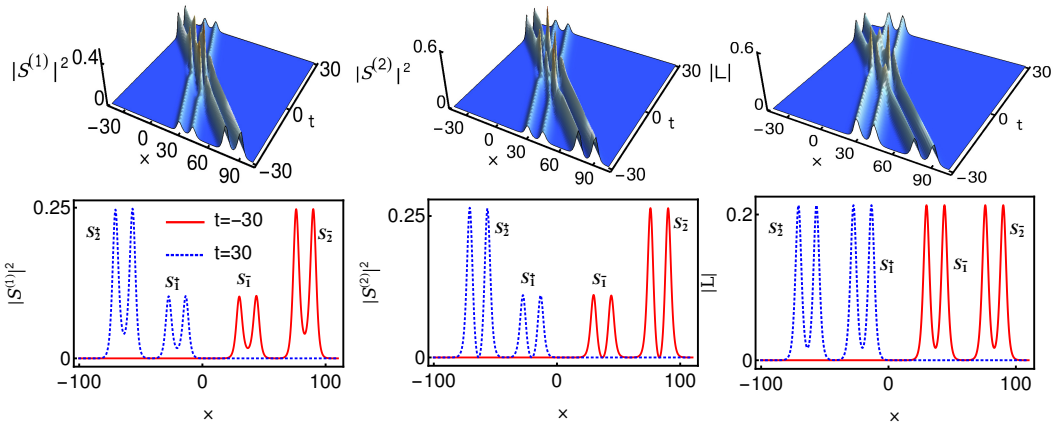

FIGURE 4.4: Elastic collision: Shape preserving collision with zero phase shift among the two symmetric double-hump solitons for the parameter values $k_1 = 0.333 - 0.5i$, $l_1 = 0.32 - 0.5i$, $k_2 = 0.333 - 1.2i$, $l_2 = 0.32 - 1.2i$, $\alpha_1^{(1)} = 0.45 + 0.5i$, $\alpha_1^{(2)} = 0.45 + 0.55i$, $\alpha_2^{(1)} = 0.45 + 0.45i$ and $\alpha_2^{(2)} = 0.45 + 0.515i$.

4.2.3 Partially nondegenerate soliton solution

We next deduce partially nondegenerate soliton solution from the complete nondegenerate two-soliton solution by imposing the wave number

restriction $k_1 = l_1$ (or $k_2 = l_2$) in Eqs. (4.24) and (4.25). Due to this restriction, the wave variables ξ_1 and η_1 are no longer independent and they get restricted as $\xi_1 = \eta_1$, while ξ_2 and η_2 continue to be distinct and independent. The Gram determinant forms of $g^{(l)}$'s and f are the same both for the partially nondegenerate soliton solution and for the complete nondegenerate two-soliton solution except that they differ in the following constituents, A_{mn}, A_{nm}, $A_{nn'}$, κ_{mn}, κ_{nm}, $\kappa_{nn'}$ and ϕ_2. Their explicit forms for the present case are given below:

$$
\begin{aligned}
A_{mn} : A_{11} &= \frac{e^{\eta_1+\eta_1^*}}{(k_1+k_1^*)},\ A_{12} = \frac{e^{\eta_1+\xi_2^*}}{(k_1+l_2^*)}, A_{21} = \frac{e^{\eta_2+\eta_1^*}}{(k_2+k_1^*)},\ A_{22} = \frac{e^{\eta_2+\xi_2^*}}{(k_2+l_2^*)},\\
A_{nm} : A_{11} &= \frac{e^{\eta_1+\eta_1^*}}{(k_1+k_1^*)},\ A_{12} = \frac{e^{\eta_1^*+\xi_2}}{(k_1^*+l_2)},\ A_{21} = \frac{e^{\eta_2^*+\eta_1}}{(k_2^*+k_1)},\ A_{22} = \frac{e^{\eta_2^*+\xi_2}}{(k_2^*+l_2)},\\
A_{nn'} : A_{11} &= \frac{e^{\eta_1+\eta_1^*}}{(k_1+k_1^*)},\ A_{12} = \frac{e^{\xi_1+\xi_2^*}}{(l_1+l_2^*)},\ A_{21} = \frac{e^{\xi_2+\eta_1^*}}{(l_2+k_1^*)},\ A_{22} = \frac{e^{\xi_2+\xi_2^*}}{(l_2+l_2^*)},\\
\kappa_{mn} : \kappa_{11} &= \frac{\psi_1^\dagger\sigma\psi_1'}{2i(k_1^2-k_1^{*2})},\ \kappa_{12} = \frac{\psi_1^\dagger\sigma\psi_2'}{2i(k_1^2-k_2^{*2})},\ \kappa_{21} = \frac{\psi_2^\dagger\sigma\psi_1'}{2i(l_2^2-k_1^{*2})},\ \kappa_{22} = \frac{\psi_2^\dagger\sigma\psi_2'}{2i(l_2^2-k_2^{*2})},\\
\kappa_{nm} : \kappa_{11} &= \frac{\psi_1'^\dagger\sigma\psi_1}{2i(k_1^2-k_1^{*2})},\ \kappa_{12} = \frac{\psi_1'^\dagger\sigma\psi_2}{2i(k_1^2-l_2^{*2})},\ \kappa_{21} = \frac{\psi_2'^\dagger\sigma\psi_1}{2i(k_2^2-k_1^{*2})},\ \kappa_{22} = \frac{\psi_2'^\dagger\sigma\psi_2}{2i(k_2^2-l_2^{*2})},\\
\kappa_{nn'} : \kappa_{11} &= \frac{\psi_1'^\dagger\sigma\psi_1'}{2i(k_1^2-k_1^{*2})},\ \kappa_{12} = \frac{\psi_1'^\dagger\sigma\psi_2'}{2i(k_1^2-l_2^{*2})},\ \kappa_{21} = \frac{\psi_2'^\dagger\sigma\psi_1'}{2i(l_2^2-k_1^{*2})},\ \kappa_{22} = \frac{\psi_2'^\dagger\sigma\psi_2'}{2i(l_2^2-l_2^{*2})},
\end{aligned}
\tag{4.26}
$$

and $\phi_2 = \begin{pmatrix} e^{\eta_1} & e^{\xi_2} \end{pmatrix}^T$. The above new class of solution permits both degenerate and nondegenerate solitons, simultanously leading to the formation of coexistence phenomenon in the present LSRI system (4.1). It is interesting to note that the coexistence phenomenon has also been discussed in the context of rogue waves [167]. The above partially nondegenerate soliton solution is described by seven arbitrary complex parameters, $\alpha_1^{(l)}$, $\alpha_2^{(l)}$, k_j, $l, j = 1, 2$ and l_2. Further, in order to get the regular (nonsingular) solution one has to fix the condition $k_{jI} < 0$, $j = 1, 2$ and $l_{2I} < 0$.

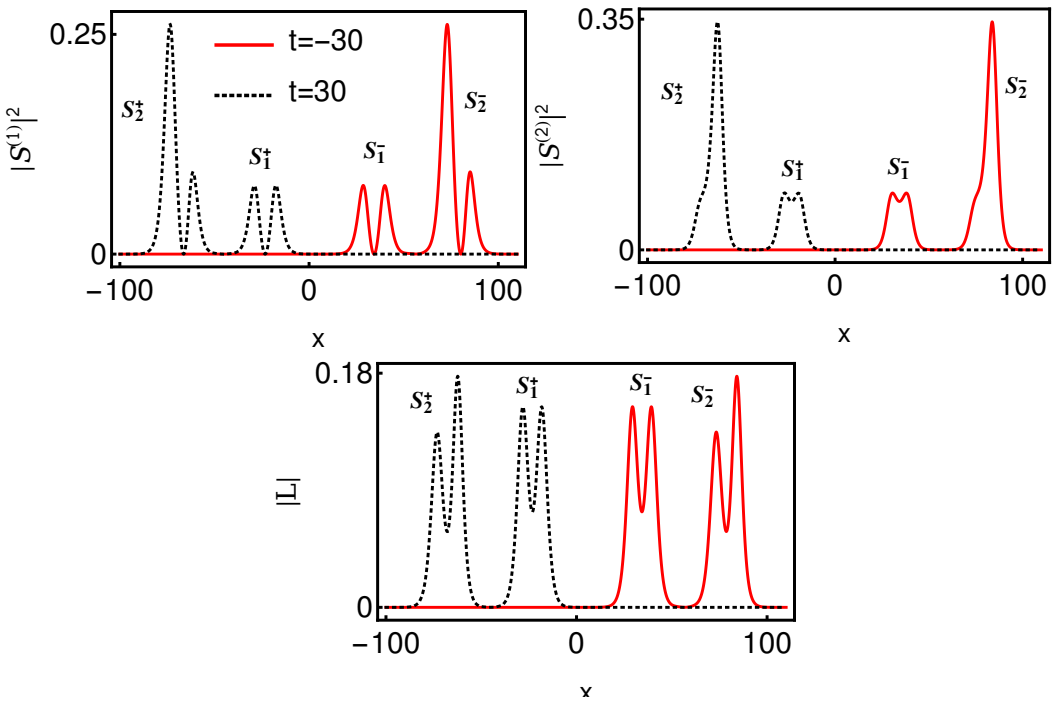

FIGURE 4.5: Elastic collision: Shape preserving collision with zero phase shift between the symmetric and asymmetric double-hump solitons. The parameter values are given in the main text.

4.3 Various types of collision dynamics of nondegenerate solitons

In this section, we analyze several interesting collision properties of the nondegenerate solitons of the system (4.1). To study the collision dynamics, it is essential to analyse the form of each of the solitons in the two soliton solution in the long time limits $t \to \pm\infty$. It can be done by performing appropriate asymptotic analysis of the completely nondegenerate two-soliton solution (4.24) and (4.25). From the analysis, we find that the nondegenerate solitons exhibit three types of collisions, namely shape preserving, shape altering and a novel shape changing collision dynamics for the cases of (i) equal velocities: $k_{jI} = l_{jI}$, $j = 1, 2$ and (ii) unequal velocities: $k_{jI} \neq l_{jI}$, $j = 1, 2$. Very interestingly, we find that the shape altering and shape changing collision scenarios belong to elastic collision which is confirmed through the following asymptotic analysis. Additionally, we observe a shape changing collision for the partially equal velocities ($k_{1I} = l_{1I}$,

$k_{2I} \neq l_{2I}$) case also. In this section, we describe the asymptotic analysis for equal velocities case only and it can be extended to unequal velocities cases as well in a similar manner. We note that the singularity condition, $k_{jI} < 0$ and $l_{jI} < 0$, enforces the two nondegenerate solitons to propagate in the same direction. Thus, the nondegenerate solitons in the system (4.1) always undergo overtaking collision. From this, it can be understood that the positive type of nonlinearity of the system (4.1) does not permit any head-on collision among the nondegenerate solitons.

4.3.1 Asymptotic analysis

We carry out an asymptotic analysis of the two-soliton solution (4.24) and (4.25) by considering the parametric choices, $k_{jI} = l_{jI} < 0$, $k_{jR}, l_{jR} > 0$, $j = 1, 2$, $k_{1I} > k_{2I}$ and $l_{1I} > l_{2I}$, which corresponds to the overtaking collision of two symmetric double-hump solitons. For other choice of parameters, similar analysis can be carried out without much difficulty. In order to deduce the asymptotic forms of nondegenerate solitons in the long time regimes, we incorporate the asymptotic behaviour of the wave variables $\eta_{jR} = k_{jR}(x - 2k_{jI}t)$ and $\xi_{jR} = l_{jR}(x - 2l_{jI}t)$, $j = 1, 2$, in the solution (4.24) and (4.25). For the above parametric choices corresponding to overtaking collision, the wave variables behave asymptotically as (i) Soliton 1 (S_1): η_{1R}, $\xi_{1R} \simeq 0$, η_{2R}, $\xi_{2R} \to \pm\infty$ as $t \pm \infty$ and (ii) Soliton 2 (S_2): η_{2R}, $\xi_{2R} \simeq 0$, η_{1R}, $\xi_{1R} \to \pm\infty$ as $t \mp \infty$. Substituting these results in Eqs. (4.24) and (4.25), we derive the following asymptotic forms of nondegenerate individual solitons.

(a) Before collision: $t \to -\infty$

Soliton 1: For soliton 1, we obtain the asymptotic forms of $S^{(l)}$, $l = 1, 2$ and L from the two-soliton solution (4.24) and 4.25) as

$$S^{(1)} \simeq \frac{4A_1^{1-}k_{1R}\sqrt{k_{1I}}e^{i\eta_{1I}}\cosh(\xi_{1R}+\phi_1^-)}{\left[a_{11}\cosh(\eta_{1R}+\xi_{1R}+\phi_1^-+\phi_2^-+c_1)+\frac{1}{a_{11}^*}\cosh(\eta_{1R}-\xi_{1R}+\phi_2^--\phi_1^-+c_2)\right]},$$
$$S^{(2)} \simeq \frac{4A_2^{1-}l_{1R}\sqrt{l_{1I}}e^{i\xi_{1I}}\cosh(\eta_{1R}+\phi_2^-)}{\left[a_{12}\cosh(\eta_{1R}+\xi_{1R}+\phi_1^-+\phi_2^-+c_1)+\frac{1}{a_{12}^*}\cosh(\eta_{1R}-\xi_{1R}+\phi_2^--\phi_1^-+c_2)\right]},$$
$$L(x,t) \simeq \frac{4}{f^2}\Big((k_{1R}^2-l_{1R}^2)+l_{1R}^2\cosh(2\eta_{1R}+2\phi_2^-+c_3)+k_{1R}^2\cosh(2\xi_{1R}+2\phi_1^-+c_4)\Big),$$
$$f = b_1\cosh(\eta_{1R}+\xi_{1R}+\phi_1^-+\phi_2^-+c_1)+b_1^{-1}\cosh(\eta_{1R}-\xi_{1R}+\phi_2^--\phi_1^-+c_2). \quad (4.27)$$

Here, $A_1^{1-} = i[\alpha_1^{(1)}/\alpha_1^{(1)^*}]^{1/2}$ and $A_2^{1-} = i[\alpha_1^{(2)}/\alpha_1^{(2)^*}]^{1/2}$. In the latter, superscript $(1-)$ represents soliton S_1 before collision and subscripts $(1,2)$ denote the two short-wave components $S^{(1)}$ and $S^{(2)}$, respectively.

Soliton 2: In this limit, the asymptotic expressions for soliton 2 in the two SW components and the long-wave component turn out to be

$$S^{(1)} \simeq \frac{4k_{2R}A_1^{2-}\sqrt{k_{2I}}e^{i(\eta_{2I}+\theta_1^-)}\cosh(\xi_{2R}+\varphi_1^-)}{\left[a_{21}\cosh(\eta_{2R}+\xi_{2R}+\varphi_1^-+\varphi_2^-+d_1)+\frac{1}{a_{21}^*}\cosh(\eta_{2R}-\xi_{2R}+\varphi_2^--\varphi_1^-+d_2)\right]},$$
$$S^{(2)} \simeq \frac{4l_{2R}A_2^{2-}\sqrt{l_{2I}}e^{i(\xi_{2I}+\theta_2^-)}\cosh(\eta_{2R}+\varphi_2^-)}{\left[a_{22}\cosh(\eta_{2R}+\xi_{2R}+\varphi_1^-+\varphi_2^-+d_1)+\frac{1}{a_{22}^*}\cosh(\eta_{2R}-\xi_{2R}+\varphi_2^--\varphi_1^-+d_2)\right]},$$
$$L(x,t) \simeq \frac{4}{f^2}\Big((k_{2R}^2-l_{2R}^2)+l_{1R}^2\cosh(2\eta_{2R}+2\varphi_1^-+d_3)+k_{2R}^2\cosh(2\xi_{2R}+2\varphi_2^-+d_4)\Big),$$
$$f = b_2\cosh(\eta_{2R}+\xi_{2R}+\varphi_1^-+\varphi_2^-+d_1)+b_2^{-1}\cosh(\eta_{2R}-\xi_{2R}+\varphi_2^--\varphi_1^-+d_2). \quad (4.28)$$

In the above, $a_{21} = \frac{(k_2^*-l_2^*)^{\frac{1}{2}}}{(k_2^*+l_2)^{\frac{1}{2}}}$, $\frac{1}{a_{21}^*} = \frac{(k_2+l_2^*)^{\frac{1}{2}}}{(k_2-l_2)^{\frac{1}{2}}}$, $a_{22} = \frac{(k_2^*-l_2^*)^{\frac{1}{2}}}{(k_2+l_2^*)^{\frac{1}{2}}}$, $\frac{1}{a_{22}^*} = \frac{(k_2^*+l_2)^{\frac{1}{2}}}{(k_2-l_2)^{\frac{1}{2}}}$,
$e^{i\theta_1^-} = \frac{(k_1-k_2)(k_1+k_2)^{\frac{1}{2}}(k_1+k_2^*)(k_2-l_1)^{\frac{1}{2}}(k_1-k_2^*)(k_2^*+l_1)^{\frac{1}{2}}}{(k_1^*-k_2^*)(k_1^*+k_2)(k_1^*+k_2^*)^{\frac{1}{2}}(k_2^*-l_1^*)^{\frac{1}{2}}(k_1^*-k_2)^{\frac{1}{2}}(k_2+l_1^*)^{\frac{1}{2}}}$,
$e^{i\theta_2^-} = \frac{(l_1-l_2)(k_1-l_2)^{\frac{1}{2}}(k_1+l_2^*)^{\frac{1}{2}}(l_1+l_2^*)(l_1+l_2)^{\frac{1}{2}}(l_1-l_2^*)^{\frac{1}{2}}}{(k_1^*-l_2^*)^{\frac{1}{2}}(l_1^*-l_2^*)(k_1^*+l_2)^{\frac{1}{2}}(l_1^*+l_2)(l_1^*+l_2^*)^{\frac{1}{2}}(l_1^*-l_2)^{\frac{1}{2}}}$,
$A_1^{2-} = [\alpha_2^{(1)}/\alpha_2^{(1)^*}]^{1/2}$, $A_2^{2-} = [\alpha_2^{(2)}/\alpha_2^{(2)^*}]^{1/2}$, $b_2 = \frac{(k_{2R}-l_{2R})^{\frac{1}{2}}}{(k_{2R}+l_{2R})^{\frac{1}{2}}}$, $d_1 = \frac{1}{2}\log\frac{(k_2^*-l_2^*)}{(k_2-l_2)}$,
$d_2 = \frac{1}{2}\log\frac{(k_2^*+l_2)}{(k_2+l_2^*)}$, $d_3 = \frac{1}{2}\log\frac{(k_2^*-l_2^*)(k_2+l_2^*)}{(k_2^*+l_2)(k_2-l_2)}$ and $d_4 = \frac{1}{2}\log\frac{(k_2^*-l_2^*)(k_2^*+l_2)}{(k_2+l_2^*)(k_2-l_2)}$.
Here, superscript $(2-)$ refers to soliton 2 (S_2) before collision.

(b) After collision: $t \to +\infty$

Soliton 1: We have deduced the following asymptotic forms of for soliton 1 in $S^{(l)}$, $l = 1,2$ and L from the two soliton solution (4.24) and 4.25) after collision as below:

$$S^{(1)} \simeq \frac{4A_1^{1+}k_{1R}\sqrt{k_{1I}}e^{i(\eta_{1I}+\theta_1^+)}\cosh(\xi_{1R}+\phi_1^+)}{\left[a_{11}\cosh(\eta_{1R}+\xi_{1R}+\phi_1^++\phi_2^++c_1)+\frac{1}{a_{11}^*}\cosh(\eta_{1R}-\xi_{1R}+\phi_2^+-\phi_1^++c_2)\right]},$$

$$S^{(2)} \simeq \frac{4A_2^{1+}l_{1R}\sqrt{l_{1I}}e^{i(\xi_{1I}+\theta_2^+)}\cosh(\eta_{1R}+\phi_2^+)}{\left[a_{12}\cosh(\eta_{1R}+\xi_{1R}+\phi_1^++\phi_2^++c_1)+\frac{1}{a_{12}^*}\cosh(\eta_{1R}-\xi_{1R}+\phi_2^+-\phi_1^++c_2)\right]},$$

$$L(x,t) \simeq \frac{4}{f^2}\Big((k_{1R}^2-l_{1R}^2)+l_{1R}^2\cosh(2\eta_{1R}+2\phi_2^++c_3)+k_{1R}^2\cosh(2\xi_{1R}+2\phi_1^++c_4)\Big),$$

$$f = b_1\cosh(\eta_{1R}+\xi_{1R}+\phi_1^++\phi_2^++c_1)+b_1^{-1}\cosh(\eta_{1R}-\xi_{1R}+\phi_2^+-\phi_1^++c_2). \quad (4.29)$$

Here, $e^{i\theta_1^+} = \frac{(k_1-k_2)(k_1-l_2)^{\frac{1}{2}}(k_1^*+k_2)(k_1^*+l_2)^{\frac{1}{2}}(k_1+k_2)^{\frac{1}{2}}(k_1^*-k_2)^{\frac{1}{2}}}{(k_1^*-k_2^*)(k_1^*-l_2^*)^{\frac{1}{2}}(k_1+k_2^*)(k_1+l_2^*)^{\frac{1}{2}}(k_1^*+k_2^*)^{\frac{1}{2}}(k_1-k_2^*)^{\frac{1}{2}}}$, $A_1^{1+} = i[\alpha_1^{(1)}/\alpha_1^{(1)^*}]^{1/2}$, $A_2^{1+} = i[\alpha_1^{(2)}/\alpha_1^{(2)^*}]^{1/2}$ and $e^{i\theta_2^+} = \frac{(l_1-l_2)(k_2-l_1)^{\frac{1}{2}}(k_2+l_1^*)^{\frac{1}{2}}(l_1^*+l_2)(l_1+l_2)^{\frac{1}{2}}(l_1^*-l_2)^{\frac{1}{2}}}{(k_2^*-l_1^*)^{\frac{1}{2}}(l_1^*-l_2^*)(k_2^*+l_1)^{\frac{1}{2}}(l_1+l_2^*)(l_1^*+l_2^*)^{\frac{1}{2}}(l_1-l_2^*)^{\frac{1}{2}}}$. In the latter, superscript (1+) represents soliton S_1 after collision and subscripts $(1,2)$ denote the two SW components $S^{(1)}$ and $S^{(2)}$, respectively.

Soliton 2: The asymptotic expressions for soliton 2 in $S^{(l)}$, $l = 1,2$ and L after collision turn out to be

$$S^{(1)} \simeq \frac{4k_{2R}A_1^{2+}\sqrt{k_{2I}}e^{i\eta_{2I}}\cosh(\xi_{2R}+\varphi_1^+)}{\left[a_{21}\cosh(\eta_{2R}+\xi_{2R}+\varphi_1^++\varphi_2^++d_1)+\frac{1}{a_{21}^*}\cosh(\eta_{2R}-\xi_{2R}+\varphi_2^+-\varphi_1^++d_2)\right]},$$

$$S^{(2)} \simeq \frac{4l_{2R}A_2^{2+}\sqrt{l_{2I}}e^{i\xi_{2I}}\cosh(\eta_{2R}+\varphi_2^+)}{\left[a_{22}\cosh(\eta_{2R}+\xi_{2R}+\varphi_1^++\varphi_2^++d_1)+\frac{1}{a_{22}^*}\cosh(\eta_{2R}-\xi_{2R}+\varphi_2^+-\varphi_1^++d_2)\right]},$$

$$L(x,t) \simeq \frac{4}{f^2}\Big((k_{2R}^2-l_{2R}^2)+l_{1R}^2\cosh(2\eta_{2R}+2\varphi_1^++d_3)+k_{2R}^2\cosh(2\xi_{2R}+2\varphi_2^++d_4)\Big),$$

$$f = b_2\cosh(\eta_{2R}+\xi_{2R}+\varphi_1^++\varphi_2^++d_1)+b_2^{-1}\cosh(\eta_{2R}-\xi_{2R}+\varphi_2^+-\varphi_1^++d_2). \quad (4.30)$$

Here, $A_1^{2+} = i[\alpha_2^{(1)}/\alpha_2^{(1)^*}]^{1/2}$, $A_2^{2+} = i[\alpha_2^{(2)}/\alpha_2^{(2)^*}]^{1/2}$. The phase constants, ϕ_j^-, ϕ_j^+, φ_j^-, φ_j^+, $j = 1,2$, appearing above are related as follows:

$$\phi_1^+ = \phi_1^- + \psi_1,\ \phi_2^+ = \phi_2^- + \psi_2,\ \varphi_1^+ = \varphi_1^- - \Psi_1,\ \varphi_2^+ = \varphi_2^- - \Psi_2, \tag{4.31}$$

where

$$\begin{aligned}
\psi_1 &= \ln \frac{|k_2 - l_1||l_1 - l_2|^2|l_1 + l_2|}{|k_2 + l_1^*||l_1 + l_2^*|^2|l_1 - l_2^*|},\ \psi_2 = \ln \frac{|k_1 - k_2|^2|k_1 + k_2||k_1 - l_2|}{|k_1 + k_2^*|^2|k_1 - k_2^*||k_1 + l_2^*|},\\
\Psi_1 &= \ln \frac{|k_1 - l_2||l_1 - l_2|^2|l_1 + l_2|}{|k_1 + l_2^*||l_1 + l_2^*|^2|l_1 - l_2^*|},\ \Psi_2 = \ln \frac{|k_2 - l_1||k_1 - k_2|^2|k_1 + k_2|}{|k_2 + l_1^*||k_1 + k_2^*|^2|k_1 - k_2^*|},\\
\phi_1^- &= \frac{1}{2}\ln \frac{(k_1 - l_1)|\alpha_1^{(2)}|^2}{2i(k_1 + l_1^*)(l_1 + l_1^*)^2(l_1 - l_1^*)},\ \phi_2^- = \frac{1}{2}\ln \frac{(l_1 - k_1)|\alpha_1^{(1)}|^2}{2i(k_1^* + l_1)(k_1 + k_1^*)^2(k_1 - k_1^*)},\\
\varphi_1^+ &= \frac{1}{2}\ln \frac{(k_2 - l_2)|\alpha_2^{(2)}|^2}{2i(k_2 + l_2^*)(l_2 + l_2^*)^2(l_2 - l_2^*)},\ \varphi_2^+ = \frac{1}{2}\ln \frac{(k_2 - l_2)|\alpha_2^{(1)}|^2}{2i(k_2^* + l_2)(k_2 + k_2^*)^2(k_2 - k_2^*)}.
\end{aligned} \tag{4.32}$$

From the above, one can easily observe that the phase terms only get changed during the collision process. As we have pointed above, the phases of each of the solitons also get changed during the collision dynamics. The total phase shift of soliton S_1 in both the SW components is calculated as

$$\begin{aligned}
\Delta\Phi_1 &= \phi_1^+ + \phi_2^+ - (\phi_1^- + \phi_2^-)\\
&= \log \frac{|k_2 - l_1||l_1 - l_2|^2|l_1 + l_2||k_1 - l_2||k_1 - k_2|^2|k_1 + k_2|}{|k_2 + l_1^*||l_1 + l_2^*|^2|l_1 - l_2^*||k_1 + l_2^*||k_1 + k_2^*|^2|k_1 - k_2^*|}.
\end{aligned} \tag{4.33}$$

Similarly the total phase shift experienced by soliton S_2 in the SW components are given by

$$\begin{aligned}
\Delta\Phi_2 &= \varphi_1^+ + \varphi_2^+ - (\varphi_1^- + \varphi_2^-)\\
&= -\log \frac{|k_2 - l_1||l_1 - l_2|^2|l_1 + l_2||k_1 - l_2||k_1 - k_2|^2|k_1 + k_2|}{|k_2 + l_1^*||l_1 + l_2^*|^2|l_1 - l_2^*||k_1 + l_2^*||k_1 + k_2^*|^2|k_1 - k_2^*|} = -\Delta\Phi_1.
\end{aligned} \tag{4.34}$$

Here, the subscript 1 and 2 in $\Delta\Phi$ denote the soliton number. The total phase shifts obtained for the SW components are the same for the LW component.

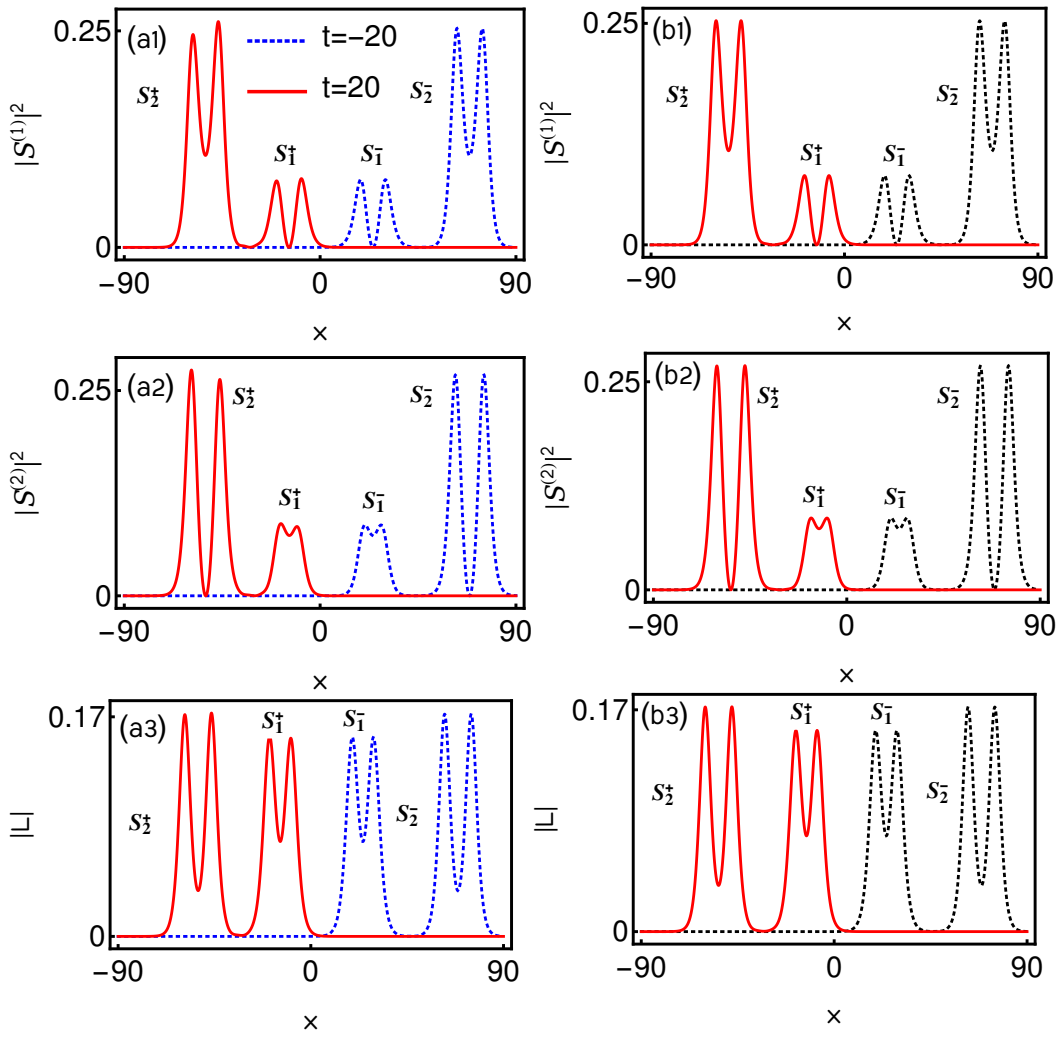

FIGURE 4.6: The column figures (a1)-(a3) represent the shape altering collision of two symmetric double-hump solitons S_1^- and S_2^- at $t = -10$ (blue dotted curves) into S_1^+ and S_2^+ at $t = +10$ (red curves) and the column figures (b1)-(b3) denote their corresponding shape preserving nature which is brought out after taking appropriate time shifts. The dotted black curves in (b1)-(b3) refer to the solitons before collision at $t = -20$, and the solitons after incorporating the appropriate finite time shifts are represented by the solid red curves. To bring back the shape preserving nature of solitons after collision we have taken the following time shifts based on Eq. (4.38): For solitons S_1 and S_2 the time shifts are performed respectively as (short wave $S^{(1)}$: $t' = 18.6525$, short wave $S^{(2)}$: $t' = 18.5791$) and ($S^{(1)}$: $t' = 20.4559$, $S^{(2)}$: $t' = 20.4266$). As far as the LW component is concerned one has to combinedly take the shifts for soliton S_1^+ ($t' = 18.6525$, $t' = 18.5791$) and soliton S_2^+ ($t' = 20.4559$, $t' = 20.4266$) in the LW component expressions (4.28) and (4.29), respectively.

4.3.2 Elastic collision: Shape-preserving, shape-altering and shape-changing collisions

The asymptotic analysis of equal velocities case ($k_{1I} = l_{1I}$ and $k_{2I} = l_{2I}$) reveals that the transition intensities, $|T_j^l|^2 = \frac{|A_j^{l+}|^2}{|A_j^{l-}|^2} = 1$, $l, j = 1, 2$, (where $A_j^{l\pm}$'s are defined in the above asymptotic analysis) always remain unimodular. Consequently, the corresponding collision among the nondegenerate solitons is always elastic in the equal velocities case. Thus, the expressions of the individual solitons should be invariant in the asymptotic time limits $t \to \pm\infty$ leading to the preservation of shapes of the nondegenerate solitons. As a result, the asymptotic expression (4.27) of soliton 1 before collision should coincide with the form (4.29). Further, to hold the elastic collision nature, the asymptotic form (4.28) of soliton 2 must also agree with Eq. (4.30). However, in view of Eq. (4.31), this is not true. Since the phase terms dramatically get varied during this collision scenario. This phase variation significantly influences the structure of the nondegenerate solitons. Therefore, to maintain the structure, the phase terms should obey the following condition:

$$\phi_j^+ = \phi_j^-, \ \varphi_j^+ = \varphi_j^-, \ j = 1, 2. \tag{4.35}$$

The above implies that the additional phase terms, ψ_j and Ψ_j, $j = 1, 2$, are equal to zero. That is

$$\psi_1 = \ln \frac{|k_2 - l_1||l_1 - l_2|^2|l_1 + l_2|}{|k_2 + l_1^*||l_1 + l_2^*|^2|l_1 - l_2^*|} = 0, \ \psi_2 = \ln \frac{|k_1 - k_2|^2|k_1 + k_2||k_1 - l_2|}{|k_1 + k_2^*|^2|k_1 - k_2^*||k_1 + l_2^*|} = 0, \tag{4.36}$$

$$\Psi_1 = \ln \frac{|k_1 - l_2||l_1 - l_2|^2|l_1 + l_2|}{|k_1 + l_2^*||l_1 + l_2^*|^2|l_1 - l_2^*|} = 0, \Psi_2 = \ln \frac{|k_2 - l_1||k_1 - k_2|^2|k_1 + k_2|}{|k_2 + l_1^*||k_1 + k_2^*|^2|k_1 - k_2^*|} = 0. \tag{4.37}$$

Physically this indicates that the nondegenerate fundamental solitons undergo shape preserving collision (or elastic collision) without a phase shift. Such a zero phase shift criterion is calculated from the above expressions (4.36) and (4.37) as

$$\frac{|k_2 + l_1^*|}{|k_2 - l_1|} - \frac{|k_1 + l_2^*|}{|k_1 - l_2|} = 0. \tag{4.38}$$

From the above, we infer that the two nondegenerate solitons pass through one another with zero phase shift whenever the criterion (4.38) (or equivalently from the phase condition Eq. (4.35)), is fulfilled by the wave numbers. This remarkable new property is not possible in the degenerate counterpart and even in the scalar nonlinear Schrödinger equation. A typical shape preserving collision with zero phase shift is demonstrated in figure 4.4. From figure 4.4, one can easily recognize that that the two symmetric double-hump solitons S_1 and S_2 are located along the lines $\eta_{1R} = k_{1R}(x - 2k_{1I}t) \simeq 0$, $\xi_{1R} = k_{1R}(x - 2k_{1I}t) \simeq 0$ and $\eta_{2R} = k_{2R}(x - 2k_{2I}t) \simeq 0$, $\xi_{2R} = k_{2R}(x - 2k_{2I}t) \simeq 0$, respectively. Around $x = 0$ they start to interact and pass through one another with almost zero phase shift. We have numerically verified this from Eq. (4.38) by calculating the value as -0.0006. It ensures that the structures (as well as phases) of the nondegenerate solitons remain constant throughout this collision process. A similar shape preserving collision scenario among the two asymmetric double-hump solitons is illustrated in figure 4.5 for the parameter values $k_1 = 0.25 - 0.5i$, $l_1 = 0.315 - 0.5i$, $k_2 = 0.25 - 1.2i$, $l_2 = 0.315 - 1.2i$, $\alpha_1^{(1)} = 0.5 + 0.5i$, $\alpha_1^{(2)} = 0.45 + 0.5i$, $\alpha_2^{(1)} = 1 + i$ and $\alpha_2^{(2)} = 0.45 + 0.5i$.

In general, the phase constants ϕ_j^+, ϕ_j^-, φ_j^+ and φ_j^-, $j = 1, 2$, do not agree with the condition (4.35) in the equal velocities case. Under this circumstance, the nondegenerate solitons undergo either shape altering collision or shape changing collision without infringing the unimodular transition intensities condition. Therefore, depending on the nature of the changes in the phase terms, the nondegenerate solitons experience slight alteration or drastic reshaping during the collision process. A typical shape altering collision is depicted in figures 4.6(a1)-(a3). To draw the figures 4.6(a1)-(a3), we fix the soliton parameters as $k_1 = 0.25 - 0.5i$, $l_1 = 0.315 - 0.5i$, $k_2 = 0.31 - 1.5i$, $l_2 = 0.28 - 1.5i$, $\alpha_1^{(1)} = 0.5 + 0.5i$, $\alpha_1^{(2)} = 0.45 + 0.5i$, $\alpha_2^{(1)} = 0.45 + 0.5i$ and $\alpha_2^{(2)} = 0.55 + 0.55i$. Then these figures show that the symmetric nature of double-hump solitons in all the three components get altered slightly into asymmetric forms after collision. However, this shape alteration can be undone, without loss of generality, by making appropriate shifts in time,

$$\left(t' = t - \frac{\psi_1}{2l_{1R}k_{1I}}, t' = t - \frac{\psi_2}{2k_{1R}k_{1I}}\right) \text{ and} \left(t' = t + \frac{\Psi_1}{2l_{2R}k_{2I}}, t' = t + \frac{\Psi_2}{2k_{2R}k_{2I}}\right) \tag{4.39}$$

in the wave variables ξ_{1R} and η_{1R} for soliton 1 and ξ_{2R} and η_{2R} for soliton 2 in the expressions (4.29) and (4.30), respectively. After effecting these time shifts in the respective asymptotic expressions, we find that the asymptotic expressions of the two nondegenerate solitons becomes identical except for unit phase factors. As a consequence, the shapes of the nondegenerate solitons are conserved asymptotically with zero phase shift thereby confirming the elastic nature of the collision. This shape preserving nature is graphically illustrated in figure 4.6(b1)-(b3).

Moreover, for $k_{1I} = l_{1I}$ and $k_{2I} = l_{2I}$, the nondegenerate solitons also exhibit a novel shape changing interaction again without violating the unity condition of the transition intensities. Very interestingly, as it is evident from Eq. (4.31), the shape changing occurs not only in the two short-wave components but it is also observed in the long-wave component as well. We display such non-trivial shape changing collision in figure 4.7(a1)-(a3) as an example, where the symmetric structure of the flattop soliton S_2 in the $S^{(1)}$ component and symmetric double-hump solitons in both the $S^{(2)}$ and L components are altered drastically as indicated by the red curves at $t = 25$. To display this figure 4.9(a1)-(a3), the parameter values are fixed as $k_1 = 0.315 - 0.5i$, $l_1 = 0.5 - 0.5i$, $k_2 = 0.45 - 1.2i$, $l_2 = 0.315 - 1.2i$, $\alpha_1^{(1)} = 0.5 + 0.5i$, $\alpha_1^{(2)} = 0.45 + 0.45i$, $\alpha_2^{(1)} = 0.45 + 0.4i$ and $\alpha_2^{(2)} = 0.65 + 0.65i$. This type of shape changing collision has not been observed earlier in the degenerate case [161]. However, as we have performed the analysis in the above case of shape altering collision, the present shape changing collision also belongs to the case of elastic collision. Thus the shape preserving nature can be retrieved by shifting the time as per Eq. (4.39). This elastic collision scenario after taking the time shifts is demonstrated in figure 4.7(b1)-(b3). Therefore, what we emphasize here is that the collision scenario among the nondegenerate solitons is always elastic regardless of the zero phase shift criterion (4.38). Further, we also demonstrate the shape changing collision in the partial velocity case $k_{1I} = l_{1I}$ and $k_{2I} \neq l_{2I}$ in figure 4.8 for the parameter values as given

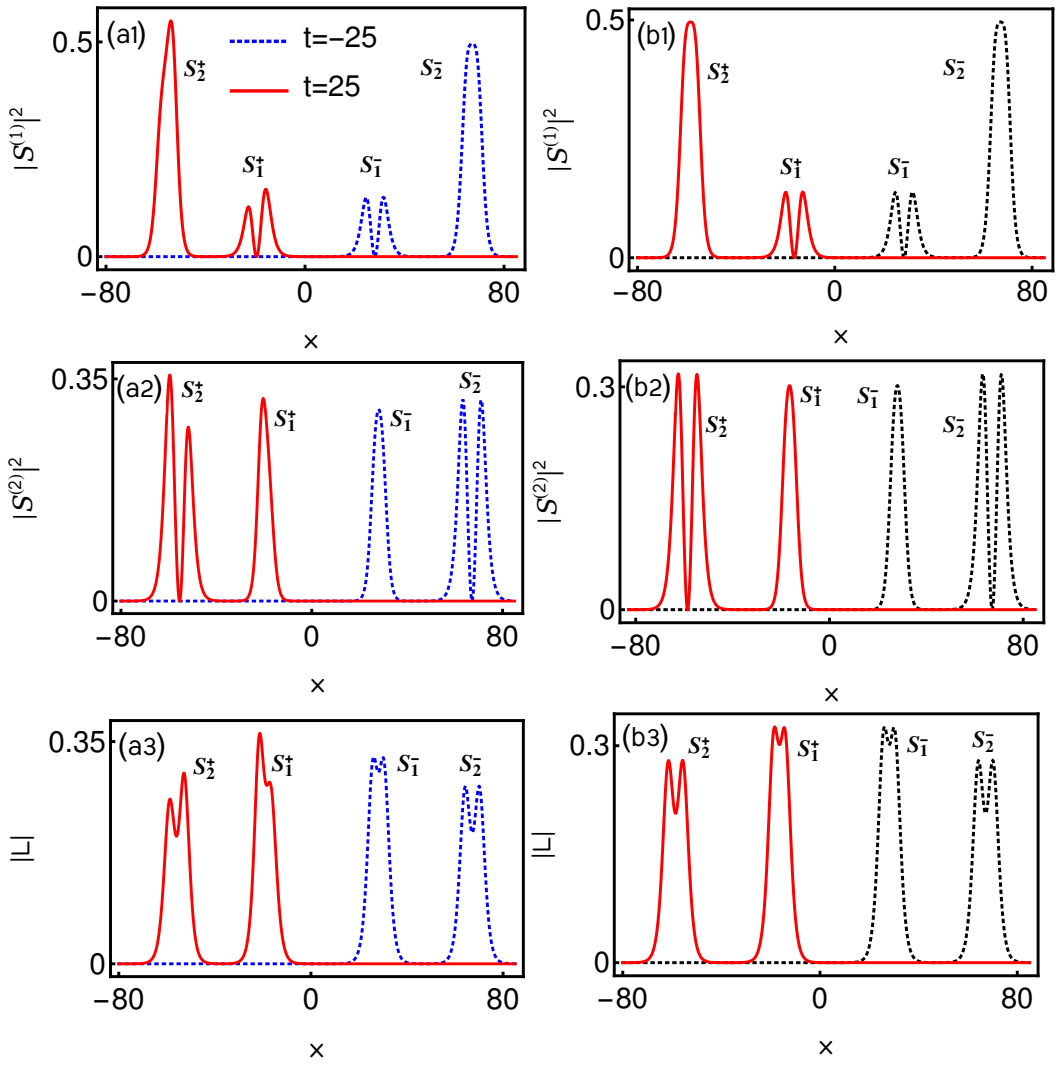

FIGURE 4.7: The column figures corresponding to (a1)-(a3) demonstrate shape changing collisions among the nondegenerate solitons whereas the figures (b1)-(b3) illustrate their corresponding shape preserving nature which is brought out after effecting the time shifts ($S^{(1)}$: $t' = 22.5772$, $S^{(2)}$: $t' = 21.962$) and ($S^{(1)}$: $t' = 26.3074$, $S^{(2)}$: $t' = 26.0926$) in the expressions (4.29) and (4.30) of both the solitons S_1 and S_2, respectively. For solitons in the LW component, one has to take the time shifts ($t' = 22.5772$, $t' = 21.962$) and ($t' = 26.3074$, $t' = 26.0926$) combinedly in Eqs. (4.29) and (4.30), respectively. In figures (b1)-(b3) black dotted curves denote the solitons before collision at $t = -25$ and the red solid line curves represent the solitons after collision with time shifts t'.

in the figure caption.

In addition to the above, the elastic collision does occur in the case of $(2, 2, 4)$-soliton solution (unequal velocities: $k_{1I} \neq l_{1I}$ and $k_{2I} \neq l_{2I}$) for the

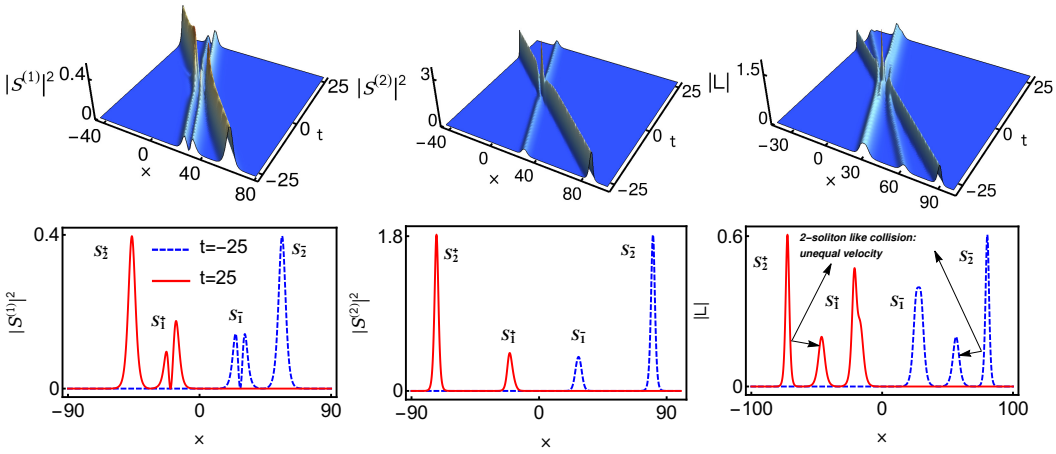

FIGURE 4.8: Shape changing collision of nondegenerate solitons in the partially equal velocity case ($k_{1I} = l_{1I}$ and $k_{2I} \neq l_{2I}$): The values are $k_1 = 0.315 - 0.5i$, $l_1 = 0.545 - 0.5i$, $k_2 = 0.315 - i$, $l_2 = 0.545 - 1.5i$, $\alpha_1^{(1)} = 0.5 + 0.5i$, $\alpha_1^{(2)} = 0.45 + 0.45i$, $\alpha_2^{(1)} = 0.5 + 0.5i$ and $\alpha_2^{(2)} = 0.45 + 0.45i$.

general choice of wave parameters. We illustrate such a collision process in figure 4.9 for the parameters given in the figure caption. From figure 4.9, it is clear that each interaction picture of the two single-humped solitons in both the SW components $S^{(1)}$ and $S^{(2)}$ reappears through the LW component. The interesting fact of this collision scenario is the structures of all the solitons do not get altered throughout the collision process thereby confirming the elastic collision.

4.4 Collision between nondegenerate and degenerate solitons: Two types of shape changing collisions

Here, we discuss the collision dynamics of nondegenerate two-soliton solution (4.24) and (4.25) under the partially nondegenerate limit $k_1 = l_1$ and $k_2 \neq l_2$. The resultant solution of the LSRI system (4.1) describes the coexistence of nondegenerate and degenerate solitons. It is of interest to study the dynamics of nondegenerate soliton in the presence of degenerate soliton and vice versa. In order to explore the underlying collision dynamics we perform an asymptotic analysis for the two-soliton solution

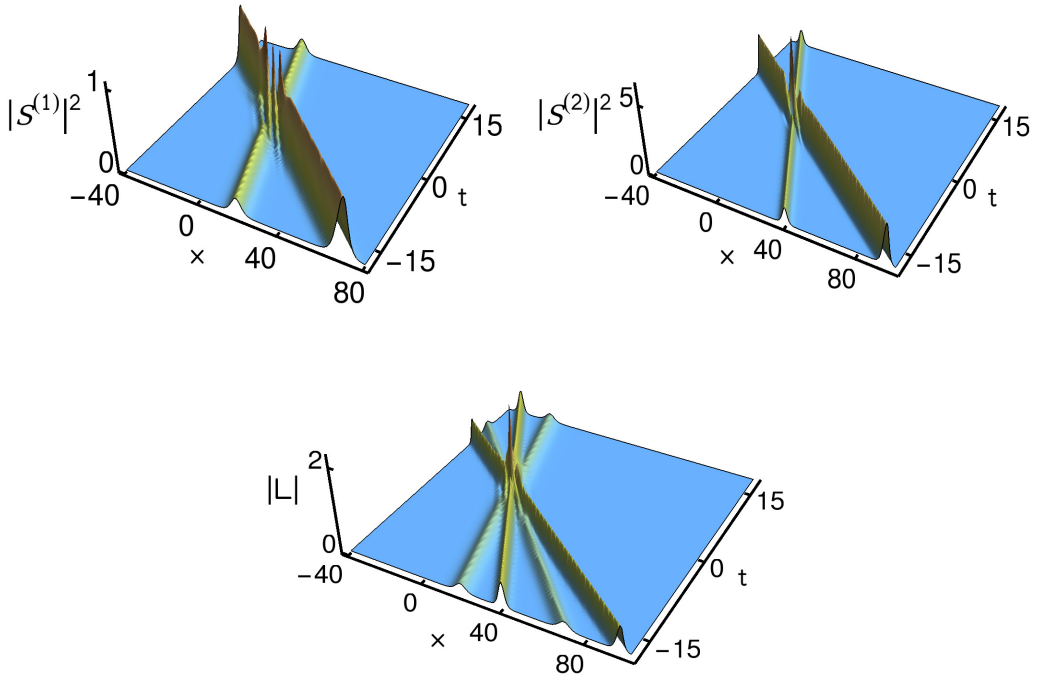

FIGURE 4.9: Elastic collision among the two nondegenerate soliton in the unequal velocities case, $k_{1I} \neq l_{1I}$ and $k_{2I} \neq l_{2I}$. The parameter values are $k_1 = 0.315 - 0.5i$, $l_1 = 0.545 - i$, $k_2 = 0.315 - 1.8i$, $l_2 = 0.545 - 2.5i$, $\alpha_1^{(1)} = 0.5 + 0.5i$, $\alpha_1^{(2)} = 0.45 + 0.45i$, $\alpha_2^{(1)} = 0.5 + 0.5i$ and $\alpha_2^{(2)} = 0.45 + 0.45i$.

(4.24) and (4.25) with the wave number restriction $k_1 = l_1$ and $k_2 \neq l_2$. By doing so, we find that the nondegenerate soliton undergoes two types of shape changing collisions. Here, we define such shape changing collisions. (i) Type-I shape changing collision is observed for the velocity condition $k_{2I} = l_{2I}$, where the initial profile structure of the nondegenerate soliton, in all the components, is either drastically changing into an asymmetric form or the initial profile structure is completely reshaped into another profile. (ii) Type-II shape changing collision is observed for the velocity choice $k_{2I} \neq l_{2I}$, where the two single-hump structured nondegenerate solitons are merged into a single-hump soliton in both the SW components while the shape of the nondegenerate soliton is preserved in the LW component. In both the collision scenarios, the degenerate soliton exhibits the usual energy exchange collision property as described in [161].

4.4.1 Asymptotic analysis

In order to explore the degenerate bright soliton collision induced shape changing behaviours of the nondegenerate soliton, we intend to analyze the partial nondegenerate two-soliton solution (4.24) and (4.25) with the elements of the Gram determinants given in Eq. (4.26) in the asymptotic limits $t \to \pm\infty$. In these limits, the resultant action provides the forms corresponding to degenerate and nondegenerate solitons. As we have pointed out in the earlier sub-section 3.1, to obtain the asymptotic forms for the present case one has to incorporate the asymptotic nature of the wave variables $\eta_{jR} = k_{jR}(t - 2k_{Ij}z)$ and $\xi_{2R} = l_{2R}(t - 2l_{2I}z)$, $j = 1, 2$, in the partially nondegenerate soliton solution. Here we note that the wave variable η_{1R} represents the degenerate soliton and η_{2R}, ξ_{2R} correspond to the nondegenerate soliton. To find the asymptotic behaviour of the above wave variables, we consider as a typical example the parametric choices, $k_{jR}, l_{2R} > 0$, $k_{jI}, l_{2I} < 0$, $j = 1, 2$, $k_{1I} > k_{2I}, l_{2I}$. For this choice, the wave variables behave asymptotically as follows: (i) degenerate bright soliton S_1: $\eta_{1R} \simeq 0$, η_{2R}, $\xi_{2R} \to \pm\infty$ as $t \to \pm\infty$ (ii) nondegenerate fundamental soliton S_2: $\eta_{2R}, \xi_{2R} \simeq 0$, $\eta_{1R} \to \pm\infty$ as $t \to \mp\infty$. By incorporating these asymptotic behaviours of the wave variables in the solution (4.24)-(4.25) with Eq. (4.26), we deduce the following asymptotic expressions for the nondegenerate and degenerate solitons.

(a) Before collision: $t \to -\infty$

Soliton 1: The asymptotic form of the degenerate soliton deduced from the partially nondegenerate soliton solution is

$$S^{(l)} \simeq \begin{pmatrix} A_1^{1-} \\ A_1^{2-} \end{pmatrix} 2k_{1R}\sqrt{k_{1I}}e^{i(\eta_{1I}+\frac{\pi}{2})}\mathrm{sech}(\eta_{1R}+\psi^-),\ l = 1, 2, \quad (4.40)$$

$$L \simeq 2k_{1R}^2\mathrm{sech}^2(\eta_{1R}+\psi^-). \quad (4.41)$$

where $A_1^{l-} = \alpha_1^{(l)}/(|\alpha_1^{(1)}|^2 + |\alpha_1^{(2)}|^2)^{1/2}$, $l = 1, 2$, $\psi^- = \frac{R}{2} = \frac{1}{2}\ln\frac{(|\alpha_1^{(1)}|^2+|\alpha_1^{(2)}|^2)}{2i(k_1+k_1^*)^2(k_1-k_1^*)}$. Here, in A_1^{l-} the subscript 1 denotes degenerate soliton S_1 and superscript

$l-$ refers to the SW components before collision.

Soliton 2: The asymptotic forms of the nondegenerate soliton S_2, which is present in both the short-wave components as well as in the long-wave component, before collision are obtained as

$$S^{(1)} \simeq \frac{1}{D_1}\left(e^{i\eta_{2I}}e^{\frac{\mu_1+\mu_3}{2}}\cosh(\xi_{2R}+\frac{\mu_3-\mu_1}{2})+e^{i\xi_{2I}}e^{\frac{\mu_2+\mu_4}{2}}\cosh(\eta_{2R}+\frac{\mu_4-\mu_2}{2})\right), \tag{4.42}$$

$$S^{(2)} \simeq \frac{1}{D_1}\left(e^{i\eta_{2I}}e^{\frac{\nu_1+\nu_3}{2}}\cosh(\xi_{2R}+\frac{\nu_3-\nu_1}{2})+e^{i\xi_{2I}}e^{\frac{\nu_2+\nu_4}{2}}\cosh(\eta_{2R}+\frac{\nu_4-\nu_2}{2})\right), \tag{4.43}$$

$$\begin{aligned} L \simeq \frac{1}{D_1^2}\Bigg(e^{\frac{\mu_5+\mu_6+\mu_7+\mu_8}{2}}\big[(k_2+k_2^*)^2\cosh(\xi_2+\xi_2^*+\frac{(\mu_7+\mu_8)-(\mu_5+\mu_6)}{2}) \\ +(l_2+l_2^*)^2\cosh(\eta_2+\eta_2^*+\frac{(\mu_6+\mu_8)-(\mu_5+\mu_7)}{2})\big]+\frac{1}{2}e^{\mu_8'} \\ +e^{\frac{\mu_5+\mu_8+\mu_9+\mu_{10}}{2}}\big[(k_2^*+l_2)^2\cosh(\eta_1+\xi_1^*+\frac{(\mu_8+\mu_{10})-(\mu_5+\mu_9)}{2}) \\ +(k_2+l_2^*)^2\cosh(\xi_2+\eta_2^*+\frac{(\mu_8+\mu_9)-(\mu_5+\mu_{10})}{2})\big] \\ +e^{\frac{\mu_6+\mu_7+\mu_9+\mu_{10}}{2}}\big[(k_2-l_2)^2\cosh(\eta_2^*-\xi_2^*+\frac{(\mu_6+\mu_9)-(\mu_7+\mu_{10})}{2}) \\ +(k_2^*-l_2^*)^2\cosh(\eta_2-\xi_2+\frac{(\mu_6+\mu_{10})-(\mu_9+\mu_7)}{2})\big]\Bigg), \end{aligned} \tag{4.44}$$

$$\begin{aligned} D_1 = e^{\frac{\mu_5+\mu_8}{2}}\cosh(\eta_{2R}+\xi_{2R}+\frac{\mu_8-\mu_5}{2})+e^{\frac{\mu_9+\mu_{10}}{2}}\cosh(i(\eta_{2I}-\xi_{2I})+\frac{\mu_{10}-\mu_9}{2}) \\ +e^{\frac{\mu_6+\mu_7}{2}}\cosh(\eta_{2R}-\xi_{2R}+\frac{\mu_6-\mu_7}{2}). \end{aligned} \tag{4.45}$$

Here, $A_2^{1-} = [\alpha_2^{(1)}/\alpha_2^{(1)^*}]^{1/2}$, $A_2^{2-} = [\alpha_2^{(2)}/\alpha_2^{(2)^*}]^{1/2}$. In the latter, the superscript $l-$, $l = 1, 2$, denotes the SW components $S^{(1)}$ and $S^{(2)}$ before collision and the subscript 2 refers the nondegenerate soliton S_2.

(b) After collision: $t \to +\infty$

Soliton 1: In this limit, the asymptotic forms for the degenerate soliton S_1 after collision are deduced as

$$S^{(l)} \simeq \begin{pmatrix} A_1^{1+} \\ A_2^{1+} \end{pmatrix} 2k_{1R}\sqrt{k_{1I}}e^{i(\eta_{1I}+\theta_l^+ +\frac{\pi}{2})}k_{1R}\mathrm{sech}(\eta_{1R}+\psi^+),\ l=1,2, \quad (4.46)$$

$$L \simeq 2k_{1R}^2\mathrm{sech}^2(\eta_{1R}+\psi^+). \quad (4.47)$$

where $A_1^{1+} = \alpha_1^{(1)}/(|\alpha_1^{(1)}|^2+\chi|\alpha_1^{(2)}|^2)^{1/2}$, $A_1^{2+} = \alpha_1^{(1)}/(|\alpha_1^{(1)}|^2\chi^{-1}+|\alpha_1^{(2)}|^2)^{1/2}$,
$\chi = (|k_1-l_2|^2|k_1+k_2^*|^2|k_1+l_2|^2|k_1-k_2^*|^2)/(|k_1-k_2|^2|k_1+l_2^*|^2|k_1+k_2|^2|k_1-l_2^*|^2)$,

$$e^{i\theta_1^+} = \frac{(k_1-k_2)(k_1^*+k_2)(k_1-l_2)^{\frac{1}{2}}(k_1^*+l_2)^{\frac{1}{2}}(k_1+k_2)^{\frac{1}{2}}(k_1^*+k_2)}{(k_1^*-k_2^*)(k_1+k_2^*)(k_1^*-l_2^*)^{\frac{1}{2}}(k_1+l_2^*)^{\frac{1}{2}}(k_1^*+k_2^*)^{\frac{1}{2}}(k_1+k_2^*)},$$

$$e^{i\theta_2^+} = \frac{(k_1-k_2)^{\frac{1}{2}}(k_1^*+k_2)^{\frac{1}{2}}(k_1-l_2)(k_1^*+l_2)(k_1+l_2)^{\frac{1}{2}}(k_1^*-l_2)^{\frac{1}{2}}}{(k_1^*-k_2^*)^{\frac{1}{2}}(k_1+k_2^*)^{\frac{1}{2}}(k_1^*-l_2^*)(k_1+l_2^*)(k_1^*+l_2^*)^{\frac{1}{2}}(k_1-l_2^*)^{\frac{1}{2}}}$$

and $\psi^+ = \frac{1}{2}\ln\frac{|k_1-k_2|^2|k_1-l_2|^2\hat{\Lambda}_3}{2i(k_1-k_1^*)(k_1+k_1*)^2|k_1-k_2^*|^2|k_1-l_2^*|^2|k_1+l_2^*|^2}$. Here, $l+$ in A_1^{l+}, $l=1,2$, refers to SW components after collision and the subscript 1 denotes the degenerate soliton S_1.

Soliton 2: Similarly the asymptotic expression for the nondegenerate soliton S_2 after collision deduced from the soliton solution (4.24) and (4.25) with the elements given in Eq. (4.26) is

$$S^{(1)} \simeq \frac{4k_{2R}\sqrt{k_{2I}}A_1^{2+}e^{i(\eta_{2I}+\frac{\pi}{2})}\cosh(\xi_{2R}+\frac{\lambda_1}{2})}{\left[a_{21}\cosh(\eta_{2R}+\xi_{2R}+\frac{\lambda_2}{2})+\frac{1}{a_{21}^*}\cosh(\eta_{2R}-\xi_{2R}+\frac{\lambda_3}{2})\right]}, \quad (4.48)$$

$$S^{(2)} \simeq \frac{4l_{2R}\sqrt{l_{2I}}A_2^{2+}e^{i(\xi_{2I}+\frac{\pi}{2})}\cosh(\eta_{2R}+\frac{\lambda_4}{2})}{\left[a_{22}\cosh(\eta_{2R}+\xi_{2R}+\frac{\lambda_2}{2})+\frac{1}{a_{22}^*}\cosh(\eta_{2R}-\xi_{2R}+\frac{\lambda_3}{2})\right]}, \quad (4.49)$$

$$L \simeq \frac{4}{D_2^2}\Bigg(k_{2R}^2\cosh(2\xi_{2R}+\frac{\lambda_4+\lambda_3-\lambda_2}{2})+\frac{1}{2}e^{\lambda_4'-(\frac{\lambda_4+\lambda_2+\lambda_3}{2})} + l_{2R}^2\cosh(2\eta_{2R}+\frac{\lambda_2+\lambda_4-\lambda_3}{2})\Bigg), \quad (4.50)$$

$$D_2 = e^{\frac{\lambda_4}{2}}\cosh(\eta_{2R}+\xi_{2R}+\frac{\lambda_4}{2})+e^{\frac{\lambda_2+\lambda_3}{2}}\cosh(\eta_{2R}-\xi_{2R}+\frac{\lambda_2-\lambda_3}{2}),$$

$$e^{\lambda_4'} = 4(k_{2R}+l_{2R})^2e^{\lambda_4}+4(k_{2R}-l_{2R})^2e^{\lambda_2+\lambda_3}, \quad (4.51)$$

where $\lambda_1 = \ln \frac{(k_2-l_2)|\alpha_2^{(2)}|^2}{2i(l_2-l_2^*)(l_2+l_2^*)^2(k_2+l_2^*)}$, $\lambda_2 = \ln \frac{|k_2-l_2|^2|\alpha_2^{(1)}|^2|\alpha_2^{(2)}|^2}{(2i)^2|k_2+l_2^*|^2(k_2-k_2^*)(l_2-l_2^*)(k_2+k_2^*)^2(l_2+l_2^*)^2}$,
$\lambda_3 = \ln \frac{|\alpha_2^{(1)}|(l_2-l_2^*)(l_2+l_2^*)^2}{|\alpha_2^{(2)}|(k_2-k_2^*)(k_2+k_2^*)^2}$, $\lambda_4 = \ln \frac{(l_2-k_2)|\alpha_2^{(1)}|^2}{2i(k_2-k_2^*)(k_2+k_2^*)^2(k_2^*+l_2)}$,
$A_2^{1+} = [\alpha_2^{(1)}/\alpha_2^{(1)^*}]^{1/2}$, $A_2^{2+} = i[\alpha_2^{(2)}/\alpha_2^{(2)^*}]^{1/2}$.

The explicit forms of all the other constants are given below.

$$e^{\mu_1} = \frac{i(k_1-k_2)\alpha_2^{(1)}\hat{\Lambda}_1}{2(k_1-k_1^*)(k_1+k_1^*)^2(k_1^*-k_2)(k_1^*+k_2)^2},\ e^{\mu_2} = \frac{i(k_1-l_2)\alpha_1^{(1)}\alpha_1^{(2)*}\alpha_2^{(2)}}{2(k_1+k_1^*)(k_1^*-l_2)(k_1^*+l_2)^2},$$

$$e^{\mu_3} = \frac{i(k_1-k_2)(k_2-l_2)|k_1-l_2|^2\alpha_2^{(1)}|\alpha_2^{(2)}|^2\hat{\Lambda}_2 e^{R_4}}{2(k_1-k_1^*)(k_1+k_1^*)^2(k_1^*-k_2)(k_1^*+k_2)^2|k_1-l_2^*|^2|k_1+l_2^*|^4(k_2+l_2^*)},$$

$$e^{\mu_4} = -\frac{i(k_1-k_2)^2(k_1+k_2)(k_1^*-k_2^*)(k_1-l_2)(k_2-l_2)\alpha_1^{(1)}\alpha_1^{(2)*}\alpha_2^{(2)}e^{R_5}}{2(k_1+k_1^*)(k_1^*+k_2)(k_1-k_2^*)(k_1^*-l_2)(k_2^*+l_2)(k_1^*+l_2)^2},$$

$$e^{\mu_5} = \frac{\hat{\Lambda}_4}{2i(k_1-k_1^*)(k_1+k_1^*)^2},\ e^{\mu_6} = \frac{i|k_1-k_2|^2\hat{\Lambda}_5 e^{R_5}}{2(k_1-k_1^*)(k_1+k_1^*)^2|k_1-k_2^*|^2|k_1+k_2^*|^4},$$

$$e^{\mu_7} = -\frac{i|k_1-l_2|^2\hat{\Lambda}_6 e^{R_4}}{2(k_1-k_1^*)(k_1+k_1^*)^2|k_1-l_2^*|^2|k_1+l_2^*|^4},\ \hat{\Lambda}_4 = \left(|\alpha_2^{(1)}|^2+|\alpha_2^{(2)}|^2\right),$$

$$e^{\mu_8} = -\frac{i|k_1-k_2|^2|k_1-l_2|^2|k_2-l_2|^2\hat{\Lambda}_3 e^{R_4+R_5}}{2(k_1-k_1^*)(k_1+k_1^*)^2|k_1-k_2^*|^2|k_1+k_2^*|^4|k_1-l_2^*|^2|k_1+l_2^*|^4|k_2+l_2^*|^2},$$

$$e^{\mu_9} = -\frac{(k_1^*-k_2^*)(k_1-l_2)\alpha_1^{(1)}\alpha_1^{(2)*}\alpha_2^{(1)*}\alpha_2^{(2)}}{4(k_1+k_1^*)(k_1-k_2^*)(k_1+k_2^*)^2(k_1^*-l_2)(k_1^*+l_2)^2(k_2^*+l_2)},$$

$$e^{\mu_{10}} = -\frac{(k_1-k_2)(k_1^*-l_2^*)\alpha_1^{(1)*}\alpha_1^{(2)}\alpha_2^{(1)}\alpha_2^{(2)*}}{4(k_1+k_1^*)(k_1^*-k_2)(k_1^*+k_2)^2(k_1-l_2^*)(k_1+l_2^*)^2(k_2+l_2^*)},$$

$$e^{\nu_1} = \frac{i(k_1-k_2)\alpha_1^{(1)*}\alpha_1^{(2)}\alpha_2^{(1)}}{2(k_1+k_1^*)(k_1^*-k_2)(k_1^*+k_2)^2},\ e^{\nu_2} = \frac{i(k_1-l_2)\alpha_2^{(2)}\hat{\Lambda}_7}{2(k_1-k_1^*)(k_1+k_1^*)^2(k_1^*-l_2)(k_1^*+l_2)^2},$$

$$e^{\nu_3} = \frac{i(k_1-k_2)(k_1-l_2)^2(k_2-l_2)(k_1+l_2)(k_1^*-l_2^*)\alpha_1^{(1)*}\alpha_1^{(2)}\alpha_2^{(1)}e^{R_4}}{2(k_1+k_1^*)(k_1^*-k_2)(k_1^*+k_2)^2(k_1^*+l_2)(k_1-l_2^*)(k_1+l_2^*)^2(k_2+l_2^*)},$$

$$e^{\nu_4} = -\frac{i|k_1-k_2|^2(k_1-l_2)(k_2-l_2)\alpha_2^{(2)}\hat{\Lambda}_8 e^{R_5}}{2(k_1-k_1^*)(k_1+k_1^*)^2|k_1-k_2^*|^2|k_1+k_2^*|^4(k_1^*-l_2)(k_1^*+l_2)^2(k_2^*+l_2)},$$

$\hat{\Lambda}_1 = \left(\varrho_{12}|\alpha_1^{(1)}|^2+\hat{\varrho}_{12}^*|\alpha_1^{(2)}|^2\right)$, $\hat{\Lambda}_2 = \left(\varrho_{12}|\bar{\gamma}_{12}|^2|\alpha_1^{(1)}|^2+\hat{\varrho}_{12}^*|\gamma_{12}|^2|\alpha_1^{(2)}|^2\right)$,
$\hat{\Lambda}_3 = \left(|\varrho_{12}|^2|\bar{\gamma}_{12}|^2|\alpha_1^{(1)}|^2+|\hat{\varrho}_{12}^*|^2|\gamma_{12}|^2|\alpha_1^{(2)}|^2\right)$, $\hat{\Lambda}_5 = \left(|\varrho_{12}|^2|\alpha_1^{(1)}|^2+|\hat{\varrho}_{12}^*|^2|\alpha_1^{(2)}|^2\right)$,
$\hat{\Lambda}_6 = \left(|\bar{\gamma}_{12}|^2|\alpha_1^{(1)}|^2+|\gamma_{12}|^2|\alpha_1^{(2)}|^2\right)$, $\hat{\Lambda}_7 = \left(\bar{\gamma}_{12}|\alpha_1^{(1)}|^2+\gamma_{12}|\alpha_1^{(2)}|^2\right)$,
$\hat{\Lambda}_8 = \left(|\varrho_{12}|^2\bar{\gamma}_{12}|\alpha_1^{(1)}|^2+|\hat{\varrho}_{12}^*|^2\gamma_{12}|\alpha_1^{(2)}|^2\right)$, $\varrho_{12} = (k_1^2-k_2^2)$, $\hat{\varrho}_{12} = (k_1^2-k_2^{*2})$,
$\gamma_{12} = (k_1^2-l_2^2)$, $\bar{\gamma_{12}} = (k_1^2-l_2^{*2})$.

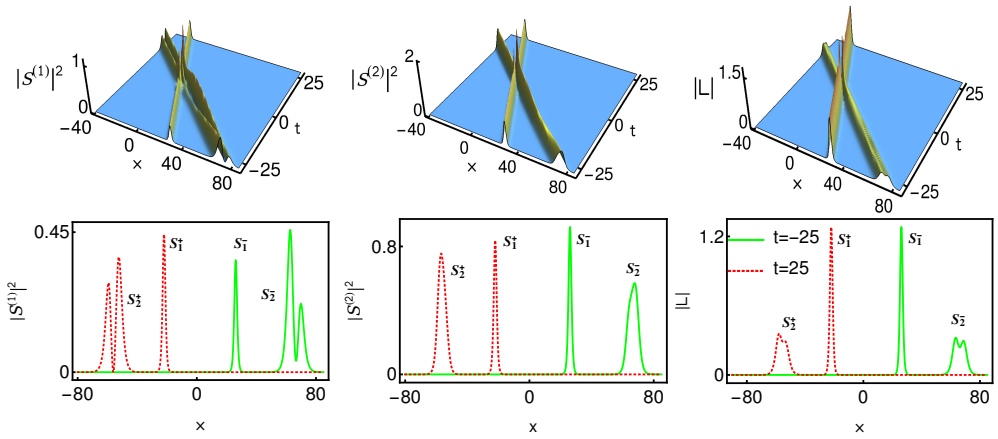

FIGURE 4.10: Type-I shape changing collision between degenerate soliton and nondegenerate soliton: To draw this figure the parameter values are fixed as follows: $k_1 = l_1 = 0.8 - 0.5i$, $k_2 = 0.315 - 1.2i$, $l_2 = 0.5 - 1.2i$, $\alpha_1^{(1)} = 0.5$, $\alpha_1^{(2)} = 0.8$, $\alpha_2^{(1)} = 0.5 + 0.5i$ and $\alpha_2^{(2)} = 0.45 + 0.45i$.

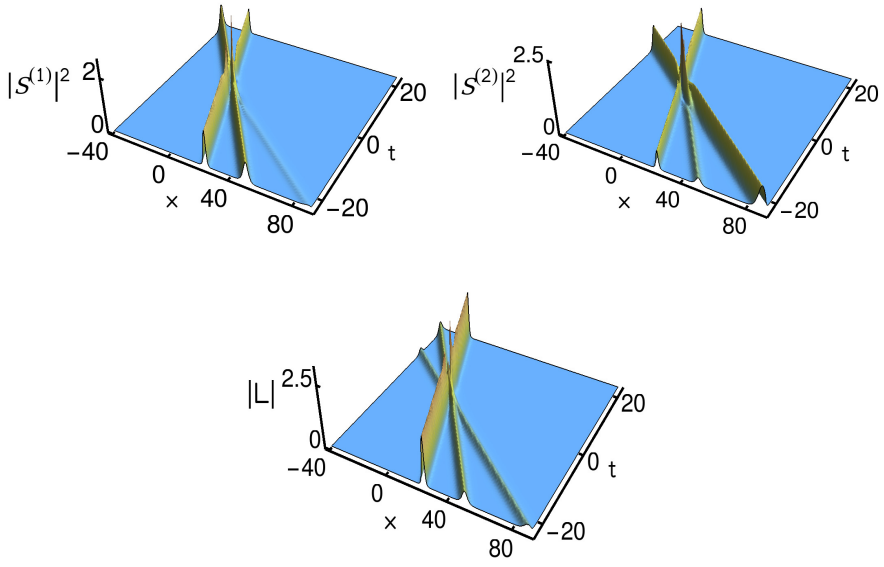

FIGURE 4.11: Type-II shape changing collision between degenerate soliton and nondegenerate soliton: To illustrate this collision we fix the complex parameter values as follows: $k_1 = l_1 = 1 - 0.5i$, $k_2 = 0.35 - 1.8i$, $l_2 = 0.5 - i$, $\alpha_1^{(1)} = 1$, $\alpha_1^{(2)} = 0.7$, $\alpha_2^{(1)} = 0.8$ and $\alpha_2^{(2)} = 0.6$.

4.4.2 Degenerate soliton collision induced shape changing property of nondegenerate soliton

As we have defined earlier, the coexisting solitons (both degenerate and nondegenerate) undergo Type-I and Type-II shape changing collisions corresponding to two distinct velocity conditions $k_{2I} = l_{2I}$ and $k_{2I} \neq l_{2I}$, respectively. In both these collision scenarios, the degenerate bright soliton strongly affects the structure of nondegenerate soliton as it is ensured from the above asymptotic analysis. As a result, the initial structure of the nondegenerate soliton S_2 is varied to a different of geometrical structure. A typical Type-I shape changing collision is depicted in figure 4.10 for $k_{2I} = l_{2I}$. In figure 4.10, it is true that the degenerate soliton S_1 undergoes energy sharing collision among the two SW components only while it interacts with the nondegenerate soliton S_2 as it has been shown in the pure degenerate case [161].

In the long-wave component, we observe elastic collision only when the degenerate soliton even collides with another class of asymmetric double-humped nondegenerate soliton. During such enegy sharing collision of the degenerate soliton, the polarization constants of SW components $A_1^{l-} = \alpha_1^{(l)}/(|\alpha_1^{(1)}|^2 + |\alpha_1^{(2)}|^2)^{1/2}, l = 1, 2$, change into $A_1^{1+} = \alpha_1^{(1)}/(|\alpha_1^{(1)}|^2 + \chi|\alpha_1^{(2)}|^2)^{1/2}$, $A_1^{2+} = \alpha_1^{(2)}/(|\alpha_1^{(1)}|^2\chi^{-1} + |\alpha_1^{(2)}|^2)^{1/2}$, where $\chi = (|k_1 - l_2|^2|k_1 + k_2^*|^2|k_1 + l_2|^2|k_1 - k_2^*|^2)/(|k_1 - k_2|^2|k_1 + l_2^*|^2|k_1 + k_2|^2|k_1 - l_2^*|^2)$. Meanwhile, the amplitude of the soliton S_1 in the long-wave component remains unchanged except for a finite phase shift. In contrast to the degenerate soliton S_1, the profile structure of the nondegenerate fundamental soliton S_2 gets dramatically altered during the collision processes as it is evident from figure 4.10. From figure 4.10, one can observe that the initial set of asymmetric double-hump profiles in the short-wave component $S^{(1)}$ and in the long-wave component L get transformed into another set of asymmetric double-hump profiles with a finite phase shift. However, in the second short-wave component, the soliton S_2 switches its asymmetric flattop profile into a single-hump profile with an enhancement of energy along with a phase shift. From the asymptotic forms, we identify that the relative separation distance or the phase terms are not maintained during this special kind of interaction.

Next, we display the Type-II shape-changing collision in figure 4.11 for $k_{2I} \neq l_{2I}$, where the degenerate soliton S_1 undergoes usual energy sharing collision as expected. However, the nondegenerate soliton S_2 exhibits unusual collision property. From figure 4.11, one can immediately notice that two single-hump solitons appear in the two short-wave components $S^{(l)}$, $l = 1, 2$, under the velocity condition $k_{2I} \neq l_{2I}$ apart from the appearance two similar solitons in the long-wave component. We do not come across the appearance of such two single-hump solitons in the short-wave components in the case of one-soliton, where a single-hump profile only emerged in both the $S^{(l)}$ components at $k_{1I} \neq l_{1I}$ (one can confirm this from figure 4.3). We also notice that the small amplitude soliton structure, in both the SW components, disappears after colliding with the degenerate soliton S_1 whereas the energy of the larger amplitude soliton is enhanced further. In other words, the two single-humped structures, in both the SW components, are merged during the collision. After the collision, they get combined into a single-hump soliton. However, very interestingly the two single-humped nondegenerate structure in the LW component propagates without any distortion thereby confirming the elastic collision nature. To characterize both Type-I and Type-II shape changing collisions, one can calculate the corresponding transition amplitudes. For both the collision scenarios, the explicit forms of the transition amplitudes turn out to be

$$T_1^1 = \frac{(|\alpha_1^{(1)}|^2 + |\alpha_1^{(2)}|^2)^{1/2}}{(|\alpha_1^{(1)}|^2 + \chi|\alpha_1^{(2)}|^2)^{1/2}}, \; T_1^2 = \frac{(|\alpha_1^{(1)}|^2 + |\alpha_1^{(2)}|^2)^{1/2}}{(|\alpha_1^{(1)}|^2\chi^{-1} + |\alpha_1^{(2)}|^2)^{1/2}}, \tag{4.52}$$

where $\chi = (|k_1 - l_2|^2|k_1 + k_2^*|^2|k_1 + l_2|^2|k_1 - k_2^*|^2)/(|k_1 - k_2|^2|k_1 + l_2^*|^2|k_1 + k_2|^2|k_1 - l_2^*|^2)$. In general, the value of χ is not equal to one. Consequently the transition amplitudes T_1^1 and T_1^2 are not unimodular. In this situation, one always comes across shape changing collision. The standard elastic collision can occur when $\chi = 1$, where the quantities T_1^1 and T_1^2 are equal to unity. We point out that one can also calculate explicitly the position shift that occurred during the collision between the degenerate and nondegenerate solitons. We wish to emphasize here that to the best of our knowledge the collision scenarios discussed above have not been reported

elsewhere in the literature for the (1+1)-dimensional two component LSRI system (4.1).

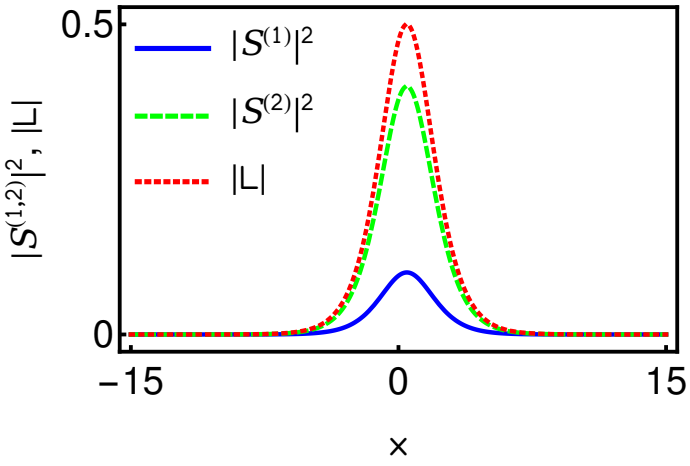

FIGURE 4.12: Single-humped degenerate fundamental soliton: $k_1 = 0.5 - 0.5i$, $\alpha_1^{(1)} = 0.5$ and $\alpha_1^{(2)} = 1$.

4.5 Degenerate soliton solutions and their collision dynamics

Here, we provide the minimal details about the already known class of degenerate soliton solutions and the underlying collision property, reported in Ref. [161] for Eq. (4.1), in order to clearly distinguish the corresponding dynamics from the dynamics of nondegenerate soliton solution (4.10)-(4.12) presented in this paper. The energy exchanging collision exhibiting degenerate fundamental bright soliton solution can be extracted from the nondegenerate one-soliton solution Eqs. (4.10)-(4.12) by imposing the restriction $k_1 = l_1$ in it. As a consequence of this constraint, the seed solutions (4.3) get restricted as $g_1^{(1)} = \alpha_1^{(1)} e^{\eta_1}$, $g_1^{(2)} = \alpha_1^{(2)} e^{\eta_1}$, $\eta_1 = k_1 x + i k_1^2 t$. This results in the degenerate one-soliton solution of the form,

$$S^{(l)} = 2A_l k_{1R} \sqrt{k_{1I}} e^{i(\eta_{1I} + \frac{\pi}{2})} \text{sech}(\eta_{1R} + \frac{R}{2}), \; L = 2k_{1R}^2 \text{sech}^2(\eta_{1R} + \frac{R}{2}). \tag{4.53}$$

Here, $A_l = \frac{\alpha_1^{(l)}}{\sqrt{|\alpha_1^{(1)}|^2 + |\alpha_1^{(2)}|^2}}$, $l = 1, 2$, $e^R = -\frac{(|\alpha_1^{(1)}|^2 + |\alpha_1^{(2)}|^2)}{16 k_{1R}^2 k_{1I}}$, $\eta_{1R} = k_{1R}(x - 2k_{1I}t)$, $\eta_{1I} = k_{1I}x + (k_{1R}^2 - k_{1I}^2)t$. In contrast to the nondegenerate soliton,

the above degenerate soliton always propagates in all the components with identical velocity $2k_{1I}$. This is because of the presence of a single complex wave number k_1 in the solution (4.53). It leads to single-hump profiles only in all the three components as we have shown in figure 4.12. The amplitudes of the degenerate soliton in the SW components and the long-wave component are $2A_l k_{1R}\sqrt{k_{1I}}$ and $2k_{1R}^2$, respectively. The central position of the soliton (for all the components) is $\frac{R}{2}$.

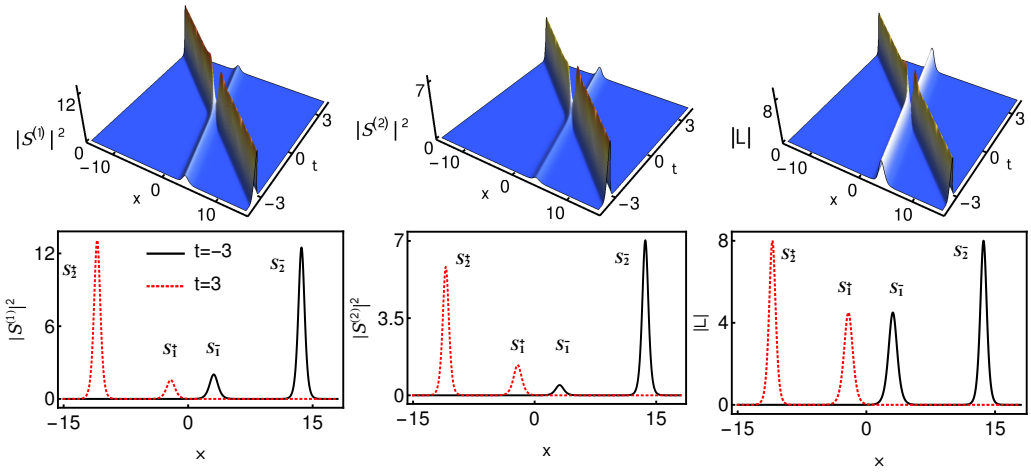

FIGURE 4.13: Energy sharing collision of two degenerate solitons: $k_1 = 1.5 - 0.5i$, $k_2 = 2 - 2i$, $\alpha_1^{(1)} = 2.5$, $\alpha_1^{(2)} = 1.2$, $\alpha_2^{(1)} = 0.9$ and $\alpha_2^{(2)} = 0.6$.

The degenerate two-soliton solution of the system (4.1) was reported in Ref. [161] by considering the seed solutions

$$g_1^{(l)} = \alpha_1^{(l)} e^{\eta_1} + \alpha_2^{(l)} e^{\eta_2},\ \eta_j = k_j x + i k_j^2 t,\ l, j = 1, 2. \tag{4.54}$$

On the other hand, it can be captured from the nondegenerate two-soliton solution (4.24) and (4.25) by imposing the restrictions $k_1 = l_1$ and $k_2 = l_2$. The resultant Gram determinat forms of the degenerate two-soliton solution contains the following elements in Eqs. (4.23),

$$\begin{aligned} A_{mm'} &= \frac{e^{\eta_m + \eta_{m'}^*}}{(k_m + k_{m'}^*)} = A_{mn} = A_{nm} = A_{nn'},\ \phi_1 = \phi_2 = \begin{pmatrix} e^{\eta_1} & e^{\eta_2} \end{pmatrix}^T, \\ \kappa_{mm'} &= \frac{\psi_m^\dagger \sigma \psi_{m'}}{2i(k_m^2 - k_{m'}^{*2})} = \kappa_{mn} = \kappa_{nm} = \kappa_{nn'},\ m, m', n, n' = 1, 2. \end{aligned} \tag{4.55}$$

The other elements are the same as the ones defined in Eqs. (4.24) and (4.25). In general, the degenerate N-soliton solution is a special case of our nondegenerate vector N-soliton solution under the restrictions, $k_i = l_i$, $i = 1, 2, ..., N$. We wish to remark here that obviously any one soliton solution will be a special case of the two-soliton solution, under the appropriate specialization of the parameters. The nondegenerate fundamental soliton solution (4.10)-(4.12) turns out be a special case of the nondegenerate two-soliton solution (4.24) and (4.25) with $\alpha_2^{(1)} = \alpha_2^{(2)} = 0$. Similarly, the degenerate fundamental soliton solution (4.53) is a special case of the degenerate two-soliton case under the restriction $\alpha_2^{(1)} = \alpha_2^{(2)} = 0$. In passing, we note that very special parametric choice turns out to be the present fundamental one soliton solution (one soliton solution presented in Eqs. (4.10)-(4.12) can be deduced from the degenerate two-soliton solution (4.55) too under the restriction $\alpha_2^{(1)} = \alpha_1^{(2)} = 0$ after renaming the resultant constants $\alpha_2^{(2)}$ as $\alpha_1^{(2)}$ and k_2 as l_1). However, as it is evident from our discussion, the properties of the nondegenerate fundamental soliton solution (4.10)-(4.12) are entirely distinct from the interacting degenerate two-soliton solution reported in Ref. [161].

As we have pointed in the previous sub-section 4.2 and by the authors of Ref. [161], the degenerate solitons of the LSRI system (4.1) undergo collision with energy redistribution among the short-wave components. Such a typical collision scenario is displayed in figure 4.13 as an example. From this figure, one can easily observe that the energy of the soliton S_2 is enhanced in the $S^{(1)}$ component and it gets suppressed in the $S^{(2)}$ component. In order to preserve the conservation of energy in both the SW components, the energy of the soliton S_1 is suppressed in the $S^{(1)}$ component and it gets enhanced in the $S^{(2)}$ component. However, the degenerate solitons in the long-wave component always undergoes elastic collision. The elastic collision is brought out in all the components by fixing the parameters as $\frac{\alpha_1^{(1)}}{\alpha_2^{(1)}} = \frac{\alpha_1^{(2)}}{\alpha_2^{(2)}}$ [161].

4.6 Nondegenerate three-soliton solution

The three-soliton solution of the system (4.1) is given below:

$$g^{(1)} = \begin{vmatrix} A_{mm'} & A_{mn} & I & \mathbf{0} & \phi_1 \\ A_{nm} & A_{nn'} & \mathbf{0} & I & \phi_2 \\ -I & \mathbf{0} & \kappa_{mm'} & \kappa_{mn} & \mathbf{0'}^T \\ \mathbf{0} & -I & \kappa_{nm} & \kappa_{nn'} & \mathbf{0'}^T \\ \mathbf{0'} & \mathbf{0'} & C_1 & \mathbf{0'} & 0 \end{vmatrix}, \; f = \begin{vmatrix} A_{mm'} & A_{mn} & I & \mathbf{0} \\ A_{nm} & A_{nn'} & \mathbf{0} & I \\ -I & \mathbf{0} & \kappa_{mm'} & \kappa_{mn} \\ \mathbf{0} & -I & \kappa_{nm} & \kappa_{nn'} \end{vmatrix} \tag{4.56}$$

$$g^{(2)} = \begin{vmatrix} A_{mm'} & A_{mn} & I & \mathbf{0} & \phi_1 \\ A_{nm} & A_{nn'} & \mathbf{0} & I & \phi_2 \\ -I & \mathbf{0} & \kappa_{mm'} & \kappa_{mn} & \mathbf{0'}^T \\ \mathbf{0} & -I & \kappa_{nm} & \kappa_{nn'} & \mathbf{0'}^T \\ \mathbf{0'} & \mathbf{0'} & \mathbf{0'} & C_2 & 0 \end{vmatrix}. \tag{4.57}$$

The various elements of the above Gram determinants are defined as

$$\begin{aligned} A_{mm'} &= \frac{e^{\eta_m+\eta^*_{m'}}}{(k_m+k^*_{m'})}, \; A_{mn} = \frac{e^{\eta_m+\xi^*_n}}{(k_m+l^*_n)}, A_{nn'} = \frac{e^{\xi_n+\xi^*_{n'}}}{(l_n+l^*_{n'})}, \; A_{nm} = \frac{e^{\eta^*_n+\xi_m}}{(k^*_n+l_m)}, \\ \kappa_{mm'} &= \frac{\psi^\dagger_m \sigma \psi_{m'}}{2i(k^2_m-k^{*2}_{m'})}, \; \kappa_{mn} = \frac{\psi^\dagger_m \sigma \psi'_n}{2i(l^2_m-k^{*2}_n)}, \; \kappa_{nm} = \frac{\psi'^\dagger_n \sigma \psi_m}{2i(k^2_n-l^{*2}_m)}, \kappa_{nn'} = \frac{\psi'^\dagger_n \sigma \psi'_{n'}}{2i(l^2_n-l^{*2}_{n'})}, \\ & \qquad m,m',n,n' = 1,2,3. \end{aligned} \tag{4.58}$$

The other elements are defined below:
$\phi_1 = \begin{pmatrix} e^{\eta_1} & e^{\eta_2} & e^{\eta_3} \end{pmatrix}^T$, $\phi_2 = \begin{pmatrix} e^{\xi_1} & e^{\xi_2} & e^{\xi_3} \end{pmatrix}^T$, $\psi_j = \begin{pmatrix} \alpha^{(1)}_j & 0 \end{pmatrix}^T$, $\psi'_j = \begin{pmatrix} 0 & \alpha^{(2)}_j \end{pmatrix}^T$, $\mathbf{0'} = \begin{pmatrix} 0 & 0 & 0 \end{pmatrix}$, $I = \sigma = \begin{pmatrix} 1 & 0 & 0 \\ 0 & 1 & 0 \\ 0 & 0 & 1 \end{pmatrix}$, $\mathbf{0} = \begin{pmatrix} 0 & 0 & 0 \\ 0 & 0 & 0 \\ 0 & 0 & 0 \end{pmatrix}$ and $C_N = -\begin{pmatrix} \alpha^{(N)}_1 & \alpha^{(N)}_2 & \alpha^{(N)}_3 \end{pmatrix}$, $j = 1,2,3$, $N = 1,2$. We remark that the

degenerate three-soliton solution can be obtained from the above nondegenerate three-soliton solution when $k_j = l_j$, $j = 1, 2, 3$. In general, mathematically to obtain the degenerate N-soliton solution from the nondegenerate N-soliton solution one needs to impose N number of restrictions on the wave bumbers $k_j = l_j$, $j = 1, 2, ..., N$.

4.7 Conclusion

In this chapter we have derived nondegenerate fundamental soliton solutions of the LSRI equations by adopting the Hirota bilinearization procedure. This general type of soliton solutions have been given in Gram determinant form for compactness. Symmetric and asymmetric profile structures of LSRI nondegenerate solitons have been demonstrated analytically and graphically. Very complicated nondegenerate two-soliton solutions of the two component LSRI system have been obtained. Also we mentioned the possibility of coexistence of nondegenerate and degenerate solitons which we called partially nondegenerate soltions. Various interesting collision behaviours (i) between nondegenerate solitons (ii) between nondegenerate and degenerate solitons have been studied in detail by the tedious asymptotic analysis. As a result of this analysis, we identified that the nondegenerate solitons exhibit three types of interaction behaviours, namely shape preserving interaction with zero phase shift, shape altering and shape changing interactions with finite phase shifts. These shape altering and shape changing interactions can also be understood as elastic interactions by taking appropriate time shifts in the asymptotic forms of the nondegenerate two-soliton solutions. In the partially nondegenerate soliton limits, two types of shape changing and energy sharing interaction have been observed. At the end, the already known class of degenerate solitons have been deduced as a subclass of our newly derived nondegenerate solitons and its profile structures, and collision properties have been mentioned briefly.

Chapter 5

Existence of Nondegenerate solitons in other coupled nonlinear Schrödinger family of systems

5.1 Introduction

In the second chapter we have studied the properties and collision dynamics of nondegenerate solitons in the Manakov system in which shape preserving, shape altering and shape changing collisions have been identified. Then we have confirmed through systematic asymptotic analysis that all these three types of collsions come under elastic collision scenario, except in the cases where degenerate solitons are involved. In Chapter 3, the effect of four wave mixing nonlinearity on the nondegenerate Manakov solitons have been analyzed. Very interestingly in chapter 4, the nondegenerate solitons in the two component long-wave short-wave resonance interaction system have been studied through the Hirota bilinearization method, where all the above mentioned three types of collision nature have been captured under appropriate wave number restrictions. Further the coexistence of degenerate and nondegenerate soliton solution simultaneously in the LSRI system is also identified. Now it is very curious to know the analytical structures and collision behaviours of nondegenerate solitons in other coupled systems like the mixed two coupled nonlinear Schrödinger system, N- coupled nonlinear Schrödinger system and coherently coupled

nonlinear Schrödinger system. In this chapter we explore some of these aspects.

This chapter is framed as follows: In section 5.2, we briefly present the nondegenerate bright solitons and their profile nature of mixed 2-CNLS system. Then the generalization of nondegenerate bright solitons admitted by N-CNLS system of Manakov type is presented in section 5.3. Also the Gram determinant solutions are deduced for the $N = 3$ and $N = 4$ cases for demonstration. Then numerical stability of triple hump nondegenerate solitons against white noise is presented in section 5.4, nondegenerate soliton solution in 2-CCNLS system is presented using the nonstandard Hirota bilinearization technique.

5.2 Nondegenerate and degenerate bright solitons in mixed 2-CNLS system

This section is essentially devoted to show the existence of nondegenerate fundamental bright solitons in the mixed 2-CNLS system or Eq. (1.10) with $\sigma_1 = +1$ and $\sigma_2 = -1$. Then the equations take the form,

$$\begin{aligned} iq_{1,z} + q_{1,tt} + 2\left(|q_1|^2 - |q_2|^2\right) q_1 = 0 \\ iq_{2,z} + q_{2,tt} + 2\left(|q_1|^2 - |q_2|^2\right) q_2 = 0 \end{aligned} \tag{5.1}$$

In this section, we also point out how the degenerate fundamental bright soliton can be captured from the obtained nondegenerate one-soliton solution and indicate its energy sharing collision. In order to write down the analytical form of nondegenerate fundamental soliton solution, one has to follow the same procedure that has been adopted to derive such a solution in the case of the Manakov system. Since the solution construction methodology has been extensively described in Refs. [77–79] and in chapter 2, here we immediately present the explicit form of nondegenerate fundamental soliton solution of the mixed 2-CNLS system. It reads as

$$q_1 = \frac{g_1^{(1)} + g_3^{(1)}}{1 + f_2 + f_4} = \frac{1}{D}(\alpha_1^{(1)} e^{\eta_1} + e^{\eta_1 + \xi_1 + \xi_1^* + \Delta_1^{(1)}}), \tag{5.2}$$

$$q_2 = \frac{g_1^{(2)} + g_3^{(2)}}{1 + f_2 + f_4} = \frac{1}{D}(\alpha_1^{(2)} e^{\xi_1} + e^{\eta_1 + \eta_1^* + \xi_1 + \Delta_1^{(2)}}). \tag{5.3}$$

Here $D = 1 + e^{\eta_1+\eta_1^*+\delta_1} + e^{\xi_1+\xi_1^*+\delta_2} + e^{\eta_1+\eta_1^*+\xi_1+\xi_1^*+\delta_{11}}$, $e^{\Delta_1^{(1)}} = -\frac{(k_1-l_1)\alpha_1^{(1)}|\alpha_1^{(2)}|^2}{(k_1+l_1^*)(l_1+l_1^*)^2}$, $e^{\Delta_1^{(2)}} = \frac{(k_1-l_1)|\alpha_1^{(1)}|^2\alpha_1^{(2)}}{(k_1+k_1^*)^2(k_1^*+l_1)}$, $e^{\delta_1} = \frac{|\alpha_1^{(1)}|^2}{(k_1+k_1^*)^2}$, $e^{\delta_2} = -\frac{|\alpha_1^{(2)}|^2}{(l_1+l_1^*)^2}$ and $e^{\delta_{11}} = -\frac{|k_1-l_1|^2|\alpha_1^{(1)}|^2|\alpha_1^{(2)}|^2}{(k_1+k_1^*)^2|k_1+l_1^*|^2(l_1+l_1^*)^2}$. Like in the Manakov system, the two complex parameters $\alpha_1^{(j)}$'s, $j = 1, 2$, and the two wave numbers k_1, and l_1 describes the behaviour of the above general form of one-soliton solution (5.2)-(5.3). By rewriting the solution (5.2)-(5.3) in hyperbolic form, as it has been done in Eqs. (2.9a) and (2.9b), we find the amplitude, velocity and central position of the soliton in the first mode is $2k_{1R}$, $2k_{1I}$ and $\frac{\phi_1}{2l_{1R}} = \frac{1}{2l_{1R}} \log \frac{(l_1-k_1|\alpha_1^{(2)}|^2)}{(k_1+l_1^*)(l_1+l_1^*)^2}$, respectively. In the second mode, the amplitude, velocity and central position of the soliton are defined by $2l_{1R}$, $2l_{1I}$ and $\frac{\phi_2}{2k_{1R}} = \frac{1}{2k_{1R}} \log \frac{(k_1-l_1|\alpha_1^{(1)}|^2)}{(k_1^*+l_1)(k_1+k_1^*)^2}$, respectively. In the mixed 2-CNLS system too, the nondegenerate fundamental soliton propagates in the two modes either with identical velocity ($v_1 = v_2 = 2k_{1I}$) or with non-identical velocity ($v_1 = 2k_{1I} \neq v_2 = 2l_{1I}$) depending on the restriction on the imaginary parts of the wave numbers k_1 and l_1. The solution (5.2)-(5.3) always shows singular behaviour due to the presence of negative sign in the constant terms e^{δ_2} and $e^{\delta_{11}}$ except for $k_1 = l_1$. This negative sign essentially arises because of the presence of defocusing nonlinearity of the mixed CNLS system. The singularity nature of the solution (5.2)-(5.3) is depicted in Figure 5.1 with the parameter values $k_1 = 1.25 + 0.45i$, $l_1 = -0.5 + 0.45i$, $\alpha_1^{(1)} = 0.3$ and $\alpha_1^{(2)} = i$. We note that the singular nature of the soliton has been recently discussed in the context of singular optics [168]. The nondegenerate higher order bright solitons can also be obtained in a similar way and one can analyse their collision dynamics.

By imposing the limit $k_1 = l_1$ in the solution (5.2)-(5.3), one can capture following degenerate fundamental vector bright soliton solution of the mixed 2-CNLS system, $q_j = k_{1R}\hat{A}_j e^{i\eta_{1I}} \mathrm{sech}(\eta_{1R} + \frac{R}{2})$, where $\eta_{1R} = k_{1R}(t -$

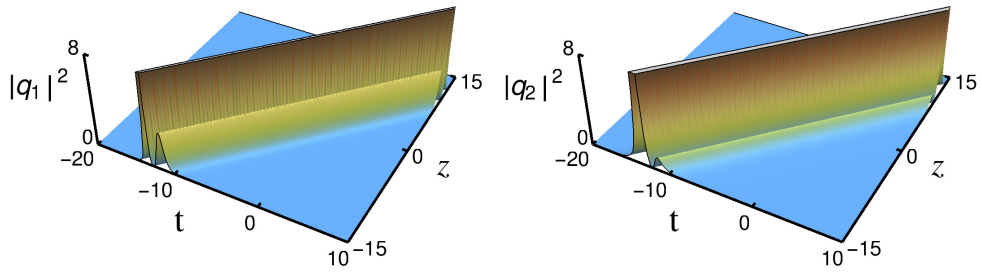

FIGURE 5.1: The singular double-hump profiles of the nondegenerate one-soliton solution (5.2)-(5.3) of the mixed 2-CNLS system.

$2k_{1I}z)$, $\eta_{1I} = k_{1I}t + (k_{1R}^2 - k_{1I}^2)z$, $\hat{A}_j = \frac{\alpha_1^{(j)}}{\sqrt{(|\alpha_1^{(1)}|^2 - |\alpha_1^{(2)}|^2)}}$, $e^R = \frac{(|\alpha_1^{(1)}|^2 - |\alpha_1^{(2)}|^2)}{(k_1 + k_1^*)^2}$, $j = 1, 2$. The latter degenerate bright soliton solution always admits the non-singular single-hump intensity profile when $|\alpha_1^{(1)}| > |\alpha_1^{(2)}|$. The degenerate multi-soliton solutions and their interesting collision property have been already discussed in [66]. The two-soliton solution of the mixed 2-CNLS system can be easily obtained by replcing B_{ij} as $B_{ij} = \kappa_{ji} = \frac{\left(\alpha_j^{(1)}\alpha_i^{(1)*} - \alpha_j^{(2)}\alpha_i^{(2)*}\right)}{(k_j + k_i^*)}$, $i, j = 1, 2$ in the degenerate two-soliton solution (2.32a)-(2.32a) of the Manakov system. However, here we indicate the special collision dynamics exhibited by the degenerate bright solitons only through a graphical demonstration as we illustrated below in Figure 5.2 for the parametric choice $k_1 = 1 - i$, $k_2 = 1.7 + I$, $\alpha_1^{(1)} = 1 + i$, $\alpha_2^{(1)} = 1 - i$, $\alpha_1^{(2)} = 0.5 + 0.3i$ and $\alpha_2^{(2)} = 0.7$. From Figure 5.2, we identify that during the collision process of the degenerate two bright solitons S_1 and S_2 in the present mixed 2-CNLS system, the intensity of the soliton S_1 is enhanced in all the modes. In contradiction to this, the intensity of the other soliton S_2 is suppressed in both the modes. Therefore, such a special property of enhancement of the intensity of a given soliton always occurs in the mixed 2-CNLS system. One may find the details of energy conservation in Ref. [66]. Additionally, we also observe the amplitude dependent phase shifts in each of the modes. This energy sharing collision is quite different from the shape changing collision of the Manakov system. The collision scenario is depicted in Figure 5.2 can be viewed as a signal amplification process, in

which the soliton S_1 refers as a signal wave and the soliton S_2 represents as a pump wave. During this amplification process, there is no external amplification medium is employed and is without the introduction of any noise [66]. We point out that the standard NLS soliton-like collision can be recovered by imposing the restriction $\frac{\alpha_1^{(1)}}{\alpha_2^{(1)}} = \frac{\alpha_1^{(2)}}{\alpha_2^{(2)}}$.

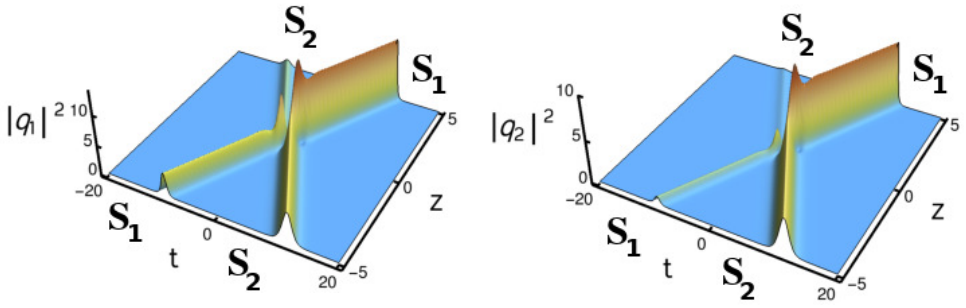

FIGURE 5.2: Energy sharing collision of degenerate two bright solitons of the mixed 2-CNLS system [66].

5.3 Nondegenerate solitons in N-CNLS system

We intend to investigate the multi-hump nature of nondegenerate fundamental solitons in the following system of multi-component nonlinear Schrödinger equations,

$$iq_{j,z} + q_{j,tt} + 2\sum_{p=1}^{N} |q_p|^2 q_j = 0, \quad j = 1, 2, ..., N, \tag{5.4}$$

by deriving their analytical forms through Hirota bilinear method. Equation (5.4) describes the optical pulse propagation in N-mode optical fibers [6] and it describes the incoherent light beam propagation in photorefractive medium [53] and so on. In the above, q_j's are complex wave envelopes propagating in N-optical modes and z and t represent the normalized distance and retarded time, respectively. We note that for $N = 2$ in Eq. (5.4),

we have studied the collision and stability properties of the nondegenerate solitons [78] and also we have identified their existence in other integrable nonlinear Schrödinger family of equations by revealing their analytical forms [79]. To derive the exact form of the nondegenerate fundamental soliton solution for the N-CNLS sytem, we bilinearize Eq. (5.4) through the dependent variable transformation, $q_j(z,t) = \frac{g^{(j)}(z,t)}{f(z,t)}$, $j = 1, 2, ..., N$ where $g^{(j)}$'s are in general complex functions and f is a real function. Substitution of this transformation in Eq. (5.4) brings out the following bilinear forms: $(iD_z + D_t^2)g^{(j)} \cdot f = 0$ and $D_t^2 f \cdot f = 2(\sum_{n=1}^{N} g^{(n)} \cdot g^{(n)*})$. Here D_z and D_t are the usual Hirota bilinear operators [155]. Then we consider the standard Hirota series expansions $g^{(j)} = \epsilon g_1^{(j)} + \epsilon^3 g_3^{(j)} + ...$, $j = 1, 2, ..., N$ and $f = 1 + \epsilon^2 f_2 + \epsilon^4 f_4 + ...$ in the solution construction process.

To obtain the nondegenerate fundamental soliton solution of Eq. (5.4) we consider the general forms of N-seed solutions, $g^{(j)} = \alpha_1^{(j)} e^{\eta_j}$, $\eta_j = k_j t + i k_j^2 z$, where $\alpha_1^{(j)}$ and k_j, $j = 1, 2, ..., N$ are complex parameters and are nonidentical in general to the N-independent linear partial differential equations, $ig_{1,z}^{(j)} + g_{1,tt}^{(j)} = 0$, $j = 1, 2, ..., N$, which arise at the lowest order of ϵ. With such general choices of seed solutions, we proceed to solve the resulting inhomogeneous linear partial differential equations successively in order to deduce the full series solution upto $g_{2N-1}^{(j)}$ in $g^{(j)}$ and f_{2N} in f. By combining the obtained forms of the unknown functions as per the series expansions we find a rather complicated form of the nondegenerate fundamental soliton solution for the N-CNLS equation. However, we have managed to rewrite it in a more compact form using the following Gram determinants [162, 163],

$$g^{(N)} = \begin{vmatrix} A & I & \phi \\ -I & B & \mathbf{0}^{\mathbf{T}} \\ \mathbf{0} & C_N & 0 \end{vmatrix}, \quad f = \begin{vmatrix} A & I \\ -I & B \end{vmatrix}, \tag{5.5}$$

where the elements of the matrices A and B are

$$A_{ij} = \frac{e^{\eta_i+\eta_j^*}}{(k_i+k_j^*)},\ B_{ij} = \kappa_{ji} = \frac{\psi_i^\dagger \sigma \psi_j}{(k_i^*+k_j)},\ C_N = -\left(\ \alpha_1^{(1)},\ \alpha_1^{(2)},\ \ldots,\ \alpha_1^{(N)}\ \right),$$
$$\psi_j = \left(\ \alpha_1^{(1)},\ \alpha_1^{(2)},\ \ldots,\ \alpha_1^{(j)}\ \right)^T, \phi = \left(\ e^{\eta_1},\ e^{\eta_2},\ \ldots,\ e^{\eta_n}\ \right)^T, j,n = 1,2,..,N.$$

In the above, $g^{(N)}$ and f are $((2^2N)+1)$ and (2^2N)th order determinants, T represents the transpose of the matrices ψ_j and ϕ, † denotes transpose complex conjugate, $\sigma = I$ is an (n × n) identity matrix, ϕ denotes (n × 1) column matrix, **0** is a (1 × n) null matrix, C_N is a (1 × n) row matrix and ψ represents a (n × 1) column matrix. In the above expressions, for the nondegenerate fundamental soliton solution the elements κ_{ji}'s do not exist ($\kappa_{ji} = 0$) in the square matrix B when $j \neq i$. Also for a given set of N and j values the corresponding elements only exist and all the other elements are equal to zero in C_N and ψ_j matrices (we have demonstrated the latter clearly for the 3-component case below). We have verified the validity of the nondegenerate fundamental soliton solution (5.5) by substituting it in the bilinear equations of Eq. (5.4) along with the following derivative formula of the determinants, $\frac{\partial M}{\partial x} = \sum_{1\leq i,j\leq n} \frac{\partial a_{i,j}}{\partial x}\frac{\partial M}{\partial a_{i,j}} = \sum_{1\leq i,j\leq n} \frac{\partial a_{i,j}}{\partial x}\Delta_{i,j}$, where $\Delta_{i,j}$'s are the cofactors of the matrix M, the bordered determinant properties and the elementary properties of the determinants [155]. This action yields a pair of Jacobi identities and thus their occurrence confirms the validity of the obtained soliton solution. Multi-hump profile nature is a special feature of the obtained nondegenerate fundamental soliton solution (5.5). Such multi-hump structures and their propagation are characterized by $2N$ arbitrary complex wave parameters. The funamental nondegenerate soliton admits a very interesting N-hump profile in the present N-CNLS system. In this system, in general, the nondegenerate solitons propagate with different velocities in different modes but one can make them to propagate with identical velocity by restricting the imaginary parts of all the wave numbers k_j, $j = 1,2,...,N$, to be equal. Interestingly, in 1976, Nogami and Warke have obtained soliton solution for the multicomponent CNLS system [169]. We note that their soliton solution corresponds to the so called partially coherent soliton (PCS) which can be checked after replacing the function $e_j = \exp(k_j x)$ by $e_j = \sqrt{2k_j a_j}\exp(k_j \bar{x}_j)$, where $\bar{x}_j = x - x_j$,

$a_j = \Pi_{j\neq i} c_{ij}$, $c_{ij} = \frac{k_i+k_j}{|k_i-k_j|}$ and k_j's are real constants, in their solution [55]. Since, the stationary N-PCS solution arises from our solution (5.5) under the parametric restrictions $\alpha_1^{(j)} = e^{\eta_{j0}}$, $j = 1, 3, 4, ..., N$ and $\alpha_1^{(2)} = -e^{\eta_{20}}$, ($\eta_{j0}$: real), $k_j = k_{jR}$, $k_{jI} = 0$, $j = 1, 2, ..., N$, the solution of Nogami and Warke [169] and its time dependent version are essentially special cases of our general solution (5.5).

It is interesting to note that if we set all the wavenumbers k_j, $j = 1, 2, ..., N$, as identical, $k_j = k_1$, $j = 1, 2, ..., N$, which corresponds to the seed solutions getting restricted as $g^{(j)} = \alpha_1^{(j)} e^{\eta_1}$, $\eta_1 = k_1 t + i k_1^2 z$, for all $j = 1, 2, ..., N$, in the fundamental soliton solution (5.5), the resultant form gets reduced to the following degenerate soliton (DS) solution for Eq. (5.4) [37] [38] as

$$(q_1, q_2, q_3, ..., q_N)^T = (A_1, A_2, A_3, ..., A_N)^T k_{1R} e^{i\eta_{1I}} \text{sech}\left(\eta_{1R} + \frac{R}{2}\right), \quad (5.6)$$

where $\eta_{1R} = k_{1R}(t - 2k_{1I}z)$, $A_j = \alpha_1^{(j)}/\Delta$ and $\Delta = ((\sum_{j=1}^{N} |\alpha_1^{(j)}|^2))^{1/2}$. Here $\alpha_1^{(j)}$, k_1, $j = 1, 2, ..., N$, are arbitrary complex parameters. Further, $k_{1R} A_j$ gives the amplitude of the jth mode, $\frac{R}{2} (= \frac{1}{2} \log \frac{\Delta}{(k_1+k_1^*)^2})$ denotes the central position of the soliton and $2k_{1I}$ is the soliton velocity [38]. It is evident that the degenerate soliton solution (5.6) always admits single-hump structure. Using this single peak intensity or power profile as signal in binary coding one cannot improve higher bit-rate in information transmission as pointed out in [19] whereas this class of degenerate solitons interestingly exhibit energy exhanging collision leading to the construction of all optical logic gates [44]. To enhance the bit-rate multi-hump pulses with symmetric and asymmetric profiles, as we describe below for 3 and 4-CNLS systems as examples, can be useful for optical communication.

In order to show the multi-hump nature of the nondegenerate soliton, here we demonstrate such special feature in the case of 3-CNLS and 4-CNLS systems. To start with, we consider the three coupled nonlinear Schrödinger equation ($N = 3$ in Eq. (5.4)). To get the nondegenerate fundamental soliton solution for this system, we consider the solutions, $g_1^{(1)} = \alpha_1^{(1)} e^{\eta_1}$, $g_1^{(2)} = \alpha_1^{(2)} e^{\eta_2}$ and $g_1^{(3)} = \alpha_1^{(3)} e^{\eta_3}$ as seed solutions to the

lowest order linear PDEs. These general form of seed solutions terminates the series expansions as $g^{(j)} = \epsilon g_1^{(j)} + \epsilon^3 g_3^{(j)} + \epsilon^5 g_5^{(j)}$, $j = 1,2,3$ and $f = 1 + \epsilon^2 f_2 + \epsilon^4 f_4 + \epsilon^6 f_6$. By rewriting the explicit forms of the obtained unknown functions in terms of Gram determinants we get the resultant forms similar to the one (Eq. (5.5)) reported above for the N-component case. We find that for the 3-CNLS system the matrices A and B are constituted by the elements, A_{ij} and B_{ij}, $i,j = 1,2,3$ and also the other matrices C_N, ψ_j and ϕ are deduced as $C_1 = \begin{pmatrix} \alpha_1^{(1)} & 0 & 0 \end{pmatrix}$, $C_2 = \begin{pmatrix} 0 & \alpha_1^{(2)} & 0 \end{pmatrix}$, $C_3 = \begin{pmatrix} 0 & 0 & \alpha_1^{(3)} \end{pmatrix}$, $\psi_1 = \begin{pmatrix} \alpha_1^{(1)} & 0 & 0 \end{pmatrix}^T$, $\psi_2 = \begin{pmatrix} 0 & \alpha_1^{(2)} & 0 \end{pmatrix}^T$, $\psi_3 = \begin{pmatrix} 0 & 0 & \alpha_1^{(3)} \end{pmatrix}^T$ and $\phi = \begin{pmatrix} e^{\eta_1} & e^{\eta_2} & e^{\eta_3} \end{pmatrix}^T$.

From the resultant Gram-determinant forms, we deduce the following triple-humped nondegenerate fundamental soliton solution for the 3-CNLS system,

$$
\begin{aligned}
q_1 &= \frac{1}{f} e^{i\eta_{1I}} \left(e^{\frac{\Delta_{51}+\rho_{11}}{2}} \cosh(\eta_{2R} + \eta_{3R} + \frac{\phi_1}{2}) + e^{\frac{\Delta_{11}+\Delta_{21}}{2}} \cosh(\eta_{2R} - \eta_{3R} + \frac{\phi_2}{2}) \right), \\
q_2 &= \frac{1}{f} e^{i\eta_{2I}} \left(e^{\frac{\Delta_{52}+\rho_{12}}{2}} \cosh(\eta_{1R} + \eta_{3R} + \frac{\psi_1}{2}) + e^{\frac{\Delta_{12}+\Delta_{22}}{2}} \cosh(\eta_{1R} - \eta_{3R} + \frac{\psi_2}{2}) \right), \\
q_3 &= \frac{1}{f} e^{i\eta_{3I}} \left(e^{\frac{\Delta_{53}+\rho_{13}}{2}} \cosh(\eta_{1R} + \eta_{2R} + \frac{\chi_1}{2}) + e^{\frac{\Delta_{13}+\Delta_{23}}{2}} \cosh(\eta_{1R} - \eta_{2R} + \frac{\chi_2}{2}) \right), \\
f &= e^{\frac{\delta_7}{2}} \cosh(\eta_{1R} + \eta_{2R} + \eta_{3R} + \frac{\delta_7}{2}) + e^{\frac{\delta_1+\delta_6}{2}} \cosh(\eta_{1R} - \eta_{2R} - \eta_{3R} + \frac{\delta_1 - \delta_6}{2}) \\
&+ e^{\frac{\delta_2+\delta_5}{2}} \cosh(\eta_{2R} - \eta_{1R} - \eta_{3R} + \frac{\delta_2 - \delta_5}{2}) + e^{\frac{\delta_3+\delta_4}{2}} \cosh(\eta_{3R} - \eta_{1R} - \eta_{2R} + \frac{\delta_3 - \delta_4}{2}),
\end{aligned} \tag{5.7}
$$

where $\eta_{jR} = k_{jR}(t - 2k_{jI}z)$, $j = 1,2,3$, $\phi_1 = \Delta_{51} - \rho_{11}$, $\phi_2 = \Delta_{11} - \Delta_{21}$, $\psi_1 = \Delta_{52} - \rho_{12}$, $\psi_2 = \Delta_{12} - \Delta_{22}$, $\chi_1 = \Delta_{53} - \rho_{13}$, $\chi_2 = \Delta_{13} - \Delta_{23}$, $\rho_{1j} = \alpha_1^{(j)}$, $j = 1,2,3$, and the other constants given above are $e^{\delta_1} = \frac{|\alpha_1^{(1)}|^2}{\Lambda_{11}}$, $e^{\delta_2} = \frac{|\alpha_1^{(2)}|^2}{\Lambda_{22}}$, $e^{\delta_3} = \frac{|\alpha_1^{(3)}|^2}{\Lambda_{33}}$, $e^{\Delta_{11}} = \frac{\alpha_1^{(1)}\varrho_{12}}{\lambda_{12}} e^{\delta_2}$, $e^{\Delta_{21}} = \frac{\alpha_1^{(1)}\varrho_{13}}{\lambda_{13}} e^{\delta_3}$, $e^{\Delta_{12}} = -\frac{\alpha_1^{(2)}\varrho_{13}}{\lambda_{12}^*} e^{\delta_1}$, $e^{\Delta_{22}} = \frac{\alpha_1^{(2)}\varrho_{23}}{\lambda_{23}} e^{\delta_3}$, $e^{\Delta_{13}} = -\frac{\alpha_1^{(3)}\varrho_{13}}{\lambda_{13}^*} e^{\delta_1}$, $e^{\Delta_{23}} = -\frac{\alpha_1^{(3)}\varrho_{23}}{\lambda_{23}^*} e^{\delta_2}$, $e^{\delta_4} = \frac{|\varrho_{12}|^2}{|\lambda_{12}|^2} e^{\delta_1+\delta_2}$, $e^{\delta_5} = \frac{|\varrho_{13}|^2}{|\lambda_{13}|^2} e^{\delta_1+\delta_3}$, $e^{\delta_6} = \frac{|\varrho_{23}|^2}{|\lambda_{23}|^2} e^{\delta_2+\delta_3}$, $e^{\delta_7} = \frac{|\varrho_{12}|^2|\varrho_{13}|^2|\varrho_{23}|^2}{|\lambda_{12}|^2|\lambda_{13}|^2|\lambda_{23}|^2} e^{\delta_1+\delta_2+\delta_3}$, $e^{\Delta_{51}} = \frac{\alpha_1^{(1)}\varrho_{12}\varrho_{13}|\varrho_{23}|^2}{\lambda_{12}\lambda_{13}|\lambda_{23}|^2} e^{\delta_2+\delta_3}$, $e^{\Delta_{52}} = -\frac{\alpha_1^{(2)}\varrho_{12}|\varrho_{13}|^2\varrho_{23}}{\lambda_{12}^*|\lambda_{13}|^2\lambda_{23}} e^{\delta_1+\delta_3}$, $e^{\Delta_{53}} = \frac{\alpha_1^{(3)}|\varrho_{12}|^2\varrho_{13}\varrho_{23}}{|\lambda_{12}|^2\lambda_{13}^*\lambda_{23}^*} e^{\delta_1+\delta_2}$,

$\Lambda_{11} = (k_1 + k_1^*)^2$, $\Lambda_{22} = (k_2 + k_2^*)^2$, $\Lambda_{33} = (k_3 + k_3^*)^2$, $\varrho_{12} = (k_1 - k_2)$, $\varrho_{13} = (k_1 - k_3)$, $\varrho_{23} = (k_2 - k_3)$, $\lambda_{12} = (k_1 + k_2^*)$, $\lambda_{13} = (k_1 + k_3^*)$ and $\lambda_{23} = (k_2 + k_3^*)$. The above nontrivial soliton solution is described by six arbitrary complex parameters, $\alpha_1^{(j)}$, k_j, $j = 1, 2, 3$. As a specific example, we can easily check that such multi-parameter solution admits a novel asymmetric triple-hump profile when we fix the velocity as $k_{1I} = k_{2I} = k_{3I} = 0.5$. The other parameter values are chosen as $k_{1R} = 0.53$, $k_{2R} = 0.5$, $k_{3R} = 0.45$, $\alpha_1^{(1)} = 0.65 + 0.65i$, $\alpha_1^{(2)} = 0.45 - 0.45i$ and $\alpha_1^{(3)} = 0.35 + 0.35i$. In Fig. 5.3 (a), we display the asymmetric triple-hump profiles in all the components for the above choice of parameter values. It is important to note that for the specific choice of parameter values, the solution (5.7) also exhibits symmetric triple-hump soliton profile. The symmetric and asymmetric nature of solution (5.7) can be identified by calculating the following relative separation distances between the solitons of the modes,

$$\Delta t_{12} = t_1 - t_2 = \frac{1}{2} \log \frac{|\alpha_1^{(1)}|^2 (k_{3R} - k_{1R})(k_{2R} + k_{3R}) k_{2R}^2}{|\alpha_1^{(2)}|^2 (k_{2R} - k_{3R})(k_{1R} + k_{3R}) k_{1R}^2}, \tag{5.8}$$

$$\Delta t_{13} = t_1 - t_3 = \frac{1}{2} \log \frac{|\alpha_1^{(1)}|^2 (k_{1R} - k_{2R})(k_{2R} + k_{3R}) k_{3R}^2}{|\alpha_1^{(3)}|^2 (k_{2R} - k_{3R})(k_{1R} + k_{2R}) k_{1R}^2}, \tag{5.9}$$

$$\Delta t_{23} = t_2 - t_3 = \frac{1}{2} \log \frac{|\alpha_1^{(2)}|^2 (k_{2R} - k_{1R})(k_{1R} + k_{3R}) k_{3R}^2}{|\alpha_1^{(3)}|^2 (k_{1R} - k_{3R})(k_{1R} + k_{2R}) k_{2R}^2}. \tag{5.10}$$

It is evident from Eqs. (5.8)-(5.10) the solution (5.7), with $k_{1I} = k_{2I} = k_{3I}$, always admits asymmetric triple-hump profiles when $\Delta t_{12} = \Delta t_{13} = \Delta t_{23} \neq 0$. In contrast to this, almost symmetric (not perfect symmetric) triple-hump profile arises in all the modes when the soliton parameters obey the condition, $\Delta t_{12} = \Delta t_{13} = \Delta t_{23} \to 0$. The double node (or multi-node) formation occurs when the relative velocities among the solitons of the modes, q_j's $j = 1, 2, 3$, do not tend to zero. Such node formation is demonstrated in Fig. 5.4 for the unequal velocity case (of the modes) in the present 3-CNLS system. We wish to point out here that the triple peak power profiles obeying the above relative separation distance condition, both symmetric and asymmetric, could be useful in the launching of the

initial signal in binary coding scheme. In the practical situation the initial profiles can vary their shape due to fiber's loss and nonlinear higher order effects. This situation cannot be avoided in a fiber. However, the solution (5.7) retains the fundamental property, namely the triple-hump soliton profile, of the nondegenerate soliton during the evolution along the fiber.

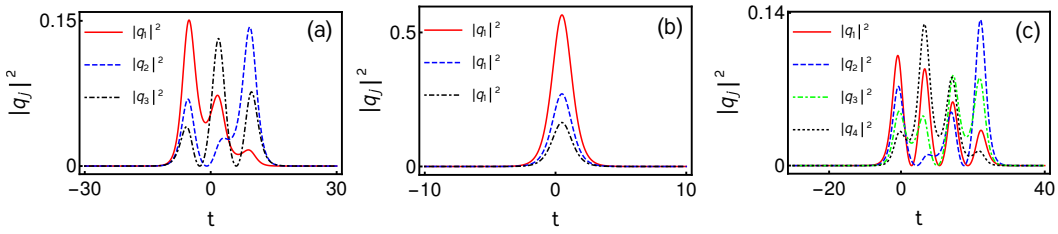

FIGURE 5.3: (a) denotes triple-hump profiles of nondegenerate fundamental soliton in the 3-CNLS system and (b) is its corresponding single-humped degenerate soliton profile. (c) represents a quadruple-humped nondegenerate soliton profiles in 4-CNLS system. The specific values of the soliton parameters are given in the text.

It is interesting to note that when we impose the condition $k_1 = k_2 = k_3$ in the solution (5.7), it turns out to be a single-humped degenerate fundamental soliton for the 3-CNLS system. This can be seen from Fig. 5.3 (b) for the values $k_1 = k_2 = k_3 = 1 + i$, $\alpha_1^{(1)} = 0.65 + 0.65i$, $\alpha_1^{(2)} = 0.45 - 0.45i$ and $\alpha_1^{(3)} = 0.35 + 0.35i$. We note that the 3-partially coherent soliton or multi-soliton complexes arise from the nondegenerate fundamental soliton solution (5.7) of the 3-CNLS system when the soliton parameters are fixed as $\alpha_1^{(1)} = e^{\eta_{10}}$, $\alpha_1^{(2)} = -e^{\eta_{20}}$, $\alpha_1^{(3)} = e^{\eta_{30}}$, $k_1 = k_{1R}$, $k_2 = k_{2R}$, $k_3 = k_{3R}$ and $k_{jI} = 0$, $j = 1, 2, 3$, where η_{j0}, $j = 1, 2, 3$, are considered as real constants [32, 38]. Next we illustrate the multi-hump nature of nondegenerate soliton in the 4-CNLS system. To obtain such solution one has to proceed with the analysis for the $N = 4$ case, as we have described in the above 3-component case. For brevity, we do not give the details of the final solution due to its complex nature. However, one can easily deduce the form of the solution from the soliton solution of the N-component case, Eq. (5.5), as given above. The final solution contains eight arbitrary complex parameters, namely $\alpha_1^{(j)}$ and k_j, $j = 1, 2, 3, 4$. These parameters play a significant role in determining the profile nature of the underlying soliton in

the 4-component case. In general, the nondegenerate one-soliton solution in the 4-CNLS system exhibits asymmetric quadruple-hump profile in all the modes. Such novel quadruple-hump profile is displayed in Fig. 5.3(c) for the parameter values $k_1 = 0.48 + 0.5i$, $k_2 = 0.5 + 0.5i$, $k_3 = 0.53 + 0.5i$, $k_4 = 0.55 + 0.5i$, $\alpha_1^{(1)} = 0.65 + 0.65i$, $\alpha_1^{(2)} = 0.55 - 0.55i$, $\alpha_1^{(3)} = 0.45 + 0.45i$ and $\alpha_1^{(4)} = 0.35 - 0.35i$.

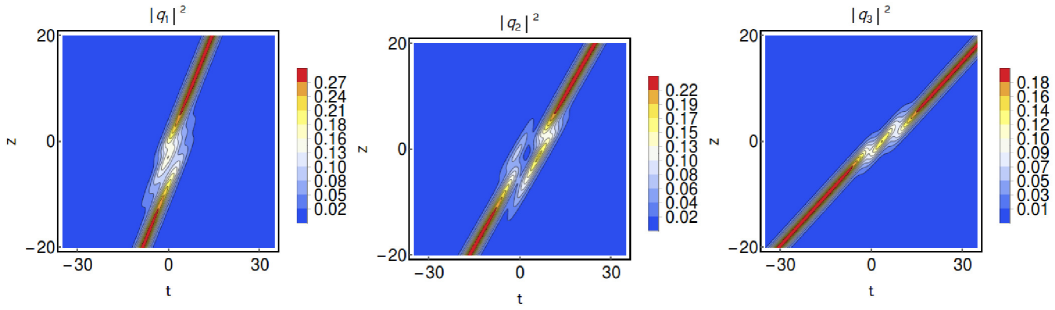

FIGURE 5.4: Double-node formation in the unequal velocities case in the profile of nondegenerate fundamental soliton in 3-CNLS system. The parameter values are $k_1 = 0.55 + 0.35i$, $k_2 = 0.5 + 0.5i$, $k_3 = 0.45 + 0.8i$ $\alpha_1^{(1)} = 0.65 + 0.65i$, $\alpha_1^{(2)} = 0.45 - 0.45i$ and $\alpha_1^{(3)} = 0.35 + 0.35i$.

We have verified the asymmetric quadruple-hump profile nature by calculating the relative separation distance, $\Delta t_{12} = \Delta t_{13} = \Delta t_{14} \neq 0$. However we do not present their explicit forms due to size limitation of the letter article. It is evident from Figs. 5.3 (a) and (c) that the nondegenerate soliton (in 3, 4 and also in the arbitrary N (> 4) CNLS systems) exhibits multi-hump nature. This multi-peak nature can increase the bit-rate in coding the information. Consequently it can help to uplift the flow of data in fiber. In the present 4-CNLS system case also multi-node forms when the relative velocities of the solitons among the modes do not tend to zero. One can also recover the already known degenerate soliton solution by fixing the condition $k_1 = k_2 = k_3 = k_4$ in the final form of nondegenerate soliton solution of the 4-CNLS system. In the following, we further report the fact that the N-CNLS system can also admit very interesting partially nondegenerate soliton solution when the wavenumbers are restricted suitably. Such partial nondegenerate soliton solutions also exhibit multi-hump profiles (but less than N in number). For instance, here we demonstrate their existence for the 3 and 4-CNLS systems and this procedure can be

generalized to the N-component case in principle. For the 3-component case, the partially nondegenerate soliton solution can be obtained by imposing the condition, $k_1 = k_2$ (or $k_1 = k_3$ or $k_2 = k_3$), on the wave numbers in the solution (5.7). This restriction reduces the asymmetric triple-hump profile, as depicted in Fig. 5.3 (a), into the asymmetric double-hump intensity profile as displayed in Fig. 5.5 (a) for the choice of parameters $k_1 = k_2 = 0.5 + 0.5i$, $k_3 = 0.45 + 0.5i$, $\alpha_1^{(1)} = 0.65 + 0.65i$, $\alpha_1^{(2)} = 0.45 - 0.45i$ and $\alpha_1^{(3)} = 0.35 + 0.35i$. The partially NDS double-hump profile is described by the following explicit form of solution, deduced from solution (5.7),

$$
\begin{aligned}
q_1 &= \frac{1}{f} e^{i\eta_{1I}} e^{\frac{\Delta_{21}+\rho_{11}}{2}} \cosh(\eta_{3R} + \frac{\Delta_{21} - \rho_{11}}{2}),\ q_3 = \frac{1}{f} e^{i\eta_{3I}} e^{\frac{\Delta+\rho_{13}}{2}} \cosh(\eta_{1R} + \frac{\Delta - \rho_{13}}{2}),\\
q_2 &= \frac{1}{f} e^{i\eta_{1I}} \Big(\frac{1}{2}[\cosh(2\eta_{1R} - \eta_{3R} + \Delta_{12}) + \sinh(2\eta_{1R} - \eta_{3R} + \Delta_{12})]\\
&\quad + e^{\frac{\Delta_{22}+\rho_{12}}{2}} \cosh(\eta_{3R} + \frac{\Delta_{22} - \rho_{12}}{2}) \Big),\\
f &= e^{\frac{\bar{\delta}_1}{2}} \cosh(\eta_{1R} + \eta_{3R} + \frac{\bar{\delta}_1}{2}) + e^{\frac{\bar{\delta}_2+\delta_3}{2}} \cosh(\eta_{1R} - \eta_{3R} + \frac{\bar{\delta}_2 - \delta_3}{2}).
\end{aligned}
\tag{5.11}
$$

In the above $e^{\bar{\delta}_1} = e^{\delta_5} + e^{\delta_6}$, $e^{\bar{\delta}_2} = e^{\delta_1} + e^{\delta_2}$, $e^{\Delta} = e^{\Delta_{13}} + e^{\Delta_{23}}$, $\eta_1 = \eta_2 = k_1 t + i k_1^2 z$, $\eta_3 = k_3 t + i k_3^2 z$ and the other constants are deduced from the constants of the solution (5.7) by imposing the condition $k_1 = k_2$ in them. We point out that one can get the degenerate soliton solution by imposing the restriction further on the wavenumbers, that is as we mentioned above $k_1 = k_2 = k_3$ leads to completely degenerate soliton solution.

It is important to note that partially nondegenerate soliton solution of the 3-CNLSE can exhibit only upto double hump profile in all the three modes due to the degeneracy among the modes and the nature of this solution is controlled by five arbitrary complex parameters.

Similarly, for the 4-CNLS equation, partially nondegenerate soliton solution can be deduced from the solution (5.5) of N-component case. However, due to the complex nature of the resultant solution we do not present the expression here. Very interestingly such solution provides the following three possibilities: (i). $k_1 = k_2$, (ii). $k_1 = k_2 = k_3$ and (iii) $k_1 = k_2 = k_3 = k_4$. The quadruple-hump soliton profile of the 4-CNLS

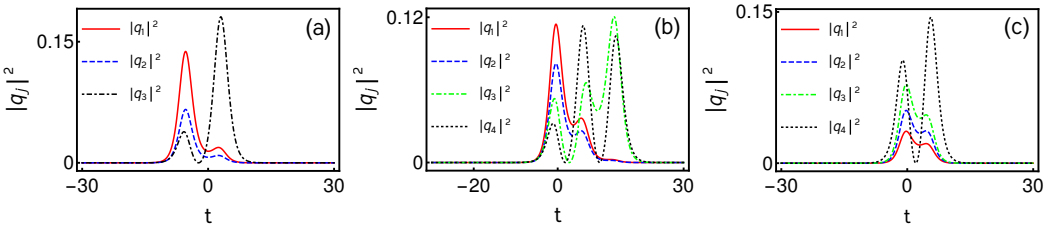

FIGURE 5.5: (a) denotes double-humped profile of the partially nondegenerate one soliton solution of 3-CNLS system. (b) and (c) represent triple and double-humped profiles of partially nondegenerate soliton solution of 4-CNLS system when the conditions $k_1 = k_2$ and $k_1 = k_2 = k_3$ on wavenumbers are imposed, respectively.

system becomes a triple-hump profile when we consider the first possibility, $k_1 = k_2$. This triple-humped partially nondegenerate soliton solution is diplayed in Fig. 5.5(b) for $k_1 = k_2 = 0.55 + 0.5i$, $k_3 = 0.5 + 0.5i$, $k_4 = 0.45 + 0.5i$, $\alpha_1^{(1)} = 0.65 + 0.65i$, $\alpha_1^{(2)} = 0.55 - 0.55i$, $\alpha_1^{(3)} = 0.45 + 0.45i$ and $\alpha_1^{(4)} = 0.35 - 0.35i$. In contrast to the latter, we observe that the double-hump soliton profile emerges while considering the second possibility, $k_1 = k_2 = k_3$, in the full nondegenerate form of solution of the 4-CNLS system. Such double-humped partially NDS solution profile is depicted in Fig. 5.5(c) for the values $k_1 = k_2 = k_3 = 0.55 + 0.5i$, $k_4 = 0.45 + 0.5i$, $\alpha_1^{(1)} = 0.35 + 0.35i$, $\alpha_1^{(2)} = 0.45 + 0.45i$, $\alpha_1^{(3)} = 0.55 + 0.55i$ and $\alpha_1^{(4)} = 0.65 - 0.65i$. The final possibilty, $k_1 = k_2 = k_3 = k_4$, corresponds to complete degeneracy. This choice brings out the completely degenerate soliton solution for the 4-CNLS system. In general, for the N-component case, one would expect $N - 1$ possibilities of choices of wave numbers. Out of these choices a single-humped complete degenerate soliton solution (5.6) arises if all the wavenumbers are equal, $k_1 = k_2 = ... = k_n$, whereas the partial nondegeneracy appears from out of the remaining $N - 2$ possibilities. Such partial nondegeneracy would bring out multi-hump profiles as we have illustrated above for the 3 and 4 component cases.

We also wish to point out the stability nature of the triple-humped nondegenerate fundamental soliton solution (5.7) of the 3-CNLS system as an example. In order to do this, we consider the Crank-Nicolson numerical algorithm [170] with different percentages of white noise as perturbations to the initial profiles. The initial profiles are considered in the

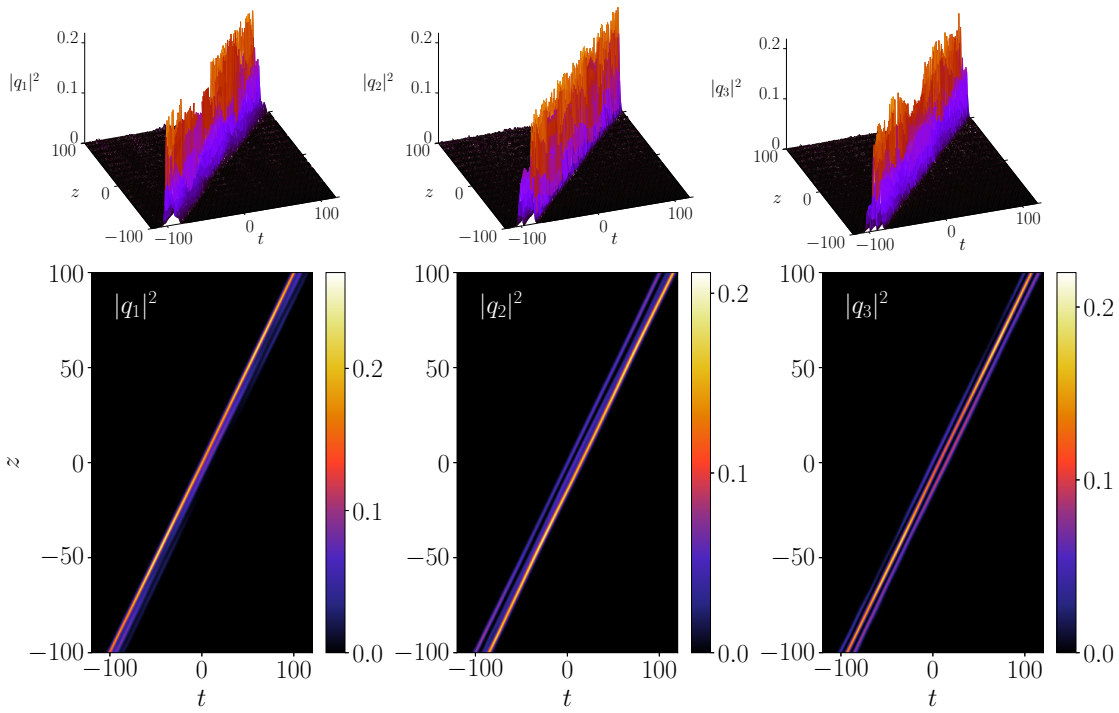

FIGURE 5.6: Numerical plots for the asymmetric nondegenerate triple hump soliton profile with 5% of white noise as perturbation. Top panel denotes the triple-hump profile of 3-dimensional surface plot and the bottom panel represents the corresponding density plots. The soliton parameters correspond to Fig. 5.3(a).

numerical analysis as $q_j(-100,t) = [1 + A\zeta(t)]q_{j,-100}(t)$, $j = 1,2,3$, where $q_{j,-100}(t)$, $j = 1,2,3$, are the initial profiles obtained from the solution (5.7) at $z = -100$. Here, A is the amplitude of the white noise which is generated from the random numbers in the interval $[-1,1]$ and $\zeta(t)$ is the noise function. The space and time step sizes are fixed in the numerical calculation, respectively, as $dz = 0.1$ and $dt = 0.2$. We also fix the domain range values for both t and z as $[-100,100]$. The triple-hump profile nature survives during the evolution even for 5% and 10% of white noise perturbations except for minor changes in the amplitude part. This is clearly demonstrated in figures 5.6 and 5.7. These figures ensure the stability of triple-humped nondegenerate soliton against perturbations of white noise. One can extend this analysis for even longer ranges of time and space without much difficulty. Similarly, we have also confirmed the

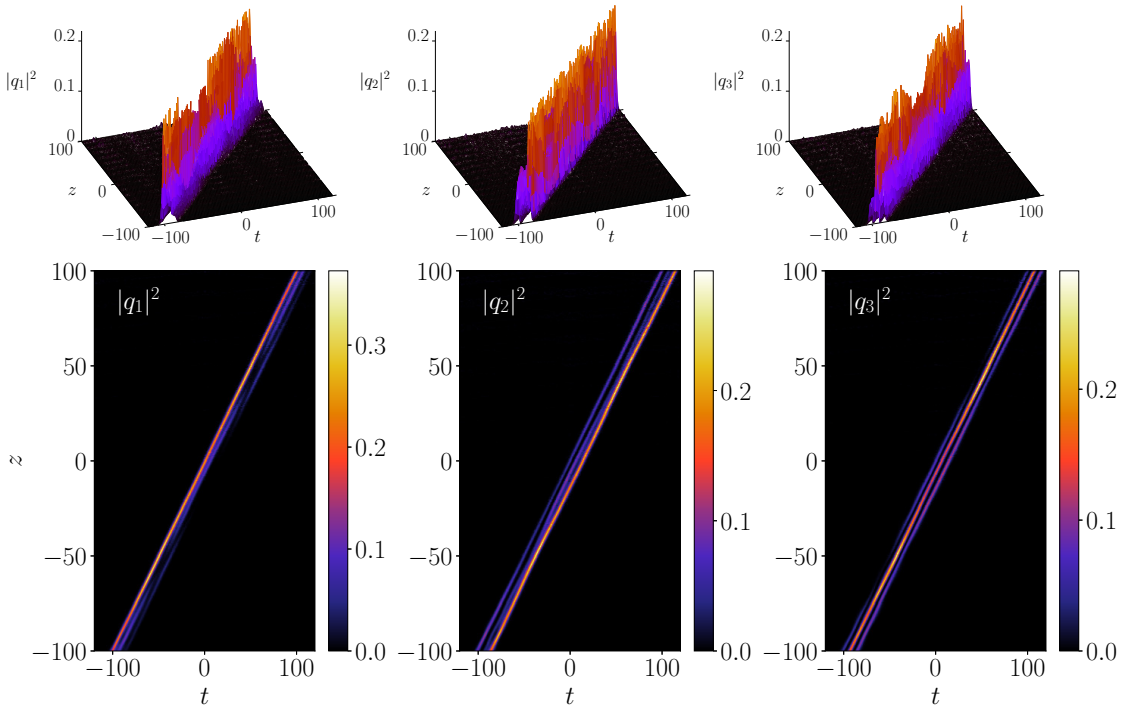

FIGURE 5.7: Numerical plots for the asymmetric nondegenerate triple hump soliton profile with 10% of white noise as perturbation.

stability of asymmetric quadruple-hump nondegenerate soliton of the 4-CNLS system as well.

5.4 Nondegenerate soliton solutions of CCNLS system

Two coherently coupled nonlinear Schrödinger equations reads as follows,

$$\begin{aligned} iq_{1,z} + q_{1,tt} + \gamma(|q_1|^2 + 2|q_2|^2)q_1 - \gamma q_2^2 q_1^* = 0, \\ iq_{2,z} + q_{2,tt} + \gamma(2|q_1|^2 + |q_2|^2)q_2 - \gamma q_1^2 q_2^* = 0. \end{aligned} \tag{5.12}$$

In order to deduce the appropriate nondegenerate soliton solution to (5.13), we introduce the bilinear transformation $q_j = \frac{g^{(j)}(z,t)}{f(z,t)}$ with an auxiliary function $s(z,t)$ [109, 110, 168]. It results in the following bilinear

equations

$$D_1 g^{(j)} \cdot f = \gamma g^{(j)*} \cdot s,\ D_2 f \cdot f = 2\gamma \sum_{j=1}^{2} |g^{(j)}|^2, s \cdot f = \sum_{j=1}^{2} (g^{(j)})^2, \quad (5.13)$$

wher $D_1 \equiv iD_z + D_t^2$ and $D_2 \equiv D_t^2$. We follow the procedure described in [109, 110] for the degenerate case but now with the seed solutions $g_1^{(1)} = \alpha_1 e^{\eta_1}$, $g_1^{(2)} = \beta_1 e^{\xi_1}$, $\eta_1 = k_1 t + ik_1^2 z$, $\xi_1 = l_1 t + il_1^2 z$. While doing so, the series expansions get truncated as $g^{(j)} = \epsilon g_1^{(j)} + \epsilon^3 g_3^{(j)} + \epsilon^5 g_5^{(j)} + \epsilon^7 g_7^{(j)}$, $f = 1 + \epsilon^2 f_2 + \epsilon^4 f_4 + \epsilon^6 f_6 + \epsilon^8 f_8$ and $s = \epsilon^2 s_2 + \epsilon^4 s_4 + \epsilon^6 s_6$. By substituting the obtained forms of the unknown functions in the truncated series expansions, we get the following general form of nondegenerate coherently coupled fundamental soliton solution of 2-CCNLS system (5.13),

$$\begin{aligned}
q_1 &= \frac{1}{f}\Big(\alpha_1 e^{\eta_1} + e^{2\eta_1+\eta_1^*+\Delta_{11}} + e^{\eta_1^*+2\xi_1+\Delta_{12}} + e^{\eta_1+\xi_1+\xi_1^*+\Delta_{13}} + e^{\eta_1+2(\eta_1^*+\xi_1)+\Delta_{14}} \\
&\quad + e^{\eta_1+2(\xi_1+\xi_1^*)+\Delta_{15}} + e^{2\eta_1+\eta_1^*+\xi_1+\xi_1^*+\Delta_{16}} + e^{2(\eta_1+\xi_1+\xi_1^*)+\eta_1^*+\Delta_{17}}\Big), \\
q_2 &= \frac{1}{f}\Big(\beta_1 e^{\xi_1} + e^{2\xi_1+\xi_1^*+\Delta_{21}} + e^{\xi_1^*+2\eta_1+\Delta_{22}} + e^{\xi_1+\eta_1+\eta_1^*+\Delta_{23}} + e^{\xi_1+2(\xi_1^*+\eta_1)+\Delta_{24}} \\
&\quad + e^{\xi_1+2(\eta_1^*+\eta_1)+\Delta_{25}} + e^{2\xi_1+\xi_1^*+\eta_1+\eta_1^*+\Delta_{26}} + e^{2(\eta_1+\eta_1^*+\xi_1)+\xi_1^*+\Delta_{27}}\Big),
\end{aligned}$$

$$\begin{aligned}
f &= 1 + e^{\eta_1+\eta_1^*+\delta_1} + e^{\xi_1+\xi_1^*+\delta_2} + e^{2(\eta_1+\eta_1^*)+\delta_3} + e^{2(\eta_1+\xi_1^*)+\delta_4} + e^{2(\xi_1+\eta_1^*)+\delta_5} \\
&\quad + e^{2(\xi_1+\xi_1^*)+\delta_6} + e^{(\eta_1+\eta_1^*+\xi_1+\xi_1^*)+\delta_7} + e^{2(\eta_1+\eta_1^*)+\xi_1+\xi_1^*+\nu_1} \\
&\quad + e^{2(\xi_1+\xi_1^*)+\eta_1+\eta_1^*+\nu_2} + e^{2(\eta_1+\eta_1^*+\xi_1+\xi_1^*)+\nu_3}. \qquad (5.14)
\end{aligned}$$

The various constants which appear in the above solution are given by

$$e^{\Delta_{11}}=\frac{\gamma\alpha_1|\alpha_1|^2}{2\kappa_{11}}, e^{\Delta_{12}}=\frac{\gamma\alpha_1^*\beta_1^2}{2\theta_1^{*2}}, e^{\Delta_{13}}=\frac{\gamma\alpha_1|\beta_1|^2\rho_1}{\theta_1 l_{11}}, e^{\Delta_{14}}=\frac{\gamma^2\rho_1^2\alpha_1^*\beta_1^2|\alpha_1|^2}{4\kappa_{11}\theta_1^{*4}},$$
$$e^{\Delta_{15}}=\frac{\gamma^2\rho_1^2\alpha_1|\beta_1|^4}{4l_{11}^2\theta_1^2}, e^{\Delta_{16}}=\frac{\gamma^2\rho_1^2\rho_1^*\alpha_1|\alpha_1|^2|\beta_1|^2}{2\kappa_{11}l_{11}\theta_1^2\theta_1^*}, e^{\Delta_{17}}=\frac{\gamma^3\rho_1^4\rho_1^{*2}\alpha_1|\alpha_1|^2|\beta_1|^4}{8\kappa_{11}l_{11}^2\theta_1^4\theta_1^{*2}},$$
$$e^{\Delta_{21}}=\frac{\gamma\beta_1|\beta_1|^2}{2l_{11}}, e^{\Delta_{22}}=\frac{\gamma\alpha_1^2\beta_1^*}{2\theta_1^2}, e^{\Delta_{23}}=-\frac{\gamma|\alpha_1|^2\beta_1\rho_1}{\theta_1^*\kappa_{11}}, e^{\Delta_{24}}=\frac{\gamma^2\rho_1^2\alpha_1^2|\beta_1|^2\alpha_1^*}{4l_{11}\theta_1^4},$$
$$e^{\Delta_{25}}=\frac{\gamma^2\rho_1^2|\alpha_1|^4\beta_1}{4\kappa_{11}^2\theta_1^{*2}}, e^{\Delta_{26}}=-\frac{\gamma^2\rho_1^2\rho_1^*\beta_1|\alpha_1|^2|\beta_1|^2}{2\kappa_{11}l_{11}\theta_1\theta_1^{*2}}, e^{\Delta_{27}}=\frac{\gamma^3\rho_1^4\rho_1^{*2}\beta_1|\alpha_1|^4|\beta_1|^2}{8\kappa_{11}^2l_{11}\theta_1^2\theta_1^{*4}},$$
$$e^{\delta_1}=\frac{\gamma|\alpha_1|^2}{\kappa_{11}}, e^{\delta_2}=\frac{\gamma|\beta_1|^2}{l_{11}}, e^{\delta_3}=\frac{\gamma^2|\alpha_1|^4}{4\kappa_{11}^2}, e^{\delta_4}=\frac{\gamma^2\alpha_1^2\beta_1^{*2}}{4\theta_1^4}, e^{\delta_5}=\frac{\gamma^2\alpha_1^{*2}\beta_1^2}{4\theta_1^{*4}},$$
$$e^{\delta_6}=\frac{\gamma^2|\beta_1|^4}{4l_{11}^2}, e^{\delta_7}=\frac{\gamma^2|\rho_1|^2|\alpha_1|^2|\beta_1|^2}{\kappa_{11}l_{11}|\theta_1|^2}, e^{\nu_1}=\frac{\gamma^3|\rho_1|^4|\alpha_1|^4|\beta_1|^2}{4\kappa_{11}^2l_{11}|\theta_1|^4},$$
$$e^{\nu_2}=\frac{\gamma^3|\rho_1|^4|\alpha_1|^2|\beta_1|^4}{4\kappa_{11}l_{11}^2|\theta_1|^2}, e^{\nu_3}=\frac{\gamma^4|\rho_1|^8|\alpha_1|^4|\beta_1|^4}{16\kappa_{11}^2l_{11}^2|\theta_1|^8}, l_{11}=(l_1+l_1^*)^2,$$
$$\theta_1=(k_1+l_1^*),\ \rho_1=(k_1-l_1),\ \kappa_{11}=(k_1+k_1^*)^2.$$

The auxiliary function is obtained as $s=\alpha_1^2e^{2\eta_1}+\beta_1^2e^{2\xi_1}+e^{2\eta_1+\xi_1+\xi_1^*+\phi_1}+e^{2\xi_1+\eta_1+\eta_1^*+\phi_2}+e^{2(\eta_1+\eta_1^*+\xi_1)+\phi_3}+e^{2(\eta_1+\xi_1^*+\xi_1)+\phi_4}$, $e^{\phi_1}=\frac{\gamma\rho_1^2\alpha_1^2|\beta_1|^2}{\theta_1^2l_{11}}$, $e^{\phi_2}=\frac{\gamma\rho_1^2\beta_1^2|\alpha_1|^2}{\theta_1^{*2}\kappa_{11}}$, $e^{\phi_3}=\frac{\gamma^2\rho_1^4\beta_1^2|\alpha_1|^4}{4\theta_1^{*4}\kappa_{11}^2}$, $e^{\phi_4}=\frac{\gamma^2\rho_1^4\alpha_1^2|\beta_1|^4}{4\theta_1^4l_{11}^2}$. The already reported degenerate coherently coupled fundamental one-soliton solution [109, 110] of Eq. (5.13) is obtained by restricting $k_1=l_1$ in Eq. (5.14). This leads to $q_1=\frac{\alpha_1e^{\eta_1}+e^{2\eta_1+\eta_1^*+\Delta_{11}}}{1+e^{\eta_1+\eta_1^*+\delta_1}+e^{2(\eta_1+\eta_1^*)+\delta_2}}$, $q_2=\frac{\beta_1e^{\eta_1}+e^{2\eta_1+\eta_1^*+\Delta_{12}}}{1+e^{\eta_1+\eta_1^*+\delta_1}+e^{2(\eta_1+\eta_1^*)+\delta_2}}$, $e^{\Delta_{11}}=\frac{\gamma\alpha_1^*(\alpha_1^2+\beta_1^2)}{2\kappa_{11}}$, $e^{\Delta_{12}}=\frac{\gamma\beta_1^*(\alpha_1^2+\beta_1^2)}{2\kappa_{11}}$, $e^{\delta_1}=\frac{\gamma(|\alpha_1|^2+|\beta_1|^2)}{\kappa_{11}}$, $e^{\delta_2}=\frac{\gamma^2|\alpha_1^2+\beta_1^2|^2}{4\kappa_{11}^2}$. The auxiliary function is reduced as $s=(\alpha_1^2+\beta_1^2)e^{2\eta_1}$.

From the solution (5.14), it is easy to identify that the shape of the nondegenerate coherently coupled fundamental soliton (5.14) is also governed by two arbitrary complex parameters α_1 and β_1 and two distinct complex wave numbers k_1 and l_1. The solution (5.14) admits various novel profiles , such as a quadruple-hump, a triple-hump, a double-hump and a single-hump profiles under appropriate restrictions on the wave parameters. This is due to the presence of additional wave number and the four wave mixing effect. As an example, we display a nontrivial breathing type

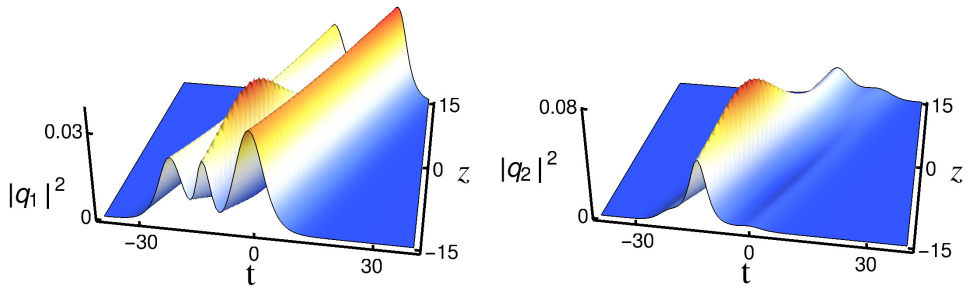

FIGURE 5.8: Breathing type triple-hump profile of nondegenerate soliton in the CCNLS system.

triple-hump shaped soliton profiles in Fig. 5.8 for the parameters $\gamma = 2$, $k_1 = 0.21 + 0.5i$, $l_1 = 0.29 + 0.5i$, $\alpha_1 = 0.95 + 0.5i$ and $\beta_1 = 0.97 - i$. By tuning the relative separation distance it is also possible to separate a single-hump and a double-hump from this triple-hump profile. However, a distinct double-hump profile only occurs in the degenerate case. This is due to the presence of a single wave number apart from two arbitrary constants α_1 and β_1. A typical degenerate flattop soliton in q_1 component and a double-hump profile in q_2 component is illustrated in Fig. 5.9 for $\gamma = 2$, $k_1 = l_1 = 0.5 + 0.5i$, $\alpha_1 = 0.72 + 0.5i$ and $\beta_1 = 0.5 - 0.42i$.

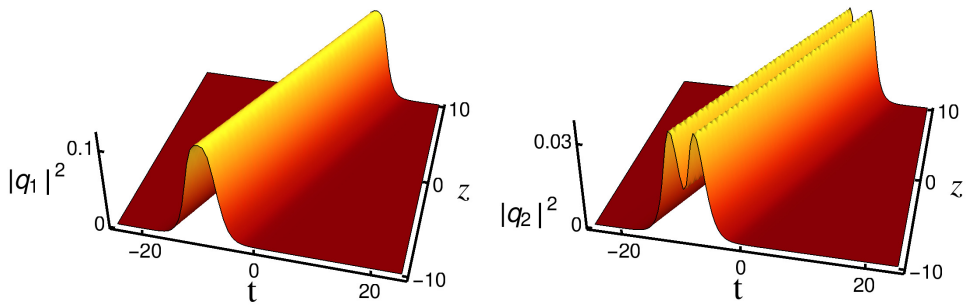

FIGURE 5.9: Flattop-double-hump profiles of degenerate solitons in the CCNLS system.

5.5 Conclusion

In this chapter we have deduced the nondegenerate one-soliton solution for the mixed 2-CNLS system using the Hirota bilinearization technique. The singular nature of the nondegenerate double hump solitons due to the presence of defocusing nonlinearity has been identified. The non-singular degenerate solitons under appropriate α parameter condition has been retained. Further the nondegenerate Manakov solitons have been generalized to N-CNLS system which interestingly admits N-humped soliton profile. This has been demonstrated with 3-CNLS (triple hump solitons) and 4-CNLS (quadraple hump solitons) systems. Also the stability of the triple hump nondegenerate solitons has been studied using Crank-Nicolson numerical algorithm against 5 percent and 10 percent white noise as perturbation. Finally the nondegenerate fundamental solitons for 2- coherently coupled nonlinear Schrödinger system have been derived through a non-standard Hirota bilinearization procedure and their breathing nature have been deduced.

Chapter 6

Summary and Future works

6.1 Summary of the thesis

In this present thesis, we have systematically analysed the new class of solitons, namely nondegenerate solitons in coupled nonlinear Schrödinger family of systems. Initially, we have started with the derivation of some of the coupled nonlinear Schrödinger family of systems which have more physical importance. We have derived nondegenerate solitons using Hirota bilinearization procedure which is the direct method to construct soliton solutions. Here nondegenerate solitons have been derived with more general form of seed solutions having nonidentical wave numbers for the bilinear equations. As a result we have obtained more general class of soliton solutions which exhibit interestingly multihump profile structures which are not possible in the already known class of soltions in the studied coupled systems. We have also recaptured the already known class of solitons with appropriate restriction on wave numbers. We designated the later as degenerate solitons. Apart from the completely nondegenerate and degenerate solitons, partially nondegenerate solitons have also been identified with suitable wave number constraint. This set of partially nondegenerate solitons allows the coexistence of nondegenerate and degenerate solitons simultaneously in all the components. As a result of our work, we understand that the partially coherent solitons can be derived from our

more general solutions with further constraints on the wave numbers. Singularity of solitons and breathing nature of solitons have also been identified with appropriate nonlinearities in the coupled nonlinear Schrödinger models. Following the above, interesting collision dynamics have been studied between nondegenerate solitons, and nondegenerate and degenerate solitons. Systematic asymptotic analysis have been carried out for all these collision scenarios. The role of polarization unit vectors have been clearly understood in the energy redistribution between the coupled modes through our detailed analysis. We strongly believe that our studies on nondegenerate solitons in coupled Schrödinger equations may open new doors in the theory of solitons. Further this may be very much useful in soliton based optical communications with enhanced data carrying capacity. In the following we summarize the concrete results which we have obtained from our series of works on nondegenerate solitons and then point out some of the future directions along similar lines.

6.2 Conclusions of the thesis

1. We have derived a general form of nondegenerate one-, two- and three-soliton solutions for the Manakov model through Hirota bilinearization method. Such new class of solitons admit various interesting profile structures. The double-hump formation is elucidated by analysing the relative velocities of the modes of the solitons. Then we have pointed out the coexistence of degenerate and nondegenerate solitons in the Manakov system by imposing a wave number restriction on the obtained two soliton solution. Then we have elucidated that the nondegenerate bright solitons possess novel collision properties. In particular, they exhibit shape preserving, shape altering and shape changing collisions. However, by performing a careful asymptotic analysis, we found that all these three types of collision scenarios can be viewed as an elastic collision. For appropriate choices of parameters, they also exhibit energy sharing collision properties. Further, we have demonstrated that the degenerate vector bright solitons of Manakov system can be captured by imposing appropriate constraints on the wave numbers. In addition to the above,

we have also explained the intriguing energy sharing collisions that occur between the degenerate vector bright solitons through graphical demonstration and analytical calculations. We have also verified the stability nature of double hump solitons even during collision using Crank-Nicolson numerical method.

2. In this chapter, we have investigated the role of the four-wave mixing effect on the structure of nondegenerate vector solitons and their collision dynamics. The fundamental, as well as higher-order nondegenerate vector soliton solutions, are derived through the Hirota bilinearization method and their forms are rewritten in a compact way using Gram determinants. Very interestingly, we found that the presence of four-wave mixing effect induced the breathing vector soliton state in both the optical modes. Then, we have observed that the nondegenerate solitons in the GCNLS system undergoes, in general, novel shape changing collision when the four-wave mixing effect strength is strong enough. On the other hand, for weak four-wave mixing effect they undergoes mere shape preserving (or shape altering) collision. Further, we have also analyzed the degenerate soliton collision induced novel shape changing property of nondegenerate vector soliton by deriving the partially nondegenerate two-soliton solution. We believe that the results reported in this chapter will be useful in nonlinear optics for manipulating light by light through collision.

3. We have derived the nondegenerate one-,two- and three-soliton solutions through the Hirota bilinear method for the two component long-wave short-wave resonance interaction system. The obtained soliton solutions are represented by Gram determinant forms. We have shown that the appearance of an additional wave number in the fundamental soliton solution brings out novel geometrical structures under the condition $k_{1I} = l_{1I}$. In addition, for $k_{1I} \neq l_{1I}$, the soliton number is increased by one in the long-wave component. The reason for the creation of additional soliton in the long-wave component is that the solitons in the two short-wave components nonlinearly interact among themselves through the LW component. Further, we

have observed that the nondegenerate solitons undergo three types of collisions, namely shape preserving with a zero phase shift, shape altering and shape changing collisions with finite phase shifts. The mechanism of the nonpreserving nature of phase terms or relative separation distances induces these novel shape altering and shape changing collision scenarios. However, they can be viewed as elastic collision only by taking time shifts in the asymptotic forms of nondegenerate solitons. Surprisingly, such type of collision property has not been observed in the degenerate counterpart though they belong to elastic collision only. Besides the above, the emergence of a coexisting nonlinear phenomenon in the two component LSRI system is also explored. We found that the existence of a partially nondegenerate soliton solution, which is a special case of the completely nondegenerate two-soliton solution, is responsible for the appearance of such a nonlinear phenomenon, where the nondegenerate soliton simultaneously exists with the degenerate soliton. We have noticed that the explicit appearance of degenerate soliton induces two types of interesting shape changing and energy sharing properties of nondegenerate soliton. Finally, we recovered the energy exchanging solitons from the nondegenerate solitons under degenerate limits. The present study on nondegenerate solitons of long-wave short-wave resonance interaction system will be useful in hydrodynamics, plasma physics, nonlinear optics and Bose-Einstein condensates.

4. We have pointed out the singularity nature of nondegenerate fundamental soliton in mixed 2- coupled nonlinear Schrödinger equations. we have also reported the existence of nondegenerate fundamental soliton solution for the N-coupled nonlinear Schrödinger equations. This new class of solitons exhibit multi-hump nature among all the modes. The existence of such special multi-humped profiles is demonstrated explicitly by considering the nondegenerate soliton solution for the 3 and 4 component cases. Very interestingly we have also shown the existence of partially nondegenerate soliton solutions by restricting the wave numbers suitably. The already known energy exchanging degenerate class of vector bright solitons is shown as a

sub-case by imposing specific restriction on the wave numbers. Finally, the stability of multi-humped nondegenerate fundamental soliton has also been verified numerically. We believe that the existence of multi-peak power nature in the nondegenerate fundamental soliton in multi-mode optical fibers may be relevant to increase the data stream in multi-level optical communication applications. Then the nondegenerate one soliton solution for 2- coherently coupled nonlinear Schrödinger equations have been derived using nonstandard Hirota bilinear procedure and breathing type triple hump and flat top soliton profiles were obtained.

6.3 Future works

1. We have studied the properties of fundamental nondegenerate soliton solutions and their two-solitons collision dynamics for focussing type 2-coupled nonlinear Schrödinger system/Manakov system, General coupled nonlinear Schrödinger system, 2-component long-wave short-wave Resonance Interaction system. Two-soliton collision dynamics of CNLS generalizations, namely 3, 4 and N-coupled equations are still open problems. Also one can study the collision dynamics of higher order solitons of the above mentioned systems.

2. It is a quite obvious question that what kind of effects will nondegenerate solitons show for other higher order nonlinear effects and their higher dimensional counterparts.

3. Nondegenerate solitons study in artificial materials like negative index materials will be of great interest due to their fascinating properties and potential applications.

4. In this present work we have constructed only the bright soliton solutions. One can derive dark soliton solutions also in appropriate cases. This work can be further extended to other interesting localized structures, namely breather and rogue wave solutions through already known systematic procedures.

5. One can also extend this study to other physically important systems like coupled Radhakrishnan-Kundu-Lakshmanan system, coupled Lakshmanan-Porsezian-Daniel system and some of the coupled real equations.

6. Mathematically this problem may be studied for more general class of initial conditions through a sophisticated Riemann–Hilbert problem approach.

7. Also in the next step, one can extend this study using numerical and experimental techniques which can suggest more useful results for the application purpose.

Bibliography

[1] M. Lakshmanan and S. Rajasekar, *Nonlinear dynamics: integrability, chaos and patterns* (Springer-Verlag, Berlin Heidelberg, 2003).

[2] D. D. J. Korteweg and D. G. de Vries, The London, Edinburgh, and Dublin Philosophical Magazine and Journal of Science **39**, 422 (1895).

[3] N. J. Zabusky and M. D. Kruskal, Physical Review Letters **15**, 240 (1965).

[4] E. Fermi, P Pasta, S Ulam, and M Tsingou, Los Alamos Scientific Laboratory Internal Report, LA 1940 (1955).

[5] Y. S. Kivshar and G. Agrawal, *Optical solitons: from fibers to photonic crystals* (Academic press, 2003).

[6] G. P. Agrawal, *Nonlinear fiber optics* (Springer, 2000).

[7] Z. Chen, M. Segev, and D. N. Christodoulides, Reports on Progress in Physics **75**, 086401 (2012).

[8] B. A. Malomed, D. Mihalache, F. Wise, and L. Torner, Journal of Optics B: Quantum and Semiclassical Optics **7**, R53 (2005).

[9] A. Hasegawa and F. Tappert, Applied Physics Letters **23**, 142 (1973).

[10] A. Hasegawa and F. Tappert, Applied Physics Letters **23**, 171 (1973).

[11] L. F. Mollenauer, R. H. Stolen, and J. P. Gordon, Physical Review Letters **45**, 1095 (1980).

[12] G. J. P. Mollenauer L F, *Nonlinear fiber optics* (Academic Press: San Diego, CA, USA, 2003).

[13] V. E. Zakharov and A. B. Shabat, Sov. Phys. JETP **37**, 823 (1973).

[14] C. S. Gardner, J. M. Greene, M. D. Kruskal, and R. M. Miura, Physical Review Letters **19**, 1095 (1967).

[15] M. J. Ablowitz, M. Ablowitz, P. Clarkson, and P. A. Clarkson, *Solitons, nonlinear evolution equations and inverse scattering*, Vol. 149 (Cambridge university press, 1991).

[16] A. Chabchoub, A. Slunyaev, N. Hoffmann, F. Dias, B. Kibler, G. Genty, J. M. Dudley, and N. Akhmediev, Frontiers in Physics, 455 (2021).

[17] J. Gordon, Optics Letters **8**, 596 (1983).

[18] F. M. Mitschke and L. F. Mollenauer, Optics Letters **12**, 355 (1987).

[19] M Stratmann, T Pagel, and F Mitschke, Physical Review Letters **95**, 143902 (2005).

[20] A Hause, H Hartwig, M Böhm, and F Mitschke, Physical Review A **78**, 063817 (2008).

[21] N. Akhmediev, G Town, and S Wabnitz, Optics Communications **104**, 385 (1994).

[22] B. A. Malomed, in *Large scale structures in nonlinear physics* (Springer, 1991), pp. 288–294.

[23] V. V. Afanasjev, B. A. Malomed, and P. Chu, Physical Review E **56**, 6020 (1997).

[24] U Al Khawaja, Physical Review E **81**, 056603 (2010).

[25] P. Grelu and J. Soto-Crespo, Journal of Optics B: Quantum and Semiclassical Optics **6**, S271 (2004).

[26] D. Tang, B Zhao, D. Shen, C Lu, W. Man, and H. Y. Tam, Physical Review A **68**, 013816 (2003).

[27] N. Akhmediev, A Ankiewicz, and J. Soto-Crespo, JOSA B **15**, 515 (1998).

[28] O. Melchert, S. Willms, S. Bose, A. Yulin, B. Roth, F. Mitschke, U. Morgner, I. Babushkin, and A. Demircan, Physical Review Letters **123**, 243905 (2019).

[29] P. Rohrmann, A. Hause, and F. Mitschke, Scientific Reports **2**, 1 (2012).

[30] M. H. Jakubowski, K. Steiglitz, and R. Squier, Physical Review E **58**, 6752 (1998).

[31] K. Steiglitz, Physical Review E **63**, 016608 (2000).

[32] N. Akhmediev and A. Ankiewicz, Chaos: An Interdisciplinary Journal of Nonlinear Science **10**, 600 (2000).

[33] F Mitschke, Handbook of Optical Fibers; Peng, G.-D., Ed, 1 (2018).

[34] R Radhakrishnan, R Sahadevan, and M. Lakshmanan, Chaos, Solitons & Fractals **5**, 2315 (1995).

[35] S. V. Manakov, Soviet Physics-JETP **38**, 248 (1974).

[36] C. R. Menyuk, IEEE journal of quantum electronics **25**, 2674 (1989).

[37] R Radhakrishnan, M Lakshmanan, and J Hietarinta, Physical Review E **56**, 2213 (1997).

[38] T Kanna and M Lakshmanan, Physical Review Letters **86**, 5043 (2001).

[39] C. Anastassiou, M. Segev, K. Steiglitz, J. Giordmaine, M. Mitchell, M.-f. Shih, S. Lan, and J. Martin, Physical Review Letters **83**, 2332 (1999).

[40] J. Kang, G. Stegeman, J. Aitchison, and N Akhmediev, Physical Review Letters **76**, 3699 (1996).

[41] D. Rand, I. Glesk, C.-S. Brès, D. A. Nolan, X. Chen, J. Koh, J. W. Fleischer, K. Steiglitz, and P. R. Prucnal, Physical Review Letters **98**, 053902 (2007).

[42] M. Soljacić, K. Steiglitz, S. M. Sears, M. Segev, M. H. Jakubowski, and R. Squier, Physical Review Letters **90**, 254102 (2003).

[43] T Kanna and M Lakshmanan, Physical Review E **67**, 046617 (2003).

[44] M Vijayajayanthi, T Kanna, K Murali, and M Lakshmanan, Physical Review E **97**, 060201 (2018).

[45] M. Segev, B. Crosignani, A. Yariv, and B. Fischer, Physical Review Letters **68**, 923 (1992).

[46] G. C. Duree Jr, J. L. Shultz, G. J. Salamo, M. Segev, A. Yariv, B. Crosignani, P. Di Porto, E. J. Sharp, and R. R. Neurgaonkar, Physical Review Letters **71**, 533 (1993).

[47] M. Segev, G. C. Valley, B. Crosignani, P. Diporto, and A. Yariv, Physical Review Letters **73**, 3211 (1994).

[48] D. N. Christodoulides and M. Carvalho, JOSA B **12**, 1628 (1995).

[49] D. Christodoulides, S. Singh, M. Carvalho, and M Segev, Applied Physics Letters **68**, 1763 (1996).

[50] Z. Chen, M. Segev, T. H. Coskun, and D. N. Christodoulides, Optics Letters **21**, 1436 (1996).

[51] Z. Chen, M. Segev, T. H. Coskun, D. N. Christodoulides, Y. S. Kivshar, and V. V. Afanasjev, Optics Letters **21**, 1821 (1996).

[52] M. Mitchell, M. Segev, and D. N. Christodoulides, Physical Review Letters **80**, 4657 (1998).

[53] N. Akhmediev, W. Królikowski, and A. Snyder, Physical Review Letters **81**, 4632 (1998).

[54] A. A. Sukhorukov and N. N. Akhmediev, Physical Review Letters **83**, 4736 (1999).

[55] A. Ankiewicz, W. Królikowski, and N. N. Akhmediev, Physical Review E **59**, 6079 (1999).

[56] W. Królikowski, N. Akhmediev, and B. Luther-Davies, Physical Review E **59**, 4654 (1999).

[57] D. N. Christodoulides and R. Joseph, Optics Letters **13**, 53 (1988).

[58] N. Akhmediev, A. Buryak, J. Soto-Crespo, and D. Andersen, JOSA B **12**, 434 (1995).

[59] B. C. Collings, S. T. Cundiff, N. Akhmediev, J. M. Soto-Crespo, K. Bergman, and W. Knox, JOSA B **17**, 354 (2000).

[60] M. Tratnik and J. Sipe, Physical Review A **38**, 2011 (1988).

[61] M. Haelterman, A. Sheppard, and A. Snyder, Optics Letters **18**, 1406 (1993).

[62] E. A. Ostrovskaya, Y. S. Kivshar, Z. Chen, and M. Segev, Optics Letters **24**, 327 (1999).

[63] J. Yang, Physica D: Nonlinear Phenomena **108**, 92 (1997).

[64] E. A. Ostrovskaya, Y. S. Kivshar, D. V. Skryabin, and W. J. Firth, Physical Review Letters **83**, 296 (1999).

[65] D. E. Pelinovsky and J. Yang, Studies in Applied Mathematics **115**, 109 (2005).

[66] T Kanna, M Lakshmanan, P. T. Dinda, and N. Akhmediev, Physical Review E **73**, 026604 (2006).

[67] M Vijayajayanthi, T Kanna, and M Lakshmanan, Physical Review A **77**, 013820 (2008).

[68] A. P. Sheppard and Y. S. Kivshar, Physical Review E **55**, 4773 (1997).

[69] R Radhakrishnan and K Aravinthan, Physical Review E **75**, 066605 (2007).

[70] R Radhakrishnan, N Manikandan, and K Aravinthan, Physical Review E **92**, 062913 (2015).

[71] B.-F. Feng, Journal of Physics A: Mathematical and Theoretical **47**, 355203 (2014).

[72] R Radhakrishnan and M. Lakshmanan, Journal of Physics A: Mathematical and General **28**, 2683 (1995).

[73] Y. Ohta, D.-S. Wang, and J. Yang, Studies in Applied Mathematics **127**, 345 (2011).

[74] P. Kevrekidis and D. Frantzeskakis, Reviews in Physics **1**, 140 (2016).

[75] Y. Song, X. Shi, C. Wu, D. Tang, and H. Zhang, Applied Physics Reviews **6**, 021313 (2019).

[76] N. Akhmediev and A. Ankiewicz, *Dissipative solitons: from optics to biology and medicine*, Vol. 751 (Springer Science & Business Media, 2008).

[77] S Stalin, R Ramakrishnan, M Senthilvelan, and M Lakshmanan, Physical Review Letters **122**, 043901 (2019).

[78] R Ramakrishnan, S Stalin, and M Lakshmanan, Physical Review E **102**, 042212 (2020).

[79] S Stalin, R Ramakrishnan, and M Lakshmanan, Physics Letters A **384**, 126201 (2020).

[80] Y.-H. Qin, L.-C. Zhao, and L. Ling, Physical Review E **100**, 022212 (2019).

[81] C.-R. Zhang, B. Tian, Q.-X. Qu, L. Liu, and H.-Y. Tian, Zeitschrift für angewandte Mathematik und Physik **71**, 1 (2020).

[82] C.-C. Ding, Y.-T. Gao, L. Hu, G.-F. Deng, and C.-Y. Zhang, Chaos, Solitons & Fractals **142**, 110363 (2021).

[83] Y.-H. Qin, L.-C. Zhao, Z.-Q. Yang, and L. Ling, Physical Review E **104**, 014201 (2021).

[84] R Ramakrishnan, S Stalin, and M Lakshmanan, Journal of Physics A: Mathematical and Theoretical **54**, 14LT01 (2021).

[85] M Lakshmanan and T Kanna, Pramana **57**, 885 (2001).

[86] V. E. Zakharov and E. Schulman, Physica D: Nonlinear Phenomena **4**, 270 (1982).

[87] D. Kaup and B. Malomed, Physical Review A **48**, 599 (1993).

[88] N Lazarides and G. Tsironis, Physical Review E **71**, 036614 (2005).

[89] V. G. Makhankov, Physics Letters A **81**, 156 (1981).

[90] V. Makhankov, N. Makhaldiani, and O. Pashaev, Physics Letters A **81**, 161 (1981).

[91] U Lindner and V. Fedyanin, Physica Status Solidi (b) **89**, 123 (1978).

[92] V. M. Perez-Garcia and J. B. Beitia, Physical Review A **72**, 033620 (2005).

[93] M. Ablowitz, B Prinari, and A. Trubatch, Inverse Problems **20**, 1217 (2004).

[94] B. Prinari, M. J. Ablowitz, and G. Biondini, Journal of Mathematical Physics **47**, 063508 (2006).

[95] G. Biondini and G. Kovačič, Journal of Mathematical Physics **55**, 031506 (2014).

[96] B. Prinari, G. Biondini, and A. D. Trubatch, Studies in Applied Mathematics **126**, 245 (2011).

[97] G. Biondini and D. Kraus, SIAM Journal on Mathematical Analysis **47**, 706 (2015).

[98] B. Prinari, F. Vitale, and G. Biondini, Journal of Mathematical Physics **56**, 071505 (2015).

[99] G. Biondini, D. K. Kraus, and B. Prinari, Communications in Mathematical Physics **348**, 475 (2016).

[100] Q.-H. Park and H. Shin, Physical Review E **61**, 3093 (2000).

[101] A. Degasperis and S. Lombardo, Journal of Physics A: Mathematical and Theoretical **40**, 961 (2007).

[102] A. Degasperis and S. Lombardo, Journal of Physics A: Mathematical and Theoretical **42**, 385206 (2009).

[103] L. Ling, L.-C. Zhao, and B. Guo, Nonlinearity **28**, 3243 (2015).

[104] L. Ling, L.-C. Zhao, and B. Guo, Communications in Nonlinear Science and Numerical Simulation **32**, 285 (2016).

[105] T. Tsuchida, arXiv preprint arXiv:1308.6623 (2013).

[106] B. Crosignani, A. Cutolo, and P. Di Porto, JOSA **72**, 1136 (1982).

[107] Q.-H. Park and H. Shin, Physical Review E **59**, 2373 (1999).

[108] N. Akhmediev and E. Ostrovskaya, Optics Communications **132**, 190 (1996).

[109] T Kanna, M Vijayajayanthi, and M Lakshmanan, Journal of Physics A: Mathematical and Theoretical **43**, 434018 (2010).

[110] T Kanna and K Sakkaravarthi, Journal of Physics A: Mathematical and Theoretical **44**, 285211 (2011).

[111] K. Kasamatsu, M. Tsubota, and M. Ueda, Physical Review Letters **93**, 250406 (2004).

[112] T Congy, A. Kamchatnov, and N Pavloff, Physical Review A **93**, 043613 (2016).

[113] R. B. Mareeswaran and T Kanna, Physics Letters A **380**, 3244 (2016).

[114] J. Ieda, T. Miyakawa, and M. Wadati, Physical Review Letters **93**, 194102 (2004).

[115] B. Prinari, A. K. Ortiz, C. van der Mee, and M. Grabowski, Studies in Applied Mathematics **141**, 308 (2018).

[116] L. Li, Z. Li, B. A. Malomed, D. Mihalache, and W. Liu, Physical Review A **72**, 033611 (2005).

[117] D.-S. Wang, D.-J. Zhang, and J. Yang, Journal of Mathematical Physics **51**, 023510 (2010).

[118] X. Lü and M. Peng, Nonlinear Dynamics **73**, 405 (2013).

[119] N. V. Priya and M Senthilvelan, Communications in Nonlinear Science and Numerical Simulation **36**, 366 (2016).

[120] A. Agalarov, V. Zhulego, and T. Gadzhimuradov, Physical Review E **91**, 042909 (2015).

[121] V. E. Zakharov et al., Sov. Phys. JETP **35**, 908 (1972).

[122] D. Benney, Studies in Applied Mathematics **56**, 81 (1977).

[123] Y. S. Kivshar, Optics Letters **17**, 1322 (1992).

[124] A. Chowdhury and J. A. Tataronis, Physical Review Letters **100**, 153905 (2008).

[125] M. J. Ablowitz, G. Biondini, and S. Blair, Physical Review E **63**, 046605 (2001).

[126] S. V. Sazonov and N. V. Ustinov, JETP letters **94**, 610 (2011).

[127] K. Nishikawa, H Hojo, K Mima, and H Ikezi, Physical Review Letters **33**, 148 (1974).

[128] N. Yajima and M. Oikawa, Progress of Theoretical Physics **56**, 1719 (1976).

[129] T. Kawahara, Journal of the Physical Society of Japan **38**, 265 (1975).

[130] T. Kawahara, N. Sugimoto, and T. Kakutani, Journal of the Physical Society of Japan **39**, 1379 (1975).

[131] V. D. Djordjevic and L. G. Redekopp, Journal of Fluid Mechanics **79**, 703 (1977).

[132] C. Koop and L. Redekopp, Journal of Fluid Mechanics **111**, 367 (1981).

[133] J. P. Boyd, Journal of Physical Oceanography **13**, 450 (1983).

[134] A. A. Zabolotskii, Journal of Experimental and Theoretical Physics **109**, 859 (2009).

[135] M Aguero, D. Frantzeskakis, and P. Kevrekidis, Journal of Physics A: Mathematical and General **39**, 7705 (2006).

[136] H. Nistazakis, D. Frantzeskakis, P. Kevrekidis, B. Malomed, and R Carretero-González, Physical Review A **77**, 033612 (2008).

[137] Y.-C. Ma and L. Redekopp, The Physics of Fluids **22**, 1872 (1979).

[138] T Kanna, K Sakkaravarthi, and K Tamilselvan, Physical Review E **88**, 062921 (2013).

[139] J. Chen, Y. Chen, B.-F. Feng, and K.-i. Maruno, Journal of the Physical Society of Japan **84**, 074001 (2015).

[140] J. Chen, Y. Chen, B.-F. Feng, and K.-i. Maruno, Journal of the Physical Society of Japan **84**, 034002 (2015).

[141] M. Oikawa, M. Okamura, and M. Funakoshi, Journal of the Physical Society of Japan **58**, 4416 (1989).

[142] Y. Ohta, K.-i. Maruno, and M. Oikawa, Journal of Physics A: Mathematical and Theoretical **40**, 7659 (2007).

[143] R Radha, C. S. Kumar, M Lakshmanan, and C. Gilson, Journal of Physics A: Mathematical and Theoretical **42**, 102002 (2009).

[144] T Kanna, M Vijayajayanthi, K Sakkaravarthi, and M Lakshmanan, Journal of Physics A: Mathematical and Theoretical **42**, 115103 (2009).

[145] K Sakkaravarthi, T Kanna, M Vijayajayanthi, and M Lakshmanan, Physical Review E **90**, 052912 (2014).

[146] T Kanna, M Vijayajayanthi, and M Lakshmanan, Physical Review E **90**, 042901 (2014).

[147] J. Chen, B.-F. Feng, Y. Chen, and Z. Ma, Nonlinear Dynamics **88**, 1273 (2017).

[148] K. Wing Chow, H. Ning Chan, D. Jacob Kedziora, and R. Hamilton James Grimshaw, Journal of the Physical Society of Japan **82**, 074001 (2013).

[149] S. Chen, P. Grelu, and J. Soto-Crespo, Physical Review E **89**, 011201 (2014).

[150] H. N. Chan, E. Ding, D. J. Kedziora, R. Grimshaw, and K. W. Chow, Nonlinear Dynamics **85**, 2827 (2016).

[151] S. Chen, J. M. Soto-Crespo, and P. Grelu, Physical Review E **90**, 033203 (2014).

[152] J. Chen, Y. Chen, B.-F. Feng, and K.-i. Maruno, Physics Letters A **379**, 1510 (2015).

[153] J. Rao, K. Porsezian, J. He, and T. Kanna, Proceedings of the Royal Society A: Mathematical, Physical and Engineering Sciences **474**, 20170627 (2018).

[154] J.-W. Yang, Y.-T. Gao, Y.-H. Sun, Y.-J. Shen, and C.-Q. Su, The European Physical Journal Plus **131**, 1 (2016).

[155] R. Hirota, *The direct method in soliton theory*, 155 (Cambridge University Press, 2004).

[156] N. N. Akhmediev, A. Ankiewicz, et al., *Nonlinear pulses and beams* (Springer, 1997).

[157] A. W. Snyder and D. J. Mitchell, Physical Review Letters **80**, 1422 (1998).

[158] A. Hasegawa, The Physics of Fluids **20**, 2155 (1977).

[159] Z.-Y. Sun, Y.-T. Gao, X. Yu, W.-J. Liu, and Y. Liu, Physical Review E **80**, 066608 (2009).

[160] S Stalin, R Ramakrishnan, and M Lakshmanan, in Photonics, Vol. 8, 7 (Multidisciplinary Digital Publishing Institute, 2021), p. 258.

[161] T Kanna, K Sakkaravarthi, and K Tamilselvan, Physical Review E **88**, 062921 (2013).

[162] M. J. Ablowitz, Y. Ohta, and A. D. Trubatch, Physics Letters A **253**, 287 (1999).

[163] M Vijayajayanthi, T Kanna, and M Lakshmanan, The European Physical Journal Special Topics **173**, 57 (2009).

[164] T. Dauxois and M. Peyrard, *Physics of solitons* (Cambridge University Press, 2006).

[165] C. Kopp and L. Redekopp, J. Fluid Mech **111**, 367 (1981).

[166] T. Bersano, V Gokhroo, M. Khamehchi, J D'Ambroise, D. Frantzeskakis, P Engels, and P. Kevrekidis, Physical Review Letters **120**, 063202 (2018).

[167] F. Baronio, A. Degasperis, M. Conforti, and S. Wabnitz, Physical Review Letters **109**, 044102 (2012).

[168] C Gilson, J Hietarinta, J Nimmo, and Y Ohta, Physical Review E **68**, 016614 (2003).

[169] Y Nogami and C. Warke, Physics Letters A **59**, 251 (1976).

[170] P. Muruganandam and S. K. Adhikari, Computer Physics Communications **180**, 1888 (2009).

Nondegenerate Solitons in Manakov System

S. Stalin, R. Ramakrishnan, M. Senthilvelan, and M. Lakshmanan*
Centre for Nonlinear Dynamics, School of Physics, Bharathidasan University, Tiruchirapalli-620 024, India

(Received 8 May 2018; revised manuscript received 29 September 2018; published 28 January 2019)

It is known that the Manakov equation which describes wave propagation in two mode optical fibers, photorefractive materials, etc., can admit solitons which allow energy redistribution between the modes on collision that also leads to logical computing. In this Letter, we point out that the Manakov system can admit a more general type of nondegenerate fundamental solitons corresponding to different wave numbers, which undergo collisions without any energy redistribution. The previously known class of solitons which allows energy redistribution among the modes turns out to be a special case corresponding to solitary waves with identical wave numbers in both the modes and traveling with the same velocity. We trace out the reason behind such a possibility and analyze the physical consequences.

DOI: 10.1103/PhysRevLett.122.043901

The discovery of solitons has created a new pathway to understand the wave propagation in many physical systems with nonlinearity [1]. In particular, the existence of optical solitons in nonlinear Kerr media [2] provoked the investigation on solitons from different perspectives, particularly from the applications point of view. By generalizing the waves propagating in an isotropic medium [3] to an anisotropic medium, a pair of coupled equations for orthogonally polarized waves has been obtained by Manakov [4,5] as

$$iq_{jz} + q_{jtt} + 2\sum_{p=1}^{2} |q_p|^2 q_j = 0, \qquad j = 1, 2, \quad (1)$$

where q_j, $j = 1, 2$, describe orthogonally polarized complex waves. Here the subscripts z and t represent the normalized distance and retarded time, respectively. Equation (1) also appears in many physical situations such as single optical field propagation in birefringent fibers [6], self-trapped incoherent light beam propagation in a photorefractive medium [7–9], and so on. The generalization of Eq. (1) to arbitrary N waves is useful to model optical pulse propagation in multimode fibers [10]. It has been identified [4] that the polarization vectors of the solitons change when orthogonally polarized waves nonlinearly interact with each other, leading to an energy exchange interaction between the modes [11]. The experimental observation of the latter has been demonstrated in Refs. [12–14]. The shape-changing collision property of such waves, which we designate here as a degenerate polarized soliton propagating with identical velocity and wave number in the two modes, gave rise to the possibility of constructing logic gates leading to all-optical computing at least in a theoretical sense [15–17]. Energy-sharing collisions among the optical vector solitons have been explored [16] by constructing multisoliton solutions explicitly to the multicomponent nonlinear Schrödinger equations. Furthermore, it has been shown that the multisoliton interaction process satisfies the Yang-Baxter relation [18]. It is clear from these studies that the shape-changing collision that occurs among the solitons with identical wave numbers in all the modes has been well understood. However, to our knowledge, studies on solitons with nonidentical wave numbers in all the modes have not been considered so far. Consequently, one would like to explore the role of such an additional wave number(s) on the soliton structures and collision scenario as well.

In the contemporary studies, a new class of multihump solitons has been identified in different physical situations. In birefringent dispersive nonlinear media, asymmetric double-hump–single-hump frozen states have been obtained [19]. Double-hump structure has been observed for the Manakov equation by considering two soliton solutions [20,21]. The first experimental observation of multihump solitons was demonstrated when the self-trapped incoherent wave packets propagate in a dispersive nonlinear medium [22]. These unusual solitons have been found in various nonlinear coupled field models [23]. The stability of multihump optical solitons has also been investigated in the case of a saturable nonlinear medium [24]. It is reported that in such a medium both two- and three-hump solitons do not survive after collision. N-self-trapped multihumped partially coherent solitons have also been explored in a photorefractive medium [25]. The coherent coupling between copropagating fields also gives rise to double-hump solitons in the coherently coupled nonlinear Schrödinger system [26]. In addition to the above, the dynamics of multihump structured solitons have also been studied in certain dissipative systems [27–30]. A double-hump phase-locked higher-order vector soliton has been observed, and its dynamics has been investigated in mode-locked fiber lasers [27,28]. Similarly in deployed fiber systems and fiber laser cavities, double-hump solitons have

been observed during the buildup process of soliton molecules [31,32].

Motivated by the above, in this Letter, we present a new class of generalized soliton solutions for the Manakov model, exhibiting various interesting structures under general parametric conditions. A fundamental double-hump soliton (as well as other structures described below) sustains its shape even after a collision with another similar soliton. This behavior is in contrast to the one which exists in saturable nonlinear media, where two and three humps do not survive after a collision. The soliton solutions presented in this Letter also have both symmetric and asymmetric natures analogous to the partially coherent solitons in a photorefractive medium. Under a specific parametric restriction on wave numbers, they degenerate into the standard Manakov solitons exhibiting shape-changing collisions [11,16].

To explore the new family of soliton solutions for Eq. (1), we consider the bilinear forms of Eq. (1) as $(iD_z+D_t^2)g^{(j)}f=0$, $j=1, 2$, and $D_t^2ff=2\sum_{n=1}^{2}g^{(n)}g^{(n)*}$, which are obtained through the dependent variable transformations $q_j=g^{(j)}/f$, $j=1, 2$. Here D_z and D_t are the well-known Hirota bilinear operators [33], and $g^{(j)}(z,t)$ are complex functions, whereas f is a real function, and $*$ denotes complex conjugation. In principle, multisoliton solutions of Eq. (1) can be constructed by solving recursively the system of linear partial differential equations which results by substituting the series expansions $g^{(j)}=\epsilon g_1^{(j)}+\epsilon^3 g_3^{(j)}+\cdots$ and $f=1+\epsilon^2 f_2+\epsilon^4 f_4+\cdots$ for the unknown functions $g^{(j)}$ and f in the bilinear forms. Here ϵ is a formal expansion parameter.

Considering two different seed solutions for $g_1^{(1)}$ and $g_1^{(2)}$ as $\alpha_1^{(1)}e^{\eta_1}$ and $\alpha_1^{(2)}e^{\xi_1}$, respectively, where $\eta_1=k_1t+ik_1^2z$, $\xi_1=l_1t+il_1^2z$, and $\alpha_1^{(j)}$, $j=1, 2$, k_1 and l_1 are, in general, independent complex wave numbers, to the resultant linear partial differential equations $(iD_z+D_t^2)g_1^{(j)}1=0$, $j=1, 2$, which arise in the lowest order of ϵ, the series expansion gets terminated as $g^{(j)}=\epsilon g_1^{(j)}+\epsilon^3 g_3^{(j)}$ and $f=1+\epsilon^2 f_2+\epsilon^4 f_4$. The explicit forms of the unknown functions present in the truncated series expansions constitute a new fundamental one soliton solution to Eq. (1) in the form

$$q_1=(\alpha_1^{(1)}e^{\eta_1}+e^{\eta_1+\xi_1+\xi_1^*+\Delta_1^{(1)}})/D_1,$$
$$q_2=(\alpha_1^{(2)}e^{\xi_1}+e^{\eta_1+\eta_1^*+\xi_1+\Delta_1^{(2)}})/D_1, \tag{2}$$

where $D_1=1+e^{\eta_1+\eta_1^*+\delta_1}+e^{\xi_1+\xi_1^*+\delta_2}+e^{\eta_1+\eta_1^*+\xi_1+\xi_1^*+\delta_{11}}$, $e^{\delta_1}=[|\alpha_1^{(1)}|^2/(k_1+k_1^*)^2]$, $e^{\delta_2}=[|\alpha_1^{(2)}|^2/(l_1+l_1^*)^2]$, $e^{\delta_{11}}=\{[|k_1-l_1|^2|\alpha_1^{(1)}|^2|\alpha_1^{(2)}|^2]/[(k_1+k_1^*)^2(k_1^*+l_1)(k_1+l_1^*)(l_1+l_1^*)^2]\}$, $e^{\Delta_1^{(1)}}=\{[(k_1-l_1)\alpha_1^{(1)}|\alpha_1^{(2)}|^2]/[(k_1+l_1^*)(l_1+l_1^*)^2]\}$, and $e^{\Delta_1^{(2)}}=-\{[(k_1-l_1)|\alpha_1^{(1)}|^2\alpha_1^{(2)}]/[(k_1+k_1^*)^2(k_1^*+l_1)]\}$. From the above, it is evident that the fundamental solitons propagating in the two modes are characterized by four arbitrary complex parameters k_1, l_1, and $\alpha_1^{(j)}$, $j=1, 2$. These nontrivial parameters determine the shape, amplitude, width, and velocity of the solitons which propagate in the Kerr media or photorefractive media. The amplitudes of the solitons that are present in the two modes q_1 and q_2 are governed by the real parts of the wave numbers k_1 and l_1, whereas velocities are described by the imaginary parts of them. Note that $\alpha_1^{(j)}$, $j=1, 2$, are related to the unit polarization vectors of the solitons in the two modes.

To identify certain special features of the obtained four complex parameter family of soliton solution (2), we first consider (for simplicity of analysis) the special case where the imaginary parts of the wave numbers $k_{1I}=l_{1I}$ but with $k_{1R}\neq l_{1R}$. The latter case yields at least the following four different symmetric wave profiles, apart from similar asymmetric wave profiles, from solution (2) by incorporating the condition $k_{1R}<l_{1R}$ with further conditions and with suitable choices of parameters (examples given in Ref. [34]): (i) single-hump–single-hump soliton, $\alpha_{1R}^{(1)}>\alpha_{1R}^{(2)}$ and $\alpha_{1I}^{(1)}=\alpha_{1I}^{(2)}$; (ii) double-hump–single-hump soliton, $\alpha_{1R}^{(1)}=\alpha_{1R}^{(2)}$ and $\alpha_{1I}^{(1)}<\alpha_{1I}^{(2)}$; (iii) double-hump-flattop soliton, $\alpha_{1R}^{(1)}=\alpha_{1R}^{(2)}$ and $\alpha_{1I}^{(1)}\approx\alpha_{1I}^{(2)}$; (iv) double-hump–double-hump soliton, $\alpha_{1R}^{(1)}>\alpha_{1R}^{(2)}$ and $\alpha_{1I}^{(1)}=\alpha_{1I}^{(2)}$. Similar conditions can be given for $k_{1R}>l_{1R}$ also. We have not listed the asymmetric wave profiles here for brevity, which also exhibit the properties discussed below. A similar classification can be made for the case $k_{1I}\neq l_{1I}$, so that the solitons propagate in the two modes with different velocities and exhibit similar interaction properties. These will be discussed separately.

To illustrate the symmetric case, we display only the intensity profile of the double-hump soliton in Fig. 1. We call the solitons that have two distinct wave numbers in both the modes as in Eq. (2) nondegenerate solitons (which can exist as different profiles as described above), while the solitons which have identical wave numbers in all the modes (which exist only in single-hump form) are designated as degenerate solitons. In particular, in the special case when $k_1=l_1$, the forms of q_j given in Eq. (2) degenerate into the standard bright soliton form [4,11]

$$q_j=\frac{\alpha_1^{(j)}e^{\eta_1}}{1+e^{\eta_1+\eta_1^*+R}}, \qquad j=1,2, \tag{3}$$

which can be rewritten as

$$q_j=k_{1R}\hat{A}_j e^{i\eta_{1I}}\mathrm{sech}\left(\eta_{1R}+\frac{R}{2}\right), \tag{4}$$

where $\eta_{1R}=k_{1R}(t-2k_{1I}z)$, $\eta_{1I}=k_{1I}t+(k_{1R}^2-k_{1I}^2)z$, $\hat{A}_j=\{[\alpha_1^{(j)}]/\sqrt{(|\alpha_1^{(1)}|^2+|\alpha_1^{(2)}|^2)}\}$,

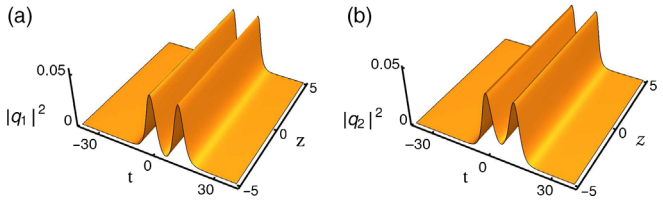

FIG. 1. Nondegenerate symmetric double-hump one soliton in the two modes: (a) and (b) denote the intensities of the components q_1 and q_2, respectively. The parameters are chosen as $k_1 = 0.316 + 0.5i$, $l_1 = 0.333 + 0.5i$, $\alpha_1^{(1)} = 0.49 + 0.45i$, and $\alpha_1^{(2)} = 0.45 + 0.45i$.

$e^R = [(|\alpha_1^{(1)}|^2 + |\alpha_1^{(2)}|^2)/(k_1 + k_1^*)^2]$, and $j = 1, 2$. Note that the above fundamental bright soliton always propagates in both the modes q_1 and q_2 with the same velocity $2k_{1I}$. The polarization vectors $(\hat{A}_1, \hat{A}_2)^\dagger$ have different amplitudes and phases, unlike the nondegenerate case where they have only different phases $[A_1 = (\alpha_1^{(1)}/\alpha_1^{(1)*})^{1/2}$, $A_2 = (\alpha_1^{(2)}/\alpha_1^{(2)*})^{1/2}]^\dagger$ [vide Eq. (2)] but the same unit amplitude. We call the above type of soliton (3) or (4) a degenerate soliton [35].

In order to understand the collision dynamics of the soliton solution of the kind (2), it is essential to construct the corresponding two-soliton solution. In the latter case, the series expansion for q_j, $j = 1, 2$, gets terminated as $g^{(j)} = \epsilon g_1^{(j)} + \epsilon^3 g_3^{(j)} + \epsilon^5 g_5^{(j)} + \epsilon^7 g_7^{(j)}$ and $f = 1 + \epsilon^2 f_2 + \epsilon^4 f_4 + \epsilon^6 f_6 + \epsilon^8 f_8$. The obtained explicit forms of $g^{(j)}$ and $f, j = 1, 2$, in the above truncated expansions constitute the nondegenerate two-soliton solution of Eq. (1), which reduces to the known form given in Ref. [11] for $k_i = l_i$, $i = 1, 2$. The complicated profiles of the present nondegenerate two-soliton solution are governed by eight arbitrary complex parameters k_j, l_j, $\alpha_1^{(j)}$, and $\alpha_2^{(j)}$, $j = 1, 2$ (see Supplemental Material [34]).

To study the collision dynamics between the nondegenerate two solitons, as an example, we again confine ourselves to the case of symmetric double-hump solitons by fixing the imaginary parts of the wave numbers as $k_{iI} = l_{iI}$, $i = 1, 2$. For other types also, a similar analysis has been carried out. By carefully examining the behavior of the obtained nondegenerate two-soliton solution in the asymptotic regimes, $z \to \pm\infty$, we find that the phases of the fundamental nondegenerate double-hump solitons in both the modes change during the collision process, while the intensities remain unchanged. This can be verified by defining the transition amplitudes as $T_j^l = (A_j^{l+}/A_j^{l-})$, $j = 1, 2$ and $l = 1, 2$, where subscript j represents the mode and superscript $l\pm$ denote the nondegenerate soliton numbers 1 and 2 designated as S_1 and S_2, respectively, in the asymptotic regimes $z \to \pm\infty$.

In the nondegenerate double-hump soliton case, the amplitudes of the solitons S_1 and S_2 in the first mode $(2k_{1R}A_1^{1-}, \{[(k_1-k_2)(k_2-l_1)^{1/2}(k_1+k_2^*)(k_2^*+l_1)^{1/2}]/[(k_1^*-k_2^*)(k_2^*-l_1^*)^{1/2}(k_1^*+k_2)(k_2+l_1^*)^{1/2}]\}2k_{2R}A_2^{1-})$ before a collision change to $(\{[(k_1-k_2)(k_1-l_2)^{1/2}(k_1^*+k_2)\times(k_1^*+l_2)^{1/2}]/[(k_1^*-k_2^*)(k_1^*-l_2^*)^{1/2}(k_1+k_2^*)(k_1+l_2^*)^{1/2}]\}\times 2k_{1R}A_1^{1+}, 2k_{2R}A_2^{1+})$ after a collision, where $A_1^{1\pm} = \sqrt{[\alpha_1^{(1)}/\alpha_1^{(1)^*}]}$ and $A_2^{1\pm} = \sqrt{[\alpha_2^{(1)}/\alpha_2^{(1)^*}]}$. Similarly in the second component, the amplitudes of the solitons S_1 and S_2 are $(2l_{1R}A_1^{2-}, \{[(l_1-l_2)(k_1-l_2)^{1/2}(l_1+l_2^*)(k_1+l_2^*)^{1/2}]/(l_1^*-l_2^*)(k_1^*-l_2^*)^{1/2}(k_1^*+l_2)^{1/2}(l_1^*+l_2)\}2l_{2R}A_2^{2-})$ before a collision which change to $(\{[(l_1-l_2)(l_1-k_2)^{1/2}\times(l_1^*+l_2)(k_2+l_1^*)^{1/2}]/[(l_1^*-l_2^*)(k_2^*-l_1^*)^{1/2}(l_1+l_2^*)\times(k_2^*+l_2)^{1/2}]\}2l_{1R}A_1^{2+}, 2l_{2R}A_2^{2+})$ after a collision, where $A_1^{2\pm} = \sqrt{[\alpha_1^{(2)}/\alpha_1^{(2)^*}]}$ and $A_2^{2\pm} = \sqrt{[\alpha_2^{(2)}/\alpha_2^{(2)^*}]}$. However, the intensity redistribution does not occur among the modes of the solitons, which can be confirmed by taking the absolute squares of the transition amplitudes which turn out to be unity, that is, $|T_j^l|^2 = 1$. This shows that, in the nondegenerate case, $k_i \neq l_i$, $i = 1, 2$, the polarization vectors do not contribute to intensity redistribution among the modes. Consequently, the double-hump solitons in each mode exhibit a shape-preserving collision corresponding to an elastic nature. This is illustrated in Fig. 2 for the parameter values given there by actually plotting the two-soliton solution (given in Supplemental Material [34]). From this figure, it is easy to identify that the intensity or energy of the double-hump solitons in the two modes propagates without change after a collision with another double-hump soliton except for a phase shift. A similar scenario exists generally for all other cases of $k_i \neq l_i$, $i = 1, 2$, the details of which will be published elsewhere. We also find that the phases of the soliton S_1 in the two modes change from $(\{[\Delta_{11} - \rho_1]/2\}, \{[\gamma_{11} - \rho_2]/2\})$ to $(\{[\Delta_{51} - \Phi_{22}]/2\}, \{[\gamma_{51} - \chi_{22}]/2\})$ during the collision process, while the phases of soliton S_2 change from $(\{[\Delta_{15} - \Theta_{11}]/2\}, \{[\gamma_{15} - \nu_{11}]/2\})$ to $(\{[\Lambda_{22} - \hat{\rho}_1]/2\}, \{[\mu_{22} - \hat{\rho}_2]/2\})$ after a collision. Here $\rho_j = \log \alpha_1^{(j)}$, $\hat{\rho}_j = \log \alpha_2^{(j)}$, $j = 1, 2$, Δ_{11}, γ_{11}, Δ_{51}, γ_{51}, Δ_{15}, Θ_{11}, γ_{15}, ν_{11}, Λ_{22} and μ_{22} are constants (see [34]).

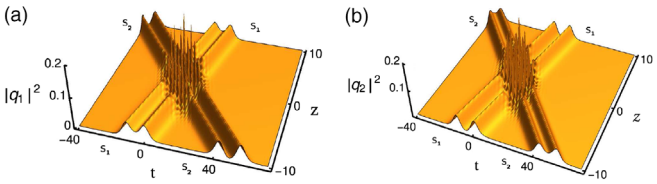

FIG. 2. Nondegenerate solitons exhibiting shape-preserving collisions: (a) and (b) denote the elastic collision of two symmetric double-hump solitons for the parametric values $k_1 = 0.333 + 0.5i$, $k_2 = 0.3$–$2.2i$, $l_1 = 0.3 + 0.5i$, $l_2 = 0.333$–$2.2i$, $\alpha_1^{(1)} = 0.45 + 0.45i$, $\alpha_2^{(1)} = 0.49 + 0.45i$, $\alpha_1^{(2)} = 0.49 + 0.45i$, and $\alpha_2^{(2)} = 0.45 + 0.45i$.

In addition to the above, we have also observed a similar shape-preserving collision in the case of a symmetric single-hump soliton when it collides with another identical soliton. The flattop soliton also preserves its structure when it collides with a symmetric double-hump soliton. However, while testing the stability property of a double-hump soliton interacting with a single-hump soliton, we come across a slightly different collision scenario. During this interaction process, the symmetric double-hump soliton experiences a strong perturbation due to the collision with the symmetric single-hump soliton. The result of their collision is reflected only in a change in the shape of the symmetric double-hump soliton into a slightly asymmetric form but without a change in energy. However, the symmetric single-hump soliton does not undergo any change (see [34]).

In contrast to the nondegenerate case, the nonlinear superposition of degenerate fundamental solitons ($k_i = l_i$, $i = 1, 2$) in the Manakov system exhibits an interesting shape-changing collision due to intensity redistribution among the modes as shown in Ref. [11]. The intensity redistribution occurs in the degenerate case due to the arbitrary polarization vectors in the two modes getting mixed up, which is illustrated in Fig. 3, where the intensity redistribution occurs because of the enhancement or suppression of intensity in any one of the modes in either one of the degenerate solitons with a corresponding suppression or enhancement of intensity of the same soliton; see Eq. (4) [11]. To hold the energy conservation between the two modes, the intensities of the two solitons S_1 and S_2 change appropriately. It is well known that the degenerate soliton or Manakov soliton [Eq. (3)] reported in Refs. [10,11], in general, exhibits a shape-changing collision through energy redistribution among the modes (except for the very special case $[\alpha_1^{(1)}/\alpha_2^{(1)}] = [\alpha_1^{(2)}/\alpha_2^{(2)}]$ [10,16], where elastic collision occurs). We have also verified the elastic nature of a double-hump soliton collision using the Crank-Nicolson method [36].

We also further wish to point out that, considering the notion dissipative solitons, they also exhibit an elastic collision property. However, this collision scenario, for example, in a fiber laser cavity, is entirely different from the one that occurs in our present case. In the fiber laser cavity, during the collision between the soliton pair (bound state or doublet) and single-soliton state (singlet), the single soliton destroys the bound state, but another pair is formed that moves away with the same velocity, leaving one of the solitons of the previously moving pair in rest [37,38]. During this collision scenario, the energy or momentum is not conserved in the dissipative system (fiber laser cavity). To bring the above elastic collision, it is essential to set up the binding energy of solitons to be nonzero, and the difference in velocities of the pair and the singlet is fixed and must be the same before and after collision [37,38]. Also, no explicit analytical form of such a dissipative soliton is available for a direct analysis.

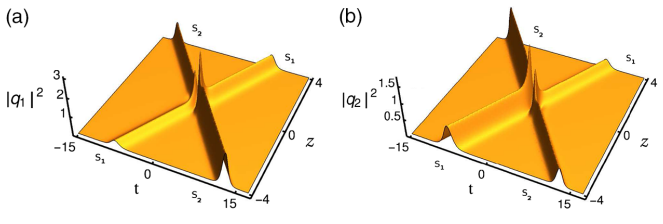

FIG. 3. Degenerate solitons exhibiting a shape-changing collision: (a) and (b) denote the energy-sharing collision in the two modes for the parametric values $k_1 = l_1 = 1 + i$, $k_2 = l_2 = 1.51 - 1.5i$, $\alpha_1^{(1)} = 0.5 + 0.5i$, and $\alpha_2^{(1)} = \alpha_1^{(2)} = \alpha_2^{(2)} = 1$.

In principle, one can construct the N-soliton solution of the nondegenerate type to the Manakov system by following the procedure given above. For the N-nondegenerate soliton, the power series expansion should be of the form $g^{(j)} = \sum_{n=1}^{2N-1} \epsilon^{2n-1} g_{2n-1}^{(j)}$ and $f = 1 + \sum_{n=1}^{2N} \epsilon^{2n} f_{2n}$. The shape of the profile will be determined by the $4N$ complex parameters which are present in the N-soliton solution. The degenerate soliton solutions can be recovered from the nondegenerate N-soliton solution by fixing the wave numbers as $k_i = l_i$, $i = 1, 2, \ldots, N$. The symmetric profile of the multinondegenerate soliton can be obtained by fixing the imaginary parts as $k_{iI} = l_{iI}$, $i = 1, 2, \ldots, N$. We also point out that the symmetric and asymmetric cases of the nondegenerate soliton solution given in Eq. (2) can be compared with a partially incoherent soliton in a photorefractive medium [25]. The profile of the partially coherent soliton is determined by only three real parameters for $N = 2$ as a special case of the degenerate soliton [10,16] (Manakov case), whereas in the present nondegenerate case, the profiles of the single soliton are governed by four complex parameters. In the incoherent limit (the number of modes is infinity), the shape of the partially coherent soliton can be arbitrary, since the number of parameters involved in the underlying analytical form is N-free real parameters. However, in the incoherent limit, the presence of $2N$ free complex parameters in the nondegenerate fundamental one soliton would bring in more complex shapes than the above-mentioned partially coherent soliton reported in the photorefractive medium.

To observe the existence of nondegenerate solitons (2) experimentally, one may consider the mutual-incoherence procedure given in Refs. [12,22] with two different laser sources of different characters (instead of a single laser source). Using polarizing beam splitters, the extraordinary beams coming out from the two laser sources can be further split into four individual incoherent fields. These four fields can act as two nondegenerate individual solitons in the two modes. Furthermore, the collision angle must be large enough to observe the elastic collision between these two nondegenerate solitons in both the modes [12,13]. The experimental procedure with a single laser can be used to

observe the Manakov solitons and multimode multihump solitons that arise in a dispersive nonlinear medium [12,22].

Finally, it is essential to point out the application of our above-reported soliton solutions. Our results open up a new possibility to investigate nondegenerate solitons in both integrable and nonintegrable systems and will give rich coherent structures when the four-wave-mixing phenomenon is taken into account. Our studies can also be extended to fiber arrays and multimode fibers where the pulse propagation is described by Manakov-type equations. Experimental observations of Manakov solitons in AlGaAs planar wave guides [13] and multihump solitons in the multimode self-induced wave guides [22] give the impression that our results will be important to an interaction of the optical field in coupled field models. The shape-preserving collision which occurs among the nondegenerate solitons can be used for the optical communication process. The double-hump nature of the nondegenerate solitons can be useful for the information process as described in the concept of a soliton molecule [31]. As far as the degenerate soliton is concerned, it has already been shown that it is useful in the computation process [15,16]. We note that under the appropriate conditions, namely, $k_{1I} \approx k_{2I}$ and $l_{1I} \approx l_{2I}$, the nondegenerate solitons reported in the present conservative system can be seen as the soliton molecule observed in the deployed fiber systems and in fiber laser cavities [31,32,39–42].

In conclusion, we have shown that the Manakov model under a general physical situation admits interesting nondegenerate solitons exhibiting shape-preserving collisions, thereby leading to explain the interaction of the elastic nature of a light-light interaction under general initial conditions. The fascinating energy-sharing collisions exhibiting the nonlinear superposition of degenerate multisolitons can be extracted from the nondegenerate soliton solutions under the specific physical restrictions, which leads to the construction of optical logic gates [15].

The authors are thankful to Dr. T. Kanna for several valuable discussions on nondegenerate solitons in coupled nonlinear Schrödinger equations. The work of R. R. and M. L. is supported by Department of Atomic Energy, National Board of Higher Mathematics [Grant No. 2/48(5)/2015/NBHM(R.P.)/R & D II/14127]. The work of M. S. is supported by the Department of Science and Technology (Grant No. EMR/2016/001818). The work of M. L. is also supported by the Department of Science and Technology-Science and Engineering Research Board Distinguished Fellowship (Grant No. SERB/F/6717/2017-18).

*Corresponding author.
lakshman@cnld.bdu.ac.in

[1] N. J. Zabusky and M. D. Kruskal, Phys. Rev. Lett. **15**, 240 (1965).
[2] A. Hasegawa, Appl. Phys. Lett. **23**, 142 (1973).
[3] V. E. Zakharov and A. B. Shabat, Sov. Phys. JETP **34**, 62 (1972).
[4] S. V. Manakov, Sov. Phys. JETP **38**, 248 (1974).
[5] Y. S. Kivshar and G. P. Agrawal, *Optical Solitons: From Fibers to Photonic Crystals* (Academic Press, San Diego, 2003).
[6] C. R. Menyuk, Opt. Lett. **12**, 614 (1987); IEEE J. Quantum Electron. **25**, 2674 (1989).
[7] D. N. Christodoulides and M. I. Carvalho, J. Opt. Soc. Am. B **12**, 1628 (1995).
[8] D. N. Christodoulides, T. H. Coskun, M. Mitchell, and M. Segev, Phys. Rev. Lett. **78**, 646 (1997).
[9] A. Ankiewicz, W. Krolikowski, and N. N. Akhmediev, Phys. Rev. E **59**, 6079 (1999).
[10] T. Kanna and M. Lakshmanan, Phys. Rev. Lett. **86**, 5043 (2001).
[11] R. Radhakrishnan, M. Lakshmanan, and J. Hietarinta, Phys. Rev. E **56**, 2213 (1997).
[12] C. Anastassiou, M. Segev, K. Steiglitz, J. A. Giordmaine, M. Mitchell, M. F. Shih, S. Lan, and J. Martin, Phys. Rev. Lett. **83**, 2332 (1999).
[13] J. U. Kang, G. I. Stegeman, J. S. Aitchison, and N. Akhmediev, Phys. Rev. Lett. **76**, 3699 (1996).
[14] D. Rand, I. Glesk, C. S. Bres, D. A. Nolan, X. Chen, J. Koh, J. W. Fleischer, K. Steiglitz, and P. R. Prucnal, Phys. Rev. Lett. **98**, 053902 (2007).
[15] M. H. Jakubowski, K. Steiglitz, and R. Squier, Phys. Rev. E **58**, 6752 (1998); K. Steiglitz, Phys. Rev. E **63**, 016608 (2000); M. Soljacic, K. Steiglitz, S. M. Sears, M. Segev, M. H. Jakubowski, and R. Squier, Phys. Rev. Lett. **90**, 254102 (2003).
[16] T. Kanna and M. Lakshmanan, Phys. Rev. E **67**, 046617 (2003).
[17] M. Vijayajayanthi, T. Kanna, K. Murali, and M. Lakshmanan, Phys. Rev. E **97**, 060201(R) (2018).
[18] M. J. Ablowitz, B. Prinari, and A. D. Trubatch, Inverse Probl. **20**, 1217 (2004).
[19] D. N. Christodoulides and R. I. Joseph, Opt. Lett. **13**, 53 (1988).
[20] M. Karlsson, D. J. Kaup, and B. A. Malomed, Phys. Rev. E **54**, 5802 (1996).
[21] C. R. Menyuk, IEEE J. Quantum Electron. **25**, 2674 (1989).
[22] M. Mitchell, Z. Chen, M. F. Shih, and M. Segev, Phys. Rev. Lett. **77**, 490 (1996); M. Mitchell and M. Segev, Nature (London) **387**, 880 (1997); M. Mitchell, M. Segev, and D. N. Christodoulides, Phys. Rev. Lett. **80**, 4657 (1998).
[23] I. A. Kolchugina *et al.*, JETP Lett. **31**, 304 (1980); M. Haelterman and A. P. Sheppard, Phys. Rev. E **49**, 3376 (1994); J. J. M. Soto-Crespo, N. Akhmediev, and A. Ankiewicz, Phys. Rev. E **51**, 3547 (1995); A. D. Boardman, K. Xie, and A. Sangarpaul, Phys. Rev. A **52**, 4099 (1995); D. Michalache, F. L. Lederer, D. Mazilu, and L.-C. Crasovan, Opt. Eng. **35**, 1616 (1996); H. He, M. J. Werner, and P. D. Drummond, Phys. Rev. E **54**, 896 (1996).
[24] E. A. Ostrovskaya, Y. S. Kivshar, D. V. Skryabin, and W. J. Firth, Phys. Rev. Lett. **83**, 296 (1999).
[25] N. Akhmediev, W. Krolikowski, and A. W. Snyder, Phys. Rev. Lett. **81**, 4632 (1998); A. Ankiewicz, W. Krolikowski, and N. N. Akhmediev, Phys. Rev. E **59**, 6079 (1999).
[26] T. Kanna, M. Vijayajayanthi, and M. Lakshmanan, J. Phys. A **43**, 434018 (2010).

[27] N. N. Akhmediev, A. V. Buryak, J. M. Soto-Crespo, and D. R. Andersen, J. Opt. Soc. Am. B **12**, 434 (1995).
[28] D. Y. Tang, H. Zhang, L. M. Zhao, and X. Wu, Phys. Rev. Lett. **101**, 153904 (2008).
[29] H. Zhang, D. Y. Tang, L. M. Zhao, and R. J. Knize, Opt. Express **18**, 4428 (2010).
[30] H. Zhang, D. Y. Tang, L. M. Zhao, and X. Wu, Phys. Rev. A **80**, 045803 (2009).
[31] M. Stratmann, T. Pagel, and F. Mitschke, Phys. Rev. Lett. **95**, 143902 (2005).
[32] G. Herink, F. Kurtz, B. Jalali, D. R. Solli, and C. Ropers, Science **356**, 50 (2017).
[33] R. Hirota, *The Direct Method in Soliton Theory* (Cambridge University Press, Cambridge, England, 2004).
[34] See Supplemental Material at http://link.aps.org/supplemental/10.1103/PhysRevLett.122.043901 for Non-degenerate and degenerate two soliton solutions, asymptotic analysis and stability of double-hump soliton and four dierent symmetric soliton proles of nondegenerate one soliton are discussed.
[35] J. Cen, F. Correa, and A. Fring, J. Phys. A **50**, 435201 (2017); S. Li, G. Biondini, and C. Schiebold, J. Math. Phys. (N.Y.) **58**, 033507 (2017).
[36] P. Muruganandam and S. K. Adhikari, Comput. Phys. Commun. **180**, 1888 (2009).
[37] Ph. Grelu and N. Akhmediev, Nat. Photonics **6**, 84 (2012).
[38] Ph. Grelu and N. Akhmediev, Opt. Express **12**, 3184 (2004).
[39] P. Rohrmann, A. Hause, and F. Mitschke, Phys. Rev. A **87**, 043834 (2013).
[40] X. Liu, X. Yao, and Y. Cui, Phys. Rev. Lett. **121**, 023905 (2018).
[41] K. Krupa, K. Nithyanandan, U. Andral, P. Tchofo-Dinda, and P. Grelu, Phys. Rev. Lett. **118**, 243901 (2017).
[42] N. Akhmediev, J. M. Soto-Crespo, M. Grapinet, and Ph. Grelu, Opt. Fibre Technol. **11**, 209 (2005).

Supplemental Material: Nondegenerate Solitons in Manakov System

S. Stalin, R. Ramakrishnan, M. Senthilvelan, and M. Lakshmanan [a]

Centre for Nonlinear Dynamics,

School of Physics, Bharathidasan University,

Tiruchirappalli-620 024, India

[a] Corresponding author E-mail: lakshman@cnld.bdu.ac.in

S.1. NONDEGENERATE TWO SOLITON SOLUTION

To explore the nondegenerate two-soliton solution of Manakov system, we adopt the Hirota's bilinear method which we have discussed in the main text. We find that the Hirota's series expansion gets truncated for the nondegenerate two-soliton solution as

$$\begin{aligned} g^{(j)} &= \epsilon g_1^{(j)} + \epsilon^3 g_3^{(j)} + \epsilon^5 g_5^{(j)} + \epsilon^7 g_7^{(j)}, j = 1, 2, \\ f &= 1 + \epsilon^2 f_2 + \epsilon^4 f_4 + \epsilon^6 f_6 + \epsilon^8 f_8. \end{aligned} \tag{1}$$

The following nondegenerate two soliton solution of Manakov system can be obtained by finding the unknown functions that are present in the above series expansions,

$$q_j = \frac{g^{(j)}}{f},\ j = 1, 2,$$

where the explicit forms of $g^{(j)}$ and f are given by

$$\begin{aligned} g^{(1)} = &\sum_{j=1}^{2} \alpha_j^{(1)} e^{\eta_j} + e^{\eta_1}\Big(\sum_{i,j=1}^{2} e^{\xi_i+\xi_j^*+\Delta_{ij}} + e^{\eta_1^*+\eta_2+\Delta_{13}} + e^{\xi_1+\xi_1^*+\xi_2+\xi_2^*+\Delta_{14}}\Big) \\ &+e^{\eta_2}\Big(\sum_{i,j=1}^{2} e^{\xi_i+\xi_j^*+\Lambda_{ij}} + e^{\eta_1+\eta_2^*+\Delta_{31}} + e^{\xi_1+\xi_1^*+\xi_2+\xi_2^*+\Delta_{41}}\Big) \\ &+e^{\eta_1+\eta_2+\eta_1^*}\Big(\sum_{i,j=1}^{2} e^{\xi_i+\xi_j^*+\Theta_{ij}} + e^{\xi_1+\xi_1^*+\xi_2+\xi_2^*+\Delta_{15}}\Big) \\ &+e^{\eta_1+\eta_2+\eta_2^*}\Big(\sum_{i,j=1}^{2} e^{\xi_i+\xi_j^*+\Phi_{ij}} + e^{\xi_1+\xi_1^*+\xi_2+\xi_2^*+\Delta_{51}}\Big), \end{aligned} \tag{2a}$$

$$\begin{aligned} g^{(2)} = &\sum_{j=1}^{2} \alpha_j^{(2)} e^{\xi_j} + e^{\xi_1}\Big(\sum_{i,j=1}^{2} e^{\eta_i+\eta_j^*+\gamma_{ij}} + e^{\xi_1^*+\xi_2+\gamma_{13}} + e^{\eta_1+\eta_1^*+\eta_2+\eta_2^*+\gamma_{14}}\Big) \\ &+e^{\xi_2}\Big(\sum_{i,j=1}^{2} e^{\eta_i+\eta_j^*+\mu_{ij}} + e^{\xi_1+\xi_2^*+\gamma_{31}} + e^{\eta_1+\eta_1^*+\eta_2+\eta_2^*+\gamma_{41}}\Big) \\ &+e^{\xi_1+\xi_2+\xi_1^*}\Big(\sum_{i,j=1}^{2} e^{\eta_i+\eta_j^*+\nu_{ij}} + e^{\eta_1+\eta_1^*+\eta_2+\eta_2^*+\gamma_{15}}\Big) \\ &+e^{\xi_1+\xi_2+\xi_2^*}\Big(\sum_{i,j=1}^{2} e^{\eta_i+\eta_j^*+\chi_{ij}} + e^{\eta_1+\eta_1^*+\eta_2+\eta_2^*+\gamma_{51}}\Big), \end{aligned} \tag{2b}$$

$$
\begin{aligned}
f = 1 &+ e^{\eta_1+\eta_1^*}\big(e^{\delta_1} + \sum_{i,j=1}^{2} e^{\xi_i+\xi_j^*+\delta_{ij}} + e^{\xi_1+\xi_1^*+\xi_2+\xi_2^*+\delta_{13}}\big) + e^{\eta_1^*+\eta_2}\big(e^{\delta_2} \\
&+ \sum_{i,j=1}^{2} e^{\xi_i+\xi_j^*+\vartheta_{ij}} + e^{\xi_1+\xi_1^*+\xi_2+\xi_2^*+\delta_{14}}\big) + e^{\eta_1+\eta_2^*}\big(e^{\delta_2^*} + \sum_{i,j=1}^{2} e^{\xi_i+\xi_j^*+\varphi_{ij}} \\
&+ e^{\xi_1+\xi_1^*+\xi_2+\xi_2^*+\delta_{15}}\big) + e^{\eta_2+\eta_2^*}\big(e^{\delta_3} + \sum_{i,j=1}^{2} e^{\xi_i+\xi_j^*+\varsigma_{ij}} + e^{\xi_1+\xi_1^*+\xi_2+\xi_2^*+\delta_{16}}\big) \\
&+ e^{\eta_1+\eta_1^*+\eta_2+\eta_2^*}\big(\sum_{i,j=1}^{2} e^{\xi_i+\xi_j^*+\phi_{ij}} + e^{\delta_{17}} + e^{\xi_1+\xi_1^*+\xi_2+\xi_2^*+\delta_{18}}\big) + \sum_{i,j=1}^{2} e^{\xi_i+\xi_j^*+\psi_{ij}} \\
&+ e^{\xi_1+\xi_1^*+\xi_2+\xi_2^*+\delta_{19}}
\end{aligned} \tag{2c}
$$

The constants that are present in the above two-soliton solution are given below,

$$
\begin{aligned}
&e^{\Delta_{11}} = \frac{\varrho_{11}\alpha_1^{(1)}\alpha_1^{(2)}\alpha_1^{(2)*}}{\tau_{11}l_{11}},\ e^{\Delta_{21}} = \frac{\varrho_{12}\alpha_1^{(1)}\alpha_1^{(2)*}\alpha_2^{(2)}}{\tau_{11}l_{21}}, e^{\Delta_{12}} = \frac{\varrho_{11}\alpha_1^{(1)}\alpha_1^{(2)}\alpha_1^{(2)*}}{\tau_{12}l_{12}}, \\
&e^{\Delta_{22}} = \frac{\varrho_{12}\alpha_1^{(1)}\alpha_2^{(2)}\alpha_2^{(2)*}}{\tau_{12}l_{22}},\ e^{\Lambda_{11}} = \frac{\varrho_{21}\alpha_2^{(1)}\alpha_1^{(2)}\alpha_1^{(2)*}}{\tau_{21}l_{11}},\ e^{\Lambda_{21}} = \frac{\varrho_{22}\alpha_2^{(1)}\alpha_2^{(2)}\alpha_1^{(2)*}}{\tau_{21}l_{21}}, \\
&e^{\Lambda_{12}} = \frac{\varrho_{21}\alpha_2^{(1)}\alpha_1^{(2)}\alpha_2^{(2)*}}{\tau_{22}l_{12}},\ e^{\Lambda_{22}} = \frac{\varrho_{22}\alpha_2^{(1)}\alpha_2^{(2)}\alpha_2^{(2)*}}{\tau_{22}l_{22}}, e^{\Delta_{13}} = \frac{\theta_1^2\alpha_1^{(1)}\alpha_1^{(1*)}\alpha_2^{(1)}}{\kappa_{21}\kappa_{11}}, \\
&e^{\Delta_{31}} = \frac{\theta_1^2\alpha_1^{(1)}\alpha_2^{(1)}\alpha_2^{(1)*}}{\kappa_{12}\kappa_{22}},\ e^{\gamma_{11}} = \frac{-\varrho_{11}\alpha_1^{(1)}\alpha_1^{(1*)}\alpha_1^{(2)}}{\tau_{11}^*\kappa_{11}},\ e^{\gamma_{21}} = \frac{-\varrho_{21}\alpha_1^{(1)*}\alpha_1^{(2)}\alpha_2^{(1)}}{\tau_{11}^*\kappa_{21}}, \\
&e^{\gamma_{12}} = \frac{-\varrho_{11}\alpha_1^{(1)}\alpha_1^{(2)}\alpha_2^{(1)*}}{\tau_{21}^*\kappa_{12}},\ e^{\gamma_{22}} = \frac{-\varrho_{21}\alpha_2^{(1)}\alpha_2^{(1)*}\alpha_1^{(2)}}{\tau_{21}^*\kappa_{22}},\ e^{\mu_{11}} = \frac{-\varrho_{12}\alpha_1^{(1)}\alpha_1^{(1)*}\alpha_2^{(2)}}{\tau_{12}^*\kappa_{11}}, \\
&e^{\mu_{21}} = \frac{-\varrho_{22}\alpha_1^{(1)*}\alpha_2^{(1)}\alpha_2^{(2)}}{\tau_{12}^*\kappa_{21}},\ e^{\mu_{12}} = \frac{-\varrho_{12}\alpha_1^{(1)}\alpha_2^{(1)*}\alpha_2^{(2)}}{\tau_{22}^*\kappa_{12}},\ e^{\mu_{22}} = \frac{-\varrho_{22}\alpha_2^{(1)}\alpha_2^{(1)*}\alpha_2^{(2)}}{\tau_{22}^*\kappa_{22}}, \\
&e^{\gamma_{13}} = \frac{\theta_2^2\alpha_1^{(2)}\alpha_1^{(2)*}\alpha_2^{(2)}}{l_{11}l_{21}},\ e^{\gamma_{31}} = \frac{\theta_2^2\alpha_1^{(2)}\alpha_2^{(2)*}\alpha_2^{(2)}}{l_{12}l_{22}},\ e^{\delta_1} = \frac{\alpha_1^{(1)}\alpha_1^{(1)*}}{\kappa_{11}},\ e^{\delta_2} = \frac{\alpha_2^{(1)}\alpha_1^{(1)*}}{\kappa_{21}}, \\
&e^{\Theta_{11}} = \frac{\theta_1^2\varrho_{11}\varrho_{11}^*\varrho_{21}\alpha_1^{(1)}\alpha_1^{(1)*}\alpha_1^{(2)}\alpha_1^{(2)*}\alpha_2^{(1)}}{\kappa_{11}\kappa_{21}\tau_{11}\tau_{11}^*\tau_{21}l_{11}},\ e^{\Theta_{21}} = \frac{\theta_1^2\varrho_{12}\varrho_{11}^*\varrho_{22}\alpha_1^{(1)}\alpha_1^{(1)*}\alpha_1^{(2)*}\alpha_2^{(1)}\alpha_2^{(2)}}{\kappa_{11}\kappa_{21}\tau_{11}\tau_{12}^*\tau_{21}l_{21}}, \\
&e^{\Theta_{12}} = \frac{\theta_1^2\varrho_{11}\varrho_{12}^*\varrho_{21}\alpha_1^{(1)}\alpha_1^{(1)*}\alpha_1^{(2)}\alpha_2^{(1)}\alpha_2^{(2)*}}{\kappa_{11}\kappa_{21}\tau_{12}\tau_{11}^*\tau_{22}l_{12}},\ e^{\Theta_{22}} = \frac{\theta_1^2\varrho_{12}\varrho_{12}^*\varrho_{22}\alpha_1^{(1)}\alpha_1^{(1)*}\alpha_2^{(1)}\alpha_2^{(2)*}\alpha_2^{(2)}}{\kappa_{11}\kappa_{21}\tau_{12}\tau_{12}^*\tau_{22}l_{22}}, \\
&e^{\Phi_{11}} = \frac{\theta_1^2\varrho_{11}\varrho_{21}^*\varrho_{21}\alpha_1^{(1)}\alpha_1^{(2)*}\alpha_1^{(2)}\alpha_2^{(1)*}\alpha_2^{(1)}}{\kappa_{12}\kappa_{22}\tau_{11}\tau_{21}^*\tau_{21}l_{11}},\ e^{\Phi_{21}} = \frac{\theta_1^2\varrho_{12}\varrho_{21}^*\varrho_{22}\alpha_1^{(1)}\alpha_1^{(2)*}\alpha_2^{(1)}\alpha_2^{(1)*}\alpha_2^{(2)}}{\kappa_{12}\kappa_{22}\tau_{11}\tau_{22}^*\tau_{21}l_{21}}, \\
&e^{\Phi_{12}} = \frac{\theta_1^2\varrho_{11}\varrho_{21}\varrho_{22}^*\alpha_1^{(1)}\alpha_1^{(2)}\alpha_2^{(1)}\alpha_2^{(1)*}\alpha_2^{(2)*}}{\kappa_{12}\kappa_{22}\tau_{12}\tau_{21}^*\tau_{22}l_{12}},\ e^{\Phi_{22}} = \frac{\theta_1^2\varrho_{12}\varrho_{22}\varrho_{22}^*\alpha_1^{(1)}\alpha_2^{(1)}\alpha_2^{(1)*}\alpha_2^{(2)}\alpha_2^{(2)*}}{\kappa_{12}\kappa_{22}\tau_{12}\tau_{22}^*\tau_{22}l_{22}}, \\
&e^{\Delta_{14}} = \frac{\theta_2^2\theta_2^{2*}\varrho_{11}\varrho_{12}\alpha_1^{(1)}\alpha_1^{(2)}\alpha_1^{(2)*}\alpha_2^{(2)}\alpha_2^{(2)*}}{\tau_{11}\tau_{12}l_{11}l_{12}l_{21}l_{22}},\ e^{\Delta_{41}} = \frac{\theta_2^2\theta_2^{2*}\varrho_{21}\varrho_{22}\alpha_1^{(2)}\alpha_1^{(2)*}\alpha_2^{(1)}\alpha_2^{(2)}\alpha_2^{(2)*}}{\tau_{21}\tau_{22}l_{11}l_{12}l_{21}l_{22}}, \\
&e^{\nu_{11}} = \frac{-\theta_2^2\varrho_{11}\varrho_{11}^*\varrho_{12}\alpha_1^{(1)}\alpha_1^{(1)*}\alpha_1^{(2)}\alpha_1^{(2)*}\alpha_2^{(2)}}{\kappa_{11}l_{11}\tau_{11}\tau_{11}^*\tau_{12}^*l_{21}},\ e^{\nu_{21}} = \frac{-\theta_2^2\varrho_{21}\varrho_{11}^*\varrho_{22}\alpha_1^{(1)*}\alpha_1^{(2)}\alpha_1^{(2)*}\alpha_2^{(1)}\alpha_2^{(2)}}{\kappa_{21}\tau_{21}\tau_{11}^*\tau_{12}^*l_{11}l_{21}},
\end{aligned}
$$

$$e^{\nu_{12}}=\frac{-\theta_2^2\varrho_{11}\varrho_{21}^*\varrho_{12}\alpha_1^{(1)}\alpha_1^{(2)*}\alpha_1^{(2)}\alpha_2^{(1)*}\alpha_2^{(2)}}{\kappa_{12}\tau_{11}\tau_{21}^*\tau_{22}^*l_{11}l_{21}},\ e^{\nu_{22}}=\frac{-\theta_2^2\varrho_{21}\varrho_{21}^*\varrho_{22}\alpha_1^{(2)}\alpha_1^{(2)*}\alpha_2^{(1)}\alpha_2^{(1)*}\alpha_2^{(2)}}{\kappa_{22}\tau_{21}\tau_{21}^*\tau_{22}^*l_{11}l_{21}},$$
$$e^{\chi_{11}}=\frac{-\theta_2^2\varrho_{11}\varrho_{12}^*\varrho_{12}\alpha_1^{(1)}\alpha_1^{(1)*}\alpha_1^{(2)}\alpha_2^{(2)*}\alpha_2^{(2)}}{\kappa_{11}\tau_{11}^*\tau_{12}^*\tau_{12}l_{12}l_{22}},\ e^{\chi_{21}}=\frac{-\theta_2^2\varrho_{21}\varrho_{12}^*\varrho_{22}\alpha_2^{(1)}\alpha_1^{(1)*}\alpha_1^{(2)}\alpha_2^{(2)*}\alpha_2^{(2)}}{\kappa_{21}\tau_{11}^*\tau_{12}^*\tau_{22}l_{12}l_{22}},$$
$$e^{\chi_{12}}=\frac{-\theta_2^2\varrho_{11}\varrho_{22}^*\varrho_{12}\alpha_1^{(1)}\alpha_2^{(1)*}\alpha_1^{(2)}\alpha_2^{(2)*}\alpha_2^{(2)}}{\kappa_{12}\tau_{21}^*\tau_{22}^*\tau_{12}l_{12}l_{22}},\ e^{\chi_{22}}=\frac{-\theta_2^2\varrho_{21}\varrho_{22}^*\varrho_{22}\alpha_2^{(1)}\alpha_2^{(1)*}\alpha_1^{(2)}\alpha_2^{(2)*}\alpha_2^{(2)}}{\kappa_{22}\tau_{21}^*\tau_{22}^*\tau_{22}l_{12}l_{22}},$$
$$e^{\gamma_{14}}=\frac{\theta_1^2\theta_1^{2*}\varrho_{11}\varrho_{21}\alpha_1^{(1)}\alpha_1^{(2)}\alpha_1^{(1)*}\alpha_2^{(1)}\alpha_2^{(1)*}}{\tau_{11}^*\tau_{21}^*\kappa_{11}\kappa_{12}\kappa_{21}\kappa_{22}},\ e^{\gamma_{41}}=\frac{\theta_1^2\theta_1^{2*}\varrho_{12}\varrho_{22}\alpha_1^{(1)}\alpha_2^{(1)}\alpha_1^{(1)*}\alpha_2^{(1)*}\alpha_2^{(2)}}{\tau_{12}^*\tau_{22}^*\kappa_{11}\kappa_{12}\kappa_{21}\kappa_{22}},$$
$$e^{\Delta_{15}}=\frac{\theta_1^2\theta_2^2\theta_2^{2*}\varrho_{11}\varrho_{21}\varrho_{12}\varrho_{22}\varrho_{11}^*\varrho_{12}^*\alpha_1^{(1)}\alpha_1^{(1)*}\alpha_1^{(2)}\alpha_1^{(2)*}\alpha_2^{(1)}\alpha_2^{(2)}\alpha_2^{(2)*}}{\kappa_{11}\kappa_{21}\tau_{11}\tau_{11}^*\tau_{21}\tau_{12}\tau_{12}^*\tau_{22}l_{11}l_{12}l_{21}l_{22}},\ e^{\delta_3}=\frac{|\alpha_2^{(1)}|^2}{\kappa_{22}},$$
$$e^{\Delta_{51}}=\frac{\theta_1^2\theta_2^2\theta_2^{2*}\varrho_{11}\varrho_{21}\varrho_{12}\varrho_{22}\varrho_{21}^*\varrho_{22}^*\alpha_1^{(1)}\alpha_1^{(2)*}\alpha_1^{(2)}\alpha_2^{(1)*}\alpha_2^{(1)}\alpha_2^{(2)}\alpha_2^{(2)*}}{\kappa_{12}\kappa_{22}\tau_{11}\tau_{21}^*\tau_{21}\tau_{12}\tau_{22}^*\tau_{22}l_{11}l_{12}l_{21}l_{22}},\ e^{\psi_{11}}=\frac{|\alpha_1^{(2)}|^2}{l_{11}},$$
$$e^{\gamma_{15}}=\frac{\theta_1^2\theta_2^2\theta_1^{2*}\varrho_{11}\varrho_{21}\varrho_{12}\varrho_{22}\varrho_{21}^*\varrho_{12}^*\alpha_1^{(1)}\alpha_1^{(1)*}\alpha_1^{(2)}\alpha_1^{(2)*}\alpha_2^{(1)}\alpha_2^{(2)}\alpha_2^{(1)*}}{\kappa_{11}\kappa_{21}\kappa_{12}\kappa_{22}\tau_{11}\tau_{11}^*\tau_{21}\tau_{12}^*\tau_{22}^*\tau_{21}^*l_{11}l_{21}},\ e^{\psi_{21}}=\frac{\alpha_1^{(2)*}\alpha_2^{(2)}}{l_{21}},$$
$$e^{\gamma_{51}}=\frac{\theta_1^2\theta_2^2\theta_1^{2*}\varrho_{11}\varrho_{21}\varrho_{12}\varrho_{22}\varrho_{22}^*\varrho_{12}^*\alpha_1^{(1)}\alpha_1^{(1)*}\alpha_1^{(2)}\alpha_2^{(1)*}\alpha_2^{(1)}\alpha_2^{(2)}\alpha_2^{(2)*}}{\kappa_{11}\kappa_{21}\kappa_{12}\kappa_{22}\tau_{22}\tau_{11}^*\tau_{12}\tau_{12}^*\tau_{22}^*\tau_{21}^*l_{12}l_{22}},\ e^{\psi_{12}}=\frac{\alpha_1^{(2)}\alpha_2^{(2)*}}{l_{12}},$$
$$e^{\delta_{18}}=\frac{\theta_1^2\theta_2^2\theta_1^{2*}\theta_2^{2*}\varrho_{11}\varrho_{21}\varrho_{12}\varrho_{22}\varrho_{11}^*\varrho_{12}^*\varrho_{21}^*\varrho_{22}^*|\alpha_1^{(1)}|^2|\alpha_1^{(2)}|^2|\alpha_2^{(1)}|^2|\alpha_2^{(2)}|^2}{\kappa_{11}\kappa_{21}\kappa_{12}\kappa_{22}|\tau_{11}|^2|\tau_{12}|^2|\tau_{21}|^2|\tau_{22}|^2l_{11}l_{21}l_{12}l_{22}},\ e^{\psi_{22}}=\frac{|\alpha_2^{(2)}|^2}{l_{22}},$$
$$e^{\delta_{11}}=\frac{|\varrho_{11}|^2|\alpha_1^{(1)}|^2|\alpha_1^{(2)}|^2}{\kappa_{11}|\tau_{11}|^2l_{11}},\ e^{\delta_{21}}=\frac{\varrho_{12}\varrho_{11}^*\alpha_1^{(1)}\alpha_1^{(1)*}\alpha_2^{(2)}\alpha_1^{(2)*}}{\kappa_{11}\tau_{11}\tau_{12}^*l_{21}},\ e^{\delta_{12}}=\frac{\varrho_{11}\varrho_{12}^*\alpha_1^{(1)}\alpha_1^{(1)*}\alpha_1^{(2)}\alpha_2^{(2)*}}{\kappa_{11}\tau_{11}^*\tau_{12}l_{12}},$$
$$e^{\delta_{22}}=\frac{|\varrho_{12}|^2|\alpha_1^{(1)}|^2|\alpha_2^{(2)}|^2}{\kappa_{11}|\tau_{12}|^2l_{22}},\ e^{\vartheta_{11}}=\frac{\varrho_{21}\varrho_{11}^*\alpha_1^{(1)*}|\alpha_1^{(2)}|^2\alpha_2^{(1)}}{\kappa_{21}\tau_{11}^*\tau_{21}l_{11}},\ e^{\vartheta_{21}}=\frac{\varrho_{22}\varrho_{11}^*\alpha_1^{(1)*}\alpha_1^{(2)*}\alpha_2^{(1)}\alpha_2^{(2)}}{\kappa_{21}\tau_{12}^*\tau_{21}l_{21}},$$
$$e^{\vartheta_{12}}=\frac{\varrho_{21}\varrho_{12}^*\alpha_1^{(1)*}\alpha_1^{(2)}\alpha_2^{(1)}\alpha_2^{(2)*}}{\kappa_{21}\tau_{11}^*\tau_{22}l_{12}},\ e^{\vartheta_{22}}=\frac{\varrho_{22}\varrho_{12}^*\alpha_1^{(1)*}\alpha_2^{(2)}\alpha_2^{(1)}\alpha_2^{(2)*}}{\kappa_{21}\tau_{12}^*\tau_{22}l_{22}},\ e^{\varphi_{11}}=\frac{\varrho_{11}\varrho_{21}^*\alpha_1^{(1)}\alpha_1^{(2)}\alpha_1^{(2)*}\alpha_2^{(1)*}}{\kappa_{12}\tau_{21}^*\tau_{11}l_{11}},$$
$$e^{\varphi_{21}}=\frac{\varrho_{12}\varrho_{21}^*\alpha_1^{(1)}\alpha_1^{(2)*}\alpha_2^{(1)*}\alpha_2^{(2)}}{\kappa_{12}\tau_{22}^*\tau_{11}l_{21}},\ e^{\varphi_{12}}=\frac{\varrho_{11}\varrho_{22}^*\alpha_1^{(1)}\alpha_1^{(2)}\alpha_2^{(2)*}\alpha_2^{(1)*}}{\kappa_{12}\tau_{21}^*\tau_{12}l_{12}},\ e^{\varphi_{22}}=\frac{\varrho_{12}\varrho_{22}^*\alpha_1^{(1)}\alpha_2^{(2)}\alpha_2^{(2)*}\alpha_2^{(1)*}}{\kappa_{12}\tau_{22}^*\tau_{12}l_{22}},$$
$$e^{\varsigma_{11}}=\frac{\varrho_{21}\varrho_{21}^*\alpha_1^{(2)}\alpha_1^{(2)*}\alpha_2^{(1)}\alpha_2^{(1)*}}{\kappa_{22}\tau_{21}^*\tau_{21}l_{11}},\ e^{\varsigma_{21}}=\frac{\varrho_{22}\varrho_{21}^*\alpha_1^{(2)*}\alpha_2^{(1)*}\alpha_2^{(1)}\alpha_2^{(2)}}{\kappa_{22}\tau_{22}^*\tau_{21}l_{21}},\ e^{\varsigma_{12}}=\frac{\varrho_{21}\varrho_{22}^*\alpha_1^{(2)}\alpha_2^{(2)*}\alpha_2^{(1)}\alpha_2^{(1)*}}{\kappa_{22}\tau_{21}^*\tau_{22}l_{12}},$$
$$e^{\varsigma_{22}}=\frac{\varrho_{22}\varrho_{22}^*\alpha_2^{(2)}\alpha_2^{(2)*}\alpha_2^{(1)}\alpha_2^{(1)*}}{\kappa_{22}\tau_{22}^*\tau_{22}l_{22}},\ e^{\delta_{17}}=\frac{\theta_1^2\theta_1^{2*}|\alpha_1^{(1)}|^2|\alpha_2^{(1)}|^2}{\kappa_{12}\kappa_{21}\kappa_{11}\kappa_{22}},\ e^{\delta_{19}}=\frac{\theta_2^2\theta_2^{2*}|\alpha_1^{(2)}|^2|\alpha_2^{(2)}|^2}{l_{12}l_{21}l_{11}l_{22}},$$
$$e^{\phi_{11}}=\frac{\theta_1^2\theta_1^{2*}\varrho_{11}\varrho_{21}\varrho_{11}^*\varrho_{21}^*|\alpha_1^{(1)}|^2|\alpha_1^{(2)}|^2|\alpha_2^{(1)}|^2}{\kappa_{12}\kappa_{21}\kappa_{11}\kappa_{22}|\tau_{11}|^2|\tau_{21}|^2l_{11}},\ e^{\phi_{21}}=\frac{\theta_1^2\theta_1^{2*}\varrho_{12}\varrho_{22}\varrho_{11}^*\varrho_{21}^*|\alpha_1^{(1)}|^2\alpha_1^{(2)*}|\alpha_2^{(1)}|^2\alpha_2^{(2)}}{\kappa_{12}\kappa_{21}\kappa_{11}\kappa_{22}\tau_{11}\tau_{21}\tau_{12}^*\tau_{22}^*l_{21}},$$
$$e^{\phi_{12}}=\frac{\theta_1^2\theta_1^{2*}\varrho_{11}\varrho_{21}\varrho_{12}^*\varrho_{22}^*|\alpha_1^{(1)}|^2\alpha_1^{(2)}|\alpha_2^{(1)}|^2\alpha_2^{(2)*}}{\kappa_{12}\kappa_{21}\kappa_{11}\kappa_{22}\tau_{11}^*\tau_{21}^*\tau_{12}\tau_{22}l_{12}},\ e^{\phi_{22}}=\frac{\theta_1^2\theta_1^{2*}\varrho_{12}\varrho_{22}\varrho_{12}^*\varrho_{22}^*|\alpha_1^{(1)}|^2|\alpha_2^{(2)}|^2|\alpha_2^{(1)}|^2}{\kappa_{12}\kappa_{21}\kappa_{11}\kappa_{22}|\tau_{12}|^2|\tau_{22}|^2l_{22}},$$
$$e^{\delta_{13}}=\frac{\theta_2^2\theta_2^{2*}\varrho_{11}\varrho_{12}\varrho_{11}^*\varrho_{12}^*|\alpha_1^{(1)}|^2|\alpha_1^{(2)}|^2|\alpha_2^{(2)}|^2}{\kappa_{11}l_{11}l_{21}l_{12}l_{22}|\tau_{11}|^2|\tau_{12}|^2},\ e^{\delta_{14}}=\frac{\theta_2^2\theta_2^{2*}\varrho_{21}\varrho_{22}\varrho_{11}^*\varrho_{12}^*\alpha_1^{(1)*}|\alpha_1^{(2)}|^2\alpha_2^{(1)}|\alpha_2^{(2)}|^2}{\kappa_{21}l_{11}l_{21}l_{12}l_{22}\tau_{11}^*\tau_{12}^*\tau_{21}\tau_{22}},$$
$$e^{\delta_{15}}=\frac{\theta_2^2\theta_2^{2*}\varrho_{11}\varrho_{12}\varrho_{21}^*\varrho_{22}^*\alpha_1^{(1)}|\alpha_1^{(2)}|^2\alpha_2^{(1)*}|\alpha_2^{(2)}|^2}{\kappa_{12}l_{11}l_{21}l_{12}l_{22}\tau_{21}^*\tau_{22}^*\tau_{11}\tau_{12}},\ e^{\delta_{16}}=\frac{\theta_2^2\theta_2^{2*}\varrho_{21}\varrho_{22}\varrho_{21}^*\varrho_{22}^*|\alpha_1^{(2)*}|^2|\alpha_2^{(1)}|^2|\alpha_2^{(2)}|^2}{\kappa_{22}l_{11}l_{21}l_{12}l_{22}\tau_{21}^*\tau_{22}^*\tau_{21}\tau_{22}},$$

$$\theta_1 = (k_1 - k_2),\ \theta_2 = (l_1 - l_2),\ \varrho_{nm} = (k_n - l_m),\ \tau_{nm} = (k_n + l_m^*),$$
$$l_{nm} = (l_n + l_m^*)^2,\ \kappa_{nm} = (k_n + k_m^*)^2,\ n, m = 1, 2.$$

S.2. DEGENERATE TWO SOLITON SOLUTION

In the limit, $k_1 = l_1$ and $k_2 = l_2$, the above given nondegenerate two-soliton solution is reduced to the following standard degenerate two-soliton solution [1], that is

$$q_j(t,z) = \frac{\alpha_1^{(j)} e^{\eta_1} + \alpha_2^{(j)} e^{\eta_2} + e^{\eta_1+\eta_1^*+\eta_2+\delta_{1j}} + e^{\eta_1+\eta_2+\eta_2^*+\delta_{2j}}}{1 + e^{\eta_1+\eta_1^*+R_1} + e^{\eta_1+\eta_2^*+\delta_0} + e^{\eta_1^*+\eta_2+\delta_0^*} + e^{\eta_2+\eta_2^*+R_2} + e^{\eta_1+\eta_1^*+\eta_2+\eta_2^*+R_3}}, \tag{3}$$

where $j = 1, 2$, $\eta_j = k_j(t + ik_j z)$, $e^{\delta_0} = \frac{k_{12}}{k_1+k_2^*}$, $e^{R_1} = \frac{k_{11}}{k_1+k_1^*}$, $e^{R_2} = \frac{k_{22}}{k_2+k_2^*}$,
$e^{\delta_{1j}} = \frac{(k_1-k_2)(\alpha_1^{(j)}k_{21}-\alpha_2^{(j)}k_{11})}{(k_1+k_1^*)(k_1^*+k_2)}$, $e^{\delta_{2j}} = \frac{(k_2-k_1)(\alpha_2^{(j)}k_{12}-\alpha_1^{(j)}k_{22})}{(k_2+k_2^*)(k_1+k_2^*)}$,
$e^{R_3} = \frac{|k_1-k_2|^2}{(k_1+k_1^*)(k_2+k_2^*)|k_1+k_2^*|^2}(k_{11}k_{22} - k_{12}k_{21})$ and $k_{il} = \frac{\mu \sum_{n=1}^{2} \alpha_i^{(n)}\alpha_i^{(n)^*}}{(k_i+k_l^*)}$, $i, l = 1, 2$, $\mu = +1$.

The energy-sharing collision of the above degenerate two-soliton solution was studied in [1].

S.3. ASYMPTOTIC ANALYSIS: SHAPE PRESERVING COLLISION OF DOUBLE-HUMP SOLITON

To study the interaction between nondegenerate solitons, we carefully perform the asymptotic analysis for the nondegenerate two soliton solution (2a)-(2c). Here, we present the asymptotic analysis for the shape preserving collision that occur between the double-hump solitons. To explore this, we consider the choice of wave parameters as $k_{1R} > l_{1R}$, $k_{2R} < l_{2R}$, $k_{1I} > k_{2I}$, $l_{1I} > l_{2I}$, $k_{1R} > k_{2R}$, $l_{1R} < l_{2R}$, $k_{1I} = l_{1I}$ and $k_{2I} = l_{2I}$. Under this parametric choice, we deduce the following asymptotic forms corresponding to two individual double-hump solitons in both the modes before and after collision can be given as follows.

Before collision: $z \to -\infty$

Soliton 1: In this limit, the asymptotic forms deduced from the two soliton solution for soliton 1 in both the modes before collision,

$$q_1 = \frac{2A_1^{1-}k_{1R}e^{i\eta_{1I}}\cosh(\xi_{1R} + \frac{\phi_1}{2})}{\Big[\frac{(k_1^*-l_1^*)^{\frac{1}{2}}}{(k_1^*+l_1)^{\frac{1}{2}}}\cosh(\eta_{1R} + \xi_{1R} + \frac{\delta_{11}}{2}) + \frac{(k_1+l_1^*)^{\frac{1}{2}}}{(k_1-l_1)^{\frac{1}{2}}}\cosh(\eta_{1R} - \xi_{1R} + \frac{\delta_1-\psi_{11}}{2})\Big]}, \tag{4a}$$

$$q_2 = \frac{2A_1^{2-}l_{1R}e^{i\xi_{1I}}\cosh(\eta_{1R} + +\frac{\phi_2}{2})}{\Big[\frac{i(k_1^*-l_1^*)^{\frac{1}{2}}}{(k_1+l_1^*)^{\frac{1}{2}}}\cosh(\eta_{1R} + \xi_{1R} + \frac{\delta_{11}}{2}) + \frac{(k_1^*+l_1)^{1/2}}{(l_1-k_1)^{1/2}}\cosh(\eta_{1R} - \xi_{1R} + \frac{\delta_1-\psi_{11}}{2})\Big]}. \tag{4b}$$

Here, $\phi_1 = \Delta_{11} - \rho_1$, $\phi_2 = \gamma_{11} - \rho_2$, $\rho_j = \log \alpha_1^{(j)}$.

Soliton 2: The asymptotic expressions for the soliton 2 in the two modes before collision turn out to be,

$$q_1 = \frac{2k_{2R}A_2^{1-}(k_1-k_2)(k_2-l_1)^{\frac{1}{2}}(k_1+k_2^*)(k_2^*+l_1)^{\frac{1}{2}}e^{i\eta_{2I}}\cosh(\xi_{2R}+\frac{\varphi_1}{2})}{(k_1^*-k_2^*)(k_2^*-l_1^*)^{\frac{1}{2}}(k_1^*+k_2)(k_2+l_1^*)^{\frac{1}{2}}\Gamma_1}, \tag{5a}$$

$$q_2 = \frac{2l_{2R}A_2^{2-}(l_1-l_2)(k_1-l_2)^{\frac{1}{2}}(k_1+l_2^*)^{\frac{1}{2}}(l_1+l_2^*)e^{i\xi_{2I}}\cosh(\eta_{2R}+\frac{\varphi_2}{2})}{(k_1^*-l_2^*)^{\frac{1}{2}}(l_1^*-l_2^*)(k_1^*+l_2)^{\frac{1}{2}}(l_1^*+l_2)\Gamma_2}. \tag{5b}$$

In the above,

$$\Gamma_1 = \big[\frac{(k_2^*-l_2^*)^{\frac{1}{2}}}{(k_2^*+l_2)^{\frac{1}{2}}}\cosh(\eta_{2R}+\xi_{2R}+\frac{\delta_{18}-\delta_{11}}{2}) + \frac{(k_2+l_2^*)^{\frac{1}{2}}}{(k_2-l_2)^{\frac{1}{2}}}\cosh(\eta_{2R}-\xi_{2R}+\frac{\phi_{11}-\delta_{15}}{2})\big],$$

$$\Gamma_2 = \big[\frac{(k_2^*-l_2^*)^{\frac{1}{2}}}{(k_1+l_2^*)^{\frac{1}{2}}}\cosh(\eta_{2R}+\xi_{2R}+\frac{\delta_{18}-\delta_{11}}{2}) + \frac{(k_2^*+l_2)^{\frac{1}{2}}}{(k_2-l_2)^{\frac{1}{2}}}\cosh(\eta_{2R}-\xi_{2R}+\frac{\phi_{11}-\delta_{15}}{2})\big],$$

$\varphi_1 = \Delta_{15} - \Theta_{11},\ \varphi_2 = \gamma_{15} - \nu_{11}.$

After collision: $z \to +\infty$

Soliton 1: The asymptotic forms for soliton 1 after collision deduced as,

$$q_1 = \frac{2k_{1R}A_1^{1+}(k_1-k_2)(k_1-l_2)^{\frac{1}{2}}(k_1^*+k_2)(k_1^*+l_2)^{\frac{1}{2}}e^{i\eta_{1I}}\cosh(\xi_{1R}+\frac{\hat{\phi}_1}{2})}{(k_1^*-k_2^*)(k_1^*-l_2^*)^{\frac{1}{2}}(k_1+k_2^*)(k_1+l_2^*)^{\frac{1}{2}}\Gamma_3}, \tag{6a}$$

$$q_2 = \frac{2l_{1R}A_1^{2+}(l_1-l_2)(k_2-l_1)^{\frac{1}{2}}(k_2+l_1^*)^{\frac{1}{2}}(l_1^*+l_2)e^{i\xi_{1I}}\cosh(\eta_{1R}+\frac{\hat{\phi}_2}{2})}{(k_2^*-l_1^*)^{\frac{1}{2}}(l_1^*-l_2^*)(k_2^*+l_1)^{\frac{1}{2}}(l_1+l_2^*)\Gamma_4}. \tag{6b}$$

Here,

$$\Gamma_3 = \big[\frac{(k_1^*-l_1^*)^{\frac{1}{2}}}{(k_1^*+l_1)^{\frac{1}{2}}}\cosh(\eta_{1R}+\xi_{1R}+\frac{\delta_{18}-\varphi_{12}}{2}) + \frac{(k_1+l_1^*)^{\frac{1}{2}}}{(k_1-l_1)^{\frac{1}{2}}}\cosh(\eta_{1R}-\xi_{1R}+\frac{\phi_{22}-\delta_{15}}{2})\big],$$

$$\Gamma_4 = \big[\frac{(k_1^*-l_1^*)^{\frac{1}{2}}}{(k_1+l_1^*)^{\frac{1}{2}}}\cosh(\eta_{1R}+\xi_{1R}+\frac{\delta_{18}-\varphi_{12}}{2}) + \frac{(k_1^*+l_1)^{\frac{1}{2}}}{(k_1-l_1)^{\frac{1}{2}}}\cosh(\eta_{1R}-\xi_{1R}+\frac{\phi_{22}-\delta_{15}}{2})\big],$$

$\hat{\phi}_1 = \Delta_{51} - \Phi_{22},\ \hat{\phi}_2 = \gamma_{51} - \chi_{22}.$

Soliton 2: The expression for soliton 2 after collision deduced from the two soliton solution is,

$$q_1 = \frac{2A_2^{1+}k_{2R}e^{i\eta_{2I}}\cosh(\xi_{2R}+\frac{\hat{\varphi}_1}{2})}{\big[\frac{(k_2^*-l_2^*)^{\frac{1}{2}}}{(k_2^*+l_2)^{\frac{1}{2}}}\cosh(\eta_{2R}+\xi_{2R}+\frac{\varsigma_{22}}{2}) + \frac{(k_2+l_2^*)^{\frac{1}{2}}}{(k_2-l_2)^{\frac{1}{2}}}\cosh(\eta_{2R}-\xi_{2R}+\frac{\delta_3-\psi_{22}}{2})\big]}, \tag{7a}$$

$$q_2 = \frac{2A_2^{2+}l_{2R}e^{i\xi_{2I}}\cosh(\eta_{2R}++\frac{\hat{\varphi}_2}{2})}{\big[\frac{i(k_2^*-l_2^*)^{\frac{1}{2}}}{(k_2+l_2^*)^{\frac{1}{2}}}\cosh(\eta_{2R}+\xi_{2R}+\frac{\varsigma_{22}}{2}) + \frac{(k_2^*+l_2)^{\frac{1}{2}}}{(l_2-k_2)^{\frac{1}{2}}}\cosh(\eta_{2R}-\xi_{2R}+\frac{\delta_3-\psi_{22}}{2})\big]}, \tag{7b}$$

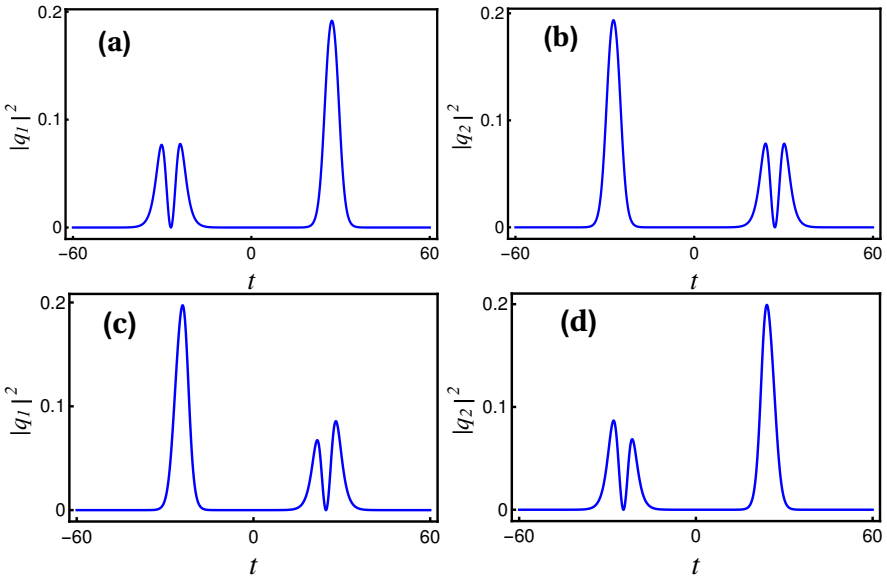

FIG. 1. Stability of double hump solitons-alteration of shape of the symmetric double hump soliton in both the modes: (a) and (b) denote the symmetric double hump soliton present in both the modes before collision. (c) and (d) exhibit that a slight asymmetry occur in the double hump soliton profiles (though the individual energies in each modes remains constant) after collision with symmetric single hump solitons. Note that the single hump soliton retains it shape. The parameter values are $k_1 = 0.55 + 0.5i$, $l_1 = 0.333 + 0.5i$, $k_2 = -0.33 + 0.5i$, $l_2 = -0.55 - 0.5i$, $\alpha_1^{(1)} = 0.5 + 0.5i$, $\alpha_2^{(1)} = -0.45 + 0.5i$, $\alpha_1^{(2)} = 0.45 + 0.5i$ and $\alpha_2^{(2)} = -0.5 + 0.5i$.

where $\hat{\varphi_1} = \Lambda_{22} - \hat{\rho}_1$, $\hat{\varphi_2} = \mu_{22} - \hat{\rho}_2$, $\hat{\rho}_j = \log \alpha_2^{(j)}$, $\eta_{jR} = k_{jR}(t - 2k_{jI}z)$, $\eta_{jI} = k_{jI}t + (k_{jR}^2 - k_{jI}^2)z$, $\xi_{jR} = l_{jR}(t - 2l_{jI}z)$, $\xi_{jI} = l_{jI}t + (l_{jR}^2 - l_{jI}^2)z$, $j = 1, 2$, and other constants appearing in the above asymptotic expressions are given in two soliton solution.

S.4. ALTERATION IN THE SHAPE OF THE SYMMETRIC DOUBLE HUMP SOLITON WHILE INTERACTING WITH A SYMMETRIC SINGLE HUMP SOLITON (WITHOUT CHANGE IN ENERGIES)

In the above, we have analysed the shape preserving collision that occurs between the two double-hump solitons [2]. However, we also come across a slightly different collision scenario while testing the stability property of a symmetric double hump soliton interacting with a symmetric single hump soliton through analytical and numerical analysis. To analyse this, we allow the double- hump soliton to interact with a symmetric single-hump soliton. As we have demon-

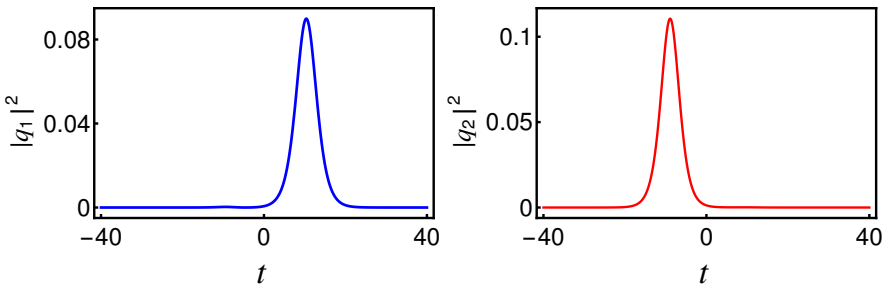

FIG. 2. Symmetric single-hump-single-hump soliton: Parameter values are $k_1 = -0.3+0.5i$, $l_1 = 0.333+0.5i$, $\alpha_1^{(1)} = 0.5+0.5i$ and $\alpha_1^{(2)} = 0.45+0.5i$.

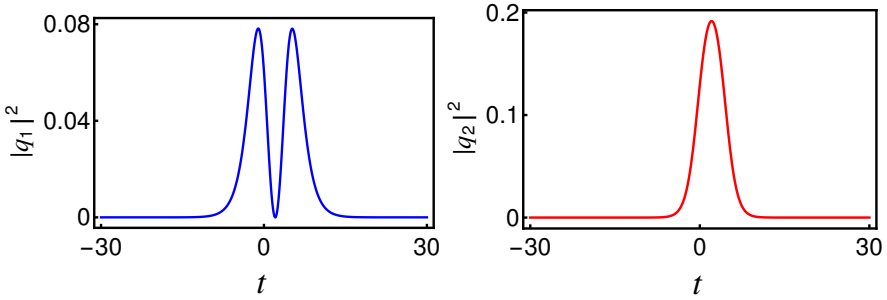

FIG. 3. Symmetric double-hump-single-hump soliton: Parameter values are $k_1 = 0.333+0.5i$, $l_1 = 0.55+0.5i$, $\alpha_1^{(1)} = 0.5+0.45i$ and $\alpha_1^{(2)} = 0.5+0.5i$.

strated in Fig. 1 in this supplement, by choosing appropriate initial conditions from our explicit analytical two-soliton solution, we locate these two solitons initially at well defined separation distance. Both the symmetric double-hump and single-hump solitons propagate steadily until they get disturbed by each other. During this interaction process, the double-hump soliton in both the modes alone experiences a strong perturbation due to the collision with the symmetric single-hump soliton. The result of their collision is reflected only in changing the shape of the symmetric double-hump soliton slightly into an asymmetric form. However, the energies of both the double-hump and single-hump solitons do not change after collision. We also confirm this collision scenario by carrying out a detailed asymptotic analysis as has been done for the double-hump soliton earlier and calculating the transition amplitudes and conservation of energy. We will present a detailed analysis of the above dynamics in the extended version. We also note that if one sets a slight asymmetry in the intensity profile of the double-hump soliton in both the modes for suitable choice of initial conditions, the asymmetric double-hump becomes symmetric when it collides with the symmetric single-hump soliton, again without change in energy.

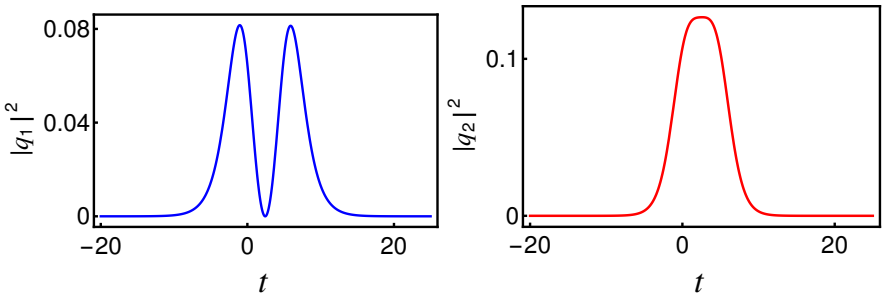

FIG. 4. Symmetric double-hump-flattop soliton: Parameter values are $k_1 = 0.35 + 0.5i$, $l_1 = 0.499 + 0.5i$, $\alpha_1^{(1)} = 0.5 + 0.51i$ and $\alpha_1^{(2)} = 0.5 + 0.5i$.

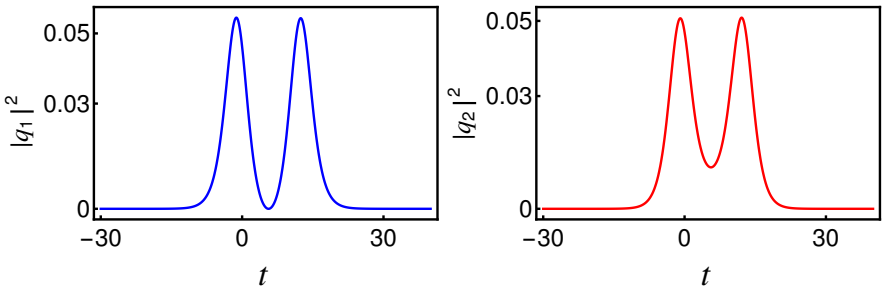

FIG. 5. Symmetric double-hump-double-hump soliton: Parameter values are $k_1 = 0.316 + 0.5i$, $l_1 = 0.333 + 0.5i$, $\alpha_1^{(1)} = 0.49 + 0.45i$ and $\alpha_1^{(2)} = 0.45 + 0.45i$.

S.5. SYMMETRIC SOLITON PROFILES OF NONDEGENERATE ONE SOLITON

We display all the four symmetric wave profiles of nondegenerate one soliton of Manakov system in Figs. (2)-(5) for appropriate choice of parameters as given in the corresponding figure captions.

[1] R. Radhakrishnan, M. Lakshmanan and J. Hietarinta, Phys. Rev. E **56**, 2213 (1997).

[2] S. Stalin, R. Ramakrishnan, M. Senthilvelan and M. Lakshmanan, Accepted for Publication in Phys. Rev. Lett. (2019).

Physics Letters A 384 (2020) 126201

Contents lists available at ScienceDirect

Physics Letters A

www.elsevier.com/locate/pla

Nondegenerate soliton solutions in certain coupled nonlinear Schrödinger systems

S. Stalin, R. Ramakrishnan, M. Lakshmanan *

Department of Nonlinear Dynamics, School of Physics, Bharathidasan University, Tiruchirappalli 620024, Tamil Nadu, India

ARTICLE INFO

Article history:
Received 13 November 2019
Received in revised form 8 December 2019
Accepted 9 December 2019
Available online 14 December 2019
Communicated by B. Malomed

Keywords:
Nondegenerate bright soliton solutions
Degenerate bright soliton solutions
Hirota bilinear method
Coupled nonlinear Schrödinger systems

ABSTRACT

In this paper, we report a more general class of nondegenerate soliton solutions, associated with two distinct wave numbers in different modes, for a certain class of physically important integrable two component nonlinear Schrödinger type equations through bilinearization procedure. In particular, we consider coupled nonlinear Schrödinger (CNLS) equations (both focusing as well as mixed type nonlinearities), coherently coupled nonlinear Schrödinger (CCNLS) equations and long-wave-short-wave resonance interaction (LSRI) system. We point out that the obtained general form of soliton solutions exhibit novel profile structures than the previously known degenerate soliton solutions corresponding to identical wave numbers in both the modes. We show that such degenerate soliton solutions can be recovered from the newly derived nondegenerate soliton solutions as limiting cases.

1. Introduction

Solitons are localized nonlinear pulses which arise in various nonlinear dispersive media due to the precise balance between nonlinearity and dispersion [1]. Such nonlinear entities remarkably exhibit energy retaining property during collision process for example in scalar nonlinear Schrödinger (NLS) equation where the fundamental soliton corresponding to intensity is always in a single-hump structure (sech function) characterized by a single wave number [2]. Similar to scalar soliton, the fascinating energy sharing collision exhibiting fundamental multicomponent/vector soliton [3,4] in certain integrable coupled nonlinear Schrödinger systems is also described by identical wave numbers in all the modes apart from distinct complex polarization vector constants [3,4]. As a consequence of this, a single-hump structure only occurs in most of the fundamental vector bright soliton solutions of various CNLS systems.

For instance Manakov type N-CNLS equations [4], mixed N-CNLS equations [5], long-wave-short-wave resonance interaction (LSRI) system [6], etc. are such cases. In contrast to such cases, the coherent coupling among the copropagating optical fields induces a special type of double-hump vector bright soliton in multicomponent CCNLS systems [7,8]. In this four wave mixing physical situation also the coherently coupled soliton governed by the same wave number arises in all the modes [7,8]. Therefore it is clear that the above mentioned degeneracy in wave numbers always persists in the previously reported vector bright solitons too [3–8].

Based on the nature of the presence of wave numbers in the multicomponent soliton solution we classify them as degenerate and nondegenerate in the present paper. We call the solitons which propagate in all the modes with identical wave numbers as degenerate vector solitons whereas the solitons with nonidentical wave numbers as nondegenerate vector solitons [9]. In this context we also note that the terminology nondegenerate solitons has been used in a different context for multi-solitons where the individual constituent solitons travel with distinct velocities in the case of scalar equations such as the Korteweg-deVries, sine-Gordon and NLS equations [10]. Then in these cases multi-solitons moving with a single velocity have been referred as degenerate solitons. This is different from our case where we designate solitons with distinct wave numbers in different modes as nondegenerate solitons [9]. In Refs. [7] and [8] one of the present authors and his collaborators have also already discussed these terminologies to classify the coherently coupled solitons as degenerate and nondegenerate based on their intensities: When the coherently coupled solitons possess the same intensity profile in both the components q_1 and q_2, they are named as degenerate while the solitons with distinct intensity profiles in the q_1 and q_2 components are referred as nondegenerate solitons [7,8]. In contrast, in the present context, the vector solitons already reported in the literature are

* Corresponding author.
E-mail address: lakshman.cnld@gmail.com (M. Lakshmanan).

https://doi.org/10.1016/j.physleta.2019.126201
0375-9601/

designated as degenerate class of solitons. In this letter, we intend to show that the above mentioned coupled systems can admit more general class of nondegenerate soliton solutions as in the case of Manakov model reported recently by us [9] which also finds applications in multicomponent Bose-Einstein condensates [11]. Very specifically we derive such new class of soliton solutions for the two component version of CNLS equations, CCNLS equations and LSRI system one by one as we describe below. Their collision property will be reported separately. The procedure we adopt in this work is essentially based on the Hirota's bilinearization method [9,12], while such solutions can also be derived using Darboux transformation method [11] or other methods like symmetry based approach [13], etc.

2. Nondegenerate bright soliton solutions of CNLS system

To start with, we consider the following coupled nonlinear Schrödinger equations,

$$iq_{j,z} + q_{j,tt} + 2\sum_{l=1}^{2}\sigma_l|q_l|^2 q_j = 0,\ \ j = 1, 2, \tag{1}$$

where $q_j,\ j = 1, 2$ represent the complex wave amplitudes, with suffices denoting usual partial derivatives. The well known Manakov system [14] arises from Eq. (1) when $\sigma_1 = \sigma_2 = 1$, whereas for $\sigma_1 = \sigma_2 = -1$ and $\sigma_1 = -\sigma_2 = 1$ turn out to be the defocusing and mixed type CNLS systems, respectively. These systems admit bright-bright soliton solutions [3,4], dark-dark/bright-dark soliton solutions [15,16] and bright-bright/bright-dark/dark-dark soliton solutions [5,17–19], respectively, as well as breather and rogue wave type solutions and nonlinear interference patterns [20]. All the above three types of CNLS equations are physically important integrable systems and appear in many physical situations [5,16].

To derive the nondegenerate bright one-soliton solutions for both the focusing and mixed type CNLS equations as well as to demonstrate the procedure for similar systems, we consider Eq. (1) with the following bilinearizing transformations $q_j(z,t) = \frac{g^{(j)}(z,t)}{f(z,t)},\ j = 1, 2$. Here $g^{(j)}$ and f are in general complex and real functions, respectively. Substituting the above transformations in Eq. (1), we obtain the bilinear forms of it as

$$D_1\ g^{(j)} \cdot f = 0,\ \ j = 1, 2,\ \ D_2\ f \cdot f = 2\sum_{l=1}^{2}\sigma_l g^{(l)} g^{(l)*}, \tag{2}$$

where $D_1 \equiv iD_z + D_t^2$ and $D_2 \equiv D_t^2$. The Hirota bilinear operators D_z and D_t are defined as [12]

$$D_z^m D_t^n G \cdot F = \left(\frac{\partial}{\partial z} - \frac{\partial}{\partial z'}\right)^m \left(\frac{\partial}{\partial t} - \frac{\partial}{\partial t'}\right)^n G(z,t) \cdot F(z,t)_{|z=z', t=t'}. \tag{3}$$

By solving the bilinear equations (3) systematically along with the series expansions,

$$g^{(j)} = \epsilon g_1^{(j)} + \epsilon^3 g_3^{(j)} + \ldots,\ \ f = 1 + \epsilon^2 f_2 + \epsilon^4 f_4 + \ldots, \tag{4}$$

for the unknown functions $g^{(j)}$ and f, we obtain the more general form of nondegenerate soliton solutions for Eq. (1) with appropriate nontrivial seed solutions. While constructing the new class of one soliton solution for Eq. (1), we find that the above series expansions get truncated as $g^{(j)} = \epsilon g_1^{(j)} + \epsilon^3 g_3^{(j)}$ and $f = 1 + \epsilon^2 f_2 + \epsilon^4 f_4$, by considering the following set of distinct initial seed solutions, $g_1^{(1)} = \alpha_1 e^{\eta_1}$, $g_1^{(2)} = \beta_1 e^{\xi_1},\ \eta_1 = k_1 t + ik_1^2 z,\ \xi_1 = l_1 t + il_1^2 z$, for the lowest order linear partial differential equations (PDEs), $ig_{1,z}^{(j)} + g_{1,tt}^{(j)} = 0,\ j = 1, 2$. In addition to the latter PDEs we obtain a system of PDEs for the unknown functions $g_3^{(j)}$, f_2 and f_4, as follows:

$$\begin{aligned}
&O(\epsilon) : D_1 g_1^{(j)} \cdot 1 = 0,\ \ O(\epsilon^2) : D_2(1 \cdot f_2 + f_2 \cdot 1) = 2(\sigma_1 g_1^{(1)} g_1^{(1)*} + \sigma_2 g_1^{(2)} g_1^{(2)*})\\
&O(\epsilon^3) : D_1(g_3^{(j)} \cdot 1 + g_1^{(j)} \cdot f_2) = 0,\ \ O(\epsilon^5) : D_1(g_3^{(j)} \cdot f_2 + g_1^{(j)} \cdot f_4) = 0,\\
&O(\epsilon^4) : D_2(1 \cdot f_4 + f_4 \cdot 1 + f_2 \cdot f_2) = 2[\sigma_1(g_1^{(1)} g_3^{(1)*} + g_3^{(1)} g_1^{(1)*}) + \sigma_2(g_1^{(2)} g_3^{(2)*} + g_3^{(2)} g_1^{(2)*})]\\
&O(\epsilon^6) : D_2(f_2 \cdot f_4 + f_4 \cdot f_2) = 2(\sigma_1 g_3^{(1)} g_3^{(1)*} + \sigma_2 g_3^{(2)} g_3^{(2)*}),\\
&O(\epsilon^7) : D_1 g_3^{(j)} \cdot f_4 = 0,\ \ O(\epsilon^8) : D_2 f_4 \cdot f_4 = 0,\ \ j = 1, 2.
\end{aligned} \tag{5}$$

The above system of PDEs admits the following solutions:

$$\begin{aligned}
&g_3^{(1)} = e^{\eta_1 + \xi_1 + \xi_1^* + \Delta_{11}},\ g_3^{(2)} = e^{\xi_1 + \eta_1 + \eta_1^* + \Delta_{12}},\ f_2 = e^{\eta_1 + \eta_1^* + \delta_1} + e^{\xi_1 + \xi_1^* + \delta_2},\\
&f_4 = e^{\eta_1 + \eta_1^* + \xi_1 + \xi_1^* + \delta_{11}},\ e^{\Delta_{11}} = \frac{\alpha_1|\beta_1|^2(k_1 - l_1)\sigma_2}{(k_1 + l_1^*)(l_1 + l_1^*)^2},\ e^{\Delta_{12}} = \frac{\beta_1|\alpha_1|^2(l_1 - k_1)\sigma_1}{(k_1^* + l_1)(k_1 + k_1^*)^2},\\
&e^{\delta_1} = \frac{|\alpha_1|^2\sigma_1}{(k_1 + k_1^*)^2},\ e^{\delta_2} = \frac{|\beta_1|^2\sigma_2}{(l_1 + l_1^*)^2},\ e^{\delta_{11}} = \frac{|\alpha_1|^2|\beta_1|^2|k_1 - l_1|^2\sigma_1\sigma_2}{|k_1 + l_1^*|^2(l_1 + l_1^*)^2(k_1 + k_1^*)^2}.
\end{aligned} \tag{6}$$

Note that the other unknown functions in the series expansions (4) are found to be zero. Hence the explicit expressions of $g_3^{(j)}$, f_2 and f_4 constitute the more general form of nondegenerate fundamental soliton solution of CNLS Eq. (1) as

$$\begin{aligned}
q_1 &= \frac{\alpha_1 e^{\eta_1} + e^{\eta_1 + \xi_1 + \xi_1^* + \Delta_{11}}}{1 + e^{\eta_1 + \eta_1^* + \delta_1} + e^{\xi_1 + \xi_1^* + \delta_2} + e^{\eta_1 + \eta_1^* + \xi_1 + \xi_1^* + \delta_{11}}},\\
q_2 &= \frac{\beta_1 e^{\xi_1} + e^{\xi_1 + \eta_1 + \eta_1^* + \Delta_{12}}}{1 + e^{\eta_1 + \eta_1^* + \delta_1} + e^{\xi_1 + \xi_1^* + \delta_2} + e^{\eta_1 + \eta_1^* + \xi_1 + \xi_1^* + \delta_{11}}},
\end{aligned} \tag{7}$$

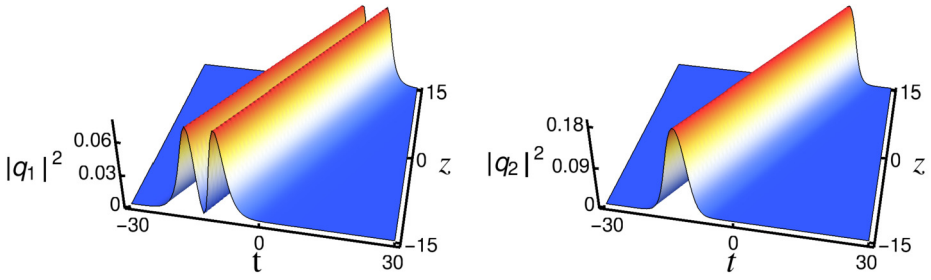

Fig. 1. Nondegenerate symmetric double-hump and single-hump soliton profiles in Manakov system.

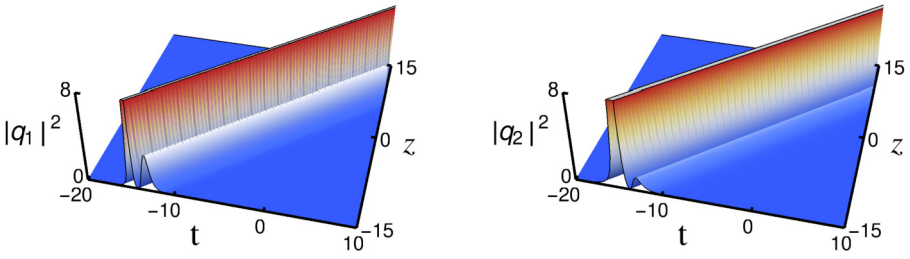

Fig. 2. Nondegenerate singular double-hump soliton profiles in mixed CNLS system.

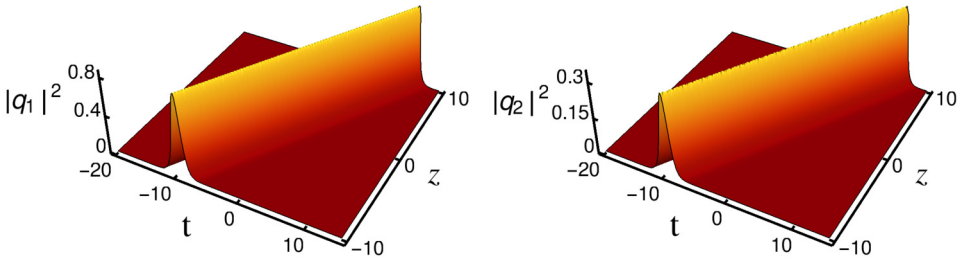

Fig. 3. Degenerate single-hump soliton profiles in Manakov system.

which is exactly of the same form as given for the Manakov equation in [9], except that in the various constants σ_1 and σ_2 appear explicitly as given in (6).

From the above, one can immediately conclude that the obtained solution is nondegenerate because of the fact that distinct wave numbers k_1 and l_1 are simultaneously present in both the expressions of q_1 and q_2. The solution (7) becomes nondegenerate one bright soliton solution of the Manakov system [9] if we fix $\sigma_1 = \sigma_2 = 1$ and for the choice $\sigma_1 = -\sigma_2 = 1$, the solution (7) is the nondegenerate fundamental soliton solution of the mixed CNLS system. In both the cases the shape of the nondegenerate soliton is described by four nontrivial complex parameters α_1, β_1, k_1 and l_1. Note that α_1 and β_1 are related to the polarization vectors, k_{1R} and l_{1R} represent the amplitudes while l_{1I} and k_{1I} denote the velocities of the solitons of the two modes q_1 and q_2, respectively.

The distinct wave numbers give rise to two physical situations by restricting the imaginary parts of them. By doing so, we find that the fundamental soliton propagates in the two modes either with identical velocities ($k_{1I} = l_{1I}$) or with non-identical velocities ($k_{1I} \neq l_{1I}$) but with ($k_{1R} \neq l_{1R}$). In the former case the nondegenerate soliton corresponding to the Manakov system admits four distinct nonsingular forms of asymmetric and symmetric profiles which include a single-hump, a double-hump and flattop profiles as we have shown in Ref. [9]. For the Manakov system, we display typical double-hump and single-hump profiles in Fig. 1 for the parameter values $k_1 = 0.333 + 0.5i$, $l_1 = 0.55 + 0.5i$, $\alpha_1 = 0.5 + 0.45i$ and $\beta_1 = 0.5 + 0.5i$. In contradiction to the Manakov system, the nondegenerate fundamental soliton in the mixed CNLS always shows singular behaviour for arbitrary choice of parameter values, except when $k_1 = l_1$. The singularity nature of double-hump soliton profile in this mixed CNLS case is illustrated in Fig. 2 for $k_1 = 1.2 + 0.5i$, $l_1 = -0.5 + 0.5i$, $\alpha_1 = 0.3$ and $\beta_1 = i$. The singularity naturally arises because of the defocusing nonlinearity of the mixed CNLS system.

If we impose $k_1 = l_1$ in Eq. (7), the forms of nondegenerate fundamental soliton reduces to the following degenerate bright soliton solution, $q_j = \frac{\alpha_1^{(j)} e^{\eta_1}}{1+e^{\eta_1+\eta_1^*+R}} \equiv A_j k_{1R} e^{i\eta_{1I}}\ \mathrm{sech}(\eta_{1R} + \frac{R}{2})$, $j = 1, 2$ for the Manakov system as well as mixed CNLS system. Here the unit polarization vectors, $A_1 = \frac{\alpha_1}{(\sigma_1|\alpha_1|^2+\sigma_2|\beta_1|^2)^{1/2}}$, $A_2 = \frac{\beta_1}{(\sigma_1|\alpha_1|^2+\sigma_2|\beta_1|^2)^{1/2}}$, $\eta_{1R} = k_{1R}(t - 2k_{1I}z)$, $\eta_{1I} = k_{1I}t + (k_{1R}^2 - k_{1I}^2)z$ and $e^R = \frac{(\sigma_1|\alpha_1|^2+\sigma_2|\beta_1|^2)}{(k_1+k_1^*)^2}$. The amplitude, velocity and the central position of the degenerate fundamental soliton are $A_j k_{1R}$, $2k_{1I}$ and $\frac{R}{2k_{1R}}$, respectively. It is an obvious fact that the degenerate bright soliton solution contains a single complex wave number k_1 which allows single-hump profile only. The degenerate fundamental soliton profile of the Manakov system is demonstrated in Fig. 3 for $k_1 = 1.1 + 0.5i$, $\alpha_1 = 1 + 0.5i$ and $\beta_1 = 0.5 + 0.5i$. Similarly for the mixed CNLS system the non-singular degenerate soliton is shown in Fig. 4 for $k_1 = 1 + 0.5i$, $\alpha_1 = 1$ and $\beta_1 = 0.5$. As shown in Ref. [5], the singularity occurs in the degenerate soliton solution of mixed CNLS case when $|\beta_1| > |\alpha_1|$.

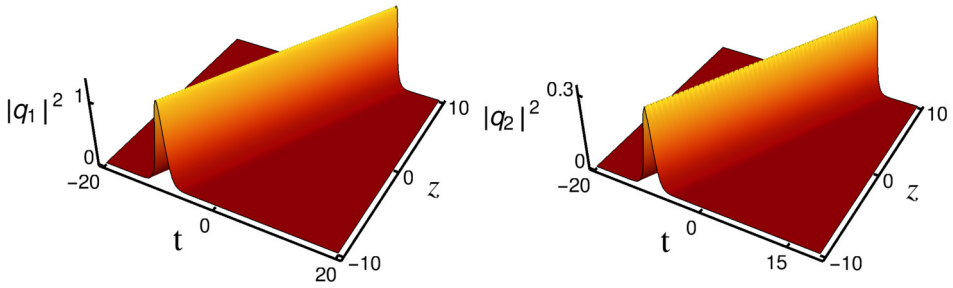

Fig. 4. Degenerate non-singular single-hump soliton profiles in mixed CNLS system.

3. Nondegenerate soliton solutions of CCNLS system

Now, we consider the following system of two coupled nonlinear Schrödinger equations with coherent coupling among the two co-propagating fields q_1 and q_2,

$$\begin{aligned} &iq_{1,z} + q_{1,tt} + \gamma(|q_1|^2 + 2|q_2|^2)q_1 - \gamma q_2^2 q_1^* = 0, \\ &iq_{2,z} + q_{2,tt} + \gamma(2|q_1|^2 + |q_2|^2)q_2 - \gamma q_1^2 q_2^* = 0. \end{aligned} \tag{8}$$

The terms inside the brackets in Eq. (8) correspond to incoherent coupling (self-phase modulation and cross-phase modulation) between the copropagating fields and the terms $q_2^2 q_1^*$ and $q_1^2 q_2^*$ correspond to the coherent coupling among the copropagating fields q_1 and q_2. We note that due to the coherent coupling effect even the degenerate fundamental soliton that is present in the underlying system admits double-hump and flattop profiles apart from the single-hump profile under appropriate parametric choices [7,8]. Very interestingly such degenerate coherently coupled soliton undergoes energy switching collision when it interacts with degenerate incoherently coupled soliton [7,8]. Equation (8) has also been shown to admit breather and rogue wave type solutions too [21,22]. Therefore it is interesting to investigate what will happen when the coherently coupled fundamental soliton is characterized by two different wave numbers.

In order to deduce the appropriate nondegenerate soliton solution to (8), we introduce the bilinear transformation $q_j = \frac{g^{(j)}(z,t)}{f(z,t)}$ with an auxiliary function $s(z,t)$ [7,8,23]. It results in the following bilinear equations

$$D_1 g^{(j)} \cdot f = \gamma g^{(j)*} \cdot s,\ D_2 f \cdot f = 2\gamma \sum_{j=1}^{2} |g^{(j)}|^2, s \cdot f = \sum_{j=1}^{2} (g^{(j)})^2, \tag{9}$$

where $D_1 \equiv iD_z + D_t^2$ and $D_2 \equiv D_t^2$. We follow the procedure described in [7,8] for the degenerate case but now with the seed solutions $g_1^{(1)} = \alpha_1 e^{\eta_1}$, $g_1^{(2)} = \beta_1 e^{\xi_1}$, $\eta_1 = k_1 t + ik_1^2 z$, $\xi_1 = l_1 t + il_1^2 z$. While doing so, the series expansions get truncated as $g^{(j)} = \epsilon g_1^{(j)} + \epsilon^3 g_3^{(j)} + \epsilon^5 g_5^{(j)} + \epsilon^7 g_7^{(j)}$, $f = 1 + \epsilon^2 f_2 + \epsilon^4 f_4 + \epsilon^6 f_6 + \epsilon^8 f_8$ and $s = \epsilon^2 s_2 + \epsilon^4 s_4 + \epsilon^6 s_6$. By substituting the obtained forms of the unknown functions in the truncated series expansions, we get the following general form of nondegenerate coherently coupled fundamental soliton solution of 2-CCNLS system (8),

$$\begin{aligned} q_1 &= \frac{1}{f}\Big(\alpha_1 e^{\eta_1} + e^{2\eta_1+\eta_1^*+\Delta_{11}} + e^{\eta_1^*+2\xi_1+\Delta_{12}} + e^{\eta_1+\xi_1+\xi_1^*+\Delta_{13}} + e^{\eta_1+2(\eta_1^*+\xi_1)+\Delta_{14}} \\ &\quad + e^{\eta_1+2(\xi_1+\xi_1^*)+\Delta_{15}} + e^{2\eta_1+\eta_1^*+\xi_1+\xi_1^*+\Delta_{16}} + e^{2(\eta_1+\xi_1+\xi_1^*)+\eta_1^*+\Delta_{17}}\Big), \\ q_2 &= \frac{1}{f}\Big(\beta_1 e^{\xi_1} + e^{2\xi_1+\xi_1^*+\Delta_{21}} + e^{\xi_1^*+2\eta_1+\Delta_{22}} + e^{\xi_1+\eta_1+\eta_1^*+\Delta_{23}} + e^{\xi_1+2(\xi_1^*+\eta_1)+\Delta_{24}} \\ &\quad + e^{\xi_1+2(\eta_1^*+\eta_1)+\Delta_{25}} + e^{2\xi_1+\xi_1^*+\eta_1+\eta_1^*+\Delta_{26}} + e^{2(\eta_1+\eta_1^*+\xi_1)+\xi_1^*+\Delta_{27}}\Big), \\ f &= 1 + e^{\eta_1+\eta_1^*+\delta_1} + e^{\xi_1+\xi_1^*+\delta_2} + e^{2(\eta_1+\eta_1^*)+\delta_3} + e^{2(\eta_1+\xi_1^*)+\delta_4} + e^{2(\xi_1+\eta_1^*)+\delta_5} \\ &\quad + e^{2(\xi_1+\xi_1^*)+\delta_6} + e^{(\eta_1+\eta_1^*+\xi_1+\xi_1^*)+\delta_7} + e^{2(\eta_1+\eta_1^*)+\xi_1+\xi_1^*+\nu_1} \\ &\quad + e^{2(\xi_1+\xi_1^*)+\eta_1+\eta_1^*+\nu_2} + e^{2(\eta_1+\eta_1^*+\xi_1+\xi_1^*)+\nu_3}. \end{aligned} \tag{10}$$

The various constants which appear in the above solution are given by

$$\begin{aligned} &e^{\Delta_{11}} = \frac{\gamma\alpha_1|\alpha_1|^2}{2\kappa_{11}}, e^{\Delta_{12}} = \frac{\gamma\alpha_1^*\beta_1^2}{2\theta_1^{*2}}, e^{\Delta_{13}} = \frac{\gamma\alpha_1|\beta_1|^2\rho_1}{\theta_1 l_{11}}, e^{\Delta_{14}} = \frac{\gamma^2\rho_1^2\alpha_1^*\beta_1^2|\alpha_1|^2}{4\kappa_{11}\theta_1^{*4}}, \\ &e^{\Delta_{15}} = \frac{\gamma^2\rho_1^2\alpha_1|\beta_1|^4}{4l_{11}^2\theta_1^2}, e^{\Delta_{16}} = \frac{\gamma^2\rho_1^2\rho_1^*\alpha_1|\alpha_1|^2|\beta_1|^2}{2\kappa_{11}l_{11}\theta_1^2\theta_1^*}, e^{\Delta_{17}} = \frac{\gamma^3\rho_1^4\rho_1^{*2}\alpha_1|\alpha_1|^2|\beta_1|^4}{8\kappa_{11}l_{11}^2\theta_1^4\theta_1^{*2}}, \\ &e^{\Delta_{21}} = \frac{\gamma\beta_1|\beta_1|^2}{2l_{11}}, e^{\Delta_{22}} = \frac{\gamma\alpha_1^2\beta_1^*}{2\theta_1^2}, e^{\Delta_{23}} = -\frac{\gamma|\alpha_1|^2\beta_1\rho_1}{\theta_1^*\kappa_{11}}, e^{\Delta_{24}} = \frac{\gamma^2\rho_1^2\alpha_1^2|\beta_1|^2\beta_1^*}{4l_{11}\theta_1^4}, \end{aligned}$$

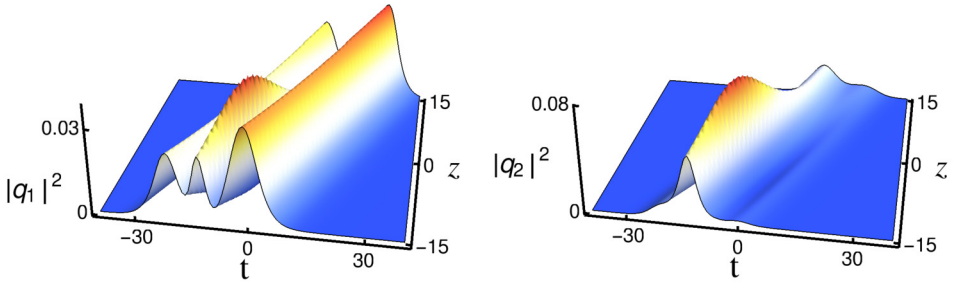

Fig. 5. Breathing type triple-hump profile of nondegenerate soliton in the CCNLS system.

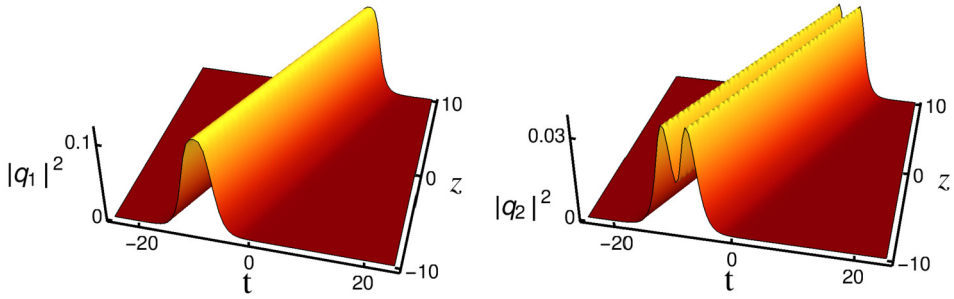

Fig. 6. Flattop-double-hump profiles of degenerate solitons in the CCNLS system.

$$e^{\Delta_{25}}=\frac{\gamma^2\rho_1^2|\alpha_1|^4\beta_1}{4\kappa_{11}^2\theta_1^{*2}}, e^{\Delta_{26}}=-\frac{\gamma^2\rho_1^2\rho_1^*\beta_1|\alpha_1|^2|\beta_1|^2}{2\kappa_{11}l_{11}\theta_1\theta_1^{*2}}, e^{\Delta_{27}}=\frac{\gamma^3\rho_1^4\rho_1^{*2}\beta_1|\alpha_1|^4|\beta_1|^2}{8\kappa_{11}^2l_{11}\theta_1^2\theta_1^{*4}},$$
$$e^{\delta_1}=\frac{\gamma|\alpha_1|^2}{\kappa_{11}}, e^{\delta_2}=\frac{\gamma|\beta_1|^2}{l_{11}}, e^{\delta_3}=\frac{\gamma^2|\alpha_1|^4}{4\kappa_{11}^2}, e^{\delta_4}=\frac{\gamma^2\alpha_1^2\beta_1^{*2}}{4\theta_1^4}, e^{\delta_5}=\frac{\gamma^2\alpha_1^{*2}\beta_1^2}{4\theta_1^{*4}},$$
$$e^{\delta_6}=\frac{\gamma^2|\beta_1|^4}{4l_{11}^2}, e^{\delta_7}=\frac{\gamma^2|\rho_1|^2|\alpha_1|^2|\beta_1|^2}{\kappa_{11}l_{11}|\theta_1|^2}, e^{\nu_1}=\frac{\gamma^3|\rho_1|^4|\alpha_1|^4|\beta_1|^2}{4\kappa_{11}^2l_{11}|\theta_1|^4},$$
$$e^{\nu_2}=\frac{\gamma^3|\rho_1|^4|\alpha_1|^2|\beta_1|^4}{4\kappa_{11}l_{11}^2|\theta_1|^4}, e^{\nu_3}=\frac{\gamma^4|\rho_1|^8|\alpha_1|^4|\beta_1|^4}{16\kappa_{11}^2l_{11}^2|\theta_1|^8}, l_{11}=(l_1+l_1^*)^2,$$
$$\theta_1=(k_1+l_1^*),\ \rho_1=(k_1-l_1),\ \kappa_{11}=(k_1+k_1^*)^2.$$

The auxiliary function is obtained as $s=\alpha_1^2e^{2\eta_1}+\beta_1^2e^{2\xi_1}+e^{2\eta_1+\xi_1+\xi_1^*+\phi_1}+e^{2\xi_1+\eta_1+\eta_1^*+\phi_2}+e^{2(\eta_1+\eta_1^*+\xi_1)+\phi_3}+e^{2(\eta_1+\xi_1^*+\xi_1)+\phi_4}$, $e^{\phi_1}=\frac{\gamma\rho_1^2\alpha_1^2|\beta_1|^2}{\theta_1^2l_{11}}$, $e^{\phi_2}=\frac{\gamma\rho_1^2\beta_1^2|\alpha_1|^2}{\theta_1^{*2}\kappa_{11}}$, $e^{\phi_3}=\frac{\gamma^2\rho_1^4\beta_1^2|\alpha_1|^4}{4\theta_1^{*4}\kappa_{11}^2}$, $e^{\phi_4}=\frac{\gamma^2\rho_1^4\alpha_1^2|\beta_1|^4}{4\theta_1^4l_{11}^2}$. The already reported degenerate coherently coupled fundamental one-soliton solution [7,8] of Eq. (8) is obtained by restricting $k_1=l_1$ in Eq. (10). This leads to $q_1=\frac{\alpha_1e^{\eta_1}+e^{2\eta_1+\eta_1^*+\Delta_{11}}}{1+e^{\eta_1+\eta_1^*+\delta_1}+e^{2(\eta_1+\eta_1^*)+\delta_2}}$, $q_2=\frac{\beta_1e^{\eta_1}+e^{2\eta_1+\eta_1^*+\Delta_{12}}}{1+e^{\eta_1+\eta_1^*+\delta_1}+e^{2(\eta_1+\eta_1^*)+\delta_2}}$, $e^{\Delta_{11}}=\frac{\gamma\alpha_1^*(\alpha_1^2+\beta_1^2)}{2\kappa_{11}}$, $e^{\Delta_{12}}=\frac{\gamma\beta_1^*(\alpha_1^2+\beta_1^2)}{2\kappa_{11}}$, $e^{\delta_1}=\frac{\gamma(|\alpha_1|^2+|\beta_1|^2)}{\kappa_{11}}$, $e^{\delta_2}=\frac{\gamma^2|\alpha_1^2+\beta_1^2|^2}{4\kappa_{11}^2}$. The auxiliary function is reduced as $s=(\alpha_1^2+\beta_1^2)e^{2\eta_1}$.

From the solution (10), it is easy to identify that the shape of the nondegenerate coherently coupled fundamental soliton (10) is also governed by two arbitrary complex parameters α_1 and β_1 and two distinct complex wave numbers k_1 and l_1. The solution (10) admits various novel profiles, such as a quadruple-hump, a triple-hump, a double-hump, a flattop and a single-hump profiles under appropriate restrictions on the wave parameters. This is due to the presence of additional wave number and the four wave mixing effect. As an example, we display a nontrivial breathing type triple-hump shaped soliton profiles in Fig. 5 for the parameters $\gamma=2$, $k_1=0.21+0.5i$, $l_1=0.29+0.5i$, $\alpha_1=0.95+0.5i$ and $\beta_1=0.97-i$. By tuning the relative separation distance it is also possible to separate a single-hump and a double-hump from this triple-hump profile. However, a distinct double-hump profile only occurs in the degenerate case. This is due to the presence of a single wave number apart from two arbitrary constants α_1 and β_1. A typical degenerate flattop soliton in q_1 component and a double-hump profile in q_2 component is illustrated in Fig. 6 for $\gamma=2$, $k_1=l_1=0.5+0.5i$, $\alpha_1=0.72+0.5i$ and $\beta_1=0.5-0.42i$.

4. Nondegenerate soliton solution of LSRI system

Finally we intend to derive the nondegenerate fundamental soliton solution for the following long-wave short-wave resonance interaction system, namely the 2-component Yajima-Oikawa system [24] with general form of nonlinearity,

$$iS_t^{(1)}+S_{xx}^{(1)}+LS^{(1)}=0,\ iS_t^{(2)}+S_{xx}^{(2)}+LS^{(2)}=0,\ L_t=\sum_{l=1}^{2}\sigma_l(|S^{(l)}|^2)_x. \tag{11}$$

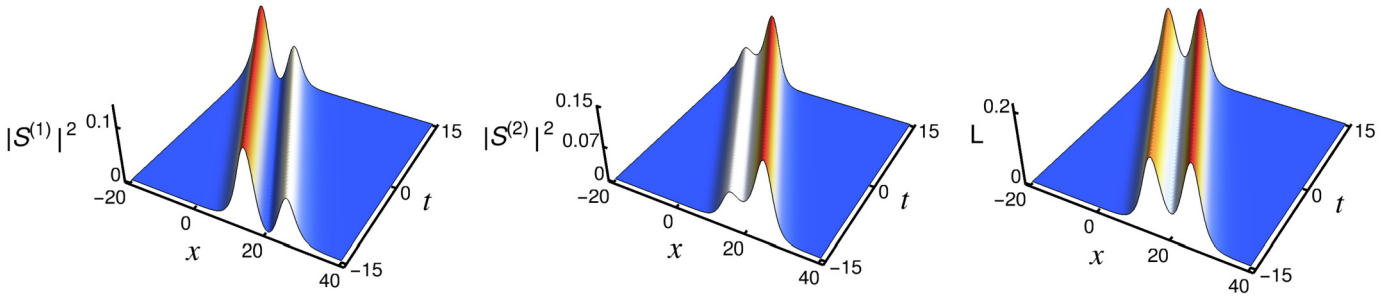

Fig. 7. Nondegenerate asymmetric double-hump soliton profiles in the two short-wave components and the long-wave component.

In the above, $S^{(l)}$'s, $l=1,2$, are short-wave components and L is the long-wave component and suffices denote partial derivatives, while σ_l's are arbitrary real parameters. Further $\sigma_l=+1$, $\sigma_l=-1$, $l=1,2$, and $\sigma_1=-\sigma_2=1$ correspond to positive, negative and mixed positive-negative nonlinearities. Both nondegenerate and degenerate solitons arise in the present short-wave components also due to the balance between their dispersion and nonlinear interactions of the short-waves with a long-wave. In contrast to the previous case, the formation of nondegenerate and degenerate solitons arises in the long-wave component due to the interaction of the short-wave components. In the present 2-component LSRI system also the solitons in the short-wave components as well as long-wave component are degenerate characterized by a single wave number. To overcome this degeneracy we take the modified form of seed solutions, involving two distinct wave numbers, in the nondegenerate soliton solution construction process. We note that the above LSRI system admits rogue wave solutions also [25].

To construct the nondegenerate one-soliton solution we again bilinearize Eq. (11) through the following transformations, $S^{(l)}(x,t)=\frac{g^{(l)}(x,t)}{f(x,t)}$, $l=1,2$, $L=2\frac{\partial^2}{\partial x^2}\ln f(x,t)$. We obtain the following bilinear forms:

$$D_1 g^{(l)}\cdot f=0, l=1,2,\ D_2 f\cdot f=\sum_{n=1}^{2}\sigma_n|g^{(n)}|^2, \tag{12}$$

where $D_1\equiv iD_t+D_x^2$ and $D_2\equiv D_xD_t$. With the modified forms of seed solutions $g_1^{(1)}=\alpha_1 e^{\eta_1}$, $g_1^{(2)}=\beta_1 e^{\xi_1}$, $\eta_1=k_1x+ik_1^2t$, $\xi_1=l_1x+il_1^2t$, we find that the series expansions which are given in [6] get terminated as $g^{(l)}=\epsilon g_1^{(l)}+\epsilon^3 g_3^{(l)}$, $f=1+\epsilon^2 f_2+\epsilon^4 f_4$. The explicit forms of the unknown functions lead to the following nondegenerate fundamental soliton solution,

$$\begin{aligned}
S^{(1)}&=\frac{g_1^{(1)}+g_3^{(1)}}{1+f_2+f_4}=\frac{\alpha_1 e^{\eta_1}+e^{\eta_1+\xi_1+\xi_1^*+\mu_{11}}}{1+e^{\eta_1+\eta_1^*+R_1}+e^{\xi_1+\xi_1^*+R_2}+e^{\eta_1+\eta_1^*+\xi_1+\xi_1^*+R_3}},\\
S^{(2)}&=\frac{g_1^{(2)}+g_3^{(2)}}{1+f_2+f_4}=\frac{\beta_1 e^{\xi_1}+e^{\xi_1+\eta_1+\eta_1^*+\mu_{12}}}{1+e^{\eta_1+\eta_1^*+R_1}+e^{\xi_1+\xi_1^*+R_2}+e^{\eta_1+\eta_1^*+\xi_1+\xi_1^*+R_3}},\\
L&=\frac{2}{f^2}\Big((k_1+k_1^*)^2e^{\eta_1+\eta_1^*+R_1}+(l_1+l_1^*)^2e^{\xi_1+\xi_1^*+R_2}+e^{\eta_1+\eta_1^*+\xi_1+\xi_1^*+R_4}\\
&\quad+(l_1+l_1^*)^2e^{2(\eta_1+\eta_1^*)+\xi_1+\xi_1^*+R_1+R_3}+(k_1+k_1^*)^2e^{\eta_1+\eta_1^*+2(\xi_1+\xi_1^*)+R_2+R_3}\Big),\\
f&=(1+e^{\eta_1+\eta_1^*+R_1}+e^{\xi_1+\xi_1^*+R_2}+e^{\eta_1+\eta_1^*+\xi_1+\xi_1^*+R_3}),
\end{aligned}\tag{13}$$

where

$$\begin{aligned}
&e^{\mu_{11}}=\frac{i\alpha_1|\beta_1|^2\sigma_2(l_1-k_1)}{2(k_1+l_1^*)(l_1-l_1^*)(l_1+l_1^*)^2},\quad e^{\mu_{12}}=\frac{i\beta_1|\alpha_1|^2\sigma_1(k_1-l_1)}{2(k_1^*+l_1)(k_1-k_1^*)(k_1+k_1^*)^2},\quad e^{R_1}=\frac{|\alpha_1|^2\sigma_1}{2i(k_1+k_1^*)^2(k_1-k_1^*)},\\
&e^{R_2}=\frac{|\beta_1|^2\sigma_2}{2i(l_1+l_1^*)^2(l_1-l_1^*)},\quad e^{R_3}=-\frac{|\alpha_1|^2|\beta_1|^2|k_1-l_1|^2\sigma_1\sigma_2}{4|k_1+l_1^*|^2(k_1-k_1^*)(l_1-l_1^*)(k_1+k_1^*)^2(l_1+l_1^*)^2},\\
&e^{R_4}=-2(k_1+k_1^*)(l_1+l_1^*)(e^{R_1+R_2}-e^{R_3})+((k_1+k_1^*)^2+(l_1+l_1^*)^2)(e^{R_1+R_2}+e^{R_3}).
\end{aligned}$$

The nondegenerate fundamental soliton in the 2-component LSRI system is also governed by four non-trivial arbitrary complex parameters α_1, β_1, k_1 and l_1. The amplitudes of the nondegenerate fundamental solitons in the short-wave components are $4k_{1R}A_1\sqrt{k_{1I}}$, $4l_{1R}A_2\sqrt{l_{1I}}$. Here $A_1=\frac{-i\sqrt{\alpha_1}}{\sqrt{\sigma_1\alpha_1^*}}$, $A_2=\frac{-i\sqrt{\beta_1}}{\sqrt{\sigma_2\beta_1^*}}$ are unit polarization vectors of the two short-wave components. In the present case the velocity of the nondegenerate fundamental soliton is characterized by the imaginary parts of the wave numbers k_1 and l_1. Very interestingly in the present LSRI system, the nondegenerate fundamental soliton exhibits amplitude dependent velocity property like the KdV-soliton. The degenerate soliton also possesses this unusual property [6]. As a consequence of this property the taller nondegenerate soliton will propagate faster than the shorter one. To get the regular solution the quantities e^{R_1}, e^{R_2} and e^{R_3} in (13) should be positive. To achive this, we fix $k_{1I},l_{1I}<0$, $k_{1I},l_{1I}>0$ and $k_{1I}<0$, $l_{1I}>0$ for the positive ($\sigma_l>0$), negative ($\sigma_l<0$) and mixed type ($\sigma_1=1$, $\sigma_2=-1$) nonlinearities, respectively. In all the three cases, we observe that the nondegenerate fundamental soliton in the present system admits double-hump profiles similar to nondegenerate soliton of Manakov system. We depict asymmetric double-hump profiles of nondegenerate one-soliton in Fig. 7 for the parameters $k_1=0.3-0.5i$, $l_1=0.35-0.5i$, $\alpha_1=0.8$, $\beta_1=0.5$ and $\sigma_1=\sigma_2=1$.

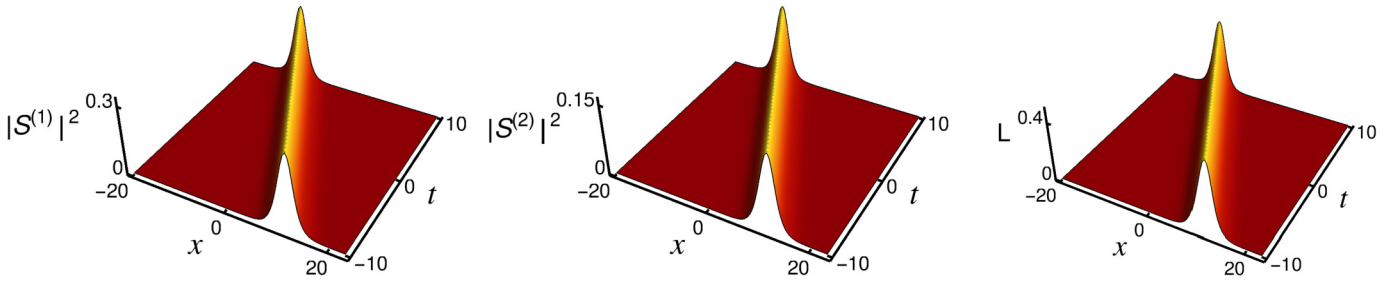

Fig. 8. Degenerate single-hump soliton profiles in both the short-wave components and the long-wave component.

We recover degenerate soliton solution of Eq. (11) by substituting the limit $k_1 = l_1$ in Eq. (13). This results in the following degenerate fundamental soliton forms: $S^{(l)} = 2A_l k_{1R}\sqrt{k_{1I}} e^{i(\eta_{1I}+\frac{\pi}{2})}\ \mathrm{sech}(\eta_{1R}+\frac{R}{2})$, $L = 2k_{1R}^2\ \mathrm{sech}^2(\eta_{1R}+\frac{R}{2})$, $l = 1, 2$. Here $A_1 = \frac{\alpha_1}{(\sigma_1|\alpha_1|^2+\sigma_2|\beta_1|^2)^{1/2}}$, $A_2 = \frac{\beta_1}{(\sigma_1|\alpha_1|^2+\sigma_2|\beta_1|^2)^{1/2}}$, $\eta_{1R} = k_{1R}(x+2k_{1I}t)$, $\eta_{1I} = k_{1I}x+(k_{1R}^2-k_{1I}^2)t$, $e^R = \frac{-(\sigma_1|\alpha_1|^2+\sigma_2|\beta_1|^2)}{16k_{1R}^2k_{1I}}$. As discussed in [6], the degenerate soliton in both the short-wave components and the long-wave component admits only a single-hump profile. A typical graph of such single-hump profile is shown in Fig. 8 for $k_1 = 0.5-0.5i$, $\alpha_1 = 0.5$, $\beta_1 = 0.35$ and $\sigma_1 = \sigma_2 = 1$.

5. Conclusion

In this work, we have thus derived more general forms of nondegenerate fundamental bright solitons corresponding to non-identical wave-numbers for certain physically important integrable coupled systems. In particular we have considered the two component version of the Manakov system, mixed CNLS system, coherently coupled NLS system and long-wave short-wave resonance interaction system. We find that the obtained nondegenerate bright soliton solution admits various novel structures compared to the corresponding degenerate counterparts. The interesting collision dynamics of such nondegenerate solitons will be presented elsewhere.

Declaration of competing interest

The authors declare that they have no known competing financial interests or personal relationships that could have appeared to influence the work reported in this paper.

Acknowledgements

The works of SS and ML are supported by the DST-SERB research project (EMR/2014/001076), Government of India. RR and ML acknowledge the financial support under a DST-SERB Distinguished Fellowship program (SB/DF/04/2017) to ML.

References

[1] Y.S. Kivshar, G.P. Agrawal, Optical Solitons: From Fibers to Photonic Crystals, Academic Press, San Diego, 2003.
[2] V.E. Zakharov, A.B. Shabat, Sov. Phys. JETP 34 (1972) 62.
[3] R. Radhakrishnan, M. Lakshmanan, J. Hietarinta, Phys. Rev. E 56 (1997) 2213.
[4] T. Kanna, M. Lakshmanan, Phys. Rev. Lett. 86 (2001) 5043.
[5] T. Kanna, M. Lakshmanan, P.T. Dinda, N. Akhmediev, Phys. Rev. E 73 (2006) 026604.
[6] T. Kanna, K. Sakkaravarthi, K. Tamilselvan, Phys. Rev. E 88 (2013) 062921.
[7] T. Kanna, M. Vijayajayanthi, M. Lakshmanan, J. Phys. A, Math. Theor. 43 (2010) 434018.
[8] T. Kanna, K. Sakkaravarthi, J. Phys. A, Math. Theor. 44 (2011) 285211.
[9] S. Stalin, R. Ramakrishnan, M. Senthilvelan, M. Lakshmanan, Phys. Rev. Lett. 122 (2019) 043901.
[10] F. Correa, A. Fring, J. High Energy Phys. 2016 (2016) 008;
J. Cen, F. Correa, A. Fring, J. Phys. A, Math. Theor. 50 (2017) 435201;
S. Li, G. Biondini, C. Schiebold, J. Math. Phys. 58 (2017) 033507.
[11] Y.H. Qin, L.C. Zhao, L. Ling, Phys. Rev. E 100 (2019) 022212.
[12] R. Hirota, The Direct Method in Soliton Theory, Cambridge University Press, Cambridge, 2004.
[13] G.W. Bluman, S. Kumei, Symmetries and Differential Equations, Springer, Berlin, 1989.
[14] S.V. Manakov, Sov. Phys. JETP 38 (1974) 248.
[15] R. Radhakrishnan, M. Lakshmanan, J. Phys. A, Math. Gen. 28 (1995) 2683.
[16] A.P. Sheppard, Y.S. Kivshar, Phys. Rev. E 55 (1997) 4773.
[17] M. Vijayajayanthi, T. Kanna, M. Lakshmanan, Phys. Rev. A 77 (2008) 013820.
[18] Y. Ohta, D.S. Wang, J. Yang, Stud. Appl. Math. 127 (2011) 345.
[19] B.F. Feng, J. Phys. A, Math. Theor. 47 (2014) 355203.
[20] Y.H. Qin, Y. Wu, L.C. Zhao, Z.Y. Yang, arXiv:1809.10926v2, 2019;
L.C. Zhao, L. Duan, P. Gao, Z.Y. Yang, Europhys. Lett. 125 (2019) 40003;
L. Ling, L.C. Zhao, Commun. Nonlinear Sci. Numer. Simul. 72 (2019) 449.
[21] C.R. Zhang, B. Tian, X.Y. Wu, Y.Q. Yuan, X.X. Du, Phys. Scr. 93 (2018) 095202.
[22] H.Q. Zhang, S.S. Yuan, Y. Wang, Mod. Phys. Lett. B 30 (2016) 1650208.
[23] C. Gilson, J. Hietarinta, J. Nimmo, Y. Ohta, Phys. Rev. E 68 (2003) 016614.
[24] N. Yajima, M. Oikawa, Prog. Theor. Phys. 56 (1976) 1719.
[25] J. Chen, Y. Chen, B.F. Feng, K.I. Maruno, Phys. Lett. A 379 (2015) 1510.

Nondegenerate solitons and their collisions in Manakov systems

R. Ramakrishnan, S. Stalin, and M. Lakshmanan*
Department of Nonlinear Dynamics, School of Physics, Bharathidasan University, Tiruchirapalli 620 024, India

(Received 8 July 2020; accepted 15 September 2020; published 12 October 2020)

Recently, we have shown that the Manakov equation can admit a more general class of nondegenerate vector solitons, which can undergo collision without any intensity redistribution in general among the modes, associated with distinct wave numbers, besides the already-known energy exchanging solitons corresponding to identical wave numbers. In the present comprehensive paper, we discuss in detail the various special features of the reported nondegenerate vector solitons. To bring out these details, we derive the exact forms of such vector one-, two-, and three-soliton solutions through Hirota bilinear method and they are rewritten in more compact forms using Gram determinants. The presence of distinct wave numbers allows the nondegenerate fundamental soliton to admit various profiles such as double-hump, flat-top, and single-hump structures. We explain the formation of double-hump structure in the fundamental soliton when the relative velocity of the two modes tends to zero. More critical analysis shows that the nondegenerate fundamental solitons can undergo shape-preserving as well as shape-altering collisions under appropriate conditions. The shape-changing collision occurs between the modes of nondegenerate solitons when the parameters are fixed suitably. Then we observe the coexistence of degenerate and nondegenerate solitons when the wave numbers are restricted appropriately in the obtained two-soliton solution. In such a situation we find the degenerate soliton induces shape-changing behavior of nondegenerate soliton during the collision process. By performing suitable asymptotic analysis we analyze the consequences that occur in each of the collision scenario. Finally, we point out that the previously known class of energy-exchanging vector bright solitons, with identical wave numbers, turns out to be a special case of nondegenerate solitons.

DOI: 10.1103/PhysRevE.102.042212

I. INTRODUCTION

The propagation of light pulses in optical Kerr media is still one of the active areas of research in nonlinear optics [1]. In particular, the fascinating dynamics of light in multimode fibers and fiber arrays has stimulated the investigation of temporal multicomponent or vector solitons over different aspects, especially from the applications point of view [2]. In the nonlinear optics context, temporal vector solitons are formed due to the balance between dispersion and Kerr nonlinearity. Mathematically these vector solitons are nothing but the solutions of certain integrable coupled nonlinear Schrödinger family of equations. There exist many types of vector solitons which have been reported so far in the literature and their dynamics have also been investigated in various physical situations. For instance, bright-bright solitons [3–5], bright-dark solitons [6–9], and dark-dark solitons [6,10] are some of the solitons which have been investigated in these systems. These vector solitons have also received considerable attention in other areas of science including Bose-Einstein condensates (BECs) [11,12], biophysics [13], plasma physics [14], and so on. Apart from the above, partially coherent solitons or soliton complexes have been reported in self-induced multimode waveguide system [15,16], while polarization-locked solitons and phase-locked solitons in fiber lasers [17] and dissipative vector solitons in certain dissipative systems [18–20] have also been analyzed in the literature.

From the above studies on vector solitons we have noted that the intensity profiles of multicomponent solitons reported, especially in the integrable coupled nonlinear Schrödinger systems, are defined by identical wave numbers in all the components. We call these vector solitons as degenerate class of solitons. As a consequence of degeneracy in the wave numbers, single-hump structured intensity profiles only emerge in these systems in general [21]. In the coherently coupled system even degenerate fundamental soliton can also admit double-hump profile when the four wave mixing process is taken into account [22,23]. However, in this case one cannot expect more than a double-hump profile. Very interestingly, our theoretical [3,4] and other experimental [24–26] studies confirm that the degenerate vector solitons undergo in general energy redistribution among the modes during the collision, except for the special case of polarization parameters satisfying specific restrictions, for example in the case of two component Manakov systems as $\frac{\alpha_1^{(1)}}{\alpha_2^{(1)}} = \frac{\alpha_1^{(2)}}{\alpha_2^{(2)}}$, where $\alpha_i^{(j)}$'s, $i, j = 1, 2$, are complex numbers related to the polarization vectors. By exploiting the fascinating shape-changing collision scenario of degenerate Manakov solitons, it has been theoretically suggested that the construction of optical logic gates is indeed possible, leading to all optical computing [27,28]. We also note that logic gates have been implemented using two stationary dissipative solitons of complex Ginzburg-Landau equation [29].

Recently in Refs. [30–32] it has been reported that multihump structured dispersion managed solitons or double-hump

*Corresponding author: lakshman@cnld.bdu.ac.in

intensity profile of soliton molecule may be useful for application in optical communications because they may provide alternative coding schemes for transmitting information with enhanced data-carrying capacity. Multihump solitons have also been identified in the literature in various physical situations [33–39]. They have been observed experimentally in a dispersive nonlinear medium [36]. Theoretically frozen double-hump states have been predicted in birefringent dispersive nonlinear media [33,34]. These solitons have been found in various nonlinear coupled field models also [37]. In the case of saturable nonlinear medium, stability of double- and triple-hump optical solitons has also been investigated [38]. Multihumped partially coherent solitons have also been investigated in photorefractive medium [15]. In addition to the above, the dynamics of double-hump solitons have also been studied in mode-locked fiber lasers [17–20]. A double-hump soliton has been observed during the buildup process of soliton molecules in deployed fiber systems and fiber laser cavities [30,40].

From the above studies, we observe that the various properties associated with the degenerate vector bright solitons of many integrable coupled field models have been well understood. However, to our knowledge, studies on fundamental solitons with nonidentical wave numbers in all the modes have not been considered so far and multihump structure solitons have also not been explored in the integrable coupled nonlinear Schrödinger type systems except in our recent work [41,42] and that of Qin *et al.* [43] on the following Manakov system [44,45]:

$$iq_{jz} + q_{jtt} + 2\sum_{p=1}^{2} |q_p|^2 q_j = 0, \quad j = 1, 2, \tag{1}$$

where q_j, $j = 1, 2$, describe orthogonally polarized complex waves in a birefringent medium. Here the subscripts z and t represent normalized distance and retarded time, respectively. Based on the above studies we are motivated to look for a class of fundamental solitons that possesses nonidentical wave numbers as well as multihump profiles, which are useful for optical soliton-based applications. We have successfully identified such a class of solitons in Ref. [41]. We call the fundamental solitons with nonidentical wave numbers as nondegenerate vector solitons [21,41]. Surprisingly, this class of vector bright solitons exhibit multihump structure (double-hump soliton arises in the present Manakov system and one can also observe N-hump soliton in the case of N-coupled Manakov type system) which may be useful for transmitting information in a highly packed manner. Therefore it is very important to investigate the role of additional wave number(s) on this class of fundamental soliton structures and collision scenario as well, which were briefly discussed in Ref. [41]. In the present comprehensive version we discuss the various properties associated with the nondegenerate solitons in a detailed manner by finding their exact analytical forms through Hirota bilinearization method. Then we discuss how the presence of additional distinct wave numbers and the cross phase modulation $(|q_1|^2 + |q_2|^2)q_j$, $j = 1, 2$, among the modes bring out double-hump profile in the structure of nondegenerate fundamental soliton. We find that the nondegenerate solitons undergo shape-preserving collision generally, as reported by us in Ref. [41], and shape-altering and shape-changing collisions for specific parametric values. Further, we figured out the coexistence of degenerate and nondegenerate solitons in the Manakov system. Such coexisting solitons undergo shape-changing collision scenarios leading to useful soliton-based signal amplification application. Finally, we show that the degenerate class of vector solitons reported in Refs. [3,4] can be deduced from the obtained nondegenerate one- and two-soliton solutions.

The structure of the paper is organized as follows: In Sec. II, we discuss the Hirota bilinear procedure in order to derive nondegenerate soliton solutions for Eq. (1). Using this procedure we obtained nondegenerate one- and two-soliton solutions in Gram-determinant forms and also identified the coexistence of degenerate and nondegenerate solitons in Sec. III. In Sec. IV we discuss the various collision properties of nondegenerate solitons. Section V deals with the collision between degenerate and nondegenerate solitons. In Sec. VI we recovered the degenerate one- and two-soliton solutions from the nondegenerate one- and two-soliton solutions by suitably restricting the wave numbers and in Sec. VII we point out the possible experimental observations of nondegenerate solitons. In Sec. VIII we summarize the results and discuss possible extension of this work. Finally, in Appendix A we present the three-soliton solution in Gram-determinant forms for completion while in Appendix B we discuss about certain asymptotic forms of solitons. In Appendix C, we introduce explicit forms of certain parameters appearing in the text. Finally, in Appendix D we discuss the numerical stability analysis of nondegenerate solitons under different strength of white noise as perturbation.

II. BILINEARIZATION

To derive the nondegenerate soliton solutions for the Manakov system we adopt the same Hirota bilinear procedure that has been already used to get degenerate vector bright soliton solutions but with appropriate form of initial seed solutions. We point out later how such a simple form of seed solutions will produce a physically important class of soliton solutions. In general, the exact soliton solutions of Eq. (1) can be obtained by introducing the bilinearizing transformation, which can be identified from the singularity structure analysis of Eq. (1) [46] as

$$q_j(z,t) = \frac{g^{(j)}(z,t)}{f(z,t)}, \quad j = 1, 2, \tag{2}$$

to Eq. (1). This results in the following set of bilinear forms of Eq. (1):

$$\left(iD_z + D_t^2\right) g^{(j)} f = 0, \quad j = 1, 2, \tag{3a}$$

$$D_t^2 f f = 2\sum_{n=1}^{2} g^{(n)} g^{(n)*}. \tag{3b}$$

Here $g^{(j)}$'s are complex functions, whereas f is a real function and $*$ denotes complex conjugation. The Hirota's bilinear operators D_z and D_t are defined [47] by the expressions $D_z^m D_t^n (ab) = (\frac{\partial}{\partial z} - \frac{\partial}{\partial z'})^m (\frac{\partial}{\partial t} - \frac{\partial}{\partial t'})^n a(z,t) b(z',t')_{|z=z',\, t=t'}$. Substituting the standard expansions

for the unknown functions $g^{(j)}$ and f,

$$g^{(j)} = \epsilon g_1^{(j)} + \epsilon^3 g_3^{(j)} + \ldots, \quad j = 1, 2,$$
$$f = 1 + \epsilon^2 f_2 + \epsilon^4 f_4 + \ldots, \tag{4}$$

in the bilinear Eqs. (3a) and (3b) one can get a system of linear partial differential equations (PDEs). Here ϵ is a formal series expansion parameter. The set of linear PDEs arises after collecting the coefficients of same powers of ϵ. By solving these linear PDEs recursively (at an appropriate order of ϵ), the resultant associated explicit forms of $g^{(j)}$'s and f constitute the soliton solutions to the underlying system (1). We note that the truncation of series expansions (4) for the nondegenerate soliton solutions is different from degenerate soliton solutions. This is essentially due to the general form of seed solutions assigned to the lowest order linear PDEs.

III. A NEW CLASS OF NONDEGENERATE SOLITON SOLUTIONS

To study the role of additional wave numbers on the structural, propagational, and collisional properties of nondegenerate soliton, it is very important to find the exact analytical form of it systematically. In this section by exploiting the procedure described above we intend to construct nondegenerate one- and two-soliton solutions which can be generalized to an arbitrary N-soliton case (for $N = 3$, see Appendix A). In principle this is possible because of the existence of a nondegenerate N-soliton solution ensured by the complete integrability property of the Manakov equation [Eq. (1)]. Then we point out the possibility of coexistence of degenerate and nondegenerate solitons by imposing certain restriction on the wave numbers in the obtained nondegenerate two-soliton solution. Further, we also point out the possibility of deriving this partially nondegenerate two-soliton solution through Hirota bilinear method. We note that to avoid too many mathematical details we provide the final form of solutions only since the nondegenerate soliton solution construction process is a lengthy one.

A. Nondegenerate fundamental soliton solution

In order to deduce the exact form of nondegenerate one-soliton solution we consider two different seed solutions for the two modes as

$$g_1^{(1)} = \alpha_1^{(1)} e^{\eta_1}, \quad g_1^{(2)} = \alpha_1^{(2)} e^{\xi_1}, \tag{5}$$

where $\eta_1 = k_1 t + i k_1^2 z$ and $\xi_1 = l_1 t + i l_1^2 z$, to the following linear PDEs:

$$i g_{1z}^{(j)} + g_{1tt}^{(j)} = 0, \quad j = 1, 2. \tag{6}$$

In (5) the complex parameters $\alpha_1^{(j)}$, $j = 1, 2$, are arbitrary. The above equations arise in the lowest order of ϵ. The presence of two distinct complex wave numbers k_1 and l_1 ($k_1 \neq l_1$, in general) in the seed solutions (5) makes the final solution a nondegenerate one. This construction procedure is different from the standard one that has been followed in earlier works on degenerate vector bright soliton solutions [3,4] where identical seed solutions of Eq. (1) [solutions (5) with $k_1 = l_1$ and distinct $\alpha_1^{(j)}$'s, $j = 1, 2$] have been used as starting seed solutions for Eq. (6). We note that such degenerate seed solutions only yield degenerate class of vector bright soliton solutions [3,4,41].

With the starting solutions (5) we allow the series expansions (4) to terminate by themselves while solving the system of linear PDEs. From this recursive process, we find that the expansions (4) get terminated for the nondegenerate fundamental soliton solution as $g^{(j)} = \epsilon g_1^{(j)} + \epsilon^3 g_3^{(j)}$ and $f = 1 + \epsilon^2 f_2 + \epsilon^4 f_4$. The explicit expressions of $g_1^{(j)}$, $g_3^{(j)}$, f_2, and f_4 constitute a general form of fundamental one-soliton solution to Eq. (1) as

$$q_1 = \frac{g_1^{(1)} + g_3^{(1)}}{1 + f_2 + f_4} = \left[\alpha_1^{(1)} e^{\eta_1} + e^{\eta_1 + \xi_1 + \xi_1^* + \Delta_1^{(1)}}\right] / D_1$$
$$q_2 = \frac{g_1^{(2)} + g_3^{(2)}}{1 + f_2 + f_4} = \left[\alpha_1^{(2)} e^{\xi_1} + e^{\eta_1 + \eta_1^* + \xi_1 + \Delta_1^{(2)}}\right] / D_1. \tag{7}$$

Here $D_1 = 1 + e^{\eta_1 + \eta_1^* + \delta_1} + e^{\xi_1 + \xi_1^* + \delta_2} + e^{\eta_1 + \eta_1^* + \xi_1 + \xi_1^* + \delta_{11}}$, $e^{\Delta_1^{(1)}} = \frac{(k_1 - l_1)\alpha_1^{(1)} |\alpha_1^{(2)}|^2}{(k_1 + l_1^*)(l_1 + l_1^*)^2}$, $e^{\Delta_1^{(2)}} = -\frac{(k_1 - l_1)|\alpha_1^{(1)}|^2 \alpha_1^{(2)}}{(k_1 + k_1^*)^2 (k_1^* + l_1)}$, $e^{\delta_1} = \frac{|\alpha_1^{(1)}|^2}{(k_1 + k_1^*)^2}$, $e^{\delta_2} = \frac{|\alpha_1^{(2)}|^2}{(l_1 + l_1^*)^2}$, and $e^{\delta_{11}} = \frac{|k_1 - l_1|^2 |\alpha_1^{(1)}|^2 |\alpha_1^{(2)}|^2}{(k_1 + k_1^*)^2 (k_1^* + l_1)(k_1 + l_1^*)(l_1 + l_1^*)^2}$. In the above one-soliton solution two distinct complex wave numbers, k_1 and l_1, occur in both the expressions of q_1 and q_2 simultanously. This confirms that the obtained solution is nondegenerate. We also note that the solution (7) can be rewritten in a more compact form using Gram determinants as

$$g^{(1)} = \begin{vmatrix} \frac{e^{\eta_1 + \eta_1^*}}{(k_1 + k_1^*)} & \frac{e^{\eta_1 + \xi_1^*}}{(k_1 + l_1^*)} & 1 & 0 & e^{\eta_1} \\ \frac{e^{\xi_1 + \eta_1^*}}{(l_1 + k_1^*)} & \frac{e^{\xi_1 + \xi_1^*}}{(l_1 + l_1^*)} & 0 & 1 & e^{\xi_1} \\ -1 & 0 & \frac{|\alpha_1^{(1)}|^2}{(k_1 + k_1^*)} & 0 & 0 \\ 0 & -1 & 0 & \frac{|\alpha_1^{(2)}|^2}{(l_1 + l_1^*)} & 0 \\ 0 & 0 & -\alpha_1^{(1)} & 0 & 0 \end{vmatrix},$$

$$g^{(2)} = \begin{vmatrix} \frac{e^{\eta_1 + \eta_1^*}}{(k_1 + k_1^*)} & \frac{e^{\eta_1 + \xi_1^*}}{(k_1 + l_1^*)} & 1 & 0 & e^{\eta_1} \\ \frac{e^{\xi_1 + \eta_1^*}}{(l_1 + k_1^*)} & \frac{e^{\xi_1 + \xi_1^*}}{(l_1 + l_1^*)} & 0 & 1 & e^{\xi_1} \\ -1 & 0 & \frac{|\alpha_1^{(1)}|^2}{(k_1 + k_1^*)} & 0 & 0 \\ 0 & -1 & 0 & \frac{|\alpha_1^{(2)}|^2}{(l_1 + l_1^*)} & 0 \\ 0 & 0 & 0 & -\alpha_1^{(2)} & 0 \end{vmatrix}, \tag{8a}$$

$$f = \begin{vmatrix} \frac{e^{\eta_1 + \eta_1^*}}{(k_1 + k_1^*)} & \frac{e^{\eta_1 + \xi_1^*}}{(k_1 + l_1^*)} & 1 & 0 \\ \frac{e^{\xi_1 + \eta_1^*}}{(l_1 + k_1^*)} & \frac{e^{\xi_1 + \xi_1^*}}{(l_1 + l_1^*)} & 0 & 1 \\ -1 & 0 & \frac{|\alpha_1^{(1)}|^2}{(k_1 + k_1^*)} & 0 \\ 0 & -1 & 0 & \frac{|\alpha_1^{(2)}|^2}{(l_1 + l_1^*)} \end{vmatrix}. \tag{8b}$$

The above Gram-determinant forms satisfy the bilinear Eqs. (3a) and (3b) as well as Manakov Eq. (1).

To investigate the various properties associated with the above fundamental soliton solution, we rewrite Eq. (7) as

$$q_1 = e^{i\eta_{1I}} e^{\frac{\Delta_1^{(1)} + \rho_1}{2}} \left\{ \cosh\left(\xi_{1R} + \frac{\phi_{1R}}{2}\right) \cos\left(\frac{\phi_{1I}}{2}\right) + i \sinh\left(\xi_{1R} + \frac{\phi_{1R}}{2}\right) \sin\left(\frac{\phi_{1I}}{2}\right) \right\} / D_2, \tag{9a}$$

$$q_2 = e^{i\xi_{1I}} e^{\frac{\Delta_1^{(2)}+\rho_2}{2}} \Big\{ \cosh\Big(\eta_{1R} + \frac{\phi_{2R}}{2}\Big) \cos\Big(\frac{\phi_{2I}}{2}\Big) + i \sinh\Big(\eta_{1R} + \frac{\phi_{2R}}{2}\Big) \sin\Big(\frac{\phi_{2I}}{2}\Big) \Big\} \Big/ D_2, \tag{9b}$$

where $D_2 = e^{\frac{\delta_{11}}{2}} \cosh(\eta_{1R} + \xi_{1R} + \frac{\delta_{11}}{2}) + e^{\frac{\delta_1+\delta_2}{2}} \cosh(\eta_{1R} - \xi_{1R} + \frac{\delta_1-\delta_2}{2})$, $\eta_{1R} = k_{1R}(t - 2k_{1I}z)$, $\eta_{1I} = k_{1I}t + (k_{1R}^2 - k_{1I}^2)z$, $\xi_{1R} = l_{1R}(t - 2l_{1I}z)$, $\xi_{1I} = l_{1I}t + (l_{1R}^2 - l_{1I}^2)z$, $\rho_j = \log \alpha_1^{(j)}$, $j = 1, 2$. Here ϕ_{1R}, ϕ_{1I}, ϕ_{2R}, and ϕ_{2I} are real and imaginary parts of $\phi_1 = \Delta_1^{(1)} - \rho_1$ and $\phi_2 = \Delta_1^{(2)} - \rho_2$, respectively, and k_{1R}, l_{1R}, k_{1I}, and l_{1I} are the real and imaginary parts of k_1 and l_1, respectively. From the above, we can write $\phi_{1R} = \frac{1}{2}\log \frac{|k_1-l_1|^2|\alpha_1^{(2)}|^4}{|k_1+l_1^*|^2(l_1+l_1^*)^4}$, $\phi_{1I} = \frac{1}{2}\log \frac{(k_1-l_1)(k_1^*+l_1)}{(k_1^*-l_1^*)(k_1+l_1^*)}$, $\phi_{2R} = \frac{1}{2}\log \frac{|l_1-k_1|^2|\alpha_1^{(1)}|^4}{|k_1+l_1^*|^2(k_1+k_1^*)^4}$, and $\phi_{2I} = \frac{1}{2}\log \frac{(l_1-k_1)(k_1+l_1^*)}{(l_1^*-k_1^*)(k_1^*+l_1)}$. The profile structures of solution (9a) and (9b) are described by the four complex parameters k_1, l_1, and $\alpha_1^{(j)}$, $j = 1, 2$. For the nondegenerate fundamental soliton in the first mode, the amplitude, velocity, and central position are found from Eq. (9a) as $2k_{1R}$, $2l_{1I}$, and $\frac{\phi_{1R}}{2l_{1R}}$, respectively. Similarly, for the soliton in the second mode they are found from Eq. (9b) as $2l_{1R}$, $2k_{1I}$, and $\frac{\phi_{2R}}{2k_{1I}}$, respectively. Note that $\alpha_1^{(j)}$, $j = 1, 2$, are related to the unit polarization vectors of the nondegenerate fundamental solitons in the two modes. They constitute different phases for the nondegenerate soliton in the two modes as $A_1 = (\alpha_1^{(1)}/\alpha_1^{(1)*})^{1/2}$ and $A_2 = (\alpha_1^{(2)}/\alpha_1^{(2)*})^{1/2}$.

To explain the various properties associated with solution (9a) and (9b) further we consider two physically important special cases where the imaginary parts of the wave numbers k_1 and l_1 are either identical with each other ($k_{1I} = l_{1I}$) or nonidentical with each other ($k_{1I} \neq l_{1I}$). Physically, this implies that the former case corresponds to solitons in the two modes traveling with identical velocities $v_1 = v_2 = 2k_{1I}$ but with $k_1 \neq l_1$, whereas the latter case corresponds to solitons which propagate in the two modes with nonidentical velocities $v_1 \neq v_2$. In the identical velocity case, the quantity ϕ_{jI}, $j = 1, 2$ becomes zero in (9a) and (9b) when $k_{1I} = l_{1I}$. This results in the following expression for the fundamental soliton propagating with single velocity, $v_{1,2} = 2k_{1I}$, in the two modes,

$$\begin{aligned} q_1 &= e^{i\eta_{1I}} e^{\frac{\Delta_1^{(1)}+\rho_1}{2}} \cosh\Big(\xi_{1R} + \frac{\phi_{1R}}{2}\Big) \Big/ D_2, \\ q_2 &= e^{i\xi_{1I}} e^{\frac{\Delta_1^{(2)}+\rho_2}{2}} \cosh\Big(\eta_{1R} + \frac{\phi_{2R}}{2}\Big) \Big/ D_2, \end{aligned} \tag{10}$$

where $D_2 = e^{\frac{\delta_{11}}{2}} \cosh(\eta_{1R} + \xi_{1R} + \frac{\delta_{11}}{2}) + e^{\frac{\delta_1+\delta_2}{2}} \cosh(\eta_{1R} - \xi_{1R} + \frac{\delta_1-\delta_2}{2})$ with $\eta_{1R} = k_{1R}(t - 2k_{1I}z)$, $\eta_{1I} = k_{1I}t + (k_{1R}^2 - k_{1I}^2)z$, $\xi_{1R} = l_{1R}(t - 2k_{1I}z)$, and $\xi_{1I} = k_{1I}t + (l_{1R}^2 - k_{1I}^2)z$. Note that the constants that appear in the above solution becomes equivalent to the one that appears in the solution (9a) and (9b) after imposing the condition $k_{1I} = l_{1I}$ in it. The solution (10) admits four types of symmetric profiles (satisfying appropriate conditions on parameters, see below) and also their corresponding asymmetric profiles. The symmetric profiles are as follows: (i) double-humps in both the modes (or a double-hump in q_1 mode and a M-type double-hump in q_2 mode), (ii) a flat-top in one mode and a double-hump in the other mode, (iii) a single-hump in the first mode and a double-hump in the second mode (or vice versa), and (iv) single-humps in both the modes. The corresponding four types of asymmetric wave profiles can be obtained by tuning the real parts of wave numbers k_1 and l_1 and the arbitrary complex parameters $\alpha_1^{(j)}$'s, $j = 1, 2$.

To illustrate the symmetric and asymmetric nature of the nondegenerate soliton in the identical velocity case we fix $k_{1I} = l_{1I} = 0.5$ in Figs. 1 and 2. The symmetric profiles are displayed in Fig. 1. The asymmetric profiles are depicted in Fig. 2 for the values of parameters indicated in Fig. 2. From Figs. 1 and 2 we observe that the transition which occurs from double-hump to single-hump is through a special flat-top profile. The flat-top profile has been considered as an intermediate soliton state. It is noted that flat-top soliton is also observed in a complex Ginzburg-Landau equation [48]. In Ref. [41] we have discussed symmetric and asymmetric nature of solution (10) by incorporating the condition $k_{1R} < l_{1R}$ [42]. However, to exhibit the generality of these structures, in the present paper, we discuss these properties for $k_{1R} > l_{1R}$. It should be pointed out here that in Ref. [43] the authors have derived this solution in the context of multicomponent BEC using Darboux transformation and they have classified density profiles as we have reported in Ref. [41] for $k_{1R} < l_{1R}$ in the context of nonlinear optics. They have also studied the stability of double-hump soliton using Bogoliubov-de Gennes excitation spectrum.

The symmetric nature of all the four cases can be confirmed by finding the extremum points of the nondegenerate one-soliton solution (10). For instance, to show that the double-hump soliton profile displayed in Fig. 1(a) is symmetric, we find the corresponding local maximum and minium points by applying the first derivative test ($\{|q_j|^2\}_t = 0$) and the second derivative test ($\{|q_j|^2\}_{tt} < 0$ or >0) to the expression of $|q_j|^2$, $j = 1, 2$, at $z = 0$. For the first mode, the three extremal points are identified, namely $t_1 = -0.9$, $t_2 = 5.5$, and $t_3 = 11.9$. We find another set of three extremal points for the second mode, namely $t_4 = -1.2$, $t_5 = 5.5$, and $t_6 = 12.2$ by setting $\{|q_2|^2\}_t = 0$. The points t_1 and t_3 correspond to the maxima (at which $\{|q_1|^2\}_{tt} < 0$) of the double-hump soliton, whereas t_2 corresponds to the minimum of the double-hump soliton. Similarly, the extremal points t_4 and t_6 represent the maxima and t_5 corresponds to the minimum of the double-hump soliton in the q_2 mode. In the first component the two maxima t_1 and t_3 are symmetrically located about the minimum point t_2. This can be easily confirmed by finding the difference between t_2 and t_1 and t_3 and t_2, that is, $t_2 - t_1 = 6.4 = t_3 - t_2$. This is true for the second component also, that is, $t_5 - t_4 = 6.7 = t_6 - t_5$. This implies that the two maxima t_4 and t_6 are located symmetrically from the minimum point t_5. Then the magnitude ($|q_1|^2$) of each hump (of the double-hump soliton) corresponding to the maxima t_1 is equal to 0.051 and t_3 is equal to 0.051. In the second mode, the magnitude ($|q_2|^2$) corresponding to t_4 is equal to 0.054 and t_6 is equal to 0.054. This confirms that the magnitude of each hump of double-hump soliton in both the modes are equal. Therefore it is evident that the double-hump soliton drawn in Fig. 1(a) is symmetric. One can easily verify from Figs. 1(c) and 1(d) that the single-hump soliton is symmetric about the local

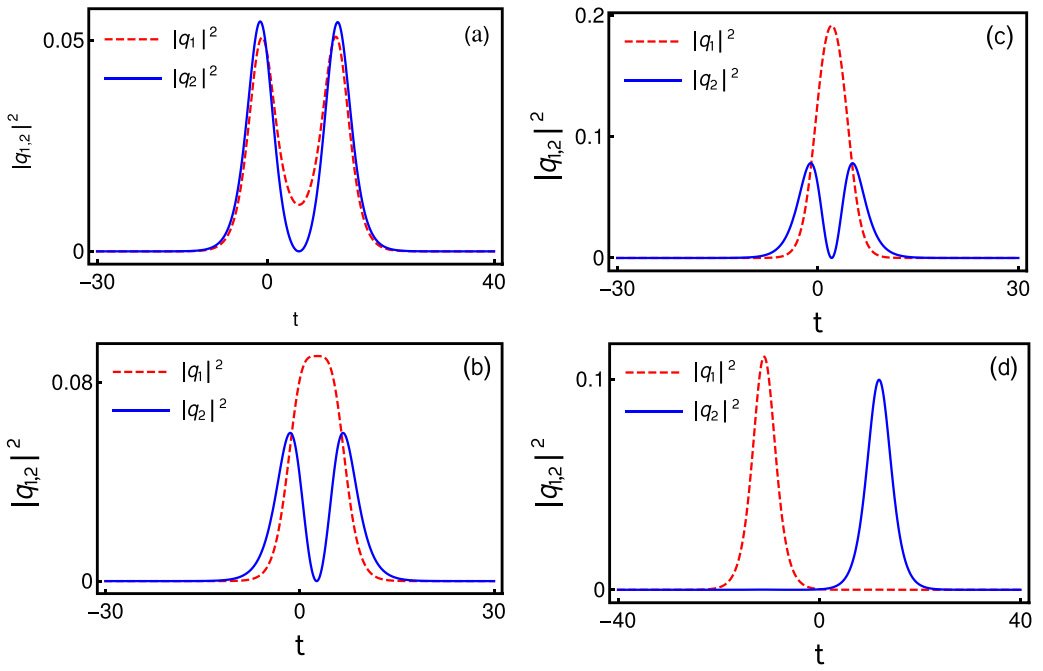

FIG. 1. Various symmetric intensity profiles of nondegenerate fundamental soliton: While (a) denotes double-hump solitons in both the modes, (b) and (c) represent flat-top-double-hump solitons and single-hump-double-hump solitons, respectively. Single-hump solitons in both the modes are illustrated in (d). The parameter values of each figures are as follows: (a) $k_1 = 0.333 + 0.5i$, $l_1 = 0.315 + 0.5i$, $\alpha_1^{(1)} = 0.45 + 0.45i$, $\alpha_1^{(2)} = 0.49 + 0.45i$. (b) $k_1 = 0.425 + 0.5i$, $l_1 = 0.3 + 0.5i$, $\alpha_1^{(1)} = 0.44 + 0.51i$, $\alpha_1^{(2)} = 0.43 + 0.5i$. (c) $k_1 = 0.55 + 0.5i$, $l_1 = 0.333 + 0.5i$, $\alpha_1^{(1)} = 0.5 + 0.5i$, $\alpha_1^{(2)} = 0.5 + 0.45i$. (d) $k_1 = 0.333 + 0.5i$, $l_1 = -0.316 + 0.5i$, $\alpha_1^{(1)} = 0.45 + 0.5i$, $\alpha_1^{(2)} = 0.5 + 0.5i$.

maximum point (and checking the half widths as well). As far as the flat-top soliton case is concerned, we have confirmed that the first derivative $\{|q_j|^2\}_t$ very slowly tends to zero near the corresponding maximum for certain number of t values. This also confirms that the presence of almost flatness and symmetric nature of the one-soliton.

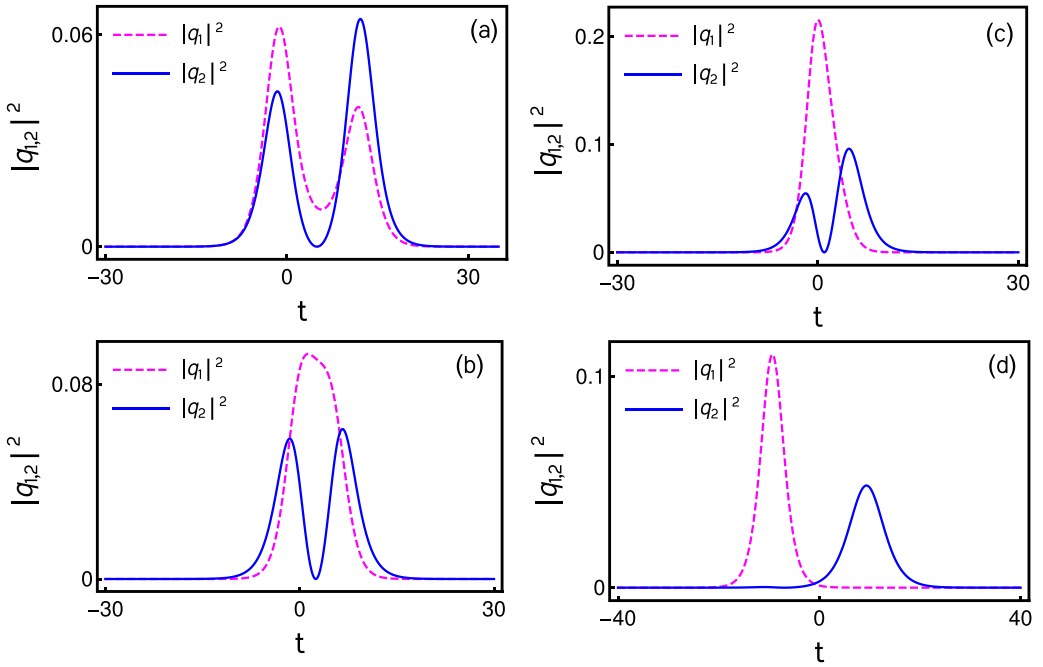

FIG. 2. Various asymmetric intensity profiles of nondegenerate fundamental soliton: Panels (a), (b), (c), and (d) represent each of figures asymmetric intensity profiles as against the symmetric profiles of Figs. 1(a)–1(d). The corresponding parameter values of each figures are as follows: (a) $k_1 = 0.333 + 0.5i$, $l_1 = 0.315 + 0.5i$, $\alpha_1^{(1)} = 0.65 + 0.45i$, $\alpha_1^{(2)} = 0.49 + 0.45i$; (b) $k_1 = 0.425 + 0.5i$, $l_1 = 0.3 + 0.5i$, $\alpha_1^{(1)} = 0.5 + 0.51i$, $\alpha_1^{(2)} = 0.43 + 0.5i$; (c) $k_1 = 0.55 + 0.5i$, $l_1 = 0.333 + 0.5i$, $\alpha_1^{(1)} = 1.2 + 0.5i$, $\alpha_1^{(2)} = 0.5 + 0.45i$; (d) $k_1 = 0.333 + 0.5i$, $l_1 = -0.22 + 0.5i$, $\alpha_1^{(1)} = 0.45 + 3i$, $\alpha_1^{(2)} = 0.5 + 0.5i$.

We also derive the conditions analytically to corroborate the symmetric and asymmetric nature of soliton solution (10) in another way. For this purpose, we intend to calculate the relative separation distance Δt_{12} between the minima of the two components (modes)

$$\Delta t_{12} = \bar{t}_1 - \bar{t}_2 = (t - t_1) - (t - t_2), \quad = \frac{\phi_{1R}}{2l_{1R}} - \frac{\phi_{2R}}{2k_{1R}}. \quad (11)$$

If the above quantity $\Delta t_{12} = 0$, then the solution (10) exhibits symmetric profiles otherwise it admits asymmetric profiles.

The explicit form of relative separation distance turns out to be

$$\Delta t_{12} = \frac{1}{2l_{1R}} \log \frac{(k_{1R} - l_{1R})|\alpha_1^{(2)}|^2}{4l_{1R}^2(k_{1R} + l_{1R})} - \frac{1}{2k_{1R}} \log \frac{(l_{1R} - k_{1R})|\alpha_1^{(1)}|^2}{4k_{1R}^2(k_{1R} + l_{1R})}. \quad (12)$$

We have explicitly calculated the relative separation distance values and confirmed the displayed profiles in Figs. 1 and 2 are symmetric and asymmetric, respectively. For instance, the Δt_{12} value corresponding to the symmetric double-hump soliton in both the modes [Fig. 1(a)] is 0.002 (to get the perfect zero value one has to fine tune the parameters suitably) and for asymmetric double-hump solitons the value is equal to 0.6493. The above calculated values reaffirm that the obtained figures are symmetric in Fig. 1(a) and asymmetric in Fig. 2(a). Similarly, one can easily confirm the symmetric and asymmetric nature of other profiles in Figs. 1 and 2 also.

In addition to the above, for the general nonidentical velocity case ($k_{1I} \neq l_{1I}$), $v_1 \neq v_2$, the distinct wave numbers k_1 and l_1 influence drastically the propagation of nondegenerate solitons in the two modes. If the relative velocity ($\Delta v_{12} = v_1 - v_2$) of the solitons between the two modes is large, then there is a node created in the structure of the fundamental solitons of both the modes [43]. This is due to the cross phase modulation between the modes. In this situation the intensity of the fast-moving soliton ($v_1 = 2l_{1I} > 0$) in the first mode starts to decrease and it gets completely suppressed after $z = 0$. At the same value of z the fast-moving soliton reappears in the second mode after a finite time. Similarly, this fact is true in the case of slow-moving soliton ($v_2 = 2k_{1I} < 0$) as well. Consequently, the intensity of solitons is unequally distributed among the two modes. This is clearly demonstrated in Fig. 3 and Figs. 4(a)–4(b). On the other hand, if the relative velocity tends to zero ($\Delta v_{12} \to 0$), then the total intensity, $I_{\text{total}} = |q_1|^2 + |q_2|^2$, of nondegenerate solitons starts to get distributed equally among the two components. As a consequence of this, a double-hump profile starts to emerge in each of the modes as displayed in Figs. 4(c)–4(d). At perfect zero relative velocity ($\Delta v_{12} = 0$), the double-hump fundamental soliton emerges completely in both the modes. As we have already pointed out in Ref. [41] the nondegenerate soliton solution exhibits symmetric and asymmetric profiles in the nonidentical velocity case also but the relative velocity of the solitons should be minimum. We have not displayed their plots here for brevity.

Recently, we found that the occurrence of multihumps depends on the number of distinct wave numbers and

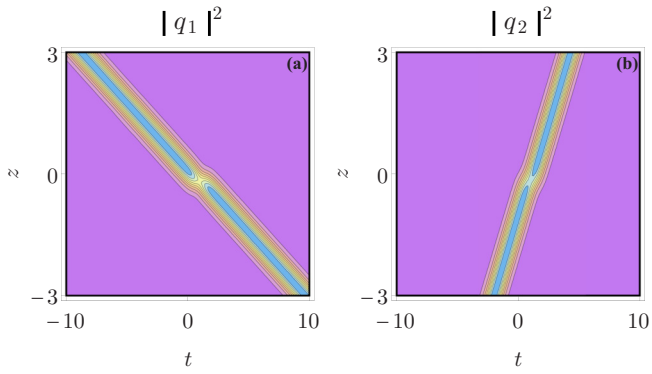

FIG. 3. Node formation in the nonidentical velocity case. The parameter values are $k_1 = 1 + 1.5i$, $l_1 = 1.5 + 0.5i$, $\alpha_1^{(1)} = 1.5 + 0.5i$, $\alpha_1^{(2)} = 0.45 + 0.5i$.

modes [49] apart from the nonlinearities. In the present two-component case, the resultant nondegenerate fundamental soliton solution (9a) and (9b) yields only a double-hump soliton. However, a triple-hump soliton and a quadruple-hump soliton are also observed in the cases of three- and four-component Manakov system cases, respectively. For the N-component case one may expect a more complicated profile, as mentioned in the case of theory of incoherent solitons [50,51], involving N-number of humps which are characterized by $2N$-complex parameters. These results will be published elsewhere. Very recently we have also reported the existence of nondegenerate fundamental solitons and their various profile structures in other integrable coupled NLS type systems [21] as well. It should be pointed out that the multihump nature of nondegenerate fundamental soliton is somewhat analogous to partially coherent solitons or soliton complexes [15,16] where such partially coherent solitons can be obtained when the number of modes is equal to the number of degenerate vector soliton solution [3,52]. We also note here that the two-partially coherent

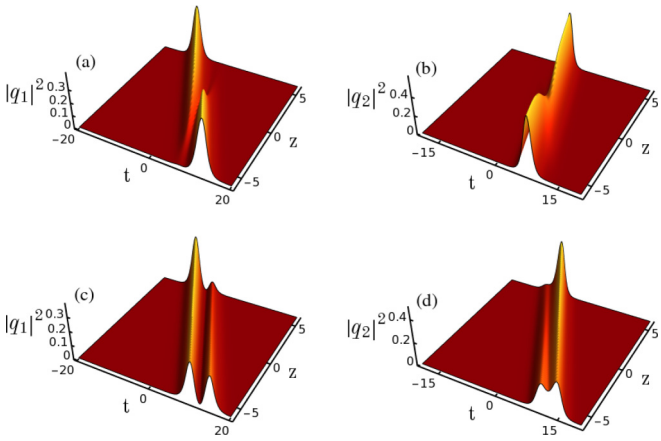

FIG. 4. Double-hump formation in the profile structure of nondegenerate fundamental soliton: Panels (a) and (b) represent the node formation in soliton profiles. Panels (c) and (d) denote the emergence of double-hump in both the modes. The corresponding parameter values for (a) and (b) are $k_1 = 0.65 - 0.85i$, $l_1 = 0.78 - 0.5i$, $\alpha_1^{(1)} = 1$, and $\alpha_1^{(2)} = 0.5$. For panels (c) and (d) the values are chosen as $k_1 = 0.65 - 0.8i$, $l_1 = 0.78 - 0.8i$, $\alpha_1^{(1)} = 1$, and $\alpha_1^{(2)} = 0.5$.

soliton can be deduced from the double-humped nondegenerate fundamental soliton (9a) and (9b) in the Manakov system by imposing the restrictions $\alpha_1^{(1)} = e^{\eta_{10}}$, $\alpha_1^{(2)} = -e^{\eta_{20}}$, $k_1 = k_{1R}$, $l_1 = k_{2R}$, $k_{1I} = l_{1I} = 0$, where η_{10} and η_{20} are real constants, in solution (7) [52]. The soliton complex reported in Ref. [53] is a special case of nondegenerate fundamental soliton solution (7) when the parameters k_1 and l_1 are chosen as real constants and $\alpha_1^{(1)} = \alpha_1^{(2)} = 1$.

B. Nondegenerate two-soliton solution

In order to investigate the collision dynamics of nondegenerate soliton of the form (7), it is essential to derive the expression for the corresponding two-soliton solution. To construct it, we consider the seed solutions as $g_1^{(1)} = \alpha_1^{(1)} e^{\eta_1} + \alpha_2^{(1)} e^{\eta_2}$ and $g_1^{(2)} = \alpha_1^{(2)} e^{\xi_1} + \alpha_2^{(2)} e^{\xi_2}$, $\eta_j = k_j t + i k_j^2 z$ and $\xi_j = l_j t + i l_j^2 z$, $j = 1, 2$, for Eqs. (6). By proceeding with the procedure given in the previous subsection along with these seed solutions we find that the series expansions for $g^{(j)}$, $j = 1, 2$, and f get terminated as $g^{(j)} = \epsilon g_1^{(j)} + \epsilon^3 g_3^{(j)} + \epsilon^5 g_5^{(j)} + \epsilon^7 g_7^{(j)}$ and $f = 1 + \epsilon^2 f_2 + \epsilon^4 f_4 + \epsilon^6 f_6 + \epsilon^8 f_8$. The other unknown functions, $g_9^{(j)}$, $g_{11}^{(j)}$, f_{10}, f_{12}, and so on, are found to be identically zero. We further note here that the termination of these perturbation series occurs at the order of ϵ^3 in $g^{(j)}$'s and at the level of ϵ^4 in f for deriving the degenerate two-soliton solution. The resulting explicit forms of the unknown functions in the truncated series expansions constitute the following nondegenerate two-soliton solution, in Gram-determinant form, to Eq. (1):

$$g^{(1)} = \begin{vmatrix} \frac{e^{\eta_1+\eta_1^*}}{(k_1+k_1^*)} & \frac{e^{\eta_1+\eta_2^*}}{(k_1+k_2^*)} & \frac{e^{\eta_1+\xi_1^*}}{(k_1+l_1^*)} & \frac{e^{\eta_1+\xi_2^*}}{(k_1+l_2^*)} & 1 & 0 & 0 & 0 & e^{\eta_1} \\ \frac{e^{\eta_2+\eta_1^*}}{(k_2+k_1^*)} & \frac{e^{\eta_2+\eta_2^*}}{(k_2+k_2^*)} & \frac{e^{\eta_2+\xi_1^*}}{(k_2+l_1^*)} & \frac{e^{\eta_2+\xi_2^*}}{(k_2+l_2^*)} & 0 & 1 & 0 & 0 & e^{\eta_2} \\ \frac{e^{\xi_1+\eta_1^*}}{(l_1+k_1^*)} & \frac{e^{\xi_1+\eta_2^*}}{(l_1+k_2^*)} & \frac{e^{\xi_1+\xi_1^*}}{(l_1+l_1^*)} & \frac{e^{\xi_1+\xi_2^*}}{(l_1+l_2^*)} & 0 & 0 & 1 & 0 & e^{\xi_1} \\ \frac{e^{\xi_2+\eta_1^*}}{(l_2+k_1^*)} & \frac{e^{\xi_2+\eta_2^*}}{(l_2+k_2^*)} & \frac{e^{\xi_2+\xi_1^*}}{(l_2+l_1^*)} & \frac{e^{\xi_2+\xi_2^*}}{(l_2+l_2^*)} & 0 & 0 & 0 & 1 & e^{\xi_2} \\ -1 & 0 & 0 & 0 & \frac{|\alpha_1^{(1)}|^2}{(k_1^*+k_1)} & \frac{\alpha_1^{(1)*}\alpha_2^{(1)}}{(k_1^*+k_2)} & 0 & 0 & 0 \\ 0 & -1 & 0 & 0 & \frac{\alpha_1^{(1)}\alpha_2^{(1)*}}{(k_2^*+k_1)} & \frac{|\alpha_2^{(1)}|^2}{(k_2+k_2^*)} & 0 & 0 & 0 \\ 0 & 0 & -1 & 0 & 0 & 0 & \frac{|\alpha_1^{(2)}|^2}{(l_1^*+l_1)} & \frac{\alpha_1^{(2)*}\alpha_2^{(2)}}{(l_1^*+l_2)} & 0 \\ 0 & 0 & 0 & -1 & 0 & 0 & \frac{\alpha_1^{(2)}\alpha_2^{(2)*}}{(l_2^*+l_1)} & \frac{|\alpha_2^{(2)}|^2}{(l_2^*+l_2)} & 0 \\ 0 & 0 & 0 & 0 & -\alpha_1^{(1)} & -\alpha_2^{(1)} & 0 & 0 & 0 \end{vmatrix}, \tag{13a}$$

$$g^{(2)} = \begin{vmatrix} \frac{e^{\eta_1+\eta_1^*}}{(k_1+k_1^*)} & \frac{e^{\eta_1+\eta_2^*}}{(k_1+k_2^*)} & \frac{e^{\eta_1+\xi_1^*}}{(k_1+l_1^*)} & \frac{e^{\eta_1+\xi_2^*}}{(k_1+l_2^*)} & 1 & 0 & 0 & 0 & e^{\eta_1} \\ \frac{e^{\eta_2+\eta_1^*}}{(k_2+k_1^*)} & \frac{e^{\eta_2+\eta_2^*}}{(k_2+k_2^*)} & \frac{e^{\eta_2+\xi_1^*}}{(k_2+l_1^*)} & \frac{e^{\eta_2+\xi_2^*}}{(k_2+l_2^*)} & 0 & 1 & 0 & 0 & e^{\eta_2} \\ \frac{e^{\xi_1+\eta_1^*}}{(l_1+k_1^*)} & \frac{e^{\xi_1+\eta_2^*}}{(l_1+k_2^*)} & \frac{e^{\xi_1+\xi_1^*}}{(l_1+l_1^*)} & \frac{e^{\xi_1+\xi_2^*}}{(l_1+l_2^*)} & 0 & 0 & 1 & 0 & e^{\xi_1} \\ \frac{e^{\xi_2+\eta_1^*}}{(l_2+k_1^*)} & \frac{e^{\xi_2+\eta_2^*}}{(l_2+k_2^*)} & \frac{e^{\xi_2+\xi_1^*}}{(l_2+l_1^*)} & \frac{e^{\xi_2+\xi_2^*}}{(l_2+l_2^*)} & 0 & 0 & 0 & 1 & e^{\xi_2} \\ -1 & 0 & 0 & 0 & \frac{|\alpha_1^{(1)}|^2}{(k_1^*+k_1)} & \frac{\alpha_1^{(1)*}\alpha_2^{(1)}}{(k_1^*+k_2)} & 0 & 0 & 0 \\ 0 & -1 & 0 & 0 & \frac{\alpha_1^{(1)}\alpha_2^{(1)*}}{(k_2^*+k_1)} & \frac{|\alpha_2^{(1)}|^2}{(k_2+k_2^*)} & 0 & 0 & 0 \\ 0 & 0 & -1 & 0 & 0 & 0 & \frac{|\alpha_1^{(2)}|^2}{(l_1^*+l_1)} & \frac{\alpha_1^{(2)*}\alpha_2^{(2)}}{(l_1^*+l_2)} & 0 \\ 0 & 0 & 0 & -1 & 0 & 0 & \frac{\alpha_1^{(2)}\alpha_2^{(2)*}}{(l_2^*+l_1)} & \frac{|\alpha_2^{(2)}|^2}{(l_2^*+l_2)} & 0 \\ 0 & 0 & 0 & 0 & 0 & 0 & -\alpha_1^{(2)} & -\alpha_2^{(2)} & 0 \end{vmatrix}, \tag{13b}$$

$$f = \begin{vmatrix} \frac{e^{\eta_1+\eta_1^*}}{(k_1+k_1^*)} & \frac{e^{\eta_1+\eta_2^*}}{(k_1+k_2^*)} & \frac{e^{\eta_1+\xi_1^*}}{(k_1+l_1^*)} & \frac{e^{\eta_1+\xi_2^*}}{(k_1+l_2^*)} & 1 & 0 & 0 & 0 \\ \frac{e^{\eta_2+\eta_1^*}}{(k_2+k_1^*)} & \frac{e^{\eta_2+\eta_2^*}}{(k_2+k_2^*)} & \frac{e^{\eta_2+\xi_1^*}}{(k_2+l_1^*)} & \frac{e^{\eta_2+\xi_2^*}}{(k_2+l_2^*)} & 0 & 1 & 0 & 0 \\ \frac{e^{\xi_1+\eta_1^*}}{(l_1+k_1^*)} & \frac{e^{\xi_1+\eta_2^*}}{(l_1+k_2^*)} & \frac{e^{\xi_1+\xi_1^*}}{(l_1+l_1^*)} & \frac{e^{\xi_1+\xi_2^*}}{(l_1+l_2^*)} & 0 & 0 & 1 & 0 \\ \frac{e^{\xi_2+\eta_1^*}}{(l_2+k_1^*)} & \frac{e^{\xi_2+\eta_2^*}}{(l_2+k_2^*)} & \frac{e^{\xi_2+\xi_1^*}}{(l_2+l_1^*)} & \frac{e^{\xi_2+\xi_2^*}}{(l_2+l_2^*)} & 0 & 0 & 0 & 1 \\ -1 & 0 & 0 & 0 & \frac{|\alpha_1^{(1)}|^2}{(k_1^*+k_1)} & \frac{\alpha_1^{(1)*}\alpha_2^{(1)}}{(k_1^*+k_2)} & 0 & 0 \\ 0 & -1 & 0 & 0 & \frac{\alpha_1^{(1)}\alpha_2^{(1)*}}{(k_2^*+k_1)} & \frac{|\alpha_2^{(1)}|^2}{(k_2+k_2^*)} & 0 & 0 \\ 0 & 0 & -1 & 0 & 0 & 0 & \frac{|\alpha_1^{(2)}|^2}{(l_1^*+l_1)} & \frac{\alpha_1^{(2)*}\alpha_2^{(2)}}{(l_1^*+l_2)} \\ 0 & 0 & 0 & -1 & 0 & 0 & \frac{\alpha_1^{(2)}\alpha_2^{(2)*}}{(l_2^*+l_1)} & \frac{|\alpha_2^{(2)}|^2}{(l_2^*+l_2)} \end{vmatrix}. \tag{13c}$$

In the above, the eight arbitrary complex parameters k_j, l_j, $\alpha_1^{(j)}$, and $\alpha_2^{(j)}$, $j = 1, 2$, define the profile shapes of the nondegenerate solitons and their various interesting collision scenarios. By generalizing the above given procedure, the nondegenerate N-soliton solution of the Manakov system can be obtained. To derive the N-nondegenerate soliton solution, the power series expansion should be as in the following form: $g^{(j)} = \sum_{n=1}^{2N-1} \epsilon^{2n-1} g_{2n-1}^{(j)}$ and $f = 1 + \sum_{n=1}^{2N} \epsilon^{2n} f_{2n}$. The $4N$ complex parameters, which are present in the N-soliton solution, determine the shape of the N-solitons. In Appendix A, we have given the three-soliton solution form explicitly using the Gram determinants.

C. Partially nondegenerate two-soliton solution

To show the possibility of occurrence of degenerate and nondegenerate solitons simultanously in the Manakov system (1), we restrict the wave numbers k_1 and l_1 (or k_2 and l_2) as $k_1 = l_1$ (or $k_2 = l_2$) but $k_2 \neq l_2$ (or $k_1 \neq l_1$) in the obtained completely nondegenerate two-soliton solution (13a)–(13c). As a consequence of this restriction, the wave variables η_1 and ξ_1 automatically get restricted as $\xi_1 = \eta_1$. By imposing such a restriction in the fully nondegenerate two-soliton solution (13a)–(13c) we deduce the following form of partially nondegenerate two-soliton solution as

$$g^{(1)} = \begin{vmatrix} \frac{e^{\eta_1+\eta_1^*}}{(k_1+k_1^*)} & \frac{e^{\eta_1+\eta_2^*}}{(k_1+k_2^*)} & \frac{e^{\eta_1+\eta_1^*}}{(k_1+k_1^*)} & \frac{e^{\eta_1+\xi_2^*}}{(k_1+l_2^*)} & 1 & 0 & 0 & 0 & e^{\eta_1} \\ \frac{e^{\eta_2+\eta_1^*}}{(k_2+k_1^*)} & \frac{e^{\eta_2+\eta_2^*}}{(k_2+k_2^*)} & \frac{e^{\eta_2+\eta_1^*}}{(k_2+k_1^*)} & \frac{e^{\eta_2+\xi_2^*}}{(k_2+l_2^*)} & 0 & 1 & 0 & 0 & e^{\eta_2} \\ \frac{e^{\eta_1+\eta_1^*}}{(k_1+k_1^*)} & \frac{e^{\eta_1+\eta_2^*}}{(k_1+k_2^*)} & \frac{e^{\eta_1+\eta_1^*}}{(k_1+k_1^*)} & \frac{e^{\eta_1+\xi_2^*}}{(k_1+l_2^*)} & 0 & 0 & 1 & 0 & e^{\eta_1} \\ \frac{e^{\xi_2+\eta_1^*}}{(l_2+k_1^*)} & \frac{e^{\xi_2+\eta_2^*}}{(l_2+k_2^*)} & \frac{e^{\xi_2+\eta_1^*}}{(l_2+k_1^*)} & \frac{e^{\xi_2+\xi_2^*}}{(l_2+l_2^*)} & 0 & 0 & 0 & 1 & e^{\xi_2} \\ -1 & 0 & 0 & 0 & \frac{|\alpha_1^{(1)}|^2}{(k_1^*+k_1)} & \frac{\alpha_1^{(1)*}\alpha_2^{(1)}}{(k_1^*+k_2)} & 0 & 0 & 0 \\ 0 & -1 & 0 & 0 & \frac{\alpha_1^{(1)}\alpha_2^{(1)*}}{(k_2^*+k_1)} & \frac{|\alpha_2^{(1)}|^2}{(k_2+k_2^*)} & 0 & 0 & 0 \\ 0 & 0 & -1 & 0 & 0 & 0 & \frac{|\alpha_1^{(2)}|^2}{(k_1^*+k_1)} & \frac{\alpha_1^{(2)*}\alpha_2^{(2)}}{(k_1^*+l_2)} & 0 \\ 0 & 0 & 0 & -1 & 0 & 0 & \frac{\alpha_1^{(2)}\alpha_2^{(2)*}}{(l_2^*+k_1)} & \frac{|\alpha_2^{(2)}|^2}{(l_2^*+l_2)} & 0 \\ 0 & 0 & 0 & 0 & -\alpha_1^{(1)} & -\alpha_2^{(1)} & 0 & 0 & 0 \end{vmatrix}, \tag{14a}$$

$$g^{(2)} = \begin{vmatrix} \frac{e^{\eta_1+\eta_1^*}}{(k_1+k_1^*)} & \frac{e^{\eta_1+\eta_2^*}}{(k_1+k_2^*)} & \frac{e^{\eta_1+\eta_1^*}}{(k_1+k_1^*)} & \frac{e^{\eta_1+\xi_2^*}}{(k_1+l_2^*)} & 1 & 0 & 0 & 0 & e^{\eta_1} \\ \frac{e^{\eta_2+\eta_1^*}}{(k_2+k_1^*)} & \frac{e^{\eta_2+\eta_2^*}}{(k_2+k_2^*)} & \frac{e^{\eta_2+\eta_1^*}}{(k_2+k_1^*)} & \frac{e^{\eta_2+\xi_2^*}}{(k_2+l_2^*)} & 0 & 1 & 0 & 0 & e^{\eta_2} \\ \frac{e^{\eta_1+\eta_1^*}}{(k_1+k_1^*)} & \frac{e^{\eta_1+\eta_2^*}}{(k_1+k_2^*)} & \frac{e^{\eta_1+\eta_1^*}}{(k_1+k_1^*)} & \frac{e^{\eta_1+\xi_2^*}}{(k_1+l_2^*)} & 0 & 0 & 1 & 0 & e^{\eta_1} \\ \frac{e^{\xi_2+\eta_1^*}}{(l_2+k_1^*)} & \frac{e^{\xi_2+\eta_2^*}}{(l_2+k_2^*)} & \frac{e^{\xi_2+\eta_1^*}}{(l_2+k_1^*)} & \frac{e^{\xi_2+\xi_2^*}}{(l_2+l_2^*)} & 0 & 0 & 0 & 1 & e^{\xi_2} \\ -1 & 0 & 0 & 0 & \frac{|\alpha_1^{(1)}|^2}{(k_1^*+k_1)} & \frac{\alpha_1^{(1)*}\alpha_2^{(1)}}{(k_1^*+k_2)} & 0 & 0 & 0 \\ 0 & -1 & 0 & 0 & \frac{\alpha_1^{(1)}\alpha_2^{(1)*}}{(k_2^*+k_1)} & \frac{|\alpha_2^{(1)}|^2}{(k_2+k_2^*)} & 0 & 0 & 0 \\ 0 & 0 & -1 & 0 & 0 & 0 & \frac{|\alpha_1^{(2)}|^2}{(k_1^*+k_1)} & \frac{\alpha_1^{(2)*}\alpha_2^{(2)}}{(k_1^*+l_2)} & 0 \\ 0 & 0 & 0 & -1 & 0 & 0 & \frac{\alpha_1^{(2)}\alpha_2^{(2)*}}{(l_2^*+k_1)} & \frac{|\alpha_2^{(2)}|^2}{(l_2^*+l_2)} & 0 \\ 0 & 0 & 0 & 0 & 0 & 0 & -\alpha_1^{(2)} & -\alpha_2^{(2)} & 0 \end{vmatrix}, \tag{14b}$$

$$f = \begin{vmatrix} \frac{e^{\eta_1+\eta_1^*}}{(k_1+k_1^*)} & \frac{e^{\eta_1+\eta_2^*}}{(k_1+k_2^*)} & \frac{e^{\eta_1+\eta_1^*}}{(k_1+k_1^*)} & \frac{e^{\eta_1+\xi_2^*}}{(k_1+l_2^*)} & 1 & 0 & 0 & 0 \\ \frac{e^{\eta_2+\eta_1^*}}{(k_2+k_1^*)} & \frac{e^{\eta_2+\eta_2^*}}{(k_2+k_2^*)} & \frac{e^{\eta_2+\eta_1^*}}{(k_2+k_1^*)} & \frac{e^{\eta_2+\xi_2^*}}{(k_2+l_2^*)} & 0 & 1 & 0 & 0 \\ \frac{e^{\eta_1+\eta_1^*}}{(k_1+k_1^*)} & \frac{e^{\eta_1+\eta_2^*}}{(k_1+k_2^*)} & \frac{e^{\eta_1+\eta_1^*}}{(k_1+k_1^*)} & \frac{e^{\eta_1+\xi_2^*}}{(k_1+l_2^*)} & 0 & 0 & 1 & 0 \\ \frac{e^{\xi_2+\eta_1^*}}{(l_2+k_1^*)} & \frac{e^{\xi_2+\eta_2^*}}{(l_2+k_2^*)} & \frac{e^{\xi_2+\eta_1^*}}{(l_2+k_1^*)} & \frac{e^{\xi_2+\xi_2^*}}{(l_2+l_2^*)} & 0 & 0 & 0 & 1 \\ -1 & 0 & 0 & 0 & \frac{|\alpha_1^{(1)}|^2}{(k_1^*+k_1)} & \frac{\alpha_1^{(1)*}\alpha_2^{(1)}}{(k_1^*+k_2)} & 0 & 0 \\ 0 & -1 & 0 & 0 & \frac{\alpha_1^{(1)}\alpha_2^{(1)*}}{(k_2^*+k_1)} & \frac{|\alpha_2^{(1)}|^2}{(k_2+k_2^*)} & 0 & 0 \\ 0 & 0 & -1 & 0 & 0 & 0 & \frac{|\alpha_1^{(2)}|^2}{(k_1^*+k_1)} & \frac{\alpha_1^{(2)*}\alpha_2^{(2)}}{(k_1^*+l_2)} \\ 0 & 0 & 0 & -1 & 0 & 0 & \frac{\alpha_1^{(2)}\alpha_2^{(2)*}}{(l_2^*+k_1)} & \frac{|\alpha_2^{(2)}|^2}{(l_2^*+l_2)} \end{vmatrix}. \tag{14c}$$

The above class of solution (14a)–(14c) can be derived through Hirota bilinear method with the following seed solutions, $g_1^{(1)} = \alpha_1^{(1)} e^{\eta_1} + \alpha_2^{(1)} e^{\eta_2}$ and $g_1^{(2)} = \alpha_1^{(2)} e^{\eta_1} + \alpha_2^{(2)} e^{\xi_2}$, $\eta_j = k_j t + i k_j^2 z$ and $\xi_2 = l_2 t + i l_2^2 z$, $j = 1, 2$, for Eqs. (6). Such coexistence

of degenerate and nondegenerate solitons and their dynamics are characterized by seven complex parameters k_j, l_2, $\alpha_1^{(j)}$, and $\alpha_2^{(j)}$, $j = 1, 2$. The interesting collision behavior of the coexisting degenerate and nondegenerate solitons is discussed in Sec. V.

IV. VARIOUS SHAPE-PRESERVING AND SHAPE-CHANGING COLLISIONS OF NONDEGENERATE SOLITONS

The several interesting collision properties associated with the nondegenerate solitons can be explored by analyzing the asymptotic forms of the two-soliton solution (13a)–(13c) of Eq. (1). By doing so, we observe that the nondegenerate solitons undergo three types of collision scenarios. For either of the two cases (i) equal velocities ($k_{1I} = l_{1I}$, $k_{2I} = l_{2I}$) and (ii) unequal velocities ($k_{1I} \neq l_{1I}$, $k_{2I} \neq l_{2I}$), the nondegenerate two solitons undergo shape-preserving, shape-altering, and shape-changing collision behaviors. Here we present the asymptotic analysis for the case of shape-preserving collision only and it can be carried out for other cases also in a similar manner.

A. Asymptotic analysis

In order to study the interaction dynamics of nondegenerate solitons completely, we perform a careful asymptotic analysis for the nondegenerate two-soliton solution (13a)–(13c) and we deduce the explicit forms of individual solitons at the limits $z \to \pm\infty$. To explore this, we consider $k_{jR}, l_{jR} > 0$, $j = 1, 2$, $k_{1I} > k_{2I}$, $l_{1I} > l_{2I}$, $k_{1I} = l_{1I}$, and $k_{2I} = l_{2I}$, which corresponds to the case of a head-on collision between the two symmetric nondegenerate solitons. In this situation the two symmetric fundamental solitons S_1 and S_2 are well separated and subsequently the asymptotic forms of the individual solitons can be deduced from the solution (13a)–(13c) by incorporating the asymptotic nature of the wave variables $\eta_{jR} = k_{jR}(t - 2k_{jI}z)$ and $\xi_{jR} = l_{jR}(t - 2l_{jI}z)$, $j = 1, 2$, in it. The wave variables η_{jR} and ξ_{jR} behave asymptotically as (i) soliton 1 (S_1): $\eta_{1R}, \xi_{1R} \simeq 0$, $\eta_{2R}, \xi_{2R} \to \mp\infty$ as $z \mp \infty$ and (ii) soliton 2 (S_2): $\eta_{2R}, \xi_{2R} \simeq 0$, $\eta_{1R}, \xi_{1R} \to \mp\infty$ as $z \pm \infty$. Correspondingly, these results lead to the following asymptotic forms of nondegenerate individual solitons.

(a) Before collision: $z \to -\infty$

Soliton 1: In this limit, the asymptotic forms of q_1 and q_2 are deduced from the two-soliton solution (13a)–(13c) for soliton 1 as follows:

$$q_1 \simeq \frac{2A_1^{1-}k_{1R}e^{i\eta_{1I}}\cosh(\xi_{1R}+\phi_1^-)}{\left[\frac{(k_1^*-l_1^*)^{\frac{1}{2}}}{(k_1^*+l_1)^{\frac{1}{2}}}\cosh(\eta_{1R}+\xi_{1R}+\phi_3^-)+\frac{(k_1+l_1^*)^{\frac{1}{2}}}{(k_1-l_1)^{\frac{1}{2}}}\cosh(\eta_{1R}-\xi_{1R}+\phi_4^-)\right]}, \tag{15a}$$

$$q_2 \simeq \frac{2A_2^{1-}l_{1R}e^{i\xi_{1I}}\cosh(\eta_{1R}+\phi_2^-)}{\left[\frac{(k_1^*-l_1^*)^{\frac{1}{2}}}{(k_1+l_1^*)^{\frac{1}{2}}}\cosh(\eta_{1R}+\xi_{1R}+\phi_3^-)+\frac{(k_1^*+l_1)^{1/2}}{(k_1-l_1)^{1/2}}\cosh(\eta_{1R}-\xi_{1R}+\phi_4^-)\right]}. \tag{15b}$$

Here $\phi_1^- = \frac{1}{2}\log\frac{(k_1-l_1)|\alpha_1^{(2)}|^2}{(k_1+l_1^*)(l_1+l_1^*)^2}$, $\phi_2^- = \frac{1}{2}\log\frac{(l_1-k_1)|\alpha_1^{(1)}|^2}{(k_1^*+l_1)(k_1+k_1^*)^2}$, $\phi_3^- = \frac{1}{2}\log\frac{|k_1-l_1|^2|\alpha_1^{(1)}|^2|\alpha_1^{(2)}|^2}{|k_1+l_1^*|^2(k_1+k_1^*)^2(l_1+l_1^*)^2}$, $\phi_4^- = \frac{1}{2}\log\frac{|\alpha_1^{(1)}|^2(l_1+l_1^*)^2}{|\alpha_1^{(2)}|^2(k_1+k_1^*)^2}$, $A_1^{1-} = [\alpha_1^{(1)}/\alpha_1^{(1)^*}]^{1/2}$ and $A_2^{1-} = i[\alpha_1^{(2)}/\alpha_1^{(2)^*}]^{1/2}$. In the latter, superscript $(1-)$ represents soliton S_1 before collision and subscripts 1 and 2 denote the two modes q_1 and q_2, respectively.

Soliton 2: The asymptotic expressions for soliton 2 in the two modes before collision turn out to be

$$q_1 \simeq \frac{2k_{2R}A_1^{2-}e^{i(\eta_{2I}+\theta_1^-)}\cosh(\xi_{2R}+\varphi_1^-)}{\left[\frac{(k_2^*-l_2^*)^{\frac{1}{2}}}{(k_2^*+l_2)^{\frac{1}{2}}}\cosh(\eta_{2R}+\xi_{2R}+\varphi_3^-)+\frac{(k_2+l_2^*)^{\frac{1}{2}}}{(k_2-l_2)^{\frac{1}{2}}}\cosh(\eta_{2R}-\xi_{2R}+\varphi_4^-)\right]}, \tag{16a}$$

$$q_2 \simeq \frac{2l_{2R}A_2^{2-}e^{i(\xi_{2I}+\theta_2^-)}\cosh(\eta_{2R}+\varphi_2^-)}{\left[\frac{(k_2^*-l_2^*)^{\frac{1}{2}}}{(k_2+l_2^*)^{\frac{1}{2}}}\cosh(\eta_{2R}+\xi_{2R}+\varphi_3^-)+\frac{(k_2^*+l_2)^{\frac{1}{2}}}{(k_2-l_2)^{\frac{1}{2}}}\cosh(\eta_{2R}-\xi_{2R}+\varphi_4^-)\right]}. \tag{16b}$$

In the above,

$$\varphi_1^- = \frac{1}{2}\log\frac{(k_2-l_2)|\alpha_2^{(2)}|^2}{(k_2+l_2^*)(l_2+l_2^*)^2}+\frac{1}{2}\log\frac{|k_1-l_2|^2|l_1-l_2|^4}{|k_1+l_2^*|^2|l_1+l_2^*|^4},$$

$$\varphi_2^- = \frac{1}{2}\log\frac{(l_2-k_2)|\alpha_2^{(1)}|^2}{(k_2^*+l_2)(k_2+k_2^*)^2}+\frac{1}{2}\log\frac{|k_2-l_1|^2|k_1-k_2|^4}{|k_2+l_1^*|^2|k_1+k_2^*|^4},$$

$$\varphi_3^- = \frac{1}{2}\log\frac{|k_2-l_2|^2|\alpha_2^{(1)}|^2|\alpha_2^{(2)}|^2}{|k_2+l_2^*|^2(k_2+k_2^*)^2(l_2+l_2^*)^2}+\frac{1}{2}\log\frac{|k_1-k_2|^4|l_1-l_2|^4|k_2-l_1|^2|k_1-l_2|^2}{|k_1+k_2^*|^4|k_2+l_1^*|^2|k_1+l_2^*|^2|l_1+l_2^*|^4},$$

$$\varphi_4^- = \frac{1}{2}\log\frac{|\alpha_2^{(1)}|^2(l_2+l_2^*)^2}{|\alpha_2^{(2)}|^2(k_2+k_2^*)^2}+\frac{1}{2}\log\frac{|k_1-k_2|^4|l_1+l_2^*|^4|k_2-l_1|^2|k_1+l_2^*|^2}{|k_1+k_2^*|^4|k_2+l_1^*|^2|k_1-l_2|^2|l_1-l_2|^4},$$

$$e^{i\theta_1^-} = \frac{(k_1-k_2)(l_1-l_2)(l_1^*+l_2)(k_2-l_1)^{\frac{1}{2}}(k_1+k_2^*)(k_2^*+l_1)^{\frac{1}{2}}}{(k_1^*-k_2^*)(l_1+l_2^*)(l_1^*-l_2^*)(k_2^*-l_1^*)^{\frac{1}{2}}(k_1^*+k_2)(k_2+l_1^*)^{\frac{1}{2}}},\ A_1^{2-} = \left[\alpha_2^{(1)}/\alpha_2^{(1)^*}\right]^{1/2},$$

$$e^{i\theta_2^-} = \frac{(l_1-l_2)(k_1-l_2)^{\frac{1}{2}}(k_1+l_2^*)^{\frac{1}{2}}(l_1+l_2^*)}{(k_1^*-l_2^*)^{\frac{1}{2}}(l_1^*-l_2^*)(k_1^*+l_2)^{\frac{1}{2}}(l_1^*+l_2)},\ A_2^{2-} = \left[\alpha_2^{(2)}/\alpha_2^{(2)^*}\right]^{1/2}.$$

Here superscript $(2-)$ refers to soliton S_2 before collision.

(b) After collision: $z \to +\infty$

Soliton 1: The asymptotic forms for soliton 1 after collision deduced as

$$q_1 \simeq \frac{2k_{1R}A_1^{1+}e^{i(\eta_{1I}+\theta_1^+)}\cosh(\xi_{1R}+\phi_1^+)}{\left[\frac{(k_1^*-l_1^*)^{\frac{1}{2}}}{(k_1^*+l_1)^{\frac{1}{2}}}\cosh\left(\eta_{1R}+\xi_{1R}+\frac{\delta_{18}-\varsigma_{22}}{2}\right)+\frac{(k_1+l_1^*)^{\frac{1}{2}}}{(k_1-l_1)^{\frac{1}{2}}}\cosh\left(\eta_{1R}-\xi_{1R}+\frac{\phi_{22}-\delta_{16}}{2}\right)\right]}, \tag{17a}$$

$$q_2 \simeq \frac{2l_{1R}A_1^{2+}e^{i(\xi_{1I}+\theta_2^+)}\cosh(\eta_{1R}+\phi_2^+)}{\left[\frac{(k_1^*-l_1^*)^{\frac{1}{2}}}{(k_1+l_1^*)^{\frac{1}{2}}}\cosh\left(\eta_{1R}+\xi_{1R}+\frac{\delta_{18}-\varsigma_{22}}{2}\right)+\frac{(k_1^*+l_1)^{\frac{1}{2}}}{(k_1-l_1)^{\frac{1}{2}}}\cosh\left(\eta_{1R}-\xi_{1R}+\frac{\phi_{22}-\delta_{16}}{2}\right)\right]}. \tag{17b}$$

Here

$$\phi_1^+ = \phi_1^- + \frac{1}{2}\log\frac{|k_2-l_1|^2|l_1-l_2|^4}{|k_2+l_1^*|^2|l_1+l_2^*|^4},\ \phi_3^+ = \phi_3^- + \frac{1}{2}\log\frac{|k_1-k_2|^4|k_2-l_1|^2|k_1-l_2|^2|l_1-l_2|^4}{|k_1+k_2^*|^4|k_2+l_1^*|^2|k_1+l_2^*|^2|l_1+l_2^*|^4},$$

$$\phi_2^+ = \phi_2^- + \frac{1}{2}\log\frac{|k_1-l_2|^2|k_1-k_2|^4}{|k_1+l_2^*|^2|k_1+k_2^*|^4},\ \phi_4^+ = \phi_4^- + \frac{1}{2}\log\frac{|k_1-k_2|^4|k_2+l_1^*|^2|k_1-l_2|^2|l_1+l_2^*|^4}{|k_1+k_2^*|^4|k_2-l_1|^2|k_1+l_2^*|^2|l_1-l_2|^4},$$

$$e^{i\theta_1^+} = \frac{(k_1-k_2)(k_1-l_2)^{\frac{1}{2}}(k_1^*+k_2)(k_1^*+l_2)^{\frac{1}{2}}}{(k_1^*-k_2^*)(k_1^*-l_2^*)^{\frac{1}{2}}(k_1+k_2^*)(k_1+l_2^*)^{\frac{1}{2}}},\ e^{i\theta_2^+} = \frac{(l_1-l_2)(k_2-l_1)^{\frac{1}{2}}(k_2+l_1^*)^{\frac{1}{2}}(l_1^*+l_2)}{(k_2^*-l_1^*)^{\frac{1}{2}}(l_1^*-l_2^*)(k_2^*+l_1)^{\frac{1}{2}}(l_1+l_2^*)},$$

$A_1^{1+} = [\alpha_1^{(1)}/\alpha_1^{(1)^*}]^{1/2}$ and $A_2^{1+} = [\alpha_1^{(2)}/\alpha_1^{(2)^*}]^{1/2}$, in which superscript $(1+)$ denotes soliton S_1 after collision.

Soliton 2: The expression for soliton 2 after collision deduced from the two-soliton solution is

$$q_1 \simeq \frac{2A_2^{1+}k_{2R}e^{i\eta_{2I}}\cosh(\xi_{2R}+\varphi_1^+)}{\left[\frac{(k_2^*-l_2^*)^{\frac{1}{2}}}{(k_2^*+l_2)^{\frac{1}{2}}}\cosh(\eta_{2R}+\xi_{2R}+\varphi_3^+)+\frac{(k_2+l_2^*)^{\frac{1}{2}}}{(k_2-l_2)^{\frac{1}{2}}}\cosh(\eta_{2R}-\xi_{2R}+\varphi_4^+)\right]}, \tag{18a}$$

$$q_2 \simeq \frac{2A_2^{2+}l_{2R}e^{i\xi_{2I}}\cosh(\eta_{2R}+\varphi_2^+)}{\left[\frac{i(k_2^*-l_2^*)^{\frac{1}{2}}}{(k_2+l_2^*)^{\frac{1}{2}}}\cosh(\eta_{2R}+\xi_{2R}+\varphi_3^+)+\frac{(k_2^*+l_2)^{\frac{1}{2}}}{(l_2-k_2)^{\frac{1}{2}}}\cosh(\eta_{2R}-\xi_{2R}+\varphi_4^+)\right]}, \tag{18b}$$

where $\varphi_1^+ = \frac{1}{2}\log\frac{(k_2-l_2)|\alpha_2^{(2)}|^2}{(k_2+l_2^*)(l_2+l_2^*)^2}$, $\varphi_2^+ = \frac{1}{2}\log\frac{(l_2-k_2)|\alpha_2^{(1)}|^2}{(k_2^*+l_2)(k_2+k_2^*)^2}$, $\varphi_3^+ = \frac{1}{2}\log\frac{|k_2-l_2|^2|\alpha_2^{(1)}|^2|\alpha_2^{(2)}|^2}{|k_2+l_2^*|^2(k_2+k_2^*)^2(l_2+l_2^*)^2}$, $\varphi_4^+ = \frac{1}{2}\log\frac{|\alpha_2^{(1)}|^2(l_2+l_2^*)^2}{|\alpha_2^{(2)}|^2(k_2+k_2^*)^2}$, $A_1^{2+} = [\alpha_2^{(1)}/\alpha_2^{(1)^*}]^{1/2}$, and $A_2^{2+} = i[\alpha_2^{(2)}/\alpha_2^{(2)^*}]^{1/2}$. In the latter, superscript $(2+)$ represents soliton S_2 after collision.

In the above, $\eta_{jR} = k_{jR}(t-2k_{jI}z)$, $\eta_{jI} = k_{jI}t + (k_{jR}^2-k_{jI}^2)z$, $\xi_{jR} = l_{jR}(t-2l_{jI}z)$, $\xi_{jI} = l_{jI}t + (l_{jR}^2-l_{jI}^2)z$, $j = 1, 2$, and that the phase terms φ_j^-, $j = 1, 2, 3, 4$ can also be rewritten as $\varphi_1^- = \varphi_1^+ + \frac{1}{2}\log\frac{|k_1-l_2|^2|l_1-l_2|^4}{|k_1+l_2^*|^2|l_1+l_2^*|^4}$, $\varphi_4^- = \varphi_4^+ + \frac{1}{2}\log\frac{|k_1-k_2|^4|l_1+l_2^*|^4|k_2-l_1|^2|k_1+l_2^*|^2}{|k_1+k_2^*|^4|k_2+l_1^*|^2|k_1-l_2|^2|l_1-l_2|^4}$, $\varphi_2^- = \varphi_2^+ + \frac{1}{2}\log\frac{|k_2-l_1|^2|k_1-k_2|^4}{|k_2+l_1^*|^2|k_1+k_2^*|^4}$, $\varphi_3^- = \varphi_3^+ + \frac{1}{2}\log\frac{|k_1-k_2|^4|l_1-l_2|^4|k_2-l_1|^2|k_1-l_2|^2}{|k_1+k_2^*|^4|k_2+l_1^*|^2|k_1+l_2^*|^2|l_1+l_2^*|^4}$. The above asymptotic analysis clearly shows that the shape-preserving collision always occurs among the nondegenerate solitons whenever the phase terms obey the conditions

$$\phi_j^- = \phi_j^+,\ \varphi_j^- = \varphi_j^+,\ j = 1, 2, 3, 4. \tag{19}$$

B. Shape-preserving and -altering collisions: Elastic collision

From the above analysis, we observe that the intensities of nondegenerate solitons S_1 and S_2 in the two modes are the same before and after collision whenever the phase conditions (19) are satisfied. This implies that the initial amplitudes do not get altered after collision $j = 1, 2$. It is also evident from the transition amplitude calculations, $T_j^l = \frac{A_j^{l+}}{A_j^{l-}}$, $j, l = 1, 2$, where the subscript j represents the modes and the superscript $l\pm$ denotes the nondegenerate soliton numbers 1 and 2 in the asymptotic regimes $z \to \pm\infty$. Again to confirm that the intensities of the nondegenerate solitons are preserved during the collision process, we calculate the transition intensities as well, $|T_j^l|^2$, $l, j = 1, 2$, which can be obtained by taking the absolute squares of the transition amplitudes T_j^l's. The transition intensities turn out to be unimodular, that is, $|T_j^l|^2 = 1$, $l, j = 1, 2$. Physically this implies that the nondegenerate solitons, for $k_{1I} = l_{1I}$, $k_{2I} = l_{2I}$, $k_1 \neq l_1$, corresponding to two distinct wave numbers undergo elastic collision without any intensity redistribution between the modes q_1 and q_2 except

for a finite phase shift. The latter confirms that the polarization vectors associated with the nondegenerate fundamental solitons do not contribute to the energy redistribution among the modes. Consequently the nondegenerate solitons in each mode exhibit elastic collision. The total intensity of each soliton is conserved which can be verfied from $|A_j^{l-}|^2 = |A_j^{l+}|^2$, $j, l = 1, 2$. In addition to this, the total intensity in each of the modes is also conserved $|A_j^{1-}|^2 + |A_j^{2-}|^2 = |A_j^{1+}|^2 + |A_j^{2+}|^2 = \text{const}$.

During the collision process, the initial phase of each of the soliton is also changed. The phase shift of soliton S_1 in the two modes gets modified after collision as

$$\Phi_1^1 = \phi_1^+ - \phi_1^- = \log \frac{|k_2 - l_1||l_1 - l_2|^2}{|k_2 + l_1^*||l_1 + l_2^*|^2},$$
$$\Phi_2^1 = \phi_2^+ - \phi_2^- = \log \frac{|k_1 - l_2||k_1 - k_2|^2}{|k_1 + l_2^*||k_1 + k_2^*|^2}. \tag{20}$$

Similarly, the phase shift suffered by soliton S_2 in the two modes are given by

$$\Phi_1^2 = \varphi_1^+ - \varphi_1^- = \log \frac{|k_1 + l_2^*||l_1 + l_2^*|^2}{|k_1 - l_2||l_1 - l_2|^2},$$
$$\Phi_2^2 = \varphi_2^+ - \varphi_2^- = \log \frac{|k_2 + l_1^*||k_1 + k_2^*|^2}{|k_2 - l_1||k_1 - k_2|^2}. \tag{21}$$

From the above expressions we conclude that the phases of all the solitons are mainly influenced by the wave numbers k_j and l_j, $j = 1, 2$, and not by the complex parameters $\alpha_1^{(j)}$'s and $\alpha_2^{(j)}$'s, $j = 1, 2$. This peculiar property of nondegenerate solitons is different in the case of degenerate vector bright solitons (see Sec. V below) where the complex parameters $\alpha_1^{(j)}$'s and $\alpha_2^{(j)}$'s, associated with polarization constants, play a crucial role in shifting the position of solitons after collision.

Further, to confirm that the profile shapes of the nondegenerate solitons S_1 and S_2 are invariant under the above elastic collision, we explicitly deduce the relative separation distance between the modes of the solitons. This is similar to the analysis which we have already discussed for the one-soliton solution to confirm the symmetric and asymmetric profile natures of the fundamental soliton. As a consequence of this analysis, one would expect that the relative separation distance values corresponding to solitons S_1 and S_2 before collision should be equal to the values after collision in order to ensure the shape-preserving nature of the collision. For this purpose, first we deduce the following expressions for relative separation distance for the solitons S_1 and S_2 before and after collisions from the asymptotic forms as

$$\Delta t_{12}^{1-} = \frac{1}{l_{1R}} \log \frac{|\alpha_1^{(2)}|(k_1 - l_1)^{1/2}}{2l_{1R}(k_1 + l_1^*)^{1/2}} - \frac{1}{k_{1R}} \log \frac{(l_1 - k_1)^{1/2}|\alpha_1^{(1)}|}{2k_{1R}(k_1^* + l_1)^{1/2}}, \tag{22a}$$

$$\Delta t_{12}^{2-} = \frac{1}{l_{2R}} \log \frac{|\alpha_2^{(2)}||k_1 - l_2|(k_2 - l_2)^{1/2}|l_1 - l_2|^2}{2l_{2R}|k_1 + l_2^*|(k_2 + l_2^*)^{1/2}|l_1 + l_2^*|^2} - \frac{1}{k_{2R}} \log \frac{|\alpha_2^{(1)}||k_1 - k_2|^2|k_2 - l_1|(l_2 - k_2)^{1/2}}{2k_{2R}|k_1 + k_2^*|^2|k_2 + l_1^*|(k_2^* + l_2)^{1/2}}, \tag{22b}$$

$$\Delta t_{12}^{1+} = \frac{1}{l_{1R}} \log \frac{|\alpha_1^{(2)}||k_2 - l_1|(k_1 - l_1)^{1/2}|l_1 - l_2|^2}{2l_{1R}|k_2 + l_1^*|(k_1 + l_1^*)^{1/2}|l_1 + l_2^*|^2} - \frac{1}{k_{1R}} \log \frac{|\alpha_1^{(1)}||k_1 - k_2|^2|k_1 - l_2|(l_1 - k_1)^{1/2}}{2k_{1R}|k_1 + k_2^*|^2|k_1 + l_2^*|(k_1^* + l_1)^{1/2}}, \tag{23a}$$

$$\Delta t_{12}^{2+} = \frac{1}{l_{2R}} \log \frac{|\alpha_2^{(2)}|(k_2 - l_2)^{1/2}}{2l_{2R}(k_2 + l_2^*)^{1/2}} - \frac{1}{k_{2R}} \log \frac{(l_2 - k_2)^{1/2}|\alpha_2^{(1)}|}{2k_{2R}(k_2^* + l_2)^{1/2}}. \tag{23b}$$

To identify the profile change of a given soliton S_1 (or S_2) during the collision, we analytically find the total change in relative separation distance by subtracting the quantity Δt_{12}^{n-} from Δt_{12}^{n+}, $n = 1, 2$. This results in the following expressions for soliton S_1:

$$\Delta t_1 = \Delta t_{12}^{1+} - \Delta t_{12}^{1-} = \frac{1}{l_{1R}} \log \frac{|k_2 - l_1||l_1 - l_2|^2}{|k_2 + l_1^*||l_1 + l_2^*|^2} - \frac{1}{k_{1R}} \log \frac{|k_1 - l_2||k_1 - k_2|^2}{|k_1 + l_2^*||k_1 + k_2^*|^2}, \tag{24}$$

and for soliton S_2,

$$\Delta t_2 = \Delta t_{12}^{2+} - \Delta t_{12}^{2-} = \frac{1}{l_{2R}} \log \frac{|k_1 - l_2||l_1 - l_2|^2}{|k_1 + l_2^*||l_1 + l_2^*|^2} - \frac{1}{k_{2R}} \log \frac{|k_2 - l_1||k_1 - k_2|^2}{|k_2 + l_1^*||k_1 + k_2^*|^2}. \tag{25}$$

To demonstrate the shape-preserving collision property of nondegenerate solitons, for the case $k_{1I} = l_{1I}$, $k_{2I} = l_{2I}$, we start with various symmetric profiles as initial conditions. In Figs. 5(a) and 5(b) we set two well-separated symmetric double-hump soliton profiles as initial profiles in both the modes. From these figures, we observe that the symmetric nature of double-hump soliton S_1 is preserved in both the modes after collision while interacting with another symmetric double-hump soliton S_2 except for a finite phase shift, which is already deduced in Eqs. (20) and (21). This can be easily verified from the asymptotic analysis itself. Further, in order to ensure the shape-preserving collision scenario of symmetric double-hump solitons we explicitly compute the numerical value of relative separation distance between the modes of each double-hump solitons by substituting all the parameter values in Eqs. (24) and (25). This action yields the final values as $\Delta t_1 = -0.0051$ and $\Delta t_2 = -0.0051$ (here we provide the values with two decimal accuracy, to get perfect zero, one has to fine tune the parameters suitably). The values reaffirm that symmetric profile struture of double-

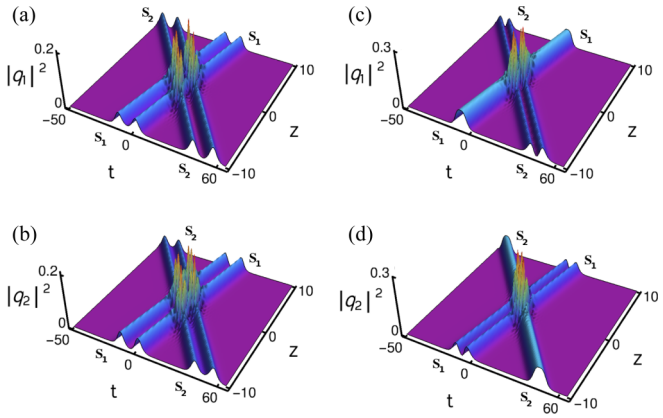

FIG. 5. Shape-preserving collision of symmetric nondegenerate solitons. The energy does not get exchanged among the nondegenerate solitons during the shape-preserving collision process: Panels (a) and (b) represent collision between two symmetric double-hump solitons. Panels (c) and (d) denote interaction among flat-top and symmetric double-hump soliton. The parameter values: [(a) and (b)] $k_1 = 0.333 + 0.5i$, $l_1 = 0.315 + 0.5i$, $k_2 = 0.315 - 2.2i$, $l_2 = 0.333 - 2.2i$, $\alpha_1^{(1)} = 0.45 + 0.45i$, $\alpha_2^{(1)} = 0.49 + 0.45i$, $\alpha_1^{(2)} = 0.49 + 0.45i$, and $\alpha_2^{(2)} = 0.45 + 0.45i$. [(c) and (d)] $k_1 = 0.43 + 0.5i$, $l_1 = 0.3 + 0.5i$, $k_2 = 0.3 - 2.2i$, $l_2 = 0.43 - 2.2i$, $\alpha_1^{(1)} = 0.45 + 0.5i$, $\alpha_2^{(1)} = 0.43 + 0.5i$, $\alpha_1^{(2)} = 0.43 + 0.5i$, and $\alpha_2^{(2)} = 0.45 + 0.5i$.

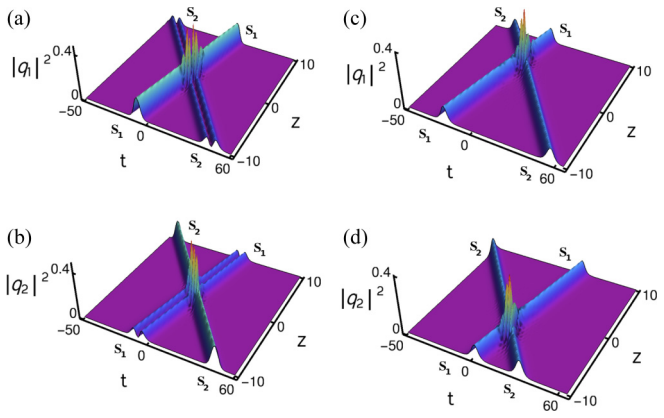

FIG. 6. Shape-preserving collision of symmetric nondegenerate solitons. Panels (a) and (b) denote collision between single-hump and double-hump solitons: The values corresponding to this collision scenario are $k_1 = 0.55 + 0.5i$, $l_1 = 0.333 + 0.5i$, $k_2 = 0.333 - 2.2i$, $l_2 = 0.55 - 2.2i$, $\alpha_1^{(1)} = 0.45 + 0.5i$, $\alpha_2^{(1)} = 0.43 + 0.5i$, $\alpha_1^{(2)} = 0.43 + 0.5i$, and $\alpha_2^{(2)} = 0.45 + 0.5i$. Panels (c) and (d) denote two single-hump solitons interaction: The corresponding parameter values are chosen as $k_1 = 0.333 + 0.5i$, $l_1 = -0.316 + 0.5i$, $k_2 = -0.316 - 2.2i$, $l_2 = 0.333 - 2.2i$, $\alpha_1^{(1)} = 0.45 + 0.51i$, $\alpha_2^{(1)} = 0.5 + 0.5i$, $\alpha_1^{(2)} = 0.5 + 0.5i$, and $\alpha_2^{(2)} = 0.45 + 0.51i$.

hump solitons are indeed preserved during the collision. This ensures further that the relative separation distance values are consistent with the shape-preserving collision condition $\phi_j^- = \phi_j^+$ and $\varphi_j^- = \varphi_j^+$, $j = 1, 2, 3, 4$, given by Eq. (19). We also show the shape-preserving collision between flat-top soliton and double-hump soliton occurs in Figs. 5(c) and 5(d). The same type of collision behavior is also observed while the symmetric single-hump soliton collides with the symmetric double-hump soliton, which is illustrated in Figs. 6(a) and 6(b). In Figs. 6(c) and 6(d) we depict the elastic collision between two symmetric single-hump solitons. From Fig. 6, we find that each soliton retains its structure during the collision scenario.

Next, we illustrate the shape-preserving collision among the asymmetric solitons. As we pointed out earlier, the nondegenerate fundamental soliton also admits asymmetric profiles for $k_{1I} = l_{1I}$. To bring out one more asymmetric soliton we set $k_{2I} = l_{2I}$ in the two-soliton solution (13a)–(13c). In order to study the shape-preserving collision of such two asymmetric solitons, first we locate asymmetric double-hump soliton S_1 along the line $\eta_{1R} = k_{1R}(t - 2k_{1I}z) \simeq 0$, $\xi_{1R} = l_{1R}(t - 2k_{1I}z) \simeq 0$ and another similar kind of soliton S_2 along the line $\eta_{2R} = k_{2R}(t - 2k_{2I}z) \simeq 0$, $\xi_{2R} = l_{2R}(t - 2k_{2I}z) \simeq 0$. These asymmetric structured double-hump solitons also preserve their structure after collision. This is clearly depicted in Figs. 7(a) and 7(b). To ensure the shape-preserving nature of asymmetric solitons, we again explicitly calculate the relative separation distance values for both the asymmetric solitons S_1 and S_2 as $\Delta t_1 = \Delta t_2 = -0.0093$. These values again confirm the shape-preserving property of the asymmetric double-hump solitons and they are indeed compatible with the shape-preserving collision condition (19). As displayed in Figs. 7(c) and 7(d), the asymmetric flat-top soliton also preserves its structure when it collides with an asymmetric double-hump soliton. In other cases also asymmetric solitons preserve their profiles. This can be confirmed from Fig. 8. Very interestingly, the shape-preserving collision also occurs even when the asymmetric double-hump soliton interacts with the symmetric double-hump soliton. This is illustrated in Fig. 9. During this collision also the standard position shift only occurs as a final outcome.

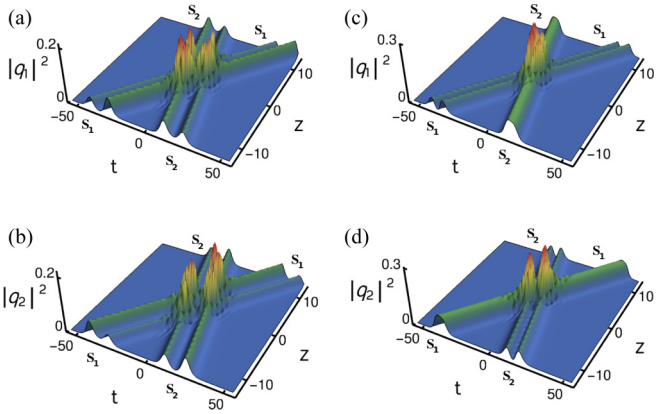

FIG. 7. Shape-preserving collision of asymmetric nondegenerate solitons. Panels (a) and (b) represent two asymmetric soliton collision: $k_1 = 0.333 - 0.5i$, $l_1 = 0.315 - 0.5i$, $k_2 = 0.315 + 1.5i$, $l_2 = 0.333 + 1.5i$, $\alpha_1^{(1)} = 0.65 + 0.45i$, $\alpha_2^{(1)} = 0.49 + 0.5i$, $\alpha_1^{(2)} = 0.49 + 0.5i$ and $\alpha_2^{(2)} = 0.65 + 0.45i$. Panels (c) and (d) denote asymmetric flat-top-double-hump soliton: The corresponding parameter values are chosen as (a): $k_1 = 0.425 - 0.5i$, $l_1 = 0.3 - 0.5i$, $k_2 = 0.3 + 1.5i$, $l_2 = 0.425 + 1.5i$, $\alpha_1^{(1)} = 0.5 + 0.51i$, $\alpha_2^{(1)} = 0.43 + 0.5i$, $\alpha_1^{(2)} = 0.43 + 0.5i$, and $\alpha_2^{(2)} = 0.5 + 0.51i$.

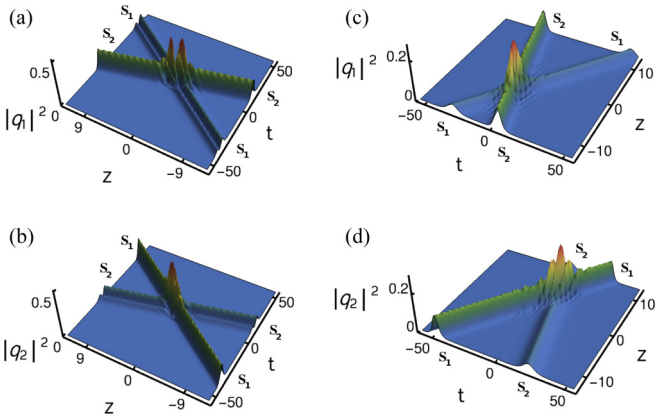

FIG. 8. Shape-preserving collision of asymmetric nondegenerate solitons. Panels (a) and (b) represent asymmetric single-hump and double-hump soliton collision: $k_1 = 0.55 - 0.5i$, $l_1 = 0.333 - 0.5i$, $k_2 = 0.333 + 1.5i$, $l_2 = 0.55 + 1.5i$, $\alpha_1^{(1)} = 1.2 + 0.5i$, $\alpha_2^{(1)} = 0.5 + 0.45i$, $\alpha_1^{(2)} = 0.5 + 0.45i$, and $\alpha_2^{(2)} = 1.2 + 0.5i$. Panels (c) and (d) denote collision of two asymmetric single-hump solitons: The parameter values of each figure are chosen as $k_1 = 0.333 - 0.5i$, $l_1 = -0.2 - 0.5i$, $k_2 = -0.2 + 1.5i$, $l_2 = 0.333 + 1.5i$, $\alpha_1^{(1)} = 0.45 + 3.0i$, $\alpha_2^{(1)} = 0.5 + 0.5i$, $\alpha_1^{(2)} = 0.5 + 0.5i$, and $\alpha_2^{(2)} = 0.45 + 3.0i$.

Then, we also come across another type of elastic collision, namely shape-altering collision for certain set of parametric choices again with $k_{1I} = l_{1I}$ and $k_{2I} = l_{2I}$. We illustrate such collision scenario in Fig. 10. We explain the profile alteration in the head-on collision between slow-moving symmetric double-hump soliton and fast-moving asymmetric double-hump soliton as displayed in Figs. 10(a) and 10(b). To draw this figure we fix the parametric choice as $k_1 = 0.41 + 0.5i$, $l_1 = 0.305 + 0.5i$, $k_2 = 0.305 - 2.2i$, $l_2 = 0.41 - 2.2i$, $\alpha_1^{(1)} = \alpha_2^{(2)} = 0.44 + 0.499i$, and $\alpha_2^{(1)} = \alpha_1^{(2)} = 0.44 + 0.5i$ in solution (13a)–(13c). From this figure, we find that while symmetric double-hump soliton S_1^- in the first mode slightly changes into an asymmetric structure, the asymmetric double-hump soliton S_2^- becomes symmetric. For this kind of shape-altering collision the parameter values corresponding to Figs. 10(a) and 10(b) are inconsistent with the condition (19), even though the unimodular condition of transition amplitudes is still preserved. A similar kind of profile alteration occurs in the second mode also. This is due to the incoherent interaction between the modes q_1 and q_2. Again, a similar type of collision property has been observed when a symmetric

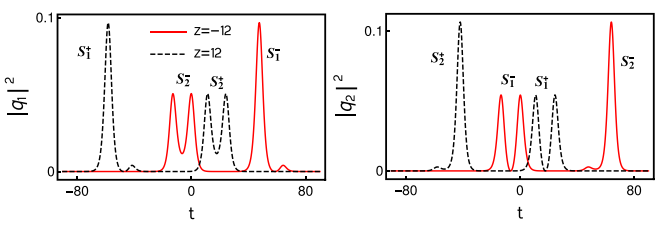

FIG. 9. Shape-preserving collision between symmetric double-hump soliton and asymmetric double-hump soliton: The parameter values are $k_1 = 0.333 + 0.5i$, $l_1 = 0.315 + 0.5i$, $k_2 = 0.315 - 2.2i$, $l_2 = 0.333 - 2.2i$, $\alpha_1^{(1)} = 0.45 + 0.45i$, $\alpha_2^{(1)} = 2.49 + 2.45i$, $\alpha_1^{(2)} = 0.49 + 0.45i$, and $\alpha_2^{(2)} = 0.45 + 0.45i$.

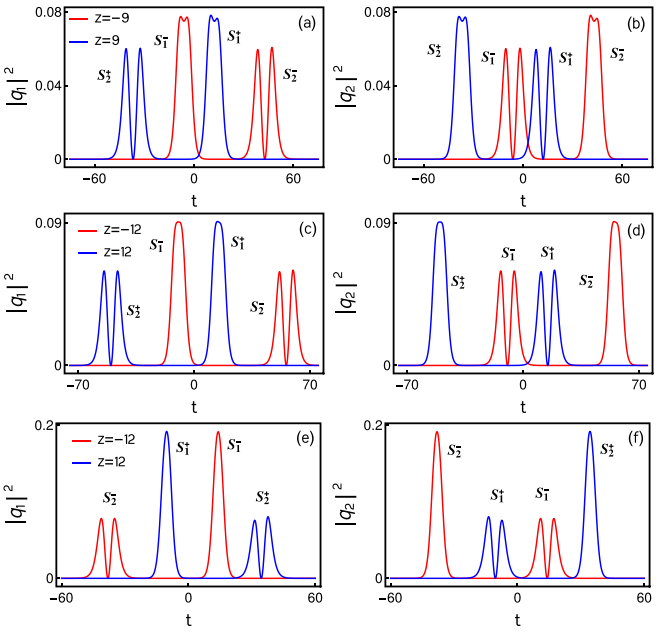

FIG. 10. Shape-altering collision: Panels (a) and (b) denote shape-altering collision between symmetric double-hump soliton and asymmetric double-hump soliton. Panels (c) and (d) refer to collision between symmetric flat-top and asymmetric double-hump soliton. Panels (e) and (f) represent interaction between single-hump and asymmetric double-hump soliton.

(or asymmetric) flat-top soliton collides with an asymmetric (or symmetric) double-hump soliton in the q_1 (or q_2) component, which is demonstrated in Figs. 10(c) and 10(d) for $k_1 = 0.425 + 0.5i$, $l_1 = 0.3 + 0.5i$, $k_2 = 0.3 - 2.2i$, $l_2 = 0.425 - 2.2i$, $\alpha_1^{(1)} = \alpha_2^{(2)} = 0.5 + 0.5i$ and $\alpha_2^{(1)} = \alpha_1^{(2)} = 0.45 + 0.5i$. In Figs. 10(e) and 10(f), we illustrate shape alteration collision between symmetric single-hump and double-hump solitons in both the components by fixing the parameter values as $k_1 = 0.55 - 0.5i$, $l_1 = 0.333 - 0.5i$, $k_2 = 0.333 + 1.5i$, $l_2 = 0.55 + 1.5i$, $\alpha_1^{(1)} = \alpha_2^{(2)} = 0.5 + 0.5i$, and $\alpha_2^{(1)} = \alpha_1^{(2)} = 0.45 + 0.5i$. In each of the modes, the collision transforms the symmetric double-hump soliton into a slightly asymmetric double-hump soliton leaving the symmetric single-hump soliton unaltered. However, in all the above cases the energy does not get redistributed among the modes even though the shape of the solitons gets altered during the collision. One can prove the unimodular nature of the transition amplitudes in these cases by following the procedure mentioned earlier in this section. As we pointed out earlier, the similar kind of shape-preserving and shape-altering collisions are also observed in the case of $k_{1I} \neq l_{1I}$ and $k_{2I} \neq l_{2I}$. Here we have not displayed their plots and their corresponding asymptotic analysis for brevity.

Additionally, in Fig. 11, we display another type of collision scenario for the velocity condition $k_{1I} = l_{1I}$, $k_{2I} \neq l_{2I}$. In this collision scenario the asymmetric double-hump solitons that are present in the two modes change dramatically. However, the single-hump solitons undergo collision without any change in their intensity profiles. Due to the incoherent coupling between the modes, the change occurred only in the profile of the double-hump soliton. One can carry out an

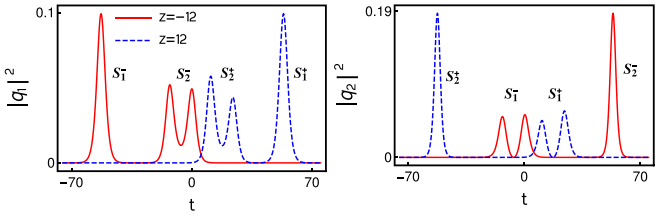

FIG. 11. Shape-changing collision between asymmetric double-hump soliton and single-hump soliton: $k_1 = 0.333 + 0.5i$, $l_1 = 0.315 + 0.5i$, $k_2 = 0.315 + 2.2i$, $l_2 = 0.433 - 2.2i$, $\alpha_1^{(1)} = \alpha_2^{(2)} = 0.5 + 0.5i$, and $\alpha_2^{(1)} = \alpha_1^{(2)} = 0.45 + 0.5i$.

appropriate asymptotic analysis for this kind of collision process also. We also note here that this kind of shape-changing collision is not observed in the degenerate case. We remark that elastic collision is also noticed in the case of dissipative solitons where a new soliton pair (doublet) is formed when the single soliton state (singlet) destroys the initial doublet state. During this interaction, energy or momentum is not conserved in the fiber laser cavity [54–56]. But the elastic collision observed in the present conservative system is entirely different from the above collision which has been observed in the dissipative system. The vector solitons in dissipative systems exhibit several interesting dynamical features, especially in fiber lasers. Fiber lasers are very useful nonlinear systems to study the formation and dynamics of temporal optical solitons experimentally. In fact several types of solitons were observed experimentally in fiber lasers. For instance, vector multisoliton operation and vector soliton interaction in an erbium-doped fiber laser [57] and a vector dark domain wall soliton has been observed in a fiber ring laser [19]. Also vector dissipative soliton operation of erbium-doped fiber lasers mode locked with atomic layer graphene was experimentally investigated [58] and the coexistence of polarization-locked and polarization rotating vector solitons in a fiber laser with a semiconductor saturable absorber mirror have been observed experimentally [59].

C. Shape-changing collision

Further, here we demonstrate the shape-changing collision scenario of nondegenerate solitons for unequal velocities, that is, $k_{1I} \neq l_{1I}$ and $k_{2I} \neq l_{2I}$ (we also note here that for appropriate choices of parameters for this unequal velocity case as pointed out above both shape-preserving and shape-altering cases do occur). During this interaction, we observe that an intensity redistribution occurs among the modes of nondegenerate fundamental solitons along with profile change. We display such a collision dynamics in Figs. 12 and 13. A typical intensity redistribution phenomenon is demonstrated in Fig. 12 when two asymmetric double-hump solitons collide with each other. To bring out this nonlinear phenomenon we choose the parameter values as $k_1 = 1.2 - 0.5i$, $l_1 = 0.8 + 0.5i$, $k_2 = 1.0 + 0.5i$, $l_2 = 1.5 - 0.5i$, $\alpha_1^{(1)} = \alpha_2^{(2)} = 0.5 + 0.51i$, and $\alpha_2^{(1)} = \alpha_1^{(2)} = 0.45 + 0.5i$. From Fig. 12, one can easily observe that the profiles of asymmetric double-hump solitons S_1 and S_2 change dramatically after collision, where the initial asymmetric solitons S_1 and S_2 lose their identities and reemerge with another set of asymmetric profiles. In

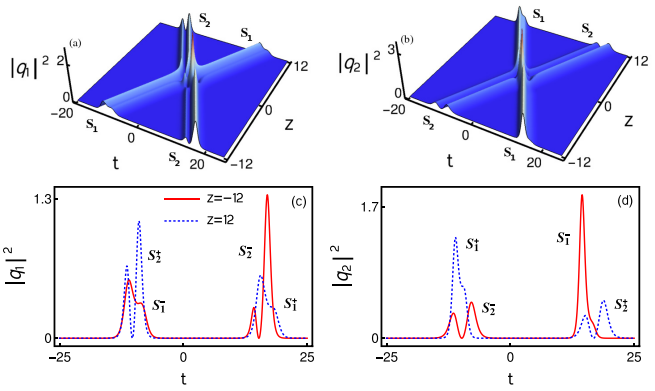

FIG. 12. Shape-changing collision between two asymmetric double-hump solitons: $k_1 = 1.2 - 0.5i$, $l_1 = 0.8 + 0.5i$ $k_2 = 1.0 + 0.5i$, $l_2 = 1.5 - 0.5i$, $\alpha_1^{(1)} = \alpha_2^{(2)} = 0.5 + 0.5i$, and $\alpha_2^{(1)} = \alpha_1^{(2)} = 0.45 + 0.5i$.

addition to the profile changes, there is also a finite intensity redistribution which takes place between the two modes of the solitons. However, the total energy of the individual solitons as well as modes is conserved in order to hold the energy conservation of system (1). A similar kind of collision is also depicted in Fig. 13, where a drastic change only occurs in the profile of asymmetric double-hump soliton but without any change in the asymmetric single-hump soliton. This can be witnessed in Fig. 13 by setting the values of the parameters as $k_1 = 0.36 + 0.5i$, $l_1 = 0.3 - 0.5i$, $k_2 = 0.5 - 2.1i$, $l_2 = 0.45 - 2.2i$, $\alpha_1^{(1)} = \alpha_2^{(2)} = 0.5 + 0.5i$, and $\alpha_2^{(1)} = 1.7 + 0.45i$, $\alpha_1^{(2)} = 0.45 + 0.5i$ in the solution (13a)–(13c). From this figure one can confirm that the intensity redistribution only occurs among the modes of the asymmetric double-hump soliton. A detailed asymptotic analysis has been carried out in order to ensure this peculiar intensity redistribution, which we have given in Appendix B. We remark that the nondegenerate solitons also exhibit shape-changing collision for the equal velocity case as well with $k_{1I} = l_{1I}$ and $k_{2I} = l_{2I}$ for appropriate choice of parameters, which are inconsistent with Eq. (19).

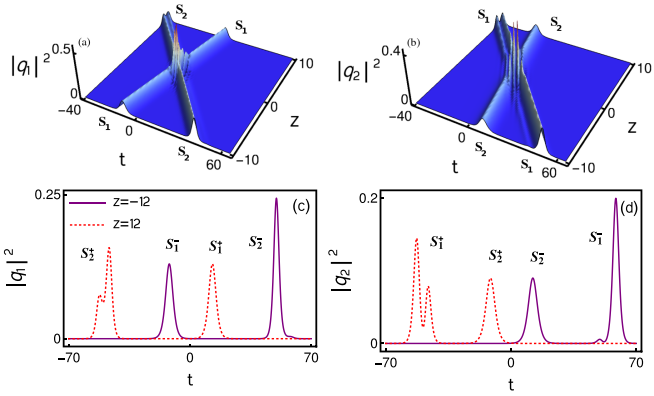

FIG. 13. Shape-changing collision between asymmetric single-hump and double-hump solitons: $k_1 = 0.36 + 0.5i$, $l_1 = 0.3 - 0.5i$ $k_2 = 0.5 - 2.1i$, $l_2 = 0.45 - 2.2i$, $\alpha_1^{(1)} = \alpha_2^{(2)} = 0.5 - 0.5i$, $\alpha_2^{(1)} = 1.7 + 0.45i$, and $\alpha_1^{(2)} = 0.45 + 0.5i$.

V. COLLISION BETWEEN NONDEGENERATE AND DEGENERATE SOLITONS

In this section, we discuss the collision among degenerate and nondegenerate solitons admitted by the two-soliton solution (13a)–(13c) of Manakov system (1) in the partial nondegenerate limit $k_1 = l_1$ and $k_2 \neq l_2$. The following asymptotic analysis assures that there is a definite energy redistribution occurs among the modes q_1 and q_2.

A. Asymptotic analysis

To elucidate this kind of collision behavior, we analyze the partial nondegenerate two-soliton solution (14a)–(14c) in the asymptotic limits $z \to \pm\infty$. The resultant action yields the asymptotic forms corresponding to degenerate and nondegenerate solitons. As we pointed out in the shape-preserving collision case, to obtain the asymptotic forms for the present case we incorporate the asymptotic nature of the wave variables $\eta_{jR} = k_{jR}(t - 2k_{jI}z)$ and $\xi_{2R} = l_{2R}(t - 2l_{2I}z)$, $j = 1, 2$, in the solution (14a)–(14c). Here the wave variable η_{1R} corresponds to the degenerate soliton and η_{2R}, ξ_{2R} correspond to the nondegenerate soliton. In order to find the asymptotic behavior of these wave variables we consider the parametric choice as $k_{1R}, k_{2R}, l_{2R} > 0$, $k_{1I} > 0$, $k_{2I}, l_{2I} < 0$, $k_{1I} > k_{2I}$, $k_{1I} > l_{2I}$. For this choice, the wave variables behave asymptotically as follows: (i) degenerate soliton S_1: $\eta_{1R} \simeq 0$, $\eta_{2R}, \xi_{2R} \to \mp\infty$ as $z \to \mp\infty$ (ii) nondegenerate soliton S_2: $\eta_{2R}, \xi_{2R} \simeq 0$, $\eta_{1R} \to \pm\infty$ as $z \to \pm\infty$. By incorporating these asymptotic behaviors of wave variables in the solution (14a)–(14c), we deduce the following asymptotic expressions for degenerate and nondegenerate solitons.

(a) Before collision: $z \to -\infty$

Soliton 1: In this limit, the asymptotic form for the degenerate soliton deduced from the partially nondegenerate two-soliton solution (14a)–(14c) is

$$q_j \simeq \begin{pmatrix} A_1^{1-} \\ A_2^{1-} \end{pmatrix} k_{1R} e^{i\eta_{1I}} \operatorname{sech}\left(\eta_{1R} + \frac{R}{2}\right), \quad j = 1, 2, \tag{26}$$

where $A_j^{1-} = \alpha_1^{(j)}/(|\alpha_1^{(1)}|^2 + |\alpha_1^{(2)}|^2)^{1/2}$, $j = 1, 2$, $R = \ln \frac{(|\alpha_1^{(1)}|^2 + |\alpha_1^{(2)}|^2)}{(k_1 + k_1^*)^2}$. Here in A_j^{1-} the superscript $1-$ denotes soliton S_1 before collision and subscript j refers to the mode number.

Soliton 2: The asymptotic expressions for the nondegenerate soliton S_2 which is present in the two modes before collision are obtained as

$$q_1 \simeq \frac{2k_{2R}A_1^{2-}}{D}\left[e^{i\xi_{2I}+\Lambda_1}\cosh\left(\eta_{2R} + \frac{\Phi_{21} - \Delta_{21}}{2}\right) + e^{i\eta_{2I}+\Lambda_2}\cosh\left(\xi_{2R} + \frac{\lambda_2 - \lambda_1}{2}\right)\right], \tag{27a}$$

$$q_2 \simeq \frac{2l_{2R}A_2^{2-}}{D}\left[e^{i\eta_{2I}+\Lambda_7}\cosh\left(\xi_{2R} + \frac{\Gamma_{21} - \gamma_{21}}{2}\right) + e^{i\xi_{2I}+\Lambda_6}\cosh\left(\eta_{2R} + \frac{\lambda_7 - \lambda_6}{2}\right)\right], \tag{27b}$$

$$D = e^{\Lambda_5}\cosh\left(\eta_{2R} - \xi_{2R} + \frac{\lambda_3 - \lambda_4}{2}\right) + e^{\Lambda_3}\cosh\left[i(\eta_{2I} - \xi_{2I}) + \frac{\vartheta_{12} - \varphi_{21}}{2}\right] + e^{\Lambda_4}\cosh\left(\eta_{2R} + \eta_{3R} + \frac{\lambda_5 - R}{2}\right).$$

Here $A_1^{2-} = [\alpha_2^{(1)}/\alpha_2^{(1)^*}]^{1/2}$ and $A_2^{2-} = [\alpha_2^{(2)}/\alpha_2^{(2)^*}]^{1/2}$. In the latter the superscript $2-$ denote nondegenerate soliton S_2 before collision.

(b) After collision: $z \to +\infty$

Soliton 1: The asymptotic forms for degenerate soliton S_1 after collision deduced from the solution (14a)–(14c) as

$$q_j \simeq \begin{pmatrix} A_1^{1+} \\ A_2^{1+} \end{pmatrix} e^{i(\eta_{1I}+\theta_j^+)} k_{1R} \operatorname{sech}\left(\eta_{1R} + \frac{R' - \varsigma_{22}}{2}\right), \quad j = 1, 2, \tag{28}$$

where $A_1^{1+} = \alpha_1^{(1)}/(|\alpha_1^{(1)}|^2 + \chi|\alpha_1^{(2)}|^2)^{1/2}$, $A_2^{1+} = \alpha_1^{(1)}/(|\alpha_1^{(1)}|^2\chi^{-1} + |\alpha_1^{(2)}|^2)^{1/2}$, $\chi = (|k_1 - l_2|^2|k_1 + k_2^*|^2)/(|k_1 - k_2|^2|k_1 + l_2^*|^2)$, $e^{i\theta_1^+} = \frac{(k_1-k_2)(k_1^*+k_2)(k_1-l_2)^{\frac{1}{2}}(k_1^*+l_2)^{\frac{1}{2}}}{(k_1^*-k_2^*)(k_1+k_2^*)(k_1^*-l_2^*)^{\frac{1}{2}}(k_1+l_2^*)^{\frac{1}{2}}}$, $e^{i\theta_2^+} = \frac{(k_1-k_2)^{\frac{1}{2}}(k_1^*+k_2)^{\frac{1}{2}}(k_1-l_2)(k_1^*+l_2)}{(k_1^*-k_2^*)^{\frac{1}{2}}(k_1+k_2^*)^{\frac{1}{2}}(k_1^*-l_2^*)(k_1+l_2^*)}$. Here $1+$ in A_1^{1+} refers to degenerate soliton S_1 after collision.

Soliton 2: Similarly the expression for the nondegenerate soliton, S_2, after collision deduced from the two-soliton solution (14a)–(14c) is

$$q_1 \simeq \frac{2k_{2R}A_1^{2+}e^{i\eta_{2I}}\cosh\left(\xi_{2R} + \frac{\Lambda_{22}-\rho_1}{2}\right)}{\left[\frac{(k_2^*-l_2^*)^{\frac{1}{2}}}{(k_2^*+l_2)^{\frac{1}{2}}}\cosh\left(\eta_{2R} + \xi_{2R} + \frac{\varsigma_{22}}{2}\right) + \frac{(k_2+l_2^*)^{\frac{1}{2}}}{(k_2-l_2)^{\frac{1}{2}}}\cosh\left(\eta_{2R} - \xi_{2R} + \frac{R_3-R_6}{2}\right)\right]}, \tag{29}$$

$$q_2 \simeq \frac{2l_{2R}A_2^{2+}e^{i\xi_{2I}}\cosh\left(\eta_{2R} + \frac{\mu_{22}-\rho_2}{2}\right)}{\left[\frac{(k_2^*-l_2^*)^{\frac{1}{2}}}{(k_2+l_2^*)^{\frac{1}{2}}}\cosh\left(\eta_{2R} + \xi_{2R} + \frac{\varsigma_{22}}{2}\right) + \frac{(k_2^*+l_2)^{\frac{1}{2}}}{(k_2-l_2)^{\frac{1}{2}}}\cosh\left(\eta_{2R} - \xi_{2R} + \frac{R_3-R_6}{2}\right)\right]}. \tag{30}$$

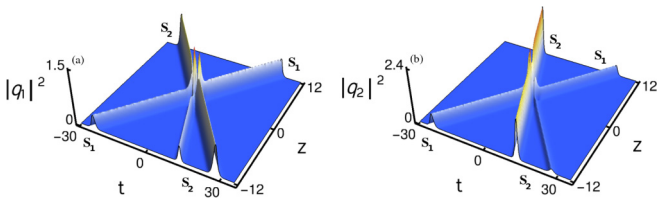

FIG. 14. Energy-sharing collision between degenerate and nondegenerate soliton: $k_1 = l_1 = 1 + i$, $k_2 = 1 - i$, $l_2 = 1.5 - 0.5i$, $\alpha_1^{(1)} = 0.8 + 0.8i$, $\alpha_2^{(2)} = 0.6 + 0.6i$, $\alpha_2^{(1)} = 0.25 + 0.25i$, and $\alpha_1^{(2)} = 1 + i$.

where $\rho_j = \log \alpha_2^{(j)}$, $j = 1, 2$, $A_1^{2+} = [\alpha_2^{(1)}/\alpha_2^{(1)^*}]^{1/2}$, and $A_2^{2+} = i[\alpha_2^{(2)}/\alpha_2^{(2)^*}]^{1/2}$. The explicit expressions of all the constants are given in Appendix C.

B. Degenerate soliton collision-induced shape-changing scenario of nondegenerate soliton

The coexistence of nondegenerate and degenerate solitons can be brought out from the partially nondegenerate soliton solution (14a)–(14c). Such coexisting solitons undergo a collision property that has been illustrated in Fig. 14. From this figure, one can observe that the intensity of the degenerate soliton S_1 is enhanced after collision in the first mode and it gets suppressed in the second mode. As we expected the degenerate soliton undergoes energy redistribution among the modes q_1 and q_2. In the degenerate soliton case, the polarization vectors, $A_j^l = \alpha_l^{(j)}/(|\alpha_1^{(1)}|^2 + |\alpha_1^{(2)}|^2)^{1/2}$, $l, j = 1, 2$, play crucial role in changing the shape of the degenerate solitons under collision, where the intensity or energy redistribution happens between the modes q_1 and q_2. As we point out in the next section, the shape-preserving collision arises in the pure degenerate case when the polarization parameters obey the condition $\frac{\alpha_1^{(1)}}{\alpha_2^{(1)}} = \frac{\alpha_1^{(2)}}{\alpha_2^{(2)}}$, where $\alpha_i^{(j)}$'s, $i, j = 1, 2$, are complex numbers related to the polarization vectors as given above. The above collision is similar to the one which occurs in the completely degenerate case [3,4]. However, this is not true in the case of nondegenerate solitons. The nondegenerate asymmetric double-hump soliton S_2 exhibits a collision property depicted in Fig. 14. In both the modes, the nondegenerate soliton S_2 experiences strong effect when it interacts with a degenerate soliton. As a result the nondegenerate soliton switches its asymmetric double-hump profile into single-hump profile with an enhancement of intensity along with a phase shift. In addition to the latter case, we also noticed that the nondegenerate soliton loses its asymmetric double-hump profile into another form of asymmetric double-hump profile when it interacts with a degenerate soliton. In the nondegenerate case, the relative separation distances (or phases) are in general not preserved during the collision. These collision properties can be understood from the corresponding asymptotic analysis given in the previous subsection. The asymptotic analysis reveals that energy redistribution occurs between modes q_1 and q_2. In order to confirm the shape-changing nature of this interesting collision process we obtain the following expression for the transition amplitudes:

$$T_1^1 = \frac{\left[|\alpha_1^{(1)}|^2 + |\alpha_1^{(2)}|^2\right]^{1/2}}{\left[|\alpha_1^{(1)}|^2 + \chi|\alpha_1^{(2)}|^2\right]^{1/2}},$$
$$T_2^1 = \frac{\left[|\alpha_1^{(1)}|^2 + |\alpha_1^{(2)}|^2\right]^{1/2}}{\left[|\alpha_1^{(1)}|^2 \chi^{-1} + |\alpha_1^{(2)}|^2\right]^{1/2}}. \tag{31}$$

In general, the transition amplitudes are not equal to unity. If the quantity T_j^l is not unimodular (for this case the constant $\chi \neq 1$), then the degenerate and nondegenerate solitons always exhibit shape-changing collision. The standard elastic collision can be recovered when $\chi = 1$. One can calculate the shift in the positions of both degenerate and nondegenerate solitons after collision from the asymptotic analysis. This kind of collision property has not been observed in the degenerate vector bright solitons of the Manakov system [3,4]. The property of enhancement of intensity in both the components of nondegenerate soliton is similar to the one observed earlier in the mixed coupled nonlinear Schrödinger system [60]. The amplification process of a single-humped nondegenerate soliton in both the modes can be viewed as an application for signal amplification where the degenerate soliton acts as a pumping wave.

VI. DEGENERATE VECTOR BRIGHT SOLITON SOLUTIONS AND THEIR COLLISION DYNAMICS

The already reported degenerate vector one-bright soliton solution of Manakov system (1) can be deduced from the one-soliton solution (7) by imposing $k_1 = l_1$ in it. The forms of q_j given in Eq. (7) degenerates into the standard bright soliton form [3,44]

$$q_j = \frac{\alpha_1^{(j)} e^{\eta_1}}{1 + e^{\eta_1 + \eta_1^* + R}}, \quad j = 1, 2, \tag{32}$$

which can be rewritten as

$$q_j = k_{1R} \hat{A}_j e^{i\eta_{1I}} \operatorname{sech}\left(\eta_{1R} + \frac{R}{2}\right), \tag{33}$$

where $\eta_{1R} = k_{1R}(t - 2k_{1I}z)$, $\eta_{1I} = k_{1I}t + (k_{1R}^2 - k_{1I}^2)z$, $\hat{A}_j = \frac{\alpha_1^{(j)}}{\sqrt{(|\alpha_1^{(1)}|^2 + |\alpha_1^{(2)}|^2)}}$, $e^R = \frac{(|\alpha_1^{(1)}|^2 + |\alpha_1^{(2)}|^2)}{(k_1 + k_1^*)^2}$, and $j = 1, 2$. Note that the above fundamental bright soliton always propagates in both the modes q_1 and q_2 with the same velocity $2k_{1I}$. The polarization vectors $(\hat{A}_1, \hat{A}_2)^\dagger$ have different amplitudes and phases, unlike the case of nondegenerate solitons where they have only different phases. The presence of single wave number k_1 in the solution (33) restricts the degenerate soliton to have a single-hump form only. A typical profile of the degenerate soliton is shown in Fig. 15. As already pointed out in Refs. [3,4] the amplitude and central position of the degenerate vector bright soliton are obtained as $2k_{1R}\hat{A}_j$, $j = 1, 2$, and $\frac{R}{2k_{1R}}$, respectively.

Further, the degenerate two-soliton solution can be deduced from the nondegenerate two-soliton solution (13a)–(13c) by applying the degenerate limits $k_1 = l_1$ and $k_2 = l_2$. This results in the following standard degenerate two-soliton

solution [3], that is,

$$q_j(t,z) = \frac{\alpha_1^{(j)} e^{\eta_1} + \alpha_2^{(j)} e^{\eta_2} + e^{\eta_1+\eta_1^*+\eta_2+\delta_{1j}} + e^{\eta_1+\eta_2+\eta_2^*+\delta_{2j}}}{1 + e^{\eta_1+\eta_1^*+R_1} + e^{\eta_1+\eta_2^*+\delta_0} + e^{\eta_1^*+\eta_2+\delta_0^*} + e^{\eta_2+\eta_2^*+R_2} + e^{\eta_1+\eta_1^*+\eta_2+\eta_2^*+R_3}}, \tag{34}$$

where $j = 1, 2$, $\eta_j = k_j(t + ik_j z)$, $e^{\delta_0} = \frac{k_{12}}{k_1+k_2^*}$, $e^{R_1} = \frac{k_{11}}{k_1+k_1^*}$, $e^{R_2} = \frac{k_{22}}{k_2+k_2^*}$, $e^{\delta_{1j}} = \frac{(k_1-k_2)(\alpha_1^{(j)}k_{21}-\alpha_2^{(j)}k_{11})}{(k_1+k_1^*)(k_1^*+k_2)}$, $e^{\delta_{2j}} = \frac{(k_2-k_1)(\alpha_2^{(j)}k_{12}-\alpha_1^{(j)}k_{22})}{(k_2+k_2^*)(k_1+k_2^*)}$, $e^{R_3} = \frac{|k_1-k_2|^2}{(k_1+k_1^*)(k_2+k_2^*)|k_1+k_2^*|^2}(k_{11}k_{22} - k_{12}k_{21})$, and $k_{il} = \frac{\mu \sum_{n=1}^{2} \alpha_i^{(n)}\alpha_l^{(n)*}}{(k_i+k_l^*)}$, $i, l = 1, 2$, $\mu = +1$. The N degenerate vector bright soliton solution can be recovered from the nondegenerate N-soliton solutions by fixing the wave numbers as $k_i = l_i$, $i = 1, 2, \ldots, N$. In passing we also note that the nondegenerate fundamental soliton solution (7) can arise when we fix the parameters $\alpha_2^{(1)} = \alpha_1^{(2)} = 0$ in Eq. (34) and rename the constants k_2 as l_1 and $\alpha_2^{(2)}$ as $\alpha_1^{(2)}$ in the resultant solution. We also note that the above degenerate two-soliton solution (34) can also be rewritten using Gram determinants from the Gram-determinant forms of nondegenerate two-soliton solution (13a)–(13c).

As reported in Refs. [3,4], the degenerate fundamental solitons ($k_i = l_i$, $i = 1, 2$) in the Manakov system undergo shape-changing collision due to intensity redistribution among the modes. The energy redistribution occurs in the degenerate case because of the polarization vectors of the two modes combine with each other. This shape-changing collision illustrated in Fig. 16 where the intensity redistribution occurs because of the enhancement of soliton S_1 in the first mode and the corresponding intensity of the same soliton is suppressed in the second mode. To hold the conservation of energy between the modes the intensity of the solitons S_2 gets suppressed in the first mode and it is enhanced in the second mode. The standard elastic collision has already been brought out in the degenerate case for the very special case $\frac{\alpha_1^{(1)}}{\alpha_2^{(1)}} = \frac{\alpha_1^{(2)}}{\alpha_2^{(2)}}$ [4,52].

VII. POSSIBLE EXPERIMENTAL OBSERVATIONS OF NONDEGENERATE SOLITONS

To experimentally observe the nondegenerate vector solitons (single-hump or double-hump solitons) one may adopt the mutual-incoherence method which has been used to observe the multihump multimode solitons experimentally (see Ref. [36]). The Manakov solitons (degenerate solitons) can also be observed by the same experimental procedure with appropriate modifications (see Ref. [24]). In the following, we briefly envisage how the procedure given in Ref. [36] can be modified to generate the single-hump or double-hump soliton (nondegenerate soliton) discussed in our work.

To generate the nondegenerate vector solitons it is essential to consider two laser sources of different characters, so that the wavelength of the first laser beam is different from the second one. Using polarizing beam splitters, each one of the laser beams can be split into ordinary and extraordinary beams. The extraordinary beam coming out from the first source can be further split into two individual fields F_{11} and F_{12} by allowing it to fall on a beam splitter. These two fields are nothing but the reflected and transmitted extraordinary beams coming out from the beam splitter. The intensities of these two fields are different. Similarly, the second beam which is coming out from the second source can also be split into two fields F_{21} and F_{22} by passing through another beam splitter. The intensities of these two fields are also different. As a result one can generate four fields that are incoherent to each other. To set the incoherence in phase among these four fields one should allow them to travel sufficient distance before coupling is performed. The fields F_{11} and F_{12} now become nondegenerate two individual solitons in the first mode whereas F_{21} and F_{22} form another set of two nondegenerate solitons in the second mode. The coupling between the fields F_{11} and F_{21} can be performed by combining them using another beam splitter. Similarly, by suitably locating another beam splitter, one can combine the fields F_{12} and F_{22}, respectively. After appropriate coupling is performed the resultant optical field beams can now be focused through two individual cylindrical lenses and the output may be recorded in an imaging system, which consists of a crystal and charge-coupled device camera. The collision between the nondegenerate two solitons in both the modes can now be seen from the recorded images.

To observe the elastic collision between nondegenerate solitons (single-hump or double-hump solitons), one must make arrangements to vanish the mutual coherence property

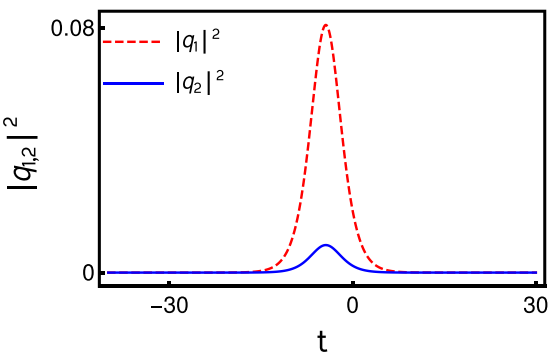

FIG. 15. Degenerate one-soliton: The values are $k_1 = 0.3 + 0.5i$, $\alpha_1^{(1)} = 1.5 + 1.5i$, and $\alpha_1^{(2)} = 0.5 + 0.5i$.

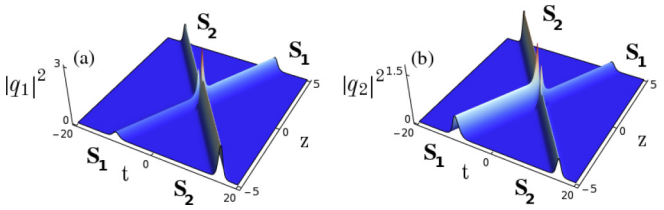

FIG. 16. Shape-changing collision of degenerate two-solitons: $k_1 = l_1 = 1 + i$, $k_2 = l_2 = 1.51 - 1.51i$, $\alpha_1^{(1)} = 0.5 + 0.5i$, and $\alpha_2^{(1)} = \alpha_1^{(2)} = \alpha_2^{(2)} = 1$.

between the solitons F_{11} and F_{12} in the first mode q_1 and F_{21} and F_{22} in the second mode q_2 (see Ref. [24]). The four optical beams are now completely independent and incoherent with one another. The collision angle at which the nondegenerate solitons interact should be sufficiently large enough. Under this situation, no energy exchange is expected to occur between the nondegenerate solitons of the two modes.

VIII. CONCLUSION

From the present study, we point out a few applications of our above reported soliton solutions. The shape-preserving collision property of the nondegenerate solitons can be used for optical communication applications. The nondegenerate solitons of Manakov system can be seen as a soliton molecule when $k_{1I} \approx k_{2I}$ and $l_{1I} \approx l_{2I}$. Therefore, as explained in the context of soliton molecule, the double-hump (or multihump) structure of the nondegenerate solitons can be useful for sending information of densely packed data [30]. Degenerate soliton collision-induced enhancement of intensity property of nondegenerate soliton is considered as signal amplification application. Recently the various properties associated with soliton molecule have been explored in the literature [30,31,40,61,62]. Also a breather wave molecule has been identified in Ref. [63]. The interesting collision property of degenerate soliton has already been shown that it is useful for optical computing [28,52]. Our results provide the possibility to investigate nondegenerate type solitons in both integrable and nonintegrable systems. The present study can also be extended to fiber arrays and multimode fibers where Manakov-type equations describe the pulse propagation. Recently we have investigated the dynamics of nondegenerate solitons in the N-coupled system and the results will be published elsewhere.

We have derived a general form of nondegenerate one-, two-, and three-soliton solutions for the Manakov model through the Hirota bilinear method. This class of solitons admits various interesting profile structures. The double-hump formation is elucidated by analyzing the relative velocities of the modes of the solitons. Then we have pointed out the coexistence of degenerate and nondegenerate solitons in the Manakov system by imposing a wave-number restriction on the obtained two-soliton solution. We have found that nondegenerate solitons undergo shape-preserving, shape-altering, and shape-changing collision scenarios for both equal velocities and unequal velocities cases. However, for the partially equal velocity case, we have demonstrated shape-changing collision. By performing appropriate asymptotic analysis, the shape-changing collision has been explained while the degenerate soliton interacts with the nondegenerate soliton. Finally, we recovered the well-known energy exchanging collision exhibiting degenerate soliton solutions from these nondegenerate one- and two-soliton solutions. We have also verified the stability nature of double-hump solitons even during collision using the Crank-Nicolson method as explained in Appendix D. It is also very interesting to investigate many possibilities of collision dynamics using a three-soliton solution as deduced in Appendix A. Now we are investigating what will happen when (i) two degenerate solitons interact with a nondegenerate soliton and (ii) two nondegenerate solitons collide with a degenerate soliton, and so on. The results will be published elsewhere.

ACKNOWLEDGMENTS

The authors are thankful to Prof. P. Muruganandam, Department of Physics, Bharathidasan University, for his personal help in verifying the shape-preserving collision nature of symmetric double-hump solitons numerically with white noise and Gaussian noise as perturbations. The work of R.R., S.S., and M.L. are supported by DST-SERB Distinguished Fellowship program under Grant No. SB/DF/04/2017.

APPENDIX A: THREE-SOLITON SOLUTION

The explicit form of nondegenerate three-soliton solution of Eq. (1) can be deduced by proceeding with the Eqs. (4) using the series representation up to orders ϵ^{11} for $g^{(N)}$ and ϵ^{12} for f. Then the solution can be expressed using Gram determinant in the following way:

$$g^{(N)} = \begin{vmatrix} A & I & \phi \\ -I & B & \mathbf{0}^T \\ \mathbf{0} & C_N & 0 \end{vmatrix}, \quad f = \begin{vmatrix} A & I \\ -I & B \end{vmatrix}, \quad N = 1, 2. \tag{A1a}$$

Here the matrices A and B are of the order (6×6) defined as

$$A = \begin{pmatrix} A_{mm'} & A_{mn} \\ A_{nm} & A_{nn'} \end{pmatrix},$$

$$B = \begin{pmatrix} \kappa_{mm'} & \kappa_{mn} \\ \kappa_{nm} & \kappa_{nn'} \end{pmatrix}, m, m', n, n' = 1, 2, 3. \tag{A1b}$$

The various elements of matrix A are obtained from the following,

$$A_{mm'} = \frac{e^{\eta_m + \eta^*_{m'}}}{(k_m + k^*_{m'})}, \; A_{mn} = \frac{e^{\eta_m + \xi^*_n}}{(k_m + l^*_n)}, \tag{A1c}$$

$$A_{nn'} = \frac{e^{\xi_n + \xi^*_{n'}}}{(l_n + l^*_{n'})}, \; A_{nm} = \frac{e^{\eta^*_n + \xi_m}}{(k^*_n + l_m)}, \; m, m', n, n' = 1, 2, 3. \tag{A1d}$$

The elements of matrix B is defined as

$$\kappa_{mm'} = \frac{\psi^\dagger_m \sigma \psi_{m'}}{(k^*_m + k_{m'})}, \; \kappa_{mn} = \frac{\psi^\dagger_m \sigma \psi'_n}{(k^*_m + l_n)},$$

$$\kappa_{nm} = \frac{\psi'^\dagger_n \sigma \psi_m}{(l^*_n + k_m)}, \; \kappa_{nn'} = \frac{\psi'^\dagger_n \sigma \psi'_{n'}}{(l^*_n + l_{n'})}. \tag{A1e}$$

In (A1e) the column matrices are $\psi_j = \binom{\alpha^{(1)}_j}{0}$, $\psi'_j = \binom{0}{\alpha^{(2)}_j}$, $j = m, m', n, n' = 1, 2, 3$, $\eta_j = k_j t + i k_j^2 z$, and $\xi_j = l_j t + i l_j^2 z$, $j = 1, 2, 3$. The other matrices in Eq. (A1a) are defined below:

$\phi = (e^{\eta_1} \; e^{\eta_2} \; e^{\eta_3} \; e^{\xi_1} \; e^{\xi_2} \; e^{\xi_3})^T$, $C_1 = -(\alpha^{(1)}_1 \; \alpha^{(1)}_2 \; \alpha^{(1)}_3 \; 0 \; 0 \; 0)$, $C_2 = -(0 \; 0 \; 0 \; \alpha^{(2)}_1 \; \alpha^{(2)}_2 \; \alpha^{(2)}_3)$, $\mathbf{0} = (0 \; 0 \; 0 \; 0 \; 0 \; 0)$, and $\sigma = I$ is a (6×6) identity matrix.

APPENDIX B: ASYMPTOTIC ANALYSIS OF SHAPE-CHANGING COLLISION OF NONDEGENERATE SOLITONS IN THE UNEQUAL VELOCITY CASE: $k_{1I} \neq l_{1I}$ AND $k_{2I} \neq l_{2I}$

To carry out the asymptotic analysis for the shape-changing collision we fix the parameters as $k_{1I} < k_{2I}, l_{1I} > l_{2I}, k_{jR}, l_{jR} > 0$, $j = 1, 2$, and $k_{1I} \neq l_{1I}$, $k_{2I} \neq l_{2I}$. For this choice the nondegenerate two-soliton solution (13a)–(13c) reduces to the following asymptotic forms:

(a) Before collision: $z \to -\infty$

Soliton 1: $(\eta_{1R}, \xi_{1R} \simeq 0,\ \eta_{2R} \to +\infty, \xi_{2R} \to -\infty)$

$$q_1 \simeq \frac{2A_1^{1-}k_{1R}e^{i(\eta_{1I}+\theta_1^{1-})}\cosh(\xi_{1R}+\psi_1^-)}{\left[\frac{(k_1^*-l_1^*)^{\frac{1}{2}}}{(k_1^*+l_1)^{\frac{1}{2}}}\cosh(\eta_{1R}+\xi_{1R}+\psi_3^-)+\frac{(k_1+l_1^*)^{\frac{1}{2}}}{(k_1-l_1)^{\frac{1}{2}}}\cosh(\eta_{1R}-\xi_{1R}+\psi_4^-)\right]}, \tag{B1a}$$

$$q_2 \simeq \frac{2A_2^{1-}l_{1R}e^{i(\xi_{1I}+\theta_2^{1-})}\cosh(\eta_{1R}+\psi_2^-)}{\left[\frac{(k_1^*-l_1^*)^{\frac{1}{2}}}{(k_1+l_1^*)^{\frac{1}{2}}}\cosh(\eta_{1R}+\xi_{1R}+\psi_3^-)+\frac{(k_1^*+l_1)^{1/2}}{(k_1-l_1)^{1/2}}\cosh(\eta_{1R}-\xi_{1R}+\psi_4^-)\right]}. \tag{B1b}$$

Here $\psi_1^- = \frac{1}{2}\log\frac{(k_1-l_1)|k_2-l_1|^2|\alpha_1^{(2)}|^2}{(k_1+l_1^*)|k_2+l_1^*|^2(l_1+l_1^*)^2}$, $\psi_2^- = \frac{1}{2}\log\frac{(l_1-k_1)|k_1-k_2|^4|\alpha_1^{(1)}|^2}{(k_1^*+l_1)|k_1+k_2^*|^4(k_1+k_1^*)^2}$, $e^{i\theta_1^{1-}} = \frac{(k_1-k_2)(k_1^*+k_2)}{(k_1^*-k_2^*)(k_1+k_2^*)}$, $\psi_4^- = \frac{1}{2}\log\frac{|k_1-k_2|^4|k_2+l_1^*|^2|\alpha_1^{(1)}|^2(l_1+l_1^*)^2}{|\alpha_1^{(2)}|^2|k_1+k_2^*|^4|k_2-l_1|^2(k_1+k_1^*)^2}$, $\psi_3^- = \frac{1}{2}\log\frac{|k_1-k_2|^4|k_1-l_1|^2|k_2-l_1|^2|\alpha_1^{(2)}|^2|\alpha_1^{(1)}|^2}{|k_1+k_2^*|^4|k_1+l_1^*|^2|k_2+l_1^*|^2(k_1+k_1^*)^2(l_1+l_1^*)^2}$, $e^{i\theta_2^{1-}} = \frac{(k_2-l_1)^{\frac{1}{2}}(k_2^*+l_1)^{\frac{1}{2}}}{(k_2^*-l_1^*)^{\frac{1}{2}}(k_2+l_1^*)^{\frac{1}{2}}}$, $A_1^{1-} = [\alpha_1^{(1)}/\alpha_1^{(1)^*}]^{1/2}$, and $A_2^{1-} = i[\alpha_1^{(2)}/\alpha_1^{(2)^*}]^{1/2}$.

Soliton 2: $(\eta_{2R}, \xi_{2R} \simeq 0,\ \eta_{1R} \to -\infty, \xi_{1R} \to +\infty)$

$$q_1 \simeq \frac{2k_{2R}A_1^{2-}e^{i(\eta_{2I}+\theta_1^{2-})}\cosh(\xi_{2R}+\chi_1^-)}{\left[\frac{(k_2^*-l_2^*)^{\frac{1}{2}}}{(k_2^*+l_2)^{\frac{1}{2}}}\cosh(\eta_{2R}+\xi_{2R}+\chi_3^-)+\frac{(k_2+l_2^*)^{\frac{1}{2}}}{(k_2-l_2)^{\frac{1}{2}}}\cosh(\eta_{2R}-\xi_{2R}+\chi_4^-)\right]}, \tag{B2a}$$

$$q_2 \simeq \frac{2l_{2R}A_2^{2-}e^{i(\xi_{2I}+\theta_2^{2-})}\cosh(\eta_{2R}+\chi_2^-)}{\left[\frac{(k_2^*-l_2^*)^{\frac{1}{2}}}{(k_2+l_2^*)^{\frac{1}{2}}}\cosh(\eta_{2R}+\xi_{2R}+\chi_3^-)+\frac{(k_2^*+l_2)^{\frac{1}{2}}}{(k_2-l_2)^{\frac{1}{2}}}\cosh(\eta_{2R}-\xi_{2R}+\chi_4^-)\right]}. \tag{B2b}$$

In the above,

$$\chi_1^- = \frac{1}{2}\log\frac{|l_1-l_2|^4(k_2-l_2)\left|\alpha_2^{(2)}\right|^2}{|l_1+l_2^*|^4(k_2+l_2^*)(l_2+l_2^*)^2},\ \chi_2^- = \frac{1}{2}\log\frac{|k_2-l_1|^2(l_2-k_2)(l_2+l_1^*)^2\left|\alpha_2^{(1)}\right|^2}{|k_2+l_1^*|^2(k_2^*+l_2)(k_2+k_1^*)^2(k_2+k_2^*)^2},$$

$$e^{i\theta_1^{2-}} = \frac{(k_2-l_1)^{\frac{1}{2}}(k_2^*+l_1)^{\frac{1}{2}}}{(k_2^*-l_1^*)^{\frac{1}{2}}(k_2+l_1^*)^{\frac{1}{2}}},\ e^{i\theta_2^{2-}} = \frac{(l_1-l_2)(l_1+l_2^*)}{(l_1^*-l_2^*)(l_1^*+l_2)},\ A_1^{2-} = \left[\alpha_2^{(1)}/\alpha_2^{(1)^*}\right]^{1/2},$$

$$\chi_3^- = \frac{1}{2}\log\frac{|l_1-l_2|^4|k_2-l_1|^2|k_2-l_2|^2\left|\alpha_2^{(1)}\right|^2\left|\alpha_2^{(2)}\right|^2}{|l_1+l_2^*|^4|k_2+l_1^*|^2|k_2+l_2^*|^2(k_2+k_2^*)^2(l_2+l_2^*)^2},\ A_2^{2-} = \left[\alpha_2^{(2)}/\alpha_2^{(2)^*}\right]^{1/2},$$

$$\chi_4^- = \frac{1}{2}\log\frac{|k_2-l_1|^2|l_1+l_2^*|^4\left|\alpha_2^{(1)}\right|^2(l_2+l_2^*)^2}{\left|\alpha_2^{(2)}\right|^2|k_2+l_1^*|^2|l_1-l_2|^4(k_2+k_2^*)^2}.$$

(b) After collision: $z \to +\infty$

Soliton 1: $(\eta_{1R}, \xi_{1R} \simeq 0,\ \eta_{2R} \to -\infty, \xi_{2R} \to +\infty)$

$$q_1 \simeq \frac{2k_{1R}A_1^{1+}e^{i(\eta_{1I}+\theta_1^{1+})}\cosh(\xi_{1R}+\psi_1^+)}{\left[\frac{(k_1^*-l_1^*)^{\frac{1}{2}}}{(k_1^*+l_1)^{\frac{1}{2}}}\cosh(\eta_{1R}+\xi_{1R}+\psi_3^+)+\frac{(k_1+l_1^*)^{\frac{1}{2}}}{(k_1-l_1)^{\frac{1}{2}}}\cosh(\eta_{1R}-\xi_{1R}+\psi_4^+)\right]}, \tag{B3a}$$

$$q_2 \simeq \frac{2l_{1R}A_1^{2+}e^{i(\xi_{1I}+\theta_2^{1+})}\cosh(\eta_{1R}+\psi_2^+)}{\left[\frac{(k_1^*-l_1^*)^{\frac{1}{2}}}{(k_1+l_1^*)^{\frac{1}{2}}}\cosh(\eta_{1R}+\xi_{1R}+\psi_3^+)+\frac{(k_1^*+l_1)^{\frac{1}{2}}}{(k_1-l_1)^{\frac{1}{2}}}\cosh(\eta_{1R}-\xi_{1R}+\psi_4^+)\right]}. \tag{B3b}$$

Here

$$\psi_1^+ = \frac{1}{2}\log\frac{|l_1-l_2|^4(k_1-l_1)\left|\alpha_1^{(2)}\right|^2}{|l_1+l_2^*|^4(k_1+l_1^*)(l_1+l_1^*)^2},\ \psi_2^+ = \frac{1}{2}\log\frac{|k_1-l_2|^2(l_1-k_1)\left|\alpha_1^{(1)}\right|^2}{|k_1+l_2^*|^2(k_1^*+l_1)(k_1+k_1^*)^2},$$

$$e^{i\theta_1^{1+}} = \frac{(k_1-l_2)^{\frac{1}{2}}(k_1^*+l_2)^{\frac{1}{2}}}{(k_1^*-l_2^*)^{\frac{1}{2}}(k_1+l_2^*)^{\frac{1}{2}}},\ e^{i\theta_2^{1+}} = \frac{(l_1-l_2)(l_1^*+l_2)}{(l_1^*-l_2^*)(l_1+l_2^*)},\ A_1^{1+} = \left[\alpha_1^{(1)}/\alpha_1^{(1)^*}\right]^{1/2}$$

$$\psi_3^+ = \frac{1}{2}\log\frac{|k_1-l_1|^2|k_1-l_2|^2|l_1-l_2|^4|\alpha_1^{(1)}|^2|\alpha_1^{(2)}|^2}{|k_1+l_1^*|^2|k_1+l_2^*|^2|l_1+l_2^*|^4(k_1+k_1^*)^2(l_1+l_1^*)^2},\ A_2^{1+} = \left[\alpha_1^{(2)}/\alpha_1^{(2)^*}\right]^{1/2}$$

$$\psi_4^+ = \frac{1}{2}\log\frac{|k_1-l_2|^2|l_1+l_2^*|^4|\alpha_1^{(1)}|^2(l_1+l_1^*)^2}{|\alpha_1^{(2)}|^2|k_1+l_2^*|^2|l_1-l_2|^4(k_1+k_1^*)^2}.$$

Soliton 2: ($\eta_{2R}, \xi_{2R} \simeq 0,\ \eta_{1R} \to +\infty, \xi_{1R} \to -\infty$)

$$q_1 \simeq \frac{2A_2^{1+}k_{2R}e^{i(\eta_{2I}+\theta_1^{2+})}\cosh(\xi_{2R}+\chi_1^+)}{\left[\frac{(k_2^*-l_2^*)^{\frac{1}{2}}}{(k_2^*+l_2)^{\frac{1}{2}}}\cosh(\eta_{2R}+\xi_{2R}+\chi_3^+)+\frac{(k_2+l_2^*)^{\frac{1}{2}}}{(k_2-l_2)^{\frac{1}{2}}}\cosh(\eta_{2R}-\xi_{2R}+\chi_4^+)\right]}, \tag{B4a}$$

$$q_2 \simeq \frac{2A_2^{2+}l_{2R}e^{i(\xi_{2I}+\theta_2^{2+})}\cosh(\eta_{2R}+\chi_2^+)}{\left[\frac{i(k_2^*-l_2^*)^{\frac{1}{2}}}{(k_2+l_2^*)^{\frac{1}{2}}}\cosh(\eta_{2R}+\xi_{2R}+\chi_3^+)+\frac{(k_2^*+l_2)^{\frac{1}{2}}}{(l_2-k_2)^{\frac{1}{2}}}\cosh(\eta_{2R}-\xi_{2R}+\chi_4^+)\right]}, \tag{B4b}$$

where $\chi_1^+ = \frac{1}{2}\log\frac{(k_2-l_2)|k_1-l_2|^2|\alpha_2^{(2)}|^2}{(k_2+l_2^*)|k_1+l_2^*|^2(l_2+l_2^*)^2}$, $\chi_2^+ = \frac{1}{2}\log\frac{\alpha_1^{(2)}|k_1-k_2|^4(k_1-l_1)(k_2-l_1)(k_1^*+l_2)|\alpha_2^{(1)}|^2}{\alpha_2^{(2)}|k_1+k_2^*|^4(k_1^*+l_1)(k_2^*+l_1)(l_2-k_1)(k_2+k_2^*)^2}$, $e^{i\theta_1^{2+}} = \frac{(k_1-k_2)(k_1+k_2^*)}{(k_1^*-k_2^*)(k_1^*+k_2)}$, $e^{i\theta_2^{2+}} = \frac{(k_1-l_2)^{\frac{1}{2}}(k_1+l_2^*)^{\frac{1}{2}}}{(k_1^*-l_2^*)^{\frac{1}{2}}(k_1^*+l_2)^{\frac{1}{2}}}$, $\chi_3^+ = \frac{1}{2}\log\frac{|k_1-k_2|^4|k_1-l_2|^2|k_2-l_2|^2|\alpha_2^{(1)}|^2|\alpha_2^{(2)}|^2}{|k_1+k_2^*|^4|k_1+l_2^*|^2|k_2+l_2^*|^2(k_2+k_2^*)^2(l_2+l_2^*)^2}$, $A_1^{2+} = [\alpha_2^{(1)}/\alpha_2^{(1)^*}]^{1/2}$, $\chi_4^+ = \frac{1}{2}\log\frac{|k_1-k_2|^4|k_1+l_2^*|^2|\alpha_2^{(1)}|^2(l_2+l_2^*)^2}{|\alpha_2^{(2)}|^2|k_1+k_2^*|^4|k_1-l_2|^2(k_2+k_2^*)^2}$, and $A_2^{2+} = i[\alpha_2^{(2)}/\alpha_2^{(2)^*}]^{1/2}$.

From the above analysis, we find that the structures of individual solitons are invariant before and after collisions except for the terms corresponding to the various phases ψ_j^-, χ_j^-, ψ_j^+, χ_j^+, $j = 1, 2, 3, 4$. For instance, from Eqs. (B1a) and (B3a), the phase terms ψ_j^-, $j = 1, 2, 3, 4$ corresponding to the first soliton in the q_1 mode change into ψ_j^+, $j = 1, 2, 3, 4$, respectively. Similar phase changes take place in the second component of the first soliton and in the structure of the second soliton as well. Consequently, the phase changes leads to the occurrence of shape-changing collision in the unequal velocity case. Therefore, in general, the shape-preserving collision does not occur in the unequal velocity case. However, it can arise when the phase terms obey the following conditions:

$$\psi_j^- = \psi_j^+,\ \chi_j^- = \chi_j^+,\ j = 1, 2, 3, 4. \tag{B5}$$

Using the complicated shape-changing collision property of nondegenerate solitons we could not identify a linear fractional transformation (as in the case of the degenerate case) in order to construct optical logic gates.

APPENDIX C: CONSTANTS WHICH APPEAR IN THE ASYMPTOTIC EXPRESSIONS IN SEC. V

The various constants which arise in the asymptotic analysis of collision between degenerate and nondegenerate solitons in Sec. V are as follows:

$$e^{\Lambda_1} = \frac{i\alpha_1^{(1)}(k_1-k_2)^{\frac{1}{2}}(k_1-l_2)^{\frac{1}{2}}(k_1^*+k_2)^{\frac{1}{2}}(k_1+k_1^*)(k_2+l_2^*)^{\frac{1}{2}}|k_1+l_2^*|^2}{\alpha_2^{(1)}(k_1^*-l_2^*)^{\frac{1}{2}}(k_2^*-l_2^*)^{\frac{1}{2}}}e^{R_5^*+\frac{R_3-R_6}{2}},$$

$$e^{\Lambda_2} = \frac{(k_1-k_2)^{\frac{1}{2}}(k_2^*+l_2)^{\frac{1}{2}}(k_1+k_2^*)\hat{\Lambda}_1\hat{\Lambda}_2}{(k_1^*-k_2^*)^{\frac{1}{2}}(k_2^*-l_2^*)^{\frac{1}{2}}(k_1^*+k_2)},\ e^{\Lambda_3} = \frac{|\alpha_1^{(1)}||\alpha_1^{(2)}|(k_1+k_1^*)(k_2+k_2^*)(l_2+l_2^*)}{|k_2-l_2|},$$

$$e^{\Lambda_4} = \left[|\alpha_1^{(1)}|^2+|\alpha_1^{(2)}|^2\right]^{1/2}\left[|\alpha_1^{(1)}|^2|k_1-k_2|^2|k_1+l_2^*|^2+|\alpha_1^{(2)}|^2|k_1-l_2|^2|k_1+k_2^*|^2\right]^{1/2},$$

$$e^{\Lambda_5} = \frac{|k_2+l_2^*|}{|k_2-l_2|}\left[|\alpha_1^{(1)}|^2|k_1+l_2^*|^2+|\alpha_1^{(2)}|^2|k_1-l_2|^2\right)^{1/2}\left(|\alpha_1^{(1)}|^2|k_1-k_2|^2+|\alpha_1^{(2)}|^2|k_1+k_2^*|^2\right]^{1/2},$$

$$e^{\Lambda_6} = \frac{(k_1-l_2)^{\frac{1}{2}}(k_2+l_2^*)^{\frac{1}{2}}(k_1+l_2^*)\hat{\Lambda}_3\hat{\Lambda}_4}{(k_1^*-l_2^*)^{\frac{1}{2}}(k_2^*-l_2^*)^{\frac{1}{2}}(k_1^*+l_2)},\ \hat{\Lambda}_1 = \left[|\alpha_1^{(1)}|^2(k_1-k_2)-|\alpha_1^{(2)}|^2(k_1^*+k_2)\right]^{1/2},$$

$$e^{\Lambda_7} = \frac{\alpha_1^{(2)}(k_1-k_2)^{\frac{1}{2}}(k_1-l_2)^{\frac{1}{2}}(k_1^*+l_2)^{\frac{1}{2}}(k_1+k_1^*)(k_2^*+l_2)^{\frac{1}{2}}|k_1+k_2^*|^2}{\alpha_2^{(2)}(k_1^*-k_2^*)^{\frac{1}{2}}(k_2^*-l_2^*)^{\frac{1}{2}}}e^{R_2^*+\frac{R_6-R_3}{2}},$$

$$\hat{\Lambda}_2 = \left[|\alpha_1^{(1)}|^2(k_1-k_2)|k_1+l_2^*|^2-|\alpha_1^{(2)}|^2|k_1-l_2|^2(k_1^*+k_2)\right]^{1/2},$$

$$\hat{\Lambda}_4 = \left[|\alpha_1^{(1)}|^2|k_1-k_2|^2(k_1^*+l_2)-|\alpha_1^{(2)}|^2(k_1-l_2)|k_1+k_2^*|^2\right]^{1/2},$$

$$\hat{\Lambda}_3 = \left[|\alpha_1^{(2)}|^2(k_1-l_2)-|\alpha_1^{(1)}|^2(k_1^*+l_2)\right]^{1/2},$$

$$e^{\frac{\Phi_{21}-\Delta_{21}}{2}} = \frac{|\alpha_2^{(1)}|(k_1-k_2)(k_2^*-k_1^*)^{\frac{1}{2}}(k_2-l_2)^{\frac{1}{2}}}{(k_1+k_2^*)(k_2+k_2^*)(k_2+k_1^*)^{\frac{1}{2}}(k_2^*+l_2)^{\frac{1}{2}}},\quad e^{\frac{\lambda_2-\lambda_1}{2}} = \frac{|\alpha_2^{(2)}||k_1-l_2|(k_2-l_2)^{\frac{1}{2}}\hat{\Lambda}_2}{(k_2+l_2^*)^{\frac{1}{2}}|k_1+l_2^*|^2(l_2+l_2^*)\hat{\Lambda}_1},$$

$$e^{\frac{\lambda_5-R}{2}} = \frac{|k_1-k_2||k_1-l_2||k_2-l_2|\hat{\Lambda}_5}{|k_1+k_2^*|^2|k_1+l_2^*|^2|k_2+l_2^*|\left(|\alpha_1^{(1)}|^2+|\alpha_1^{(2)}|^2\right)^{1/2}}e^{\frac{R_3+R_6}{2}},$$

$$e^{\frac{\vartheta_{12}-\varphi_{21}}{2}} = \frac{(k_2-k_1)^{\frac{1}{2}}(k_1^*-l_2^*)^{\frac{1}{2}}(k_2^*+l_2)^{\frac{1}{2}}}{(k_2+l_2^*)^{\frac{1}{2}}(k_2^*-k_1^*)^{\frac{1}{2}}(k_1-l_2)^{\frac{1}{2}}}e^{\frac{R_2^*+R_5-(R_2+R_5^*)}{2}},\quad e^{\frac{\lambda_3-\lambda_4}{2}} = \frac{|k_1-k_2|\hat{\Lambda}_6|k_1+l_2^*|^2e^{\frac{R_3-R_6}{2}}}{|k_1+k_2^*|^2|k_1-l_2|\hat{\Lambda}_7},$$

$$e^{\frac{\Gamma_{21}-\gamma_{21}}{2}} = \frac{(k_2-l_2)^{\frac{1}{2}}(k_1-l_2)(k_1^*-l_2^*)^{\frac{1}{2}}}{(k_2+l_2^*)^{\frac{1}{2}}(k_1+l_2^*)(k_1^*+l_2)^{\frac{1}{2}}}e^{\frac{R_6}{2}},\quad e^{\frac{\lambda_7-\lambda_6}{2}} = \frac{(k_1-k_2)(k_2-l_2)^{\frac{1}{2}}\hat{\Lambda}_4}{|k_1+k_2^*|^2(k_2^*+l_2)^{\frac{1}{2}}\hat{\Lambda}_3}e^{\frac{R_3}{2}},$$

$$\hat{\Lambda}_5 = \left[|\alpha_1^{(1)}|^2|k_1-k_2|^2|k_1+l_2^*|^2+|\alpha_1^{(2)}|^2|k_1-l_2|^2|k_1+k_2^*|^2\right]^{1/2},$$

$$e^{\frac{R'-\varsigma_{22}}{2}} = \frac{|k_1-k_2||k_1-l_2|\hat{\Lambda}_5}{|k_1+k_2^*|^2|k_1+l_2^*|^2(k_1+k_1^*)},\quad e^{\frac{\varsigma_{22}}{2}} = \frac{|k_2-l_2|}{|k_2+l_2^*|}e^{\frac{R_3+R_6}{2}},\quad e^{\frac{R_3-R_6}{2}} = \frac{|\alpha_2^{(1)}|(l_2+l_2^*)}{|\alpha_2^{(2)}|(k_2+k_2^*)},$$

$$\hat{\Lambda}_6 = \left[|\alpha_1^{(1)}|^2|k_1-k_2|^2+|\alpha_1^{(2)}|^2|k_1+k_2^*|^2\right]^{1/2},\quad \hat{\Lambda}_7 = \left[|\alpha_1^{(1)}|^2|k_1+l_2^*|^2+|\alpha_1^{(2)}|^2|k_1-l_2|^2\right]^{1/2},$$

$$e^{\frac{\Lambda_{22}-\rho_1}{2}} = \frac{(k_2-l_2)^{\frac{1}{2}}}{(k_2+l_2^*)^{\frac{1}{2}}}e^{\frac{R_6}{2}},\quad e^{\frac{\mu_{22}-\rho_2}{2}} = \frac{(l_2-k_2)^{\frac{1}{2}}}{(k_2^*+l_2)^{\frac{1}{2}}}e^{\frac{R_3}{2}},\quad e^{R_1} = \frac{|\alpha_1^{(1)}|^2}{(k_1+k_1^*)^2},\quad e^{R_2} = \frac{\alpha_1^{(1)}\alpha_2^{(1)*}}{(k_1+k_2^*)^2},$$

$$e^{R_3} = \frac{|\alpha_2^{(1)}|^2}{(k_2+k_2^*)^2},\quad e^{R_4} = \frac{|\alpha_1^{(2)}|^2}{(k_1+k_1^*)^2},\quad e^{R_5} = \frac{\alpha_1^{(2)}\alpha_2^{(2)*}}{(k_1+l_2^*)^2},\quad e^{R_6} = \frac{|\alpha_2^{(2)}|^2}{(l_2+l_2^*)^2}.$$

APPENDIX D: NUMERICAL STABILITY ANALYSIS CORRESPONDING TO FIGS. 5(a) AND 5(b) UNDER PERTURBATION

In this Appendix, we wish to point out the stability nature of the obtained nondegenerate soliton solutions numerically using Crank-Nicolson procedure [64] even under the addition of suitable white noise or Gaussian noise to the initial conditions. Specifically, we consider the shape-preserving collision of symmetric double-hump solitons discussed in Fig. 5. For this purpose, we have considered the Manakov system (1) with the initial conditions,

$$q_j(-10,t) = [1+A\zeta(t)]q_{j,-10}(t),\ \ j=1,2. \qquad \text{(D1)}$$

In the above, $q_{j,-10}$'s, $j=1,2$, are the initial profile obtained from the nondegenerate two-soliton solution Eqs. (13a)–(13c) at $z=-10$. Here A is the amplitude of the white noise and $\zeta(t)$ represents the noise or fluctuation function. The white noise was created by generating random numbers in the interval $[-1,1]$. To fix the initial profile in the numerical algorithm, we consider the same complex parameter values which are given for the Figs. 5(a) and 5(b) in Sec. IV. We also consider the space and time step sizes, respectively, as $dz=0.1$ and $dt=0.001$ in the numerical algorithm. To study the collision scenario of double-hump solitons [Figs. 17(a) and 17(b)] under perturbation we fix the domain ranges for t and z as $[-45,45]$ and $[-10,10]$, respectively.

First, we consider 10% ($A=0.1$) of random perturbation on the intial solution of the Manakov system. For this strength of perturbation, we observe no significant change in the profile as well as in the dynamics of the nondegenerate solitons apart from a slight change, which is insignificant, in the amplitudes of double-hump solitons after the collision. This is illustrated in Figs. 17(c) and 17(d). Then we study the stability with 20% white noise ($A=0.2$), which is a stronger perturbation, for the double-hump solitons. Such a study is demonstrated

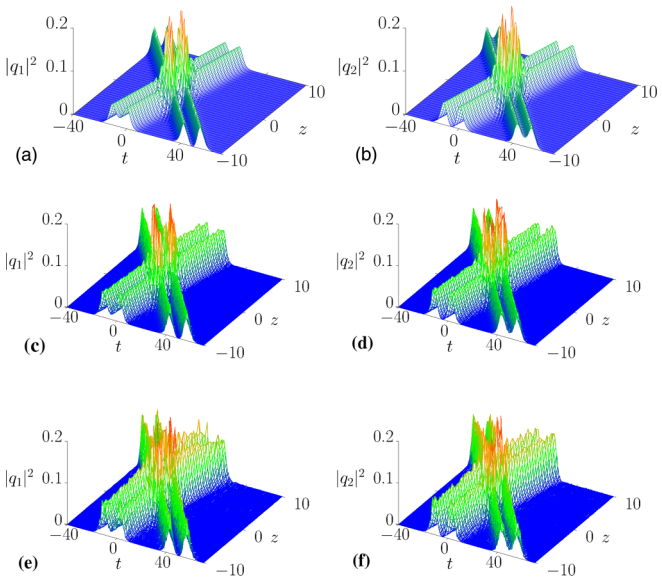

FIG. 17. Numerical plots of shape-preserving collision of nondegenerate symmetric double-hump solitons with 10% and 20% white noise as perturbations. Panels (a) and (b) denote the elastic collision of two symmetric double-hump solitons without perturbation. Panels (c) and (d) denote the collision with 10% white noise. Panels (e) and (f) represent the collision with 20% strong white noise as perturbation.

in Figs. 17(e) and 17(f). The numerical analysis shows that the double-hump soliton profiles still survive after the collision under as strong as 20% perturbation apart from a slight distortion in the amplitudes. This ensures the stability of nondegenerate solitons against perturbations of the above type of noise.

Similarly, we have also verified the stability of nondegenerate solitons with Gaussian noise perturbation as well.

[1] Y. S. Kivshar and G. P. Agrawal, *Optical Solitons: From Fibers to Photonic Crystals* (Academic Press, San Diego, 2003).

[2] G. P. Agrawal, *Applications of Nonlinear Fiber Optics* (Academic Press, San Diego, 2001).

[3] R. Radhakrishnan, M. Lakshmanan, and J. Hietarinta, Phys. Rev. E **56**, 2213 (1997).

[4] T. Kanna and M. Lakshmanan, Phys. Rev. Lett. **86**, 5043 (2001).

[5] M. J. Ablowitz, B. Prinari, and A. D. Trubatch, Inv. Probl. **20**, 1217 (2004).

[6] R. Radhakrishnan and M. Lakshmanan, J. Phys. A: Math. Gen **28**, 2683 (1995).

[7] A. P. Sheppard and Y. S. Kivshar, Phys. Rev. E **55**, 4773 (1997).

[8] M. Vijayajayanthi, T. Kanna, and M. Lakshmanan, Phys. Rev. A **77**, 013820 (2008).

[9] B. F. Feng, J. Phys. A: Math. Theor. **47**, 355203 (2014).

[10] Y. Ohta, D. S. Wang, and J. Yang, Stud. Appl. Math. **127**, 345 (2011).

[11] P. G. Kevrekidis and D. J. Frantzeskakis, Rev. Phys. **1**, 140 (2016).

[12] D. J. Frantzeskakis, J. Phys. A: Math. Theor. **43**, 213001 (2010).

[13] A. C. Scott, Phys. Scr. **29**, 279 (1984).

[14] B. Crosignani, A. Cutolo, and P. D. Porto, J. Opt. Soc. Am. **72**, 1136 (1982).

[15] N. Akhmediev, W. Krolikowski, and A. W. Snyder, Phys. Rev. Lett. **81**, 4632 (1998).

[16] A. Ankiewicz, W. Krolikowski, and N. N. Akhmediev, Phys. Rev. E **59**, 6079 (1999).

[17] N. N. Akhmediev, A. V. Buryak, J. M. Soto-Crespo, and D. R. Andersen, J. Opt. Soc. Am. B **12**, 434 (1995).

[18] D. Y. Tang, H. Zhang, L. M. Zhao, and X. Wu, Phys. Rev. Lett. **101**, 153904 (2008).

[19] H. Zhang, D. Y. Tang, L. M. Zhao, and R. J. Knize, Opt. Express **18**, 4428 (2010).

[20] H. Zhang, D. Y. Tang, L. M. Zhao, and X. Wu, Phys. Rev. A **80**, 045803 (2009).

[21] S. Stalin, R. Ramakrishnan, and M. Lakshmanan, Phys. Lett. A **384**, 126201 (2020).

[22] T. Kanna, M. Vijayajayanthi, and M. Lakshmanan, J. Phys. A: Math. Theor. **43**, 434018 (2010).

[23] T. Kanna and K. Sakkaravarthi, J. Phys. A: Math. Theor. **44**, 285211 (2011).

[24] C. Anastassiou, M. Segev, K. Steiglitz, J. A. Giordmaine, M. Mitchell, M. F. Shih, S. Lan, and J. Martin, Phys. Rev. Lett. **83**, 2332 (1999).

[25] J. U. Kang, G. I. Stegeman, J. S. Aitchison, and N. Akhmediev, Phys. Rev. Lett. **76**, 3699 (1996).

[26] D. Rand, I. Glesk, C. S. Bres, D. A. Nolan, X. Chen, J. Koh, J. W. Fleischer, K. Steiglitz, and P. R. Prucnal, Phys. Rev. Lett. **98**, 053902 (2007).

[27] M. Vijayajayanthi, T. Kanna, K. Murali, and M. Lakshmanan, Phys. Rev. E **97**, 060201(R) (2018).

[28] M. H. Jakubowski, K. Steiglitz, and R. Squier, Phys. Rev. E **58**, 6752 (1998); K. Steiglitz, *ibid.* **63**, 016608 (2000); M. Soljacic, K. Steiglitz, S. M. Sears, M. Segev, M. H. Jakubowski, and R. Squier, Phys. Rev. Lett. **90**, 254102 (2003).

[29] B. A. Kochetov, I. Vasylieva, A. Butrym, and V. R. Tuz, Phys. Rev. E **99**, 052214 (2019).

[30] M. Stratmann, T. Pagel, and F. Mitschke, Phys. Rev. Lett. **95**, 143902 (2005).

[31] P. Rohrmann, A. Hause, and F. Mitschke, Phys. Rev. A **87**, 043834 (2013).

[32] O. Melchert, S. Willms, S. Bose, A. Yulin, B. Roth, F. Mitschke, U. Morgner, I. Babushkin, and A. Demircan, Phys. Rev. Lett. **123**, 243905 (2019).

[33] D. N. Christodoulides and R. I. Joseph, Opt. Lett. **13**, 53 (1988).

[34] M. Karlsson, D. J. Kaup, and B. A. Malomed, Phys. Rev. E **54**, 5802 (1996).

[35] C. R. Menyuk, IEEE J. Quant. Electron. **25**, 2674 (1989).

[36] M. Mitchell, Z. Chen, M. F. Shih, and M. Segev, Phys. Rev. Lett. **77**, 490 (1996); M. Mitchell and M. Segev, Nature (Lond.) **387**, 880 (1997); M. Mitchell, M. Segev, and D. N. Christodoulides, Phys. Rev. Lett. **80**, 4657 (1998).

[37] I. A. Kolchugina V. A. Mironov, and A. M. Sergeev, JETP Lett. **31**, 304 (1980); M. Haelterman and A. P. Sheppard, Phys. Rev. E **49**, 3376 (1994); J. J. M. Soto-Crespo, N. Akhmediev, and A. Ankiewicz, *ibid.* **51**, 3547 (1995); A. D. Boardman, K. Xie, and A. Sangarpaul, Phys. Rev. A **52**, 4099 (1995); D. Michalache, F. L. Lederer, D. Mazilu, and L. C. Crasovan, Opt. Eng. **35**, 1616 (1996); H. He, M. J. Werner, and P. D. Drummond, Phys. Rev. E **54**, 896 (1996).

[38] E. A. Ostrovskaya, Y. S. Kivshar, D. V. Skryabin, and W. J. Firth, Phys. Rev. Lett. **83**, 296 (1999); D. E. Pelinovsky and J. Yang, Stud. Appl. Math. **115**, 109 (2005).

[39] J. Yang, Physica D **108**, 92 (1997).

[40] G. Herink, F. Kurtz, B. Jalali, D. R. Solli, and C. Ropers, Science **356**, 50 (2017).

[41] S. Stalin, R. Ramakrishnan, M. Senthilvelan, and M. Lakshmanan, Phys. Rev. Lett. **122**, 043901 (2019).

[42] See Supplemental Material at http://link.aps.org/supplemental/10.1103/PhysRevLett.122.043901 for $k_{1R} < l_{1R}$ the symmetric and asymmetric nature of nondegenerate one-soliton solution are discussed.

[43] Y. H. Qin, L. C. Zhao, and L. Ling, Phys. Rev. E **100**, 022212 (2019).

[44] S. V. Manakov, Zh. Eksp. Teor. Fiz. **67**, 543 (1974) [Sov. Phys. JETP **38**, 248 (1974)].

[45] M. J. Ablowitz, B. Prinari, and A. D. Trubatch, *Discrete and Continuous Nonlinear Schrödinger Systems* (Cambridge University Press, Cambridge, UK, 2003).

[46] R. Radhakrishnan, R. Sahadevan, and M. Lakshmanan, Chaos, Solitons Fract. **5**, 2315 (1995).

[47] R. Hirota, *The Direct Method in Soliton Theory* (Cambridge University Press, Cambridge, UK, 2004).

[48] N. Akhmediev and A. Ankiewicz, *Solitons: Nonlinear Pulses and Beams* (Chapman & Hall, London, 1997).

[49] R. Ramakrishnan, S. Stalin, and M. Lakshmanan (unpublished).
[50] A. W. Snyder and D. J. Mitchell, Phys. Rev. Lett. **80**, 1422 (1998).
[51] A. Hasegawa, Phys. Fluids **20**, 2155 (1977).
[52] T. Kanna and M. Lakshmanan, Phys. Rev. E **67**, 046617 (2003).
[53] Z. Y. Sun, Y. T. Gao, X. Yu, W. J. Liu, and Y. Liu, Phys. Rev. E **80**, 066608 (2009).
[54] Ph. Grelu and N. Akhmediev, Nat. Photon. **6**, 84 (2012).
[55] N. Akhmediev, J. M. Soto-Crespo, M. Grapinet, and Ph. Grelu, Opt. Fibre Technol. **11**, 209 (2005).
[56] Ph. Grelu and N. Akhmediev, Opt. Express **12**, 3184 (2004).
[57] Y. F. Song, L. Li, H. Zhang, D. Y. Shen, D. Y. Tang, and K. P. Loh, Opt. Express **21**, 10010 (2013).
[58] H. Zhang, D. Y. Tang, L. Zhao, Q. Bao, and K. P. Loh, Opt. Commun. **283**, 3334 (2010).
[59] Y. Song, X. Shi, C. Wu, H. Zhang, and D. Y. Tang, Appl. Phys. Rev. **6**, 021313 (2019).
[60] T. Kanna, M. Lakshmanan, P. T. Dinda, and N. Akhmediev, Phys. Rev. E **73**, 026604 (2006).
[61] X. Liu, X. Yao, and Y. Cui, Phys. Rev. Lett. **121**, 023905 (2018).
[62] K. Krupa, K. Nithyanandan, U. Andral, P. Tchofo-Dinda, and P. Grelu, Phys. Rev. Lett. **118**, 243901 (2017).
[63] G. Xu, A. Gelash, A. Chabchoub, V. Zakharov, and B. Kibler, Phys. Rev. Lett. **122**, 084101 (2019).
[64] P. Muruganandam and S. K. Adhikari, Comput. Phys. Commun. **180**, 1888 (2009).

Letters

IOP Publishing

Journal of Physics A: Mathematical and Theoretical

J. Phys. A: Math. Theor. **54** (2021) 14LT01 (11pp)

https://doi.org/10.1088/1751-8121/abe6bb

Letter

Multihumped nondegenerate fundamental bright solitons in *N*-coupled nonlinear Schrödinger system

R Ramakrishnan, S Stalin* and M Lakshmanan

Department of Nonlinear Dynamics, Bharathidasan University, Tiruchirappalli-620024, Tamilnadu, India

E-mail: stalin.cnld@gmail.com and lakshman.cnld@gmail.com

Received 28 November 2020, revised 10 February 2021
Accepted for publication 16 February 2021
Published 19 March 2021

Abstract

In this letter we report the existence of nondegenerate fundamental bright soliton solution for coupled multi-component nonlinear Schrödinger equations of Manakov type. To derive this class of nondegenerate vector soliton solutions, we adopt the Hirota bilinear method with appropriate general class of seed solutions. Very interestingly the obtained nondegenerate fundamental soliton solution of the *N*-coupled nonlinear Schrödinger (CNLS) system admits multi-hump natured intensity profiles. We explicitly demonstrate this specific property by considering the nondegenerate soliton (NDS) solutions for 3 and 4-CNLS systems. We also point out the existence of a special class of partially NDS solutions by imposing appropriate restrictions on the wavenumbers in the already obtained completely NDS solution. Such class of soliton solutions can also exhibit multi-hump profile structures. Finally, we present the stability analysis of nondegenerate fundamental soliton of the 3-CNLS system as an example. The numerical results confirm the stability of triple-humped profile nature against perturbations of 5% and 10% white noise. The multi-hump nature of nondegenerate fundamental soliton solution will be useful in multi-level optical communication applications with enhanced flow of data in multi-mode fibers.

Keywords: Hirota bilinear method, nondegenerate solitons, degenerate solitons, vector bright solitons, coupled nonlinear Schrödinger equations

(Some figures may appear in colour only in the online journal)

Multi-level optical communication with high bit-rate data transmission is a hotly debated topic and is a challenging task in optical communication applications. Using wavelength division multiplexing scheme, the conventional binary data transmission approaches its limit [1],

*Author to whom any correspondence should be addressed.

where the maximum data-carrying rate of the fiber is restricted by Shannon's theorem [2] due to channel capacity crunch. In the conventional binary data coding, the presence of light pulse is represented by logical '1' and logical '0' corresponds to its absence. However, the demand for fiber's information carrying capacity is increasing day by day. To improve the underlying technology it has been proposed that soliton assisted fiber-optic telecommunication will play a crucial role in determining the future communication systems. Several coding schemes have been proposed in the past to develop this technology: for example, solitons [3], which are stable localized nonlinear wave solutions of nonlinear Schrödinger equation, are being proposed as constituting a model for optical pulse propagation in fibers as natural bits for coding the information. Recently, the existence of soliton molecules in dispersion-managed fiber [4] has been demonstrated and their possible usefulness in optical telecommunications technology with enhanced data carrying capacity has been pointed out [5]. Soliton molecule is a bound soliton state which can be formed when two antiphase solitons persist at a stable equilibrium separation distance, where the interaction force is null among the individuals. Such stable equilibrium manifests this bound state structure, reminiscent of a diatomic molecule in condensed matter physics. The binding force arises between the constituents of the soliton compound due to the Kerr nonlinearity [6, 7] and the detailed mechanism can be found in reference [8]. The existence of two-pulse and three-pulse molecules complete the next level of alphabet of symbols. Such soliton molecules allow coding of two-bits of information simultaneously in a single time slot. In this way, the soliton molecules increase the flow of data in fibers. It should be noted here that the initial shape (symmetric peaks with equal intensities) of soliton molecules changes due to various losses in the fiber and its intrinsic nonlinearities. However, their fundamental properties do not change during the evolution. Apart from the above, the concept of soliton molecules has been discussed earlier in detail in the context of non-dispersion managed fiber [9–11] and in fiber lasers [12–14]. In addition to the above, multi-soliton complexes in multimode fibers have also been discussed for increasing the bit-rate in multi-level coding of information [15–17].

Very recently we have identified a new class of nondegenerate vector bright solitons [18], with double-hump nature characterized by two distinct wavenumbers, for the Manakov system [19]. Basically the Manakov system is a model for propagation of orthogonally polarized optical waves in birefringent fiber, where the solitons undergo collision without energy redistribution in general among the modes depending upon the choice of soliton parameters [18, 20]. However, they encounter shape changing collision for suitable choice of parameters whenever they interact with themselves or when they collide with degenerate vector brights solitons, that is solitons with single-peak intensity profile described by identical wavenumbers in both the modes [21]. Such nondegenerate solitons (NDSs) exhibit multi-hump profiles, as we describe below in the present letter, in the case of N-coupled nonlinear Schrödinger (CNLS) system which may be relevant for optical communication applications. By exploiting the multi-peaks, with different peak powers, the nature of NDSs can be made useful to code the two bits of information as described in [1] in the next level of binary coding. To the best of our knowledge study on NDSs in multi-mode fibers or fiber arrays is missing in the literature and their existence in multi-component nonlinear Schrödinger system and their usefulness in the context of higher bit-rate information transmission applications have not been reported. In addition, the underlying interesting analytical forms of NDSs and their geometrical profiles have not been revealed so far in the literature and they need to be analysed in detail.

In this letter, we intend to investigate the multi-hump nature of nondegenerate fundamental solitons in the following system of multi-component nonlinear Schrödinger equations

$$\mathrm{i}q_{j,z} + q_{j,tt} + 2\sum_{p=1}^{N} |q_p|^2 q_j = 0, \quad j = 1, 2, \ldots, N, \tag{1}$$

by deriving their analytical forms through Hirota bilinear method. Equation (1) describes the optical pulse propagation in N-mode optical fibers [22] and it describes the incoherent light beam propagation in photorefractive medium [16] and so on. In the above, q_j's are complex wave envelopes propagating in N-optical modes and z and t represent the normalized distance and retarded time, respectively. We note that for $N = 2$ in equation (1), we have studied the collision and stability properties of the NDSs [21] and also we have identified their existence in other integrable nonlinear Schrödinger family of equations by revealing their analytical forms [23]. To derive the exact form of the nondegenerate fundamental soliton solution for the N-CNLS system, we bilinearize equation (1) through the dependent variable transformation, $q_j(z,t) = \frac{g^{(j)}(z,t)}{f(z,t)}$, $j = 1, 2, \ldots, N$ where $g^{(j)}$'s are in general complex functions and f is a real function. Substitution of this transformation in equation (1) brings out the following bilinear forms: $(\mathrm{i}D_z + D_t^2)g^{(j)} \cdot f = 0$ and $D_t^2 f \cdot f = 2(\sum_{n=1}^{N} g^{(n)} \cdot g^{(n)*})$. Here D_z and D_t are the usual Hirota bilinear operators [24]. Then we consider the standard Hirota series expansions $g^{(j)} = \epsilon g_1^{(j)} + \epsilon^3 g_3^{(j)} + \cdots$, $j = 1, 2, \ldots, N$ and $f = 1 + \epsilon^2 f_2 + \epsilon^4 f_4 + \cdots$ in the solution construction process.

To obtain the nondegenerate fundamental soliton solution of equation (1) we consider the general forms of N-seed solutions, $g^{(j)} = \alpha_1^{(j)} \mathrm{e}^{\eta_j}$, $\eta_j = k_j t + \mathrm{i}k_j^2 z$, where $\alpha_1^{(j)}$ and k_j, $j = 1, 2, \ldots, N$ are complex parameters and are nonidentical in general to the N-independent linear partial differential equations, $\mathrm{i}g_{1,z}^{(j)} + g_{1,tt}^{(j)} = 0$, $j = 1, 2, \ldots, N$, which arise at the lowest order of ϵ. With such general choices of seed solutions, we proceed to solve the resulting inhomogeneous linear partial differential equations successively in order to deduce the full series solution up to $g_{2N-1}^{(j)}$ in $g^{(j)}$ and f_{2N} in f. By combining the obtained forms of the unknown functions as per the series expansions we find a rather complicated form of the nondegenerate fundamental soliton solution for the N-CNLS equation. However, we have managed to rewrite it in a more compact form using the following Gram determinants [25, 26],

$$g^{(N)} = \begin{vmatrix} A & I & \phi \\ -I & B & \mathbf{0}^{\mathrm{T}} \\ \mathbf{0} & C_N & 0 \end{vmatrix}, \qquad f = \begin{vmatrix} A & I \\ -I & B \end{vmatrix}, \tag{2}$$

where the elements of the matrices A and B are

$$A_{ij} = \frac{\mathrm{e}^{\eta_i + \eta_j^*}}{(k_i + k_j^*)}, \qquad B_{ij} = \kappa_{ji} = \frac{\psi_i^\dagger \sigma \psi_j}{(k_i^* + k_j)},$$
$$C_N = -\left(\alpha_1^{(1)}, \alpha_1^{(2)}, \ldots, \alpha_1^{(N)}\right),$$
$$\psi_j = \left(\alpha_1^{(1)}, \alpha_1^{(2)}, \ldots, \alpha_1^{(j)}\right)^{\mathrm{T}},$$
$$\phi = \left(\mathrm{e}^{\eta_1}, \mathrm{e}^{\eta_2}, \ldots, \mathrm{e}^{\eta_n}\right)^{\mathrm{T}}, \quad j, n = 1, 2, \ldots, N.$$

In the above, $g^{(N)}$ and f are $((2^2N) + 1)$ and (2^2N)th order determinants, T represents the transpose of the matrices ψ_j and ϕ, $\dagger$ denotes transpose complex conjugate, $\sigma = I$ is an $(n \times n)$ identity matrix, ϕ denotes $(n \times 1)$ column matrix, $\mathbf{0}$ is a $(1 \times n)$ null matrix, C_N is a (1

$\times\ n$) row matrix and ψ represents a $(n \times 1)$ column matrix. In the above expressions, for the nondegenerate fundamental soliton solution the elements κ_{ji}'s do not exist ($\kappa_{ji} = 0$) in the square matrix B when $j \neq i$. Also for a given set of N and j values the corresponding elements only exist and all the other elements are equal to zero in C_N and ψ_j matrices (we have demonstrated the latter clearly for the three-component case below). We have verified the validity of the nondegenerate fundamental soliton solution (2) by substituting it in the bilinear equations of equation (1) along with the following derivative formula of the determinants, $\frac{\partial M}{\partial x} = \sum_{1\leqslant i,j\leqslant n} \frac{\partial a_{i,j}}{\partial x}\frac{\partial M}{\partial a_{i,j}} = \sum_{1\leqslant i,j\leqslant n} \frac{\partial a_{i,j}}{\partial x}\Delta_{i,j}$, where $\Delta_{i,j}$'s are the cofactors of the matrix M, the bordered determinant properties and the elementary properties of the determinants [24]. This action yields a pair of Jacobi identities and thus their occurrence confirms the validity of the obtained soliton solution. Multi-hump profile nature is a special feature of the obtained nondegenerate fundamental soliton solution (2). Such multi-hump structures and their propagation are characterized by $2N$ arbitrary complex wave parameters. The fundamental NDS admits a very interesting N-hump profile in the present N-CNLS system. In this system, in general, the NDSs propagate with different velocities in different modes but one can make them to propagate with identical velocity by restricting the imaginary parts of all the wave numbers k_j, $j = 1, 2, \ldots, N$, to be equal. Interestingly, in 1976, Nogami and Warke have obtained soliton solution for the multicomponent CNLS system [29]. We note that their soliton solution corresponds to the so called partially coherent soliton (PCS) which can be checked after replacing the function $e_j = \exp(k_j x)$ by $e_j = \sqrt{2k_j a_j}\,\exp(k_j \bar{x}_j)$, where $\bar{x}_j = x - x_j$, $a_j = \Pi_{j\neq i} c_{ij}$, $c_{ij} = \frac{k_i + k_j}{|k_i - k_j|}$ and k_j's are real constants, in their solution [30]. Since, the stationary N-PCS solution arises from our solution (2) under the parametric restrictions $\alpha_1^{(j)} = \mathrm{e}^{\eta_{j0}}$, $j = 1, 3, 4, \ldots, N$ and $\alpha_1^{(2)} = -\mathrm{e}^{\eta_{20}}$, ($\eta_{j0}$: real), $k_j = k_{jR}$, $k_{jI} = 0$, $j = 1, 2, \ldots, N$, the solution of Nogami and Warke [29] and its time dependent version are essentially special cases of our general solution (2).

It is interesting to note that if we set all the wavenumbers k_j, $j = 1, 2, \ldots, N$, as identical, $k_j = k_1$, $j = 1, 2, \ldots, N$, which corresponds to the seed solutions getting restricted as $g^{(j)} = \alpha_1^{(j)}\,\mathrm{e}^{\eta_1}$, $\eta_1 = k_1 t + \mathrm{i}k_1^2 z$, for all $j = 1, 2, \ldots, N$, in the fundamental soliton solution (2), the resultant form gets reduced to the following degenerate soliton (DS) solution for equation (1) [27, 28] as

$$(q_1, q_2, q_3, \ldots, q_N)^{\mathrm{T}} = (A_1, A_2, A_3, \ldots, A_N)^{\mathrm{T}} k_{1R}\,\mathrm{e}^{\mathrm{i}\eta_{1I}}\,\mathrm{sech}\left(\eta_{1R} + \frac{R}{2}\right), \tag{3}$$

where $\eta_{1R} = k_{1R}(t - 2k_{1I}z)$, $A_j = \alpha_1^{(j)}/\Delta$ and $\Delta = ((\sum_{j=1}^{N} |\alpha_1^{(j)}|^2))^{1/2}$. Here $\alpha_1^{(j)}$, k_1, $j = 1, 2, \ldots, N$, are arbitrary complex parameters. Further, $k_{1R}A_j$ gives the amplitude of the jth mode, $\frac{R}{2}(= \frac{1}{2}\log\frac{\Delta}{(k_1 + k_1^*)^2})$ denotes the central position of the soliton and $2k_{1I}$ is the soliton velocity [28]. It is evident that the DS solution (3) always admits single-hump structure. Using this single peak intensity or power profile as signal in binary coding one cannot improve higher bit-rate in information transmission as pointed out in [4] whereas this class of DSs interestingly exhibit energy exchanging collision leading to the construction of all optical logic gates [31]. To enhance the bit-rate multi-hump pulses with symmetric and asymmetric profiles, as we describe below for 3 and 4-CNLS systems as examples, can be useful for optical communication.

In order to show the multi-hump nature of the NDS, here we demonstrate such special feature in the case of 3-CNLS and 4-CNLS systems. To start with, we consider the three CNLS equation ($N = 3$ in equation (1)). To get the nondegenerate fundamental soliton solution for this system, we consider the solutions, $g_1^{(1)} = \alpha_1^{(1)}\,\mathrm{e}^{\eta_1}$, $g_1^{(2)} = \alpha_1^{(2)}\,\mathrm{e}^{\eta_2}$ and $g_1^{(3)} = \alpha_1^{(3)}\,\mathrm{e}^{\eta_3}$ as seed solutions to the lowest order linear PDEs. These general form of seed solutions terminates the

series expansions as $g^{(j)} = \epsilon g_1^{(j)} + \epsilon^3 g_3^{(j)} + \epsilon^5 g_5^{(j)}$, $j = 1, 2, 3$ and $f = 1 + \epsilon^2 f_2 + \epsilon^4 f_4 + \epsilon^6 f_6$. By rewriting the explicit forms of the obtained unknown functions in terms of Gram determinants we get the resultant forms similar to the one (equation (2)) reported above for the N-component case. We find that for the 3-CNLS system the matrices A and B are constituted by the elements, A_{ij} and B_{ij}, $i, j = 1, 2, 3$ and also the other matrices C_N, ψ_j and ϕ are deduced as $C_1 = \begin{pmatrix}\alpha_1^{(1)} & 0 & 0\end{pmatrix}$, $C_2 = \begin{pmatrix}0 & \alpha_1^{(2)} & 0\end{pmatrix}$, $C_3 = \begin{pmatrix}0 & 0 & \alpha_1^{(3)}\end{pmatrix}$, $\psi_1 = \begin{pmatrix}\alpha_1^{(1)} & 0 & 0\end{pmatrix}^{\mathrm{T}}$, $\psi_2 = \begin{pmatrix}0 & \alpha_1^{(2)} & 0\end{pmatrix}^{\mathrm{T}}$, $\psi_3 = \begin{pmatrix}0 & 0 & \alpha_1^{(3)}\end{pmatrix}^{\mathrm{T}}$ and $\phi = \begin{pmatrix}\mathrm{e}^{\eta_1} & \mathrm{e}^{\eta_2} & \mathrm{e}^{\eta_3}\end{pmatrix}^{\mathrm{T}}$. From the resultant Gram-determinant forms, we deduce the following triple-humped nondegenerate fundamental soliton solution for the 3-CNLS system,

$$
\begin{aligned}
q_1 &= \frac{1}{f}\mathrm{e}^{\mathrm{i}\eta_{1I}}\left(\mathrm{e}^{\frac{\Delta_{51}+\rho_{11}}{2}}\cosh\left(\eta_{2R}+\eta_{3R}+\frac{\phi_1}{2}\right)+\mathrm{e}^{\frac{\Delta_{11}+\Delta_{21}}{2}}\cosh\left(\eta_{2R}-\eta_{3R}+\frac{\phi_2}{2}\right)\right),\\
q_2 &= \frac{1}{f}\mathrm{e}^{\mathrm{i}\eta_{2I}}\left(\mathrm{e}^{\frac{\Delta_{52}+\rho_{12}}{2}}\cosh\left(\eta_{1R}+\eta_{3R}+\frac{\psi_1}{2}\right)+\mathrm{e}^{\frac{\Delta_{12}+\Delta_{22}}{2}}\cosh\left(\eta_{1R}-\eta_{3R}+\frac{\psi_2}{2}\right)\right),\\
q_3 &= \frac{1}{f}\mathrm{e}^{\mathrm{i}\eta_{3I}}\left(\mathrm{e}^{\frac{\Delta_{53}+\rho_{13}}{2}}\cosh\left(\eta_{1R}+\eta_{2R}+\frac{\chi_1}{2}\right)+\mathrm{e}^{\frac{\Delta_{13}+\Delta_{23}}{2}}\cosh\left(\eta_{1R}-\eta_{2R}+\frac{\chi_2}{2}\right)\right),\\
f &= \mathrm{e}^{\frac{\delta_7}{2}}\cosh\left(\eta_{1R}+\eta_{2R}+\eta_{3R}+\frac{\delta_7}{2}\right)+\mathrm{e}^{\frac{\delta_1+\delta_6}{2}}\cosh\left(\eta_{1R}-\eta_{2R}-\eta_{3R}+\frac{\delta_1-\delta_6}{2}\right)\\
&\quad+\mathrm{e}^{\frac{\delta_2+\delta_5}{2}}\cosh\left(\eta_{2R}-\eta_{1R}-\eta_{3R}+\frac{\delta_2-\delta_5}{2}\right)+\mathrm{e}^{\frac{\delta_3+\delta_4}{2}}\cosh\left(\eta_{3R}-\eta_{1R}-\eta_{2R}+\frac{\delta_3-\delta_4}{2}\right),
\end{aligned}
\tag{4}
$$

where $\eta_{jR} = k_{jR}(t - 2k_{jI}z)$, $j = 1, 2, 3$, $\phi_1 = \Delta_{51} - \rho_{11}$, $\phi_2 = \Delta_{11} - \Delta_{21}$, $\psi_1 = \Delta_{52} - \rho_{12}$, $\psi_2 = \Delta_{12} - \Delta_{22}$, $\chi_1 = \Delta_{53} - \rho_{13}$, $\chi_2 = \Delta_{13} - \Delta_{23}$, $\rho_{1j} = \log\alpha_1^{(j)}$, $j = 1, 2, 3$, and the other constants given above are $\mathrm{e}^{\delta_1} = \frac{|\alpha_1^{(1)}|^2}{\Lambda_{11}}$, $\mathrm{e}^{\delta_2} = \frac{|\alpha_1^{(2)}|^2}{\Lambda_{22}}$, $\mathrm{e}^{\delta_3} = \frac{|\alpha_1^{(3)}|^2}{\Lambda_{33}}$, $\mathrm{e}^{\Delta_{11}} = \frac{\alpha_1^{(1)}\varrho_{12}}{\lambda_{12}}\mathrm{e}^{\delta_2}$, $\mathrm{e}^{\Delta_{21}} = \frac{\alpha_1^{(1)}\varrho_{13}}{\lambda_{13}}\mathrm{e}^{\delta_3}$, $\mathrm{e}^{\Delta_{12}} = -\frac{\alpha_1^{(2)}\varrho_{13}}{\lambda_{12}^*}\mathrm{e}^{\delta_1}$, $\mathrm{e}^{\Delta_{22}} = \frac{\alpha_1^{(2)}\varrho_{23}}{\lambda_{23}}\mathrm{e}^{\delta_3}$, $\mathrm{e}^{\Delta_{13}} = -\frac{\alpha_1^{(3)}\varrho_{13}}{\lambda_{13}^*}\mathrm{e}^{\delta_1}$, $\mathrm{e}^{\Delta_{23}} = -\frac{\alpha_1^{(3)}\varrho_{23}}{\lambda_{23}^*}\mathrm{e}^{\delta_2}$, $\mathrm{e}^{\delta_4} = \frac{|\varrho_{12}|^2}{|\lambda_{12}|^2}\mathrm{e}^{\delta_1+\delta_2}$, $\mathrm{e}^{\delta_5} = \frac{|\varrho_{13}|^2}{|\lambda_{13}|^2}\mathrm{e}^{\delta_1+\delta_3}$, $\mathrm{e}^{\delta_6} = \frac{|\varrho_{23}|^2}{|\lambda_{23}|^2}\mathrm{e}^{\delta_2+\delta_3}$, $\mathrm{e}^{\delta_7} = \frac{|\varrho_{12}|^2|\varrho_{13}|^2|\varrho_{23}|^2}{|\lambda_{12}|^2|\lambda_{13}|^2|\lambda_{23}|^2}\mathrm{e}^{\delta_1+\delta_2+\delta_3}$, $\mathrm{e}^{\Delta_{51}} = \frac{\alpha_1^{(1)}\varrho_{12}\varrho_{13}|\varrho_{23}|^2}{\lambda_{12}\lambda_{13}|\lambda_{23}|^2}\mathrm{e}^{\delta_2+\delta_3}$, $\mathrm{e}^{\Delta_{52}} = -\frac{\alpha_1^{(2)}\varrho_{12}|\varrho_{13}|^2\varrho_{23}}{\lambda_{12}^*|\lambda_{13}|^2\lambda_{23}}\mathrm{e}^{\delta_1+\delta_3}$, $\mathrm{e}^{\Delta_{53}} = \frac{\alpha_1^{(3)}|\varrho_{12}|^2\varrho_{13}\varrho_{23}}{|\lambda_{12}|^2\lambda_{13}^*\lambda_{23}^*}\mathrm{e}^{\delta_1+\delta_2}$, $\Lambda_{11} = (k_1 + k_1^*)^2$, $\Lambda_{22} = (k_2 + k_2^*)^2$, $\Lambda_{33} = (k_3 + k_3^*)^2$, $\varrho_{12} = (k_1 - k_2)$, $\varrho_{13} = (k_1 - k_3)$, $\varrho_{23} = (k_2 - k_3)$, $\lambda_{12} = (k_1 + k_2^*)$, $\lambda_{13} = (k_1 + k_3^*)$ and $\lambda_{23} = (k_2 + k_3^*)$. The above nontrivial soliton solution is described by six arbitrary complex parameters, $\alpha_1^{(j)}$, k_j, $j = 1, 2, 3$. As a specific example, we can easily check that such multi-parameter solution admits a novel asymmetric triple-hump profile when we fix the velocity as $k_{1I} = k_{2I} = k_{3I} = 0.5$. The other parameter values are chosen as $k_{1R} = 0.53$, $k_{2R} = 0.5$, $k_{3R} = 0.45$, $\alpha_1^{(1)} = 0.65 + 0.65\mathrm{i}$, $\alpha_1^{(2)} = 0.45 - 0.45\mathrm{i}$ and $\alpha_1^{(3)} = 0.35 + 0.35\mathrm{i}$. In figure 1(a), we display the asymmetric triple-hump profiles in all the components for the above choice of parameter values. It is important to note that for the specific choice of parameter values, the solution (4) also exhibits symmetric triple-hump soliton profile. The symmetric and asymmetric nature of solution (4)

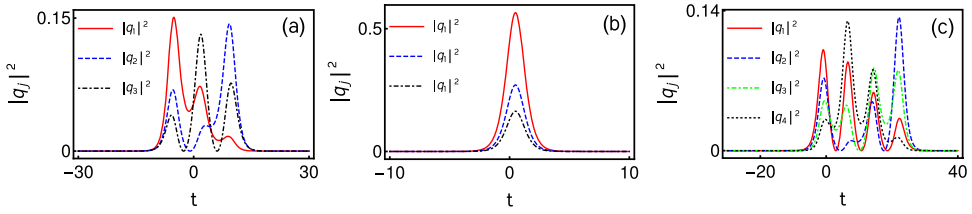

Figure 1. (a) Denotes triple-hump profiles of nondegenerate fundamental soliton in the 3-CNLS system and (b) is its corresponding single-humped DS profile. (c) Represents a quadruple-humped NDS profiles in 4-CNLS system. The specific values of the soliton parameters are given in the text.

can be identified by calculating the following relative separation distances between the solitons of the modes,

$$\Delta t_{12} = t_1 - t_2 = \frac{1}{2}\log\frac{|\alpha_1^{(1)}|^2(k_{3R}-k_{1R})(k_{2R}+k_{3R})k_{2R}^2}{|\alpha_1^{(2)}|^2(k_{2R}-k_{3R})(k_{1R}+k_{3R})k_{1R}^2}, \tag{5a}$$

$$\Delta t_{13} = t_1 - t_3 = \frac{1}{2}\log\frac{|\alpha_1^{(1)}|^2(k_{1R}-k_{2R})(k_{2R}+k_{3R})k_{3R}^2}{|\alpha_1^{(3)}|^2(k_{2R}-k_{3R})(k_{1R}+k_{2R})k_{1R}^2}, \tag{5b}$$

$$\Delta t_{23} = t_2 - t_3 = \frac{1}{2}\log\frac{|\alpha_1^{(2)}|^2(k_{2R}-k_{1R})(k_{1R}+k_{3R})k_{3R}^2}{|\alpha_1^{(3)}|^2(k_{1R}-k_{3R})(k_{1R}+k_{2R})k_{2R}^2}. \tag{5c}$$

It is evident from equations (5a)–(5c) the solution (4), with $k_{1I} = k_{2I} = k_{3I}$, always admits asymmetric triple-hump profiles when $\Delta t_{12} = \Delta t_{13} = \Delta t_{23} \neq 0$. In contrast to this, almost symmetric (not perfect symmetric) triple-hump profile arises in all the modes when the soliton parameters obey the condition, $\Delta t_{12} = \Delta t_{13} = \Delta t_{23} \to 0$. The double node (or multi-node) formation occurs when the relative velocities among the solitons of the modes, q_j's $j = 1, 2, 3$, do not tend to zero. Such node formation is demonstrated in figure 2 for the unequal velocity case (of the modes) in the present 3-CNLS system. We wish to point out here that the triple peak power profiles obeying the above relative separation distance condition, both symmetric and asymmetric, could be useful in the launching of the initial signal in binary coding scheme. In the practical situation the initial profiles can vary their shape due to fiber's loss and nonlinear higher order effects. This situation cannot be avoided in a fiber. However, the solution (4) retains the fundamental property, namely the triple-hump soliton profile, of the NDS during the evolution along the fiber. It is interesting to note that when we impose the condition $k_1 = k_2 = k_3$ in the solution (4), it turns out to be a single-humped degenerate fundamental soliton for the 3-CNLS system. This can be seen from figure 1(b) for the values $k_1 = k_2 = k_3 = 1 + \mathrm{i}$, $\alpha_1^{(1)} = 0.65 + 0.65\mathrm{i}$, $\alpha_1^{(2)} = 0.45 - 0.45\mathrm{i}$ and $\alpha_1^{(3)} = 0.35 + 0.35\mathrm{i}$. We note that the three-PCS or multi-soliton complexes arise from the nondegenerate fundamental soliton solution (4) of the 3-CNLS system when the soliton parameters are fixed as $\alpha_1^{(1)} = \mathrm{e}^{\eta_{10}}$, $\alpha_1^{(2)} = -\mathrm{e}^{\eta_{20}}$, $\alpha_1^{(3)} = \mathrm{e}^{\eta_{30}}$, $k_1 = k_{1R}$, $k_2 = k_{2R}$, $k_3 = k_{3R}$ and $k_{jI} = 0$, $j = 1, 2, 3$, where η_{j0}, $j = 1, 2, 3$, are considered as real constants [15, 28].

Next we illustrate the multi-hump nature of NDS in the 4-CNLS system. To obtain such solution one has to proceed with the analysis for the $N = 4$ case, as we have described in the above three-component case. For brevity, we do not give the details of the final solution due to its complex nature. However, one can easily deduce the form of the solution from the soliton solution of the N-component case, equation (2), as given above. The final solution

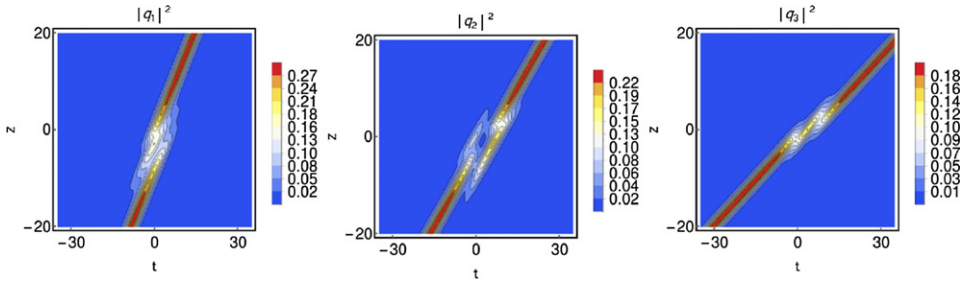

Figure 2. Double-node formation in the unequal velocities case in the profile of nondegenerate fundamental soliton in 3-CNLS system. The parameter values are $k_1 = 0.55 + 0.35\mathrm{i}$, $k_2 = 0.5 + 0.5\mathrm{i}$, $k_3 = 0.45 + 0.8\mathrm{i}\alpha_1^{(1)} = 0.65 + 0.65\mathrm{i}$, $\alpha_1^{(2)} = 0.45 - 0.45\mathrm{i}$ and $\alpha_1^{(3)} = 0.35 + 0.35\mathrm{i}$.

contains eight arbitrary complex parameters, namely $\alpha_1^{(j)}$ and k_j, $j = 1, 2, 3, 4$. These parameters play a significant role in determining the profile nature of the underlying soliton in the four-component case. In general, the nondegenerate one-soliton solution in the 4-CNLS system exhibits asymmetric quadruple-hump profile in all the modes. Such novel quadruple-hump profile is displayed in figure 1(c) for the parameter values $k_1 = 0.48 + 0.5\mathrm{i}$, $k_2 = 0.5 + 0.5\mathrm{i}$, $k_3 = 0.53 + 0.5\mathrm{i}$, $k_4 = 0.55 + 0.5\mathrm{i}$, $\alpha_1^{(1)} = 0.65 + 0.65\mathrm{i}$, $\alpha_1^{(2)} = 0.55 - 0.55\mathrm{i}$, $\alpha_1^{(3)} = 0.45 + 0.45\mathrm{i}$ and $\alpha_1^{(4)} = 0.35 - 0.35\mathrm{i}$. We have verified the asymmetric quadruple-hump profile nature by calculating the relative separation distance, $\Delta t_{12} = \Delta t_{13} = \Delta t_{14} \neq 0$. However we do not present their explicit forms due to size limitation of the letter article. It is evident from figures 1(a) and (c) that the NDS (in 3, 4 and also in the arbitrary N (>4) CNLS systems) exhibits multi-hump nature. This multi-peak nature can increase the bit-rate in coding the information. Consequently it can help to uplift the flow of data in fiber. In the present 4-CNLS system case also multi-node forms when the relative velocities of the solitons among the modes do not tend to zero. One can also recover the already known DS solution by fixing the condition $k_1 = k_2 = k_3 = k_4$ in the final form of NDS solution of the 4-CNLS system.

In the following, we further report the fact that the N-CNLS system can also admit very interesting partially NDS solution when the wavenumbers are restricted suitably. Such partial NDS solutions also exhibit multi-hump profiles (but less than N in number). For instance, here we demonstrate their existence for the 3 and 4-CNLS systems and this procedure can be generalized to the N-component case in principle. For the three-component case, the partially NDS solution can be obtained by imposing the condition, $k_1 = k_2$ (or $k_1 = k_3$ or $k_2 = k_3$), on the wave numbers in the solution (4). This restriction reduces the asymmetric triple-hump profile, as depicted in figure 1(a), into the asymmetric double-hump intensity profile as displayed in figure 3(a) for the choice of parameters $k_1 = k_2 = 0.5 + 0.5\mathrm{i}$, $k_3 = 0.45 + 0.5\mathrm{i}$, $\alpha_1^{(1)} = 0.65 + 0.65\mathrm{i}$, $\alpha_1^{(2)} = 0.45 - 0.45\mathrm{i}$ and $\alpha_1^{(3)} = 0.35 + 0.35\mathrm{i}$. The partially NDS double-hump profile is described by the following explicit form of solution, deduced from solution (4),

$$q_1 = \frac{1}{f} e^{i\eta_{1I}} e^{\frac{\Delta_{21}+\rho_{11}}{2}} \cosh\left(\eta_{3R} + \frac{\Delta_{21} - \rho_{11}}{2}\right),$$

$$q_3 = \frac{1}{f} e^{i\eta_{3I}} e^{\frac{\Delta+\rho_{13}}{2}} \cosh\left(\eta_{1R} + \frac{\Delta - \rho_{13}}{2}\right),$$

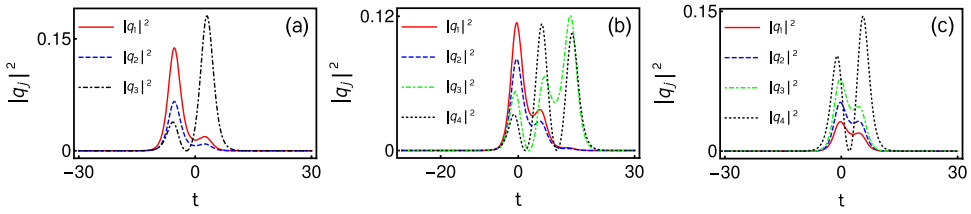

Figure 3. (a) Denotes double-humped profile of the partially nondegenerate one soliton solution of 3-CNLS system. (b) and (c) represent triple and double-humped profiles of partially NDS solution of 4-CNLS system when the conditions $k_1 = k_2$ and $k_1 = k_2 = k_3$ on wavenumbers are imposed, respectively.

$$q_2 = \frac{1}{f} e^{i\eta_{1I}} \left(\frac{1}{2} [\cosh(2\eta_{1R} - \eta_{3R} + \Delta_{12}) + \sinh(2\eta_{1R} - \eta_{3R} + \Delta_{12})] + e^{\frac{\Delta_{22}+\rho_{12}}{2}} \cosh\left(\eta_{3R} + \frac{\Delta_{22} - \rho_{12}}{2}\right)\right),$$

$$f = e^{\frac{\bar{\delta}_1}{2}} \cosh\left(\eta_{1R} + \eta_{3R} + \frac{\bar{\delta}_1}{2}\right) + e^{\frac{\bar{\delta}_2+\delta_3}{2}} \cosh\left(\eta_{1R} - \eta_{3R} + \frac{\bar{\delta}_2 - \delta_3}{2}\right). \quad (6)$$

In the above $e^{\bar{\delta}_1} = e^{\delta_5} + e^{\delta_6}$, $e^{\bar{\delta}_2} = e^{\delta_1} + e^{\delta_2}$, $e^{\Delta} = e^{\Delta_{13}} + e^{\Delta_{23}}$, $\eta_1 = \eta_2 = k_1 t + ik_1^2 z$, $\eta_3 = k_3 t + ik_3^2 z$ and the other constants are deduced from the constants of the solution (4) by imposing the condition $k_1 = k_2$ in them. We point out that one can get the DS solution by imposing the restriction further on the wavenumbers, that is as we mentioned above $k_1 = k_2 = k_3$ leads to completely DS solution. It is important to note that partially NDS solution of the 3-CNLSE can exhibit only up to double hump profile in all the three modes due to the degeneracy among the modes and the nature of this solution is controlled by five arbitrary complex parameters.

Similarly, for the 4-CNLS equation, partially NDS solution can be deduced from the solution (2) of N-component case. However, due to the complex nature of the resultant solution we do not present the expression here. Very interestingly such solution provides the following three possibilities: (i) $k_1 = k_2$, (ii) $k_1 = k_2 = k_3$ and (iii) $k_1 = k_2 = k_3 = k_4$. The quadruple-hump soliton profile of the 4-CNLS system becomes a triple-hump profile when we consider the first possibility, $k_1 = k_2$. This triple-humped partially NDS solution is diplayed in figure 3(b) for $k_1 = k_2 = 0.55 + 0.5i$, $k_3 = 0.5 + 0.5i$, $k_4 = 0.45 + 0.5i$, $\alpha_1^{(1)} = 0.65 + 0.65i$, $\alpha_1^{(2)} = 0.55 - 0.55i$, $\alpha_1^{(3)} = 0.45 + 0.45i$ and $\alpha_1^{(4)} = 0.35 - 0.35i$. In contrast to the latter, we observe that the double-hump soliton profile emerges while considering the second possibility, $k_1 = k_2 = k_3$, in the full nondegenerate form of solution of the 4-CNLS system. Such double-humped partially NDS solution profile is depicted in figure 3(c) for the values $k_1 = k_2 = k_3 = 0.55 + 0.5i$, $k_4 = 0.45 + 0.5i$, $\alpha_1^{(1)} = 0.35 + 0.35i$, $\alpha_1^{(2)} = 0.45 + 0.45i$, $\alpha_1^{(3)} = 0.55 + 0.55i$ and $\alpha_1^{(4)} = 0.65 - 0.65i$. The final possibility, $k_1 = k_2 = k_3 = k_4$, corresponds to complete degeneracy. This choice brings out the completely DS solution for the 4-CNLS system. In general, for the N-component case, one would expect $N - 1$ possibilities of choices of wave numbers. Out of these choices a single-humped complete DS solution (3) arises if all the wavenumbers are equal, $k_1 = k_2 = \cdots = k_n$, whereas the partial nondegeneracy appears from out of the remaining $N - 2$ possibilities. Such partial nondegeneracy would

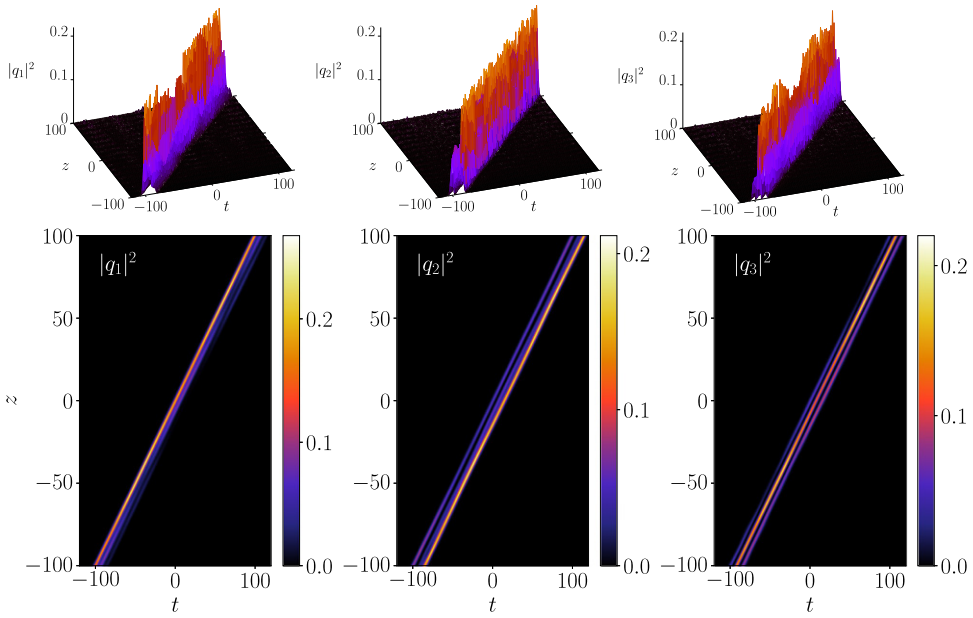

Figure 4. Numerical plots for the asymmetric nondegenerate triple hump soliton profile with 5% of white noise as perturbation. Top panel denotes the triple-hump profile of three-dimensional surface plot and the bottom panel represents the corresponding density plots. The soliton parameters correspond to figure 1(a).

bring out multi-hump profiles as we have illustrated above for the three and four component cases.

We also wish to point out the stability nature of the triple-humped nondegenerate fundamental soliton solution (4) of the 3-CNLS system as an example. In order to do this, we consider the Crank–Nicolson numerical algorithm [32] with different percentages of white noise as perturbations to the initial profiles. The initial profiles are considered in the numerical analysis as $q_j(-100, t) = [1 + A\zeta(t)]q_{j,-100}(t)$, $j = 1, 2, 3$, where $q_{j,-100}(t)$, $j = 1, 2, 3$, are the initial profiles obtained from the solution (4) at $z = -100$. Here, A is the amplitude of the white noise which is generated from the random numbers in the interval $[-1, 1]$ and $\zeta(t)$ is the noise function. The space and time step sizes are fixed in the numerical calculation, respectively, as $\mathrm{d}z = 0.1$ and $\mathrm{d}t = 0.2$. We also fix the domain range values for both t and z as $[-100, 100]$. The triple-hump profile nature survives during the evolution even for 5% and 10% of white noise perturbations except for minor changes in the amplitude part. This is clearly demonstrated in figures 4 and 5. These figures ensure the stability of triple-humped NDS against perturbations of white noise. One can extend this analysis for even longer ranges of time and space without much difficulty. Similarly, we have also confirmed the stability of asymmetric quadruple-hump NDS of the 4-CNLS system as well.

In this paper, we reported the existence of nondegenerate fundamental soliton solution for the N-CNLS equation (1). This new class of solitons exhibit multi-hump nature among all the modes. The existence of such special multi-humped profiles is demonstrated explicitly by considering the NDS solution for the three and four component cases. Very interestingly we have also shown the existence of partially NDS solutions by restricting the wave numbers suitably. The already known energy exchanging degenerate class of vector bright solitons is

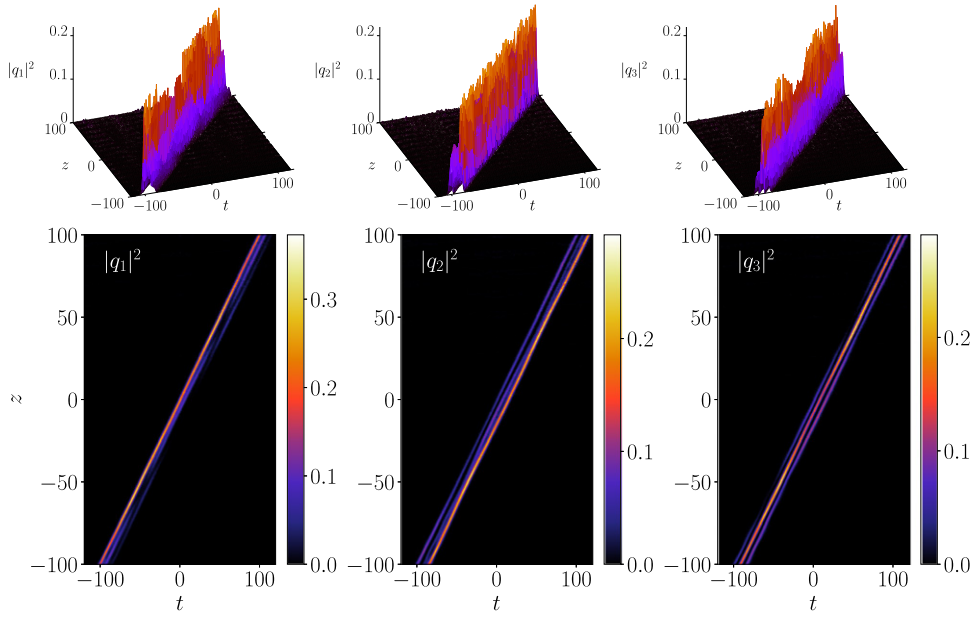

Figure 5. Numerical plots for the asymmetric nondegenerate triple hump soliton profile with 10% of white noise as perturbation.

shown as a sub-case by imposing specific restriction on the wave numbers. Finally, the stability of multi-humped nondegenerate fundamental soliton has also been verified numerically. In a subsequent work we have planned to report the interesting collision properties of these NDSs. We believe that the existence of multi-peak power nature in the nondegenerate fundamental soliton in multi-mode optical fibers may be relevant to increase the data stream in multi-level optical communication applications.

Acknowledgments

The authors are thankful to Prof. P Muruganandam, Department of Physics, Bharathidasan University, Tiruchirapalli-620024 for verifying the multi-hump nature of NDSs numerically with white noise as perturbation. RR, SS and ML acknowledge the financial support in the form of DST-SERB Distinguished Fellowship program to ML under the Grant No. SB/DF/04/2017.

Data availability statement

All data that support the findings of this study are included within the article (and any supplementary files).

ORCID iDs

S Stalin https://orcid.org/0000-0002-7651-4011
M Lakshmanan https://orcid.org/0000-0001-6687-4251

References

[1] Rohrmann P, Hause A and Mitschke F 2012 *Sci. Rep.* **2** 866
[2] Shannon C E 1948 A mathematical theory of communication *Bell Syst. Tech. J.* **27** 379–423
[3] Dauxois T and Peyrard M 2006 *Physics of Solitons* (Cambridge: Cambridge University Press)
[4] Stratmann M, Pagel T and Mitschke F 2005 *Phys. Rev. Lett.* **95** 143902
[5] Melchert O, Willms S, Bose S, Yulin A, Roth B, Mitschke F, Morgner U, Babushkin I and Demircan A 2019 *Phys. Rev. Lett.* **123** 243905
[6] Gordon J P 1983 *Opt. Lett.* **8** 596
[7] Mitschke F M and Mollenauer L F 1987 *Opt. Lett.* **12** 355
[8] Hause A, Hartwig H, Böhm M and Mitschke F 2008 *Phys. Rev.* A **78** 063817
[9] Akhmediev N N, Town G and Wabnitz S 1994 *Opt. Commun.* **104** 385
[10] Malomed B A 1991 *Phys. Rev.* A **44** 6954
[11] Khawaja U A 2010 *Phys. Rev.* E **81** 056603
[12] Grelu P and Soto-Crespo J M 2004 *J. Opt. B: Quantum SemiClass. Opt.* **6** S271
[13] Tang D Y, Zhao B, Shen D Y, Lu C, Man W S and Tam H Y 2003 *Phys. Rev.* A **68** 013816
[14] Akhmediev N N, Ankiewicz A and Soto-Crespo J M 1998 *J. Opt. Soc. Am.* B **15** 515
[15] Akhmediev N and Ankiewicz A 2000 *Chaos* **10** 600–12
[16] Akhmediev N, Królikowski W and Snyder A W 1998 *Phys. Rev. Lett.* **81** 4632
[17] Sukhorukov A A and Akhmediev N N 1999 *Phys. Rev. Lett.* **83** 4736
[18] Stalin S, Ramakrishnan R, Senthilvelan M and Lakshmanan M 2019 *Phys. Rev. Lett.* **122** 043901
[19] Manakov S V 1974 *Sov. Phys. JETP* **38** 248
[20] Qin Y H, Zhao L C and Ling L 2019 *Phys. Rev.* E **100** 022212
[21] Ramakrishnan R, Stalin S and Lakshmanan M 2020 *Phys. Rev.* E **102** 042212
[22] Agrawal G P 1995 *Nonlinear Fiber Optics* 2nd edn (New York: Academic)
[23] Stalin S, Ramakrishnan R and Lakshmanan M 2020 *Phys. Lett.* A **384** 126201
[24] Hirota R 2004 *The Direct Method in Soliton Theory* (Cambridge: Cambridge University Press)
[25] Ablowitz M J, Ohta Y and David Trubatch A 1999 *Phys. Lett.* A **253** 287
[26] Vijayajayanthi M, Kanna T and Lakshmanan M 2009 *Eur. Phys. J. Spec. Top.* **173** 57–80
[27] Radhakrishnan R, Lakshmanan M and Hietarinta J 1997 *Phys. Rev.* E **56** 2213
[28] Kanna T and Lakshmanan M 2001 *Phys. Rev. Lett.* **86** 5043
[29] Nogami Y and Warke C S 1976 *Phys. Lett.* A **59** 251
[30] Ankiewicz A, Królikowski W and Akhmediev N N 1999 *Phys. Rev.* E **59** 6079
[31] Vijayajayanthi M, Kanna T, Murali K and Lakshmanan M 2018 *Phys. Rev.* E **97** 060201
[32] Muruganandam P and Adhikari S K 2009 *Comput. Phys. Commun.* **180** 1888

photonics

MDPI

Review

Nondegenerate Bright Solitons in Coupled Nonlinear Schrödinger Systems: Recent Developments on Optical Vector Solitons

S. Stalin †, R. Ramakrishnan † and M. Lakshmanan *,†

Department of Nonlinear Dynamics, School of Physics, Bharathidasan University, Tiruchirappalli 620024, Tamil Nadu, India; stalin@cnld.bdu.ac.in (S.S.); ramki@cnld.bdu.ac.in (R.R.)

* Correspondence: lakshman.cnld@gmail.com or lakshman@cnld.bdu.ac.in

† These authors contributed equally to this work.

Abstract: Nonlinear dynamics of an optical pulse or a beam continue to be one of the active areas of research in the field of optical solitons. Especially, in multi-mode fibers or fiber arrays and photorefractive materials, the vector solitons display rich nonlinear phenomena. Due to their fascinating and intriguing novel properties, the theory of optical vector solitons has been developed considerably both from theoretical and experimental points of view leading to soliton-based promising potential applications. Mathematically, the dynamics of vector solitons can be understood from the framework of the coupled nonlinear Schrödinger (CNLS) family of equations. In the recent past, many types of vector solitons have been identified both in the integrable and non-integrable CNLS framework. In this article, we review some of the recent progress in understanding the dynamics of the so called nondegenerate vector bright solitons in nonlinear optics, where the fundamental soliton can have more than one propagation constant. We address this theme by considering the integrable two coupled nonlinear Schrödinger family of equations, namely the Manakov system, mixed 2-CNLS system (or focusing-defocusing CNLS system), coherently coupled nonlinear Schrödinger (CCNLS) system, generalized coupled nonlinear Schrödinger (GCNLS) system and two-component long-wave short-wave resonance interaction (LSRI) system. In these models, we discuss the existence of nondegenerate vector solitons and their associated novel multi-hump geometrical profile nature by deriving their analytical forms through the Hirota bilinear method. Then we reveal the novel collision properties of the nondegenerate solitons in the Manakov system as an example. The asymptotic analysis shows that the nondegenerate solitons, in general, undergo three types of elastic collisions without any energy redistribution among the modes. Furthermore, we show that the energy sharing collision exhibiting vector solitons arises as a special case of the newly reported nondegenerate vector solitons. Finally, we point out the possible further developments in this subject and potential applications.

Keywords: integrable coupled nonlinear Schrödinger models; nondegenerate vector bright solitons; degenerate vector bright solitons

Citation: Stalin, S.; Ramakrishnan, R.; Lakshmanan, M. Nondegenerate Bright Solitons in Coupled Nonlinear Schrödinger Systems: Recent Developments on Optical Vector Solitons. *Photonics* **2021**, *8*, 258. https://doi.org/10.3390/photonics8070258

Received: 9 June 2021
Accepted: 27 June 2021
Published: 5 July 2021

1. Introduction

Solitons are stable localized nonlinear wave packets which can propagate without distortion over long distances. After the discovery of solitons in the numerical experiments on the Fermi–Pasta–Ulam–Tsingou anharmonic lattice problem [1,2], the field of solitons and related nonlinear phenomena flourished and advanced by the invaluable discoveries in nonlinear optics. The concept of solitons is not only reserved for nonlinear optics, but it ubiquitously appears in many branches of physics, including hydrodynamics, Bose–Einstein condensates, plasma physics, particle physics, and even astrophysics apart from the mathematical interest in the theory of integrable nonlinear partial differential equations. In optics, in general, an optical pulse or a beam has a natural property to spread while it propagates in a linear medium because the Fourier components of the pulse or the

beam start to travel with distinct velocities. The spreading occurs in the temporal domain because of the material dispersion while in the spatial domain it is due to diffraction. In some cases, the spreading takes place due to the combined effects of dispersion and diffraction. However, a stable localized wave packet forms when this linear effect is balanced by the nonlinear response of the medium. Such a stable light wave envelope is known as the optical soliton. Optical soliton can be further classified as (i) spatial soliton, (ii) temporal soliton and (iii) spatio-temporal soliton depending on the nature of formation mechanism [3]. The evolution of optical soliton, whether it is a spatial or temporal one, in $(1+1)$-dimensional setting is described by the ubiquitous nonlinear Schrödinger (NLS) equation. For instance, the dimensionless NLS equation, derived from the Maxwell's equations under slowly varying envelope approximation, for the optical field propagation in a single mode optical fiber turns out to be [4].

$$iq_z - \mathrm{sgn}(\mathrm{K}'')q_{tt} + 2|q|^2 q = 0,\ K'' = \left(\frac{\partial^2 K}{\partial \omega^2}\right)_{\omega=\omega_0} = \frac{1}{v_g^2}. \tag{1}$$

In the temporal soliton case, where the soliton evolution is confined along the optical fiber, $q(z,t)$ is the complex wave amplitude and the independent variables z and t denote normalized distance along the fiber and retarded time, respectively. In addition, $q_z = \frac{\partial q}{\partial z}$ and $q_{tt} = \frac{\partial^2 q}{\partial t^2}$. Here, the sign of the group velocity dispersion (GVD) or simply the coefficient of the second derivative in time, in Equation (1), characterizes the nature of the fiber dispersion. If $K'' < 0$, then the dispersion is anomalous whereas the dispersion is normal for $K'' > 0$. The nonlinearity in Equation (1) arises due to the self phase modulation (SPM), where the intensity of light induces a change in the refractive index of the medium $\Delta n(I) = n_0(\omega) + n_2|E|^2 = n_0 + n_2 I$, where n_0 refers to the linear refractive index and n_2 is the nonlinear refractive index of the medium due to Kerr effect, which gives rise to an intensity-dependent phase modulation. On the other hand, the spatial soliton is a self-trapped optical beam that guides itself by inducing a waveguide during the stable propagation in a photorefractive medium without diffraction. Here, the diffraction is exactly balanced by the nonlinearly induced self-focusing effect. In this context, the independent variables, z and t in Equation (1), correspond to transverse spatial coordinates. Since this review will focus on the theoretical aspects of vector bright solitons of certain coupled integrable field models that emerge in optical fiber systems, the readers can find a detailed discussion on the development and advancement of both spatial and spatio-temporal solitons in the interesting review articles by Chen et al. [5] and by Malomed et al. [6], respectively.

In 1973, Hasegawa and Tappert theoretically demonstrated that the lossless fibers can admit bright soliton structure, which exhibits an intensity maximum in the time domain when the GVD regime is anomalous [7]. They have also shown that the dark soliton, with the intensity minimum or dip on a constant wave background field, arises in the normal GVD regime [8]. After this theoretical work, in 1980, Mollenauer and his coworkers succeeded experimentally in observing the optical soliton in a fiber [9]. These discoveries clearly demonstrated how an abstract mathematical concept can turn into a practical use. Both these theoretical and experimental works have opened up a new possibility of using the ultra-short optical pulses in long distance communication applications [10]. On the other hand, the mathematical interest in understanding the analytical structure of the underlying integrable models intensified after the NLS equation was solved by Zakharov and Shabat through a more sophisticated inverse scattering transform (IST) method [11], developed earlier by Gardner et al. for the celebrated Korteweg–deVries equation [12]. Now, it is well known that the NLS Equation (1) is a completely integrable infinite dimensional Hamiltonian system having special mathematical properties like an infinite number of conserved quantities and Lax pair [13]. We note that in [11] the authors had derived a double-pole solution, which has recently received attention in the theory of rogue-waves for describing the Peregrine breather on the zero background field of the

NLS equation [14], by considering the merging of two simple poles in the complex plane. The interesting fact of the temporal bright solitons of the scalar NLS equation is that they exhibit particle-like elastic collision.

Apart from the above fundamental aspects, in 1983, Gordon had predicted that when two or more light pulses propagate in a nonlinear optical fiber, they exert forces, either attractive or repulsive, on their neighbors [15]. This has been experimentally verified by Mitschke and Mollenauer in [16]. Such a study brought out a special kind of soliton state, namely the bound soliton state or soliton molecule [17]. A soliton molecule is a bound soliton state that can be formed when two solitons persist at a stable equilibrium separation distance, where the interaction force is zero among the individuals. Such a stable equilibrium manifests as this bound state structure, reminiscent of a diatomic molecule in chemical physics. The binding force arises between the constituents of the soliton composite due to the Kerr nonlinearity [15,16] and the detailed mechanism can be found in Ref. [18]. This special kind of soliton state has been extensively studied in non-dispersion managed fibers [19–25]. Recently, the existence of soliton molecules in dispersion-managed fiber [17] and their usefulness in optical telecommunications with enhanced data carrying capacity have been pointed out [26,27]. However, in order to elevate the transmission capacity of the optical telecommunication systems, it is necessary to consider multichannel bit-parallel wavelength fiber networks and wavelength division multiplexing schemes, where the light pulses propagate in multi channels simultaneously. In fact, practically even in a single mode fiber the bending and strains or birefringence induce two orthogonal polarization modes. To pursue this kind of practical application, one has to essentially understand the problem of the intermodal interaction of solitons. Therefore the contribution of the interaction of copropagating modes must be taken into account. In fact, there is no surprise other than the standard elastic collision of the bright solitons in single mode optical fibers. In contrast to this, the bright soliton structure in two mode fibers or in a single mode fiber with birefringence property or even in multimode fibers display rich propagation and collisional properties. Due to these fascinating features and intriguing collision dynamics, vector solitons receive intense attention among researchers. Apart from the several interesting properties, vector solitons have also been found in a variety of applications, including soliton-based optical computing [28,29], multi-level optical communication with enhanced bit-rate transmission [30], soliton based signal processing systems [31] and so on.

Vector solitons are fascinating nonlinear objects in which a given soliton is split among two or more components. In other words, a vector soliton with two or more polarization components coupled together maintains its shape during propagation. Such vector solitons are also named as multicolour solitons. The dynamics of vector solitons is usually understandable within the framework of coupled nonlinear Schrödinger (CNLS) equations. In general, the CNLS equations are non-integrable and they become integrable for specific choices of parameters [32]. Therefore, mathematically vector solitons arise as solutions of the CNLS equations. Like in the scalar NLS equation, the optical vector solitons are formed due to an exact balance between the dispersion/diffraction and the self-phase modulation and cross-phase modulation. This interesting class of optical solitons was first predicted by Manakov in 1974, where he derived the one-soliton solution and made an asymptotic analysis for the two-soliton solution through the IST method, by introducing a set of two CNLS equations for the nonlinear interaction of the two orthogonally polarized optical waves in birefringent fibers [33]. The Manakov system is essentially an integrable system, where the strength of the nonlinear interactions within and between the components are equal. Vector optical solitary wave propagation in birefringent fiber was first theoretically studied by Menyuk by considering a pair of non-integrable CNLS equations [34]. Very interestingly one of the present authors (ML) along with Radhakrishnan and Hietarinta theoretically predicted that the bright solitons of the Manakov model exhibit novel energy sharing collision through intensity redistribution [35]. They explicitly demonstrated this fascinating collision scenario by analyzing the two bright soliton solution derived through the Hirota bilinear method. Then this study was extended to N-CNLS equations by Kanna

and Lakshmanan in [36], where there is a lot of exciting possibilities for the occurrence of energy redistribution among the N-modes that have been reported. This theoretical development was experimentally verified in [37–39] and, subsequently, it gave rise to the possibility of constructing all optical logic gates [28,29,40–42]. The discovery of photorefractive solitons [43–46] and the subsequent experimental developments [47–50] have substantially enriched our knowledge on vector solitons. It is known that a set of N-CNLS equations describes the beam propagation in a Kerr-like photorefractive medium [51–54]. Furthermore, the experimental studies on vector solitons in photorefractive media as well as in dispersive media during the past three decades demand investigation of physical and mathematical aspects of CNLS equations even more rigorously.

It is very important to point out that there exist many types of vector solitons that have been reported so far for both integrable and non-integrable CNLS type equations. For instance, in the non-integrable cases, a temporal light pulse composed of orthogonally polarized components propagate with common group velocity and it is called group velocity-locked soliton [55]. On the other hand, if the two polarization components of the soliton are locked in phase, then such a vector soliton has been called a phase-locked soliton [56], whereas for the polarization-locked vector soliton [57], the relative phase between the components is locked at $\pm\frac{\pi}{2}$ but across the pulse, the polarization state profile is not uniform. However, that profile is invariant with propagation. Apart from the above, other types of vector solitary waves have been reported in birefringent fibers [58–61] and in saturable nonlinear medium [62,63], where the stability of multi-hump solitons has been reported. In the integrable cases, bright–bright solitons [33,35,36,64], bright–dark or dark–bright solitons [65–69] and dark–dark solitons [70,71] were documented in the context of nonlinear optics and their novel properties in multicomponent BECs have also been investigated considerably [72]. In a photorefractive medium, partially coherent solitons or soliton complexes were identified in the N-CNLS system, and their special properties were revealed by Akhmediev and his collaborators in [30,51–54]. Apart from the above, during the last decade, a large volume of work has been dedicated to the temporal optical solitons (both theoretically and experimentally) by considering the fiber lasers, which has been reported as a very useful nonlinear system to study the dynamics and formation of temporal optical solitons [73]. There exist different types of optical solitons in dissipative systems too and their various properties have been explored in [74].

From the above studies on vector solitons, especially in integrable coupled nonlinear Schrödinger models, we have identified that there exists a degeneracy in the structure of the bright solitons as we have explained below in Section 3. That is, the solitons in two-mode fibers or in multi-mode fibers propagate with identical wave numbers. In order to avoid this degeneracy, we introduce two non-identical propagation constants appropriately in the structure of the fundamental bright solitons of the 2-CNLS equation to start with. Consequently, the degeneracy is removed and it leads to a new class of fundamental bright solitons, namely nondegenerate fundamental vector bright solitons [75]. For the first time, we have shown that such an inclusion of additional distinct propagation constants brings out a general form of vector bright soliton solution to the several integrable CNLS systems [76,77], namely the Manakov system or 2-CNLS system, mixed 2-CNLS system (with one mode in the anomalous dispersion regime and the other mode in the normal dispersion regime), two-component coherently coupled NLS system, generalized CNLS system, and two-component long-wave short-wave resonance interaction system [77]. We note that very recently the nondegenerate solitons have also been studied in other contexts as well. For instance, in multi-component BECs [78] using the Darboux transformation method, in the coupled Fokas–Lenells system [79] and in the AB-system [80] such nondegenerate solitons have been identified. We also note that a multi-valley dark nondegenerate soliton has been studied in the context of multicomponent repulsive BECs [81]. In this paper, we critically review the existence and their salient novel features of the general form of nondegenerate vector bright solitons in the above class of two-component nonlinear Schrödinger systems. Then we also critically analyze their novel collision properties with the Manakov system

as an example. Furthermore, we also discuss in detail the corresponding already known degenerate vector bright solitons and their intriguing collisional properties. Additionally, we also illustrate the multi-hump nature of the nondegenerate fundamental bright solitons in the N-CNLS system [82].

The outline of this review paper is as follows. In Section 2, we quickly point out the derivation of 2-CNLS equations in the context of multi-mode fibers and introduce the various coupled integrable models and their physical importance. In Section 3, we clearly distinguish how the vector bright soliton reported so far in the literature for the integrable coupled NLS family type equations may be considered as a special case of the fundamental nondegenerate bright soliton solution derived recently by us. In Section 4, we discuss the nondegenerate soliton solutions of the Manakov system and analyze their underlying novel collision dynamics. In this section, we also describe the degenerate soliton solutions and their interesting energy sharing collision apart from mentioning the possible experimental realization and the multi-hump nature of the nondegenerate fundamental bright solitons in the N-CNLS system. Then in Section 5, we describe the properties and the existence of the nondegenerate fundamental bright soliton of the mixed CNLS system. We also discuss the collision dynamics of the degenerate solitons by pointing out their explicit analytical forms. In Section 6, we discuss the existence of both nondegenerate and degenerate fundamental bright solitons in the coherently coupled NLS system and point out the energy switching collision scenario of degenerate bright solitons. Furthermore, we illustrate the existence of the nondegenerate bright soliton in the generalized coupled nonlinear Schrödinger system and point out its degenerate limit in Section 7. Then, in Section 8, we also elucidate the existence of the nondegenerate soliton in the two-component (1+1)-dimensional LSRI system. Finally, in Section 9, we summarize the results and provide a possible future outlook.

2. Derivation of CNLS Equations and Other Integrable CNLS Type Models

In general, the interaction between two or more co-propagating optical modes is governed by the coupled nonlinear Schrödinger family of equations. The derivation of one such CNLS equations starts from Maxwell's equations for electromagnetic wave propagation in a dielectric medium,

$$\nabla^2\vec{E} - \frac{1}{c^2}\frac{\partial^2\vec{E}}{\partial t^2} = -\mu_0\frac{\partial^2\vec{P}}{\partial t^2}, \tag{2}$$

where $\vec{E}(\vec{r},t)$ is the electric field, $\vec{P}(\vec{r},t)$ is the induced polarization, μ_0 is the permeability of free space and c is the velocity of light. The induced polarization $\vec{P}(\vec{r},t)$ contains both a linear part and a nonlinear part. That is $\vec{P}(\vec{r},t) = \vec{P}_L(\vec{r},t) + \vec{P}_{NL}(\vec{r},t)$. The linear and nonlinear induced polarizations are defined as

$$\vec{P}_L(\vec{r},t) = \epsilon_0\int_{-\infty}^{+\infty}\chi^{(1)}(t-t')\vec{E}(\vec{r},t')dt', \tag{3a}$$

$$\vec{P}_{NL}(\vec{r},t) = \epsilon_0\int_{-\infty}^{+\infty}\int_{-\infty}^{+\infty}\int_{-\infty}^{+\infty}\chi^{(3)}(t-t_1,t-t_2,t-t_3)\vec{E}(\vec{r},t_1)\vec{E}(\vec{r},t_2)\vec{E}(\vec{r},t_3)dt_1dt_2dt_3. \tag{3b}$$

Here, ϵ_0 is the permitivity of the free space and $\chi^{(j)}$ is the jth order suceptibility tensor of rank $(j+1)$ [4,83]. For elliptically birefringent fibers, the electric field $\vec{E}(\vec{r},t)$ can be written as

$$\vec{E}(\vec{r},t) = \frac{1}{2}\Big(\hat{e}_1E_1(z,t) + \hat{e}_2E_2(z,t)\Big)e^{-i\omega_0t} + c.c. \tag{4}$$

In the above, the variables z and t denote the direction of propagation and retarded time, respectively, and $c.c$ stands for complex conjugation. The orthonormal vectors $\hat{e}_1$ and $\hat{e}_2$ are expressed as, $\hat{e}_1 = \frac{\hat{x}+ir\hat{y}}{\sqrt{1+r^2}}$ and $\hat{e}_2 = \frac{r\hat{x}-i\hat{y}}{\sqrt{1+r^2}}$, where r is a measure of the extent of

ellipticity and $\hat{x}$ and $\hat{y}$ are unit polarization vectors along x and y directions, respectively. In Equation (4), E_1 and E_2 are complex amplitudes of the polarization components at frequency ω_0. The nonlinear polarization can be obtained by substituting the expression of the electric field $\vec{E}(\vec{r},t)$ from Equation (4) in Equations (3a) and (3b). The electric-field components are written under slowly varying approximation as

$$E_j(z,t) = F_j(x,y)Q_j(z,t)e^{iK_{0j}z},\ j=1,2, \tag{5}$$

where $F_j(x,y)$ are the fiber distribution function in the transverse directions x and y and K_{0j}, $j=1,2$ are the propagation constants for the two modes. By doing so, the following coupled equations are obtained for $Q_j(z,t)$:

$$iQ_{1,z} + \frac{i}{v_{g1}}Q_{1,t} - \frac{k''}{2}Q_{1,tt} + \mu(|Q_1|^2 + B|Q_2|^2)Q_1 = 0, \tag{6a}$$

$$iQ_{2,z} + \frac{i}{v_{g2}}Q_{2,t} - \frac{k''}{2}Q_{2,tt} + \mu(|Q_1|^2 + B|Q_2|^2)Q_2 = 0. \tag{6b}$$

Here, $k'' = \left(\frac{\partial^2 k}{\partial \omega^2}\right)_{\omega=\omega_0}$ accounts for the group velocity dispersion, μ is the nonlinearity coefficient and v_{g1} and v_{g2} are the group velocities of the two co-propagating modes, respectively. The constant $B = \frac{2+2\sin^2\theta}{2+\cos^2\theta}$ is the cross-phase modulation coupling parameter, where θ is the angle of ellipticity which varies between 0 and $\frac{\pi}{2}$. Here, we have assumed that the fiber has a strong birefringent nature. Under three sets of consecutive transformations (detailed derivation can be found in [83]), we obtain the following dimensionless 2-CNLS equation with the integrability restriction $B=1$ [32], which is obtained from the Painlevé analysis,

$$iq_{1,z} + q_{1,tt} + 2\mu(|q_1|^2 + |q_2|^2)q_1 = 0, \tag{7a}$$

$$iq_{2,z} + q_{2,tt} + 2\mu(|q_1|^2 + |q_2|^2)q_2 = 0. \tag{7b}$$

The above set of CNLS equations constitutes the completely integrable system introduced by Manakov to describe the propagation of an intense electromagnetic pulse in a birefringent fiber [33]. The system (7a) and (7b) is well discussed in nonlinear optics and in other areas of physics. In this review, we also wish to consider another 2-CNLS equation which is a variant of the Manakov system, namely the mixed coupled nonlinear Schrödinger system or Zakharov and Schulman system [64,84]. One can write both the mixed CNLS equation and Manakov equation in a unified form as given below:

$$iq_{j,z} + q_{j,tt} + 2\Big(\sigma_1|q_1|^2 + \sigma_2|q_2|^2\Big)q_j = 0, \qquad j=1,2. \tag{8}$$

In Equation (8), σ_1 and σ_2 are the strength of the SPM and cross-phase modulation (XPM) nonlinearities. If $\sigma_1 = \sigma_2 = +1$, the above equation becomes the Manakov equation (focusing type 2-CNLS equations), where the two optical fields q_1 and q_2 propagate in the anomalous dispersion regimes [33], whereas, for $\sigma_1 = \sigma_2 = -1$, they propagate in the normal dispersion regimes or in other words, the resultant model (8) turns out to be the defocusing Manakov system [70]. For the other choice, $\sigma_1 = +1$ and $\sigma_2 = -1$, the system (8) becomes the mixed-CNLS system [64], in which the SPM is positive and the XPM is negative in both the modes, where the first mode q_1 is propagating in the anomalous dispersion regime while the second mode q_2 is propagating in the normal dispersion regime. Both the focusing and defocusing Manakov models also find applications in attractive and repulsive multicomponent BECs [72]. We note that the soliton trapping and daughter wave (shadow) formation have been reported [85] using the bright soliton solutions of the Manakov system. Radhakrishnan and Lakshmanan have derived the dark–dark soliton solution [70] and Sheppard and Kivshar have obtained bright–dark soliton solution [65] to the above system. In the latter case, the authors have pointed out the existence of

breathing bound states. Furthermore, it has been shown that the mixed CNLS system models the electromagnetic pulse propagation in isotropic and homogeneous nonlinear left handed materials [86]. By taking into account the electron–phonon interaction and in the long-wavelength approximation, the mixed-CNLS system can also be obtained as the modified Hubbard model (Lindner–Fedyanin system) [87–89]. The mixed CNLS system is also realized in two species BECs for a suitable choice of interspecies and intraspecies interactions [90]. We point out that the IST method and Darboux transformation method have been rigorously developed to obtain the bright–bright, dark–dark and bright–dark soliton solutions of the multicomponent focusing, defocusing and mixed CNLS systems [91–103].

Next, we consider the two-component coherently coupled nonlinear Schrödinger equation, which arises due to the coherent effects of the coupling among the copropagating optical fields. In general, an ultrashort pulse propagation in non-ideal weakly birefringent multimode fibers and optical beam propagation in low anisotropic Kerr type nonlinear media are described by the following two-component non-integrable CCNLS system [3,104,105];

$$iq_{1,z} + \delta q_{1,tt} - \mu q_1 + (|q_1|^2 + \sigma|q_2|^2)q_1 + \lambda q_2^2 q_1^* = 0, \tag{9a}$$
$$iq_{2,z} + \delta q_{2,tt} + \mu q_2 + (\sigma|q_1|^2 + |q_2|^2)q_2 + \lambda q_1^2 q_2^* = 0. \tag{9b}$$

The above equation also appears in isotropic Kerr-type nonlinear gyrotropic medium [106]. In the above q_1 and q_2 are two coherently coupled orthogonally polarized modes, z and t are the propagation direction and transverse direction, respectively, μ is the degree of birefringence, σ and λ are the incoherent and coherent coupling parameters, respectively, and δ is the group velocity dispersion. The nonlinearities arise in Equation (9) due to SPM ($|q_j|^2 q_j$, $j = 1, 2$), XPM ($\sigma|q_k|^2 q_j$, $j, k = 1, 2$, $j \neq k$) and four-wave mixing effect ($\lambda q_k^2 q_j^*$, $j, k = 1, 2$, $j \neq k$). Equation (9) is shown to be integrable for a specific choice of system parameters (δ, μ, σ and λ) [105] and soliton solutions were derived by linearly superposing the soliton solutions of the two nonlinear Schrödinger equations through a transformation. The corresponding integrable two-component CCNLS system (2-CCNLS system) is

$$iq_{1,z} + q_{1,tt} + \gamma(|q_1|^2 + 2|q_2|^2)q_1 - \gamma q_2^2 q_1^* = 0, \tag{10a}$$
$$iq_{2,z} + q_{2,tt} + \gamma(2|q_1|^2 + |q_2|^2)q_2 - \gamma q_1^2 q_2^* = 0. \tag{10b}$$

Interestingly, Kanna et al. [107] have derived the fundamental and two bright soliton solutions of (10) and its multicomponent version [108] by developing a non-standard Hirota bilinearization procedure. They have classified the fundamental bright soliton as incoherently coupled soliton (ICS) and coherently coupled soliton (CCS) based on a condition on the parameters in the auxiliary function. A novel double-hump soliton profile arises in these CCNLS systems due to the coherent coupling among the two copropagating optical fields. Furthermore, they have also demonstrated a fascinating energy switching collision during the interaction of ICS and CCS [107,108]. We remark that the CCNLS type equations are useful in studying the dynamics of solitons in spinor BECs and coherently coupled BECs [109–111] also. A similar type of CCNLS equation has been identified in the context of spinor BEC and is shown to be integrable [112–114].

Next, we wish to examine the bright soliton solutions of the general coupled nonlinear Schrödinger (GCNLS) system [115], namely

$$iq_{1,z} + q_{1,tt} + 2(a|q_1|^2 + c|q_2|^2 + bq_1 q_2^* + b^* q_1^* q_2)q_1 = 0, \tag{11a}$$
$$iq_{2,z} + q_{2,tt} + 2(a|q_1|^2 + c|q_2|^2 + bq_1 q_2^* + b^* q_1^* q_2)q_2 = 0. \tag{11b}$$

In the above GCNLS equations, a and c account for the strength of the SPM and XPM nonlinearities whereas the complex parameter b in the phase dependent terms, $bq_1 q_2^* + b^* q_1^* q_2$, describes the four-wave mixing effect that arises in multichannel communication systems [4]. When $a = c$ and $b = 0$ the system (11a) and (11b) reduces to the Manakov

system (or Equation (8) with $\sigma_1 = \sigma_2 = +1$). Then, if $a = -c$ and $b = 0$ the GCNLS system becomes the mixed-CNLS model. This GCNLS system has received considerable attention recently in both mathematical and physical aspects [115–118]. The integrability properties of the system (11a) and (11b) have been studied in [115] in which the N-soliton solution was obtained through the Riemann–Hilbert method. The GCNLS system is shown to be integrable through Weiss–Tabor–Carnevale (WTC) test [116]. In [117], bright and dark-soliton solutions were obtained through the Hirota bilinear method. By relating the GCNLS system with the Manakov and Makhankov vector models, using a transformation ($q_1 = \psi_1 - b^*\psi_2$ and $q_2 = a\psi_2$), the authors in [118] have constructed bright–bright, dark–dark and a quasibreather–dark soliton solutions.

Finally, for our investigation, we also wish to take into account the following coupled nonlinear Schrödinger type equations, namely the two-component long-wave short-wave resonance interaction system,

$$iS_t^{(1)} + S_{xx}^{(1)} + LS^{(1)} = 0,\ iS_t^{(2)} + S_{xx}^{(2)} + LS^{(2)} = 0,\ L_t = \sum_{l=1}^{2}(|S^{(l)}|^2)_x. \tag{12}$$

In the above, $S^{(l)}$'s, $l = 1, 2$, are short-wave (SW) components, L is the long-wave (LW) component and suffixes x and t denote partial derivatives with respect to spatial and temporal coordinates, respectively. The above LSRI system arises whenever the phase velocity of the low-frequency long-wave matches with the group velocity of the high-frequency short-waves [119,120]. In Equation (12), the formation of soliton in the SW components is due to the exact balance between its dispersion by the nonlinear interaction of the LW with the SW. At the same time, the formation and evolution of the soliton in the LW components is determined by the self-interaction of the SWs. The above LSRI system (12) has considerable physical relevance in nonlinear optics [121–124], plasma physics [125,126], hydrodynamics [120,127–131] and BECs [132–134]. The LSRI system originally arose from the pioneering study of nonlinear resonant interaction of the plasma waves by Zakharov [119], where generalized Zakharov equations were deduced to describe Langmuir waves. Such generalized Zakharov equations were reduced to a $(1 + 1)$-dimensional Yajima–Oikawa equation for describing the one-dimensional two-layer fluid flow [126] for which soliton solutions were obtained through the IST method. Benney has also derived a single-component LSRI system for modelling the dynamics of short capillary gravity waves and gravity waves in deep water [120]. After these works, there has been a large amount of work in the direction of LSRI involving $(1 + 1)$ and $(2 + 1)$-dimensional single component and multi-component cases [135–152]. In nonlinear optics, the single component LSRI system was deduced from the coupled nonlinear Schrödinger equations describing the interaction of two optical modes under small amplitude asymptotic expansion [121]. In the negative refractive index media, the LSRI process has been investigated [122]. We wish to point out that the bright soliton solutions for the general multi-component LSRI system have been derived through the Hirota bilinear method [136]. In this paper, the authors have demonstrated two types of energy sharing collisions for two different choices of nonlinearity coefficients. Considering the collisions of solitons in these cases one finds that the solitons appearing in the LW component always exhibit elastic collision whereas the solitons in the SW components always undergo energy sharing collisions.

In this review, we investigate the existence of nondegenerate vector bright solitons and their novel properties in the above described five interesting integrable coupled field models.

3. Statement of the Problem

As we pointed out in Section 1, the fundamental (and even higher order) bright soliton solutions which have been already reported for the integrable coupled nonlinear Schrödinger family of equations are degenerate. Here, by degenerate, we mean that the fundamental bright soliton nature is characterized by a single wave number in all the

modes or components. The presence of identical wave numbers in all the modes restricts the motion as well as the structure of the fundamental bright soliton in most of the CNLS-type equations. Thus, the bright solitons propagate in all the modes with identical velocity apart from the distinct polarization vector constants. Such a constrained motion always persists in most of the fundamental bright soliton solutions of various CNLS systems. As a consequence of this degeneracy, a single-hump structure only emerges in the fundamental bright soliton profile. In order to demonstrate this clearly, in the following, we consider the fundamental bright soliton solution of the Manakov system:

$$q_j = \frac{\alpha_1^{(j)} e^{\eta_1}}{1 + e^{\eta_1 + \eta_1^* + R}} \equiv A_j k_{1R} e^{i\eta_{1I}} \operatorname{sech}(\eta_{1R} + \frac{R}{2}),\ j = 1, 2. \tag{13}$$

Here A_j's are the unit polarization vectors, $A_j = \frac{\alpha_1^{(j)}}{(|\alpha_1|^2 + |\beta_1|^2)^{1/2}}$, $j = 1, 2$, the wave variable η_1 $(= \eta_{1R} + i\eta_{1I})$, $\eta_{1R} = k_{1R}(t - 2k_{1I}z)$, $\eta_{1I} = k_{1I}t + (k_{1R}^2 - k_{1I}^2)z$ and $e^R = \frac{(|\alpha_1|^2 + |\beta_1|^2)}{(k_1 + k_1^*)^2}$. From the above expression for the one-soliton solution, it is evident that the fundamental soliton is described by only one complex wave number k_1. Consequently, the single-hump soliton propagates in the two modes, q_1 and q_2, with identical velocity $v = 2k_{1I}$. A similar situation always persists in the other coupled field models mentioned above and their generalizations. For instance, the N-component Manakov type system [36], the mixed N-CNLS system [64], the GCNLS system [115,117], and the multi-component LSRI system [126,136] are such cases. However, in contrast to such cases, the coherent coupling among the copropagating optical fields induces a special type of double-hump vector bright soliton in the CCNLS system [107,108]. In this four wave mixing physical situation also the coherently coupled soliton is governed by an identical propagation constant in all the modes. Therefore, it is clear that the above mentioned degeneracy in propagation constants always persist in all the previously reported vector bright solitons.

In order to differentiate the above class of vector bright solitons from more general fundamental solitons, we classify them as degenerate and nondegenerate solitons based on the absence or presence of more than one wave number in the multi-component soliton solution. We call the solitons which propagate in all the modes with identical wave number as degenerate vector solitons whereas the solitons with nonidentical wave numbers as nondegenerate vector solitons. From the above literature, it is clear that the vector bright solitons with identical wave numbers have been well understood. However, the studies on solitons with non-identical propagation constants in all the modes have not been considered until recently. Therefore one would like to investigate the role of additional wave number(s) on the vector bright soliton structures and collision scenario as well. With this motivation, we plan to look for a class of fundamental soliton solutions, in a more general form, which possesses more than one distinct propagation constants. Recently, we have successfully identified such a general class of fundamental vector bright soliton solutions for a wide class of physically important CNLS type equations using the Hirota bilinear method. In this review, we briefly describe the novel properties, including the various collision properties, associated with the nondegenerate vector bright solitons of the Manakov system by deriving their analytical forms through the bilinearization method. Then we point out the existence of such nondegenerate solitons in other coupled systems, namely the N-CNLS system, mixed 2-CNLS system, 2-CCNLS system, GCNLS system and two-component LSRI system. In these systems, we also specify how the degenerate bright soliton solution arises as a special case of the nondegenerate soliton solution and point out their fascinating energy sharing collisions.

4. Nondegenerate Solitons and Their Collisions in Manakov System

To begin, we derive the nondegenerate bright soliton solutions of the Manakov system (Equation (8) with $\sigma_1 = \sigma_2 = 1$) using the Hirota bilinear method. In order to obtain this new class of soliton solutions, we first bilinearize the Manakov system with the

bilinearizing transformation, $q_j = \frac{g^{(j)}(z,t)}{f(z,t)}$, $j = 1,2$, where $g^{(j)}$'s are complex functions and f is a real function. It leads to the following bilinear forms of Equation (8), namely $(iD_z + D_t^2)g^{(j)} \cdot f = 0$, $j = 1,2$, $D_t^2 f \cdot f = 2\sum_{n=1}^{2} g^{(n)} g^{(n)*}$, where $*$ denotes complex conjugation. Here, the Hirota's bilinear operators D_z and D_t are defined [153] as $D_z^m D_t^n (a \cdot b) = \left(\frac{\partial}{\partial z} - \frac{\partial}{\partial z'}\right)^m \left(\frac{\partial}{\partial t} - \frac{\partial}{\partial t'}\right)^n a(z,t) b(z',t')_{|z=z',\, t=t'}$. Substituting the standard Hirota series expansions for the unknown functions $g^{(j)} = \epsilon g_1^{(j)} + \epsilon^3 g_3^{(j)} + ...$, $j = 1,2$, and $f = 1 + \epsilon^2 f_2 + \epsilon^4 f_4 + ...$ in the above bilinear equations, one can obtain a system of linear partial differential equations (PDEs). Here ϵ is the series expansion parameter. These linear PDEs arise after collecting the coefficients of the same powers of ϵ, and they can be solved recursively for every order of ϵ with the general forms of seed solutions. The resultant associated explicit expressions for $g^{(j)}$'s and f constitute the soliton solutions to the underlying Manakov system (8).

4.1. Nondegenerate Fundamental Soliton Solution of the Manakov System

The exact form of the nondegenerate fundamental soliton solution can be obtained by considering the two different seed solutions for the two modes as

$$g_1^{(1)} = \alpha_1^{(1)} e^{\eta_1},\ g_1^{(2)} = \alpha_1^{(2)} e^{\xi_1},\ \eta_1 = k_1 t + i k_1^2 z,\ \xi_1 = l_1 t + i l_1^2 z, \tag{14}$$

to the following lowest order linear PDEs, $i g_{1z}^{(j)} + g_{1tt}^{(j)} = 0$, $j = 1,2$. In the above k_1, l_1, $\alpha_1^{(j)}$, $j = 1,2$, are distinct complex parameters. The presence of two distinct complex wave numbers k_1 and l_1 ($k_1 \neq l_1$, in general) in Equation (14) makes the final solution as nondegenerate one. However, the identical seed solutions, that is the solutions (14) with $k_1 = l_1$ but different $\alpha_1^{(j)}$'s $j = 1,2$, have been used so far to derive the vector bright soliton solutions [35]. With the general forms of starting solutions (14), we allow the series expansions of the unknown functions $g^{(j)}$ and f to terminate themselves while solving the system of linear PDEs. We find that the series expansions become truncated as $g^{(j)} = \epsilon g_1^{(j)} + \epsilon^3 g_3^{(j)}$ and $f = 1 + \epsilon^2 f_2 + \epsilon^4 f_4$. With the explicit forms of unknown functions $g_3^{(j)}$, f_2 and f_4, finally we obtain the following a new fundamental one-soliton solution for the Manakov system,

$$q_1 = \frac{g_1^{(1)} + g_3^{(1)}}{1 + f_2 + f_4} = \frac{1}{D}(\alpha_1^{(1)} e^{\eta_1} + e^{\eta_1 + \xi_1 + \xi_1^* + \Delta_1^{(1)}}), \tag{15a}$$

$$q_2 = \frac{g_1^{(2)} + g_3^{(2)}}{1 + f_2 + f_4} = \frac{1}{D}(\alpha_1^{(2)} e^{\xi_1} + e^{\eta_1 + \eta_1^* + \xi_1 + \Delta_1^{(2)}}). \tag{15b}$$

Here $D = 1 + e^{\eta_1 + \eta_1^* + \delta_1} + e^{\xi_1 + \xi_1^* + \delta_2} + e^{\eta_1 + \eta_1^* + \xi_1 + \xi_1^* + \delta_{11}}$, $e^{\Delta_1^{(1)}} = \frac{(k_1 - l_1)\alpha_1^{(1)} |\alpha_1^{(2)}|^2}{(k_1 + l_1^*)(l_1 + l_1^*)^2}$, $e^{\Delta_1^{(2)}} = -\frac{(k_1 - l_1)|\alpha_1^{(1)}|^2 \alpha_1^{(2)}}{(k_1 + k_1^*)^2 (k_1^* + l_1)}$, $e^{\delta_1} = \frac{|\alpha_1^{(1)}|^2}{(k_1 + k_1^*)^2}$, $e^{\delta_2} = \frac{|\alpha_1^{(2)}|^2}{(l_1 + l_1^*)^2}$ and $e^{\delta_{11}} = \frac{|k_1 - l_1|^2 |\alpha_1^{(1)}|^2 |\alpha_1^{(2)}|^2}{(k_1 + k_1^*)^2 (k_1^* + l_1)(k_1 + l_1^*)(l_1 + l_1^*)^2}$. The above one-soliton solution possesses two distinct complex wave numbers, k_1 and l_1, which appear in both the expressions of q_1 and q_2 simultaneously. This confirms that the obtained

soliton solution is nondegenerate. The fundamental soliton solution (15a) and (15b) can also be rewritten using Gram determinant forms as well [154,155],

$$g^{(1)} = \begin{vmatrix} \frac{e^{\eta_1+\eta_1^*}}{(k_1+k_1^*)} & \frac{e^{\eta_1+\xi_1^*}}{(k_1+l_1^*)} & 1 & 0 & e^{\eta_1} \\ \frac{e^{\xi_1+\eta_1^*}}{(l_1+k_1^*)} & \frac{e^{\xi_1+\xi_1^*}}{(l_1+l_1^*)} & 0 & 1 & e^{\xi_1} \\ -1 & 0 & \frac{|\alpha_1^{(1)}|^2}{(k_1+k_1^*)} & 0 & 0 \\ 0 & -1 & 0 & \frac{|\alpha_1^{(2)}|^2}{(l_1+l_1^*)} & 0 \\ 0 & 0 & -\alpha_1^{(1)} & 0 & 0 \end{vmatrix}, \tag{16a}$$

$$g^{(2)} = \begin{vmatrix} \frac{e^{\eta_1+\eta_1^*}}{(k_1+k_1^*)} & \frac{e^{\eta_1+\xi_1^*}}{(k_1+l_1^*)} & 1 & 0 & e^{\eta_1} \\ \frac{e^{\xi_1+\eta_1^*}}{(l_1+k_1^*)} & \frac{e^{\xi_1+\xi_1^*}}{(l_1+l_1^*)} & 0 & 1 & e^{\xi_1} \\ -1 & 0 & \frac{|\alpha_1^{(1)}|^2}{(k_1+k_1^*)} & 0 & 0 \\ 0 & -1 & 0 & \frac{|\alpha_1^{(2)}|^2}{(l_1+l_1^*)} & 0 \\ 0 & 0 & 0 & -\alpha_1^{(2)} & 0 \end{vmatrix}, \tag{16b}$$

$$f = \begin{vmatrix} \frac{e^{\eta_1+\eta_1^*}}{(k_1+k_1^*)} & \frac{e^{\eta_1+\xi_1^*}}{(k_1+l_1^*)} & 1 & 0 \\ \frac{e^{\xi_1+\eta_1^*}}{(l_1+k_1^*)} & \frac{e^{\xi_1+\xi_1^*}}{(l_1+l_1^*)} & 0 & 1 \\ -1 & 0 & \frac{|\alpha_1^{(1)}|^2}{(k_1+k_1^*)} & 0 \\ 0 & -1 & 0 & \frac{|\alpha_1^{(2)}|^2}{(l_1+l_1^*)} \end{vmatrix}. \tag{16c}$$

The above Gram determinant forms indeed satisfy the bilinear equations as well as the Manakov Equation (8).

To explain the properties associated with the solution (15a) and (15b), we rewrite it in hyperbolic form as

$$q_1 = \frac{2k_{1R}A_1 e^{i\eta_{1I}}[\cosh(\xi_{1R}+\phi_{1R})\cos\phi_{1I} + i\sinh(\xi_{1R}+\phi_{1R})\sin\phi_{1I}]}{\left[a_{11}\cosh(\eta_{1R}+\xi_{1R}+\phi_1+\phi_2+c_1) + \frac{1}{a_{11}^*}\cosh(\eta_{1R}-\xi_{1R}+\phi_2-\phi_1+c_2)\right]}, \tag{17a}$$

$$q_2 = \frac{2l_{1R}A_2 e^{i\xi_{1I}}[\cosh(\eta_{1R}+\phi_{2R})\cos\phi_{2I} + i\sinh(\eta_{1R}+\phi_{2R})\sin\phi_{2I}]}{\left[a_{12}\cosh(\eta_{1R}+\xi_{1R}+\phi_1+\phi_2+c_1) + \frac{1}{a_{12}^*}\cosh(\eta_{1R}-\xi_{1R}+\phi_2-\phi_1+c_2)\right]}, \tag{17b}$$

where $a_{11} = \frac{(k_1^*-l_1^*)^{\frac{1}{2}}}{(k_1^*+l_1)^{\frac{1}{2}}}$, $a_{12} = \frac{(k_1^*-l_1^*)^{\frac{1}{2}}}{(k_1+l_1^*)^{\frac{1}{2}}}$, $c_1 = \frac{1}{2}\log\frac{(k_1^*-l_1^*)}{(l_1-k_1)}$, $c_2 = \frac{1}{2}\log\frac{(k_1-l_1)(k_1^*+l_1)}{(l_1-k_1)(k_1+l_1^*)}$, $\phi_1 = \frac{1}{2}\log\frac{(k_1-l_1)|\alpha_1^{(2)}|^2}{(k_1+l_1^*)(l_1+l_1)^2}$, $\phi_2 = \frac{1}{2}\log\frac{(l_1-k_1)|\alpha_1^{(1)}|^2}{(k_1^*+l_1)(k_1+k_1)^2}$, $\eta_{1R} = k_{1R}(t-2k_{1I}z)$, $\eta_{1I} = k_{1I}t + (k_{1R}^2-k_{1I}^2)z$, $\xi_{1R} = l_{1R}(t-2l_{1I}z)$, $\xi_{1I} = l_{1I}t + (l_{1R}^2-l_{1I}^2)z$, $A_1 = [\alpha_1^{(1)}/\alpha_1^{(1)*}]^{1/2}$, $A_2 = i[\alpha_1^{(2)}/\alpha_1^{(2)*}]^{1/2}$. Here, ϕ_{1R}, ϕ_{2R}, ϕ_{1I} and ϕ_{2I} are real and imaginary parts of ϕ_1 and ϕ_2, respectively, and k_{1R}, l_{1R}, k_{1I} and l_{1I} denote the real and imaginary parts of k_1 and l_1, respectively. The geometrical structure of the solution (17a) and (17b) is described by the four complex parameters k_1, l_1, $\alpha_1^{(j)}$, $j = 1, 2$. The nondegenerate fundamental bright soliton solution (17a) and (17b) either propagates with identical velocity $k_{1I} = l_{1I}$ or with

non-identical velocities $k_{1I} \neq l_{1I}$ in the two modes q_1 and q_2. In the identical velocity case, the quantity $\phi_{jI} = 0$, $j = 1, 2$ in (17a) and (17b) when $k_{1I} = l_{1I}$. This results in the forms

$$q_1 = \frac{2k_{1R}A_1 e^{i\eta_{1I}} \cosh(\xi_{1R} + \phi_{1R})}{\left[a_{11}\cosh(\eta_{1R} + \xi_{1R} + \phi_1 + \phi_2 + c_1) + \frac{1}{a_{11}^*}\cosh(\eta_{1R} - \xi_{1R} + \phi_2 - \phi_1 + c_2)\right]}, \quad (18a)$$

$$q_2 = \frac{2l_{1R}A_2 e^{i\xi_{1I}} \cosh(\eta_{1R} + \phi_{2R})}{\left[a_{12}\cosh(\eta_{1R} + \xi_{1R} + \phi_1 + \phi_2 + c_1) + \frac{1}{a_{12}^*}\cosh(\eta_{1R} - \xi_{1R} + \phi_2 - \phi_1 + c_2)\right]}, \quad (18b)$$

where $\eta_{1R} = k_{1R}(t - 2k_{1I}z)$, $\eta_{1I} = k_{1I}t + (k_{1R}^2 - k_{1I}^2)z$, $\xi_{1R} = l_{1R}(t - 2k_{1I}z)$, $\xi_{1I} = k_{1I}t + (l_{1R}^2 - k_{1I}^2)z$. The amplitude, velocity and central position of the nondegenerate fundamental soliton in the first mode are found from Equation (18a) as $2k_{1R}$, $2l_{1I}$ and $\frac{\phi_{1R}}{l_{1R}}$, respectively. Similarly they are found for the soliton in the second mode from Equation (18b) as $2l_{1R}$, $2k_{1I}$ and $\frac{\phi_{2R}}{k_{1R}}$, respectively. The solution (18a) and (18b) admits both the symmetric and asymmetric profiles, including a double-hump, a flat top and a single-hump profiles. We have displayed a combination of these three types of symmetric profiles (and their corresponding asymmetric profiles also) in our recent paper [76]. However, here, we display a typical novel double-hump, a flat top and a single-hump profile in Figure 1.

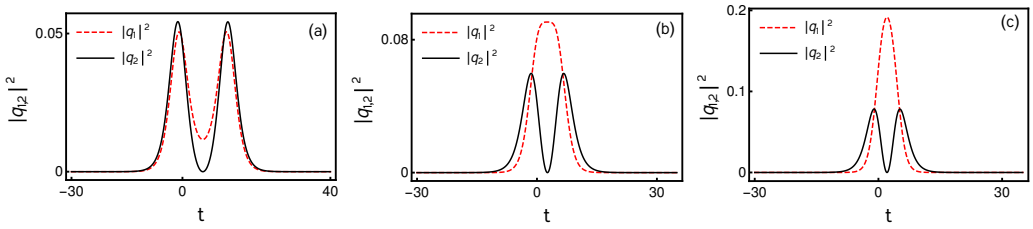

Figure 1. Symmetric intensity profiles of nondegenerate fundamental bright soliton solution (18a) and (18b): while (**a**) denotes double-hump soliton in both the modes, (**b**) represents a flat-top in q_1 mode and a double-hump in q_2 mode and (**c**) denotes a single-hump in q_1 mode and double-hump in q_2 mode. The parameter values of each figures are: (**a**): $k_1 = 0.333 + 0.5i$, $l_1 = 0.315 + 0.5i$, $\alpha_1^{(1)} = 0.45 + 0.45i$, $\alpha_1^{(2)} = 0.49 + 0.45i$. (**b**): $k_1 = 0.425 + 0.5i$, $l_1 = 0.3 + 0.5i$, $\alpha_1^{(1)} = 0.44 + 0.51i$, $\alpha_1^{(2)} = 0.43 + 0.5i$. (**c**): $k_1 = 0.55 + 0.5i$, $l_1 = 0.333 + 0.5i$, $\alpha_1^{(1)} = 0.5 + 0.5i$, $\alpha_1^{(2)} = 0.5 + 0.45i$.

The symmetric and asymmetric nature of the solution (18a) and (18b) can be confirmed by calculating either the relative separation distance between the minima of the two modes or by finding the corresponding extremum points from it. We remark that the double-hump formation occurs in the structure of nondegenerate one-bright soliton solution (17a) and (17b) when the relative velocity of the solitons in the two modes tends to zero. That is $\Delta v = v_1 - v_2 = 2(l_{1I} - k_{1I}) \to 0$. One can find the various special features associated with the obtained nondegenerate fundamental soliton solution (17a) and (17b) further in Ref. [76].

4.2. Nondegenerate Two-Soliton Solution

To obtain the nondegenerate two-soliton solution of Manakov Equation (8) we proceed with the procedure given in the previous subsection along with the following seed solutions, $g_1^{(1)} = \alpha_1^{(1)}e^{\eta_1} + \alpha_2^{(1)}e^{\eta_2}$ and $g_1^{(2)} = \alpha_1^{(2)}e^{\xi_1} + \alpha_2^{(2)}e^{\xi_2}$, $\eta_j = k_j t + ik_j^2 z$ and $\xi_j = l_j t + il_j^2 z$, $j = 1, 2$. We find that the series expansions for $g^{(j)}$, $j = 1, 2$, and f are terminated as $g^{(j)} = \epsilon g_1^{(j)} + \epsilon^3 g_3^{(j)} + \epsilon^5 g_5^{(j)} + \epsilon^7 g_7^{(j)}$ and $f = 1 + \epsilon^2 f_2 + \epsilon^4 f_4 + \epsilon^6 f_6 + \epsilon^8 f_8$. Here we assume that all the k_j's and l_j's, $j = 1, 2$, are distinct. The explicit forms of the obtained unknown functions in the truncated series expansions constitute the following nondegenerate two-soliton solution and it can be expressed using Gram determinants in the following way:

$$g^{(N)} = \begin{vmatrix} A & I & \phi \\ -I & B & \mathbf{0}^T \\ \mathbf{0} & C_N & 0 \end{vmatrix}, \quad f = \begin{vmatrix} A & I \\ -I & B \end{vmatrix}, \quad N = 1, 2. \tag{19}$$

Here the matrices A and B are of the order (4×4) defined as $A = \begin{pmatrix} A_{mm'} & A_{mn} \\ A_{nm} & A_{nn'} \end{pmatrix}$, $B = \begin{pmatrix} \kappa_{mm'} & \kappa_{mn} \\ \kappa_{nm} & \kappa_{nn'} \end{pmatrix}$, $m, m', n, n' = 1, 2$. The various elements of the matrix A can be obtained from the following, $A_{mm'} = \frac{e^{\eta_m + \eta^*_{m'}}}{(k_m + k^*_{m'})}$, $A_{mn} = \frac{e^{\eta_m + \xi^*_n}}{(k_m + l^*_n)}$, $A_{nn'} = \frac{e^{\xi_n + \xi^*_{n'}}}{(l_n + l^*_{n'})}$, $A_{nm} = \frac{e^{\eta^*_n + \xi_m}}{(k^*_n + l_m)}$, $m, m', n, n' = 1, 2$. The elements of the matrix B are $\kappa_{mm'} = \frac{\psi^\dagger_m \sigma \psi_{m'}}{(k^*_m + k_{m'})}$, $\kappa_{mn} = \frac{\psi^\dagger_m \sigma \psi'_n}{(k^*_m + k_n)}$, $\kappa_{nm} = \frac{\psi'^\dagger_n \sigma \psi_m}{(l^*_n + k_m)}$, $\kappa_{nn'} = \frac{\psi'^\dagger_n \sigma \psi'_{n'}}{(l^*_n + l_{n'})}$. In the latter, the column matrices are defined as $\psi_j = \begin{pmatrix} \alpha^{(1)}_j \\ 0 \end{pmatrix}$, $\psi'_j = \begin{pmatrix} 0 \\ \alpha^{(2)}_j \end{pmatrix}$, $j = m, m', n, n' = 1, 2$, $\eta_j = k_j t + i k_j^2 z$ and $\xi_j = l_j t + i l_j^2 z$, $j = 1, 2$. The other matrices in Equation (3) are defined as $\phi = \begin{pmatrix} e^{\eta_1} & e^{\eta_2} & e^{\xi_1} & e^{\xi_2} \end{pmatrix}^T$, $C_1 = -\begin{pmatrix} \alpha^{(1)}_1 & \alpha^{(1)}_2 & 0 & 0 \end{pmatrix}$, $C_2 = -\begin{pmatrix} 0 & 0 & \alpha^{(2)}_1 & \alpha^{(2)}_2 \end{pmatrix}$, $\mathbf{0} = \begin{pmatrix} 0 & 0 & 0 & 0 \end{pmatrix}$ and $\sigma = I$ is a (4×4) identity matrix. The presence of eight arbitrary complex parameters k_j, l_j, $\alpha^{(j)}_1$ and $\alpha^{(j)}_2$, $j = 1, 2$, define the profile shapes of the nondegenerate two solitons and their interesting collision scenarios. In addition to the above, we also find that the Manakov system also admits degenerate and nondegenerate solitons simultaneously under the wave number restriction $k_1 = l_1$ (or $k_2 = l_2$) but $k_2 \neq l_2$ (or $k_1 \neq l_1$). Such a special kind of partially nondegenerate two-soliton solution can be deduced by fixing the latter wave number restriction in the completely nondegenerate two-soliton solution (19). This partially nondegenerate soliton solution can also be derived through the Hirota bilinear method. To derive this solution one has to assume the following seed solutions, $g^{(1)}_1 = \alpha^{(1)}_1 e^{\eta_1} + \alpha^{(1)}_2 e^{\eta_2}$ and $g^{(2)}_1 = \alpha^{(2)}_1 e^{\eta_1} + \alpha^{(2)}_2 e^{\xi_2}$, $\eta_j = k_j t + i k_j^2 z$ and $\xi_2 = l_2 t + i l_2^2 z$, $j = 1, 2$, in the solution construction process. The resultant coexistence soliton solution and its dynamics are characterized by only seven complex parameters k_j, l_2, $\alpha^{(j)}_1$ and $\alpha^{(j)}_2$, $j = 1, 2$.

4.3. Various Types of Collision Dynamics of Nondegenerate Solitons

In order to understand the interesting collision properties associated with the nondegenerate solitons, one has to analyze the asymptotic forms of the complete nondegenerate two-soliton solution (19) of the Manakov equation. By doing so, we observe that the nondegenerate solitons in general exhibit three types of collision scenarios, namely shape preserving, shape altering and shape changing collision behaviors, for either of the two cases (i) Equal velocities: $k_{1I} = l_{1I}$, $k_{2I} = l_{2I}$ and (ii) Unequal velocities: $k_{1I} \neq l_{1I}$, $k_{2I} \neq l_{2I}$. To facilitate the understanding of these collision properties, here we present the asymptotic analysis for the case of equal velocities only and it can be performed for unequal velocities case also in a similar manner.

4.3.1. Asymptotic Analysis

We perform a careful asymptotic analysis for the nondegenerate two soliton solution (19) in order to understand the interaction dynamics of the nondegenerate solitons completely. We deduce the explicit expressions for the individual solitons at the asymptotic limits $z \to \pm\infty$. To explore this, we consider as a typical example $k_{jR}, l_{jR} > 0$, $j = 1, 2$, $k_{1I} > k_{2I}$, $l_{1I} > l_{2I}$, $k_{1I} = l_{1I}$ and $k_{2I} = l_{2I}$, that corresponds to head-on collision between the two nondegenerate solitons. In this situation, the two fundamental solitons S_1 and S_2 are well separated and subsequently the asymptotic forms of the individual nondegenerate solitons can be deduced from the solution (19) by incorporating the following asymptotic nature of the wave variables $\xi_{jR} = l_{jR}(t - 2l_{jI} z)$ and $\eta_{jR} = k_{jR}(t - 2k_{jI} z)$, $j = 1, 2$, in it. The

wave variables η_{jR} and ξ_{jR} behave asymptotically as (i) Soliton 1 (S_1): $\eta_{1R}, \xi_{1R} \simeq 0$, $\eta_{2R}, \xi_{2R} \to \mp\infty$ as $z \mp \infty$ and (ii) Soliton 2 (S_2): $\eta_{2R}, \xi_{2R} \simeq 0$, $\eta_{1R}, \xi_{1R} \to \mp\infty$ as $z \pm \infty$. Correspondingly, these results lead to the following asymptotic expressions of nondegenerate individual solitons.

(a) Before collision: $z \to -\infty$

Soliton 1: In this limit, the asymptotic forms of q_1 and q_2 are deduced from the two soliton solutions (19) for soliton 1 as below:

$$q_1 \simeq \frac{2A_1^{1-}k_{1R}e^{i\eta_{1I}}\cosh(\xi_{1R}+\phi_1^-)}{\left[a_{11}\cosh(\eta_{1R}+\xi_{1R}+\phi_1^-+\phi_2^-+c_1)+\frac{1}{a_{11}^*}\cosh(\eta_{1R}-\xi_{1R}+\phi_2^--\phi_1^-+c_2)\right]}, \quad (20a)$$

$$q_2 \simeq \frac{2A_2^{1-}l_{1R}e^{i\xi_{1I}}\cosh(\eta_{1R}+\phi_2^-)}{\left[a_{12}\cosh(\eta_{1R}+\xi_{1R}+\phi_1^-+\phi_2^-+c_1)+\frac{1}{a_{12}^*}\cosh(\eta_{1R}-\xi_{1R}+\phi_2^--\phi_1^-+c_2)\right]}. \quad (20b)$$

Here, $a_{11} = \frac{(k_1^*-l_1^*)^{\frac{1}{2}}}{(k_1^*+l_1)^{\frac{1}{2}}}$, $a_{12} = \frac{(k_1^*-l_1^*)^{\frac{1}{2}}}{(k_1+l_1^*)^{\frac{1}{2}}}$, $\phi_1^- = \frac{1}{2}\log\frac{(k_1-l_1)|\alpha_1^{(2)}|^2}{(k_1+l_1^*)(l_1+l_1^*)^2}$, $\phi_2^- = \frac{1}{2}\log\frac{(l_1-k_1)|\alpha_1^{(1)}|^2}{(k_1^*+l_1)(k_1+k_1^*)^2}$, $A_1^{1-} = [\alpha_1^{(1)}/\alpha_1^{(1)^*}]^{1/2}$ and $A_2^{1-} = i[\alpha_1^{(2)}/\alpha_1^{(2)^*}]^{1/2}$. In the latter, superscript $(1-)$ represents soliton S_1 before collision and subscript $(1,2)$ denotes the two modes q_1 and q_2, respectively.

Soliton 2: The asymptotic expressions for soliton 2 in the two modes before collision turn out to be

$$q_1 \simeq \frac{2k_{2R}A_1^{2-}e^{i(\eta_{2I}+\theta_1^-)}\cosh(\xi_{2R}+\varphi_1^-)}{\left[a_{21}\cosh(\eta_{2R}+\xi_{2R}+\varphi_1^-+\varphi_2^-+c_3)+\frac{1}{a_{21}^*}\cosh(\eta_{2R}-\xi_{2R}+\varphi_2^--\varphi_1^-+c_4)\right]}, \quad (21a)$$

$$q_2 \simeq \frac{2l_{2R}A_2^{2-}e^{i(\xi_{2I}+\theta_2^-)}\cosh(\eta_{2R}+\varphi_2^-)}{\left[a_{22}\cosh(\eta_{2R}+\xi_{2R}+\varphi_1^-+\varphi_2^-+c_3)+\frac{1}{a_{22}^*}\cosh(\eta_{2R}-\xi_{2R}+\varphi_2^--\varphi_1^-+c_4)\right]}. \quad (21b)$$

In the above, $a_{21} = \frac{(k_2^*-l_2^*)^{\frac{1}{2}}}{(k_2^*+l_2)^{\frac{1}{2}}}$, $a_{22} = \frac{(k_2^*-l_2^*)^{\frac{1}{2}}}{(k_2+l_2^*)^{\frac{1}{2}}}$, $c_3 = \frac{1}{2}\log\frac{(k_2^*-l_2^*)}{(l_2-k_2)}$, $c_4 = \frac{1}{2}\log\frac{(k_2-l_2)(k_2^*+l_2)}{(l_2-k_2)(k_2+l_2^*)}$, $\varphi_1^- = \frac{1}{2}\log\frac{(k_2-l_2)|\alpha_2^{(2)}|^2}{(k_2+l_2^*)(l_2+l_2^*)^2} + \Psi_1$, $\Psi_1 = \frac{1}{2}\log\frac{|k_1-l_2|^2|l_1-l_2|^4}{|k_1+l_2^*|^2|l_1+l_2^*|^4}$, $\varphi_2^- = \frac{1}{2}\log\frac{(l_2-k_2)|\alpha_2^{(1)}|^2}{(k_2^*+l_2)(k_2+k_2^*)^2} + \Psi_2$, $\Psi_2 = \frac{1}{2}\log\frac{|k_2-l_1|^2|k_1-k_2|^4}{|k_2+l_1^*|^2|k_1+k_2^*|^4}$, $e^{i\theta_1^-} = \frac{(k_1-k_2)(l_1-l_2)(l_1^*+l_2)(k_2-l_1)^{\frac{1}{2}}(k_1+k_2^*)(k_2^*+l_1)^{\frac{1}{2}}}{(k_1^*-k_2^*)(l_1+l_2^*)(l_1^*-l_2^*)(k_2^*-l_1^*)^{\frac{1}{2}}(k_1^*+k_2)(k_2+l_1^*)^{\frac{1}{2}}}$, $A_1^{2-} = [\alpha_2^{(1)}/\alpha_2^{(1)^*}]^{1/2}$, $A_2^{2-} = [\alpha_2^{(2)}/\alpha_2^{(2)^*}]^{1/2}$, $e^{i\theta_2^-} = \frac{(l_1-l_2)(k_1-l_2)^{\frac{1}{2}}(k_1+l_2^*)^{\frac{1}{2}}(l_1+l_2^*)}{(k_1^*-l_2^*)^{\frac{1}{2}}(l_1^*-l_2^*)(k_1^*+l_2)^{\frac{1}{2}}(l_1^*+l_2)}$. Here, superscript $(2-)$ refers to soliton S_2 before collision.

(b) After collision: $z \to +\infty$

Soliton 1: The asymptotic form for soliton 1 after collision is deduced as,

$$q_1 \simeq \frac{2k_{1R}A_1^{1+}e^{i(\eta_{1I}+\theta_1^+)}\cosh(\xi_{1R}+\phi_1^+)}{\left[a_{11}\cosh(\eta_{1R}+\xi_{1R}+\phi_1^++\phi_2^++c_1)+\frac{1}{a_{11}^*}\cosh(\eta_{1R}-\xi_{1R}+\phi_2^+-\phi_1^++c_2)\right]}, \quad (22a)$$

$$q_2 \simeq \frac{2l_{1R}A_1^{2+}e^{i(\xi_{1I}+\theta_2^+)}\cosh(\eta_{1R}+\phi_2^+)}{\left[a_{12}\cosh(\eta_{1R}+\xi_{1R}+\phi_1^++\phi_2^++c_1)+\frac{1}{a_{12}^*}\cosh(\eta_{1R}-\xi_{1R}+\phi_2^+-\phi_1^++c_2)\right]}. \quad (22b)$$

Here, $\phi_1^+ = \phi_1^- + \psi_1$, $\psi_1 = \frac{1}{2}\log\frac{|k_2-l_1|^2|l_1-l_2|^4}{|k_2+l_1^*|^2|l_1+l_2^*|^4}$, $\phi_2^+ = \phi_2^- + \psi_2$, $\psi_2 = \frac{1}{2}\log\frac{|k_1-l_2|^2|k_1-k_2|^4}{|k_1+l_2^*|^2|k_1+k_2^*|^4}$, $e^{i\theta_1^+} = \frac{(k_1-k_2)(k_1-l_2)^{\frac{1}{2}}(k_1^*+k_2)(k_1^*+l_2)^{\frac{1}{2}}}{(k_1^*-k_2^*)(k_1^*-l_2^*)^{\frac{1}{2}}(k_1+k_2^*)(k_1+l_2^*)^{\frac{1}{2}}}$,

$e^{i\theta_2^+} = \frac{(l_1-l_2)(k_2-l_1)^{\frac{1}{2}}(k_2+l_1^*)^{\frac{1}{2}}(l_1^*+l_2)}{(k_2^*-l_1^*)^{\frac{1}{2}}(l_1^*-l_2^*)(k_2^*+l_1)^{\frac{1}{2}}(l_1+l_2^*)}$, $A_1^{1+} = [\alpha_1^{(1)}/\alpha_1^{(1)^*}]^{1/2}$ and $A_2^{1+} = [\alpha_1^{(2)}/\alpha_1^{(2)^*}]^{1/2}$, in which superscript $(1+)$ denotes soliton S_1 after collision.

Soliton 2: The expression for soliton 2 after collision deduced from the two soliton solutions is

$$q_1 \simeq \frac{2A_2^{1+}k_{2R}e^{i\eta_{2I}}\cosh(\xi_{2R}+\varphi_1^+)}{[a_{21}\cosh(\eta_{2R}+\xi_{2R}+\varphi_1^++\varphi_2^++c_3)+\frac{1}{a_{21}^*}\cosh(\eta_{2R}-\xi_{2R}+\varphi_2^+-\varphi_1^++c_4)]}, \quad (23a)$$

$$q_2 \simeq \frac{2A_2^{2+}l_{2R}e^{i\xi_{2I}}\cosh(\eta_{2R}+\varphi_2^+)}{[a_{22}\cosh(\eta_{2R}+\xi_{2R}+\varphi_1^++\varphi_2^++c_3)+\frac{1}{a_{22}^*}\cosh(\eta_{2R}-\xi_{2R}+\varphi_2^+-\varphi_1^++c_4)]}, \quad (23b)$$

where $\varphi_1^+ = \frac{1}{2}\log\frac{(k_2-l_2)|\alpha_2^{(2)}|^2}{(k_2+l_2^*)(l_2+l_2^*)^2}$, $\varphi_2^+ = \frac{1}{2}\log\frac{(l_2-k_2)|\alpha_2^{(1)}|^2}{(k_2^*+l_2)(k_2+k_2^*)^2}$, $\varphi_3^+ = \frac{1}{2}\log\frac{|k_2-l_2|^2|\alpha_2^{(1)}|^2|\alpha_2^{(2)}|^2}{|k_2+l_2^*|^2(k_2+k_2^*)^2(l_2+l_2^*)^2}$, $\varphi_4^+ = \frac{1}{2}\log\frac{|\alpha_2^{(1)}|^2(l_2+l_2^*)^2}{|\alpha_2^{(2)}|^2(k_2+k_2^*)^2}$, $A_1^{2+} = [\alpha_2^{(1)}/\alpha_2^{(1)^*}]^{1/2}$ and $A_2^{2+} = i[\alpha_2^{(2)}/\alpha_2^{(2)^*}]^{1/2}$. In the latter, superscript $(2+)$ represents soliton S_2 after collision.

In the above, $\eta_{jI} = k_{jI}t + (k_{jR}^2 - k_{jI}^2)z$, $\xi_{jI} = l_{jI}t + (l_{jR}^2 - l_{jI}^2)z$, $j = 1,2$, and the phase terms φ_j^-, $j = 1,2$, can also be rewritten as $\varphi_1^- = \varphi_1^+ + \Psi_1$, $\varphi_2^- = \varphi_2^+ + \Psi_2$. The above asymptotic analysis clearly shows that there is a definite drastic alteration in the phase terms only. It can be identified from the following relations among the phase terms before and after collisions. That is,

$$\phi_1^+ = \phi_1^- + \psi_1,\ \phi_2^+ = \phi_2^- + \psi_2,\ \varphi_1^+ = \varphi_1^- - \Psi_1,\ \varphi_2^+ = \varphi_2^- - \Psi_2. \quad (24)$$

The above relations imply that the initial structures of the nondegenerate two solitons are preserved except for the phase terms. From this, we infer that they undergo either shape preserving collision with zero phase shift or shape changing collision with a finite phase shift. In addition to this, a special shape altering collision can also occur with a small phase shift. The zero phase shift condition, deduced from Equation (24), turns out to be

$$\phi_j^+ = \phi_j^-,\ \varphi_j^+ = \varphi_j^-,\ j = 1,2. \quad (25)$$

In order to follow the above condition, the additional phase constants $\psi_j's$ and Ψ_j's should be maintained as zero. That is,

$$\psi_1 = \frac{1}{2}\log\frac{|k_2-l_1|^2|l_1-l_2|^4}{|k_2+l_1^*|^2|l_1+l_2^*|^4} = 0,\ \psi_2 = \frac{1}{2}\log\frac{|k_1-l_2|^2|k_1-k_2|^4}{|k_1+l_2^*|^2|k_1+k_2^*|^4} = 0. \quad (26a)$$

$$\Psi_1 = \frac{1}{2}\log\frac{|k_1-l_2|^2|l_1-l_2|^4}{|k_1+l_2^*|^2|l_1+l_2^*|^4} = 0,\ \Psi_2 = \frac{1}{2}\log\frac{|k_2-l_1|^2|k_1-k_2|^4}{|k_2+l_1^*|^2|k_1+k_2^*|^4} = 0. \quad (26b)$$

From the above, we deduce the following criterion, corresponding to the conditions (25), for the occurrence of shape preserving collision with zero phase shift,

$$\frac{|k_2+l_1^*|^2}{|k_2-l_1|^2}| - \frac{|k_1+l_2^*|^2}{|k_1-l_2|^2} = 0. \quad (27)$$

As a result, whenever the conditions (25) or equivalently the criterion (27), are satisfied the nondegenerate bright solitons exhibit shape preserving collision with a zero phase shift. Otherwise, they undergo shape altering and shape changing collisions, as discussed in the following. Furthermore, the shape changing (and altering) collision scenario also belongs to the elastic collision as we describe below.

The above analysis clearly demonstrates that during the collision process the initial phase of each of the soliton is changed. The total phase shift of soliton S_1 in the two modes after collision becomes

$$\begin{aligned}\Delta\Phi_1 &= (\phi_1^+ + \phi_2^+) - (\phi_1^- + \phi_2^-) = \psi_1 + \psi_2 \\ &= \frac{1}{2}\log\frac{|k_2 - l_1|^2|l_1 - l_2|^4|k_1 - l_2|^2|k_1 - k_2|^4}{|k_2 + l_1^*|^2|l_1 + l_2^*|^4|k_1 + l_2^*|^2|k_1 + k_2^*|^4}.\end{aligned} \tag{28a}$$

Similarly the total phase shift suffered by soliton S_2 in the two modes is

$$\begin{aligned}\Delta\Phi_2 &= (\varphi_1^+ + \varphi_2^+) - (\varphi_1^- + \varphi_2^-) = -(\Psi_1 + \Psi_2) \\ &= -\frac{1}{2}\log\frac{|k_1 - l_2|^2|l_1 - l_2|^4|k_2 - l_1|^2|k_1 - k_2|^4}{|k_1 + l_2^*|^2|l_1 + l_2^*|^4|k_2 + l_1^*|^2|k_1 + k_2^*|^4} = -(\psi_1 + \psi_2) = -\Delta\Phi_1.\end{aligned} \tag{28b}$$

From the above expressions, we conclude that the phases of all the solitons are mainly influenced by the wave numbers k_j and l_j, $j = 1, 2$, and not by the complex parameters $\alpha_1^{(j)}$'s and $\alpha_2^{(j)}$'s, $j = 1, 2$. This peculiar property of nondegenerate solitons is different in the case of degenerate vector bright solitons [35,36], see also Section 4.6 below, where the complex parameters $\alpha_1^{(j)}$'s and $\alpha_2^{(j)}$'s, associated with polarization constants, play a crucial role in shifting the position of solitons after the collision.

4.3.2. Elastic Collision: Shape Preserving, Shape Altering and Shape Changing Collisions

From the above asymptotic analysis, we observe that the intensities of nondegenerate solitons S_1 and S_2 in the two modes are the same before and after collision in the equal velocities case, $k_{1I} = l_{1I}$ and $k_{2I} = l_{2I}$. To confirm this, we calculate the transition intensities (using the expressions for the transition amplitudes $T_j^i = \frac{A_j^{i+}}{A_j^{i-}}$, $i, j = 1, 2$), $|T_1^1|^2 = \frac{|A_1^{1+}|^2}{|A_1^{1-}|^2}$, $|T_2^1|^2 = \frac{|A_2^{1+}|^2}{|A_2^{1-}|^2}$, $|T_1^2|^2 = \frac{|A_1^{2+}|^2}{|A_1^{2-}|^2}$ and $|T_2^2|^2 = \frac{2|A_2^{2+}|^2}{2|A_2^{2-}|^2}$. The various expressions deduced for the different A_j^i's previously confirm that the transition intensities are unimodular. That is, $|T_j^l|^2 = 1$, $j, l = 1, 2$. Thus, the collision scenario that occurs among the nondegenerate solitons, in general, is always elastic. So, the nondegenerate solitons, for $k_{1I} = l_{1I}$, $k_{2I} = l_{2I}$, (but $k_1 \neq l_1$, $k_2 \neq l_2$) corresponding to two distinct wave numbers in general undergo elastic collision without any intensity redistribution between the modes q_1 and q_2. However, it is clear from Equation (24), that the changes that occur in the phase terms do alter the structure of the nondegenerate solitons during the collision scenario. Consequently, there is a possibility of shape altering and shape changing collisions occurring, without violating the unimodular conditions of transition intensities, in the equal velocities case, apart from the earlier mentioned shape preserving collision. A typical shape-preserving collision is displayed in Figure 2, in which we set two well separated symmetric double-hump soliton profiles as initial profiles in both the modes at $z = -10$. The initial structures of the two double-hump solitons are preserved after the collision. It is evident from the dashed red curves drawn at $z = +10$ in Figure 2. In addition to this, we have also verified that the wave parameters k_j and l_j, $j = 1, 2$, that are given in the caption of Figure 2, satisfy the zero phase shift criterion (27). The obtained numerical value from Equation (27) is equal to -0.0064 (nearly equal to) 0. This value physically implies that during the collision the two double-humped nondegenerate bright solitons pass through one another without a phase shift and emerge from the collision unaltered in shape, amplitude and velocity. This remarkable property has not been observed earlier in the cases of scalar NLS bright solitons as well as in the degenerate vector bright solitons [35,36]. Very interestingly, a similar zero phase shift shape preserving collision also occurs even when the symmetric double-hump soliton interacts with an asymmetric double-hump soliton. Such collision is illustrated in Figure 3.

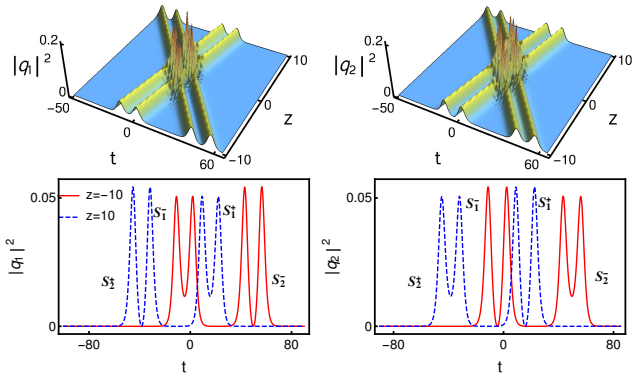

Figure 2. Shape preserving collision of two symmetric double-hump solitons—the energy is not exchanged among the nondegenerate solitons during the collision process. The parameter values are $k_1 = 0.333 + 0.5i$, $l_1 = 0.315 + 0.5i$, $k_2 = 0.315 - 2.2i$, $l_2 = 0.333 - 2.2i$, $\alpha_1^{(1)} = 0.45 + 0.45i$, $\alpha_2^{(1)} = 0.49 + 0.45i$, $\alpha_1^{(2)} = 0.49 + 0.45i$ and $\alpha_2^{(2)} = 0.45 + 0.45i$.

In this case, the total intensity of each soliton is conserved which can be verified from the relations $|A_j^{l-}|^2 = |A_j^{l+}|^2$, $j, l = 1, 2$. In addition to this, the total intensity in each of the modes is also conserved, that is $|A_j^{1-}|^2 + |A_j^{2-}|^2 = |A_j^{1+}|^2 + |A_j^{2+}|^2 =$ constant.

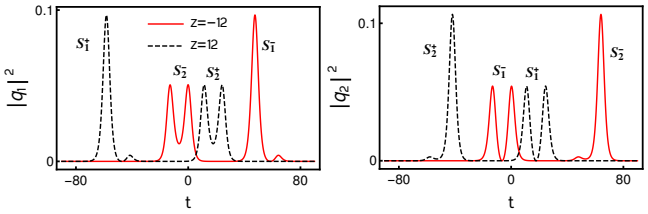

Figure 3. Shape preserving collision between a symmetric double-hump soliton and an asymmetric double-hump soliton: the parameter values are $k_1 = 0.333 + 0.5i$, $l_1 = 0.315 + 0.5i$, $k_2 = 0.315 - 2.2i$, $l_2 = 0.333 - 2.2i$, $\alpha_1^{(1)} = 0.45 + 0.45i$, $\alpha_2^{(1)} = 2.49 + 2.45i$, $\alpha_1^{(2)} = 0.49 + 0.45i$ and $\alpha_2^{(2)} = 0.45 + 0.45i$.

Then, we also come across another type of elastic collision, namely shape altering collision for certain sets of parametric choices again with $k_{1I} = l_{1I}$ and $k_{2I} = l_{2I}$. To demonstrate this collision scenario in Figure 4, we fix the parameter values as $k_1 = 0.425 + 0.5i$, $l_1 = 0.3 + 0.5i$, $k_2 = 0.3 - 2.2i$, $l_2 = 0.425 - 2.2i$, $\alpha_1^{(1)} = \alpha_2^{(2)} = 0.5 + 0.5i$ and $\alpha_2^{(1)} = \alpha_1^{(2)} = 0.45 + 0.5i$. From this figure, one can observe that a symmetric (or asymmetric) flattop soliton collides with an asymmetric (or symmetric) double-hump soliton in the q_1 (or q_2) component. As a result, the symmetric flattop profile in the q_1 mode is modified slightly as the asymmetric flattop profile and slightly asymmetric double-hump soliton S_2^- becomes a symmetric double-hump soliton. Similarly, while the symmetric double-hump soliton S_1^- in the q_2 mode changes slightly into an asymmetric structure, the asymmetric flattop soliton S_2^- becomes symmetric. As we pointed out earlier, this kind of shape alteration essentially arises in the structures of nondegenerate bright solitons is due to the phase conditions (24). However, the shape preserving nature of the nondegenerate solitons can be brought out by taking appropriate position shifts based on the expressions (22a) and (22b) and (23a) and (23b). For example, the expressions (22a) and (22b) of soliton 1 after collision exactly coincide with the expressions (20a) and (20b) after substituting $z' = z - \frac{\psi_1}{2l_{1R}k_{1I}}$ and $z' = z - \frac{\psi_2}{2k_{1R}k_{1I}}$, respectively, in it. Similarly, for the soliton 2, the expressions (23a) and (23b) exactly match with the expressions (21a) and (21b) after taking the position shifts $z' = z + \frac{\Psi_1}{2l_{2R}k_{2I}}$ and $z' = z + \frac{\Psi_2}{2k_{2R}k_{2I}}$, respectively, into account. Correspondingly, the shapes of the nondegenerate solitons are preserved. A typical example of this transition is illustrated in Figure 4c,d, where the initial profiles are

retained after taking the shifts in the positions of solitons. This is also true in the case of shape changing collision. Here, we have not displayed the shape changing collisions and their corresponding position shift plots for brevity.

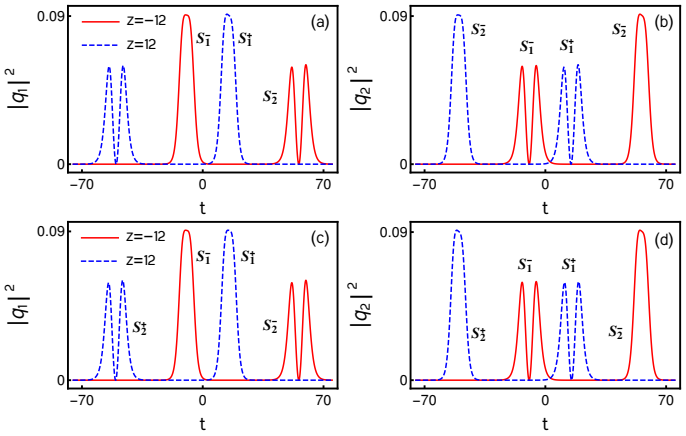

Figure 4. (**a**–**d**) A typical shape altering collision is displayed in the top panels. Their corresponding shape preserving nature is brought out in the bottom panels after taking a pair of position shifts, ($z' = z - \frac{\psi_1}{2l_{1R}k_{1I}} = 12.3053$, $z' = z - \frac{\psi_2}{2k_{1R}k_{1I}} = 12.27$) and ($z' = z + \frac{\Psi_1}{2l_{2R}k_{2I}} = 12.0614$, $z' = z + \frac{\Psi_2}{2k_{2R}k_{2I}} = 12.0694$) in the expressions (22a) and (22b) of soliton 1 and the expressions (23a) and (23b) of soliton 2, respectively.

4.4. Collision between Nondegenerate and Degenerate Solitons

In this sub-section, we discuss the collision among the degenerate and nondegenerate solitons admitted by the two-soliton solution (19) of the Manakov system (8) in the partial nondegenerate limit $k_1 = l_1$ and $k_2 \neq l_2$. The following asymptotic analysis assures that there is a definite energy redistribution occurs among the modes q_1 and q_2.

4.4.1. Asymptotic Analysis

To elucidate this new kind of collision behavior, we analyze the partially nondegenerate two-soliton solution (19) in the asymptotic limits $z \to \pm\infty$. The resultant action yields the asymptotic forms corresponding to degenerate and nondegenerate solitons. To obtain the asymptotic forms for the present case we incorporate the asymptotic nature of the wave variables $\eta_{jR} = k_{jR}(t - 2k_{Ij}z)$ and $\xi_{2R} = l_{2R}(t - 2l_{2I}z)$, $j = 1, 2$, in the solution (19). Here the wave variable η_{1R} corresponds to the degenerate soliton and η_{2R}, ξ_{2R} correspond to the nondegenerate soliton. In order to find the asymptotic behavior of these wave variables we consider the parametric choice as $k_{1R}, k_{2R}, l_{2R} > 0$, $k_{1I} > 0$, $k_{2I}, l_{2I} < 0$, $k_{1I} > k_{2I}, k_{1I} > l_{2I}$. For this choice, the wave variables behave asymptotically as follows: (i) degenerate soliton S_1: $\eta_{1R} \simeq 0$, η_{2R},$\xi_{2R} \to \mp\infty$ as $z \to \mp\infty$ (ii) nondegenerate soliton S_2: $\eta_{2R}, \xi_{2R} \simeq 0$, $\eta_{1R} \to \pm\infty$ as $z \to \pm\infty$. By incorporating these asymptotic behaviors of wave variables in the solution (19), we deduce the following asymptotic expressions for degenerate and nondegenerate solitons.

(a) Before collision: $z \to -\infty$

Soliton 1: In this limit, the asymptotic form for the degenerate soliton deduced from the partially nondegenerate two soliton solution (19) is

$$q_j \simeq \begin{pmatrix} A_1^{1-} \\ \\ A_2^{1-} \end{pmatrix} k_{1R} e^{i\eta_{1I}} \operatorname{sech}(\eta_{1R} + \frac{R}{2}),\ j = 1, 2, \tag{29}$$

where $A_j^{1-} = \alpha_1^{(j)} / (|\alpha_1^{(1)}|^2 + |\alpha_1^{(2)}|^2)^{1/2}$, $j = 1, 2$, $R = \ln \frac{(|\alpha_1^{(1)}|^2 + |\alpha_1^{(2)}|^2)}{(k_1 + k_1^*)^2}$. Here, in A_j^{1-} the superscript $1-$ denotes soliton S_1 before collision and subscript j refers to the mode number.

Soliton 2: The asymptotic expressions for the nondegenerate soliton S_2 which is present in the two modes before collision are obtained as

$$q_1 \simeq \frac{2k_{2R}A_1^{2-}}{D}\left(e^{i\xi_{2I}+\Lambda_1}\cosh(\eta_{2R}+\frac{\Phi_{21}-\Delta_{21}}{2})+e^{i\eta_{2I}+\Lambda_2}\cosh(\xi_{2R}+\frac{\lambda_2-\lambda_1}{2})\right), \quad (30a)$$

$$q_2 \simeq \frac{2l_{2R}A_2^{2-}}{D}\left(e^{i\eta_{2I}+\Lambda_7}\cosh(\xi_{2R}+\frac{\Gamma_{21}-\gamma_{21}}{2})+e^{i\xi_{2I}+\Lambda_6}\cosh(\eta_{2R}+\frac{\lambda_7-\lambda_6}{2})\right), \quad (30b)$$

$$D = e^{\Lambda_5}\cosh(\eta_{2R}-\xi_{2R}+\frac{\lambda_3-\lambda_4}{2})+e^{\Lambda_3}\cosh(i(\eta_{2I}-\xi_{2I})+\frac{\vartheta_{12}-\varphi_{21}}{2})$$
$$+e^{\Lambda_4}\cosh(\eta_{2R}+\eta_{3R}+\frac{\lambda_5-R}{2}).$$

Here, $A_1^{2-}=[\alpha_2^{(1)}/\alpha_2^{(1)^*}]^{1/2}$, $A_2^{2-}=[\alpha_2^{(2)}/\alpha_2^{(2)^*}]^{1/2}$. In the latter the superscript $2-$ denote nondegenerate soliton S_2 before collision. The various other constants appearing in Equation (30) are defined in the Appendix A.

(b) After collision: $z \to +\infty$

Soliton 1: The asymptotic forms for degenerate soliton S_1 after collision deduced from the solution (19) (with $k_1 = l_1$ and $k_2 \neq l_2$) as,

$$q_j \simeq \begin{pmatrix} A_1^{1+} \\ \\ A_2^{1+} \end{pmatrix} e^{i(\eta_{1I}+\theta_j^+)}k_{1R}\,\mathrm{sech}(\eta_{1R}+\frac{R'-\varsigma_{22}}{2}),\ j=1,2, \quad (31)$$

where $A_1^{1+}=\alpha_1^{(1)}/(|\alpha_1^{(1)}|^2+\chi|\alpha_1^{(2)}|^2)^{1/2}$, $A_2^{1+}=\alpha_1^{(2)}/(|\alpha_1^{(1)}|^2\chi^{-1}+|\alpha_1^{(2)}|^2)^{1/2}$, $\chi=(|k_1-l_2|^2|k_1+k_2^*|^2)/(|k_1-k_2|^2|k_1+l_2^*|^2)$, $e^{i\theta_1^+}=\frac{(k_1-k_2)(k_1^*+k_2)(k_1-l_2)^{\frac{1}{2}}(k_1^*+l_2)^{\frac{1}{2}}}{(k_1^*-k_2^*)(k_1+k_2^*)(k_1^*-l_2^*)^{\frac{1}{2}}(k_1+l_2^*)^{\frac{1}{2}}}$, $e^{i\theta_2^+}=\frac{(k_1-k_2)^{\frac{1}{2}}(k_1^*+k_2)^{\frac{1}{2}}(k_1-l_2)(k_1^*+l_2)}{(k_1^*-k_2^*)^{\frac{1}{2}}(k_1+k_2^*)^{\frac{1}{2}}(k_1^*-l_2^*)(k_1+l_2^*)}$. Here $1+$ in A_1^{1+} refers to degenerate soliton S_1 after collision.

Soliton 2: Similarly the expression for the nondegenerate soliton, S_2, after collision deduced from the two soliton solution (19) (with $k_1 = l_1$ and $k_2 \neq l_2$) is

$$q_1 \simeq \frac{2k_{2R}A_1^{2+}e^{i\eta_{2I}}\cosh(\xi_{2R}+\frac{\Lambda_{22}-\rho_1}{2})}{\left[\frac{(k_2^*-l_2^*)^{\frac{1}{2}}}{(k_2^*+l_2)^{\frac{1}{2}}}\cosh(\eta_{2R}+\xi_{2R}+\frac{\varsigma_{22}}{2})+\frac{(k_2+l_2^*)^{\frac{1}{2}}}{(k_2-l_2)^{\frac{1}{2}}}\cosh(\eta_{2R}-\xi_{2R}+\frac{R_3-R_6}{2})\right]}, \quad (32a)$$

$$q_2 \simeq \frac{2l_{2R}A_2^{2+}e^{i\xi_{2I}}\cosh(\eta_{2R}+\frac{\mu_{22}-\rho_2}{2})}{\left[\frac{(k_2^*-l_2^*)^{\frac{1}{2}}}{(k_2+l_2^*)^{\frac{1}{2}}}\cosh(\eta_{2R}+\xi_{2R}+\frac{\varsigma_{22}}{2})+\frac{(k_2^*+l_2)^{\frac{1}{2}}}{(k_2-l_2)^{\frac{1}{2}}}\cosh(\eta_{2R}-\xi_{2R}+\frac{R_3-R_6}{2})\right]}. \quad (32b)$$

where $\rho_j=\log\alpha_2^{(j)}$, $j=1,2$, $A_1^{2+}=[\alpha_2^{(1)}/\alpha_2^{(1)^*}]^{1/2}$, $A_2^{2+}=i[\alpha_2^{(2)}/\alpha_2^{(2)^*}]^{1/2}$. The explicit expressions of all the undefined constants are given in Appendix A.

4.5. Degenerate Soliton Collision Induced Shape Changing Scenario of Nondegenerate Soliton

The coexistence of nondegenerate and degenerate solitons can be realized from the partially nondegenerate limit of the soliton solution (19) (with $k_1 = l_1$ and $k_2 \neq l_2$). Such coexisting solitons undergo a novel collision property, which has been illustrated in Figure 5. From this figure, one can observe that the intensity of the degenerate soliton S_1 is enhanced after collision in the q_1 mode and it is suppressed in the q_2 mode. As we expected, like in the complete degenerate case [35,41], the degenerate soliton undergoes energy redistribution among both the modes. In this case, the polarization vectors, $A_j^l=\alpha_l^{(j)}/(|\alpha_1^{(1)}|^2+|\alpha_1^{(2)}|^2)^{1/2}$, $l,j=1,2$, play a crucial role in changing the shape of the degenerate solitons under collision, where the intensity redistribution occurs between the

modes q_1 and q_2. As we have pointed out below in the next subsection, the shape preserving collision arises in the pure degenerate case when the polarization parameters obey the condition, $\frac{\alpha_1^{(1)}}{\alpha_2^{(1)}} = \frac{\alpha_1^{(2)}}{\alpha_2^{(2)}}$, where $\alpha_i^{(j)}$'s, $i, j = 1, 2$, are complex parameters related to the polarization vectors as given above. However, this collision property is not true in the case of nondegenerate solitons as we have depicted in Figure 5. As a result, the nondegenerate soliton S_2 switches its asymmetric double-hump profile into a single-hump profile along with a phase shift. In addition, we also noticed from the asymptotic expressions (30a) and (30b) and (32a) and (32b), that the asymmetric double-hump profile of nondegenerate soliton is transformed into another form of an asymmetric double-hump profile when it interacts with a degenerate soliton for a specific choice of parameter values. In the nondegenerate case, the relative separation distances (or phases) are in general not preserved during the collision. Therefore the mechanism behind the occurrence of shape preserving and shape changing collisions in the nondegenerate solitons is quite new. These novel collision properties can be understood from the corresponding asymptotic analysis given in the previous subsection. The analysis reveals that energy redistribution occurs between the modes q_1 and q_2. In order to confirm the shape changing nature of this interesting collision scenario, we obtain the following expression for the transition amplitudes,

$$T_1^1 = \frac{(|\alpha_1^{(1)}|^2 + |\alpha_1^{(2)}|^2)^{1/2}}{(|\alpha_1^{(1)}|^2 + \chi|\alpha_1^{(2)}|^2)^{1/2}}, \; T_2^1 = \frac{(|\alpha_1^{(1)}|^2 + |\alpha_1^{(2)}|^2)^{1/2}}{(|\alpha_1^{(1)}|^2\chi^{-1} + |\alpha_1^{(2)}|^2)^{1/2}}. \tag{33}$$

In general, the transition amplitudes are not equal to unity. If the quantity T_j^l is not unimodular (for this case the constant $\chi \neq 1$), then the degenerate and nondegenerate solitons always exhibit shape changing collision. The standard elastic collision can be recovered when $\chi = 1$. One can calculate the shift in the positions of both degenerate and nondegenerate solitons after collision from the asymptotic analysis. This new kind of collision property has not been observed in the degenerate vector bright solitons of the Manakov system [35,41].

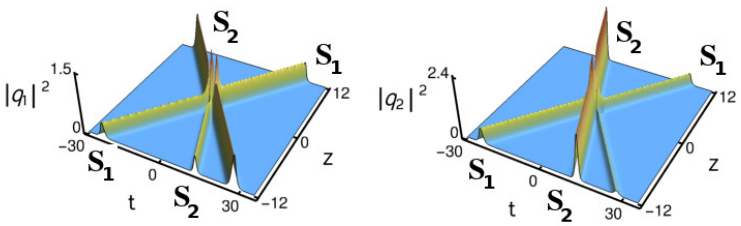

Figure 5. Shape changing collision between a degenerate and nondegenerate soliton: $k_1 = l_1 = 1 + i$, $k_2 = 1 - i$, $l_2 = 1.5 - 0.5i$, $\alpha_1^{(1)} = 0.8 + 0.8i$, $\alpha_2^{(2)} = 0.6 + 0.6i$, $\alpha_2^{(1)} = 0.25 + 0.25i$, $\alpha_1^{(2)} = 1 + i$.

4.6. Degenerate Bright Solitons and Their Shape Changing/Energy Redistribution Collision in the Manakov System

The already reported degenerate vector one-bright soliton solution of the Manakov system (8) can be deduced from the one-soliton solution (15a) and (15b) by imposing the condition $k_1 = l_1$ in it. The forms of q_j given in Equations (15a) and (15b) degenerate into the standard bright soliton form [35,41]

$$q_j = \frac{\alpha_1^{(j)} e^{\eta_1}}{1 + e^{\eta_1 + \eta_1^* + R}}, \; j = 1, 2, \tag{34}$$

which can be rewritten as

$$q_j = k_{1R} \hat{A}_j e^{i\eta_{1I}} \operatorname{sech}(\eta_{1R} + \frac{R}{2}), \tag{35}$$

where $\eta_{1R} = k_{1R}(t - 2k_{1I}z)$, $\eta_{1I} = k_{1I}t + (k_{1R}^2 - k_{1I}^2)z$, $\hat{A}_j = \frac{\alpha_1^{(j)}}{\sqrt{(|\alpha_1^{(1)}|^2+|\alpha_1^{(2)}|^2)}}$, $e^R = \frac{(|\alpha_1^{(1)}|^2+|\alpha_1^{(2)}|^2)}{(k_1+k_1^*)^2}$, $j = 1,2$. Note that the above fundamental bright soliton always propagates in both the modes q_1 and q_2 with the same velocity $2k_{1I}$. The polarization vectors $(\hat{A}_1, \hat{A}_2)^\dagger$ have different amplitudes and phases, unlike the case of nondegenerate solitons where they have only different unit phases. The presence of a single wave number k_1 in the solution (35) restricts the degenerate soliton to have a single-hump form only. A typical profile of the degenerate soliton is shown in Figure 6. As already pointed out in [35,41], the amplitude and central position of the degenerate vector bright soliton are obtained as $2k_{1R}\hat{A}_j$, $j = 1,2$ and $\frac{R}{2k_{1R}}$, respectively.

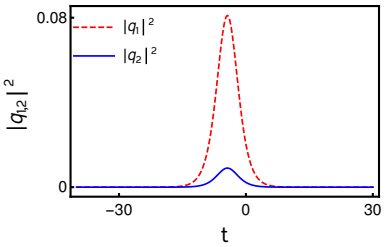

Figure 6. Degenerate one-soliton of the Manakov equation: the values of the parameters are $k_1 = 0.3 + 0.5i$, $\alpha_1^{(1)} = 1.5 + 1.5i$, $\alpha_1^{(2)} = 0.5 + 0.5i$.

Furthermore, the degenerate two-soliton solution can be deduced from the nondegenerate two-soliton solution (19) by applying the degenerate limits $k_1 = l_1$ and $k_2 = l_2$. This degenerate two-soliton solution of the Manakov system is obtained in [35]. The two-soliton solution can be compactly written in terms of Gram determinants as

$$q_j = \frac{g^{(j)}}{f}, \quad j = 1,2, \tag{36a}$$

where

$$g^{(j)} = \begin{vmatrix} A_{11} & A_{12} & 1 & 0 & e^{\eta_1} \\ A_{21} & A_{22} & 0 & 1 & e^{\eta_2} \\ -1 & 0 & B_{11} & B_{12} & 0 \\ 0 & -1 & B_{21} & B_{22} & 0 \\ 0 & 0 & -\alpha_1^{(j)} & -\alpha_2^{(j)} & 0 \end{vmatrix}, \quad f = \begin{vmatrix} A_{11} & A_{12} & 1 & 0 \\ A_{21} & A_{22} & 0 & 1 \\ -1 & 0 & B_{11} & B_{12} \\ 0 & -1 & B_{21} & B_{22} \end{vmatrix}, \tag{36b}$$

in which $A_{ij} = \frac{e^{\eta_i+\eta_j^*}}{k_i+k_j^*}$, and $B_{ij} = \kappa_{ji} = \frac{\left(\alpha_j^{(1)}\alpha_i^{(1)*} + \alpha_j^{(2)}\alpha_i^{(2)*}\right)}{(k_j+k_i^*)}$, $i,j = 1,2$. The above degenerate bright two-soliton solution is characterized by six arbitrary complex parameters $k_1, k_2, \alpha_1^{(j)}$ and $\alpha_2^{(j)}$, $j = 1,2$.

By fixing the wave numbers as $k_i = l_i, i = 1,2,...,N$, the N degenerate vector bright soliton solution can be recovered from the nondegenerate N-soliton solutions. In passing we, also note that the nondegenerate one-soliton solution (15a) and (15b) can arise when we fix the parameters $\alpha_2^{(1)} = \alpha_1^{(2)} = 0$ in Equations (36a) and (36b) and rename the constants k_2 as l_1 and $\alpha_2^{(2)}$ as $\alpha_1^{(2)}$ in the resultant solution. We also note that the above degenerate two-soliton solution (36a) and (36b) can also be rewritten from the Gram determinant forms of the nondegenerate two-soliton solution (19).

As reported in [35,36,41], the degenerate fundamental solitons ($k_i = l_i$, $i = 1,2$) in the Manakov system undergo shape changing collision due to the intensity redistribution among the modes. The energy redistribution occurs in the degenerate case because the polarization vectors of the two modes combine with each other in a specific way. This shape changing collision is illustrated in Figure 7 where the intensity redistribution occurs because

of the enhancement of soliton S_1 in the first mode and the corresponding suppression of the intensity of the same soliton in the second mode. To hold the conservation of energy between the modes, the intensity of the soliton S_2 is suppressed in the first mode and it is enhanced in the second mode. The standard elastic collision occurs (as already noted) for the very special choice of parameters, namely $\frac{\alpha_1^{(1)}}{\alpha_2^{(1)}} = \frac{\alpha_1^{(2)}}{\alpha_2^{(2)}}$ [35,36].

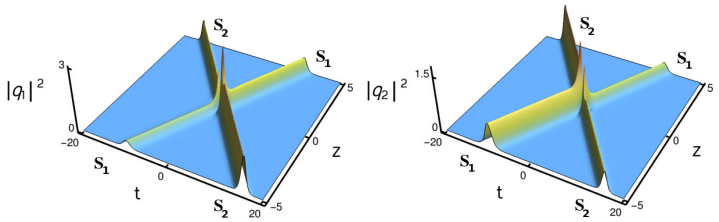

Figure 7. Shape changing collision of the degenerate two-solitons: $k_1 = l_1 = 1 + i$, $k_2 = l_2 = 1.51 - 1.51i$, $\alpha_1^{(1)} = 0.5 + 0.5i$, $\alpha_2^{(1)} = \alpha_1^{(2)} = \alpha_2^{(2)} = 1$.

4.7. Possible Experimental Realization of Nondegenerate Solitons

To experimentally observe the nondegenerate vector solitons (single hump/double hump solitons) in the Manakov system, one may adopt the mutual-incoherence method that has been used to observe the multi-hump multi-mode solitons experimentally (Ref. [50]). The Manakov solitons (degenerate solitons) can also be observed by the same experimental procedure with appropriate modifications (Ref. [37]). In the following, we briefly envisage how the procedure given in Ref. [50] can be redesigned to generate the double-humped nondegenerate soliton as it has been discussed in our work [76].

To observe the nondegenerate vector solitons experimentally, it is essential to consider two laser sources with different properties so that the wavelength of the second laser beam is different from the first one. Using polarizing beam splitters, each one of the laser beams can be split into ordinary and extraordinary beams. The extraordinary beam coming out from the first source can be further split into two individual fields F_{11} and F_{12} by allowing it to fall on a beam splitter. These two fields are nothing but the reflected and transmitted extraordinary beams coming out from the beam splitter. The intensities of these two fields are different. Similarly, the second beam which is coming out from the second source can also be split into two fields F_{21} and F_{22} by passing through another beam splitter. The intensities of these two fields are also different. As a result, one can generate four fields that are incoherent to each other. To set the incoherence in phase among these four fields, one should allow them to travel a sufficient distance before the coupling is performed. The fields F_{11} and F_{12} now become nondegenerate two individual solitons in the first mode, whereas F_{21} and F_{22} form another set of two nondegenerate solitons in the second mode. The coupling between the fields F_{11} and F_{21} can be performed by combining them using another beam splitter. Similarly, by suitably locating another beam splitter, one can combine the fields F_{12} and F_{22}, respectively. After appropriate coupling is performed, the resultant optical field beams can now be focused through two individual cylindrical lenses and the output may be recorded in an imaging system, which consists of a crystal and CCD camera. The collision between the nondegenerate two-solitons in both the modes can now be seen from the recorded images.

To observe the elastic collision between double-humped nondegenerate solitons, one must make arrangements to vanish the mutual coherence property between the solitons F_{11} and F_{12} in the first mode q_1 and F_{21} and F_{22} in the second mode q_2 (Ref. [37]). The four optical beams are now completely independent and incoherent with one another. The collision angle at which the nondegenerate solitons interact should be sufficiently large enough. Under this situation, no energy exchange is expected to occur between the nondegenerate solitons of the two modes. This experimental procedure can also be used

to realize multi-humped nondegenerate vector solitons in the N-CNLS system but with appropriate modification in the initial conditions.

4.8. Multi-Humped Nondegenerate Fundamental Bright Soliton Solution in N-CNLS System

In this sub-section, we explore the existence of the nondegenerate fundamental bright soliton solution for coupled multi-component nonlinear Schrödinger equations of Manakov type [36,82]. Here, we intend to point out the multi-hump nature of the nondegenerate fundamental solitons in the following system of multi-component nonlinear Schrödinger equations,

$$iq_{j,z} + q_{j,tt} + 2\sum_{p=1}^{N} |q_p|^2 q_j = 0, \quad j = 1, 2, ..., N. \tag{37}$$

Here, straight away we provide the nondegenerate fundamental soliton solution of the above N-CNLS system, which is derived through the Hirota bilinear method. We note that for detailed derivation one can refer to our recent paper [82]. The nondegenerate fundamental bright soliton solution $q_j = \frac{g^{(j)}}{f}, j = 1, 2, ..., N$, of the N-CNLS system written in a more compact form using the following Gram determinants

$$g^{(N)} = \begin{vmatrix} A & I & \phi \\ -I & B & \mathbf{0^T} \\ \mathbf{0} & C_N & 0 \end{vmatrix}, \quad f = \begin{vmatrix} A & I \\ -I & B \end{vmatrix}, \tag{38}$$

where the elements of the matrices A and B are

$$A_{ij} = \frac{e^{\eta_i + \eta_j^*}}{(k_i + k_j^*)}, \; B_{ij} = \kappa_{ji} = \frac{\psi_i^\dagger \sigma \psi_j}{(k_i^* + k_j)}, \; C_N = -\left(\alpha_1^{(1)}, \quad \alpha_1^{(2)}, \quad \ldots, \quad \alpha_1^{(N)} \right),$$

$$\psi_j = \left(\alpha_1^{(1)}, \quad \alpha_1^{(2)}, \quad \ldots, \quad \alpha_1^{(j)} \right)^T, \phi = \left(e^{\eta_1}, \quad e^{\eta_2}, \quad \ldots, \quad e^{\eta_n} \right)^T, j, n = 1, 2, .., N.$$

In the above, $g^{(N)}$ and f are $((2^2N) + 1)$ and (2^2N)th order determinants, respectively. When $j \neq i$, the elements κ_{ji} in the square matrix B do not exist ($\kappa_{ji} = 0$). Then, in the above fundamental soliton solution T denotes the transpose of the matrices ψ_j and ϕ, † represents transpose complex conjugate, $\sigma = I$ is an (n × n) identity matrix, ϕ is a (n × 1) column matrix, $\mathbf{0}$ is a (1 × n) null matrix, C_N is a (1 × n) row matrix and ψ represents a (n × 1) column matrix. Furthermore, for a given set of N and j values, the corresponding elements only exist and all the other elements are equal to zero in ψ_j and C_N matrices. We have verified the reliability of the nondegenerate fundamental soliton solution (38) by substituting it into the bilinear equations of the N-CNLS system along with the following derivative formula of the determinants, $\frac{\partial M}{\partial x} = \sum_{1 \leq i,j \leq n} \frac{\partial a_{i,j}}{\partial x} \frac{\partial M}{\partial a_{i,j}} = \sum_{1 \leq i,j \leq n} \frac{\partial a_{i,j}}{\partial x} \Delta_{i,j}$, where $\Delta_{i,j}$'s are the cofactors of the matrix M, the elementary properties of the determinants and the bordered determinant properties [153,155]. This action produces a pair of Jacobi identities and thus their occurrence confirms the validity of the obtained soliton solution. A multi-hump profile nature is a special feature of the obtained nondegenerate fundamental soliton solution (38). Such multi-hump structures and their propagation are characterized by $2N$ arbitrary complex wave parameters. The fundamental nondegenerate soliton admits a very interesting N-hump profile in the present N-CNLS system. The number of peaks or humps in the intensity profile of the nondegenerate fundamental soliton solution of the N-CNLS system is essentially equal to the number of wave numbers or equivalently the number of components involved. In this system, in general, the nondegenerate solitons propagate with different velocities in different modes but one can make them propagate with identical velocity by restricting the imaginary parts of all the wave numbers k_j, $j = 1, 2, ..., N$, to be equal. We wish to note that the degenerate fundamental bright soliton solution of the N-CNLS system can be obtained by setting all the wavenumbers k_j ,

$j = 1, 2, ..., N$, as identical, $k_j = k_1$, $j = 1, 2, ..., N$. It leads to single-hump intensity profiles only in all the modes [36]. Very interestingly, the N-CNLS system (9) also admits a special kind of multi-humped partially nondegenerate fundamental soliton solution for a smaller number of restrictions on the wave numbers, as we have explained in [82]. Consequently, in this partially nondegenerate case, the number of humps is not equal to the number of components.

In order to indicate the multi-hump nature of the nondegenerate soliton, here we demonstrate this special feature in the case of 3-CNLS and 4-CNLS systems. As a specific example, we can easily check that this multi-parameter solution admits a novel asymmetric triple-hump profile in the case of the 3-CNLS system when we fix the velocity as $k_{1I} = k_{2I} = k_{3I} = 0.5$. The other parameter values are chosen as $k_{1R} = 0.53$, $k_{2R} = 0.5$, $k_{3R} = 0.45$, $\alpha_1^{(1)} = 0.65 + 0.65i$, $\alpha_1^{(2)} = 0.45 - 0.45i$ and $\alpha_1^{(3)} = 0.35 + 0.35i$. In Figure 8a, we display the asymmetric triple-hump profiles in all the components for the above choice of parameter values. Then, the nondegenerate one-soliton solution in the 4-CNLS system exhibits an asymmetric quadruple-hump profile in all the modes. This novel quadruple-hump profile is displayed in Figure 8b for the parameter values $k_1 = 0.48 + 0.5i$, $k_2 = 0.5 + 0.5i$, $k_3 = 0.53 + 0.5i$, $k_4 = 0.55 + 0.5i$, $\alpha_1^{(1)} = 0.65 + 0.65i$, $\alpha_1^{(2)} = 0.55 - 0.55i$, $\alpha_1^{(3)} = 0.45 + 0.45i$ and $\alpha_1^{(4)} = 0.35 - 0.35i$. We remark that the nondegenerate fundamental soliton solution reduces to a double-humped partially nondegenerate soliton by considering a restriction $k_1 = k_2$ (or $k_2 = k_3$) [82].

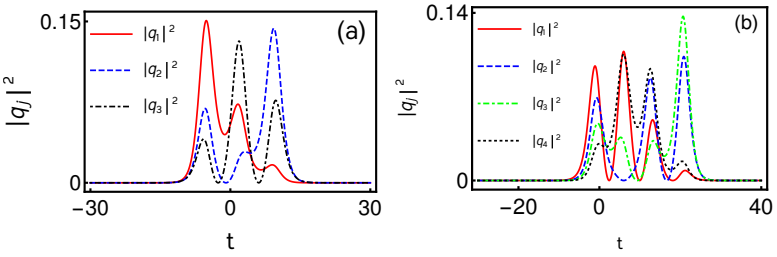

Figure 8. (**a**) Denotes triple-hump profile of the nondegenerate fundamental soliton in the 3-CNLS system and (**b**) represents a quadruple-humped nondegenerate soliton profiles in the 4-CNLS system.

In general, to derive nondegenerate N-soliton solution of the N-CNLS system, we have to consider a more general form of the starting solutions $g_1^{(j)} = \sum_{l,j=1}^{N} \alpha_l^{(j)} e^{\eta_l^{(j)}}$, $\eta_l^{(j)} = k_l^{(j)} t + i k_l^{(j)2} z$ to the lowest order set of N linear PDEs $i g_{1,z}^{(j)} + g_{1,tt}^{(j)} = 0$, $j = 1, 2, ..., N$. This choice of initial seed solutions yields a very complicated nondegenerate N-soliton solution. We do not provide the details of this intricate form here for brevity and they will be published elsewhere.

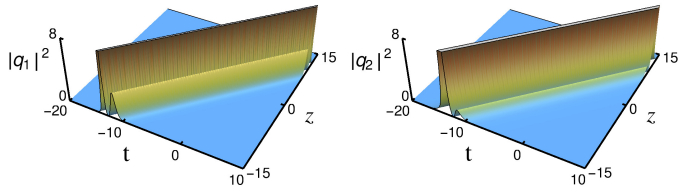

Figure 9. The singular double-hump profiles of the nondegenerate one-soliton solution (39a) and (39b) of the mixed 2-CNLS system.

5. Nondegenerate and Degenerate Bright Solitons in the Mixed 2-CNLS System

This section is essentially devoted to showing the existence of nondegenerate fundamental bright solitons in the mixed 2-CNLS system or Equation (8) with $\sigma_1 = +1$ and $\sigma_2 = -1$. In this section, we also point out how the degenerate fundamental bright soliton can be captured from the obtained nondegenerate one-soliton solution and indicate its

energy sharing collision. In order to write down the analytical form of the nondegenerate fundamental soliton solution, one has to follow the same procedure that has been adopted to derive such a solution in the case of the Manakov system. Since the solution construction methodology has been extensively described in References [75–77] and in the earlier section, here we immediately present the explicit form of the nondegenerate fundamental soliton solution of the mixed 2-CNLS system. It reads as

$$q_1 = \frac{g_1^{(1)} + g_3^{(1)}}{1 + f_2 + f_4} = \frac{1}{D}(\alpha_1^{(1)} e^{\eta_1} + e^{\eta_1+\xi_1+\xi_1^*+\Delta_1^{(1)}}), \tag{39a}$$

$$q_2 = \frac{g_1^{(2)} + g_3^{(2)}}{1 + f_2 + f_4} = \frac{1}{D}(\alpha_1^{(2)} e^{\xi_1} + e^{\eta_1+\eta_1^*+\xi_1+\Delta_1^{(2)}}). \tag{39b}$$

Here $D = 1 + e^{\eta_1+\eta_1^*+\delta_1} + e^{\xi_1+\xi_1^*+\delta_2} + e^{\eta_1+\eta_1^*+\xi_1+\xi_1^*+\delta_{11}}$, $e^{\Delta_1^{(1)}} = -\frac{(k_1-l_1)\alpha_1^{(1)}|\alpha_1^{(2)}|^2}{(k_1+l_1^*)(l_1+l_1^*)^2}$, $e^{\Delta_1^{(2)}} = \frac{(k_1-l_1)|\alpha_1^{(1)}|^2\alpha_1^{(2)}}{(k_1+k_1^*)^2(k_1^*+l_1)}$, $e^{\delta_1} = \frac{|\alpha_1^{(1)}|^2}{(k_1+k_1^*)^2}$, $e^{\delta_2} = -\frac{|\alpha_1^{(2)}|^2}{(l_1+l_1^*)^2}$ and $e^{\delta_{11}} = -\frac{|k_1-l_1|^2|\alpha_1^{(1)}|^2|\alpha_1^{(2)}|^2}{(k_1+k_1^*)^2|k_1+l_1^*|^2(l_1+l_1^*)^2}$. Like in the Manakov system, the two complex parameters $\alpha_1^{(j)}$'s, $j = 1, 2$, and the two wave numbers k_1, and l_1 describes the behavior of the above general form of the one-soliton solution (39a) and (39b). By rewriting the solution (39a) and (39b) in hyperbolic form, as has been done in Equations (17a) and (17b), we find that the amplitude, velocity and central position of the soliton in the first mode is $2k_{1R}$, $2k_{1I}$ and $\frac{\phi_1}{2l_{1R}} = \frac{1}{2l_{1R}} \log \frac{(l_1-k_1|\alpha_1^{(2)}|^2)}{(k_1+l_1^*)(l_1+l_1^*)^2}$, respectively. In the second mode, the amplitude, velocity and central position of the soliton are defined by $2l_{1R}$, $2l_{1I}$ and $\frac{\phi_2}{2k_{1R}} = \frac{1}{2k_{1R}} \log \frac{(k_1-l_1|\alpha_1^{(1)}|^2)}{(k_1^*+l_1)(k_1+k_1^*)^2}$, respectively. In the mixed 2-CNLS system too, the nondegenerate fundamental soliton propagates in the two modes either with identical velocity ($v_1 = v_2 = 2k_{1I}$) or with non-identical velocity ($v_1 = 2k_{1I} \neq v_2 = 2l_{1I}$) depending on the restriction on the imaginary parts of the wave numbers k_1 and l_1. The solution (39a) and (39b) always shows singular behavior due to the presence of the negative sign in the constant terms e^{δ_2} and $e^{\delta_{11}}$ except for $k_1 = l_1$. This negative sign essentially arises because of the presence of defocusing nonlinearity of the mixed CNLS system. The singularity nature of the solution (39a) and (39b) is depicted in Figure 9 with the parameter values $k_1 = 1.25 + 0.45i$, $l_1 = -0.5 + 0.45i$, $\alpha_1^{(1)} = 0.3$ and $\alpha_1^{(2)} = i$. We note that the singular nature of the soliton has been recently discussed in the context of singular optics [156]. The nondegenerate higher order bright solitons can also be obtained in a similar way and one can analyze their collision dynamics.

By imposing the limit $k_1 = l_1$ in the solution (39a) and (39b), one can capture the following degenerate fundamental vector bright soliton solution of the mixed 2-CNLS system, $q_j = k_{1R}\hat{A}_j e^{i\eta_{1I}} \operatorname{sech}(\eta_{1R} + \frac{R}{2})$, where $\eta_{1R} = k_{1R}(t - 2k_{1I}z)$, $\eta_{1I} = k_{1I}t + (k_{1R}^2 - k_{1I}^2)z$, $\hat{A}_j = \frac{\alpha_1^{(j)}}{\sqrt{(|\alpha_1^{(1)}|^2 - |\alpha_1^{(2)}|^2)}}$, $e^R = \frac{(|\alpha_1^{(1)}|^2 - |\alpha_1^{(2)}|^2)}{(k_1+k_1^*)^2}$, $j = 1, 2$. The latter degenerate bright soliton solution always admits the non-singular single-hump intensity profile when $|\alpha_1^{(1)}| > |\alpha_1^{(2)}|$. The degenerate multi-soliton solutions and their interesting collision properties have been already discussed in [64]. The two-soliton solution of the mixed 2-CNLS system can be easily obtained by replacing B_{ij} with $B_{ij} = \kappa_{ji} = \frac{\left(\alpha_j^{(1)}\alpha_i^{(1)*} - \alpha_j^{(2)}\alpha_i^{(2)*}\right)}{(k_j + k_i^*)}$, $i, j = 1, 2$ in the degenerate two-soliton solution (36a) and (36b) of the Manakov system. However, here we indicate the special collision dynamics exhibited by the degenerate bright solitons only through a graphical demonstration as we illustrated below in Figure 10 for the parametric choice $k_1 = 1 - i$, $k_2 = 1.7 + I$, $\alpha_1^{(1)} = 1 + i$, $\alpha_2^{(1)} = 1 - i$, $\alpha_1^{(2)} = 0.5 + 0.3i$ and $\alpha_2^{(2)} = 0.7$. From Figure 10, we identify that during the collision process of the degenerate two bright solitons S_1 and S_2 in the present mixed 2-CNLS system, the intensity of the soliton S_1 is enhanced in all the modes. In contradiction to this, the intensity of the other soliton

S_2 is suppressed in both the modes. Therefore, such a special property of enhancement of the intensity of a given soliton always occurs in the mixed 2-CNLS system. One may find the details of energy conservation in Ref. [64]. Additionally, we also observe the amplitude dependent phase shifts in each of the modes. This energy sharing collision is quite different from the shape changing collision of the Manakov system. The collision scenario is depicted in Figure 10 can be viewed as a signal amplification process, in which the soliton S_1 refers as a signal wave and the soliton S_2 represents as a pump wave. During this amplification process, there is no external amplification medium is employed and is without the introduction of any noise [64]. We point out that the standard NLS soliton-like collision can be recovered by imposing the restriction $\frac{\alpha_1^{(1)}}{\alpha_2^{(1)}} = \frac{\alpha_1^{(2)}}{\alpha_2^{(2)}}$.

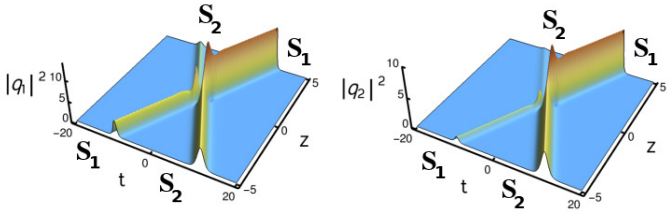

Figure 10. Energy sharing collision of degenerate two bright solitons of the mixed 2-CNLS system [64].

6. Existence of Nondegenerate and Degenerate Bright Solitons in Two-Component Coherently Coupled Nonlinear Schrödinger System

Now, we intend to derive a more general form of nondegenerate fundamental bright soliton solution of the two-component CCNLS system (10). In this section, we also mention the already known degenerate one bright soliton solution and illustrate its fascinating energy switching collision property through a graphical demonstration. To obtain the explicit forms of the nondegenerate soliton solution, we adopt a non-standard bilinearization procedure in which an appropriate number of auxiliary functions have been introduced to match the number of bilinear equations with the number of bilinearizing variables. This procedure was developed by Gilson et al. [157] for the Sasa–Satsuma higher order nonlinear Schrödinger equations and by Kanna et al. [107,108] for the coherently coupled nonlinear Schrödinger equations. By adopting this technique, we obtain the following correct bilinear equations of system (10) through the bilinearizing transformation $q_j = \frac{g^{(j)}}{f}$, $j = 1, 2$, to Equation (10) with the introduction of an auxiliary function s. The set of bilinear equations are

$$D_1(g^{(j)} \cdot f) = \gamma s g^{(j)*},\ j = 1,2,\ D_2(f \cdot f) = 2\gamma\left(\sum_{j=1}^{2} |g^{(j)}|^2\right),\ s \cdot f = \sum_{j=1}^{2} (g^{(j)})^2, \tag{40}$$

where $D_1 = iD_z + D_t^2$ and $D_2 = D_t^2$. Here $g^{(j)}$'s and f are complex and real functions, respectively, $*$ denotes the complex conjugate. After the bilinearization, essentially we follow the procedure that has been described in [107] for the degenerate case but now with the general forms of seed solutions $g_1^{(1)} = \alpha_1 e^{\eta_1}$, $g_1^{(2)} = \beta_1 e^{\xi_1}$, $\eta_1 = k_1 t + ik_1^2 z$, $\xi_1 = l_1 t + il_1^2 z$. While doing so, the series expansions are truncated as $g^{(j)} = \epsilon g_1^{(j)} + \epsilon^3 g_3^{(j)} + \epsilon^5 g_5^{(j)} + \epsilon^7 g_7^{(j)}$, $f = 1 + \epsilon^2 f_2 + \epsilon^4 f_4 + \epsilon^6 f_6 + \epsilon^8 f_8$ and $s = \epsilon^2 s_2 + \epsilon^4 s_4 + \epsilon^6 s_6$. By substituting the obtained forms of the unknown functions in the appropriate places, we obtain the

following a more general form of nondegenerate coherently coupled fundamental bright soliton solution of the 2-CCNLS system (10),

$$\begin{aligned}
q_1(z,t) &= \frac{1}{f}\Big(\alpha_1 e^{\eta_1} + e^{2\eta_1+\eta_1^*+\Delta_{11}} + e^{\eta_1^*+2\xi_1+\Delta_{12}} + e^{\eta_1+\xi_1+\xi_1^*+\Delta_{13}} + e^{\eta_1+2(\eta_1^*+\xi_1)+\Delta_{14}} \\
&\quad + e^{\eta_1+2(\xi_1+\xi_1^*)+\Delta_{15}} + e^{2\eta_1+\eta_1^*+\xi_1+\xi_1^*+\Delta_{16}} + e^{2(\eta_1+\xi_1+\xi_1^*)+\eta_1^*+\Delta_{17}}\Big), \\
q_2(z,t) &= \frac{1}{f}\Big(\beta_1 e^{\xi_1} + e^{2\xi_1+\xi_1^*+\Delta_{21}} + e^{\xi_1^*+2\eta_1+\Delta_{22}} + e^{\xi_1+\eta_1+\eta_1^*+\Delta_{23}} + e^{\xi_1+2(\xi_1^*+\eta_1)+\Delta_{24}} \\
&\quad + e^{\xi_1+2(\eta_1^*+\eta_1)+\Delta_{25}} + e^{2\xi_1+\xi_1^*+\eta_1+\eta_1^*+\Delta_{26}} + e^{2(\eta_1+\eta_1^*+\xi_1)+\xi_1^*+\Delta_{27}}\Big), \\
f &= 1 + e^{\eta_1+\eta_1^*+\delta_1} + e^{\xi_1+\xi_1^*+\delta_2} + e^{2(\eta_1+\eta_1^*)+\delta_3} + e^{2(\eta_1+\xi_1^*)+\delta_4} + e^{2(\xi_1+\eta_1^*)+\delta_5} \\
&\quad + e^{2(\xi_1+\xi_1^*)+\delta_6} + e^{(\eta_1+\eta_1^*+\xi_1+\xi_1^*)+\delta_7} + e^{2(\eta_1+\eta_1^*)+\xi_1+\xi_1^*+\nu_1} \\
&\quad + e^{2(\xi_1+\xi_1^*)+\eta_1+\eta_1^*+\nu_2} + e^{2(\eta_1+\eta_1^*+\xi_1+\xi_1^*)+\nu_3}.
\end{aligned} \tag{41}$$

The various constants which appear in the above solution are defined by

$$\begin{aligned}
&e^{\Delta_{11}} = \frac{\gamma\alpha_1|\alpha_1|^2}{2\kappa_{11}}, e^{\Delta_{12}} = \frac{\gamma\alpha_1^*\beta_1^2}{2\theta_1^{*2}}, e^{\Delta_{13}} = \frac{\gamma\alpha_1|\beta_1|^2\rho_1}{\theta_1 l_{11}}, e^{\Delta_{14}} = \frac{\gamma^2\rho_1^2\alpha_1^*\beta_1^2|\alpha_1|^2}{4\kappa_{11}\theta_1^{*4}}, \\
&e^{\Delta_{15}} = \frac{\gamma^2\rho_1^2\alpha_1|\beta_1|^4}{4l_{11}^2\theta_1^2}, e^{\Delta_{16}} = \frac{\gamma^2\rho_1^2\rho_1^*\alpha_1|\alpha_1|^2|\beta_1|^2}{2\kappa_{11}l_{11}\theta_1^2\theta_1^*}, e^{\Delta_{17}} = \frac{\gamma^3\rho_1^4\rho_1^{*2}\alpha_1|\alpha_1|^2|\beta_1|^4}{8\kappa_{11}l_{11}^2\theta_1^4\theta_1^{*2}}, \\
&e^{\Delta_{21}} = \frac{\gamma\beta_1|\beta_1|^2}{2l_{11}}, e^{\Delta_{22}} = \frac{\gamma\alpha_1^2\beta_1^*}{2\theta_1^2}, e^{\Delta_{23}} = -\frac{\gamma|\alpha_1|^2\beta_1\rho_1}{\theta_1^*\kappa_{11}}, e^{\Delta_{24}} = \frac{\gamma^2\rho_1^2\alpha_1^2|\beta_1|^2\alpha_1^*}{4l_{11}\theta_1^4}, \\
&e^{\Delta_{25}} = \frac{\gamma^2\rho_1^2|\alpha_1|^4\beta_1}{4\kappa_{11}^2\theta_1^{*2}}, e^{\Delta_{26}} = -\frac{\gamma^2\rho_1^2\rho_1^*\beta_1|\alpha_1|^2|\beta_1|^2}{2\kappa_{11}l_{11}\theta_1\theta_1^{*2}}, e^{\Delta_{27}} = \frac{\gamma^3\rho_1^4\rho_1^{*2}\beta_1|\alpha_1|^4|\beta_1|^2}{8\kappa_{11}^2l_{11}\theta_1^2\theta_1^{*4}}, \\
&e^{\delta_1} = \frac{\gamma|\alpha_1|^2}{\kappa_{11}}, e^{\delta_2} = \frac{\gamma|\beta_1|^2}{l_{11}}, e^{\delta_3} = \frac{\gamma^2|\alpha_1|^4}{4\kappa_{11}^2}, e^{\delta_4} = \frac{\gamma^2\alpha_1^2\beta_1^{*2}}{4\theta_1^4}, e^{\delta_5} = \frac{\gamma^2\alpha_1^{*2}\beta_1^2}{4\theta_1^{*4}}, \\
&e^{\delta_6} = \frac{\gamma^2|\beta_1|^4}{4l_{11}^2}, e^{\delta_7} = \frac{\gamma^2|\rho_1|^2|\alpha_1|^2|\beta_1|^2}{\kappa_{11}l_{11}|\theta_1|^2}, e^{\nu_1} = \frac{\gamma^3|\rho_1|^4|\alpha_1|^4|\beta_1|^2}{4\kappa_{11}^2l_{11}|\theta_1|^4}, \\
&e^{\nu_2} = \frac{\gamma^3|\rho_1|^4|\alpha_1|^2|\beta_1|^4}{4\kappa_{11}l_{11}^2|\theta_1|^2}, e^{\nu_3} = \frac{\gamma^4|\rho_1|^8|\alpha_1|^4|\beta_1|^4}{16\kappa_{11}^2l_{11}^2|\theta_1|^8}, l_{11} = (l_1+l_1^*)^2, \\
&\theta_1 = (k_1+l_1^*),\ \rho_1 = (k_1-l_1),\ \kappa_{11} = (k_1+k_1^*)^2.
\end{aligned}$$

The auxiliary function $s(z,t)$ is found to be, $s = \alpha_1^2 e^{2\eta_1} + \beta_1^2 e^{2\xi_1} + e^{2\eta_1+\xi_1+\xi_1^*+\phi_1} + e^{2\xi_1+\eta_1+\eta_1^*+\phi_2} + e^{2(\eta_1+\eta_1^*+\xi_1)+\phi_3} + e^{2(\eta_1+\xi_1^*+\xi_1)+\phi_4}$, $e^{\phi_1} = \frac{\gamma\rho_1^2\alpha_1^2|\beta_1|^2}{\theta_1^2 l_{11}}$, $e^{\phi_2} = \frac{\gamma\rho_1^2\beta_1^2|\alpha_1|^2}{\theta_1^{*2}\kappa_{11}}$, $e^{\phi_3} = \frac{\gamma^2\rho_1^4\beta_1^2|\alpha_1|^4}{4\theta_1^{*4}\kappa_{11}^2}$, $e^{\phi_4} = \frac{\gamma^2\rho_1^4\alpha_1^2|\beta_1|^4}{4\theta_1^4 l_{11}^2}$. The shape of the coherently coupled nondegenerate fundamental soliton solution (41) is governed by the four complex parameters k_1, l_1, α_1 and β_1. Due to the presence of coherent coupling among the two fields q_1 and q_2 (or four-wave mixing effect) and the additional wave number, the solution (41) admits rich geometrical structures, such as a breather, a quadruple-hump, a triple-hump, a double-hump, a flattop and a single-hump profiles under a suitable choice of parameter values. We display a novel non-trivial breathing nondegenerate fundamental soliton profile in Figure 11. To draw this figure, we fixed the parametric values as $\gamma = 4$, $k_1 = 2.5 + 0.5i$, $l_1 = 1.65 + 0.5i$, $\alpha_1 = 0.5 + 0.5i$ and $\beta_1 = 1 - i$. The breathing nature of the multi-hump profile of the nondegenerate soliton in the present 2-CCNLS system cannot be observed in the degenerate case [107,108], as described below. We note that one can also derive the nondegenerate multi-soliton solutions to the 2-CCNLS system. However, the resultant expressions will be cumbersome due to the presence of the four-wave mixing effect.

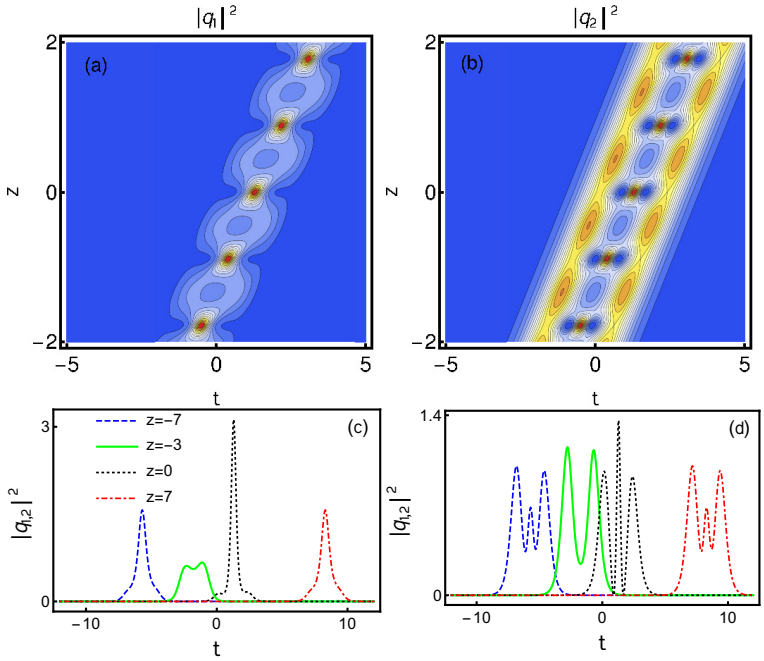

Figure 11. The figures (**a**,**b**) denote the contour plots of the breathing non-degenerate fundamental bright soliton of the 2-CCNLS system and the corresponding line plots are drawn for various z values in figures (**c**,**d**).

In order to obtain the degenerate one-soliton solution, one has to impose the wave number restriction $k_1 = l_1$ in Equation (41). This results in the following explicit degenerate bright one-soliton solution,

$$q_1 = \frac{\alpha_1 e^{\eta_1} + e^{2\eta_1+\eta_1^*+\Delta_1}}{1 + e^{\eta_1+\eta_1^*+R_1} + e^{2\eta_1+2\eta_1^*+\delta_{11}}},\ q_2 = \frac{\beta_1 e^{\eta_1} + e^{2\eta_1+\eta_1^*+\Delta_2}}{1 + e^{\eta_1+\eta_1^*+R_1} + e^{2\eta_1+2\eta_1^*+\delta_{11}}}, \tag{42}$$

where the auxiliary function is reduced to the form $s = (\alpha_1^2 + \beta_1^2)e^{2\eta_1}$. Here, $\eta_1 = k_1(t + ik_1 z)$, $e^{\Delta_1} = \frac{\gamma\alpha_1^*(\alpha_1^2+\beta_1^2)}{2(k_1+k_1^*)^2}$, $e^{\Delta_2} = \frac{\gamma\beta_1^*(\alpha_1^2+\beta_1^2)}{2(k_1+k_1^*)^2}$, $e^{R_1} = \frac{\gamma(|\alpha_1|^2+|\beta_1|^2)}{(k_1+k_1^*)^2}$, $e^{\delta_{11}} = \frac{\gamma^2(\alpha_1^2+\beta_1^2)(\alpha_1^{*2}+\beta_1^{*2})}{4(k_1+k_1^*)^4}$. The above degenerate solution (42) is characterized by only two complex parameters α_1 and β_1 and a single complex wave number k_1. We point out that the degenerate solution (42) is classified as a coherently coupled bright soliton and an incoherently coupled bright soliton depending on the presence/absence of the auxiliary function s [107]. If the restriction, $\alpha_1^2 + \beta_1^2 = 0$ is imposed, where the auxiliary function s becomes zero, in the solution (42), then the resultant solution is called ICS [107]. Due to this restriction, the coherent coupling among the fields q_1 and q_2 vanishes. Under the latter restriction, the analytical form of ICS is reduced from the solution (42) as

$$q_1 = A_1 \operatorname{sech}(\eta_{1R} + \frac{R_1}{2})e^{i\eta_{1I}},\ q_2 = \pm q_1. \tag{43}$$

Here, $A_1 = \frac{\alpha_1}{2}e^{-\frac{R_1}{2}}$, $R_1 = \log\left(\frac{2\gamma|\alpha_1|^2}{(k_1+k_1^*)^2}\right)$, $\eta_{1R} = k_{1R}(t - 2k_{1I}z)$ and $\eta_{1I} = k_{1I}t + (k_{1I}^2 - k_{1R}^2)z$. From the above solution, it is evident that the ICS always admits a 'sech'-type intensity profile only. However, very interestingly, a novel double-hump profile arises in the degenerate case when the auxiliary function is non-zero. That is, for $\alpha_1^2 + \beta_1^2 \neq 0$ the coherent coupling among the optical fields is established. Thus, the solution (42) admits the double-hump profile as demonstrated below in Figure 12. However, in the degenerate case, even the presence of single wave number k_1 and the four wave mixing effect can induce only the double-hump profile apart from a flattop profile. We do not present the

degenerate two-soliton solution of the 2-CCNLS system for brevity. However, the explicit form of the degenerate two-soliton solution has been given in [107,108].

In addition to the above, we wish to specify the fascinating shape changing collision of degenerate solitons in the 2-CCNLS system. Especially, we discuss the collision between the coherently coupled soliton (42) and incoherently coupled soliton (43). As an example, we illustrate such a novel collision scenario in Figure 13. In order to display both CCS and ICS in this figure we choose the parametric values as $\gamma = 2$, $k_1 = 1.9 + i$, $k_2 = 2.1 - i$, $\alpha_1 = 0.5i$, $\alpha_2 = 0.5 + 0.5i$, $\beta_1 = 1.5$ and $\beta_2 = 0.5 - 0.5i$. In Figure 13, we refer the soliton S_1 as CCS and the soliton S_2 as ICS. This figure clearly explains that the CCS S_1 encounters intensity/energy switching in all the modes. In contradiction to this, the ICS S_2 undergoes elastic collision with a finite phase shift as specified in [107]. Consequently, the CCS S_1 switches its double-hump intensity profile to the single-hump profile in the first component and it is reversed in the second component without affecting the structure of ICS S_2. In this type of energy switching collision scenario, the energy in the individual component is not conserved. However, the total energy, $\int_{-\infty}^{+\infty}(|q_1|^2 + |q_2|^2)dt$, is conserved. The detailed discussion on this collision scenario and its asymptotic analysis has been carried out in [108]. We also note that elastic collision always occurs during the collision among the two coherently coupled solitons and it is true in the case of collision between two incoherently coupled solitons too. We remark that the generalization of the above outcome for the multi-component CCNLS system has been established in [108] with exciting results.

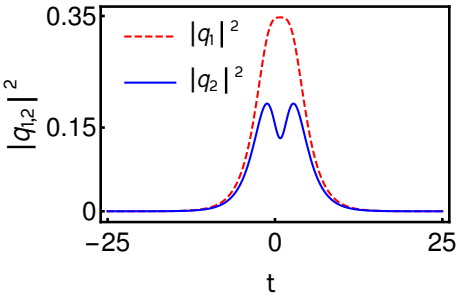

Figure 12. A typical degenerate bright soliton profile in the 2-CCNLS system is drawn for the values $\gamma = 2$, $k_1 = 0.5 + 0.5i$,$\alpha_1 = 0.72 + 0.5i$ and $\beta_1 = 0.5 - 0.42i$.

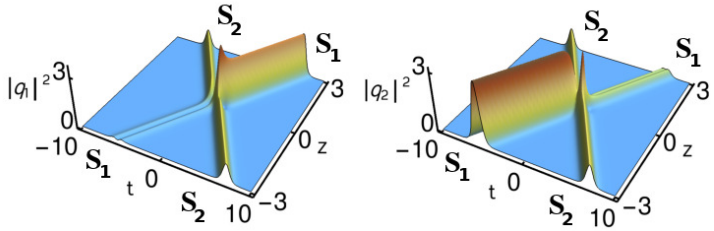

Figure 13. Energy switching collision between CCS and ICS in a 2-CCNLS system [107,108].

7. Fundamental Vector Bright Solitons in a GCNLS System

To construct both the nondegenerate and degenerate fundamental vector bright soliton solutions of the GCNLS system (11a) and (11b), we consider the bilinear forms, $(iD_z + D_t^2)g^{(j)} \cdot f = 0$, $j = 1,2$, $D_t^2 f \cdot f = 2(ag^{(1)}g^{(1)*} + cg^{(2)}g^{(2)*} + bg^{(1)}g^{(2)*} + b^*g^{(1)*}g^{(2)})$, which result from substituting the dependent variable transformation $q_j = \frac{g^{(j)}(z,t)}{f(z,t)}$, $j = 1,2$, to Equations (11a) and (11b). Here $g^{(j)}$'s are complex functions and f is a real function. By following the same procedure that has been outlined in Section 4.1, we obtain the general

form of nondegenerate fundamental bright soliton solution of the GCNLS system (11a) and (11b) as [158]

$$q_1 = \frac{g_1^{(1)} + g_3^{(1)}}{1 + f_2 + f_4} = \frac{1}{D}(\alpha_1^{(1)} e^{\eta_1} + e^{\eta_1+\xi_1+\xi_1^*+\nu_{11}} + e^{\eta_1+\eta_1^*+\xi_1+\nu_{12}}), \tag{44a}$$

$$q_2 = \frac{g_1^{(2)} + g_3^{(2)}}{1 + f_2 + f_4} = \frac{1}{D}(\alpha_1^{(1)} e^{\eta_1} + e^{\eta_1+\xi_1+\xi_1^*+\nu_{21}} + e^{\eta_1+\eta_1^*+\xi_1+\nu_{22}}), \tag{44b}$$

$$D = 1 + e^{\eta_1+\eta_1^*+\delta_1} + e^{\eta_1+\xi_1^*+\delta_2} + e^{\eta_1^*+\xi_1+\delta_2^*} + e^{\xi_1+\xi_1^*+\delta_3} + e^{\eta_1+\eta_1^*+\xi_1+\xi_1^*+\delta_4}.$$

Here, $\eta_1 = k_1(t + ik_1 z)$, $\xi_1 = l_1(t + il_1 z)$, $e^{\nu_{11}} = \frac{c(k_1-l_1)\alpha_1^{(1)}|\alpha_1^{(2)}|^2}{(k_1+l_1^*)(l_1+l_1^*)^2}$, $e^{\nu_{12}} = \frac{b^*(k_1-l_1)\alpha_1^{(2)}|\alpha_1^{(1)}|^2}{(k_1+k_1^*)(l_1+k_1^*)^2}$, $e^{\nu_{21}} = -\frac{b(k_1-l_1)\alpha_1^{(1)}|\alpha_1^{(2)}|^2}{(l_1+l_1^*)(k_1+l_1^*)^2}$, $e^{\nu_{22}} = -\frac{a(k_1-l_1)\alpha_1^{(2)}|\alpha_1^{(1)}|^2}{(k_1+k_1^*)^2(l_1+k_1^*)}$, $e^{\delta_1} = \frac{a|\alpha_1^{(1)}|^2}{(k_1+k_1^*)^2}$, $e^{\delta_2} = \frac{b\alpha_1^{(1)}\alpha_1^{(2)*}}{(k_1+l_1^*)^2}$, $e^{\delta_3} = \frac{c|\alpha_1^{(2)}|^2}{(l_1+l_1^*)^2}$ and $e^{\delta_4} = \frac{|k_1-l_1|^2|\alpha_1^{(1)}|^2|\alpha_1^{(2)}|^2(ac|k_1+l_1^*|^2-|b|^2(k_1+k_1^*)(l_1+l_1^*))}{(k_1+k_1^*)^2(k_1^*+l_1)^2(k_1+l_1^*)^2(l_1+l_1^*)^2}$. Under the restrictions, ($a = c = 1, b = 0$) and ($a = 1, c = -1, b = 0$) the solution (44a) and (44b) of GCNLS system exactly coincides with the nondegenerate one-soliton solution of the Manakov system and mixed 2-CNLS system, respectively. In the present GCNLS system, the properties of the nondegenerate fundamental bright soliton solution (44a) and (44b) is determined by the four complex parameters $\alpha_1^{(j)}$, $j = 1, 2$, k_1 and l_1 apart from the system parameters a (SPM), c (XMP) and b (the four wave mixing effect). The nondegenerate one-soliton solution admits singularity whenever either one of the signs of SPM (a) and XPM (c) is negative or if both are negative. Additionally, the condition $(ac|k_1 + l_1^*|^2 - |b|^2(k_1 + k_1^*)(l_1 + l_1^*)) > 0$ should also be maintained to obtain a regular soliton solution of the GCNLS system. The solution exhibits a double-hump or a single-hump intensity profile for suitable choices of parameter values. Very surprisingly, like in the case of the 2-CCNLS system, the presence of a four-wave mixing term and an additional wave number induces breather formation in the structure of nondegenerate fundamental soliton. A typical breathing behavior along the z direction is displayed in Figure 14. This kind of breathing soliton is not observed in the Manakov and mixed CNLS cases.

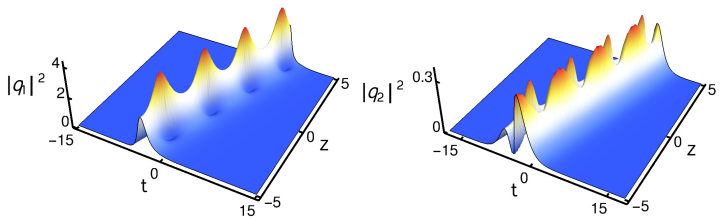

Figure 14. Breathing nondegenerate fundamental soliton in the GCNLS system. Here the parameters are $k_1 = 1.65 + 0.5i$, $l_1 = 0.45 + 0.5i$, $\alpha_1^{(1)} = 0.35 + 0.35 + i$, $\alpha_1^{(2)} = 0.5 + 0.5i$, $a = c = 1$ and $b = 0.5 - 0.5i$.

The degenerate bright soliton solution is recovered by incorporating the limit $k_1 = l_1$ in the solution (44a) and (44b). It leads to the following expressions of the degenerate bright soliton solution [117], $q_j = A_j k_{1R}\,\mathrm{sech}(\eta_{1R} + \frac{R_1}{2})e^{i\eta_{1I}}$, $A_j = \frac{\alpha_1^{(j)}}{(a|\alpha_1^{(1)}|^2+c|\alpha_1^{(2)}|^2+b\alpha_1^{(1)}\alpha_1^{(2)*}+b^*\alpha_1^{(1)*}\alpha_1^{(2)})^{1/2}}$, $e^{R_1} = \frac{(a|\alpha_1^{(1)}|^2+c|\alpha_1^{(2)}|^2+b\alpha_1^{(1)}\alpha_1^{(2)*}+b^*\alpha_1^{(1)*}\alpha_1^{(2)})}{(k_1+k_1^*)^2}$, $\eta_{1R} = k_{1R}(t - 2k_{1I}z)$, $\eta_{1I} = k_{1I}t + (k_{1R}^2 - k_{1I}^2)z$. The latter expressions ensure that the degenerate fundamental soliton always admits a single-hump profile characterized by three complex constants k_1 and $\alpha_1^{(j)}$'s. The degenerate two-soliton solution can be easily obtained by replacing the form of $B_{ji} = \kappa_{ij} = \frac{(a\alpha_i^{(1)}\alpha_j^{(1)*}+c\alpha_i^{(2)}\alpha_j^{(2)*}+b\alpha_i^{(1)}\alpha_j^{(2)*}+b^*\alpha_j^{(1)*}\alpha_i^{(2)})}{(k_i+k_j^*)}$, $i, j = 1, 2$, into Equations (36a) and (36b). With arbitrary values of b, the degenerate two solitons undergo two types of shape changing

collisions corresponding to two different choices: (i) Manakov type shape changing collision for $a, c > 0$, (ii) a mixed 2-CNLS type shape changing collision for $a > 0$, $c < 0$. We do not provide the corresponding collision plots for brevity. We wish to point out that the degenerate bright solitons also undergo a special collision scenario, where the two degenerate solitons in each of the components do not pass through each other, whereas they bounce off each other when they start to collide. This type of bright soliton collision scenario is referred to as soliton reflection in the literature [115,118].

8. Nondegenerate and Degenerate Bright Solitons in Two Component LSRI System

Finally, we intend to construct the nondegenerate fundamental soliton solution for the two-component long-wave short-wave resonance interaction system, namely the two-component Yajima–Oikawa system [77,126]. To derive the nondegenerate one-soliton solution we again bilinearize Equation (12) through the following dependent variable transformations, $S^{(l)}(x,t) = \frac{g^{(l)}(x,t)}{f(x,t)}$, $l = 1,2$, $L = 2\frac{\partial^2}{\partial x^2}\ln f(x,t)$. By doing so, we obtain the following bilinear equations:

$$D_1 g^{(l)} \cdot f = 0, l = 1,2,\ D_2 f \cdot f = \sum_{n=1}^{2} |g^{(n)}|^2, \tag{45}$$

where $D_1 \equiv iD_t + D_x^2$ and $D_2 \equiv D_x D_t$. With the modified forms of seed solutions $g_1^{(1)} = \alpha_1 e^{\eta_1}$, $g_1^{(2)} = \beta_1 e^{\xi_1}$, $\eta_1 = k_1 x + ik_1^2 t$, $\xi_1 = l_1 x + il_1^2 t$, we find that the series expansions that are given in [77] are terminated as $g^{(l)} = \epsilon g_1^{(l)} + \epsilon^3 g_3^{(l)}$, $f = 1 + \epsilon^2 f_2 + \epsilon^4 f_4$. The explicit forms of the unknown functions lead to the following nondegenerate fundamental soliton solution,

$$S^{(1)} = \frac{g_1^{(1)} + g_3^{(1)}}{1 + f_2 + f_4} = \frac{\alpha_1 e^{\eta_1} + e^{\eta_1+\xi_1+\xi_1^*+\mu_{11}}}{1 + e^{\eta_1+\eta_1^*+R_1} + e^{\xi_1+\xi_1^*+R_2} + e^{\eta_1+\eta_1^*+\xi_1+\xi_1^*+R_3}}, \tag{46a}$$

$$S^{(2)} = \frac{g_1^{(2)} + g_3^{(2)}}{1 + f_2 + f_4} = \frac{\beta_1 e^{\xi_1} + e^{\xi_1+\eta_1+\eta_1^*+\mu_{12}}}{1 + e^{\eta_1+\eta_1^*+R_1} + e^{\xi_1+\xi_1^*+R_2} + e^{\eta_1+\eta_1^*+\xi_1+\xi_1^*+R_3}}, \tag{46b}$$

$$L = \frac{2}{f^2}\Big((k_1+k_1^*)^2 e^{\eta_1+\eta_1^*+R_1} + (l_1+l_1^*)^2 e^{\xi_1+\xi_1^*+R_2} + e^{\eta_1+\eta_1^*+\xi_1+\xi_1^*+R_4} + e^{2(\eta_1+\eta_1^*)+\xi_1+\xi_1^*+R_1+R_3} + e^{\eta_1+\eta_1^*+2(\xi_1+\xi_1^*)+R_2+R_3}\Big), \tag{46c}$$

$$f = (1 + e^{\eta_1+\eta_1^*+R_1} + e^{\xi_1+\xi_1^*+R_2} + e^{\eta_1+\eta_1^*+\xi_1+\xi_1^*+R_3}),$$

where $e^{\mu_{11}} = \frac{i\alpha_1|\beta_1|^2(l_1-k_1)}{2(k_1+l_1^*)(l_1-l_1^*)(l_1+l_1^*)^2}$, $e^{\mu_{12}} = \frac{i\beta_1|\alpha_1|^2(k_1-l_1)}{2(k_1^*+l_1)(k_1-k_1^*)(k_1+k_1^*)^2}$, $e^{R_1} = \frac{|\alpha_1|^2}{2i(k_1+k_1^*)^2(k_1-k_1^*)}$, $e^{R_2} = \frac{|\beta_1|^2}{2i(l_1+l_1^*)^2(l_1-l_1^*)}$, $e^{R_3} = -\frac{|\alpha_1|^2|\beta_1|^2|k_1-l_1|^2}{4|k_1+l_1^*|^2(k_1-k_1^*)(l_1-l_1^*)(k_1+k_1^*)^2(l_1+l_1^*)^2}$, $e^{R_4} = -2(k_1+k_1^*)(l_1+l_1^*)(e^{R_1+R_2} - e^{R_3}) + ((k_1+k_1^*)^2 + (l_1+l_1^*)^2)(e^{R_1+R_2} + e^{R_3})$. The above the nondegenerate one-soliton solution in the two-component LSRI system is also governed by the four arbitrary complex parameters k_1, l_1, α_1 and β_1. The solution (46a)–(46c) admits both regular and singular solutions. To obtain the non-singular solution, the quantities e^{R_1}, e^{R_2} and e^{R_3} should be positive definite. Consequently, the imaginary parts of the wave numbers k_1 and l_1 are restricted as $k_{1I}, l_{1I} < 0$. For this reason, the nondegenerate soliton in the present LSRI system always propagates in the same direction. It has been shown in [77] that the velocity of the soliton is described by the imaginary parts of wave numbers k_1 and l_1. Then, the amplitudes of the nondegenerate soliton in the short-wave components $S^{(1)}$ and $S^{(2)}$ are found to be $4k_{1R}A_1\sqrt{k_{1I}}$ and $4l_{1R}A_2\sqrt{l_{1I}}$, respectively, where $A_1 = \frac{i\alpha_1^{1/2}}{\alpha_1^{1/2*}}$ and $A_2 = \frac{i\beta_1^{1/2}}{\beta_1^{1/2*}}$. From the expressions for the amplitudes, we find that the nondegenerate one-soliton in the present LSRI system (12) exhibits the amplitude-dependent velocity

property as in the KdV-soliton. The solution (46a) and (46b) exhibits double-hump, flattop and single-hump profiles depending on the appropriate choice of parameters. A typical asymmetric double-hump profile is illustrated in Figure 15 with the parameter values $k_1 = 0.35 - 0.5i$, $l_1 = 0.315 - 0.5i$, $\alpha_1 = 0.5 + i$, $\beta_1 = 0.45 + 0.5i$.

We wish to point out that the explicit compact forms of higher-order nondegenerate soliton solutions have also been very recently obtained by us [159]. As in the Manakov system, we also find that the nondegenerate solitons in the present two-component LSRI system (12) also in general exhibit three kinds of elastic collisions, namely shape preserving collision with zero phase shift and shape altering and shape changing collisions with a finite phase shifts. Remarkably, during the shape preserving collision, the two nondegenerate solitons pass through one another without any change in phase shift. In contrast to this collision scenario, the alteration in phase shift leads to a change in the profile structure of the solitons after collision. However, as we have demonstrated in the case of the Manakov system, the shape of the solitons will be restored after considering appropriate time shifts. In addition, the unity condition of the transition intensities also validates that both shape altering and shape changing collisions also belong to the case of elastic collision [159]. As in the case of the Manakov equation, here also we can identify two partially nondegenerate solitons, when the wave numbers satisfy the condition $k_1 = l_1$ and $k_2 \neq l_2$, as an example, and the collision of the nondegenerate soliton with the degenerate soliton exhibits a novel energy exchange collision as demonstrated in [159].

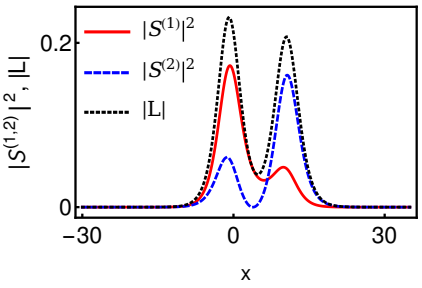

Figure 15. Asymmetric double-hump profile of the nondegenerate fundamental soliton in a 2-component LSRI system.

We capture the degenerate soliton solution of Equation (12) by substituting the limit $k_1 = l_1$ in Equation (46a–c). This results in the following degenerate fundamental soliton forms [136]: $S^{(l)} = 2A_l k_{1R}\sqrt{k_{1I}} e^{i(\eta_{1I}+\frac{\pi}{2})}\,\mathrm{sech}(\eta_{1R}+\frac{R}{2})$, $L = 2k_{1R}^2\,\mathrm{sech}^2(\eta_{1R}+\frac{R}{2})$, $l = 1,2$. Here $A_1 = \frac{\alpha_1}{(|\alpha_1|^2+|\beta_1|^2)^{1/2}}$, $A_2 = \frac{\beta_1}{(|\alpha_1|^2+|\beta_1|^2)^{1/2}}$, $\eta_{1R} = k_{1R}(t + 2k_{1I}z)$, $\eta_{1I} = k_{1I}t + (k_{1R}^2 - k_{1I}^2)z$, $e^R = \frac{-(|\alpha_1|^2+|\beta_1|^2)}{16k_{1R}^2 k_{1I}}$. The degenerate soliton always admits a single-hump profile in both the SW components as well as in the LW component. The amplitude of the soliton in the SW and LW components are $2A_l k_{1R}\sqrt{k_{1I}}$, $2k_{1R}^2$, respectively. Their velocity and the central position are identified as $2k_{1I}$ and $\frac{R}{2k_{1R}}$, respectively. From this, it is known that the degenerate bright soliton also exhibits the amplitude-dependent velocity property, since the velocity explicitly appears in the amplitude part of the soliton. The explicit expression for the degenerate two bright soliton solution of the 2-LSRI system (12) can be identified from [136].

As has been demonstrated in Ref. [136], the degenerate bright solitons undergo energy sharing collision through energy redistribution among the SW components. We demonstrate this energy sharing collision in Figure 16. It is evident from this figure that the intensity of the soliton S_1 is suppressed in the $S^{(1)}$ component after collision with the soliton S_2. In addition it is enhanced in the second SW component $S^{(2)}$. In order to hold the conservation of energy, the intensity of the soliton S_2 is enhanced in the $S^{(1)}$ SW component and it is suppressed in the $S^{(2)}$ SW component. However, in the degenerate case, the solitons in the LW component always undergo elastic collision. The standard elastic collision can occur in both the SW components for the choice $\frac{\alpha_1}{\alpha_2} = \frac{\beta_1}{\beta_2}$ [136].

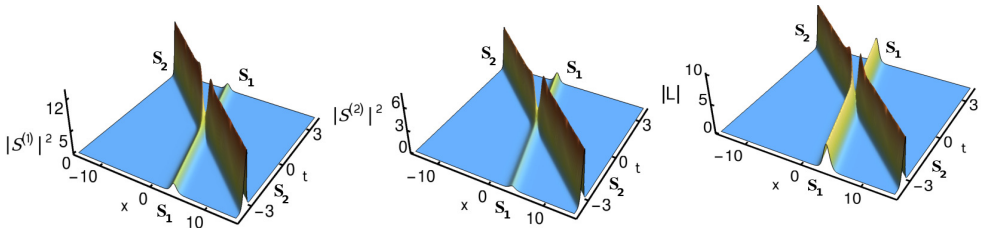

Figure 16. Energy sharing collision among the degenerate solitons in a 2-component LSRI system. The parameter values are $k_1 = 1.5 - 0.5i$, $k_2 = 2 - 2i$, $\alpha_1^{(1)} = 2.5$, $\alpha_1^{(2)} = 1.2$, $\alpha_2^{(1)} = 0.95$ and $\alpha_2^{(2)} = 0.6$.

9. Summary and Outlook

In summary, we have shown that the coupled nonlinear Schrödinger family of equations, namely the Manakov system or 2-CNLS system, N-CNLS system, mixed 2-CNLS system, 2-CCNLS system, GCNLS system and the 2-component LSRI system, can admit a more general form of fundamental bright soliton solution with non-identical propagation constants. In these systems, the obtained nondegenerate one-soliton solution admits novel geometrical structures which are not possible in the degenerate counterparts. Very surprisingly, the nondegenerate fundamental soliton in the N-CNLS system exhibits a novel intricate N-hump intensity profile. Then we elucidated that the nondegenerate bright solitons possess novel collision properties. In particular, they exhibit shape preserving, shape altering and shape changing collisions. However, by performing a careful asymptotic analysis, we found that all these three types of collision scenarios can be viewed as an elastic collision. For appropriate choices of parameters, they also exhibit energy sharing collision properties. Furthermore, we demonstrated that the degenerate vector bright solitons of all the CNLS systems can be captured by imposing appropriate constraints on the wave numbers. In addition to the above, we also explained the various intriguing energy sharing collisions that occur between the degenerate vector bright solitons through graphical demonstration and analytical calculations. From the application point of view, the multi-hump nature of the nondegenerate solitons will be useful to enhance the flow of data in multi-level optical communication applications. On the other hand, the energy sharing collision properties of the degenerate vector solitons are utilized to construct all the optical logic gates and they are also useful in optical switching device applications.

We also wish to note here that the light pulse spread naturally occurs while it propagates in an optical fiber due to the intrinsic properties of the fibers. This spreading or limitation usually occurs due to various fiber losses and fiber deformations. Practically, one cannot completely achieve stable propagation of information in laboratories. To overcome this difficulty a number of schemes have been proposed in the literature. Recently, the usage of dispersion managed solitons in optical communication has also been described to address this problem. In addition, the concept of soliton molecules and multi-soliton complexes have also been suggested to improve the data flow in optical fibers. In view of these facts, the multi-hump nature of the nondegenerate vector solitons is expected to be useful in enhancing the data flow in multi-level communication applications and in overcoming practical limitations.

Although the existence of nondegenerate vector bright solitons have been pointed out in several CNLS families of equations, much remains to be uncovered, especially with higher-order nonlinear effects, such as third order dispersion, self-steepening and stimulated Raman scattering and so on. It is evident from our study that much work is needed to study the collision properties associated with the newly derived vector solitons. From the current level of research activity, we believe that the area of nondegenerate vector solitons will continue to develop in future.

Author Contributions: Conceptualization, S.S., R.R. and M.L.; methodology, S.S. and R.R.; validation, S.S., R.R. and M.L.; writing—original draft preparation, S.S. and R.R.; writing—review and editing, S.S. and M.L.; supervision, M.L.; project administration, M.L.; funding acquisition, M.L. All authors have read and agreed to the published version of the manuscript.

Funding: This research received no external funding.

Acknowledgments: The works of S.S., R.R. and M.L. are supported by the DST-SERB Distinguished Fellowship program to ML under the Grant No. SB/DF/04/2017. RR is also grateful to Council of Scientific and Industrial Research, Government of India, for their support in the form of a Senior Research Fellowship (09/475(0203)/2020-EMR-I).

Conflicts of Interest: The authors declare no conflict of interest.

Appendix A. Constants That Appear in the Asymptotic Expressions in Section 4.4.1

The various constants which arise in the asymptotic analysis of collision between degenerate and nondegenerate solitons in Section 4.4.1 are given below.

$$e^{\Lambda_1}=\frac{i\alpha_1^{(1)}(k_1-k_2)^{\frac{1}{2}}(k_1-l_2)^{\frac{1}{2}}(k_1^*+k_2)^{\frac{1}{2}}(k_1+k_1^*)(k_2+l_2^*)^{\frac{1}{2}}|k_1+l_2^*|^2}{\alpha_2^{(1)}(k_1^*-l_2^*)^{\frac{1}{2}}(k_2^*-l_2^*)^{\frac{1}{2}}}e^{R_5^*+\frac{R_3-R_6}{2}},$$

$$e^{\Lambda_2}=\frac{(k_1-k_2)^{\frac{1}{2}}(k_2^*+l_2)^{\frac{1}{2}}(k_1+k_2^*)\hat{\Lambda}_1\hat{\Lambda}_2}{(k_1^*-k_2^*)^{\frac{1}{2}}(k_2^*-l_2^*)^{\frac{1}{2}}(k_1^*+k_2)},\ e^{\Lambda_3}=\frac{|\alpha_1^{(1)}||\alpha_1^{(2)}|(k_1+k_1^*)(k_2+k_2^*)(l_2+l_2^*)}{|k_2-l_2|},$$

$$e^{\Lambda_4}=(|\alpha_1^{(1)}|^2+|\alpha_1^{(2)}|^2)^{1/2}(|\alpha_1^{(1)}|^2|k_1-k_2|^2|k_1+l_2^*|^2+|\alpha_1^{(2)}|^2|k_1-l_2|^2|k_1+k_2^*|^2)^{1/2},$$

$$e^{\Lambda_5}=\frac{|k_2+l_2^*|}{|k_2-l_2|}(|\alpha_1^{(1)}|^2|k_1+l_2^*|^2+|\alpha_1^{(2)}|^2|k_1-l_2|^2)^{1/2}(|\alpha_1^{(1)}|^2|k_1-k_2|^2+|\alpha_1^{(2)}|^2|k_1+k_2^*|^2)^{1/2},$$

$$e^{\Lambda_6}=\frac{(k_1-l_2)^{\frac{1}{2}}(k_2+l_2^*)^{\frac{1}{2}}(k_1+l_2^*)\hat{\Lambda}_3\hat{\Lambda}_4}{(k_1^*-l_2^*)^{\frac{1}{2}}(k_2^*-l_2^*)^{\frac{1}{2}}(k_1^*+l_2)},\ \hat{\Lambda}_1=(|\alpha_1^{(1)}|^2(k_1-k_2)-|\alpha_1^{(2)}|^2(k_1^*+k_2))^{1/2},$$

$$e^{\Lambda_7}=\frac{\alpha_1^{(2)}(k_1-k_2)^{\frac{1}{2}}(k_1-l_2)^{\frac{1}{2}}(k_1^*+l_2)^{\frac{1}{2}}(k_1+k_1^*)(k_2^*+l_2)^{\frac{1}{2}}|k_1+k_2^*|^2}{\alpha_2^{(2)}(k_1^*-k_2^*)^{\frac{1}{2}}(k_2^*-l_2^*)^{\frac{1}{2}}}e^{R_2^*+\frac{R_6-R_3}{2}},$$

$$\hat{\Lambda}_2=(|\alpha_1^{(1)}|^2(k_1-k_2)|k_1+l_2^*|^2-|\alpha_1^{(2)}|^2|k_1-l_2|^2(k_1^*+k_2))^{1/2},$$

$$\hat{\Lambda}_4=(|\alpha_1^{(1)}|^2|k_1-k_2|^2(k_1^*+l_2)-|\alpha_1^{(2)}|^2(k_1-l_2)|k_1+k_2^*|^2)^{1/2},$$

$$\hat{\Lambda}_3=(|\alpha_1^{(2)}|^2(k_1-l_2)-|\alpha_1^{(1)}|^2(k_1^*+l_2))^{1/2},$$

$$e^{\frac{\Phi_{21}-\Delta_{21}}{2}}=\frac{|\alpha_2^{(1)}|(k_1-k_2)(k_2^*-k_1^*)^{\frac{1}{2}}(k_2-l_2)^{\frac{1}{2}}}{(k_1+k_2^*)(k_2+k_2^*)(k_2+k_1^*)^{\frac{1}{2}}(k_2^*+l_2)^{\frac{1}{2}}},\ e^{\frac{\lambda_2-\lambda_1}{2}}=\frac{|\alpha_2^{(2)}||k_1-l_2|(k_2-l_2)^{\frac{1}{2}}\hat{\Lambda}_2}{(k_2+l_2^*)^{\frac{1}{2}}|k_1+l_2^*|^2(l_2+l_2^*)\hat{\Lambda}_1},$$

$$e^{\frac{\lambda_5-R}{2}}=\frac{|k_1-k_2||k_1-l_2||k_2-l_2|\hat{\Lambda}_5}{|k_1+k_2^*|^2|k_1+l_2^*|^2|k_2+l_2^*|(|\alpha_1^{(1)}|^2+|\alpha_1^{(2)}|^2)^{1/2}}e^{\frac{R_3+R_6}{2}},$$

$$e^{\frac{\vartheta_{12}-\varphi_{21}}{2}}=\frac{(k_2-k_1)^{\frac{1}{2}}(k_1^*-l_2^*)^{\frac{1}{2}}(k_2^*+l_2)^{\frac{1}{2}}}{(k_2+l_2^*)^{\frac{1}{2}}(k_2^*-k_1^*)^{\frac{1}{2}}(k_1-l_2)^{\frac{1}{2}}}e^{\frac{R_2^*+R_5-(R_2+R_5^*)}{2}},\ e^{\frac{\lambda_3-\lambda_4}{2}}=\frac{|k_1-k_2|\hat{\Lambda}_6|k_1+l_2^*|^2e^{\frac{R_3-R_6}{2}}}{|k_1+k_2^*|^2|k_1-l_2|\hat{\Lambda}_7},$$

$$e^{\frac{\Gamma_{21}-\gamma_{21}}{2}}=\frac{(k_2-l_2)^{\frac{1}{2}}(k_1-l_2)(k_1^*-l_2^*)^{\frac{1}{2}}}{(k_2+l_2^*)^{\frac{1}{2}}(k_1+l_2^*)(k_1^*+l_2)^{\frac{1}{2}}}e^{\frac{R_6}{2}},\ e^{\frac{\lambda_7-\lambda_6}{2}}=\frac{(k_1-k_2)(k_2-l_2)^{\frac{1}{2}}\hat{\Lambda}_4}{|k_1+k_2^*|^2(k_2^*+l_2)^{\frac{1}{2}}\hat{\Lambda}_3}e^{\frac{R_3}{2}},$$

$$\hat{\Lambda}_5=(|\alpha_1^{(1)}|^2|k_1-k_2|^2|k_1+l_2^*|^2+|\alpha_1^{(2)}|^2|k_1-l_2|^2|k_1+k_2^*|^2)^{1/2},$$

$$e^{\frac{R'-\varsigma_{22}}{2}}=\frac{|k_1-k_2||k_1-l_2|\hat{\Lambda}_5}{|k_1+k_2^*|^2|k_1+l_2^*|^2(k_1+k_1^*)},\ e^{\frac{\varsigma_{22}}{2}}=\frac{|k_2-l_2|}{|k_2+l_2^*|}e^{\frac{R_3+R_6}{2}},\ e^{\frac{R_3-R_6}{2}}=\frac{|\alpha_2^{(1)}|(l_2+l_2^*)}{|\alpha_2^{(2)}|(k_2+k_2^*)},$$

$$\hat{\Lambda}_6=(|\alpha_1^{(1)}|^2|k_1-k_2|^2+|\alpha_1^{(2)}|^2|k_1+k_2^*|^2)^{1/2},\ \hat{\Lambda}_7=(|\alpha_1^{(1)}|^2|k_1+l_2^*|^2+|\alpha_1^{(2)}|^2|k_1-l_2|^2)^{1/2},$$

$$e^{\frac{\Lambda_{22}-\rho_1}{2}}=\frac{(k_2-l_2)^{\frac{1}{2}}}{(k_2+l_2^*)^{\frac{1}{2}}}e^{\frac{R_6}{2}},\ e^{\frac{\mu_{22}-\rho_2}{2}}=\frac{(l_2-k_2)^{\frac{1}{2}}}{(k_2^*+l_2)^{\frac{1}{2}}}e^{\frac{R_3}{2}},\ e^{R_1}=\frac{|\alpha_1^{(1)}|^2}{(k_1+k_1^*)^2},\ e^{R_2}=\frac{\alpha_1^{(1)}\alpha_2^{(1)*}}{(k_1+k_2^*)^2},$$

$$e^{R_3}=\frac{|\alpha_2^{(1)}|^2}{(k_2+k_2^*)^2},\ e^{R_4}=\frac{|\alpha_1^{(2)}|^2}{(k_1+k_1^*)^2},\ e^{R_5}=\frac{\alpha_1^{(2)}\alpha_2^{(2)*}}{(k_1+l_2^*)^2},\ e^{R_6}=\frac{|\alpha_2^{(2)}|^2}{(l_2+l_2^*)^2}.$$

References

1. Zabusky, N.J.; Kruskal, M.D. Interaction of "Solitons" in a Collisionless Plasma and the Recurrence of Initial States. *Phys. Rev. Lett.* **1965**, *15*, 240–243. [CrossRef]
2. Dauxois, T. Fermi, Pasta, Ulam and a mysterious lady. *Phys. Today* **2008**, *61*, 55–57. [CrossRef]
3. Kivshar, Y.; Agrawal, G.P. *Optical Solitons: From Fibers to Photonic Crystals*, 1st ed.; Academic Press: San Diego, CA, USA, 2003.
4. Agrawal, G.P. *Nonlinear Fiber Optics*, 5th ed.; Academic Press: Oxford, UK, 2013.
5. Chen, Z.; Segev, M.; Christodoulides, D.N. Optical spatial solitons: Historical overview and recent advances. *Rep. Prog. Phys.* **2012**, *75*, 086401. [CrossRef]
6. Malomed, B.A.; Mihalache, D.; Wise, F.; Torner, L. Spatiotemporal optical solitons. *J. Opt. B Quantum Semiclass. Opt.* **2005**, *7*, R53–R72. [CrossRef]
7. Hasegawa, A.; Tappert, F. Transmission of stationary nonlinear optical pulses in dispersive dielectric fibers. I. Anomalous dispersion. *Appl. Phys. Lett.* **1973**, *23*, 142. [CrossRef]
8. Hasegawa, A.; Tappert, F. Transmission of stationary nonlinear optical pulses in dispersive dielectric fibers. II. Normal dispersion. *Appl. Phys. Lett.* **1973**, *23*, 171. [CrossRef]
9. Mollenauer, L.F.; Stolen, R.H.; Gordon, J.P. Experimental Observation of Picosecond Pulse Narrowing and Solitons in Optical Fibers. *Phys. Rev. Lett.* **1980**, *45*, 1095. [CrossRef]
10. Mollenauer, L.F.; Gordon, J.P. *Nonlinear Fiber Optics*, 1st ed.; Academic Press: San Diego, CA, USA, 2006.
11. Zakharov, V.E.; Shabat, A.B. Interaction between solitons in a stable medium. *Sov. Phys. JETP* **1973**, *37*, 823–828.
12. Gardner, C.S.; Green, G.; Kruskal, M.; Miura, R. Method for solving the Korteweg-deVries equation. *Phys. Rev. Lett.* **1967**, *19*, 1095. [CrossRef]
13. Ablowitz, M.J.; Clarkson, P.A. *Solitons, Nonlinear Evolution Equations and Inverse Scattering*, 1st ed.; Cambridge University Press: Cambridge, UK, 1991.
14. Chabchoub, A.; Slunyaev, A.; Hoffmann, N.; Dias, F.; Kibler, B.; Genty, G.; Dudley, J.M.; Akhmediev, N. The Peregrine breather on the zero-background limit as the two-soliton degenerate solution: An experimental study. *arXiv* **2020**, arXiv:2011.13252.
15. Gordon, J.P. Interaction forces among solitons in optical fibers. *Opt. Lett.* **1983**, *8*, 596–598. [CrossRef]
16. Mitschke, F.M.; Mollenauer, L.F. Experimental observation of interaction forces between solitons in optical fibers. *Opt. Lett.* **1987**, *12*, 355. [CrossRef] [PubMed]
17. Stratmann, M.; Pagel, T.; Mitschke, F.M. Experimental Observation of Temporal Soliton Molecules. *Phys. Rev. Lett.* **2005**, *95*, 143902. [CrossRef]
18. Hause, A.; Hartwig, H.; Böhm, M.; Mitschke, F.M. Binding mechanism of temporal soliton molecules. *Phys. Rev. A* **2008**, *78*, 063817. [CrossRef]
19. Akhmediev, N.; Town, G.; Wabnitz, S. Soliton coding based on shape invariant interacting soliton packets: The three-soliton case. *Opt. Commun.* **1994**, *104*, 385. [CrossRef]
20. Malomed, B.A. Bound solitons in the nonlinear Schrödinger/Ginzburg-Landau equation. In *Large Scale Structures in Nonlinear Physics. Lecture Notes in Physics*; Fournier, J.D., Sulem, P.L., Eds.; Springer: Berlin/Heidelberg, Germany, 1991; p. 392.
21. Afanasjev, V.V.; Malomed, B.A.; Chu, P.L. Stability of bound states of pulses in the Ginzburg-Landau equations. *Phys. Rev. E* **1997**, *56*, 6020. [CrossRef]
22. Khawaja, U.A. Stability and dynamics of two-soliton molecules. *Phys. Rev. E* **2010**, *81*, 056603. [CrossRef] [PubMed]
23. Grelu, P.; Soto-Crespo, J.M. Multisoliton states and pulse fragmentation in a passively mode-locked fibre laser. *J. Opt. B Quantum SemiClass. Opt.* **2004**, *6*, S271. [CrossRef]
24. Tang, D.Y.; Zhao, B.; Shen, D.Y.; Lu, C.; Man, W.S.; Tam, H.Y. Compound pulse solitons in a fiber ring laser. *Phys. Rev. A* **2003**, *68*, 013816. [CrossRef]
25. Akhmediev, N.N.; Ankiewicz, A.; Soto-Crespo, J.M. Stable soliton pairs in optical transmission lines and fiber lasers. *J. Opt. Soc. Am. B* **1998**, *15*, 515. [CrossRef]
26. Melchert, O.; Willms, S.; Bose, S.; Yulin, A.; Roth, B.; Mitschke, F.M.; Morgner, U.; Babushkin, I.; Demircan, A. Soliton Molecules with Two Frequencies. *Phys. Rev. Lett.* **2019**, *123*, 243905. [CrossRef]
27. Rohrmann, P.; Hause, A.; Mitschke, F. Solitons Beyond Binary: Possibility of Fibre-Optic Transmission of Two Bits per Clock Period. *Sci. Rep.* **2012**, *2*, 866. [CrossRef]
28. Jakubowski, M.H.; Steiglitz, K.; Squier, R. State transformations of colliding optical solitons and possible application to computation in bulk media. *Phys. Rev. E* **1998**, *58*, 6752. [CrossRef]
29. Steiglitz, K. Time-gated Manakov spatial solitons are computationally universal. *Phys. Rev. E* **2000**, *63*, 016608. [CrossRef]
30. Akhmediev, N.; Ankiewicz, A. Multi-soliton complexes. *Chaos* **2000**, *10*, 600. [CrossRef] [PubMed]
31. Mitschke, F. A Brief History of Fiber-Optic Soliton Transmission. In *Handbook of Optical Fibers*; Peng, G.-D., Ed.; Springer: Singapore, 2017; pp. 1–47.
32. Radhakrishnan, R.; Sahadevan, R.; Lakshmanan, M. Integrability and singularity structure of coupled nonlinear Schródinger equations. *Chaos Solitons Fractals* **1995**, *5*, 2315. [CrossRef]
33. Manakov, S.V. On the theory of two-dimensional stationary self-focusing of electromagnetic waves. *Sov. Phys. JETP* **1974**, *38*, 248.
34. Menyuk, C.R. Pulse propagation in an elliptically birefringent Kerr medium. *IEEE J. Quantum Electron.* **1989**, *25*, 2674. [CrossRef]

35. Radhakrishnan, R.; Lakshmanan, M.; Hietarinta, J. Inelastic collision and switching of coupled bright solitons in optical fibers. *Phys. Rev. E* **1997**, *56*, 2213. [CrossRef]
36. Kanna, T.; Lakshmanan, M. Exact soliton solutions, shape changing collisions, and partially coherent solitons in coupled nonlinear Schrödinger equations. *Phys. Rev. Lett.* **2001**, *86*, 5043. [CrossRef] [PubMed]
37. Anastassiou, C.; Segev, M.; Steiglitz, K.; Giordmaine, J.A.; Mitchell, M.; Shih, M.F.; Lan, S.; Martin, J. Energy-exchange interactions between colliding vector solitons. *Phys. Rev. Lett.* **1999**, *83*, 2332. [CrossRef]
38. Kang, J.U.; Stegeman, G.I.; Aitchison, J.S.; Akhmediev, N. Observation of Manakov spatial solitons in AlGaAs planar waveguides. *Phys. Rev. Lett.* **1996**, *76*, 3699. [CrossRef]
39. Rand, D.; Glesk, I.; Bres, C.S.; Nolan, D.A.; Chen, X.; Koh, J.; Fleischer, J.W.; Steiglitz, K.; Prucnal, P. R. Observation of temporal vector soliton propagation and collision in birefringent fiber. *Phys. Rev. Lett.* **2007**, *98*, 053902. [CrossRef] [PubMed]
40. Soljacic, M.; Steiglitz, K.; Sears, S.M.; Segev, M.; Jakubowski, M.H.; Squier, R. Collisions of Two Solitons in an Arbitrary Number of Coupled Nonlinear Schrödinger Equations. *Phys. Rev. Lett.* **2003**, *90*, 254102. [CrossRef] [PubMed]
41. Kanna, T.; Lakshmanan, M. Exact soliton solutions of coupled nonlinear Schrödinger equations: Shape-changing collisions, logic gates, and partially coherent solitons. *Phys. Rev. E* **2003**, *67*, 046617. [CrossRef] [PubMed]
42. Vijayajayanthi, M.; Kanna, T.; Murali, K.; Lakshmanan, M. Harnessing energy-sharing collisions of Manakov solitons to implement universal NOR and OR logic gates. *Phys. Rev. E* **2018**, *97*, 060201(R). [CrossRef] [PubMed]
43. Segev, M.; Crosignani, B.; Yariv, A.; Fischer, B. Spatial solitons in photorefractive media. *Phys. Rev. Lett.* **1992**, *68*, 923. [CrossRef] [PubMed]
44. Duree, G.C.; Shultz, J.L.; Segev, M.; Yariv, A.; Crosignani, B.; Porto, P.D.; Sharp, E.J.; Neurgaonkar, R.R. Observation of self-trapping of an optical beam due to the photorefractive effect. *Phys. Rev. Lett.* **1993**, *71*, 533. [CrossRef]
45. Segev, M.; Valley, G.C.; Crosignani, B.; DiPorto, P.; Yariv, A. Steady-State Spatial Screening Solitons in Photorefractive Materials with External Applied Field. *Phys. Rev. Lett.* **1994**, *73*, 3211. [CrossRef] [PubMed]
46. Christodoulides, D.N.; Carvalho, M.I. Bright, dark, and gray spatial soliton states in photorefractive media. *J. Opt. Soc. Am. B* **1995**, *12*, 1628. [CrossRef]
47. Christodoulides, D.N.; Singh, S.R.; Carvalho, M.I. Incoherently coupled soliton pairs in biased photorefractive crystals. *Appl. Phys. Lett.* **1996**, *68*, 1763. [CrossRef]
48. Chen, Z.; Segev, M.; Coskun, T.H.; Christodoulides, D.N. Observation of incoherently coupled photorefractive spatial soliton pairs. *Opt. Lett.* **1996**, *21*, 1436. [CrossRef] [PubMed]
49. Chen, Z.; Segev, M.; Coskun, T.H.; Christodoulides, D.N.; Kivshar, Y.S.; Afanasjev, V.V. Incoherently coupled dark–bright photorefractive solitons. *Opt. Lett.* **1996**, *21*, 1821. [CrossRef]
50. Mitchell, M.; Segev, M.; Christodoulides, D.N. Observation of multihump multimode solitons. *Phys. Rev. Lett.* **1998**, *80*, 4657. [CrossRef]
51. Akhmediev, N.; Królikowski, W.; Snyder, A.W. Partially coherent colitons of variable shape. *Phys. Rev. Lett.* **1998**, *81*, 4632. [CrossRef]
52. Ankiewicz, A.; Królikowski, W.; Akhmediev, N. Partially coherent solitons of variable shape in a slow Kerr-like medium: Exact solutions. *Phys. Rev. E* **1999**, *59*, 6079. [CrossRef] [PubMed]
53. Sukhorukov, A.A.; Akhmediev, N. Coherent and Incoherent Contributions to Multisoliton Complexes. *Phys. Rev. Lett.* **1999**, *83*, 4736. [CrossRef]
54. Królikowski, W.; Akhmediev, N.; Luther-Davies, B. Collision-induced shape transformations of partially coherent solitons. *Phys. Rev. E* **1999**, *59*, 4654. [CrossRef]
55. Christodoulides, D.N.; Joseph, R.I. Vector solitons in birefringent nonlinear dispersive media. *Opt. Lett.* **1988**, *13*, 53. [CrossRef]
56. Akhmediev, N.N.; Buryak, A.V.; Soto-Crespo, J.M.; Andersen, D.R. Phase-locked stationary soliton states in birefringent nonlinear optical fibers. *J. Opt. Soc. Am. B* **1995**, *12*, 434. [CrossRef]
57. Collings, B.C.; Cundiff, S.T.; Akhmediev, N.N.; Soto-Crespo, J.M.; Bergman, K.; Knox, W.H. Polarization-locked temporal vector solitons in a fiber laser: Experiment. *J. Opt. Soc. Am. B* **2000**, *17*, 354. [CrossRef]
58. Tratnik, M.V.; Sipe, J.E. Bound solitary waves in a birefringent optical fiber. *Phys. Rev. A* **1988**, *38*, 2011. [CrossRef]
59. Haelterman, M.; Sheppard, A.P.; Snyder, A.W. Bound-vector solitary waves in isotropic nonlinear dispersive media. *Opt. Lett.* **1993**, *18*, 1406. [CrossRef]
60. Yang, J. Classification of the solitary waves in coupled nonlinear Schrödinger equations. *Phys. D Nonlinear Phenom.* **1997**, *108*, 92. [CrossRef]
61. Elena, A.; Ostrovskaya, E.A.; Kivshar, Y.S.; Chen, Z.; Segev, M. Interaction between vector solitons and solitonic gluons. *Opt. Lett.* **1999**, *24*, 327.
62. Ostrovskaya, E.A.; Kivshar, Y.S.; Skryabin, D.V.; Firth, W.J. Stability of Multihump Optical Solitons. *Phys. Rev. Lett.* **1999**, *83*, 296. [CrossRef]
63. Pelinovsky, D.E.; Yang, J. Instabilities of multihump vector solitons in coupled nonlinear Schrödinger equations. *Stud. Appl. Math.* **2005**, *115*, 109. [CrossRef]
64. Kanna, T.; Lakshmanan, M.; Dinda, P.T.; Akhmediev, N. Soliton collisions with shape change by intensity redistribution in mixed coupled nonlinear Schrödinger equations. *Phys. Rev. E* **2006**, *73*, 026604. [CrossRef] [PubMed]
65. Sheppard, A.P.; Kivshar, Y.S. Polarized dark solitons in isotropic Kerr media. *Phys. Rev. E* **1997**, *55*, 4773. [CrossRef]

66. Radhakrishnan, R.; Aravinthan, K. Spatial vector soliton and its collisions in isotropic self-defocusing Kerr media. *Phys. Rev. E* **2007**, *75*, 066605. [CrossRef]
67. Radhakrishnan, R.; Manikandan, N.; Aravinthan, K. Energy-exchange collisions of dark-bright-bright vector solitons. *Phys. Rev. E* **2015**, *92*, 062913. [CrossRef] [PubMed]
68. Vijayajayanthi, M.; Kanna, T.; Lakshmanan, M. Bright-dark solitons and their collisions in mixed N-coupled nonlinear Schrödinger equations. *Phys. Rev. A* **2008**, *77*, 013820. [CrossRef]
69. Feng, B.F. General N-soliton solution to a vector nonlinear Schrödinger equation. *J. Phys. A Math. Theor.* **2014**, *47*, 355203. [CrossRef]
70. Radhakrishnan, R.; Lakshmanan, M. Bright and dark soliton solutions to coupled nonlinear Schrödinger equations. *J. Phy. A Math. Gen.* **1995**, *28*, 2683. [CrossRef]
71. Ohta, Y.; Wang, D.S.; Yang, J. General *N*-Dark-Dark Solitons in the Coupled Nonlinear Schrödinger Equations. *Stud. Appl. Math.* **2011**, *127*, 345. [CrossRef]
72. Kevrekidis, P.G.; Frantzeskakis, D.J. Solitons in coupled nonlinear Schrödinger models: A survey of recent developments. *Rev. Phys.* **2016**, *1*, 140. [CrossRef]
73. Song, Y.; Shi, X.; Wu, C.; Tang, D.; Zhang, H. Recent Progress of study on optical solitons in fiber lasers. *Appl. Phys. Rev.* **2019**, *6*, 021313. [CrossRef]
74. Akhmediev, N.; Ankiewicz, A. *Dissipative Solitons*; Springer: Berlin/Heidelberg, Germany, 2005.
75. Stalin, S.; Ramakrishnan, R.; Senthilvelan, M.; Lakshmanan, M. Nondegenerate solitons in Manakov system. *Phys. Rev. Lett.* **2019**, *122*, 043901. [CrossRef]
76. Ramakrishnan, R.; Stalin, S.; Lakshmanan, M. Nondegenerate solitons and their collisions in Manakov systems. *Phys. Rev. E* **2020**, *102*, 042212. [CrossRef] [PubMed]
77. Stalin, S.; Ramakrishnan, R.; Lakshmanan, M. Nondegenerate soliton solutions in certain coupled nonlinear Schrödinger systems. *Phys. Lett. A* **2020**, *384*, 126201. [CrossRef]
78. Qin, Y.H.; Zhao, L.C.; Ling, L. Nondegenerate bound-state solitons in multicomponent Bose-Einstein condensates. *Phys. Rev. E* **2019**, *100*, 022212. [CrossRef]
79. Zhang, C.R.; Tian, B.; Qu, Q.X.; Liu, L.; Tian, H.Y. Vector bright solitons and their interactions of the couple Fokas-Lenells system in a birefringent optical fiber. *Z. Angew. Math. Phys.* **2020**, *71*, 18. [CrossRef]
80. Ding, C.C.; Gao, Y.T.; Hu, L.; Deng, G.F.; Zhang, C.Y. Vector bright soliton interactions of the two-component AB system in a baroclinic fluid. *Chaos Solitons Fractals* **2021**, *142*, 110363. [CrossRef]
81. Qin, Y.H.; Zhao, L.C.; Yang, Z.Q.; Ling, L. Multivalley dark solitons in multicomponent Bose-Einstein condensates with repulsive interactions. *arXiv* **2021**, arXiv:2102.10507.
82. Ramakrishnan, R.; Stalin, S.; Lakshmanan, M. Multihumped nondegenerate fundamental bright solitons in N-coupled nonlinear Schrödinger system. *J. Phys. A Math. Theor.* **2021**, *54*, 14LT01. [CrossRef]
83. Lakshmanan, M.; Kanna, T. Shape changing collisions of optical solitons, universal logic gates and partially coherent solitons in coupled nonlinear Schrödinger equations. *Pramana J. Phys.* **2001**, *57*, 885. [CrossRef]
84. Zakharov, V.E.; Schulman, E.I. To the integrability of the system of two coupled nonlinear Schrödinger equations. *Phys. D* **1982**, *4*, 270. [CrossRef]
85. Kaup, D.J.; Malomed, B.A. Soliton trapping and daughter waves in the Manakov model. *Phys. Rev. E* **1993**, *48*, 599. [CrossRef] [PubMed]
86. Lazarides, N.; Tsironis, G.P. Coupled nonlinear Schrödinger field equations for electromagnetic wave propagation in nonlinear left-handed materials. *Phys. Rev. E* **2005**, *71*, 036614. [CrossRef]
87. Makhankov, V.G. Quasi-classical solitons in the Lindner-Fedyanin model-"hole"-like excitations. *Phys. Lett. A* **1981**, *81*, 156. [CrossRef]
88. Makhankov, V.G.;Makhaldiani, N.V.; Pashaev, O.K. On the integrability and isotopic structure of the one-dimensional Hubbard model in the long wave approximation. *Phys. Lett. A* **1981**, *81*, 161. [CrossRef]
89. Lindner, U.; Fedyanin, V. Solitons in a one-dimensional modified Hubbard model. *Phys. Status Solidi B* **1978**, *89*, 123. [CrossRef]
90. Pérez-García, V.M.; Beitia, J.B. Symbiotic solitons in heteronuclear multicomponent Bose-Einstein condensates. *Phys. Rev. A* **2005**, *72*, 033620. [CrossRef]
91. Ablowitz, M.J.; Prinari, B.; Trubatch, A.D. Soliton interactions in the vector NLS equation. *Inverse Probl.* **2004**, *20*, 1217. [CrossRef]
92. Prinari, B.; Ablowitz, M.J.; Biondini, G. Inverse scattering transform for the vector nonlinear Schrödinger equation with nonvanishing boundary conditions. *J. Math. Phys.* **2006**, *47*, 063508. [CrossRef]
93. Prinari, B.; Biondini, G.; Trubatch, A.D. Inverse scattering transform for the multi-component Nonlinear Schrödinger equation with nonzero boundary conditions. *Stud. Appl. Math.* **2011**, *126*, 245. [CrossRef]
94. Biondini, G.; Kovacic, G. Inverse scattering transform for the focusing nonlinear Schrödinger equation with nonzero boundary conditions. *J. Math. Phys.* **2014**, *55*, 031506. [CrossRef]
95. Biondini, G.; Kraus, D. Inverse Scattering transform for the defocusing Manakov system with nonzero boundary conditions. *SIAM J. Math. Anal.* **2015**, *47*, 706. [CrossRef]
96. Prinari, B.; Vitale, F.; Biondini, G. Dark-bright soliton solutions with nontrivial polarization interactions for the three-component defocusing nonlinear Schrödinger equation with nonzero boundary conditions. *J. Math. Phys.* **2015**, *56*, 071505. [CrossRef]

97. Biondini, G.; Kraus, D.K.; Prinari, B. The three-component defocusing nonlinear Schrödinger equation with nonzero boundary conditions. *Commun. Math. Phys.* **2016**, *348*, 475–533. [CrossRef]
98. Park, Q.H.; Shin, H.J. Systematic construction of multicomponent optical solitons. *Phys. Rev. E* **2000**, *61*, 3093. [CrossRef]
99. Degasperis, A.; Lombardo, S. Multicomponent integrable wave equations: I. Darboux-dressing transformation *J. Phys. A Math. Theor.* **2007**, *40*, 961. [CrossRef]
100. Degasperis, A.; Lombardo, S. Multicomponent integrable wave equations: II. Soliton solutions. *J. Phys. A Math. Theor.* **2009**, *42*, 385206. [CrossRef]
101. Ling, L.; Zhao, L.C.; Guo, B. Darboux transformation and multi-dark soliton for N-component nonlinear Schrödinger equations. *Nonlinearity* **2015**, *28*, 3243. [CrossRef]
102. Ling, L.; Zhao, L.C.; Guo, B. Darboux transformation and classification of solution for mixed coupled nonlinear Schrödinger equations. *Commun. Nonlin. Sci. Numer. Simul.* **2016**, *32*, 285. [CrossRef]
103. Tsuchida, T. Exact solutions of multicomponent nonlinear Schrödinger equations under general plane-wave boundary conditions. *arXiv* **2013**, arXiv:1308.6623v2.
104. Crosignani, B.; Cutolo, A.; Porto, P.D. Coupled-mode theory of nonlinear propagation in multimode and single-mode fibers: Envelope solitons and self-confinement. *J. Opt. Soc. Am.* **1982**, *72*, 1136. [CrossRef]
105. Park, Q.H.; Shin, H.J. Painlevé analysis of the coupled nonlinear Schrödinger equation for polarized optical waves in an isotropic medium. *Phys. Rev. E* **1999**, *59*, 2373. [CrossRef]
106. Akhmediev, N.N.; Ostrovskaya, E.A. Elliptically polarized spatial solitons in cubic gyrotropic materials. *Opt. Commun.* **1996**, *132*, 190. [CrossRef]
107. Kanna, T.; Vijayajayanthi, M.; Lakshmanan, M. Coherently coupled bright optical solitons and their collisions. *J. Phys. A Math. Theor.* **2010**, *43*, 434018. [CrossRef]
108. Kanna, T.; Sakkaravarthi, K. Multicomponent coherently coupled and incoherently coupled solitons and their collisions. *J. Phys. A Math. Theor.* **2011**, *44*, 285211. [CrossRef]
109. Kasamatsu, K.; Tsubota, M.; Ueda, M. Vortex molecules in coherently coupled two-component Bose-Einstein condensates. *Phys. Rev. Lett.* **2004**, *93*, 250406. [CrossRef] [PubMed]
110. Congy, T.; Kamchatnov, A.M.; Pavloff, N. Nonlinear waves in coherently coupled Bose-Einstein condensates. *Phys. Rev. A* **2016**, *93*, 043613. [CrossRef]
111. Babu Mareeswaran, R.; Kanna, T. Superposed nonlinear waves in coherently coupled Bose-Einstein condensates. *Phys. Lett. A* **2016**, *380*, 3244. [CrossRef]
112. Ieda, J.; Miyakawa, T.; Wadati, M. Exact Analysis of Soliton Dynamics in Spinor Bose—Einstein Condensates. *Phys. Rev Lett.* **2004**, *93*, 194102. [CrossRef]
113. Prinari, B.; Ortiz, A.K.; van der Mee, C.; Grabowski, M. Inverse Scattering Transform and Solitons for Square Matrix Nonlinear Schrödinger Equations. *Stud. Appl. Math.* **2018**, *141*, 308. [CrossRef]
114. Li, L.; Li, Z.; Malomed, B.; Mihalache, D.; Liu, W. Exact Soliton Solutions and Nonlinear Modulation Instability in Spinor Bose-Einstein Condensates. *Phys. Rev. A* **2005**, *72*, 033611. [CrossRef]
115. Wang, D.S.; Zhang, D.J.; Yang, J. Integrable properties of the general coupled nonlinear Schrödinger equations. *J. Math. Phys.* **2010**, *51*, 023510. [CrossRef]
116. lü, M.; Peng, M. Painlevé-integrability and explicit solutions of the general two-coupled nonlinear Schrödinger system in the optical fiber communications. *Nonlinear. Dyn.* **2013**, *73*, 405. [CrossRef]
117. Vishnu Priya, N.; Senthilvelan, M. N-bright-bright and N-dark-dark solitons of the coupled generalized nonlinear Schrödinger equations. *Commun. Nonlin. Sci. Numer. Simul.* **2016**, *36*, 366. [CrossRef]
118. Agalarov, A.; Zhulego, V.; Gadzhimuradov, T. Bright, dark, and mixed vector soliton solutions of the general coupled nonlinear Schrödinger equations. *Phys. Rev. E* **2015**, *91*, 042909. [CrossRef]
119. Zakharov, V.E. Collapse of Langmuir waves. *Sov. Phys. JETP* **1972**, *35*, 908.
120. Benny, D.J. A General Theory for Interactions Between Short and Long Waves. *Stud. Appl. Math.* **1977**, *56*, 81. [CrossRef]
121. Kivshar, Y.S. Stable vector solitons composed of bright and dark pulses. *Opt. Lett.* **1992**, *17*, 1322. [CrossRef]
122. Chowdhury, A. Tataronis, J.A. Long wave–short wave resonance in nonlinear negative refractive index media. *Phys. Rev. Lett.* **2008**, *100*, 153905. [CrossRef]
123. Ablowitz, M.J.; Biondini, G.; Blair, S. Nonlinear Schrödinger equations with mean terms in nonresonant multidimensional quadratic materials. *Phys. Rev. E* **2001**, *63*, 046605. [CrossRef] [PubMed]
124. Sazonov, S.V.; Ustinov, N.V. Vector solitons generated by the long wave-short wave interaction. *JETP Lett.* **2011**, *94*, 610. [CrossRef]
125. Nishikawa, K.; Hojo, H.; Mima, K.; Ikezi, H. Coupled nonlinear electron-plasma and ion-acoustic waves. *Phys. Rev. Lett.* **1974**, *33*, 148. [CrossRef]
126. Yajima, N.; Oikawa, M. Formation and interaction of sonic-Langmuir solitons: Inverse scattering method. *Prog. Theor. Phys.* **1976**, *56*, 1719. [CrossRef]
127. Kawahara, T. Nonlinear self-modulation of capillary-gravity waves on liquid layer. *J. Phys. Soc. Jpn.* **1975**, *38*, 265. [CrossRef]
128. Kawahara, T.; Sugimoto, N.; Kakutani, T. Nonlinear interaction between short and long capillary-gravity waves. *J. Phys. Soc. Jpn.* **1975**, *39*, 1379. [CrossRef]
129. Djordjevic, V.D.; Redekopp, L.G. On two-dimensional packets of capillary-gravity waves. *J. Fluid Mech.* **1977**, *79*, 703. [CrossRef]

130. Kopp, C.G.; Redekopp, L.G. The interaction of long and short internal gravity waves: Theory and experiment. *J. Fluid. Mech.* **1981**, *111*, 367. [CrossRef]
131. Boyd, J.P. Long wave/short wave resonance in equatorial waves. *J. Phys. Oceanogr.* **1982**, *13*, 450. [CrossRef]
132. Zabolotskii, A.A. Resonant interaction between a localized fast wave and a slow wave with constant asymptotic amplitude. *JETP* **2009**, *109*, 859. [CrossRef]
133. Aguero, M.; Frantzeskakis, D.J.; Kevrekidis, P.G. Asymptotic reductions of two coupled (2+1)-dimensional nonlinear Schrödinger equations: Application to Bose-Einstein condensates. *J. Phys. A Math. Gen.* **2006**, *39*, 7705. [CrossRef]
134. Niztazakis, H.E.; Frantzeskakis, D.J.; Kevrekidis, P.G.; Malomed, B.A.; González, R.C. Bright-dark soliton complexes in spinor Bose-Einstein condensates. *Phys. Rev. A* **2008**, *77*, 033612. [CrossRef]
135. Ma, Y.C.; Redekopp, L.G. Some solutions pertaining to the resonant interaction of long and short waves. *Phys. Fluids* **1979**, *22*, 1872. [CrossRef]
136. Kanna, T.; Sakkaravarthi, K.; Tamilselvan, K. General multicomponent Yajima-Oikawa system: Painlevé analysis, soliton solutions, and energy-sharing collisions. *Phys. Rev. E* **2013**, *88*, 062921. [CrossRef]
137. Chen, J.; Chen, Y.; Feng, B.F.; Maruno, K.I. General mixed multi-soliton solutions to one-dimensional multicomponent Yajima-Oikawa system. *J. Phys. Soc. Jpn.* **2015**, *84*, 074001. [CrossRef]
138. Chen, J.; Chen, Y.; Feng, B.F.; Maruno, K.I. Multi-dark soliton solutions of the two-dimensional multi-component Yajima-Oikawa systems. *J. Phys. Soc. Jpn.* **2015**, *84*, 034002. [CrossRef]
139. Oikawa, M.; Okamura, M.; Funakoshi, M. Two-dimensional resonant interaction between long and short waves. *J. Phys. Soc. Jpn.* **1989**, *58*, 4416. [CrossRef]
140. Ohta, Y.; Maruno, K.; Oikawa, M. Two-component analogue of two-dimensional long wave-short wave resonance interaction equations: A derivation and solutions. *J. Phys. A Math. Theor.* **2007**, *40*, 7659. [CrossRef]
141. Radha, R.; Senthil Kumar, C.; Lakshmanan, M.; Gilson, C.R. The collision of multimode dromions and a firewall in the two-component long-wave-short-wave resonance interaction equation. *J. Phys. A Math. Theor.* **2009**, *42*, 102002. [CrossRef]
142. Kanna, T.; Vijayajayanthi, M.; Sakkaravarthi, K.; Lakshmanan, M. Higher dimensional bright solitons and their collisions in a multicomponent long wave-short wave system. *J. Phys. A Math.Theor.* **2009**, *42*, 115103. [CrossRef]
143. Sakkaravarthi, K.; Kanna, T.; Vijayajayanthi, M.; Lakshmanan, M. Multicomponent long-wave-short-wave resonance interaction system: Bright solitons, energy-sharing collisions, and resonant solitons. *Phys. Rev. E* **2014**, *90*, 052912. [CrossRef]
144. Kanna, T.; Vijayajayanthi, M.; Lakshmanan, M. Mixed solitons in a $(2+1)$-dimensional multicomponent long-wave-short-wave system. *Phys. Rev. E* **2014**, *90*, 042901. [CrossRef]
145. Chen, J.; Feng, B.F.; Chen, Y.; Ma, Z. General bright-dark soliton solution to $(2+1)$-dimensional multi-component long-wave-short-wave resonance interaction system. *Nonlinear Dyn.* **2017**, *88*, 1273. [CrossRef]
146. Chow, K.W.; Chan, H.N.; Kedzioara, D.J.; Grimshaw, R.H.J. Rogue wave modes for the long wave-short wave resonance model. *J. Phys. Soc. Jpn.* **2013**, *82*, 074001. [CrossRef]
147. Chen, S.; Grelu, P.; Soto-Crespo, J.M. Dark-and bright-rogue-wave solutions for media with long-wave-short-wave resonance. *Phys. Rev. E* **2014**, *89*, 011201(R). [CrossRef] [PubMed]
148. Chan, H.N.; Ding, E.; Kedzioara, D.J.; Grimshaw, R.H.J.; Chow, K.W. Rogue waves for a long wave–short wave resonance model with multiple short waves. *Nonlinear Dyn.* **2016**, *85*, 2827. [CrossRef]
149. Chen, S.; Soto-Crespo, J.M.; Grelu, P. Coexisting rogue waves within the $(2+1)$-component long-wave-short-wave resonance. *Phys. Rev. E* **2014**, *90*, 033203. [CrossRef]
150. Chen, J.; Chen, Y.; Feng, B.F.; Maruno, K.I. Rational solutions to two-and one-dimensional multicomponent Yajima-Oikawa systems. *Phys. Lett. A* **2015**, *379*, 1510. [CrossRef]
151. Rao, J.; Porsezian, K.; He, J.; Kanna, T. Dynamics of lumps and dark-dark solitons in the multi-component long-wave-short-wave resonance interaction system. *Proc. R. Soc. A* **2018**, *474*, 20170627. [CrossRef]
152. Yang, J.W.; Gao, Y.T.; Sun, Y.H.; Shen, Y.J.; Su, C.Q. Higher-order rogue waves with new spatial distributions for the $(2+1)$-dimensional two-component long-wave-short-wave resonance interaction system. *Eur. Phys. J. Plus* **2016**, *131*, 416. [CrossRef]
153. Hirota, R. *The Direct Method in Soliton Theory*; Cambridge University Press: Cambridge, UK, 2004.
154. Ablowitz, M.J.; Ohta, Y.; Trubatch, A.D. On discretizations of the vector nonlinear Schrödinger equation. *Phys. Lett. A* **1999**, *253*, 287. [CrossRef]
155. Vijayajayanthi, M.; Kanna, T.; Lakshmanan, M. Multisoliton solutions and energy sharing collisions in coupled nonlinear Schrödinger equations with focusing, defocusing and mixed type nonlinearities. *Eur. Phys. J. Spec. Top.* **2009**, *173*, 57. [CrossRef]
156. Gilson, C.; Hietarinta, J.; Nimmo, J.; Ohta, Y. Sasa-Satsuma higher-order nonlinear Schrödinger equation and its bilinearization and multisoliton solutions. *Phys. Rev. E* **2003**, *68*, 016614. [CrossRef] [PubMed]
157. Sakaguchi, H.; Malomed, B.A. Singular solitons. *Phys. Rev. E* **2020**, *101*, 012211. [CrossRef] [PubMed]
158. Ramakrishnan, R.; Stalin, S.; Lakshmanan, M. Dynamics of nondegenerate solitons in generalized coupled nonlinear Schrödinger system. **2021**, Unpublished.
159. Stalin, S.; Ramakrishnan, R.; Lakshmanan, M. Dynamics of nondegenerate solitons in long-wave short-wave resonance interaction system. **2021**, Unpublished.

Dynamics of nondegenerate solitons in long-wave short-wave resonance interaction system

S. Stalin†, R. Ramakrishnan and M. Lakshmanan‡

Department of Nonlinear Dynamics, Bharathidasan University, Tiruchirappalli - 620 024, Tamilnadu, India.

E-mail: ‡ lakshman.cnld@gmail.com

E-mail: †stalin.cnld@gmail.com (Corresponding Author)

Abstract. In this paper, we point out that the two-component long wave-short wave resonance interaction (LSRI) system can admit a more general form of nondegenerate fundamental soliton solution than the one that is known in the literature and consequently its higher-order generalized soliton solutions as well. To derive this class of soliton solutions through the Hirota bilinear method we consider the more general form of admissible seed solutions with nonidentical distinct propagation constants. The resultant general fundamental soliton solution admits a double-hump or a single-hump profile structure including a special flattop profile form when the soliton propagates in all the components with identical velocities. Interestingly, in the case of nonidentical velocities, the soliton number is increased to two in the long-wave (LW) component, while a single-humped soliton propagates in the two short-wave (SW) components. We also express the obtained nondegenerate one-, two- and three-soliton solutions in a compact way using Gram-determinants. It is also established that the nondegenerate solitons in contrast to the degenerate case (with identical wave numbers) can undergo three types of elastic collision scenarios: (i) shape preserving, (ii) shape altering and (iii) a novel shape changing collision, depending on the choice of soliton parameters. In addition, we also point out the coexistence of nondegenerate and degenerate solitons simultanously along with the consequences. We also indicate the physical realizations of these general solitons in hydrodynamics, nonlinear optics and Bose-Einstein condensates.

1. Introduction

Resonance is a natural phenomenon which occurs in both linear and nonlinear dynamical systems under special conditions on the frequencies [1]. This parametric process has been widely observed ranging from simple harmonic motion in mechanical systems to more complicated ultra-short pulse dynamics in optical systems. In this sequence, the interaction among the nonlinear waves induces one such fascinating resonance phenomenon called the long wave-short wave resonance interaction modelled by a set of coupled nonlinear Schrödinger type equations. In this paper, we intend to derive a

more general form of bright soliton solutions for the following LSRI model, namely two component long-wave short-wave resonance interaction system,

$$iS_t^{(1)} + S_{xx}^{(1)} + LS^{(1)} = 0,\ iS_t^{(2)} + S_{xx}^{(2)} + LS^{(2)} = 0,\ L_t = \sum_{l=1}^{2}(|S^{(l)}|^2)_x. \qquad (1)$$

In the above, L is the long-wave and $S^{(l)}$'s, $l = 1, 2$, are the short-waves. The suffixes x and t denote partial derivatives with respect to the spatial and temporal coordinates, respectively. Soliton formation essentially takes place in the evolution equations of SWs, that is the first two of the equations in Eq. (1), due to the interplay between the nonlinearities and their corresponding dispersions, namely second order spatial derivative terms. The nonlinearities arise in these equations while the long-wave interacts with the short-waves. At the same time, the self interaction of the SWs defines the soliton formation in the long-wave evolution equation as specified by the last of the equations in Eq. (1). Physically the system (1) appears whenever the phase velocity of the long-wave ($v_{p,LW}$) almost matches with the group velocity of the short-waves ($v_{g,SW} = \frac{d\omega}{dk}$). This resonance condition was originally derived by Zakharov in the study on Langmuir waves in plasmas [2] and it was also derived by Benney during the investigation on the interaction between capillary gravity waves and gravity waves in deep water [3].

The long-wave short-wave resonance phenomenon was identified in several physical situations. For instance, in plasma physics, the LSRI process was observed during the nonlinear resonance interaction of an electron-plasma wave and an ion-sound wave [4]. In Ref. [5], Yajima and Oikawa have shown that the unidirectional propagation of Langmuir waves coupled with ion-sound waves is modelled by the single component LSRI system, where they have established the integrability of the system by obtaining the soliton solutions using a more sophisticated inverse scattering transform method [6]. Due to this, the system (1) is also referred as Yajima-Oikawa (YO) system in the literature. In the context of the fluid dynamics, the LSRI was noticed during the evolution of the short and long capillary gravity waves in deep water [3], in uniform water depth [7] and in finite depth-water [8]. Such a fascinating resonance phenomenon was verified experimentally in three layer fluid flow [9]. In addition to this, the phenomenon was discussed in [10] when ultralong equatorial Rossby waves get coupled with the short gravity waves. The LSRI process has been reported in the nonlinear optics context also, especially in an optical fiber, where a single component YO system is reduced from the coupled nonlinear Schrödinger equations describing the interaction of two optical modes under small amplitude asymptotic expansion [11]. In negative refractive index media [12], the three-wave mixing process leads to the formation of LSRI, where two degenerate short-waves propagate in the negative index branch while a long wave stays in the positive index branch. It should be noted that several evolution equations and their solutions have been obtained in nonresonant quadratic nonlinear media [13]. The dynamics of quasi-resonant two-frequency short pulses and a long-wave is described by Eq. (1) [14] and multicomponent version of Eq. (1) finds potential applications in spinor Bose-

Einstein condensates (BECs) [15]. By employing a multi-scale expansion procedure, the higher dimensional LSRI system has been derived for describing the dynamics of binary disk-shaped BECs [16], and also to study the dynamics of bright-dark soliton complexes in spinor BECs the YO system has been derived in [17]. Multicomponent YO type equations have been derived in the study of magon-phonon interaction [18]. Therefore, the system considered in the present paper is physically very important and analysing its solutions is useful for studying this peculiar resonance property in the above described nonlinear media.

It is important to point out that there are several nonlinear wave solutions which have been reported in the literature for the integrable long wave-short wave resonance interaction model and its variants [19–29, 31–37]. For the one-dimensional single component YO system, both bright and dark soliton solutions were derived in [19]. Interestingly energy sharing collisions among the single-humped bright solitons of the $(1 + 1)$-dimensional multicomponent LSRI system have been brought out in [20]. For this system, such shape changing collision scenario is demonstrated in [21] by deriving the mixed bright-dark soliton solutions. In this case, the authors set up bright solitons in the two SW components in order to observe the shape changing collision. In contrast to this, the dark soliton solutions of the multicomponent LSRI system always exhibit elastic collision [22]. It is noted that for the two layer fluid flow the one and two-dimensional versions of LSRI systems were obtained and bright and dark type soliton solutions were derived [23]. Ohta et al. have deduced the two- component analogue of the two-dimensional LSRI system by considering the nonlinear interactions of dispersive waves on three channels and they have obtained soliton solutions in Wronskian form for the corresponding two-dimensional model [24]. This system is shown to be integrable through Painlevé analysis and the dromion solutions were obtained using Painlevé truncation method [25]. Very interestingly, one of the present authors (ML) and his collaborators demonstrated the energy sharing collisions of bright solitons in the two-dimensional integrable versions of the multicomponent LSRI system by deriving their explicit solutions through the Hirota bilinear method [26,27] and they have also shown that the formation of resonant solitons in this higher-dimensional system [27]. Mixed bright-dark soliton solutions and their collision dynamics for this $(2 + 1)$-dimensional system have been studied in [28,29]. For this system, multi-dark soliton solutions and their elastic collision have also been studied [22]. Apart from the above studies, rogue waves, a wave which is localized both in space and in time and appearing from nowhere and disappearing without a trace modelled by simple lowest order rational solution [30] and its various interesting dynamical patterns, have been reported for the LSRI system ranging from $(1 + 1)$ and $(2 + 1)$-dimensional single component to multi-component cases [31–37].

From the above studies, we carefully identify that the fundamental bright solitons reported so far in the literature for the two-component YO system (1) correspond to degenerate solitons with identical wave numbers in all the components, as we have pointed out recently in [38,39] for the case of Manakov system and in Eq. (29) of

section 5 of the present paper. By introducing non-identical propagation constants appropriately we have removed the degeneracy in the structure of the fundamental bright soliton solutions of the Manakov system. For the first time, we have shown that such an inclusion of additional distinct propagation constants brings out a new class of fundamental bright solitons, namely nondegenerate fundamental solitons, characterized by non-identical wave numbers in all the modes [38]. As we have demonstrated in [38,39], this new class of fundamental solitons for the Manakov system undergoes novel collision properties. To the best of our knowledge, such nondegenerate solitons have not been predicted so far in the literature for the $(1+1)$-dimensional long wave-short wave resonance interaction system (1) and their fascinating dynamics remains to be unravelled. With this motivation, in this paper, we aim to derive the nondegenerate multi-soliton solutions with the general forms of seed solutions through the Hirota bilinear method. We find that the obtained nondegenerate solitons possess remarkable collisional properties for an appropriate choice of soliton parameters. In particular, they exhibit shape preserving collision with a zero phase shift, and shape altering and shape changing collisions with finite phase shifts. However, by taking the time shift in the asymptotic expressions, we show that all these three cases belong to elastic collision only. This special feature is not observed earlier in the degenerate counterpart. Further, we deduce another special type of two soliton solution from the obtained completely nondegenerate two-soliton solution. This new type of partially nondegenerate soliton solution displays an interesting coexistence phenomenon, where the degenerate soliton coexists with a nondegenerate soliton. This class of soliton solution undergoes two types of shape changing collision scenarios. Finally, we point out the degenerate fundamental and multi-bright soliton solutions can be captured from the nondegenerate fundamental and multi-soliton solutions, respectively, under restrictions on the wave numbers. We note that the existence of nondegenerate fundamental soliton solution for other integrable coupled nonlinear Schrödinger systems has also been reported recently by us using the Hirota bilinear method [40] and in Ref. [41] the nondegenerate solitons have been discussed in the context of BEC using Darboux transformation method. Very recently, we have shown that the nondegenerate soliton solution exhibits multihump profile structures in N-coupled nonlinear Schrödinger system [42] as well. Further, we have also shown that the $\mathcal{PT}$-symmetric nonlocal two coupled NLS system also admits both nondegenerate and degenerate soliton solutions [43]. It is interesting to note that the nondegenerate solitons also have been reported in the coupled Fokas-Lenells system [44] using Darboux transformation and in the two component AB system, [37,45] by following our work [38].

The plan of the paper is as follows: In Section 2, we present the nondegenerate one and two-soliton solutions of the system (1) apart from pointing out the existence of partially nondegenerate soliton solution. In this section, we also discuss the various properties associated with the nondegenerate fundamental soliton. Section 3 deals with the investigation of the three types of elastic collision scenarios with appropriate asymptotic analysis and suitable graphical demonstrations. The degenerate soliton

collision induced novel shape changing properties of the nondegenerate soliton is analysed in Section 4. In Section 5, we point out that the degenerate one- and two-soliton solutions can be captured as a limiting case of the nondegenerate one- and two-soliton solutions under appropriate wave number restrictions. In Section 6, we summarize the results. For completeness, in Appendix A, we provide the nondegenerate three-soliton solution in Gram determinant forms. In Appendix B, we present the explicit forms of constants appearing in the asymptotic analysis of collision dynamics between degenerate and nondegenerate solitons.

2. Nondegenerate soliton solutions

We construct the nondegenerate multi-soliton solution by bilinearizing Eq. (1) through the dependent variable transformations, $S^{(l)}(x,t) = \frac{g^{(l)}(x,t)}{f(x,t)}$, $l = 1, 2$, $L = 2\frac{\partial^2}{\partial x^2} \ln f(x,t)$. This action yields the following bilinear forms of Eq. (1),

$$D_1 g^{(l)} \cdot f = 0, \ l = 1, 2, \ D_2 f \cdot f = \sum_{n=1}^{2} |g^{(n)}|^2, \tag{2}$$

where $D_1 \equiv iD_t + D_x^2$ and $D_2 \equiv D_x D_t$. Here D_t and D_x are the Hirota bilinear operators defined by $D_x^m D_t^n (a \cdot b) = \left(\frac{\partial}{\partial x} - \frac{\partial}{\partial x'}\right)^m \left(\frac{\partial}{\partial t} - \frac{\partial}{\partial t'}\right)^n a(x,t) b(x',t')|_{x=x',\ t=t'}$ [46]. In principle, the soliton solutions (with vanishing boundary condition $S^{(l)} \to 0$, $l = 1, 2$ and $L \to 0$ as $x \to \pm\infty$) of Eq. (1) can be derived by solving a system of linear partial differential equations (PDEs), which appear at various orders of ϵ while substituting the series expansions $g^{(l)} = \epsilon g_1^{(l)} + \epsilon^3 g_3^{(l)} + ..., \ l = 1, 2$, $f = 1 + \epsilon^2 f_2 + \epsilon^4 f_4 + ...$ in the bilinear forms (2). The explicit forms of the functions $g^{(l)}$'s and f lead to various soliton solutions to the underlying LSRI system (1).

2.1. Nondegenerate one-soliton solution

To derive the nondegenerate fundamental soliton solution we start with the more general form of seed solutions,

$$g_1^{(1)} = \alpha_1^{(1)} e^{\eta_1}, \ g_1^{(2)} = \alpha_1^{(2)} e^{\xi_1}, \ \eta_1 = k_1 x + i k_1^2 t, \ \xi_1 = l_1 x + i l_1^2 t, \tag{3}$$

where $\alpha_1^{(l)}$'s, k_1 and l_1 are arbitrary complex constants, for the lowest order linear PDEs,

$$i g_{1,t}^{(1)} + g_{1,xx}^{(1)} = 0, \ i g_{1,t}^{(2)} + g_{1,xx}^{(2)} = 0. \tag{4}$$

From the above, one can notice that the functions $g^{(1)}$ and $g^{(2)}$ considered in Eq. (3) are two distinct solutions. This is because of the independent nature of the two linear PDEs specified above in Eq. (4) and so their solutions should be expressed in general in terms of two independent functions as given in Eq. (3) above with arbitrary wave numbers k_1, l_1, where in general $k_1 \neq l_1$. The general forms of the seed solutions with distinct propagation constants will bring out a physically meaningful class of fundamental soliton solutions as we describe below. Such a possibility has not been considered so far in the literature for the (1+1)-dimensional integrable two component LSRI system as far as our

knowledge goes except in our earlier papers [38–40, 42, 47]. What has been considered so far is only the restricted class of seed solutions, that is the wave number restricted seed solutions, namely $g_1^{(1)} = \alpha_1^{(1)} e^{\eta_1}$, $g_1^{(2)} = \alpha_1^{(2)} e^{\eta_1}$, $\eta_1 = k_1 x + i k_1^2 t$ (one can get this set of seed solutions straightforwardly by setting the condition $k_1 = l_1$ in (3)). Even such restricted seed solutions have been shown to yield interesting energy sharing collision properties of solitons [20]. So what we emphasize here is that the vector bright solitons reported so far in the literature are achieved by considering such a limited class of seed solutions only. With the general forms of seed solutions (3), we solve the following system of linear inhomogeneous partial differential equations:

$$O(\epsilon^0) : 0 = 0,\ O(\epsilon^2) : D_2(1 \cdot f_2 + f_2 \cdot 1) = g_1^{(1)} g_1^{(1)*} + g_1^{(2)} g_1^{(2)*}, \tag{5a}$$

$$O(\epsilon^3) : D_1 g_3^{(l)} \cdot 1 = -D_1 g_1^{(l)} \cdot f_2, \tag{5b}$$

$$O(\epsilon^4) : D_2(1 \cdot f_4 + f_4 \cdot 1) = -D_2 f_2 \cdot f_2 + g_1^{(1)} g_3^{(1)*} + g_3^{(1)} g_1^{(1)*} + g_1^{(2)} g_3^{(2)*} + g_3^{(2)} g_1^{(2)*}, \tag{5c}$$

$$O(\epsilon^5) : D_1 g_5^{(l)} \cdot 1 = -D_1 (g_1^{(l)} \cdot f_4 + g_3^{(l)} \cdot f_2),\ l = 1, 2, \tag{5d}$$

$$\begin{aligned} O(\epsilon^6) : D_2(1 \cdot f_6 + f_6 \cdot 1) = &-D_2(f_4 \cdot f_2 + f_2 \cdot f_4) + g_1^{(1)} g_5^{(1)*} + g_3^{(1)} g_3^{(1)*} + g_5^{(1)} g_1^{(1)*} \\ &+ g_1^{(2)} g_5^{(2)*} + g_3^{(2)} g_3^{(2)*} + g_5^{(2)} g_1^{(2)*}, \end{aligned} \tag{5e}$$

and etc. By doing so, we find the explicit forms of the unknown functions f_2, $g_3^{(l)}$, $l = 1, 2$, and f_4 as $f_2 = e^{\eta_1 + \eta_1^* + R_1} + e^{\xi_1 + \xi_1^* + R_2}$, $g_3^{(1)} = e^{\eta_1 + \xi_1 + \xi_1^* + \Delta_1}$, $g_3^{(2)} = e^{\xi_1 + \eta_1 + \eta_1^* + \Delta_2}$, $f_4 = e^{\eta_1 + \eta_1^* + \xi_1 + \xi_1^* + R_3}$, where $e^{R_1} = \frac{|\alpha_1^{(1)}|^2}{2i(k_1 + k_1^*)^2 (k_1 - k_1^*)}$, $e^{R_2} = \frac{|\alpha_1^{(2)}|^2}{2i(l_1 + l_1^*)^2 (l_1 - l_1^*)}$, $e^{\Delta_1} = \frac{i\alpha_1^{(1)} |\alpha_1^{(2)}|^2 (l_1 - k_1)}{2(k_1 + l_1^*)(l_1 - l_1^*)(l_1 + l_1^*)^2}$, $e^{\Delta_2} = \frac{i\alpha_1^{(2)} |\alpha_1^{(1)}|^2 (k_1 - l_1)}{2(k_1^* + l_1)(k_1 - k_1^*)(k_1 + k_1^*)^2}$, $e^{R_3} = -\frac{|\alpha_1^{(1)}|^2 |\alpha_1^{(2)}|^2 |k_1 - l_1|^2}{4|k_1 + l_1^*|^2 (k_1 - k_1^*)(l_1 - l_1^*)(k_1 + k_1^*)^2 (l_1 + l_1^*)^2}$. We note that the right hand sides of all the remaining linear PDEs identically vanish upon substitution of the obtained functions $g_1^{(l)}$, $g_3^{(l)}$, $l = 1, 2$, f_2 and f_4. Consequently, one can take $g_5^{(l)} = g_7^{(l)} = ... = 0$, $l = 1, 2$, and $f_6 = f_8 = ... = 0$. Thus in the series all $g_i^{(l)} = 0$ for $i \geq 5$ and all $f_j = 0$, $j \geq 6$. Therefore, ultimately the series converges at the $O(\epsilon^3)$ in the function $g^{(l)}(x, t)$ while the series terminates at the $O(\epsilon^4)$ in $f(x, t)$: $g^{(l)} = \epsilon g_1^{(l)} + \epsilon^3 g_3^{(l)}$, $l = 1, 2$, $f = 1 + \epsilon^2 f_2 + \epsilon^4 f_4$. We also note that the small parameter ϵ can be fixed as 1 (as it can be subsumed with the parameters $\alpha_1^{(1)}$ and $\alpha_1^{(2)}$), without loss of generality. Thus the above procedure makes the infinite expansion to terminate with a finite number of terms only and hence the solution can be summed up into an exact one. Finally, the resultant explicit forms of the unknown functions constitute the nondegenerate fundamental soliton solution for the system (1), which reads as,

$$S^{(1)}(x, t) = \frac{g_1^{(1)} + g_3^{(1)}}{1 + f_2 + f_4} = \frac{\alpha_1^{(1)} e^{\eta_1} + e^{\eta_1 + \xi_1 + \xi_1^* + \Delta_1}}{1 + e^{\eta_1 + \eta_1^* + R_1} + e^{\xi_1 + \xi_1^* + R_2} + e^{\eta_1 + \eta_1^* + \xi_1 + \xi_1^* + R_3}}, \tag{6a}$$

$$S^{(2)}(x, t) = \frac{g_1^{(2)} + g_3^{(2)}}{1 + f_2 + f_4} = \frac{\alpha_1^{(2)} e^{\xi_1} + e^{\xi_1 + \eta_1 + \eta_1^* + \Delta_2}}{1 + e^{\eta_1 + \eta_1^* + R_1} + e^{\xi_1 + \xi_1^* + R_2} + e^{\eta_1 + \eta_1^* + \xi_1 + \xi_1^* + R_3}}, \tag{6b}$$

$$L(x, t) = 2 \frac{\partial^2}{\partial x^2} \ln(1 + e^{\eta_1 + \eta_1^* + R_1} + e^{\xi_1 + \xi_1^* + R_2} + e^{\eta_1 + \eta_1^* + \xi_1 + \xi_1^* + R_3}). \tag{6c}$$

Using Gram determinants [48, 49], we can rewrite the above soliton solution in a

more compact form as $S^{(1)}=\frac{g^{(1)}}{f}$, $S^{(2)}=\frac{g^{(2)}}{f}$, $L=2\frac{\partial^2}{\partial x^2}\ln f$, where

$$g^{(1)}=\begin{vmatrix} \frac{e^{\eta_1+\eta_1^*}}{(k_1+k_1^*)} & \frac{e^{\eta_1+\xi_1^*}}{(k_1+l_1^*)} & 1 & 0 & e^{\eta_1} \\ \frac{e^{\xi_1+\eta_1^*}}{(l_1+k_1^*)} & \frac{e^{\xi_1+\xi_1^*}}{(l_1+l_1^*)} & 0 & 1 & e^{\xi_1} \\ -1 & 0 & \frac{|\alpha_1^{(1)}|^2}{2i(k_1^2-k_1^{*2})} & 0 & 0 \\ 0 & -1 & 0 & \frac{|\alpha_1^{(2)}|^2}{2i(l_1^2-l_1^{*2})} & 0 \\ 0 & 0 & -\alpha_1^{(1)} & 0 & 0 \end{vmatrix}, \tag{7a}$$

$$g^{(2)}=\begin{vmatrix} \frac{e^{\eta_1+\eta_1^*}}{(k_1+k_1^*)} & \frac{e^{\eta_1+\xi_1^*}}{(k_1+l_1^*)} & 1 & 0 & e^{\eta_1} \\ \frac{e^{\xi_1+\eta_1^*}}{(l_1+k_1^*)} & \frac{e^{\xi_1+\xi_1^*}}{(l_1+l_1^*)} & 0 & 1 & e^{\xi_1} \\ -1 & 0 & \frac{|\alpha_1^{(1)}|^2}{2i(k_1^2-k_1^{*2})} & 0 & 0 \\ 0 & -1 & 0 & \frac{|\alpha_1^{(2)}|^2}{2i(l_1^2-l_1^{*2})} & 0 \\ 0 & 0 & 0 & -\alpha_1^{(2)} & 0 \end{vmatrix}, \tag{7b}$$

$$f=\begin{vmatrix} \frac{e^{\eta_1+\eta_1^*}}{(k_1+k_1^*)} & \frac{e^{\eta_1+\xi_1^*}}{(k_1+l_1^*)} & 1 & 0 \\ \frac{e^{\xi_1+\eta_1^*}}{(l_1+k_1^*)} & \frac{e^{\xi_1+\xi_1^*}}{(l_1+l_1^*)} & 0 & 1 \\ -1 & 0 & \frac{|\alpha_1^{(1)}|^2}{2i(k_1^2-k_1^{*2})} & 0 \\ 0 & -1 & 0 & \frac{|\alpha_1^{(2)}|^2}{2i(l_1^2-l_1^{*2})} \end{vmatrix}. \tag{7c}$$

We find that the above forms of Gram determinants satisfy the two component LSRI system (1) as well as the bilinear equations (2). In order to analyse the various special properties of the nondegenerate one-soliton solution of Eq. (1), we obtain the following expression for the one-soliton solution by rewriting Eqs. (6a)-(6c) in hyperbolic forms,

$$S^{(1)}=\frac{4k_{1R}\sqrt{k_{1I}}A_1e^{i(\eta_{1I}+\frac{\pi}{2})}[\cosh(\xi_{1R}+\varphi_{1R})\cos\varphi_{1I}+i\sinh(\xi_{1R}+\varphi_{1R})\sin\varphi_{1I}]}{[a_{11}\cosh(\eta_{1R}+\xi_{1R}+\varphi_1+\varphi_2+c_1)+\frac{1}{a_{11}^*}\cosh(\eta_{1R}-\xi_{1R}+\varphi_2-\varphi_1+c_2)]}, \tag{8a}$$

$$S^{(2)}=\frac{4l_{1R}\sqrt{l_{1I}}A_2e^{i(\xi_{1I}+\frac{\pi}{2})}[\cosh(\eta_{1R}+\varphi_{2R})\cos\varphi_{2I}+i\sinh(\eta_{1R}+\varphi_{2R})\sin\varphi_{2I}]}{[a_{12}\cosh(\eta_{1R}+\xi_{1R}+\varphi_1+\varphi_2+c_1)+\frac{1}{a_{12}^*}\cosh(\eta_{1R}-\xi_{1R}+\varphi_2-\varphi_1+c_2)]}, \tag{8b}$$

$$L=\frac{4k_{1R}^2\cosh(2\xi_{1R}+2\varphi_1+c_4)+4l_{1R}^2\cosh(2\eta_{1R}+2\varphi_2+c_3)+\frac{1}{2}e^{R_3'-(\frac{R_1+R_2+R_3}{2})}}{[\Lambda\cosh(\eta_{1R}+\xi_{1R}+\varphi_1+\varphi_2+c_1)+\Lambda^{-1}\cosh(\eta_{1R}-\xi_{1R}+\varphi_2-\varphi_1+c_2)]^2}, \tag{8c}$$

$$e^{R_3'}=4(k_{1R}+l_{1R})^2e^{R_3}+4(k_{1R}-l_{1R})^2e^{R_1+R_2},$$

where $a_{11}=\frac{(k_1^*-l_1^*)^{\frac{1}{2}}}{(k_1^*+l_1)^{\frac{1}{2}}}$, $a_{12}=\frac{(k_1^*-l_1^*)^{\frac{1}{2}}}{(k_1+l_1^*)^{\frac{1}{2}}}$, $\Lambda=\frac{1}{2}\log\frac{|k_1-l_1|}{|k_1+l_1^*|}$, $c_1=\frac{1}{2}\log\frac{(k_1^*-l_1^*)}{(l_1-k_1)}$, $c_2=\frac{1}{2}\log\frac{(k_1-l_1)(k_1^*+l_1)}{(l_1-k_1)(k_1+l_1^*)}$, $c_3=\frac{1}{2}\log\frac{(l_1^*-k_1^*)(k_1^*+l_1)}{(k_1+l_1^*)(l_1-k_1)}$, $c_4=\frac{1}{2}\log\frac{(k_1^*-l_1^*)(k_1+l_1^*)}{(k_1^*+l_1)(k_1-l_1)}$, $\eta_{1R}=k_{1R}(x-2k_{1I}t)$, $\eta_{1I}=k_{1I}x+(k_{1R}^2-k_{1I}^2)t$, $\xi_{1R}=l_{1R}(x-2l_{1I}t)$, $\xi_{1I}=l_{1I}x+(l_{1R}^2-l_{1I}^2)t$, $A_1=[\alpha_1^{(1)}/\alpha_1^{(1)*}]^{1/2}$, $A_2=i[\alpha_1^{(2)}/\alpha_1^{(2)*}]^{1/2}$, and the other constants can be calculated using the constants that are defined below Eqs. (6a)-(6c). Here, φ_{1R}, φ_{2R}, φ_{1I} and φ_{2I} are real and imaginary parts of $\varphi_1=\frac{\Delta_1-\rho_1}{2}$ and $\varphi_2=\frac{\Delta_2-\rho_2}{2}$, $e^{\rho_l}=\alpha_1^{(l)}$, $l=1,2$, respectively and k_{1R}, l_{1R}, k_{1I} and l_{1I} denote the real and imaginary parts of k_1 and l_1, respectively. The four arbitrary complex parameters, $\alpha_1^{(l)}$'s, $l=1,2$, k_1 and l_1, determine the structure of

the nondegenerate fundamental soliton solution (8*a*)-(8*c*) of the two component LSRI system (1).

In general, the amplitudes of the soliton in the short-wave components are $4k_{1R}\sqrt{k_{1I}}A_1$ and $4l_{1R}\sqrt{l_{1I}}A_2$, respectively, and their velocities in their respective SW components are $2k_{1I}$ and $2l_{1I}$. On the other hand, the amplitude and the velocity of the soliton in the LW component mainly depend on the real and imaginary parts of both the wave numbers k_1 and l_1, respectively. From the above, one can easily notice that the amplitudes of the SW components explicitly depend on the velocity of the soliton. This interesting amplitude dependent velocity property is analogous to the property of the Korteweg-de Vries (KdV) soliton of the form $u(x,t) = \frac{c}{2}\,\mathrm{sech}^2\frac{\sqrt{c}}{2}(x-ct)$. Here c is the velocity of the KdV soliton [1,50]. Consequently, like the degenerate bright solitons, the taller nondegenerate solitons also travel faster than the smaller ones, as pointed out in Section 5 and in Ref. [20]. We note that the nondegenerate fundamental soliton in the Manakov system does not possess this velocity-dependent amplitude property [38,39]. The solution (8*a*)-(8*c*) shows both regular and singular behaviour. The singularity property of the solution is determined by the quantities e^{R_1}, e^{R_2} and e^{R_3}. The regular soliton solution arises for the case when both k_{1I} and $l_{1I} < 0$. In this case, the quantities, e^{R_1}, e^{R_2} and $e^{R_3} > 0$ whereas the solution (8*a*)-(8*c*) displays singularity for k_{1I} and/or $l_{1I} > 0$.

The nondegenerate one-soliton solution (8*a*)-(8*c*) is classified as follows depending on the choice of the velocity conditions:
(i) For $k_{1I} = l_{1I}$, we designate the one-soliton solution as $(1,1,1)$-soliton solution, where all the components $(S^{(1)}, S^{(2)}, L)$ consist of only one soliton with double-hump or flattop or single-hump structured profile.
(ii) On the other hand, we refer the solution (8*a*)-(8*c*) with $k_{1I} \neq l_{1I}$ as $(1,1,2)$-soliton solution, where both the short-wave components $S^{(1)}$ and $S^{(2)}$ possess one humped localized structures only while the long-wave component contains two single-hump structured profiles like the 2-soliton solution of the NLS equation. We will discuss each one of these cases separately in the following.

In the equal velocity case, the soliton in the SW components propagates with identical velocities but with different amplitudes. For this case, the imaginary parts of φ_j's are equal to zero. That is, $\varphi_{jI} = 0$, $j = 1,2$. This property reduces the solution (8*a*)-(8*c*) into the following form of $(1,1,1)$-soliton solution,

$$S^{(1)} = \frac{4k_{1R}\sqrt{k_{1I}}A_1 e^{i(\eta_{1I}+\frac{\pi}{2})}\cosh(\xi_{1R}+\varphi_{1R})}{[b_1\cosh(\eta_{1R}+\xi_{1R}+\varphi_1+\varphi_2+c_1)+\frac{1}{b_1}\cosh(\eta_{1R}-\xi_{1R}+\varphi_2-\varphi_1+c_2)]}, \quad (9a)$$

$$S^{(2)} = \frac{4l_{1R}\sqrt{k_{1I}}A_2 e^{i(\xi_{1I}+\frac{\pi}{2})}\cosh(\eta_{1R}+\varphi_{2R})}{[b_1\cosh(\eta_{1R}+\xi_{1R}+\varphi_1+\varphi_2+c_1)+\frac{1}{b_1}\cosh(\eta_{1R}-\xi_{1R}+\varphi_2-\varphi_1+c_2)]}, \quad (9b)$$

$$L = \frac{4k_{1R}^2\cosh(2\xi_{1R}+2\varphi_1+c_4)+4l_{1R}^2\cosh(2\eta_{1R}+2\varphi_2+c_3)+4(k_{1R}^2-l_{1R}^2)}{[b_1\cosh(\eta_{1R}+\xi_{1R}+\varphi_1+\varphi_2+c_1)+b_1^{-1}\cosh(\eta_{1R}-\xi_{1R}+\varphi_2-\varphi_1+c_2)]^2}, \quad (9c)$$

where $b_1 = \frac{(k_{1R}-l_{1R})^{\frac{1}{2}}}{(k_{1R}+l_{1R})^{\frac{1}{2}}}$, $\eta_{1R} = k_{1R}(x-2k_{1I}t)$, $\eta_{1I} = k_{1I}x+(k_{1R}^2-k_{1I}^2)t$, $\xi_{1R} = l_{1R}(x-2k_{1I}t)$,

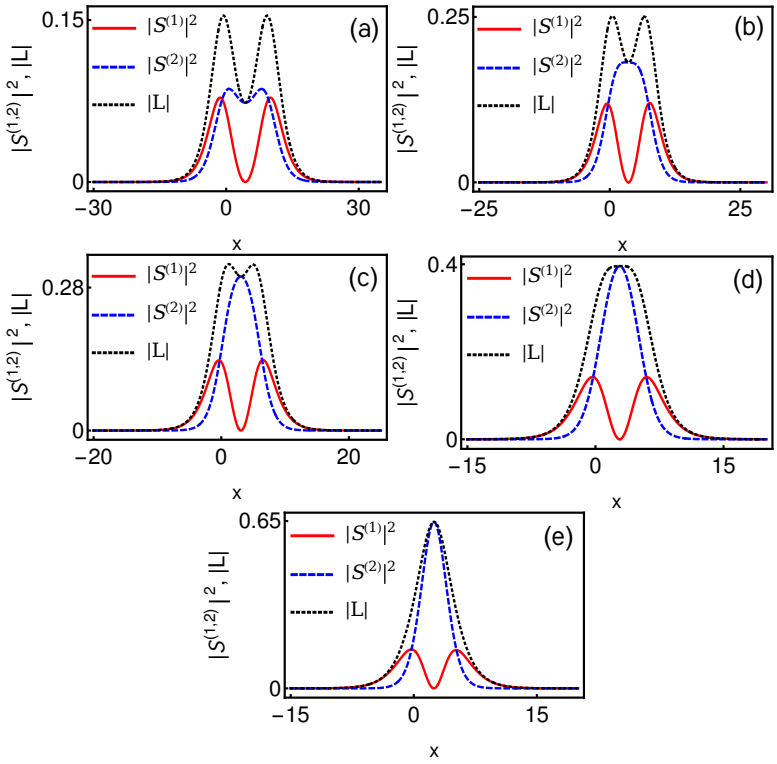

Figure 1. Five types of symmetric profiles of the nondegenerate fundamental soliton solution (8*a*)-(8*c*) with $k_{1I} = l_{1I}$ or (9*a*)-(9*c*): While (a) represents double-hump profiles in all the components, (b) denotes double-hump profiles in $S^{(1)}$ and L components and a flattop profile in $S^{(2)}$ componenet, (c) indicates double-hump profiles in $S^{(1)}$ and L components and a single-hump profile in $S^{(2)}$ componenet, (d) represents double-hump in $S^{(1)}$ component, single-hump in $S^{(2)}$ component and a flattop profile in L componnet and (e) denotes double-hump profile in $S^{(1)}$ and single-hump profiles in both $S^{(2)}$ and L components. The parameter values of each one of the cases are as follows: (a) $k_1 = 0.25 - 0.5i$, $l_1 = 0.315 - 0.5i$, $\alpha_1^{(1)} = 0.5 + 0.5i$ and $\alpha_1^{(2)} = 0.45 + 0.5i$. (b) $k_1 = 0.3 - 0.5i$, $l_1 = 0.425 - 0.5i$, $\alpha_1^{(1)} = 0.43 + 0.55i$ and $\alpha_1^{(2)} = 0.45 + 0.45i$. (c) $k_1 = 0.315 - 0.5i$, $l_1 = 0.5 - 0.5i$, $\alpha_1^{(1)} = 0.5 + 0.5i$ and $\alpha_1^{(2)} = 0.45 + 0.45i$. (d) $k_1 = 0.315 - 0.5i$, $l_1 = 0.545 - 0.5i$, $\alpha_1^{(1)} = 0.5 + 0.5i$ and $\alpha_1^{(2)} = 0.45 + 0.5i$. (e) $k_1 = 0.315 - 0.5i$, $l_1 = 0.65 - 0.5i$, $\alpha_1^{(1)} = 0.5 + 0.5i$ and $\alpha_1^{(2)} = 0.45 + 0.5i$.

$\xi_{1I} = k_{1I}x + (l_{1R}^2 - k_{1I}^2)t$.

From the above solution, we find a relation between the short-wave components and the long-wave component and it turns out to be

$$|S^{(1)}|^2 + |S^{(2)}|^2 = -2k_{1I}L. \tag{10}$$

The latter relation confirms that the above type of linear superposition of intensities of the two short-wave components accounts for the formation of interesting soliton structure in the long-wave component. The special solutions (9*a*)-(9*c*) with the condition $k_{1R} < l_{1R}$ admits five types of symmetric profiles which we have displayed in figure 1. The symmetric profiles are classified as follows: (i) Double-humps in all the components, (ii) double-humps in $S^{(1)}$ and long-wave components and a flattop in the $S^{(2)}$ component,

(iii) double-humps in $S^{(1)}$ and long-wave components and a single-hump in the $S^{(2)}$ component, (iv) double-hump in $S^{(1)}$ component, single-hump in $S^{(2)}$ component and a flattop profile in the long-wave component and (v) double-hump in $S^{(1)}$ component and single-humps in both the $S^{(2)}$ and long-wave components. In order to demonstrate all the above five cases we fix $k_{1I} = l_{1I} = -0.5 < 0$ in figure 1. From figure 1, one can observe that the transition which occurs from double-hump to single-hump or from single-hump to double-hump is through a special flattop profile. The corresponding asymmetric profiles are illustrated in figure 2 for the parameter values as specified there. This can be achieved by tuning either the real parts of the wave numbers k_1 and l_1 or by tuning the complex parameters $\alpha_1^{(l)}$'s. One can also bring out a double-hump and a flattop profile in the $S^{(1)}$ ($S^{(2)}$ and L as well) component by considering another possibility, namely $k_{1I} = l_{1I} < 0$ and $k_{1R} > l_{1R}$.

Further, one can confirm the symmetric and asymmetric nature of the $(1, 1, 1)$ solution (9*a*)-(9*c*), by finding the extremum points as we have analyzed the profile nature of the nondegenerate soliton solution in the Manakov system [39]. In the following, we explain this analysis for the symmetric double-hump soliton profile, displayed in figure 1(a), of the LSRI system (1): First, we find the local maximum and minimum points by applying the first derivative test ($\{|S^{(j)}|^2\}_x = 0$, $\{|L|\}_x = 0$) and the second derivative test ($\{|S^{(j)}|^2\}_{xx}, \{|L|\}_{xx} < 0$ or > 0) to the expressions of $|S^{(j)}|^2$, $j = 1, 2$, and $|L|$, at $t = 0$. As a result, for the first SW component, three extremal points are identified, namely $x_1 = -1.4$, $x_2 = 4.3$ and $x_3 = 9.99$. Then we found another set of three extremal points, $x_4 = 0.6$, $x_5 = 4.3$ and $x_6 = 8.09$, for the second SW component. We also identified another set of three extremal points, $x_7 = -0.6$, $x_8 = 4.29$ and $x_9 = 9.2$, for the LW component by setting $\{|L|\}_x = 0$. While the points x_2, x_5 and x_8 correspond to minima, the points, (x_1, x_3), (x_4, x_6), and (x_7, x_9) correspond to maximum points. In all the components, the minimum points x_2, x_5 and x_8 are located at equal distances from the two maximum points (x_1, x_3), (x_4, x_6) and (x_7, x_9), respectively. This can be easily confirmed by finding their differences. For instance, in the $S^{(1)}$-component, $x_1 - x_2 = -5.7 = x_2 - x_3$. This is true for both the SW component $S^{(2)}$ and the LW component L also. That is for $S^{(2)}$: $x_4 - x_5 = -3.7 \approx x_5 - x_6 = -3.79$ and for L: $x_7 - x_8 = -4.89 \approx x_8 - x_9 = -4.91$. Then the intensity, $|S^{(1)}|^2$, of each hump, of the double-hump soliton, corresponding to maxima x_1 and x_3 are equal to 0.078. Similarly, in the second SW component, the magnitude of the intensity corresponding to the maximum points x_4 and x_6 are equal to 0.086. We also obtain the magnitudes corresponding to the maxima x_7 and x_8 are equal to 0.154. The above analysis confirms that the double-hump soliton profiles displayed in figure 1(a) are symmetric. In addition, one can also verify the symmetric nature of the single-hump soliton about the local maximum point and checking the half widths as well. For the flat-top soliton case, we have confirmed that the first derivative $\{|S^{(l)}|^2\}_x$, $l = 1, 2$, and $\{|L|\}_x$, very slowly tends to zero, for a certain number of x values, near the corresponding maximum. This also confirms that the presence of almost flatness and symmetric nature of the one-soliton. By following the above procedure, one can also verify the asymmetric nature of the

solution (9*a*)-(9*c*).

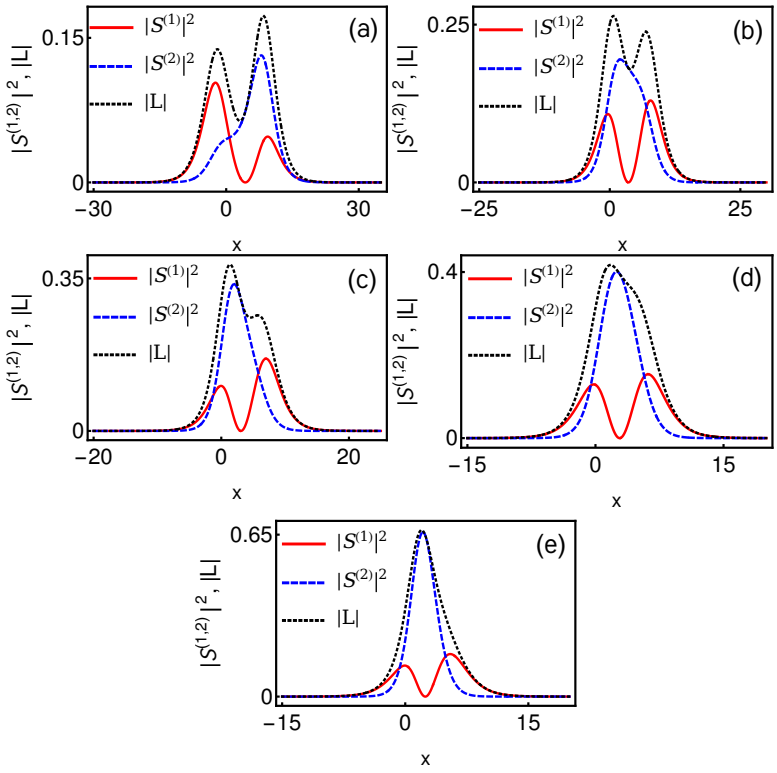

Figure 2. Panels (a), (b), (c), (d) and (e) denote asymmetric profiles corresponding to the symmetric profiles of Fig. 1(a)-1(e) with $k_{1I} = l_{1I}$. The parameter values of each of the cases are as follows: (a) $k_1 = 0.25 - 0.5i$, $l_1 = 0.315 - 0.5i$, $\alpha_1^{(1)} = 0.5 + i$ and $\alpha_1^{(2)} = 0.45 + 0.5i$. (b) $k_1 = 0.3 - 0.5i$, $l_1 = 0.425 - 0.5i$, $\alpha_1^{(1)} = 0.3 + 0.55i$ and $\alpha_1^{(2)} = 0.45 + 0.45i$. (c) $k_1 = 0.315 - 0.5i$, $l_1 = 0.5 - 0.5i$, $\alpha_1^{(1)} = 0.15 + 0.5i$ and $\alpha_1^{(2)} = 0.45 + 0.45i$. (d) $k_1 = 0.315 - 0.5i$, $l_1 = 0.545 - 0.5i$, $\alpha_1^{(1)} = 0.38 + 0.5i$ and $\alpha_1^{(2)} = 0.45 + 0.5i$. (e) $k_1 = 0.315 - 0.5i$, $l_1 = 0.65 - 0.5i$, $\alpha_1^{(1)} = 0.25 + 0.5i$ and $\alpha_1^{(2)} = 0.45 + 0.5i$.

Next, we consider the $(1, 1, 2)$-soliton solution, that is the solution (8*a*)-(8*c*) with $k_{1I} \neq l_{1I}$. In this situation, the soliton in the two short-wave components (as well as in the long-wave component) propagate with distinct velocities as we have displayed in figure 3. As it is evident from this figure that distinct single-humped one-soliton structures always occur in each of the short-wave components and they propagate from $+x$ to $-x$ direction (but with different localizations). However, surprisingly the two single-hump structured solitons of the SW component emerge in the LW component and they interact like the two soliton solution of the scalar NLS case. Each of the single-humped structures of the soliton in the SW components $S^{(1)}$ and $S^{(2)}$ interact through the LW component as dictated by the nonlinearity of the LW component. This special nonlinear phenomenon occurs because of the nondegeneracy property of the fundamental soliton solution (8*a*)-(8*c*) of the LSRI system (1). To the best of our knowledge, this special kind of phenomenon has not been observed earlier in the present $(1 + 1)$-dimensional two-component LSRI system and its multicomponent version. A

similar kind of soliton nature is also observed in the Wronskian solutions, derived by Ohta et al., for the two-component $(2+1)$-dimensional LSRI system [24]. Although the authors have graphically demonstrated the $(1,1,2)$ and $(2,2,4)$ soliton solutions in [24], the complete analysis of such soliton solutions and their associated many novel results are still missing in the literature. We have systematically analyzed the $(1,1,2)$ and $(2,2,4)$ soliton solutions of the $(2+1)$-dimensional multicomponent LSRI system by expressing their exact analytical forms in terms of Gram determinants and the results will be published elsewhere [51]. Moreover, it is shown in Ref. [26] that the Wronskian solutions $(N, M, N+M)$ reported in [24] have also been deduced from the degenerate soliton solutions (m, m, m). However, the dynamical properties of the Wronskian solutions, as graphically illustrated in [24], are distinct from the degenerate soliton solutions as explained in [26]. We point out that the double-hump soliton profile emerges in all the components when the relative velocity $2(l_{1I} - k_{1I})$ tends to zero. In other words, the double-hump formation will occur if $l_{1I} \approx k_{1I}$.

To experimentally generate the nondegenerate vector solitons one may consider three channels of nonlinear dispersive medium or triple mode nonlinear optical fiber [24], where the two light pulses are in the anomalous dispersion regime and the remaining pulse is in the normal dispersion regime. By introducing the intermodal interactions in such a way one can make the short-wave modes (anamalous dispersion regime) to interact with the long-wave mode (normal dispersion regime). In this situation, it is essential to consider two laser sources of different characters so that the frequency of the first laser beam is different from the second one. By sending the extraordinary mutual incoherent optical beam, coming out from both the sources, to the short-wave channels along with the appropriate coupling on the long-wave channel, it is possible to create the nondegenerate solitons. In this situation, the group velocities $v_g = \frac{d\omega}{dk}$ of the optical beam in the short-wave channels should be equal to the phase velocity v_p of the long-wave channel. Under this resonance condition, the nondegenerate solitons in the short-wave optical modes can be created and made to interact with the soliton in the long-wave mode. In the fluid dynamics context also one can observe the nondegenerate solitons by considering a three-layer system [9] of homogeneous fluids having different densities. In this circumstance, it is possible to achieve the problem of resonance interaction of a long interfacial wave and a short surface waves. By a proper choice of the various densities and layer thicknesses, one may tune the three-layer system to a resonant condition whereby the group velocity of the shorter surface waves and the phase velocity of the longer interfacial wave are nearly equal. Thus, all of the physics relevant to the nondegenerate solitons can be identified from this simple three-layer fluid system. On the other hand, it is also possible to create the nondegenerate solitons in spinor BECs by tuning the hyperfine states of the ^{87}Rb atoms [54] whenever the group velocities of the short-waves are equal to the phase velocity of the long-wave.

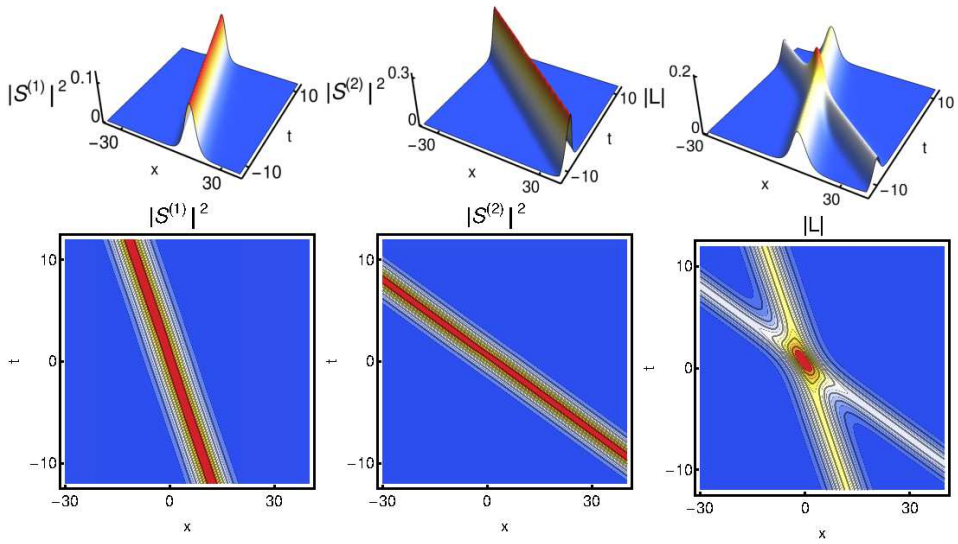

Figure 3. Nondegenerate one-soliton $(1,1,2)$ with unequal velocities. The parameter values are $k_1 = 0.25 - 0.5i$, $l_1 = 0.2 - 2i$, $\alpha_1^{(1)} = 0.45 + 0.5i$ and $\alpha_1^{(2)} = 0.5 + 0.5i$.

2.2. Completely nondegenerate two-soliton solution

To construct the completely nondegenerate two-soliton solution, we consider the seed solutions of the following forms,

$$\begin{aligned} g_1^{(1)} &= \alpha_1^{(1)} e^{\eta_1} + \alpha_2^{(1)} e^{\eta_2},\ \eta_1 = k_1 x + i k_1^2 t,\ \eta_2 = k_2 x + i k_2^2 t, \\ g_1^{(2)} &= \alpha_1^{(2)} e^{\xi_1} + \alpha_2^{(2)} e^{\xi_2},\ \xi_1 = l_1 x + i l_1^2 t,\ \xi_2 = l_2 x + i l_2^2 t, \end{aligned} \tag{11}$$

for Eqs. (4). Here we treat the four arbitrary constants k_1, k_2, l_1 and l_2 as distinct from one another, in general, apart from the other four distinct complex constants $\alpha_1^{(l)}$ and $\alpha_2^{(l)}$, $l = 1, 2$. For the two-soliton solution, we find that the above seed solutions terminate the series expansions as $g^{(l)} = \epsilon g_1^{(l)} + \epsilon^3 g_3^{(l)} + \epsilon^5 g_5^{(l)} + \epsilon^7 g_7^{(l)}$, $l = 1, 2$, $f = 1 + \epsilon^2 f_2 + \epsilon^4 f_4 + \epsilon^6 f_6 + \epsilon^8 f_8$, while solving the resulting inhomogeneous linear partial differential equations recursively. The explicit Gram determinat forms of $g^{(l)}$'s and f can be written as

$$g^{(1)} = \begin{vmatrix} A_{mm'} & A_{mn} & I & \mathbf{0} & \phi_1 \\ A_{nm} & A_{nn'} & \mathbf{0} & I & \phi_2 \\ -I & \mathbf{0} & \kappa_{mm'} & \kappa_{mn} & \mathbf{0'}^T \\ \mathbf{0} & -I & \kappa_{nm} & \kappa_{nn'} & \mathbf{0'}^T \\ \mathbf{0'} & \mathbf{0'} & C_1 & \mathbf{0'} & 0 \end{vmatrix},\ f = \begin{vmatrix} A_{mm'} & A_{mn} & I & \mathbf{0} \\ A_{nm} & A_{nn'} & \mathbf{0} & I \\ -I & \mathbf{0} & \kappa_{mm'} & \kappa_{mn} \\ \mathbf{0} & -I & \kappa_{nm} & \kappa_{nn'} \end{vmatrix}, \tag{12a}$$

$$g^{(2)} = \begin{vmatrix} A_{mm'} & A_{mn} & I & \mathbf{0} & \phi_1 \\ A_{nm} & A_{nn'} & \mathbf{0} & I & \phi_2 \\ -I & \mathbf{0} & \kappa_{mm'} & \kappa_{mn} & \mathbf{0'}^T \\ \mathbf{0} & -I & \kappa_{nm} & \kappa_{nn'} & \mathbf{0'}^T \\ \mathbf{0'} & \mathbf{0'} & \mathbf{0'} & C_2 & 0 \end{vmatrix}. \tag{12b}$$

The various elements are defined as

$$A_{mm'} = \frac{e^{\eta_m+\eta^*_{m'}}}{(k_m+k^*_{m'})},\ A_{mn} = \frac{e^{\eta_m+\xi^*_n}}{(k_m+l^*_n)}, A_{nn'} = \frac{e^{\xi_n+\xi^*_{n'}}}{(l_n+l^*_{n'})},\ A_{nm} = \frac{e^{\eta^*_n+\xi_m}}{(k^*_n+l_m)},$$

$$\kappa_{mm'} = \frac{\psi^\dagger_m\sigma\psi_{m'}}{2i(k^2_m-k^{*2}_{m'})},\ \kappa_{mn} = \frac{\psi^\dagger_m\sigma\psi'_n}{2i(l^2_m-k^{*2}_n)},\ \kappa_{nm} = \frac{\psi'^\dagger_n\sigma\psi_m}{2i(k^2_n-l^{*2}_m)},$$

$$\kappa_{nn'} = \frac{\psi'^\dagger_n\sigma\psi'_{n'}}{2i(l^2_n-l^{*2}_{n'})},\ m,m',n,n' = 1,2.$$

The other elements are defined below:
$\phi_1 = \begin{pmatrix} e^{\eta_1} & e^{\eta_2} \end{pmatrix}^T$, $\phi_2 = \begin{pmatrix} e^{\xi_1} & e^{\xi_2} \end{pmatrix}^T$, $\psi_j = \begin{pmatrix} \alpha^{(1)}_j & 0 \end{pmatrix}^T$, $\psi'_j = \begin{pmatrix} 0 & \alpha^{(2)}_j \end{pmatrix}^T$, $\mathbf{0}' = \begin{pmatrix} 0 & 0 \end{pmatrix}$, $I = \sigma = \begin{pmatrix} 1 & 0 \\ 0 & 1 \end{pmatrix}$, $\mathbf{0} = \begin{pmatrix} 0 & 0 \\ 0 & 0 \end{pmatrix}$ and $C_N = -\begin{pmatrix} \alpha^{(N)}_1 & \alpha^{(N)}_2 \end{pmatrix}$, $j, N = 1,2$. Note that in the above the $g^{(j)}$'s are (9×9) determinants and f is a (8×8) determinant. The collision dynamics and the structure of the nondegenerate two-solitons are characterized by eight arbitrary complex constants, $\alpha^{(j)}_1$, $\alpha^{(j)}_2$, k_j and l_j, $j = 1,2$. The singularity of the two-soliton solution mainly depends on the function f. To get the non-singluar solution, the function f should be positive definite ($f > 0$). This restricts the imaginary parts of the wave numbers, k_{jI} and l_{jI}, $j = 1,2$ as negative. That is $k_{jI}, l_{jI} < 0$. Further, the complete nondegenerate two-soliton solution (12*a*) and (12*b*) is classified as $(2,2,2)$-soliton solution ($k_{jI} = l_{jI}$, $j = 1,2$) and $(2,2,4)$-soliton solution ($k_{jI} \neq l_{jI}$, $j = 1,2$). We have also given the completely nondegenerate three-soliton solution in Appendix A for the system (1) using the Gram-determinants.

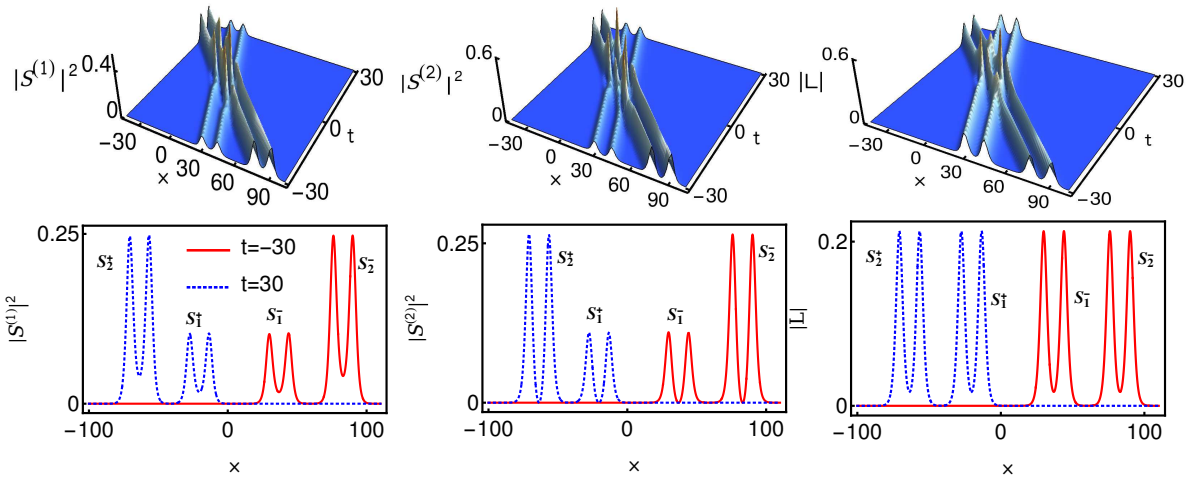

Figure 4. Elastic collision: Shape preserving collision with zero phase shift among the two symmetric double-hump solitons for the parameter values $k_1 = 0.333 - 0.5i$, $l_1 = 0.32-0.5i$, $k_2 = 0.333-1.2i$, $l_2 = 0.32-1.2i$, $\alpha^{(1)}_1 = 0.45+0.5i$, $\alpha^{(2)}_1 = 0.45+0.55i$, $\alpha^{(1)}_2 = 0.45 + 0.45i$ and $\alpha^{(2)}_2 = 0.45 + 0.515i$.

2.3. Partially nondegenerate soliton solution

We next deduce partially nondegenerate soliton solution from the complete nondegenerate two-soliton solution by imposing the wave number restriction $k_1 = l_1$ (or $k_2 = l_2$) in Eqs. (12*a*) and (12*b*). Due to this restriction, the wave variables ξ_1 and η_1 are no longer independent and they get restricted as $\xi_1 = \eta_1$, while ξ_2 and η_2 continue to be distinct and independent. The Gram determinant forms of $g^{(l)}$'s and f are the same both for the partially nondegenerate soliton solution and for the complete nondegenerate two-soliton solution except that they differ in the following constituents, A_{mn}, A_{nm}, $A_{nn'}$, κ_{mn}, κ_{nm}, $\kappa_{nn'}$ and ϕ_2. Their explicit forms for the present case are given below:

$$
\begin{aligned}
A_{mn} &: A_{11} = \frac{e^{\eta_1+\eta_1^*}}{(k_1+k_1^*)},\ A_{12} = \frac{e^{\eta_1+\xi_2^*}}{(k_1+l_2^*)}, A_{21} = \frac{e^{\eta_2+\eta_1^*}}{(k_2+k_1^*)},\ A_{22} = \frac{e^{\eta_2+\xi_2^*}}{(k_2+l_2^*)},\\
A_{nm} &: A_{11} = \frac{e^{\eta_1+\eta_1^*}}{(k_1+k_1^*)},\ A_{12} = \frac{e^{\eta_1^*+\xi_2}}{(k_1^*+l_2)},\ A_{21} = \frac{e^{\eta_2^*+\eta_1}}{(k_2^*+k_1)},\ A_{22} = \frac{e^{\eta_2^*+\xi_2}}{(k_2^*+l_2)},\\
A_{nn'} &: A_{11} = \frac{e^{\eta_1+\eta_1^*}}{(k_1+k_1^*)},\ A_{12} = \frac{e^{\xi_1+\xi_2^*}}{(l_1+l_2^*)},\ A_{21} = \frac{e^{\xi_2+\eta_1^*}}{(l_2+k_1^*)},\ A_{22} = \frac{e^{\xi_2+\xi_2^*}}{(l_2+l_2^*)},\\
\kappa_{mn} &: \kappa_{11} = \frac{\psi_1^\dagger\sigma\psi_1'}{2i(k_1^2-k_1^{*2})},\ \kappa_{12} = \frac{\psi_1^\dagger\sigma\psi_2'}{2i(k_1^2-k_2^{*2})},\ \kappa_{21} = \frac{\psi_2^\dagger\sigma\psi_1'}{2i(l_2^2-k_1^{*2})},\ \kappa_{22} = \frac{\psi_2^\dagger\sigma\psi_2'}{2i(l_2^2-k_2^{*2})},\\
\kappa_{nm} &: \kappa_{11} = \frac{\psi_1^{'\dagger}\sigma\psi_1}{2i(k_1^2-k_1^{*2})},\ \kappa_{12} = \frac{\psi_1^{'\dagger}\sigma\psi_2}{2i(k_1^2-l_2^{*2})},\ \kappa_{21} = \frac{\psi_2^{'\dagger}\sigma\psi_1}{2i(k_2^2-k_1^{*2})},\ \kappa_{22} = \frac{\psi_2^{'\dagger}\sigma\psi_2}{2i(k_2^2-l_2^{*2})},\\
\kappa_{nn'} &: \kappa_{11} = \frac{\psi_1^{'\dagger}\sigma\psi_1'}{2i(k_1^2-k_1^{*2})},\ \kappa_{12} = \frac{\psi_1^{'\dagger}\sigma\psi_2'}{2i(k_1^2-l_2^{*2})},\ \kappa_{21} = \frac{\psi_2^{'\dagger}\sigma\psi_1'}{2i(l_2^2-k_1^{*2})},\ \kappa_{22} = \frac{\psi_2^{'\dagger}\sigma\psi_2'}{2i(l_2^2-l_2^{*2})},
\end{aligned}
\tag{13}
$$

and $\phi_2 = \begin{pmatrix} e^{\eta_1} & e^{\xi_2} \end{pmatrix}^T$. The above new class of solution permits both degenerate and nondegenerate solitons, simultanously leading to the formation of coexistence phenomenon in the present LSRI system (1). It is interesting to note that the coexistence phenomenon has also been discussed in the context of rogue waves [52]. The above partially nondegenerate soliton solution is described by seven arbitrary complex parameters, $\alpha_1^{(l)}$, $\alpha_2^{(l)}$, k_j, $l, j = 1, 2$ and l_2. Further, in order to get the regular (nonsingular) solution one has to fix the condition $k_{jI} < 0$, $j = 1, 2$ and $l_{2I} < 0$.

3. Various types of collision dynamics of nondegenerate solitons

In this section, we analyze several interesting collision properties of the nondegenerate solitons of the system (1). To study the collision dynamics, it is essential to analyse the form of each of the solitons in the two soliton solution in the long time limits $t \to \pm\infty$. It can be done by performing appropriate asymptotic analysis of the completely nondegenerate two-soliton solution (12*a*) and (12*b*). From the analysis, we find that the nondegenerate solitons exhibit three types of collisions, namely shape preserving, shape altering and a novel shape changing collision dynamics for the cases of (i) equal velocities: $k_{jI} = l_{jI}$, $j = 1, 2$ and (ii) unequal velocities: $k_{jI} \neq l_{jI}$, $j = 1, 2$.

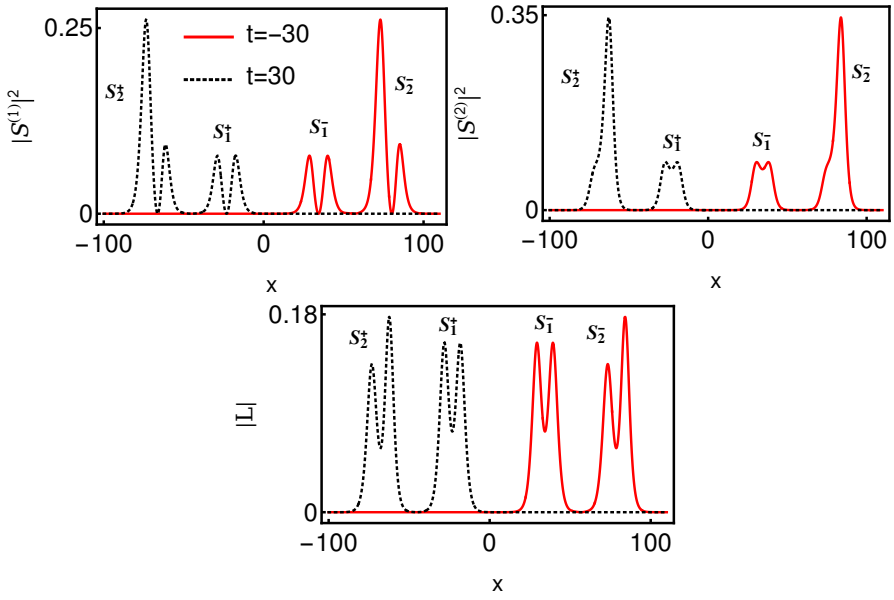

Figure 5. Elastic collision: Shape preserving collision with zero phase shift between the symmetric and asymmetric double-hump solitons. The parameter values are given in the main text.

Very interestingly, we find that the shape altering and shape changing collision scenarios belong to elastic collision which is confirmed through the following asymptotic analysis. Additionally, we observe a shape changing collision for the partially equal velocities ($k_{1I} = l_{1I}$, $k_{2I} \neq l_{2I}$) case also. In this section, we describe the asymptotic analysis for equal velocities case only and it can be extended to unequal velocities cases as well in a similar manner. We note that the singularity condition, $k_{jI} < 0$ and $l_{jI} < 0$, enforces the two nondegenerate solitons to propagate in the same direction. Thus, the nondegenerate solitons in the system (1) always undergo overtaking collision. From this, it can be understood that the positive type of nonlinearity of the system (1) does not permit any head-on collision among the nondegenerate solitons.

3.1. Asymptotic analysis

We carry out an asymptotic analysis of the two-soliton solution (12*a*) and (12*b*) by considering the parametric choices, $k_{jI} = l_{jI} < 0$, $k_{jR}, l_{jR} > 0$, $j = 1, 2$, $k_{1I} > k_{2I}$ and $l_{1I} > l_{2I}$, which corresponds to the overtaking collision of two symmetric double-hump solitons. For other choice of parameters, similar analysis can be carried out without much difficulty. In order to deduce the asymptotic forms of nondegenerate solitons in the long time regimes, we incorporate the asymptotic behaviour of the wave variables $\eta_{jR} = k_{jR}(x - 2k_{jI}t)$ and $\xi_{jR} = l_{jR}(x - 2l_{jI}t)$, $j = 1, 2$, in the solution (12*a*) and (12*b*). For the above parametric choices corresponding to overtaking collision, the wave variables behave asymptotically as (i) Soliton 1 (S_1): η_{1R}, $\xi_{1R} \simeq 0$, η_{2R}, $\xi_{2R} \to \pm\infty$ as $t \pm \infty$ and (ii) Soliton 2 (S_2): η_{2R}, $\xi_{2R} \simeq 0$, η_{1R}, $\xi_{1R} \to \pm\infty$ as $t \mp \infty$. Substituting these results in Eqs. (12*a*) and (12*b*), we derive the following asymptotic forms of nondegenerate

individual solitons.

(a) Before collision: $t \to -\infty$

Soliton 1: For soliton 1, we obtain the asymptotic forms of $S^{(l)}$, $l = 1, 2$ and L from the two-soliton solution (12*a*) and 12*b*) as

$$S^{(1)} \simeq \frac{4A_1^{1-}k_{1R}\sqrt{k_{1I}}e^{i\eta_{1I}}\cosh(\xi_{1R}+\phi_1^-)}{[a_{11}\cosh(\eta_{1R}+\xi_{1R}+\phi_1^-+\phi_2^-+c_1)+\frac{1}{a_{11}^*}\cosh(\eta_{1R}-\xi_{1R}+\phi_2^--\phi_1^-+c_2)]},$$

$$S^{(2)} \simeq \frac{4A_2^{1-}l_{1R}\sqrt{l_{1I}}e^{i\xi_{1I}}\cosh(\eta_{1R}+\phi_2^-)}{[a_{12}\cosh(\eta_{1R}+\xi_{1R}+\phi_1^-+\phi_2^-+c_1)+\frac{1}{a_{12}^*}\cosh(\eta_{1R}-\xi_{1R}+\phi_2^--\phi_1^-+c_2)]},$$

$$L(x,t) \simeq \frac{4}{f^2}\Big((k_{1R}^2-l_{1R}^2)+l_{1R}^2\cosh(2\eta_{1R}+2\phi_2^-+c_3)+k_{1R}^2\cosh(2\xi_{1R}+2\phi_1^-+c_4)\Big),$$

$$f = b_1\cosh(\eta_{1R}+\xi_{1R}+\phi_1^-+\phi_2^-+c_1)+b_1^{-1}\cosh(\eta_{1R}-\xi_{1R}+\phi_2^--\phi_1^-+c_2). \quad (14)$$

Here, $A_1^{1-} = i[\alpha_1^{(1)}/\alpha_1^{(1)^*}]^{1/2}$ and $A_2^{1-} = i[\alpha_1^{(2)}/\alpha_1^{(2)^*}]^{1/2}$. In the latter, superscript $(1-)$ represents soliton S_1 before collision and subscripts $(1,2)$ denote the two short-wave components $S^{(1)}$ and $S^{(2)}$, respectively.

Soliton 2: In this limit, the asymptotic expressions for soliton 2 in the two SW components and the long-wave component turn out to be

$$S^{(1)} \simeq \frac{4k_{2R}A_1^{2-}\sqrt{k_{2I}}e^{i(\eta_{2I}+\theta_1^-)}\cosh(\xi_{2R}+\varphi_1^-)}{[a_{21}\cosh(\eta_{2R}+\xi_{2R}+\varphi_1^-+\varphi_2^-+d_1)+\frac{1}{a_{21}^*}\cosh(\eta_{2R}-\xi_{2R}+\varphi_2^--\varphi_1^-+d_2)]},$$

$$S^{(2)} \simeq \frac{4l_{2R}A_2^{2-}\sqrt{l_{2I}}e^{i(\xi_{2I}+\theta_2^-)}\cosh(\eta_{2R}+\varphi_2^-)}{[a_{22}\cosh(\eta_{2R}+\xi_{2R}+\varphi_1^-+\varphi_2^-+d_1)+\frac{1}{a_{22}^*}\cosh(\eta_{2R}-\xi_{2R}+\varphi_2^--\varphi_1^-+d_2)]},$$

$$L(x,t) \simeq \frac{4}{f^2}\Big((k_{2R}^2-l_{2R}^2)+l_{1R}^2\cosh(2\eta_{2R}+2\varphi_1^-+d_3)+k_{2R}^2\cosh(2\xi_{2R}+2\varphi_2^-+d_4)\Big),$$

$$f = b_2\cosh(\eta_{2R}+\xi_{2R}+\varphi_1^-+\varphi_2^-+d_1)+b_2^{-1}\cosh(\eta_{2R}-\xi_{2R}+\varphi_2^--\varphi_1^-+d_2). \quad (15)$$

In the above, $a_{21} = \frac{(k_2^*-l_2^*)^{\frac{1}{2}}}{(k_2^*+l_2)^{\frac{1}{2}}}$, $\frac{1}{a_{21}^*} = \frac{(k_2+l_2^*)^{\frac{1}{2}}}{(k_2-l_2)^{\frac{1}{2}}}$, $a_{22} = \frac{(k_2^*-l_2^*)^{\frac{1}{2}}}{(k_2+l_2^*)^{\frac{1}{2}}}$, $\frac{1}{a_{22}^*} = \frac{(k_2^*+l_2)^{\frac{1}{2}}}{(k_2-l_2)^{\frac{1}{2}}}$, $e^{i\theta_1^-} = \frac{(k_1-k_2)(k_1+k_2)^{\frac{1}{2}}(k_1+k_2^*)(k_2-l_1)^{\frac{1}{2}}(k_1-k_2^*)(k_2^*+l_1)^{\frac{1}{2}}}{(k_1^*-k_2^*)(k_1^*+k_2)(k_1^*+k_2^*)^{\frac{1}{2}}(k_2^*-l_1^*)^{\frac{1}{2}}(k_1^*-k_2)^{\frac{1}{2}}(k_2+l_1^*)^{\frac{1}{2}}}$, $e^{i\theta_2^-} = \frac{(l_1-l_2)(k_1-l_2)^{\frac{1}{2}}(k_1+l_2^*)^{\frac{1}{2}}(l_1+l_2^*)(l_1+l_2)^{\frac{1}{2}}(l_1-l_2^*)^{\frac{1}{2}}}{(k_1^*-l_2^*)^{\frac{1}{2}}(l_1^*-l_2^*)(k_1^*+l_2)^{\frac{1}{2}}(l_1^*+l_2)(l_1^*+l_2^*)^{\frac{1}{2}}(l_1^*-l_2)^{\frac{1}{2}}}$, $A_1^{2-} = [\alpha_2^{(1)}/\alpha_2^{(1)^*}]^{1/2}$, $A_2^{2-} = [\alpha_2^{(2)}/\alpha_2^{(2)^*}]^{1/2}$, $b_2 = \frac{(k_{2R}-l_{2R})^{\frac{1}{2}}}{(k_{2R}+l_{2R})^{\frac{1}{2}}}$, $d_1 = \frac{1}{2}\log\frac{(k_2^*-l_2^*)}{(k_2-l_2)}$, $d_2 = \frac{1}{2}\log\frac{(k_2^*+l_2)}{(k_2+l_2^*)}$, $d_3 = \frac{1}{2}\log\frac{(k_2^*-l_2^*)(k_2+l_2^*)}{(k_2^*+l_2)(k_2-l_2)}$ and $d_4 = \frac{1}{2}\log\frac{(k_2^*-l_2^*)(k_2^*+l_2)}{(k_2+l_2^*)(k_2-l_2)}$. Here, superscript $(2-)$ refers to soliton 2 (S_2) before collision.

(b) After collision: $t \to +\infty$

Soliton 1: We have deduced the following asymptotic forms of for soliton 1 in $S^{(l)}$, $l = 1, 2$ and L from the two soliton solution (12*a*) and 12*b*) after collision as below:

$$S^{(1)} \simeq \frac{4A_1^{1+}k_{1R}\sqrt{k_{1I}}e^{i(\eta_{1I}+\theta_1^+)}\cosh(\xi_{1R}+\phi_1^+)}{[a_{11}\cosh(\eta_{1R}+\xi_{1R}+\phi_1^++\phi_2^++c_1)+\frac{1}{a_{11}^*}\cosh(\eta_{1R}-\xi_{1R}+\phi_2^+-\phi_1^++c_2)]},$$

$$S^{(2)} \simeq \frac{4A_2^{1+}l_{1R}\sqrt{l_{1I}}e^{i(\xi_{1I}+\theta_2^+)}\cosh(\eta_{1R}+\phi_2^+)}{[a_{12}\cosh(\eta_{1R}+\xi_{1R}+\phi_1^++\phi_2^++c_1)+\frac{1}{a_{12}^*}\cosh(\eta_{1R}-\xi_{1R}+\phi_2^+-\phi_1^++c_2)]},$$

$$L(x,t) \simeq \frac{4}{f^2}\Big((k_{1R}^2-l_{1R}^2)+l_{1R}^2\cosh(2\eta_{1R}+2\phi_2^++c_3)+k_{1R}^2\cosh(2\xi_{1R}+2\phi_1^++c_4)\Big),$$

$$f = b_1 \cosh(\eta_{1R} + \xi_{1R} + \phi_1^+ + \phi_2^+ + c_1) + b_1^{-1} \cosh(\eta_{1R} - \xi_{1R} + \phi_2^+ - \phi_1^+ + c_2). \tag{16}$$

Here, $e^{i\theta_1^+} = \frac{(k_1-k_2)(k_1-l_2)^{\frac{1}{2}}(k_1^*+k_2)(k_1^*+l_2)^{\frac{1}{2}}(k_1+k_2)^{\frac{1}{2}}(k_1^*-k_2)^{\frac{1}{2}}}{(k_1^*-k_2^*)(k_1^*-l_2^*)^{\frac{1}{2}}(k_1+k_2^*)(k_1+l_2^*)^{\frac{1}{2}}(k_1^*+k_2^*)^{\frac{1}{2}}(k_1-k_2^*)^{\frac{1}{2}}}$, $A_1^{1+} = i[\alpha_1^{(1)}/\alpha_1^{(1)^*}]^{1/2}$, $A_2^{1+} = i[\alpha_1^{(2)}/\alpha_1^{(2)^*}]^{1/2}$ and $e^{i\theta_2^+} = \frac{(l_1-l_2)(k_2-l_1)^{\frac{1}{2}}(k_2+l_1^*)^{\frac{1}{2}}(l_1^*+l_2)(l_1+l_2)^{\frac{1}{2}}(l_1^*-l_2)^{\frac{1}{2}}}{(k_2^*-l_1^*)^{\frac{1}{2}}(l_1^*-l_2^*)(k_2^*+l_1)^{\frac{1}{2}}(l_1+l_2^*)(l_1^*+l_2^*)^{\frac{1}{2}}(l_1-l_2^*)^{\frac{1}{2}}}$. In the latter, superscript (1+) represents soliton S_1 after collision and subscripts $(1,2)$ denote the two SW components $S^{(1)}$ and $S^{(2)}$, respectively.

Soliton 2: The asymptotic expressions for soliton 2 in $S^{(l)}$, $l = 1, 2$ and L after collision turn out to be

$$S^{(1)} \simeq \frac{4k_{2R}A_1^{2+}\sqrt{k_{2I}}e^{i\eta_{2I}}\cosh(\xi_{2R}+\varphi_1^+)}{[a_{21}\cosh(\eta_{2R}+\xi_{2R}+\varphi_1^+ + \varphi_2^+ + d_1) + \frac{1}{a_{21}^*}\cosh(\eta_{2R}-\xi_{2R}+\varphi_2^+ - \varphi_1^+ + d_2)]},$$

$$S^{(2)} \simeq \frac{4l_{2R}A_2^{2+}\sqrt{l_{2I}}e^{i\xi_{2I}}\cosh(\eta_{2R}+\varphi_2^+)}{[a_{22}\cosh(\eta_{2R}+\xi_{2R}+\varphi_1^+ + \varphi_2^+ + d_1) + \frac{1}{a_{22}^*}\cosh(\eta_{2R}-\xi_{2R}+\varphi_2^+ - \varphi_1^+ + d_2)]},$$

$$L(x,t) \simeq \frac{4}{f^2}\Big((k_{2R}^2 - l_{2R}^2) + l_{1R}^2\cosh(2\eta_{2R} + 2\varphi_1^+ + d_3) + k_{2R}^2\cosh(2\xi_{2R} + 2\varphi_2^+ + d_4)\Big),$$

$$f = b_2\cosh(\eta_{2R}+\xi_{2R}+\varphi_1^+ + \varphi_2^+ + d_1) + b_2^{-1}\cosh(\eta_{2R}-\xi_{2R}+\varphi_2^+ - \varphi_1^+ + d_2). \tag{17}$$

Here, $A_1^{2+} = i[\alpha_2^{(1)}/\alpha_2^{(1)^*}]^{1/2}$, $A_2^{2+} = i[\alpha_2^{(2)}/\alpha_2^{(2)^*}]^{1/2}$. The phase constants, ϕ_j^-, ϕ_j^+, φ_j^-, φ_j^+, $j = 1, 2$, appearing above are related as follows:

$$\phi_1^+ = \phi_1^- + \psi_1,\ \phi_2^+ = \phi_2^- + \psi_2,\ \varphi_1^+ = \varphi_1^- - \Psi_1,\ \varphi_2^+ = \varphi_2^- - \Psi_2, \tag{18a}$$

where

$$\psi_1 = \ln\frac{|k_2-l_1||l_1-l_2|^2|l_1+l_2|}{|k_2+l_1^*||l_1+l_2^*|^2|l_1-l_2^*|},\ \psi_2 = \ln\frac{|k_1-k_2|^2|k_1+k_2||k_1-l_2|}{|k_1+k_2^*|^2|k_1-k_2^*||k_1+l_2^*|},$$

$$\Psi_1 = \ln\frac{|k_1-l_2||l_1-l_2|^2|l_1+l_2|}{|k_1+l_2^*||l_1+l_2^*|^2|l_1-l_2^*|},\ \Psi_2 = \ln\frac{|k_2-l_1||k_1-k_2|^2|k_1+k_2|}{|k_2+l_1^*||k_1+k_2^*|^2|k_1-k_2^*|}, \tag{18b}$$

$$\phi_1^- = \frac{1}{2}\ln\frac{(k_1-l_1)|\alpha_1^{(2)}|^2}{2i(k_1+l_1^*)(l_1+l_1^*)^2(l_1-l_1^*)},\ \phi_2^- = \frac{1}{2}\ln\frac{(l_1-k_1)|\alpha_1^{(1)}|^2}{2i(k_1^*+l_1)(k_1+k_1^*)^2(k_1-k_1^*)},$$

$$\varphi_1^+ = \frac{1}{2}\ln\frac{(k_2-l_2)|\alpha_2^{(2)}|^2}{2i(k_2+l_2^*)(l_2+l_2^*)^2(l_2-l_2^*)},\ \varphi_2^+ = \frac{1}{2}\ln\frac{(k_2-l_2)|\alpha_2^{(1)}|^2}{2i(k_2^*+l_2)(k_2+k_2^*)^2(k_2-k_2^*)}.$$

From the above, one can easily observe that the phase terms only get changed during the collision process. As we have pointed above, the phases of each of the solitons also get changed during the collision dynamics. The total phase shift of soliton S_1 in both the SW components is calculated as

$$\begin{aligned}\Delta\Phi_1 &= \phi_1^+ + \phi_2^+ - (\phi_1^- + \phi_2^-)\\ &= \log\frac{|k_2-l_1||l_1-l_2|^2|l_1+l_2||k_1-l_2||k_1-k_2|^2|k_1+k_2|}{|k_2+l_1^*||l_1+l_2^*|^2|l_1-l_2^*||k_1+l_2^*||k_1+k_2^*|^2|k_1-k_2^*|}.\end{aligned} \tag{19a}$$

Similarly the total phase shift experienced by soliton S_2 in the SW components are given by

$$\begin{aligned}\Delta\Phi_2 &= \varphi_1^+ + \varphi_2^+ - (\varphi_1^- + \varphi_2^-)\\ &= -\log\frac{|k_2-l_1||l_1-l_2|^2|l_1+l_2||k_1-l_2||k_1-k_2|^2|k_1+k_2|}{|k_2+l_1^*||l_1+l_2^*|^2|l_1-l_2^*||k_1+l_2^*||k_1+k_2^*|^2|k_1-k_2^*|} = -\Delta\Phi_1.\end{aligned} \tag{19b}$$

Here, the subscript 1 and 2 in $\Delta\Phi$ denote the soliton number. The total phase shifts obtained for the SW components are the same for the LW component.

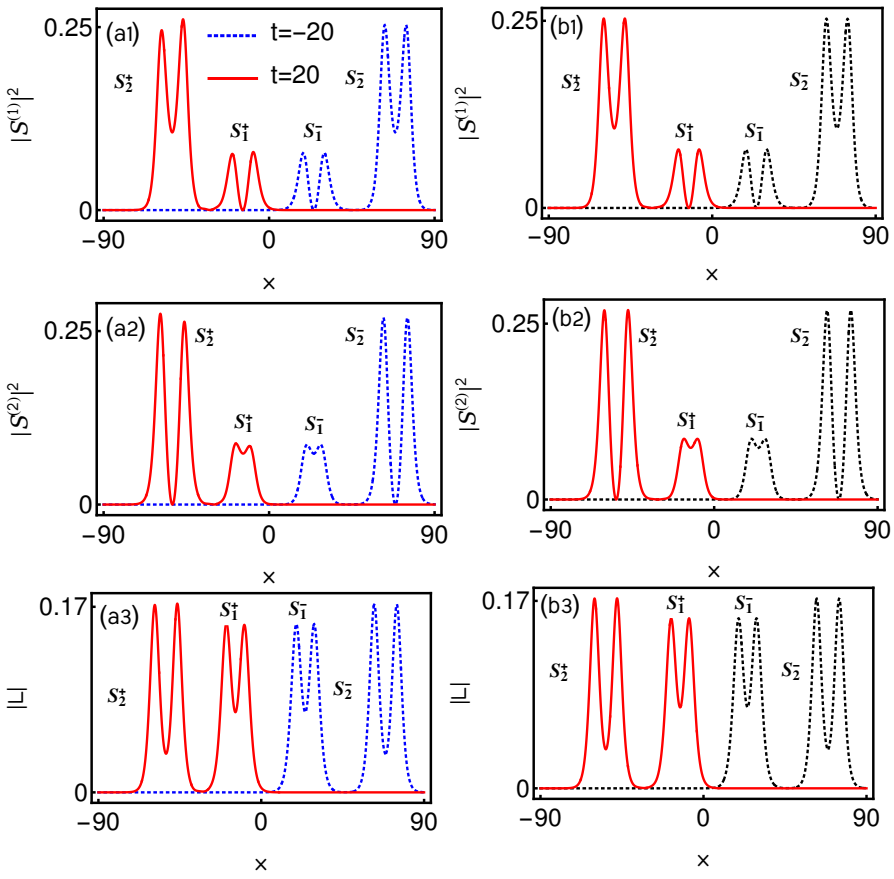

Figure 6. The column figures (a1)-(a3) represent the shape altering collision of two symmetric double-hump solitons S_1^- and S_2^- at $t = -10$ (blue dotted curves) into S_1^+ and S_2^+ at $t = +10$ (red curves) and the column figures (b1)-(b3) denote their corresponding shape preserving nature which is brought out after taking appropriate time shifts. The dotted black curves in (b1)-(b3) refer to the solitons before collision at $t = -20$, and the solitons after incorporating the appropriate finite time shifts are represented by the solid red curves. To bring back the shape preserving nature of solitons after collision we have taken the following time shifts based on Eq. (22): For solitons S_1 and S_2 the time shifts are performed respectively as (short wave $S^{(1)}$: $t' = 18.6525$, short wave $S^{(2)}$: $t' = 18.5791$) and ($S^{(1)}$: $t' = 20.4559$, $S^{(2)}$: $t' = 20.4266$). As far as the LW component is concerned one has to combinedly take the shifts for soliton S_1^+ ($t' = 18.6525$, $t' = 18.5791$) and soliton S_2^+ ($t' = 20.4559$, $t' = 20.4266$) in the LW component expressions (16) and (17), respectively.

3.2. Elastic collision: Shape-preserving, shape-altering and shape-changing collisions

The asymptotic analysis of equal velocities case ($k_{1I} = l_{1I}$ and $k_{2I} = l_{2I}$) reveals that the transition intensities, $|T_j^l|^2 = \frac{|A_j^{l+}|^2}{|A_j^{l-}|^2} = 1$, $l, j = 1, 2$, (where $A_j^{l\pm}$'s are defined in the above asymptotic analysis) always remain unimodular. Consequently, the corresponding

collision among the nondegenerate solitons is always elastic in the equal velocities case. Thus, the expressions of the individual solitons should be invariant in the asymptotic time limits $t \to \pm\infty$ leading to the preservation of shapes of the nondegenerate solitons. As a result, the asymptotic expression (14) of soliton 1 before collision should coincide with the form (16). Further, to hold the elastic collision nature, the asymptotic form (15) of soliton 2 must also agree with Eq. (17). However, in view of Eq. (18*a*), this is not true. Since the phase terms dramatically get varied during this collision scenario. This phase variation significantly influences the structure of the nondegenerate solitons. Therefore, to maintain the structure, the phase terms should obey the following condition:

$$\phi_j^+ = \phi_j^-,\ \varphi_j^+ = \varphi_j^-,\ j = 1, 2. \tag{20}$$

The above implies that the additional phase terms, ψ_j and Ψ_j, $j = 1, 2$, are equal to zero. That is

$$\psi_1 = \ln \frac{|k_2 - l_1||l_1 - l_2|^2|l_1 + l_2|}{|k_2 + l_1^*||l_1 + l_2^*|^2|l_1 - l_2^*|} = 0,\ \psi_2 = \ln \frac{|k_1 - k_2|^2|k_1 + k_2||k_1 - l_2|}{|k_1 + k_2^*|^2|k_1 - k_2^*||k_1 + l_2^*|} = 0, \tag{21a}$$

$$\Psi_1 = \ln \frac{|k_1 - l_2||l_1 - l_2|^2|l_1 + l_2|}{|k_1 + l_2^*||l_1 + l_2^*|^2|l_1 - l_2^*|} = 0, \Psi_2 = \ln \frac{|k_2 - l_1||k_1 - k_2|^2|k_1 + k_2|}{|k_2 + l_1^*||k_1 + k_2^*|^2|k_1 - k_2^*|} = 0. \tag{21b}$$

Physically this indicates that the nondegenerate fundamental solitons undergo shape preserving collision (or elastic collision) without a phase shift. Such a zero phase shift criterion is calculated from the above expressions (21*a*) and (21*b*) as

$$\frac{|k_2 + l_1^*|}{|k_2 - l_1|} - \frac{|k_1 + l_2^*|}{|k_1 - l_2|} = 0. \tag{22}$$

From the above, we infer that the two nondegenerate solitons pass through one another with zero phase shift whenever the criterion (22) (or equivalently from the phase condition Eq. (20)), is fulfilled by the wave numbers. This remarkable new property is not possible in the degenerate counterpart and even in the scalar nonlinear Schrödinger equation. A typical shape preserving collision with zero phase shift is demonstrated in figure 4. From figure 4, one can easily recognize that that the two symmetric double-hump solitons S_1 and S_2 are located along the lines $\eta_{1R} = k_{1R}(x - 2k_{1I}t) \simeq 0$, $\xi_{1R} = k_{1R}(x - 2k_{1I}t) \simeq 0$ and $\eta_{2R} = k_{2R}(x - 2k_{2I}t) \simeq 0$, $\xi_{2R} = k_{2R}(x - 2k_{2I}t) \simeq 0$, respectively. Around $x = 0$ they start to interact and pass through one another with almost zero phase shift. We have numerically verified this from Eq. (22) by calculating the value as -0.0006. It ensures that the structures (as well as phases) of the nondegenerate solitons remain constant throughout this collision process. A similar shape preserving collision scenario among the two asymmetric double-hump solitons is illustrated in figure 5 for the parameter values $k_1 = 0.25 - 0.5i$, $l_1 = 0.315 - 0.5i$, $k_2 = 0.25 - 1.2i$, $l_2 = 0.315 - 1.2i$, $\alpha_1^{(1)} = 0.5 + 0.5i$, $\alpha_1^{(2)} = 0.45 + 0.5i$, $\alpha_2^{(1)} = 1 + i$ and $\alpha_2^{(2)} = 0.45 + 0.5i$.

In general, the phase constants ϕ_j^+, ϕ_j^-, φ_j^+ and φ_j^-, $j = 1, 2$, do not agree with the condition (20) in the equal velocities case. Under this circumstance, the nondegenerate solitons undergo either shape altering collision or shape changing collision without infringing the unimodular transition intensities condition. Therefore, depending on the

nature of the changes in the phase terms, the nondegenerate solitons experience slight alteration or drastic reshaping during the collision process. A typical shape altering collision is depicted in figures 6(a1)-(a3). To draw the figures 6(a1)-(a3), we fix the soliton parameters as $k_1 = 0.25-0.5i$, $l_1 = 0.315-0.5i$, $k_2 = 0.31-1.5i$, $l_2 = 0.28-1.5i$, $\alpha_1^{(1)} = 0.5+0.5i$, $\alpha_1^{(2)} = 0.45+0.5i$, $\alpha_2^{(1)} = 0.45+0.5i$ and $\alpha_2^{(2)} = 0.55+0.55i$. Then these figures show that the symmetric nature of double-hump solitons in all the three components get altered slightly into asymmetric forms after collision. However, this shape alteration can be undone, without loss of generality, by making appropriate shifts in time,

$$\left(t' = t - \frac{\psi_1}{2l_{1R}k_{1I}}, t' = t - \frac{\psi_2}{2k_{1R}k_{1I}}\right) \text{ and} \left(t' = t + \frac{\Psi_1}{2l_{2R}k_{2I}}, t' = t + \frac{\Psi_2}{2k_{2R}k_{2I}}\right) \tag{23}$$

in the wave variables ξ_{1R} and η_{1R} for soliton 1 and ξ_{2R} and η_{2R} for soliton 2 in the expressions (16) and (17), respectively. After effecting these time shifts in the respective asymptotic expressions, we find that the asymptotic expressions of the two nondegenerate solitons becomes identical except for unit phase factors. As a consequence, the shapes of the nondegenerate solitons are conserved asymptotically with zero phase shift thereby confirming the elastic nature of the collision. This shape preserving nature is graphically illustrated in figure 6(b1)-(b3). Moreover, for $k_{1I} = l_{1I}$ and $k_{2I} = l_{2I}$, the nondegenerate solitons also exhibit a novel shape changing interaction again without violating the unity condition of the transition intensities. Very interestingly, as it is evident from Eq. (18*a*), the shape changing occurs not only in the two short-wave components but it is also observed in the long-wave component as well. We display such non-trivial shape changing collision in figure 7(a1)-(a3) as an example, where the symmetric structure of the flattop soliton S_2 in the $S^{(1)}$ component and symmetric double-hump solitons in both the $S^{(2)}$ and L components are altered drastically as indicated by the red curves at $t = 25$. To display this figure 9(a1)-(a3), the parameter values are fixed as $k_1 = 0.315-0.5i$, $l_1 = 0.5-0.5i$, $k_2 = 0.45-1.2i$, $l_2 = 0.315-1.2i$, $\alpha_1^{(1)} = 0.5+0.5i$, $\alpha_1^{(2)} = 0.45+0.45i$, $\alpha_2^{(1)} = 0.45+0.4i$ and $\alpha_2^{(2)} = 0.65+0.65i$. This type of shape changing collision has not been observed earlier in the degenerate case [20]. However, as we have performed the analysis in the above case of shape altering collision, the present shape changing collision also belongs to the case of elastic collision. Thus the shape preserving nature can be retrieved by shifting the time as per Eq. (23). This elastic collision scenario after taking the time shifts is demonstrated in figure 7(b1)-(b3). Therefore, what we emphasize here is that the collision scenario among the nondegenerate solitons is always elastic regardless of the zero phase shift criterion (22). Further, we also demonstrate the shape changing collision in the partial velocity case $k_{1I} = l_{1I}$ and $k_{2I} \neq l_{2I}$ in figure 8 for the parameter values as given in the figure caption.

In addition to the above, the elastic collision does occur in the case of $(2,2,4)$-soliton solution (unequal velocities: $k_{1I} \neq l_{1I}$ and $k_{2I} \neq l_{2I}$) for the general choice of wave parameters. We illustrate such a collision process in figure 9 for the parameters given in the figure caption. From figure 9, it is clear that each interaction picture of the

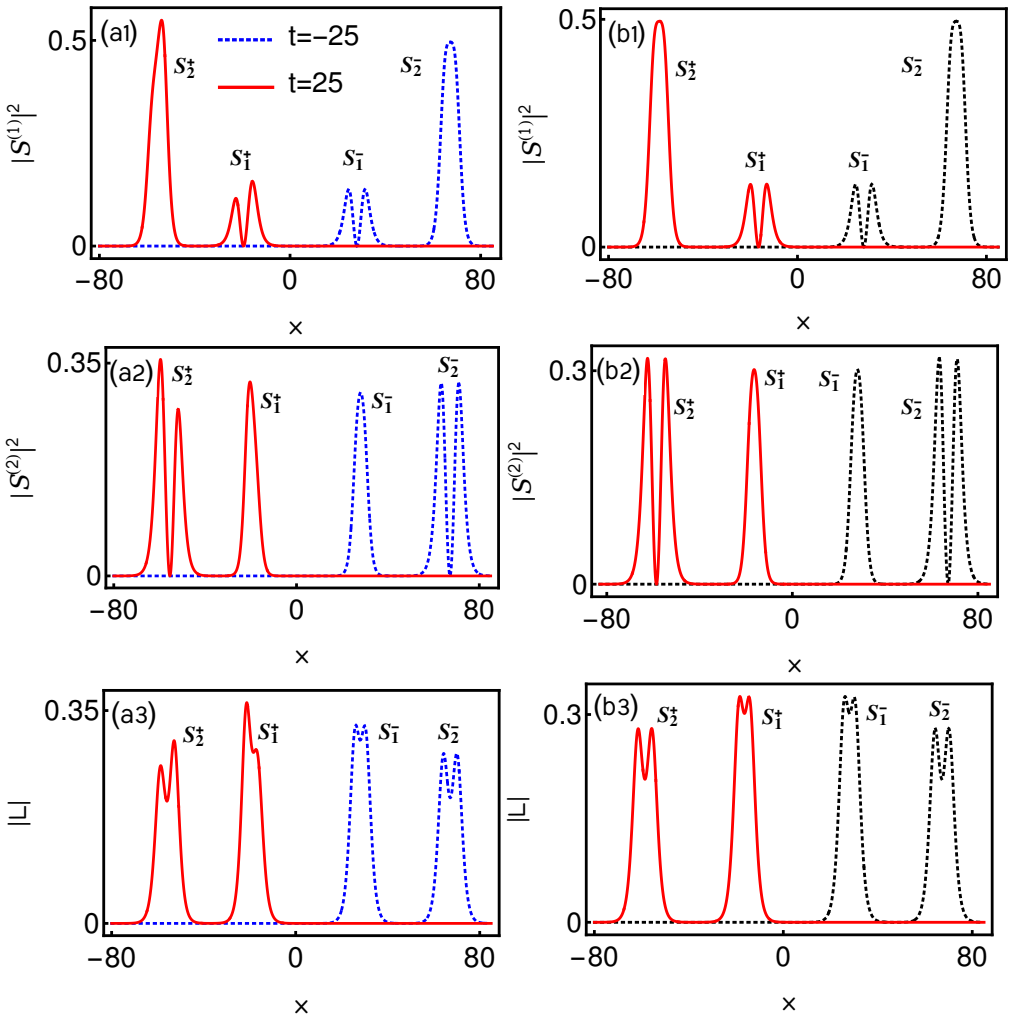

Figure 7. The column figures corresponding to (a1)-(a3) demonstrate shape changing collisions among the nondegenerate solitons whereas the figures (b1)-(b3) illustrate their corresponding shape preserving nature which is brought out after effecting the time shifts ($S^{(1)}$: $t' = 22.5772$, $S^{(2)}$: $t' = 21.962$) and ($S^{(1)}$: $t' = 26.3074$, $S^{(2)}$: $t' = 26.0926$) in the expressions (16) and (17) of both the solitons S_1 and S_2, respectively. For solitons in the LW component, one has to take the time shifts ($t' = 22.5772$, $t' = 21.962$) and ($t' = 26.3074$, $t' = 26.0926$) combinedly in Eqs. (16) and (17), respectively. In figures (b1)-(b3) black dotted curves denote the solitons before collision at $t = -25$ and the red solid line curves represent the solitons after collision with time shifts t'.

two single-humped solitons in both the SW components $S^{(1)}$ and $S^{(2)}$ reappears through the LW component. The interesting fact of this collision scenario is the structures of all the solitons do not get altered throughout the collision process thereby confirming the elastic collision.

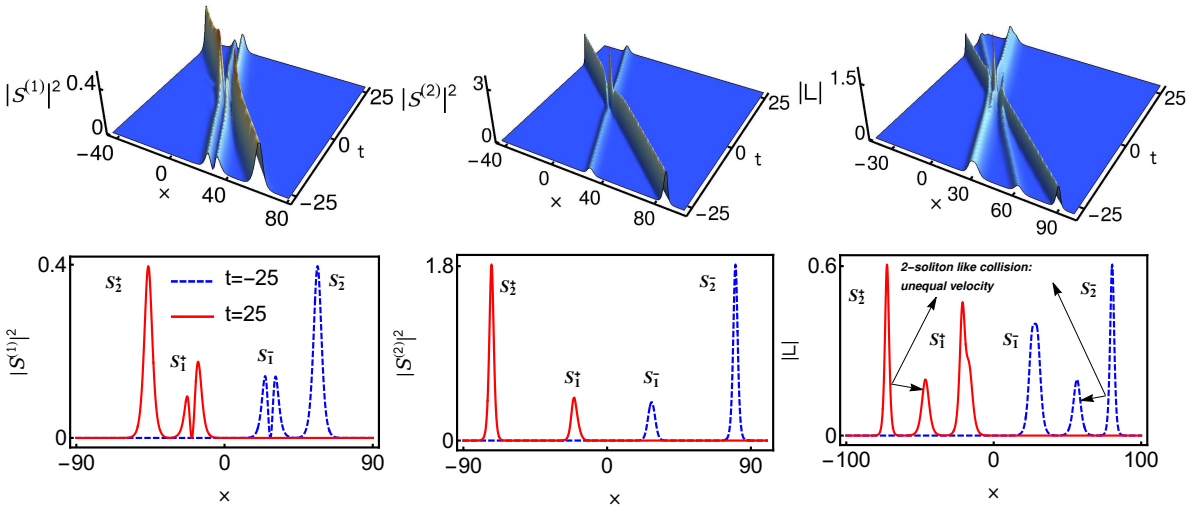

Figure 8. Shape changing collision of nondegenerate solitons in the partially equal velocity case ($k_{1I} = l_{1I}$ and $k_{2I} \neq l_{2I}$): The values are $k_1 = 0.315 - 0.5i$, $l_1 = 0.545 - 0.5i$, $k_2 = 0.315 - i$, $l_2 = 0.545 - 1.5i$, $\alpha_1^{(1)} = 0.5 + 0.5i$, $\alpha_1^{(2)} = 0.45 + 0.45i$, $\alpha_2^{(1)} = 0.5 + 0.5i$ and $\alpha_2^{(2)} = 0.45 + 0.45i$.

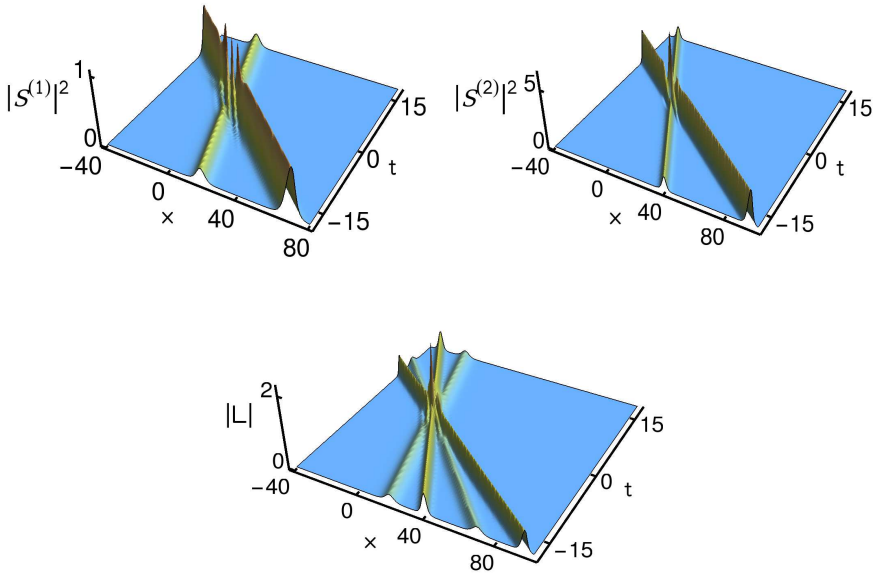

Figure 9. Elastic collision among the two nondegenerate soliton in the unequal velocities case, $k_{1I} \neq l_{1I}$ and $k_{2I} \neq l_{2I}$. The parameter values are $k_1 = 0.315 - 0.5i$, $l_1 = 0.545 - i$, $k_2 = 0.315 - 1.8i$, $l_2 = 0.545 - 2.5i$, $\alpha_1^{(1)} = 0.5 + 0.5i$, $\alpha_1^{(2)} = 0.45 + 0.45i$, $\alpha_2^{(1)} = 0.5 + 0.5i$ and $\alpha_2^{(2)} = 0.45 + 0.45i$.

4. Collision between nondegenerate and degenerate solitons: Two types of shape changing collisions

Here, we discuss the collision dynamics of nondegenerate two-soliton solution (12*a*) and (12*b*) under the partially nondegenerate limit $k_1 = l_1$ and $k_2 \neq l_2$. The resultant solution of the LSRI system (1) describes the coexistence of nondegenerate and degenerate solitons. It is of interest to study the dynamics of nondegenerate soliton in the presence of degenerate soliton and vice versa. In order to explore the underlying collision dynamics we perform an asymptotic analysis for the two-soliton solution (12*a*) and (12*b*) with the wave number restriction $k_1 = l_1$ and $k_2 \neq l_2$. By doing so, we find that the nondegenerate soliton undergoes two types of shape changing collisions. Here, we define such shape changing collisions. (i) Type-I shape changing collision is observed for the velocity condition $k_{2I} = l_{2I}$, where the initial profile structure of the nondegenerate soliton, in all the components, is either drastically changing into an asymmetric form or the initial profile structure is completely reshaped into another profile. (ii) Type-II shape changing collision is observed for the velocity choice $k_{2I} \neq l_{2I}$, where the two single-hump structured nondegenerate solitons are merged into a single-hump soliton in both the SW components while the shape of the nondegenerate soliton is preserved in the LW component. In both the collision scenarios, the degenerate soliton exhibits the usual energy exchange collision property as described in [20].

4.1. Asymptotic analysis

In order to explore the degenerate bright soliton collision induced shape changing behaviours of the nondegenerate soliton, we intend to analyze the partial nondegenerate two-soliton solution (12*a*) and (12*b*) with the elements of the Gram determinants given in Eq. (13) in the asymptotic limits $t \to \pm\infty$. In these limits, the resultant action provides the forms corresponding to degenerate and nondegenerate solitons. As we have pointed out in the earlier sub-section 3.1, to obtain the asymptotic forms for the present case one has to incorporate the asymptotic nature of the wave variables $\eta_{jR} = k_{jR}(t - 2k_{Ij}z)$ and $\xi_{2R} = l_{2R}(t - 2l_{2I}z)$, $j = 1, 2$, in the partially nondegenerate soliton solution. Here we note that the wave variable η_{1R} represents the degenerate soliton and η_{2R}, ξ_{2R} correspond to the nondegenerate soliton. To find the asymptotic behaviour of the above wave variables, we consider as a typical example the parametric choices, $k_{jR}, l_{2R} > 0$, $k_{jI}, l_{2I} < 0$, $j = 1, 2$, $k_{1I} > k_{2I}, l_{2I}$. For this choice, the wave variables behave asymptotically as follows: (i) degenerate bright soliton S_1: $\eta_{1R} \simeq 0$, η_{2R}, $\xi_{2R} \to \pm\infty$ as $t \to \pm\infty$ (ii) nondegenerate fundamental soliton S_2: $\eta_{2R}, \xi_{2R} \simeq 0$, $\eta_{1R} \to \pm\infty$ as $t \to \mp\infty$. By incorporating these asymptotic behaviours of the wave variables in the solution (12*a*)-(12*b*) with Eq. (13), we deduce the following asymptotic expressions for the nondegenerate and degenerate solitons.

(a) Before collision: $t \to -\infty$

Soliton 1: The asymptotic form of the degenerate soliton deduced from the partially

nondegenerate soliton solution is

$$S^{(l)} \simeq \begin{pmatrix} A_1^{1-} \\ A_1^{2-} \end{pmatrix} 2k_{1R}\sqrt{k_{1I}}e^{i(\eta_{1I}+\frac{\pi}{2})}\,\mathrm{sech}(\eta_{1R}+\psi^-),\ l=1,2, \tag{24a}$$

$$L \simeq 2k_{1R}^2\,\mathrm{sech}^2(\eta_{1R}+\psi^-). \tag{24b}$$

where $A_1^{l-}=\alpha_1^{(l)}/(|\alpha_1^{(1)}|^2+|\alpha_1^{(2)}|^2)^{1/2}$, $l=1,2$, $\psi^-=\frac{R}{2}=\frac{1}{2}\ln\frac{(|\alpha_1^{(1)}|^2+|\alpha_1^{(2)}|^2)}{2i(k_1+k_1^*)^2(k_1-k_1^*)}$. Here, in A_1^{l-} the subscript 1 denotes degenerate soliton S_1 and superscript $l-$ refers to the SW components before collision.

Soliton 2: The asymptotic forms of the nondegenerate soliton S_2, which is present in both the short-wave components as well as in the long-wave component, before collision are obtained as

$$S^{(1)} \simeq \frac{1}{D_1}\Big(e^{i\eta_{2I}}e^{\frac{\mu_1+\mu_3}{2}}\cosh(\xi_{2R}+\frac{\mu_3-\mu_1}{2})+e^{i\xi_{2I}}e^{\frac{\mu_2+\mu_4}{2}}\cosh(\eta_{2R}+\frac{\mu_4-\mu_2}{2})\Big), \tag{25a}$$

$$S^{(2)} \simeq \frac{1}{D_1}\Big(e^{i\eta_{2I}}e^{\frac{\nu_1+\nu_3}{2}}\cosh(\xi_{2R}+\frac{\nu_3-\nu_1}{2})+e^{i\xi_{2I}}e^{\frac{\nu_2+\nu_4}{2}}\cosh(\eta_{2R}+\frac{\nu_4-\nu_2}{2})\Big), \tag{25b}$$

$$\begin{aligned} L \simeq \frac{1}{D_1^2}\Big(&e^{\frac{\mu_5+\mu_6+\mu_7+\mu_8}{2}}[(k_2+k_2^*)^2\cosh(\xi_2+\xi_2^*+\frac{(\mu_7+\mu_8)-(\mu_5+\mu_6)}{2})\\ &+(l_2+l_2^*)^2\cosh(\eta_2+\eta_2^*+\frac{(\mu_6+\mu_8)-(\mu_5+\mu_7)}{2})]+\frac{1}{2}e^{\mu_8'}\\ &+e^{\frac{\mu_5+\mu_8+\mu_9+\mu_{10}}{2}}[(k_2^*+l_2)^2\cosh(\eta_1+\xi_1^*+\frac{(\mu_8+\mu_{10})-(\mu_5+\mu_9)}{2})\\ &+(k_2+l_2^*)^2\cosh(\xi_2+\eta_2^*+\frac{(\mu_8+\mu_9)-(\mu_5+\mu_{10})}{2})]\\ &+e^{\frac{\mu_6+\mu_7+\mu_9+\mu_{10}}{2}}[(k_2-l_2)^2\cosh(\eta_2^*-\xi_2^*+\frac{(\mu_6+\mu_9)-(\mu_7+\mu_{10})}{2})\\ &+(k_2^*-l_2^*)^2\cosh(\eta_2-\xi_2+\frac{(\mu_6+\mu_{10})-(\mu_9+\mu_7)}{2})]\Big), \end{aligned} \tag{25c}$$

$$\begin{aligned} D_1 = {}& e^{\frac{\mu_5+\mu_8}{2}}\cosh(\eta_{2R}+\xi_{2R}+\frac{\mu_8-\mu_5}{2})+e^{\frac{\mu_9+\mu_{10}}{2}}\cosh(i(\eta_{2I}-\xi_{2I})+\frac{\mu_{10}-\mu_9}{2})\\ &+e^{\frac{\mu_6+\mu_7}{2}}\cosh(\eta_{2R}-\xi_{2R}+\frac{\mu_6-\mu_7}{2}). \end{aligned} \tag{25d}$$

Here, $A_2^{1-}=[\alpha_2^{(1)}/\alpha_2^{(1)^*}]^{1/2}$, $A_2^{2-}=[\alpha_2^{(2)}/\alpha_2^{(2)^*}]^{1/2}$. In the latter, the superscript $l-$, $l=1,2$, denotes the SW components $S^{(1)}$ and $S^{(2)}$ before collision and the subscript 2 refers the nondegenerate soliton S_2.

(b) After collision: $t\to+\infty$

Soliton 1: In this limit, the asymptotic forms for the degenerate soliton S_1 after collision are deduced as

$$S^{(l)} \simeq \begin{pmatrix} A_1^{1+} \\ A_2^{1+} \end{pmatrix} 2k_{1R}\sqrt{k_{1I}}e^{i(\eta_{1I}+\theta_l^++\frac{\pi}{2})}k_{1R}\,\mathrm{sech}(\eta_{1R}+\psi^+),\ l=1,2, \tag{26a}$$

$$L \simeq 2k_{1R}^2\,\mathrm{sech}^2(\eta_{1R}+\psi^+). \tag{26b}$$

where $A_1^{1+}=\alpha_1^{(1)}/(|\alpha_1^{(1)}|^2+\chi|\alpha_1^{(2)}|^2)^{1/2}$, $A_1^{2+}=\alpha_1^{(1)}/(|\alpha_1^{(1)}|^2\chi^{-1}+|\alpha_1^{(2)}|^2)^{1/2}$, $\chi=(|k_1-l_2|^2|k_1+k_2^*|^2|k_1+l_2|^2|k_1-k_2^*|^2)/(|k_1-k_2|^2|k_1+l_2^*|^2|k_1+k_2|^2|k_1-l_2^*|^2)$, $e^{i\theta_1^+}=$

$\frac{(k_1-k_2)(k_1^*+k_2)(k_1-l_2)^{\frac{1}{2}}(k_1^*+l_2)^{\frac{1}{2}}(k_1+k_2)^{\frac{1}{2}}(k_1^*+k_2)}{(k_1^*-k_2^*)(k_1+k_2^*)(k_1^*-l_2^*)^{\frac{1}{2}}(k_1+l_2^*)^{\frac{1}{2}}(k_1^*+k_2^*)^{\frac{1}{2}}(k_1+k_2^*)}$, $e^{i\theta_2^+} = \frac{(k_1-k_2)^{\frac{1}{2}}(k_1^*+k_2)^{\frac{1}{2}}(k_1-l_2)(k_1^*+l_2)(k_1+l_2)^{\frac{1}{2}}(k_1^*-l_2)^{\frac{1}{2}}}{(k_1^*-k_2^*)^{\frac{1}{2}}(k_1+k_2^*)^{\frac{1}{2}}(k_1^*-l_2^*)(k_1+l_2^*)(k_1^*+l_2^*)^{\frac{1}{2}}(k_1-l_2^*)^{\frac{1}{2}}}$ and $\psi^+ = \frac{1}{2}\ln\frac{|k_1-k_2|^2|k_1-l_2|^2\hat{\Lambda}_3}{2i(k_1-k_1^*)(k_1+k_1*)^2|k_1-k_2^*|^2|k_1-l_2^*|^2|k_1+l_2^*|^2}$. Here, $l+$ in A_1^{l+}, $l = 1, 2$, refers to SW components after collision and the subscript 1 denotes the degenerate soliton S_1.

Soliton 2: Similarly the asymptotic expression for the nondegenerate soliton S_2 after collision deduced from the soliton solution (12*a*) and (12*b*) with the elements given in Eq. (13) is

$$S^{(1)} \simeq \frac{4k_{2R}\sqrt{k_{2I}}A_1^{2+}e^{i(\eta_{2I}+\frac{\pi}{2})}\cosh(\xi_{2R}+\frac{\lambda_1}{2})}{[a_{21}\cosh(\eta_{2R}+\xi_{2R}+\frac{\lambda_2}{2})+\frac{1}{a_{21}^*}\cosh(\eta_{2R}-\xi_{2R}+\frac{\lambda_3}{2})]}, \tag{27a}$$

$$S^{(2)} \simeq \frac{4l_{2R}\sqrt{l_{2I}}A_2^{2+}e^{i(\xi_{2I}+\frac{\pi}{2})}\cosh(\eta_{2R}+\frac{\lambda_4}{2})}{[a_{22}\cosh(\eta_{2R}+\xi_{2R}+\frac{\lambda_2}{2})+\frac{1}{a_{22}^*}\cosh(\eta_{2R}-\xi_{2R}+\frac{\lambda_3}{2})]}, \tag{27b}$$

$$L \simeq \frac{4}{D_2^2}\Big(k_{2R}^2\cosh(2\xi_{2R}+\frac{\lambda_4+\lambda_3-\lambda_2}{2})+\frac{1}{2}e^{\lambda_4'-(\frac{\lambda_4+\lambda_2+\lambda_3}{2})} + l_{2R}^2\cosh(2\eta_{2R}+\frac{\lambda_2+\lambda_4-\lambda_3}{2})\Big), \tag{27c}$$

$$D_2 = e^{\frac{\lambda_4}{2}}\cosh(\eta_{2R}+\xi_{2R}+\frac{\lambda_4}{2})+e^{\frac{\lambda_2+\lambda_3}{2}}\cosh(\eta_{2R}-\xi_{2R}+\frac{\lambda_2-\lambda_3}{2}),$$

$$e^{\lambda_4'} = 4(k_{2R}+l_{2R})^2e^{\lambda_4}+4(k_{2R}-l_{2R})^2e^{\lambda_2+\lambda_3},$$

where $\lambda_1 = \ln\frac{(k_2-l_2)|\alpha_2^{(2)}|^2}{2i(l_2-l_2^*)(l_2+l_2^*)^2(k_2+l_2^*)}$, $\lambda_2 = \ln\frac{|k_2-l_2|^2|\alpha_2^{(1)}|^2|\alpha_2^{(2)}|^2}{(2i)^2|k_2+l_2^*|^2(k_2-k_2^*)(l_2-l_2^*)(k_2+k_2^*)^2(l_2+l_2^*)^2}$, $\lambda_3 = \ln\frac{|\alpha_2^{(1)}|(l_2-l_2^*)(l_2+l_2^*)^2}{|\alpha_2^{(2)}|(k_2-k_2^*)(k_2+k_2^*)^2}$, $\lambda_4 = \ln\frac{(l_2-k_2)|\alpha_2^{(1)}|^2}{2i(k_2-k_2^*)(k_2+k_2^*)^2(k_2^*+l_2)}$, $A_2^{1+} = [\alpha_2^{(1)}/\alpha_2^{(1)^*}]^{1/2}$, $A_2^{2+} = i[\alpha_2^{(2)}/\alpha_2^{(2)^*}]^{1/2}$. The explicit forms of all the other constants are given in Appendix C.

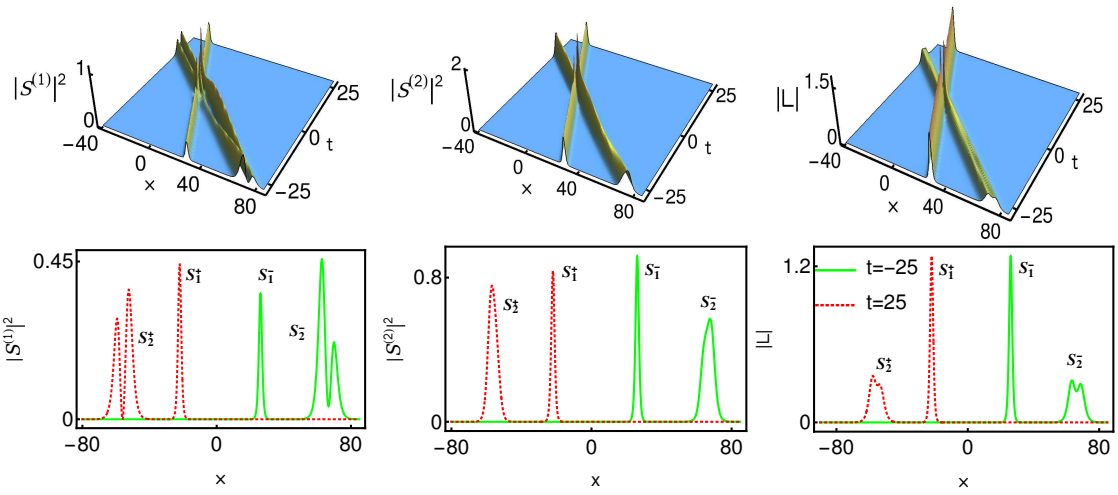

Figure 10. Type-I shape changing collision between degenerate soliton and nondegenerate soliton: To draw this figure the parameter values are fixed as follows: $k_1 = l_1 = 0.8 - 0.5i$, $k_2 = 0.315 - 1.2i$, $l_2 = 0.5 - 1.2i$, $\alpha_1^{(1)} = 0.5$, $\alpha_1^{(2)} = 0.8$, $\alpha_2^{(1)} = 0.5 + 0.5i$ and $\alpha_2^{(2)} = 0.45 + 0.45i$.

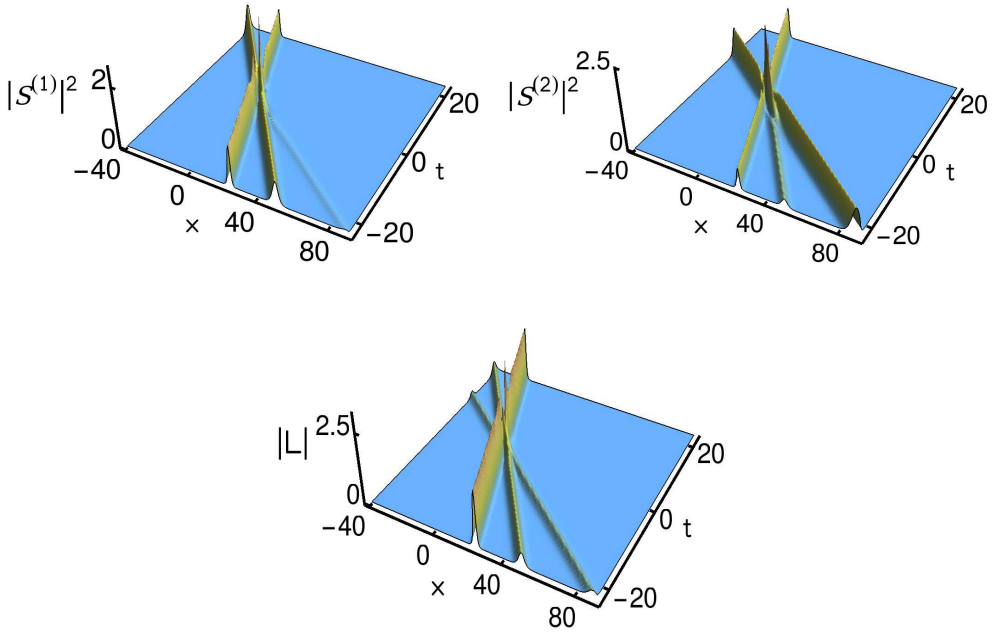

Figure 11. Type-II shape changing collision between degenerate soliton and nondegenerate soliton: To illustrate this collision we fix the complex parameter values as follows: $k_1 = l_1 = 1 - 0.5i$, $k_2 = 0.35 - 1.8i$, $l_2 = 0.5 - i$, $\alpha_1^{(1)} = 1$, $\alpha_1^{(2)} = 0.7$, $\alpha_2^{(1)} = 0.8$ and $\alpha_2^{(2)} = 0.6$.

4.2. Degenerate soliton collision induced shape changing property of nondegenerate soliton

As we have defined earlier, the coexisting solitons (both degenerate and nondegenerate) undergo Type-I and Type-II shape changing collisions corresponding to two distinct velocity conditions $k_{2I} = l_{2I}$ and $k_{2I} \neq l_{2I}$, respectively. In both these collision scenarios, the degenerate bright soliton strongly affects the structure of nondegenerate soliton as it is ensured from the above asymptotic analysis. As a result, the initial structure of the nondegenerate soliton S_2 is varied to a different of geometrical structure. A typical Type-I shape changing collision is depicted in figure 10 for $k_{2I} = l_{2I}$. In figure 10, it is true that the degenerate soliton S_1 undergoes energy sharing collision among the two SW components only while it interacts with the nondegenerate soliton S_2 as it has been shown in the pure degenerate case [20]. In the long-wave component, we observe elastic collision only when the degenerate soliton even collides with another class of asymmetric double-humped nondegenerate soliton. During such enegy sharing collision of the degenerate soliton, the polarization constants of SW components $A_1^{l-} = \alpha_1^{(l)}/(|\alpha_1^{(1)}|^2 + |\alpha_1^{(2)}|^2)^{1/2}$, $l = 1, 2$, change into $A_1^{1+} = \alpha_1^{(1)}/(|\alpha_1^{(1)}|^2 + \chi|\alpha_1^{(2)}|^2)^{1/2}$, $A_1^{2+} = \alpha_1^{(2)}/(|\alpha_1^{(1)}|^2\chi^{-1} + |\alpha_1^{(2)}|^2)^{1/2}$, where $\chi = (|k_1 - l_2|^2|k_1 + k_2^*|^2|k_1 + l_2|^2|k_1 - k_2^*|^2)/(|k_1 - k_2|^2|k_1 + l_2^*|^2|k_1 + k_2|^2|k_1 - l_2^*|^2)$. Meanwhile, the amplitude of the soliton S_1 in the long-wave component remains unchanged except for a finite phase shift. In contrast to the

degenerate soliton S_1, the profile structure of the nondegenerate fundamental soliton S_2 gets dramatically altered during the collision processes as it is evident from figure 10. From figure 10, one can observe that the initial set of asymmetric double-hump profiles in the short-wave component $S^{(1)}$ and in the long-wave component L get transformed into another set of asymmetric double-hump profiles with a finite phase shift. However, in the second short-wave component, the soliton S_2 switches its asymmetric flattop profile into a single-hump profile with an enhancement of energy along with a phase shift. From the asymptotic forms, we identify that the relative separation distance or the phase terms are not maintained during this special kind of interaction.

Next, we display the Type-II shape-changing collision in figure 11 for $k_{2I} \neq l_{2I}$, where the degenerate soliton S_1 undergoes usual energy sharing collision as expected. However, the nondegenerate soliton S_2 exhibits unusual collision property. From figure 11, one can immediately notice that two single-hump solitons appear in the two short-wave components $S^{(l)}$, $l = 1, 2$, under the velocity condition $k_{2I} \neq l_{2I}$ apart from the appearance two similar solitons in the long-wave component. We do not come across the appearance of such two single-hump solitons in the short-wave components in the case of one-soliton, where a single-hump profile only emerged in both the $S^{(l)}$ components at $k_{1I} \neq l_{1I}$ (one can confirm this from figure 3). We also notice that the small amplitude soliton structure, in both the SW components, disappears after colliding with the degenerate soliton S_1 whereas the energy of the larger amplitude soliton is enhanced further. In other words, the two single-humped structures, in both the SW components, are merged during the collision. After the collision, they get combined into a single-hump soliton. However, very interestingly the two single-humped nondegenerate structure in the LW component propagates without any distortion thereby confirming the elastic collision nature. To characterize both Type-I and Type-II shape changing collisions, one can calculate the corresponding transition amplitudes. For both the collision scenarios, the explicit forms of the transition amplitudes turn out to be

$$T_1^1 = \frac{(|\alpha_1^{(1)}|^2 + |\alpha_1^{(2)}|^2)^{1/2}}{(|\alpha_1^{(1)}|^2 + \chi|\alpha_1^{(2)}|^2)^{1/2}}, \quad T_1^2 = \frac{(|\alpha_1^{(1)}|^2 + |\alpha_1^{(2)}|^2)^{1/2}}{(|\alpha_1^{(1)}|^2\chi^{-1} + |\alpha_1^{(2)}|^2)^{1/2}}, \tag{28}$$

where $\chi = (|k_1-l_2|^2|k_1+k_2^*|^2|k_1+l_2|^2|k_1-k_2^*|^2)/(|k_1-k_2|^2|k_1+l_2^*|^2|k_1+k_2|^2|k_1-l_2^*|^2)$. In general, the value of χ is not equal to one. Consequently the transition amplitudes T_1^1 and T_1^2 are not unimodular. In this situation, one always comes across shape changing collision. The standard elastic collision can occur when $\chi = 1$, where the quantities T_1^1 and T_1^2 are equal to unity. We point out that one can also calculate explicitly the position shift that occurred during the collision between the degenerate and nondegenerate solitons. We wish to emphasize here that to the best of our knowledge the collision scenarios discussed above have not been reported elsewhere in the literature for the (1+1)-dimensional two component LSRI system (1).

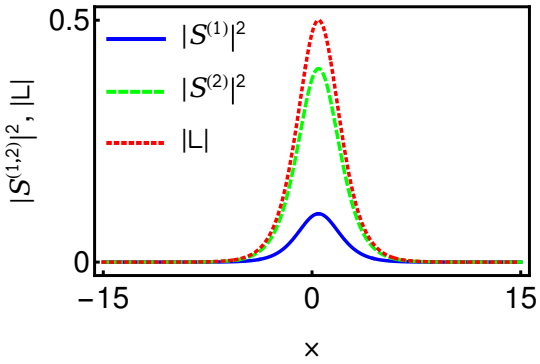

Figure 12. Single-humped degenerate fundamental soliton: $k_1 = 0.5 - 0.5i$, $\alpha_1^{(1)} = 0.5$ and $\alpha_1^{(2)} = 1$.

5. Degenerate-soliton solutions and their collision dynamics

Here, we provide the minimal details about the already known class of degenerate soliton solutions and the underlying collision property, reported in Ref. [20] for Eq. (1), in order to clearly distinguish the corresponding dynamics from the dynamics of nondegenerate soliton solution (6*a*)-(6*c*) presented in this paper. The energy exchanging collision exhibiting degenerate fundamental bright soliton solution can be extracted from the nondegenerate one-soliton solution Eqs. (6*a*)-(6*c*) by imposing the restriction $k_1 = l_1$ in it. As a consequence of this constraint, the seed solutions (3) get restricted as $g_1^{(1)} = \alpha_1^{(1)} e^{\eta_1}$, $g_1^{(2)} = \alpha_1^{(2)} e^{\eta_1}$, $\eta_1 = k_1 x + i k_1^2 t$. This results in the degenerate one-soliton solution of the form,

$$S^{(l)} = 2A_l k_{1R}\sqrt{k_{1I}} e^{i(\eta_{1I}+\frac{\pi}{2})}\ \mathrm{sech}(\eta_{1R}+\frac{R}{2}),\ L = 2k_{1R}^2\ \mathrm{sech}^2(\eta_{1R}+\frac{R}{2}). \tag{29}$$

Here, $A_l = \frac{\alpha_1^{(l)}}{\sqrt{|\alpha_1^{(1)}|^2+|\alpha_1^{(2)}|^2}}$, $l = 1, 2$, $e^R = -\frac{(|\alpha_1^{(1)}|^2+|\alpha_1^{(2)}|^2)}{16k_{1R}^2 k_{1I}}$, $\eta_{1R} = k_{1R}(x - 2k_{1I}t)$, $\eta_{1I} = k_{1I}x + (k_{1R}^2 - k_{1I}^2)t$. In contrast to the nondegenerate soliton, the above degenerate soliton always propagates in all the components with identical velocity $2k_{1I}$. This is because of the presence of a single complex wave number k_1 in the solution (29). It leads to single-hump profiles only in all the three components as we have shown in figure 12. The amplitudes of the degenerate soliton in the SW components and the long-wave component are $2A_l k_{1R}\sqrt{k_{1I}}$ and $2k_{1R}^2$, respectively. The central position of the soliton (for all the components) is $\frac{R}{2}$.

The degenerate two-soliton solution of the system (1) was reported in Ref. [20] by considering the seed solutions

$$g_1^{(l)} = \alpha_1^{(l)} e^{\eta_1} + \alpha_2^{(l)} e^{\eta_2},\ \eta_j = k_j x + i k_j^2 t,\ l, j = 1, 2. \tag{30}$$

On the other hand, it can be captured from the nondegenerate two-soliton solution (12*a*) and (12*b*) by imposing the restrictions $k_1 = l_1$ and $k_2 = l_2$. The resultant Gram determinat forms of the degenerate two-soliton solution contains the following elements

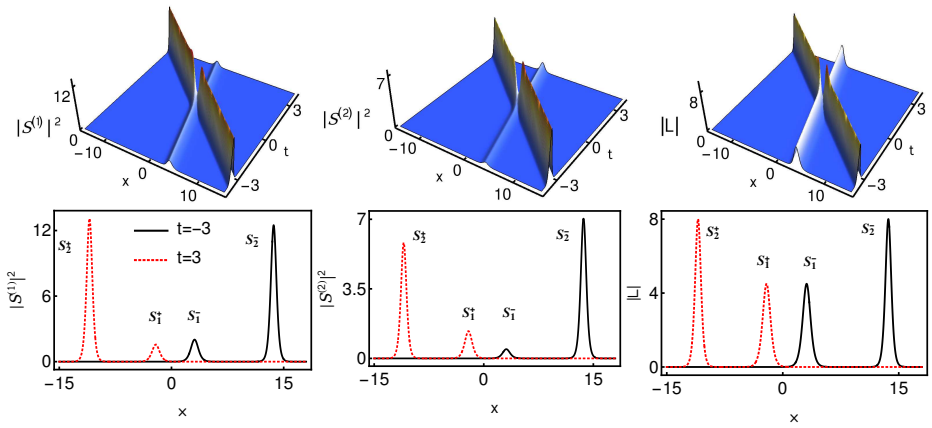

Figure 13. Energy sharing collision of two degenerate solitons: $k_1 = 1.5 - 0.5i$, $k_2 = 2 - 2i$, $\alpha_1^{(1)} = 2.5$, $\alpha_1^{(2)} = 1.2$, $\alpha_2^{(1)} = 0.9$ and $\alpha_2^{(2)} = 0.6$.

in Eqs. (11),

$$A_{mm'} = \frac{e^{\eta_m + \eta^*_{m'}}}{(k_m + k^*_{m'})} = A_{mn} = A_{nm} = A_{nn'},\ \phi_1 = \phi_2 = \begin{pmatrix} e^{\eta_1} & e^{\eta_2} \end{pmatrix}^T,$$
$$\kappa_{mm'} = \frac{\psi^\dagger_m \sigma \psi_{m'}}{2i(k^2_m - k^{*2}_{m'})} = \kappa_{mn} = \kappa_{nm} = \kappa_{nn'},\ m, m', n, n' = 1, 2. \tag{31}$$

The other elements are the same as the ones defined in Eqs. (12*a*) and (12*b*). In general, the degenerate N-soliton solution is a special case of our nondegenerate vector N-soliton solution under the restrictions, $k_i = l_i$, $i = 1, 2, ..., N$. We wish to remark here that obviously any one soliton solution will be a special case of the two-soliton solution, under the appropriate specialization of the parameters. The nondegenerate fundamental soliton solution (6*a*)-(6*c*) turns out be a special case of the nondegenerate two-soliton solution (12*a*) and (12*b*) with $\alpha_2^{(1)} = \alpha_2^{(2)} = 0$. Similarly, the degenerate fundamental soliton solution (29) is a special case of the degenerate two-soliton case under the restriction $\alpha_2^{(1)} = \alpha_2^{(2)} = 0$. In passing, we note that very special parametric choice turns out to be the present fundamental one soliton solution (one soliton solution presented in Eqs. (6*a*)-(6*c*) can be deduced from the degenerate two-soliton solution (31) too under the restriction $\alpha_2^{(1)} = \alpha_1^{(2)} = 0$ after renaming the resultant constants $\alpha_2^{(2)}$ as $\alpha_1^{(2)}$ and k_2 as l_1). However, as it is evident from our discussion, the properties of the nondegenerate fundamental soliton solution (6*a*)-(6*c*) are entirely distinct from the interacting degenerate two-soliton solution reported in Ref. [20].

As we have pointed in the previous sub-section 4.2 and by the authors of Ref. [20], the degenerate solitons of the LSRI system (1) undergo collision with energy redistribution among the short-wave components. Such a typical collision scenario is displayed in figure 13 as an example. From this figure, one can easily observe that the energy of the soliton S_2 is enhanced in the $S^{(1)}$ component and it gets suppressed in the $S^{(2)}$ component. In order to preserve the conservation of energy in both the SW components, the energy of the soliton S_1 is suppressed in the $S^{(1)}$ component and it gets enhanced in the $S^{(2)}$ component. However, the degenerate solitons in the long-wave

component always undergoes elastic collision. The elastic collision is brought out in all the components by fixing the parameters as $\frac{\alpha_1^{(1)}}{\alpha_2^{(1)}} = \frac{\alpha_1^{(2)}}{\alpha_2^{(2)}}$ [20].

6. Conclusion

We have derived the nondegenerate one-,two- and three-soliton solutions through the Hirota bilinear method for the two component long wave short-wave resonance interaction system. The obtained soliton solutions are represented by Gram determinant forms. We have shown that the appearance of an additional wave number in the fundamental soliton solution brings out novel geometrical structures under the condition $k_{1I} = l_{1I}$. In addition, for $k_{1I} \neq l_{1I}$, the soliton number is increased by one in the long-wave component. The reason for the creation of additional soliton in the long-wave component is that the solitons in the two short-wave components nonlinearly interact among themselves through the LW component. Further, we have observed that the nondegenerate solitons undergo three types of collisions, namely shape preserving with a zero phase shift, shape altering and shape changing collisions with finite phase shifts. The mechanism of the nonpreserving nature of phase terms or relative separation distances induces these novel shape altering and shape changing collision scenarios. However, they can be viewed as elastic collision only by taking time shifts in the asymptotic forms of nondegenerate solitons. Surprisingly, such type of collision property has not been observed in the degenerate counterpart though they belong to elastic collision only. Besides this, the emergence of a coexisting nonlinear phenomenon in the two component LSRI system is also explored. We found that the existence of a partially nondegenerate soliton solution, which is a special case of the completely nondegenerate two-soliton solution, is responsible for the appearance of such a nonlinear phenomenon, where the nondegenerate soliton simultaneously exists with the degenerate soliton. We have noticed that the explicit appearance of degenerate soliton induces two types of interesting shape changing and energy sharing properties of nondegenerate soliton. Finally, we recovered the energy exchanging solitons from the nondegenerate solitons under degenerate limits. The present study on nondegenerate solitons of long wave-short wave resonance interaction system will be useful in hydrodynamics, plasma physics, nonlinear optics and Bose-Einstein condensates.

Acknowledgements

The works of SS, RR and ML are supported by the DST-SERB Distinguished Fellowship program to ML under the Grant No. SB/DF/04/2017. RR also grateful to Council of Scientific and Industrial Research, Government of India, for their support in the form of a Senior Research Fellowship (09/475(0203)/2020-EMR-I).

Appendix A. Three-soliton solution

The three-soliton solution of the system (1) is given below:

$$g^{(1)}=\begin{vmatrix} A_{mm'} & A_{mn} & I & \mathbf{0} & \phi_1 \\ A_{nm} & A_{nn'} & \mathbf{0} & I & \phi_2 \\ -I & \mathbf{0} & \kappa_{mm'} & \kappa_{mn} & \mathbf{0'}^T \\ \mathbf{0} & -I & \kappa_{nm} & \kappa_{nn'} & \mathbf{0'}^T \\ \mathbf{0'} & \mathbf{0'} & C_1 & \mathbf{0'} & 0 \end{vmatrix},\ f=\begin{vmatrix} A_{mm'} & A_{mn} & I & \mathbf{0} \\ A_{nm} & A_{nn'} & \mathbf{0} & I \\ -I & \mathbf{0} & \kappa_{mm'} & \kappa_{mn} \\ \mathbf{0} & -I & \kappa_{nm} & \kappa_{nn'} \end{vmatrix}, \quad \text{(A.1)}$$

$$g^{(2)}=\begin{vmatrix} A_{mm'} & A_{mn} & I & \mathbf{0} & \phi_1 \\ A_{nm} & A_{nn'} & \mathbf{0} & I & \phi_2 \\ -I & \mathbf{0} & \kappa_{mm'} & \kappa_{mn} & \mathbf{0'}^T \\ \mathbf{0} & -I & \kappa_{nm} & \kappa_{nn'} & \mathbf{0'}^T \\ \mathbf{0'} & \mathbf{0'} & \mathbf{0'} & C_2 & 0 \end{vmatrix}. \quad \text{(A.2)}$$

The various elements of the above Gram determinants are defined as

$$A_{mm'}=\frac{e^{\eta_m+\eta^*_{m'}}}{(k_m+k^*_{m'})},\ A_{mn}=\frac{e^{\eta_m+\xi^*_n}}{(k_m+l^*_n)}, A_{nn'}=\frac{e^{\xi_n+\xi^*_{n'}}}{(l_n+l^*_{n'})},\ A_{nm}=\frac{e^{\eta^*_n+\xi_m}}{(k^*_n+l_m)},$$

$$\kappa_{mm'}=\frac{\psi^\dagger_m\sigma\psi_{m'}}{2i(k^2_m-k^{*2}_{m'})},\ \kappa_{mn}=\frac{\psi^\dagger_m\sigma\psi'_n}{2i(l^2_m-k^{*2}_n)},\ \kappa_{nm}=\frac{\psi'^\dagger_n\sigma\psi_m}{2i(k^2_n-l^{*2}_m)},$$

$$\kappa_{nn'}=\frac{\psi'^\dagger_n\sigma\psi'_{n'}}{2i(l^2_n-l^{*2}_{n'})},\ m,m',n,n'=1,2,3.$$

The other elements are defined below:
$\phi_1 = \begin{pmatrix} e^{\eta_1} & e^{\eta_2} & e^{\eta_3} \end{pmatrix}^T$, $\phi_2 = \begin{pmatrix} e^{\xi_1} & e^{\xi_2} & e^{\xi_3} \end{pmatrix}^T$, $\psi_j = \begin{pmatrix} \alpha^{(1)}_j & 0 \end{pmatrix}^T$, $\psi'_j = \begin{pmatrix} 0 & \alpha^{(2)}_j \end{pmatrix}^T$, $\mathbf{0'} = \begin{pmatrix} 0 & 0 & 0 \end{pmatrix}$, $I = \sigma = \begin{pmatrix} 1 & 0 & 0 \\ 0 & 1 & 0 \\ 0 & 0 & 1 \end{pmatrix}$, $\mathbf{0} = \begin{pmatrix} 0 & 0 & 0 \\ 0 & 0 & 0 \\ 0 & 0 & 0 \end{pmatrix}$ and $C_N = -\begin{pmatrix} \alpha^{(N)}_1 & \alpha^{(N)}_2 & \alpha^{(N)}_3 \end{pmatrix}$, $j=1,2,3$, $N=1,2$. We remark that the degenerate three-soliton solution can be obtained from the above nondegenerate three-soliton solution when $k_j=l_j$, $j=1,2,3$. In general, mathematically to obtain the degenerate N-soliton solution from the nondegenerate N-soliton solution one needs to impose N number of restrictions on the wave bumbers $k_j=l_j$, $j=1,2,...,N$.

Appendix B. Constants which arise in the asymptotic analysis of collision dynamics of degenerate and nondegenerate solitons

$$e^{\mu_1}=\frac{i(k_1-k_2)\alpha^{(1)}_2\hat{\Lambda}_1}{2(k_1-k^*_1)(k_1+k^*_1)^2(k^*_1-k_2)(k^*_1+k_2)^2},\ e^{\mu_2}=\frac{i(k_1-l_2)\alpha^{(1)}_1\alpha^{(2)*}_1\alpha^{(2)}_2}{2(k_1+k^*_1)(k^*_1-l_2)(k^*_1+l_2)^2},$$

$$e^{\mu_3}=\frac{i(k_1-k_2)(k_2-l_2)|k_1-l_2|^2\alpha^{(1)}_2|\alpha^{(2)}_2|^2\hat{\Lambda}_2e^{R_4}}{2(k_1-k^*_1)(k_1+k^*_1)^2(k^*_1-k_2)(k^*_1+k_2)^2|k_1-l^*_2|^2|k_1+l^*_2|^4(k_2+l^*_2)},$$

$$e^{\mu_4}=-\frac{i(k_1-k_2)^2(k_1+k_2)(k^*_1-k^*_2)(k_1-l_2)(k_2-l_2)\alpha^{(1)}_1\alpha^{(2)*}_1\alpha^{(2)}_2e^{R_5}}{2(k_1+k^*_1)(k^*_1+k_2)(k_1-k^*_2)(k^*_1-l_2)(k^*_2+l_2)(k^*_1+l_2)^2},$$

$$e^{\mu_5}=\frac{\hat{\Lambda}_4}{2i(k_1-k_1^*)(k_1+k_1^*)^2},\ e^{\mu_6}=\frac{i|k_1-k_2|^2\hat{\Lambda}_5e^{R_5}}{2(k_1-k_1^*)(k_1+k_1^*)^2|k_1-k_2^*|^2|k_1+k_2^*|^4},$$
$$e^{\mu_7}=-\frac{i|k_1-l_2|^2\hat{\Lambda}_6e^{R_4}}{2(k_1-k_1^*)(k_1+k_1^*)^2|k_1-l_2^*|^2|k_1+l_2^*|^4},\ \hat{\Lambda}_4=(|\alpha_2^{(1)}|^2+|\alpha_2^{(2)}|^2),$$
$$e^{\mu_8}=-\frac{i|k_1-k_2|^2|k_1-l_2|^2|k_2-l_2|^2\hat{\Lambda}_3e^{R_4+R_5}}{2(k_1-k_1^*)(k_1+k_1^*)^2|k_1-k_2^*|^2|k_1+k_2^*|^4|k_1-l_2^*|^2|k_1+l_2^*|^4|k_2+l_2^*|^2},$$
$$e^{\mu_9}=-\frac{(k_1^*-k_2^*)(k_1-l_2)\alpha_1^{(1)}\alpha_1^{(2)*}\alpha_2^{(1)*}\alpha_2^{(2)}}{4(k_1+k_1^*)(k_1-k_2^*)(k_1+k_2^*)^2(k_1^*-l_2)(k_1^*+l_2)^2(k_2^*+l_2)},$$
$$e^{\mu_{10}}=-\frac{(k_1-k_2)(k_1^*-l_2^*)\alpha_1^{(1)*}\alpha_1^{(2)}\alpha_2^{(1)}\alpha_2^{(2)*}}{4(k_1+k_1^*)(k_1^*-k_2)(k_1^*+k_2)^2(k_1-l_2^*)(k_1+l_2^*)^2(k_2+l_2^*)},$$
$$e^{\nu_1}=\frac{i(k_1-k_2)\alpha_1^{(1)*}\alpha_1^{(2)}\alpha_2^{(1)}}{2(k_1+k_1^*)(k_1^*-k_2)(k_1^*+k_2)^2},\ e^{\nu_2}=\frac{i(k_1-l_2)\alpha_2^{(2)}\hat{\Lambda}_7}{2(k_1-k_1^*)(k_1+k_1^*)^2(k_1^*-l_2)(k_1^*+l_2)^2},$$
$$e^{\nu_3}=\frac{i(k_1-k_2)(k_1-l_2)^2(k_2-l_2)(k_1+l_2)(k_1^*-l_2^*)\alpha_1^{(1)*}\alpha_1^{(2)}\alpha_2^{(1)}e^{R_4}}{2(k_1+k_1^*)(k_1^*-k_2)(k_1^*+k_2)^2(k_1^*+l_2)(k_1-l_2^*)(k_1+l_2^*)^2(k_2+l_2^*)},$$
$$e^{\nu_4}=-\frac{i|k_1-k_2|^2(k_1-l_2)(k_2-l_2)\alpha_2^{(2)}\hat{\Lambda}_8e^{R_5}}{2(k_1-k_1^*)(k_1+k_1^*)^2|k_1-k_2^*|^2|k_1+k_2^*|^4(k_1^*-l_2)(k_1^*+l_2)^2(k_2^*+l_2)},$$
$$\hat{\Lambda}_1=(\varrho_{12}|\alpha_1^{(1)}|^2+\hat{\varrho}_{12}^*|\alpha_1^{(2)}|^2),\ \hat{\Lambda}_2=(\varrho_{12}|\bar{\gamma}_{12}|^2|\alpha_1^{(1)}|^2+\hat{\varrho}_{12}^*|\gamma_{12}|^2|\alpha_1^{(2)}|^2),$$
$$\hat{\Lambda}_3=(|\varrho_{12}|^2|\bar{\gamma}_{12}|^2|\alpha_1^{(1)}|^2+|\hat{\varrho}_{12}^*|^2|\gamma_{12}|^2|\alpha_1^{(2)}|^2),\ \hat{\Lambda}_5=(|\varrho_{12}|^2|\alpha_1^{(1)}|^2+|\hat{\varrho}_{12}^*|^2|\alpha_1^{(2)}|^2),$$
$$\hat{\Lambda}_6=(|\bar{\gamma}_{12}|^2|\alpha_1^{(1)}|^2+|\gamma_{12}|^2|\alpha_1^{(2)}|^2),\ \hat{\Lambda}_7=(\bar{\gamma}_{12}|\alpha_1^{(1)}|^2+\gamma_{12}|\alpha_1^{(2)}|^2),$$
$$\hat{\Lambda}_8=(|\varrho_{12}|^2\bar{\gamma}_{12}|\alpha_1^{(1)}|^2+|\hat{\varrho}_{12}^*|^2\gamma_{12}|\alpha_1^{(2)}|^2),\ \varrho_{12}=(k_1^2-k_2^2),\ \hat{\varrho}_{12}=(k_1^2-k_2^{*2}),$$
$$\gamma_{12}=(k_1^2-l_2^2),\ \bar{\gamma_{12}}=(k_1^2-l_2^{*2}). \tag{2.1}$$

References

[1] Lakshmanan M, Rajasekar S 2003, *Nonlinear Dynamics, Integrability, Chaos and Patterns* (Springer-Verlag, Berlin Heidelberg).

[2] Zakharov V E 1972, *Sov. Phys. JETP* **35**, 908 [*Zh. Eksp. Teor. Fiz.* **62**, 1745 (1972)].

[3] D. J. Benny D J 1977, *Stud. Appl. Math.* **56**, 81.

[4] Nishikawa K, Hojo H, Mima K and Ikezi H 1974, *Phys. Rev. Lett.* **33**, 148

[5] Yajima N and Oikawa M, 1976 *Prog. Theor. Phys.* **56**, 1719.

[6] Ablowitz M J and Clarkson P A, 1991 *Solitons, Nonlinear Evolution Equations and Inverse Scattering* (Cambridge University Press, Cambridge)

[7] Kawahara T 1975, *J. Phys. Soc. Japan* **38** 265; Kawahara T, Sugimoto N and Kakutani T, *J. Phys. Soc. Japan* **39** 1379.

[8] R. H. J. Grimshaw, *Stud. Appl. Math.* **56**, 241 (1977); V. D. Djordjevic and L. G. Redekopp, *J. Fluid Mech.* **79**, 703 (1977);

[9] Kopp C G and Redekopp L G (1981), *J. Fluid. Mech.*, **111**, 367.

[10] Boyd J P (1982) *J. Phys. Oceanogr.* **13**, 450.

[11] Kivshar Y S 1992, *Opt. Lett.* **17**, 1322.

[12] A. Chowdhury and J. A. Tataronis 2008, *Phys. Rev. Lett.* **100**, 153905.

[13] Ablowitz M J, Biondini G, Blair S 2001, *Phys. Rev. E* **63** 046605.

[14] Sazonov S V and Ustinov N V 2011, *JETP Lett.* **94**, 610 (2011).

[15] Zabolotskii A A 2009, *Phys. Rev. A* **80**, 063616; Zabolotskii A A 2009, *JETP* **109**, 859.

[16] Aguero M, Frantzeskakis D J and Kevrekidis P G 2006, *J. Phys. A: Math. Gen.* **39**, 7705.

[17] Niztazakis H E, Frantzeskakis D J, Kevrekidis P G, Malomed B A, González R C 2008, *Phys. Rev. A*, **77**, 033612.

[18] Myrzakulov R, Pashaev O K and Kholmurodov Kh. T 1986, *Phys. Scr.* **33**, 378.

[19] Ma Y C 1978, *Stud. Appl. Math.* **59**, 201; Ma Y C and Redekopp L G 1979, *Phys. Fluids* **22**, 1872;

[20] Kanna T, Sakkaravarthi K, and Tamilselvan K 2013, *Phys. Rev. E* **88**, 062921.

[21] Chen J, Chen Y, Feng B F, and Maruno K I 2015, *J. Phys. Soc. Jpn.* **84**, 074001.

[22] Chen J, Chen Y, Feng B F, and Maruno K I 2015, *J. Phys. Soc. Jpn.* **84**, 034002.

[23] Funakoshi M and Oikawa M 1983, *J. Phys. Soc. Japan* **52**, 1982 (1983); Oikawa M, Okamura M and Funakoshi M 1989, *J. Phys. Soc. Japan* **58** 4416

[24] Ohta Y, Maruno K and Oikawa M 2007 *J. Phys. A: Math. Theor.* **40** 7659

[25] Radha R, Senthil Kumar C, Lakshmanan M and Gilson C R 2009, *J. Phys. A: Math. Theor.* **42**, 102002.

[26] Kanna T, Vijayajayanthi M, Sakkaravarthi K and Lakshmanan M 2009, *J. Phys. A: Math.Theor.* **42**, 115103.

[27] Sakkaravarthi K, Kanna T, Vijayajayanthi M and M. Lakshmanan 2014, *Phys. Rev. E* **90**, 052912.

[28] Kanna T, Vijayajayanthi M and Lakshmanan M 2014, *Phys. Rev. E* **90** 042901.

[29] Chen J, Feng B F, Chen Y, and Ma Z 2017, *Nonlinear Dyn.* **88**, 1273.

[30] Akhmediev N, Ankiewicz A and Taki M 2009, *Phys. Lett. A* **373**, 675.

[31] Chow K W, Chan H N, Kedzioara D J, and Grimshaw R H J 2013, *J. Phys. Soc. Japan* **82**, 074001.

[32] Chen S, Grelu P and Soto-Crespo J M 2014, *Phys. Rev. E* **89** 011201(R).

[33] Chan H N, Ding E, Kedzioara D J, Grimshaw R H J and Chow K W 2016, *Nonlinear Dyn.* **85**, 2827.

[34] Chen S, Soto-Crespo J M and Grelu P 2014, *Phys. Rev. E* **90** 033203.

[35] Chen J, Chen Y, Feng B F, and Maruno K I 2015, *Phys. Lett. A* **379**, 1510.

[36] Rao J, Porsezian K, He J and Kanna T 2018, *Proc. R. Soc. A* **474** 20170627.

[37] Yang J W, Gao Y T, Sun Y H, Shen Y J and Su C Q 2016, *Eur. Phys. J. Plus* **131** 416.

[38] Stalin S, Ramakrishnan R, Senthilvelan M and Lakshmanan M 2019, *Phys. Rev. Lett.* **122** 043901

[39] Ramakrishnan R, Stalin S, and Lakshmanan M 2020, *Phys. Rev. E* **102** 042212.

[40] Stalin S, Ramakrishnan R and Lakshmanan M 2020, *Phys. Lett. A* **384**, 126201.

[41] Qin Y H, Zhao L C and Ling L 2019, *Phys. Rev. E* **100** 022212.

[42] Ramakrishnan R, Stalin S, and Lakshmanan M 2021, *J. Phys. A: Math. Theor.* **54** 14LT01.

[43] Stalin S, Senthilvelan M and Lakshmanan M 2019, *Nonlinear Dyn.* **95** 343.

[44] Zhang C R, Tian B, Qu Q X, Liu L and Tian H Y 2020, *Z. Angew. Math. Phys.* **71**, 18.

[45] Ding C C, Gao Y T, Hu L, Deng G F and Zhang C Y 2021, *Chaos, Solitons & Fractals* **142**, 110363.

[46] Hirota R 2004 *The Direct Method in Soliton Theory* (Cambridge: Cambridge University Press)

[47] Stalin S, Ramakrishnan R and Lakshmanan M 2021, *Photonics* **8**, 258.

[48] Ablowitz M J, Ohta Y and Trubatch A D 1999, *Phys. Lett. A* **253**, 287.

[49] Vijayajayanthi M, Kanna T and Lakshmanan M 2009, *Eur. Phys. J. Special Topics* **173**, 57.

[50] Dauxois T and Peyrard M 2006, *Physics of Solitons*, (Cambridge University Press).

[51] Stalin S, Ramakrishnan R and Lakshmanan M 2020, *unpublished*.

[52] Baronio F, Degasperis A, Conforti M and Wabnitz S (2012), *Phys. Rev. Lett.* **109**, 044102

[53] Degasperis A, Conforti M, Baronio F and Wabnitz S 2006 *Phys. Rev. Lett.* **97** 093901

[54] Bersano, T M, Gokhroo V, Khamehchi M A, D'Ambroise J, Frantzeskakis D J, Engels P and Kevrekidis P G 2018 *Phys. Rev. Lett.* **120** 063202.